Durham University

Durham E-Theses

Biostratigraphical constraints (calcareous nannofossils) on the Late Cretaceous to Late Miocene evolution of S.W. Cyprus.

Morse, Trevor John

How to cite:

Morse, Trevor John (1996) *Biostratigraphical constraints (calcareous nannofossils) on the Late Cretaceous to Late Miocene evolution of S.W. Cyprus.*, Durham theses, Durham University. Available at Durham E-Theses Online: http://etheses.dur.ac.uk/1565/

Use policy

The full-text may be used and/or reproduced, and given to third parties in any format or medium, without prior permission or charge, for personal research or study, educational, or not-for-profit purposes provided that:

- a full bibliographic reference is made to the original source
- a link is made to the metadata record in Durham E-Theses
- the full-text is not changed in any way

The full-text must not be sold in any format or medium without the formal permission of the copyright holders.

Please consult the full Durham E-Theses policy for further details.

Academic Support Office, The Palatine Centre, Durham University, Stockton Road, Durham, DH1 3LE
e-mail: e-theses.admin@durham.ac.uk Tel: +44 0191 334 6107
http://etheses.dur.ac.uk

BIOSTRATIGRAPHICAL CONSTRAINTS (CALCAREOUS NANNOFOSSILS) ON THE LATE CRETACEOUS TO LATE MIOCENE EVOLUTION OF S. W. CYPRUS.

Trevor John Morse BSc. Hons (Dunelm)

(St. Cuthbert's Society)

PART I

A thesis submitted in part fulfillment
of the requirements for the degree of
Doctor of Philosophy.

The copyright of this thesis rests with the author.
No quotation from it should be published without
his prior written consent and information derived
from it should be acknowledged.

10 MAR 1997

Department of Geological Sciences
University of Durham
AUGUST 1996

Frontispiece. Satellite infrared image of Cyprus. Irrigated fields appear as vibrant red, pine forests as dark red, dry vegetation as yellow, towns as greyish blue, limestone soils as white and reddish soils as green (centre fold, Executive Review, Cyprus Airways, Winter 1991).

DEDICATION

Anthony George Waterfield

1949-1979

His untimely end was my beginning

ACKNOWLEDGEMENTS

Firstly I must thank my wife Lynn and our children Joanne, Kathryn (Katy) and David, for their support and understanding over the last five years, whilst I was carrying out my PhD studies, plus the three years before as an undergraduate. Thank you is not really enough.

Further thanks go to Lynn for sacrificing the family holidays over three field seasons, so as to act as my field assistant, sorry about the bees.

Special thanks to my supervisors Drs R. E. Swarbrick and H. A. Armstrong for their assistance, patience and guidance throughout the length of the project.

The financial support is acknowledged from the Natural Environmental Research Council, with respect to the research studentship (GT4/91/GS/32).

I am grateful to the technical staff within the Department at Durham, for their much need assistance. To Julie, George and Ron for your services in the field of thin sections; To Gerry for his assistance in producing the photographic plates for the thesis; To Carol and Claire for my administrative needs; To Karen in the drawing office for advice and assistance with my drawing requirements; To you all thank you. Last but not least Mr 'fixit' Dave Asbery for his assistance in all those little things that helped to make my stay a comfortable one, and when added together, special thanks are well deserved.

Thank you to David Hirst and the Open University for employing me over the last Eight summer school seasons. Without the revenue, my studies would have been fraught with many financial worries. With a special thank you from Lynn and family (I am not sure if the thank you is for the financial gain or for keeping me occupied over summer months).

Cyprus is a very special island. To attempt to understand what makes it tick, you must live in one of the villages, away from the flesh spots of the coast. Every Easter, a bit like our Christmas, everybody goes home to family. At Easter weekend the villages become alive, where there were five families, there would be twenty plus. During my first field season, Lynn and I was staying at the village of Mamonia over Easter weekend, to both of us this experience represented the real Cyprus. To all Cypriots thank you for your friendship, especially those in Mamonia, our adopted Cypriot home.

Thank you to those members of the Cyprus Geological Survey, who gave their advice and assistance during my field seasons in Cyprus, with a special thank you to Costos Xenophontos, who arranged our stay in Mamonia.

Thank you Dick for introducing me to Cyprus. I am saving up so that I can spend that year there and grow tired of the place (never).

Thank you to the staff, at the Biomedical Electron Microscopy unit, University of Newcastle. Especially Angus Parker and Phil Bradley for the training and assistance they gave, on the Scanning Electron Microscope, plus photographic work.

Eight years is a long time to spend in any one place as a student, so it is with much regret that I cannot mention by name all the students, postgraduates and members of staff, both academic and technical, who have contributed along with those mentioned above, to making those eight years, very special memories. Thank you for your help, guidance, advise, friendship, laughter and for allowing me to be part of the departmental family.

COPYRIGHT

The copyright of this thesis rests with the author. No quotation from it should be published without prior written consent and any information derived from it should be acknowledged.

© 1996 Trevor J. Morse

DECLARATION

No part of this thesis has been previously submitted for a degree at this university or any other university. The work described in this thesis is entirely that of the author except where reference is made to previous published or unpublished work.

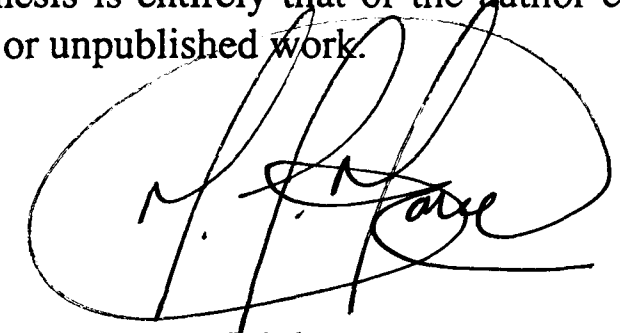

Trevor J. Morse,
Dept. of Geological Sciences,
University of Durham.
AUGUST 1996.

CONTENTS

PART I

Title page. . . . . i.
Frontispiece. . . . . ii.
Dedication. . . . . iii.
Acknowledgements. . . . . iv.
Copyright and Declaration. . . . . v.
Contents. . . . . vi.
Abstract. . . . . xii.

CHAPTER 1.
INTRODUCTION, OBJECTIVES AND THESIS OUTLINE.

1.1 Introduction. . . . . 1.
1.2 Objectives. . . . . 5.
1.3 Thesis Outline.
1.3.1 Chapter 2. . . . . 5.
1.3.2 Chapter 3. . . . . 6.
1.3.3 Chapter 4. . . . . 6.
1.3.4 Chapter 5. . . . . 6.
1.3.5 Chapter 6. . . . . 6.
1.3.6 Chapter 7. . . . . 6.
1.3.7 Appendix A. . . . . 6.
1.3.8 Appendix B. . . . . 6.
1.3.9 Appendix C. . . . . 7.
1.3.10 Appendix D. . . . . 7.
1.3.11 Appendix E. . . . . 7.

CHAPTER 2.
INTRODUCTION TO CYPRUS AND ITS GEOLOGY.

2.1 Introduction. . . . . 8.
2.2 Allochthonous Basement Terranes. . . . . 8.
2.2.1 Kyrenia basement terrane. . . . . 10.

2.2.2 Mesaoria Basin. . . . . 10.
2.2.3 Troodos basement terrane. . . . . 10.
2.2.4 Southern Troodos Transform Fault Zone. . . . 13.
2.2.5 Anti-Troodos basement terrane. . . . . 13.
2.2.6 S.W. Cyprus and Mamonia basement terranes. . . 13.
2.3 Lithostratigraphy and Past Biostratigraphical Research. . . 16.
2.3.1 Sediments associated with the Troodos Basement terrane and fragments. . . . . 16.
2.3.1.1 Perapedhi Formation. . . . . 16.
2.3.1.2 Kannaviou Formation. . . . . 17.
2.3.2 Neo-autochthonous sedimentary cover. . . . 19.
2.3.2.1 Sedimentary melange deposits. . . . 19.
2.3.2.1.1 Moni Formation. . . . . 20.
2.3.2.1.2 Paralimini Melange. . . . . 21.
2.3.2.1.3 Dhrousha Melange. . . . . 22.
2.3.2.1.4 Kathikas Formation. . . . . 23.
2.3.2.2 Calcareous and evaporite sediments. . . . 24.
2.3.2.2.1 Lefkara Formation. . . . . 24.
Lower Member. . . . . 26.
Middle Member (Chalk and Chert unit). . . 28.
Middle Member (Massive Chalk unit). . . 30.
Upper Member. . . . . 32.
2.3.2.2.2 Pakhna Formation. . . . . 33.
Chalks. . . . . 33.
Terra Limestone Member. . . . 35.
Koronia Limestone Member. . . . 36.
2.3.2.2.3 Kalavasos Formation. . . . . 37.
2.3.2.2.4 Pissouri Formation. . . . . 38.
2.4 Major Tectonic Events. . . . . 38.
2.4.1 The Mamonia Complex (Mamonia basement fragments). 39.
2.4.2 Juxtapositioning of the Mamonia and Troodos basement terranes. . . . . 39.
2.4.3 Rotation of the Troodos micro plate. . . . 40.
2.4.4 Kyrenia - D1 Tectonic event. . . . . 40.

2.4.5 Kyrenia - D2 Tectonic event. . . . . 41.
2.4.6 Polis Graben. . . . . 41.
2.4.7 Yerasa Fold Belt. . . . . 41.
2.4.8 Kyrenia - D3 Tectonic event. . . . . 42.
2.4.9 Peyia Half Graben. . . . . 42.
2.4.10 Rapid uplift, Troodos Massif.. . . . . 43.
2.4.11 Subduction. . . . . 43.

CHAPTER 3.
INTRODUCTION TO CALCAREOUS NANNOFOSSILS AND SYSTEMATICS.

3.1 Introduction. . . . . 44.
3.2 History of Research. . . . . 45.
3.3 Systematic Palaeontology.
3.3.1 Construction. . . . . 45.
3.3.2 Classification and definitions. . . . . 45.
3.3.3 Biostratigraphical zonal schemes. . . . . 47.

CHAPTER 4.
BIOSTRATIGRAPHY OF THE LATE CRETACEOUS (CAMPANIAN TO MAASTRICHTIAN) SEDIMENTARY COVER OF S. W. CYPRUS.

4.1 Introduction. . . . . 52.
4.2 Sampling Strategy and Localities. . . . . 52.
4.3 Biostratigraphy. . . . . 55.
4.3.1 Kannaviou Formation. . . . . 56.
4.3.2 Moni Formation. . . . . 57.
4.3.3 Kathikas Formation. . . . . 61.
4.3.4 Lefkara Formation (Lower Member). . . . . 64.
4.4 Summary. . . . . 72.

4.5 Systematic Descriptions. . . . . 74.
Plate 1. . . . . 98.
Plate 2. . . . . 100.
Plate 3. . . . . 102.

CHAPTER 5.
BIOSTRATIGRAPHY OF THE PALAEOCENE AND EOCENE NEO-AUTOCHTHONOUS SEDIMENTARY COVER OF S. W. CYPRUS.

5.1 Introduction. . . . . 105.
5.2 Sampling Strategy and Localities. . . . . 105.
5.3 Biostratigraphy. . . . . 107.
5.3.1 Lefkara Formation, Middle Member,
Chalk and Chert unit (Palaeocene). . . . . 113.
5.3.1.1 Mid Palaeocene. . . . . 114.
5.3.1.2 Late Palaeocene. . . . . 117.
5.3.1.3 Outcrop pattern. . . . . 117.
5.3.2 Lefkara Formation, Middle Member,
Chalk and Chert unit (Eocene). . . . . 118.
5.3.3 Lefkara Formation, Middle Member,
Massive Chalk unit (Eocene). . . . . 120.
5.4 Summary. . . . . 123.
5.5 Systematic Descriptions. . . . . 125.
Plate 4. . . . . 163.
Plate 5. . . . . 165.
Plate 6. . . . . 168.
Plate 7. . . . . 171.
Plate 8. . . . . 173.

CHAPTER 6.
BIOSTRATIGRAPHY OF THE MIOCENE NEO-AUTOCHTHONOUS SEDIMENTARY COVER OF S. W. CYPRUS.

6.1 Introduction. . . . . 175.

6.2 Sampling Strategy and Localities. . . . . 175.
6.3 Biostratigraphy. . . . . 177.
6.3.1 Pakhna Formation chalks. . . . . 184.
6.3.2 Pakhna Formation, Terra Limestone Member. . . 188.
6.3.3 Pakhna Formation, Kottaphi Hill measured section. . 189.
6.3.4 Pissouri Formation (Myrtou Marls). . . . 190.
6.4 Summary. . . . . 191.
6.5 Systematic Descriptions. . . . . 192.
Plate 9. . . . . 219.
Plate 10. . . . . 222.
Plate 11. . . . . 225.

CHAPTER 7.
DISCUSSION AND IMPLICATIONS.

7.1 Introduction. . . . . 227.
7.2 Conformable and Unconformable Contacts. . . . . 227.
7.3 Sedimentary Outcrop Patterns of S.W. Cyprus.
7.3.1 Kannaviou Formation. . . . . 232.
7.3.2 Kathikas Formation and Dhrousha Melange. . . 232.
7.3.3 Lefkara Formation, Lower Member. . . . 238.
7.3.4 Lefkara Formation, Middle Member, Chalk and Chert unit. . 238.
7.3.5 Lefkara Formation, Middle Member, Massive Chalk unit. . 239.
7.3.6 Lefkara Formation, Upper Member. . . . 239.
7.3.7 Pakhna Formation. . . . . 239.
7.3.8 Kalavasos Formation. . . . . 241.
7.3.9 Pissouri Formation. . . . . 241.
7.3.10 General observations.
7.3.10.1 Kannaviou Formation. . . . . 241.
7.3.10.2 Southern Mamonia basement fragment. . . 242.
7.3.10.3 Overall observation of the outcrop pattern. . . 242.
7.4 Lateral Movement (Major Lineaments). . . . . 243.
7.5 The Juxtapositioning and Anticlockwise Rotation Events. . . 244.

7.6 Subduction Zone History of Cyprus. . . . . 245.
7.7 Conclusion. 249

REFERENCES. . . . . . 253.

PART II

APPENDICES.

Title page. . . . . 1.
Contents. . . . . 2.

APPENDIX A. Sampling and Processing. . . . . 3.
APPENDIX B. Calcareous Nannofossil Identification Key
to Family Level. . . . . 8.
APPENDIX C. Deep sea Drilling Project and Ocean Drilling project
Relating to Calcareous Nannofossils. . . . 63.
APPENDIX D. Calcareous Nannofossil Glossary. . . . 75.
APPENDIX E. Sample Data. . . . . 79.

ABSTRACT

BIOSTRATIGRAPHICAL CONSTRAINTS (CALCAREOUS NANNOFOSSILS) ON THE LATE CRETACEOUS TO LATE MIOCENE EVOLUTION OF S. W. CYPRUS

Trevor John Morse

PhD. Thesis, Department of Geological Sciences, University of Durham

In S.W. Cyprus, the sedimentary formations of the Late Cretaceous to Holocene neo-autochthonous sedimentary cover, which unconformably overlie the Mamonia and Troodos basements, are biostatigraphically poorly constrained. The age of the sediments overlying the basement, is critical to providing constraints on the timing of the juxtapositioning of the basement terranes, which may also be closely linked to the anticlockwise rotation of the Troodos micro plate. In addition the biostratigraphy is a valuable tool in establishing the post-juxtapositioning evolution of S.W. Cyprus, in particular relating to its emergence from a deep sea setting.

The relative biostratigraphical data using calcareous nannofossils, have provided revised age dates for all sedimentary formations of Late Miocene age and older. Relative to the early juxtapositioning history, the age of the Kannaviou Formation as Campanian (CC18-CC23a) and the Kathikas Formation as early Maastrichtian (CC23b-CC25a) is confirmed, but a new unit of the Moni Formation, termed the Dhrousha Melange has been recognised/proposed, and dated as late Campanian to early Maastrichtian (CC23-CC25a). Several new unconformable contacts have been recognised. Three new unconformable contacts are found in the Lefkara Formation, Middle Member, Chalk and Chert unit, as mid Palaeocene (NP5), Late Palaeocene (NP8/NP9 boundary) and Early Eocene (NP12-NP15, diachronous), and one unconformable contact at the base of the Lefkara Formation, Middle Member, Massive Chalk unit as Late Eocene (NP16). In addition the diachroneity of the base of the Pissouri Formation has been revised NN10-NN11) for S.W. Cyprus. Finally a new outcrop of the Pakhna Formation, Terra Limestone Member at Petra-tou-Romiou extends the known limits of this unit within S.W. Cyprus.

There are a number of implications for the geological evolution of S.W. Cyprus. The melange units of the Moni and Kathikas Formations are coeval and relate to a common tectonic event that is early Maastrichtian. The Lefkara Formation, Lower Member intercalates with the Kathikas Formation to form the pelagic chalk interbeds. The presence of the Kathikas Formation straddling the major lineaments, suggests the ?initial stages of juxtaposition of the Mamonia and Troodos basements had ceased by early Maastrichtian times. This would coincide with cessation of the first phase of anticlockwise rotation (60°) of the Troodos micro plate. The presence of the Lefkara Formation, Middle Member, Massive Chalk unit straddling the major lineaments in the southern part of S.W. Cyprus, indicates cessation of the ?final stages of the juxtaposition event by Late Eocene times, which is also coincident with the termination of anticlockwise rotation. The evaporites of the Kalavasos Formation in the Polemi Basin are Tortonian, older than other evaporite basin deposits in Cyprus and elsewhere (Messinian).

Distribution of the pre-Late Miocene sediments in S.W. Cyprus show variable sedimentation across the area. In some areas there are hiatuses, possibly related to the influence of a structural high, centred around an early positive area created during the Mamonia-Troodos juxtaposition. It is clear that this early basement geometry strongly influenced sedimentation, but diminished in its control by ?Late Oligocene. The outcrop patterns displayed by the surviving sedimentary packages, bounded by unconformities are seen to overstep one another, younging in a north westerly direction preserving the underlying older sedimentary packages, to rest on the basement, similar to that seen against the northern margin of the Troodos Massif.

The trend of the north-west and west younging directions of the sedimentary packages seen in S.W. Cyprus and against the northern margin of the Troodos Massif respectively, offer evidence for the north dipping subduction zone to have migrated southwards, i.e. from the Kyrenia lineament to the south side of Cyprus by the Early Paleocene. The subducting African plate could have controlled the differential movement of the allochthonous basement terranes and fragments by uplift at the south western edge of the overriding European plate.

CHAPTER 1

INTRODUCTION, OBJECTIVES AND THESIS OUTLINE

1.1 Introduction

In the late 50's and 60's, detailed geological field studies and systematic mapping were carried out, centred in the main around the Troodos Massif (Fig. 1.1; Mt. Olympus), on the allochthonous basement terranes of Cyprus, including their associated sediments and the overlying relatively undisturbed sedimentary formations (Fig. 1.2), of the neo-autochthonous Late Cretaceous (Maastrichtian) to Holocene sedimentary cover. The research resulted in the publication of memoirs, reports and maps by the Cyprus Geological Survey. Publications relating to the circum-Troodos Massif, making reference to the neo-autochthonous sedimentary cover (Wilson, 1959; Bagnall, 1960; Bear, 1960; Bear and Morel, 1960; Carr and Bear, 1960; Gass, 1960; Pantazis, 1967; Lilljequist, 1969; Turner, 1971), have reported unconformities representing large gaps in the sedimentary succession. However, against the southern margin of the Troodos Massif, there is evidence (Bagnall, 1960; Bear and Morel, 1960; Pantazis, 1967) to suggest the sedimentary succession is more complete, than that seen against the northern margin.

The overall observation of the outcrop pattern displayed by the neo-autochthonous sedimentary cover, against the margins of the Troodos Massif, is that the sedimentary succession thickens in a north easterly direction away from the northern margin (Cleintuar *et al.*, 1977) and in a southerly direction away from the southern margin (Bagnall, 1960; Bear and Morel, 1960; Pantazis, 1967). However, against the south western margin and in the area of S.W. Cyprus, the outcrop pattern appears to be more complex than that seen against the other two margins and the explanation, may be due to the presence of the Mamonia and Troodos basement fragments (Fig. 1.3) which could have had an affect on the depositional history of the neo-autochthonous sedimentary cover.

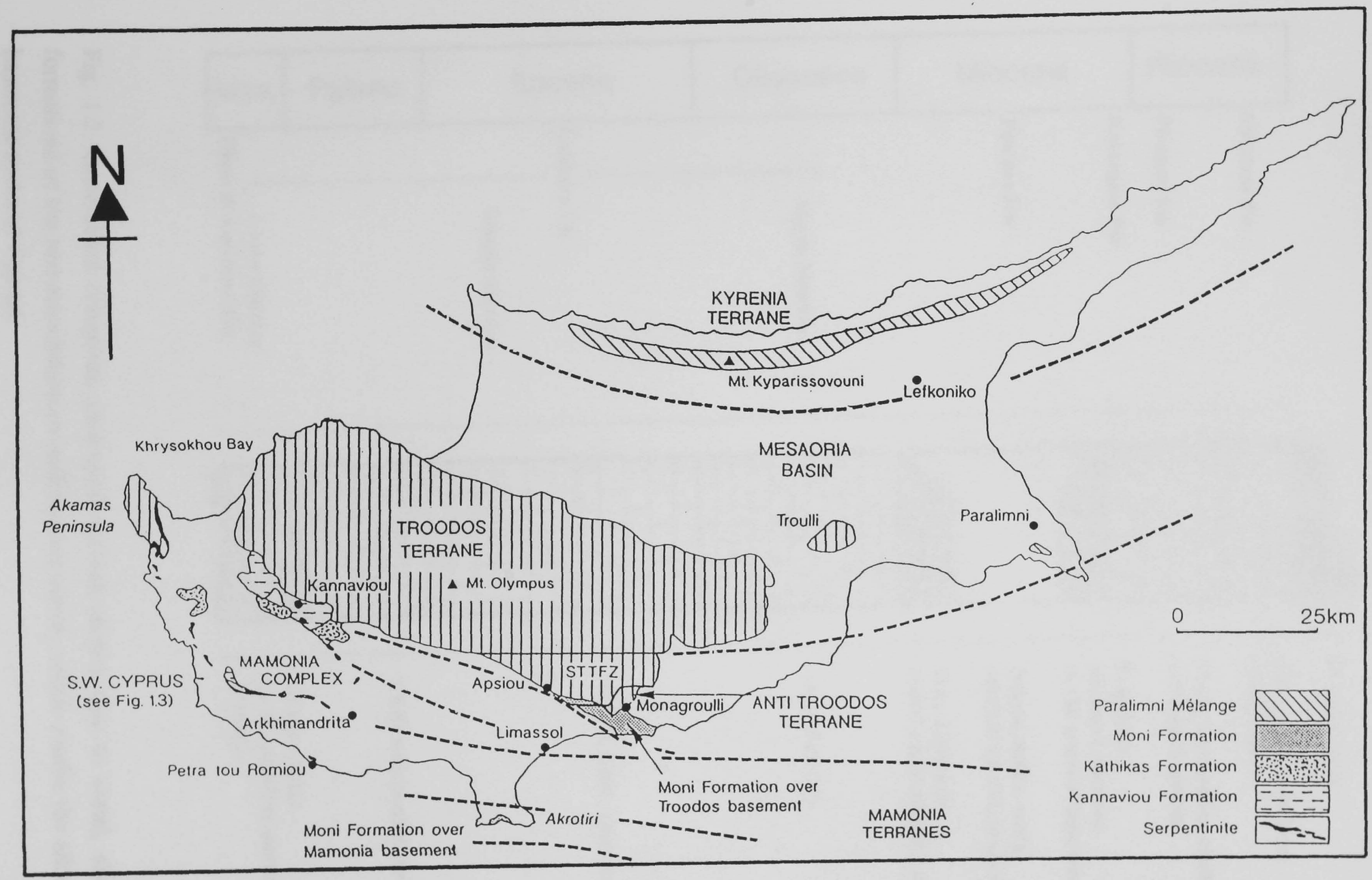

Fig. 1.1. Map of Cyprus, showing the boundaries of the individual allochthonous basement terranes (modified from Gass *et al.*, 1994 and including geophysical research by Kempler, 1994).

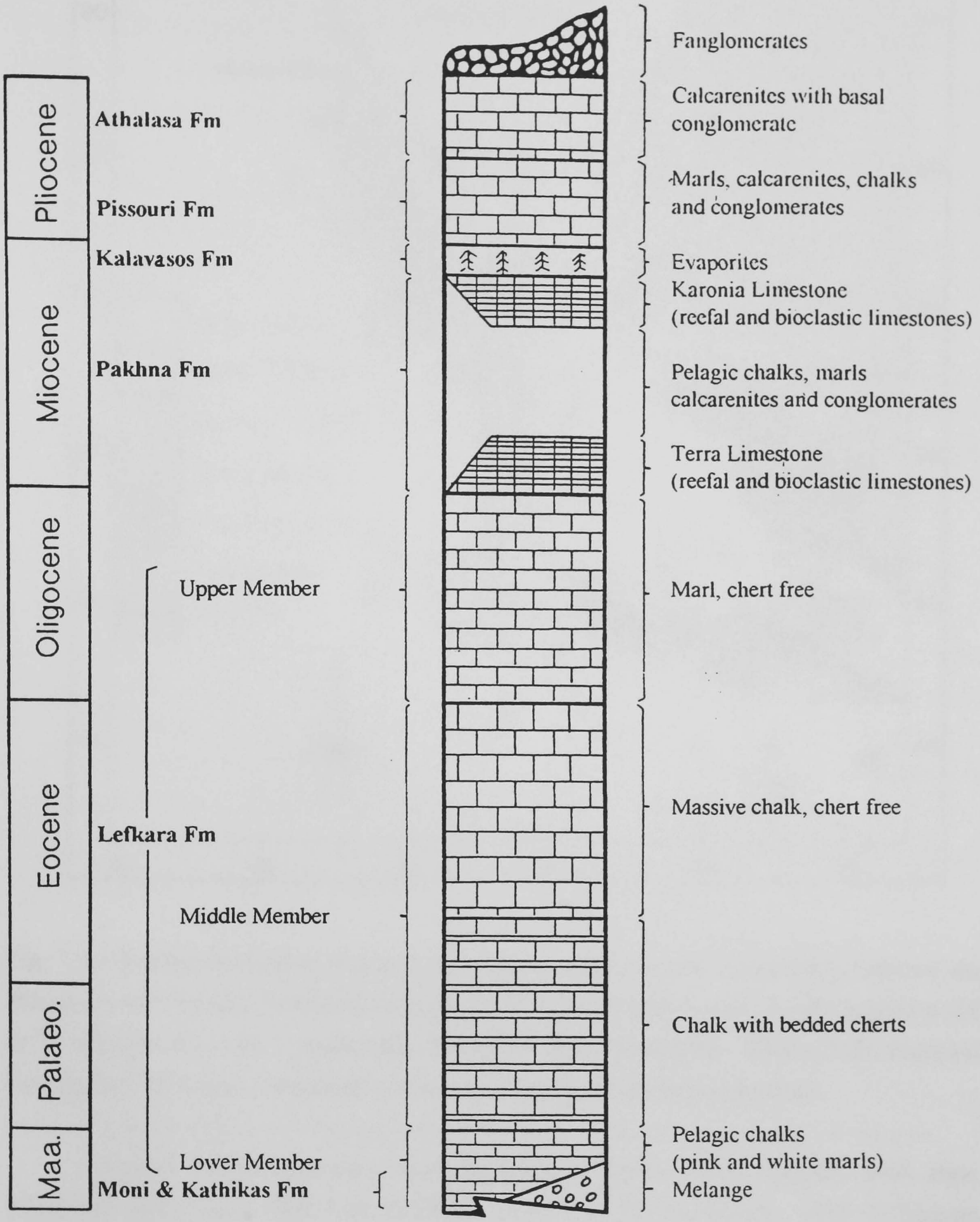

Fig. 1.2. Generalised composite geological vertical section (not to scale), showing the formations of the neo-autochthonous sedimentary cover, which overlie the allochthonous basement rocks of Cyprus.

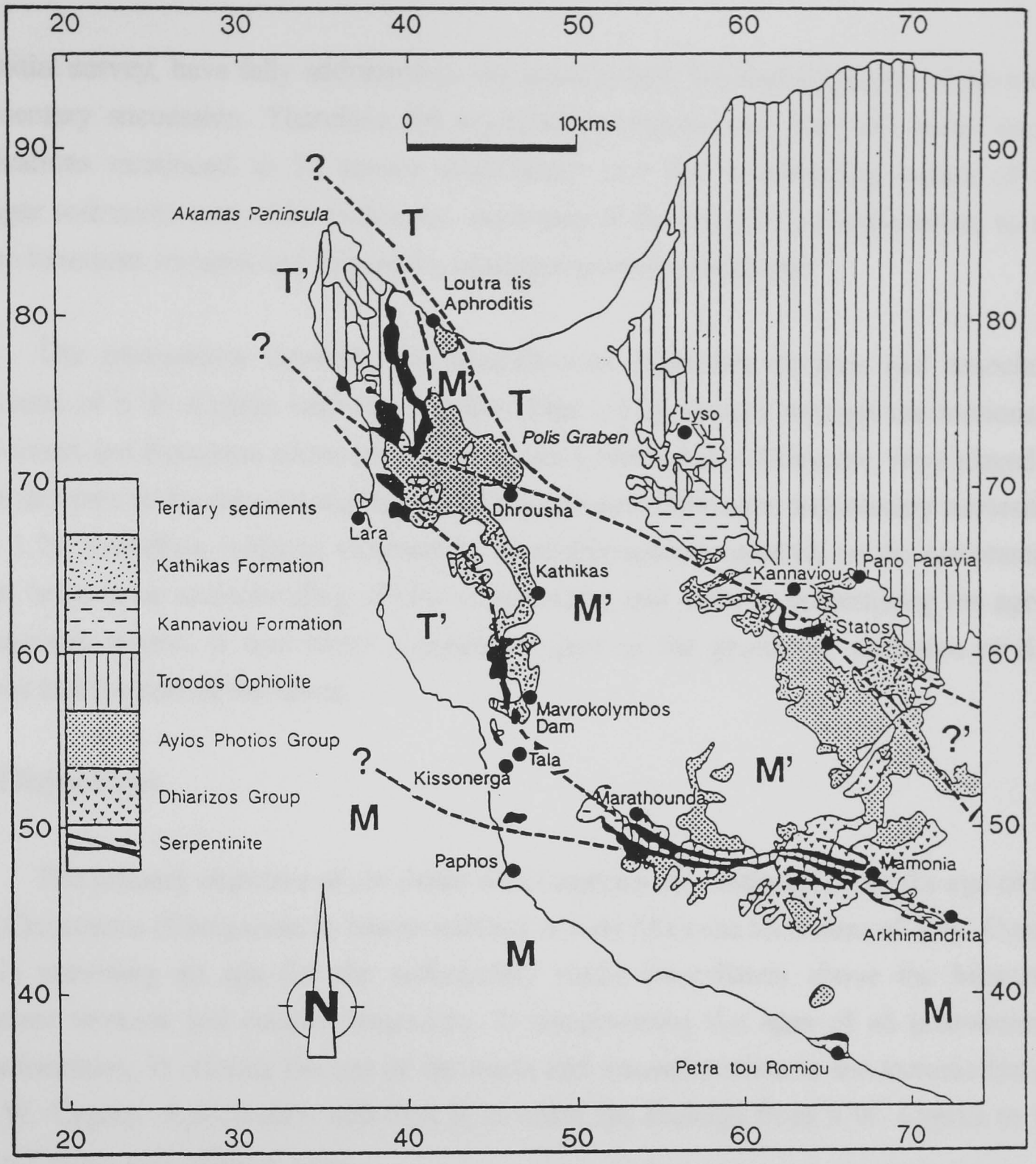

Fig. 1.3. General geological map of S.W. Cyprus, showing the relationship between the Mamonia and Troodos basement terranes (M & T respectively), and related fragments (M' & T' respectively and ?' uncertain) (modified from Swarbrick, 1980). N.B. Kathikas Formation and Tertiary sediments = Neo-autochthonous sedimentary cover.

Since the initial systematic mapping survey (Wilson, 1959; Bagnall, 1960; Bear, 1960; Bear and Morel, 1960; Carr and Bear, 1960; Gass, 1960; Pantazis, 1967; Lilljequist, 1969; Turner, 1971), research has continued through to the present day on the circum-Troodos Massif neo-autochthonous sedimentary cover, resulting in a number of publications (e.g. Mantis, 1970; Robertson and Hudson, 1974; Baroz and Bizon, 1977; Cleintuar *et al.*, 1977; Robertson, 1977a; Follows and Robertson, 1990; Gass *et al.*, 1994; Payne and Robertson, 1995 etc.). However, none of the publications, including those of

the initial survey, have fully addressed in any great detail the biostratigraphy of the entire sedimentary succession. Therefore the reported unconformities from the initial survey publications continued to be poorly constrained and the overstepping nature of the younger sediments over older sediments, separated in the main by unconformities, to rest on the basement terranes and fragments, remained poorly understood.

The interactions between the allochthonous basement terranes and associated fragments of S.W. Cyprus with one another (Figs 1.1,3), caused through the motions of the African and European plates between the Late Cretaceous to Holocene, have played an important part in the depositional history of the neo-autochthonous sedimentary succession (Fig. 1.2). Therefore evidence obtained by biostratigraphical research on the sedimentary cover, helps in an understanding of time relationships and assist in constraining the age of the tectonic events. It also forms a significant part of the geological evolution of S.W Cyprus and the rest of the island.

1.2 Objectives

The primary objective of the thesis is to constrain biostratigraphically the age of the Late Cretaceous (Campanian to Maastrichtian) to Late Miocene tectonism of S.W. Cyprus by: 1) providing an age for the sedimentary rocks immediately above the Mesozoic basement terranes and relative fragments; 2) documenting the ages of all post-tectonic unconformities; 3) relating the age of the rocks and unconformities to the tectonic history of S.W. Cyprus. A secondary objective is to relate the findings from S.W. Cyprus to the rest of Cyprus and offshore areas.

To achieve the primary objective, the biostratigraphy was focused on the analysis of calcareous nannofossil. Techniques were developed for processing and preparation, which includes extracting and mounting the material in readiness for recognition and identification of individual species, under light and scanning electron microscope conditions (Appendix A, Sampling and Processing).

1.3 Thesis Outline

1.3.1 Chapter 2, starts with a brief geographical introduction, after which goes on to describe each individual allochthonous basement terrane, that makes up the island of Cyprus, including their eastward extension offshore to the mainlands of Turkey and Syria. The relatively undisturbed formations of the neo-autochthonous sedimentary cover which

unconformably overlies the allochthonous Mamonia and Troodos basement terranes and fragments are also described. The tectonic events which have affected the depositional history of the neo-autochthonous sedimentary cover of Cyprus, during the Late Cretaceous to Holocene are reviewed.

1.3.2 Chapter 3, provides an introduction and description of the microfossil group, coccoliths and nannoliths which together are termed calcareous nannofossils. It covers the history of research and the systematic palaeontological approach employed within the thesis.

1.3.3 Chapter 4, covers the Late Cretaceous (Campanian to Maastrichtian) calcareous nannofossil biostratigraphical data, observed in samples collected from the Kannaviou, Kathikas, Moni (Dhrousha Melange) and Lefkara (Lower Member) Formations, including discussion and summary of findings.

1.3.4 Chapter 5, covers the Palaeocene and Eocene calcareous nannofossil biostratigraphical data, observed in samples collected from the Lefkara Formation, Middle Member (Chalk and Chert and Massive Chalk units), including discussion and summary of findings.

1.3.5 Chapter 6, covers the Late Oligocene to Miocene calcareous nannofossil biostratigraphical data, observed in samples collected from the Pakhna and Pissouri (Mrytou Marls) Formations, including discussion and summary of findings.

1.3.6 Chapter 7, provides discussion, making reference to the findings of chapters 4, 5 and 6 and fieldwork of past researchers. The data relating to the conformable and unconformable contacts, and outcrop patterns are formalised, so that their implications with respect to uplift, subsidence and ?lateral movement at the major lineaments, in connection with the juxtapositioning and anticlockwise rotation events can be reviewed. Also the effects caused by a subduction zone to the south of Cyprus from Early Palaeocene onwards is explored.

1.3.7 Appendix A, Sampling and Processing, covers the strategy behind the fieldwork and sampling programme, the dissaggregation techniques employed during the project so as to free the calcareous nannofossils from the sample, and the mounting of the material obtained so that it can be examined under light and scanning electron microscopes.

1.3.8 Appendix B, Calcareous Nannofossil Identification Key to Family Level, leads the researcher through four possible levels of search to achieve recognition: 1. Morphology of the overall shape; 2. Distinguishing features of the family within the overall shape; 3. Detailed description of each family in alphabetical order; 4. A miscellaneous section covering calcareous nannofossils of holococcolith type construction and Incertae sedis.

1.3.9 Appendix C, Deep Sea Drilling Project and Ocean Drilling Project Chapters Relating to Calcareous Nannofossils, provides information in the form of a table giving volume, year of publication, chapter, page, plates (if available), chronological range of calcareous nannofossils reported and author(s).

1.3.10 Appendix D, Calcareous Nannofossil Glossary, has been formulated to assist undergraduates, postgraduates and academics with little or no experience in the terminology employed to describe calcareous nannofossils.

1.3.11 Appendix E, Sample Data, contains tables which make reference to sampling, processing, fieldwork records and research data, which have been split into three sections: 1) Data tables, comprising three separate tables displaying information in numerical order, according to processing number, sample number and new locality number; 2) Distribution tables, comprising five separate age related tables (Late Cretaceous, Palaeocene, Mid to Late Eocene, Early Miocene and Late Miocene) in numerical order according to processing number only; 3) Miscellaneous section, comprising one table displaying information in numerical order according to processing number, making reference to samples which were processed to reconnaissance level only.

Footnotes

1) The chronostratigraphic framework employed throughout the thesis, is that proposed by Harland *et al.* (1989).

2) It is the intention of the author to bring together Appendices B, C and D of the thesis, after submission and along with further refinements, into one internal publication, for the use by the Department of Geological Sciences at the University of Durham. To assist future undergraduates, post-graduates and academics in the recognition of calcareous nannofossils.

CHAPTER 2

INTRODUCTION TO CYPRUS AND ITS GEOLOGY

2.1 Introduction

Cyprus is the third largest (9250 km²) and most easterly island, after Sicily and Sardinia in the Mediterranean, being located south of Turkey and west of Syria. The main physical features of the island (Fig. 2.1) are the long narrow Kyrenia (Pentadaktylos) Range rising to 1024m at Mt. Kyparissovouni and trends south-west to north-east running parallel to the northern coastline, forming a 'panhandle' in the north-east. The Troodos Range which forms the bulk of the central area of the island, trends west to east, rising to 1951m at Mt. Olympus and is separated from the Kyrenia Range by the low lying alluvial Mesaoria plain. In the south-west there is an inclined plateau with north facing scarps in the south and to the north a valley that drains into Khrysokhou Bay. There are no perennial freshwater lakes or rivers, just numerous water courses which are dry during summer and autumn. Cyprus has a typical Mediterranean climate with hot dry summers, were temperatures can exceed 38°C (cooler in the mountains) and warm winters with the rainy season between late October and February (snow on the high ground). Pine trees and shrubs are the main vegetation that is associated with the high ground and extensive agriculture on the low lying plains.

2.2 Allochthonous Basement Terranes

Offshore geophysical research (Kempler, 1994), to the south and east of Cyprus towards the Levant coastline, has located lineaments which are associated with onshore lineaments seen in south-east Turkey, Syria and Cyprus. The research confirms the basement of Cyprus to be a series of west to east trending arcuate allochthonous basement terranes and associated fragments (S.W. Cyprus), bounded by major lineaments and are from north to south (Fig. 2.1): The Kyrenia basement terrane; The Mesaoria Basin; The Troodos basement terrane; The South Troodos Transform Fault Zone, including the Anti-Troodos basement terrane; S.W. Cyprus, which is made up of several basement fragments which are associated with the Troodos and Mamonia basement terranes to the north and south respectively.

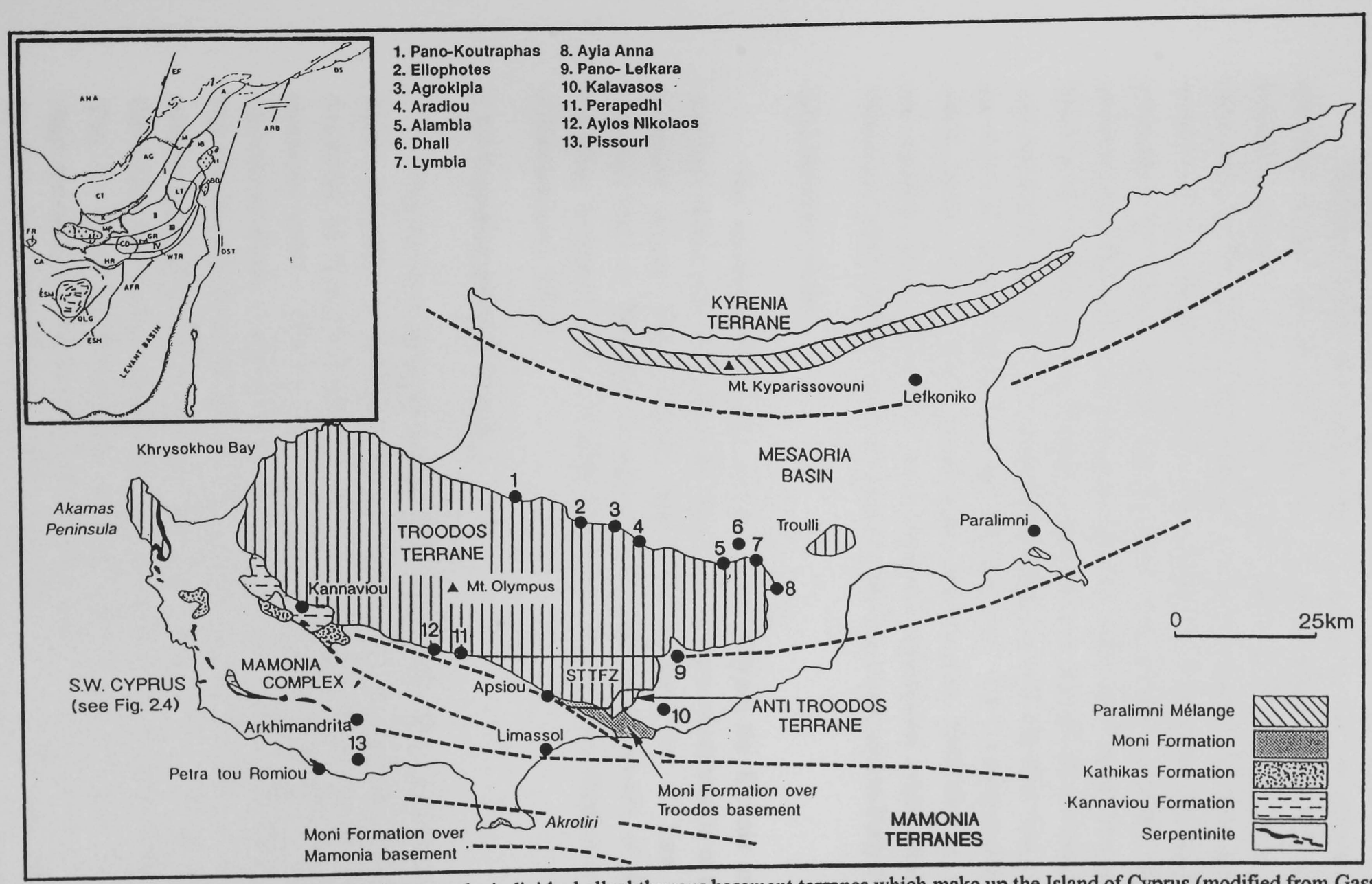

Fig. 2.1. Map showing the relationship between the individual allochthonous basement terranes which make up the Island of Cyprus (modified from Gass *et al.*, 1994 and including geophysical research by Kempler, 1994). Inset, Map showing eastward extension of the allochthonous basement terranes (Kempler, 1994). A=Andirin, AF=Arakapas Fault, AFR=African Plate, AG=Gulf of Adana, ANA= Anatolia Plate, ARB=Arabia Plate, BB=Baer-Bassit ophiolite, BS=Bitlis Suture, CA=Cypriot Arc, CD=Cyprus Depression, CT=Cilicia Trough, DST=Deep Sea Transform, EAF=East Anatolian Fault, EF=Ecemis Fault, ESH=Eratosthenes Structural High, ESM=Eratosthenes Seamount, FR=Florence Rise, GR=Gelendzhik Rise, H=Hatay ophiolite, HR=Hecataeus Ridge, IB=Iskenderun Basin, K=Kyrenia Range, LT=Latakia Trough, M=Misis, MP=Mesaoria Plain, QLG=quadrilateral graben, T=Troodos ophiolite, WTR=West Tartus Ridge, I=Kyrinia-Misis, II=Famagusta-Hatay, III=Kiti-Baer-Bassit, IV=Hecataeus-Latakia.

2.2.1 Kyrenia basement terrane

The Kyrenia basement terrane (Fig. 2.1) forms the western section of a narrow structural arcuate terrane stretching for several hundreds of kilometres in length, extending eastwards offshore towards the Misis Mountains of south-east Turkey (Robertson and Woodcock 1986; Kempler, 1994). The Kyrenia basement terrane has the structure of a small alpine type fold-and-thrust belt (Robertson and Xenophontos 1993), dominated by steeply dipping thrust slices, that partially straddles the northern termination of basement rock, similar to that seen within the Troodos basement terrane. They consist of Mesozoic and Tertiary sediments with deposits of subordinate volcanic and metamorphic rocks. The sedimentary sequence is split into four rock groups, with the oldest to youngest being the Trypa (Henson *et al.*, 1949), Lapithos (Henson *et al.*, 1949), Kithrea (Weiler, 1965) and Mesaoria (Henson *et al.*, 1949) Groups. The Groups are separated by unconformities which represent deformation events (Robertson and Woodcock 1986), which have occurred during the Late Cretaceous to Early Pliocene.

2.2.2 Mesaoria Basin

The Mesaoria Basin (Fig 2.1) is located between the Kyrenia and Troodos mountain ranges, with the floor of the basin forming the northern margin of the Troodos basement terrane. The sediments that infill the basin are of Late Cretaceous (Maastrichtian) to Holocene in age (Fig 2.2) and overlie basalts of the Troodos Ophiolite Complex (Fig. 2.3) and bentonitic clays of the Kannaviou Formation (Cleintaur *et al.*, 1977).

2.2.3 Troodos basement terrane

The Troodos basement terrane (Fig. 2.1) currently forms the central part of the island. Research by Kempler (1994) suggest that the Troodos basement terrane (including the floor of the Mesaoria Basin), forms the western section of an arcuate structural terrane, which extends eastwards through the Latakia Trough and the Iskenderum Basin of south-eastern Turkey, to include the Hatay Ophiolite Complex. The Troodos basement terrane has been interpreted as an ophiolite, a remnant piece of oceanic crust (Gass, 1968; Moores and Vine 1971), which formed above a Late Cretaceous Neo-Tethyan subduction zone, and termed the Troodos Ophiolite Complex (Fig. 2.3). Recent Ur/Pb age-dating by Mukasa and Ludden (1987), on the late forming plagiogranites, gave a date of c. 91.6 Ma (Cenomanian-Turonian, Late Cretaceous) for the formation of the Troodos Ophiolite Complex. Since its formation the terrane has undergone 90° of anticlockwise rotation between the Late Cretaceous (late Campanian)

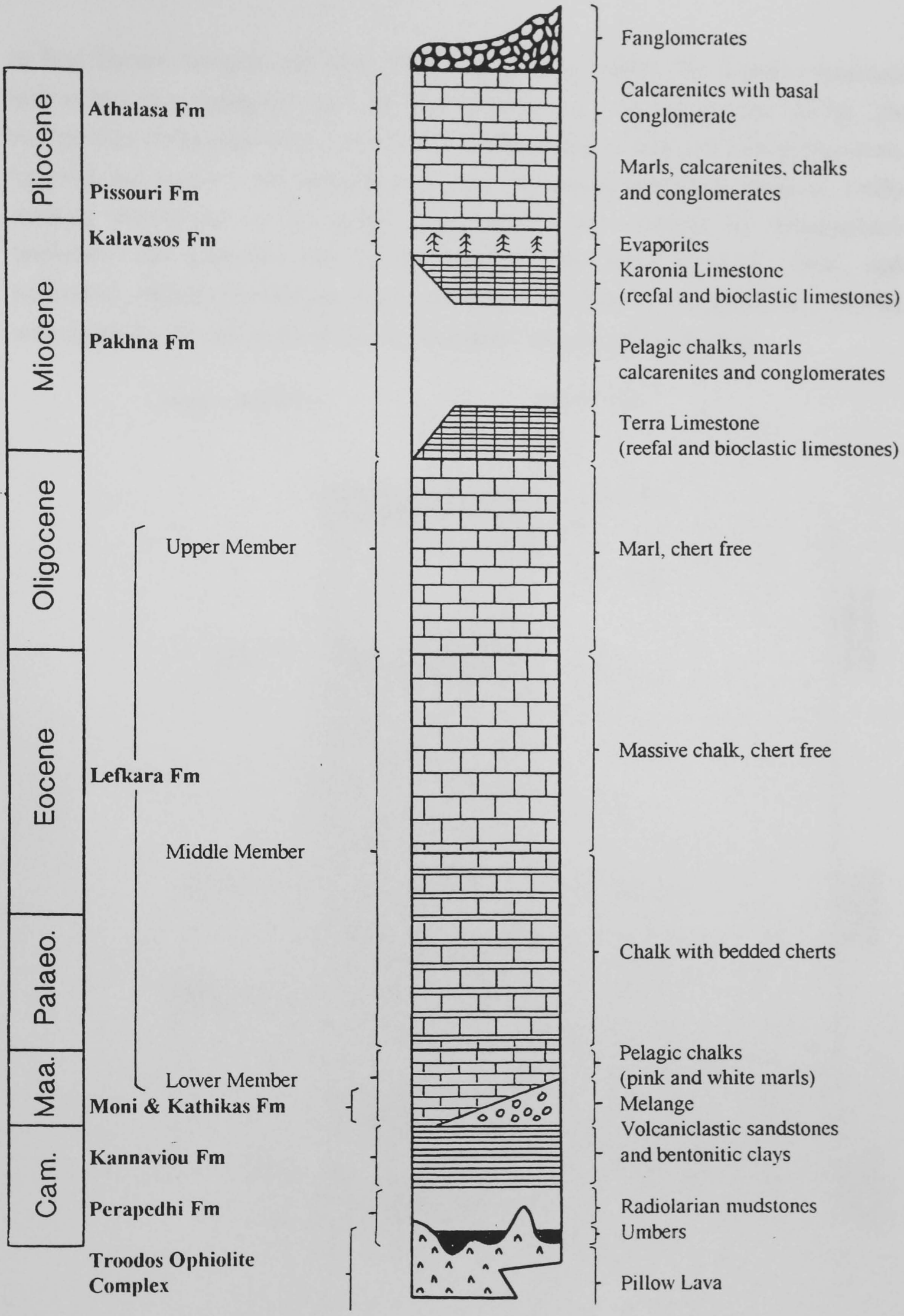

Fig. 2.2. Generalised composite geological vertical section (not to scale) of the neo-autochthonous sedimentary cover, overlying the Kannaviou and Perapedhi Formations, the associated sediments of the Troodos basement terrane (Troodos Ophiolite Complex).

to Mid Eocene (Moores and Vine, 1971; Clube *et al.*, 1985). The Troodos basement terrane has also undergone rapid uplift during the last 2 Ma (Robertson 1977a). The sedimentary cover associated with the Troodos basement terrane and related fragments, includes the umbers and radiolarites of the Perapedhi Formation (Wilson, 1959), infilling depressions in the pillow lava surface, then overlain by volcaniclastic sandstones and bentonitic clays of the Kannaviou Formation (Lapiérre, 1968), with particularly thick deposits in the south and south-west of the island (Robertson, 1977b), and capped by the sediments of the neo-autochthonous sedimentary cover.

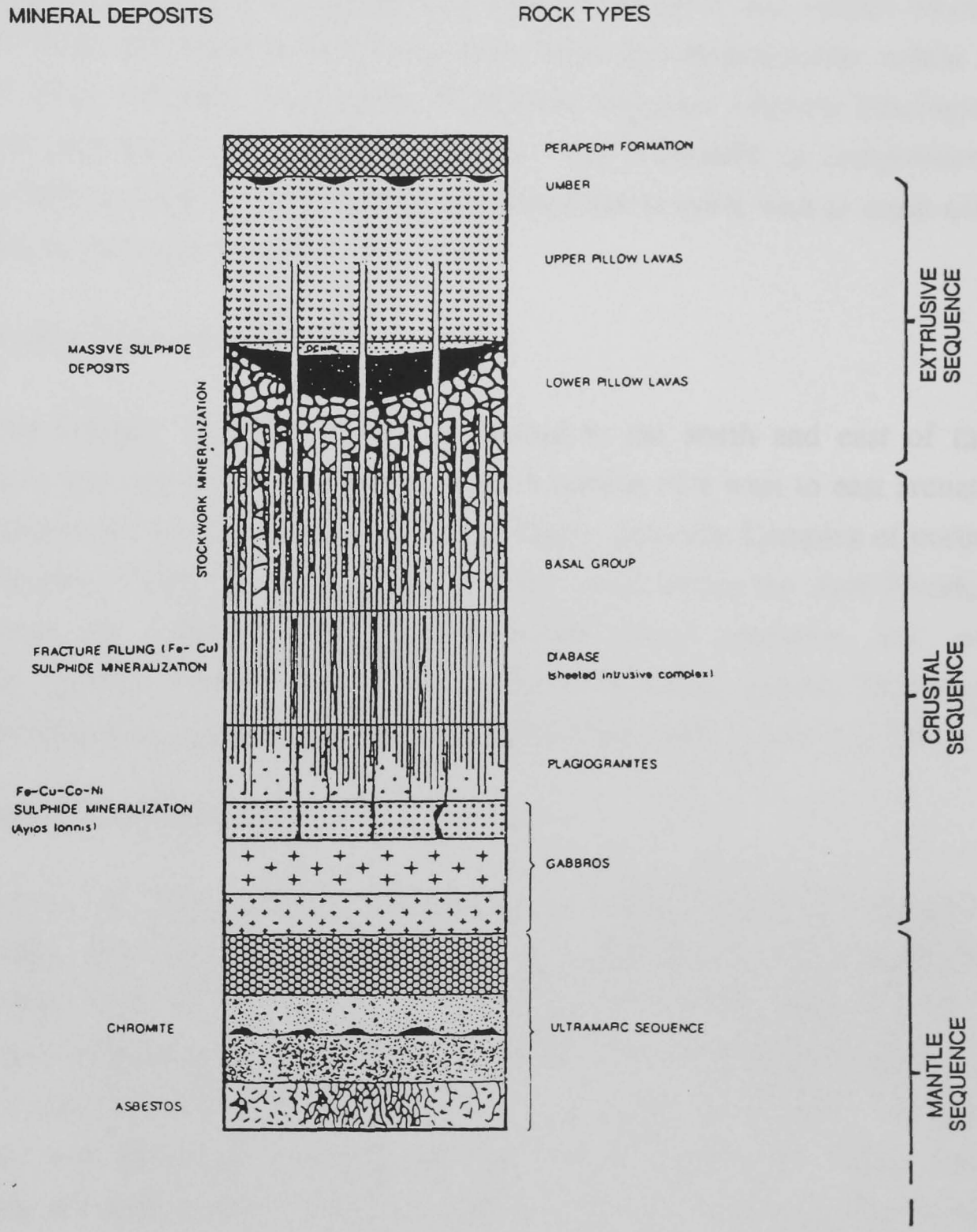

Fig. 2.3. Generalised lithological column of the Troodos Ophiolite Complex, the major rock component of the Troodos basement terrane and fragments (modified from Constantinou, 1980).

2.2.4 Southern Troodos Transform Fault Zone (STTFZ)

The STTFZ is located to the south of the main Troodos basement terrane (Fig. 2.1), it is a west to east sublinear feature which is 10km wide in the west and narrows to 5km in the east. Research by Gass *et al.* (1994), indicate the rocks within the area bear little resemblance to the standard ophiolite stratigraphy, because of the chaotically juxtaposed and distributed variety of lithologies within the zone. Gass *et al.* (1994) recognised two distinct lithostratigraphic groups. Firstly, the older 'Axis Sequence' which is identical to the Troodos and Anti-Troodos basement terranes, in terms of lithology, magmatic structure and petrology, is exposed as titled and rotated blocks which resulted from deformation associated with strike-slip displacement within a transform fault zone. Secondly, the younger 'Transform Sequence' contains lithologies of plutonic and hypabyssal rocks, which are mafic and ultramafic in composition, including a volcanic sequence, these have been emplaced due to north-west to south-east crustal extension at an active transform fault zone.

2.2.5 Anti-Troodos basement terrane

The Anti-Troodos basement terrane is located to the south and east of the STTFZ (Fig. 2.1) and together they form the western section of a west to east arcuate terrane, that extends eastwards offshore to the Baer-Bassit Ophiolite Complex of north-west Syria (Kempler, 1994). The succession of rocks found within the Anti-Troodos basement terrane are typical of an axis-generated crustal sequence and are macroscopically similar to those seen in the Troodos basement terrane. However, microscopically there are compositional differences (Remond 1986; Gass *et al.*, 1994).

2.2.6 S.W. Cyprus and Mamonia basement terranes

The area of S.W. Cyprus (Fig. 2.4) comprises five arcuate basement fragments, trending generally north-west to south-east, and are separating their lithologically associated Troodos (Fig. 2.3; Troodos Ophiolite Complex) and Mamonia (Fig. 2.5; Mamonia Complex) basement terranes (Fig. 2.1), to the north and south respectively, trending west to east. The Mamonia basement terrane is seen as two separate structural units (Fig. 2.1), with the narrow southern basement terrane (Kempler, 1994), seen onshore forming the high ground, running parallel to the southern coastline of the Akrotiri peninsula (Fig. 2.1). Both the southern and northern Mamonia basement terranes extend eastwards offshore towards the Levant coastline. Vertical to high angle faults separate the Mamonia and Troodos basement terranes and related fragments,

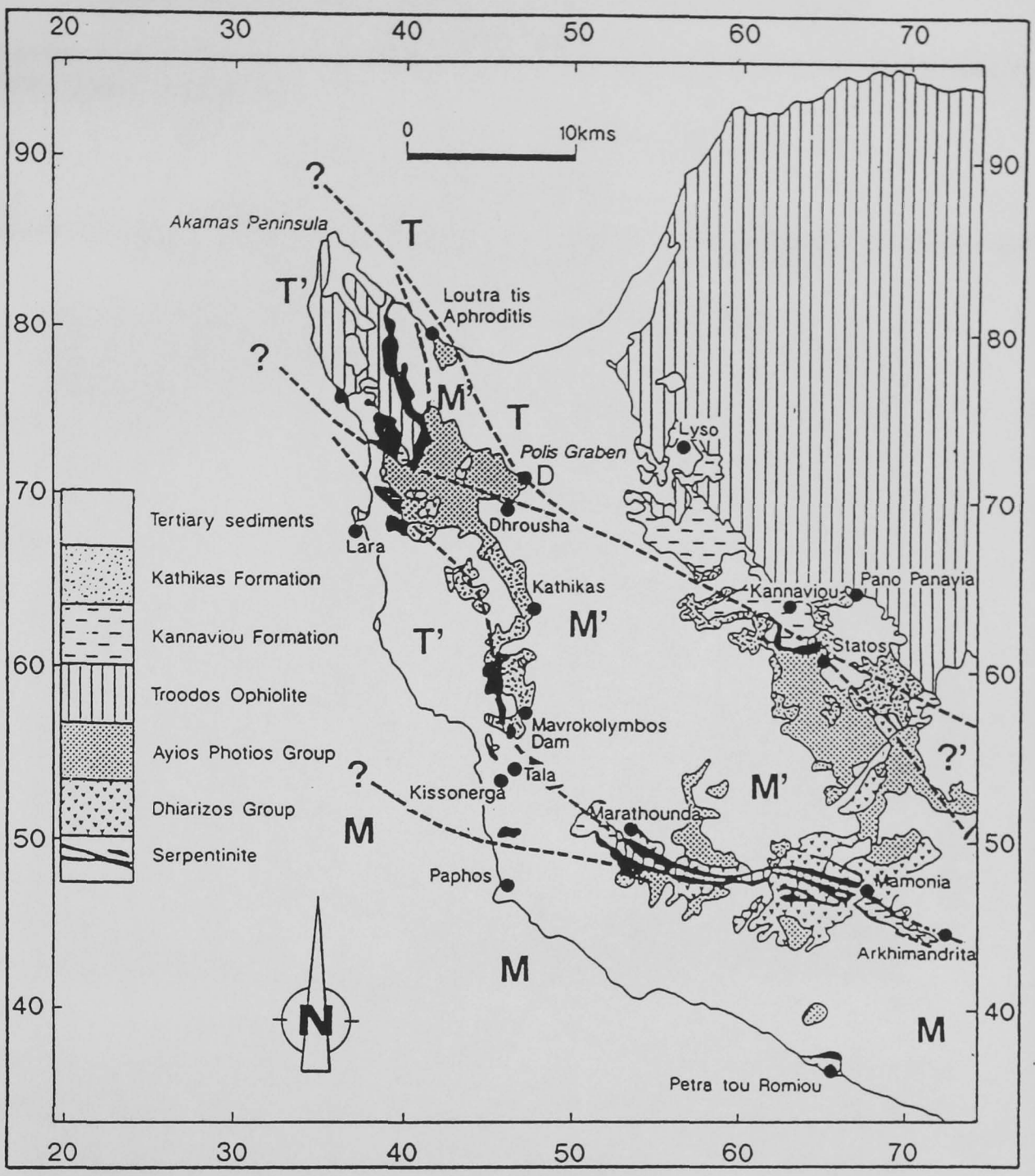

Fig. 2.4. General geological map of S.W. Cyprus, showing the Mamonia and Troodos basement terranes (M and T respectively) sandwiching the five Mamonia and Troodos basement fragments (M', T' respectively and ?' uncertain) (modified from Swarbrick 1980). N.B. Kathikas Formation and Tertiary sediments = neo-autochthonous sedimentary cover. D = Dhrousha Melange outcrop.

---

containing screens of serpentinite. The lava of the Troodos related basement fragments, have petrological and geochemical similarities to the lava of the Southern Troodos Transform Fault Zone (Cameron 1985; Malpas and Xenophontos, 1987; Malpas *et al.*, 1992,1993). The lithologies relating to the Mamonia basement terranes and associated fragments (Mamonia Complex, Fig. 2.5), were assigned by Swarbrick and Robertson (1980) to two groups, the oceanic sequence of the Dhiarizos Group, comprising basic lava and deep water pelagic sediments, and the continental sequence of the Ayios Photios Group comprising deep water continental slope and rise sediments. Both groups are Late Triassic to Early Cretaceous in age. On two occasions the rocks have suffered

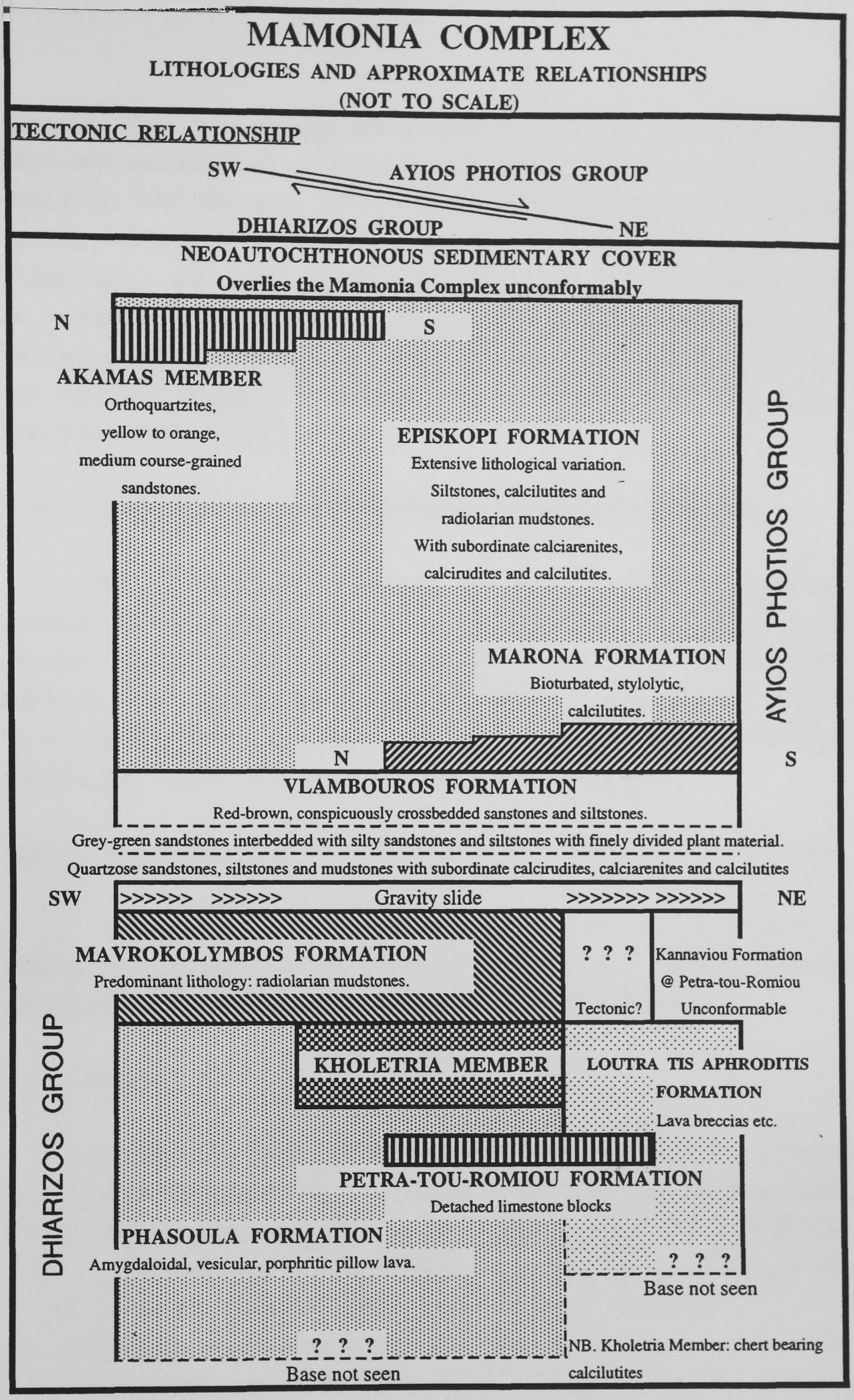

Fig. 2.5. The approximate lithological and tectonic relationships between the Groups, Formations and Members that make up the Mamonia Complex, based on research carried out by Swarbrick and Robertson (1980).

disruption. First by a possible gravity slide of post early Late Cretaceous in age (Robertson and Woodcock, 1979; Swarbrick, 1980). Second by transpressional activity (Swarbrick, 1993; Gass *et al.*, 1994), involving the juxtapositioning of the Mamonia and Troodos basement terranes, which may include the first phase of anticlockwise rotation of the Troodos and Anti-Troodos basement terranes, during the Campanian (Morris *et al.*, 1990) and early Maastrichtian. The latter disruption caused the formation of the melange deposits belonging to the Kathikas and Moni (and may include the Paralimini and Dhrousha Melanges) Formations which are the basal formations of the neo-autochthonous sedimentary cover.

2.3 Lithostratigraphy and Past Biostratigraphical Research

The Late Cretaceous to Holocene sedimentary succession, is split into two sections. The basal Perapedhi and Kannaviou Formations exclusively overlie the Troodos basement terrane and related fragments. In contrast the localised basal sedimentary melange deposits, coupled with the overlying calcareous sediments form the neo-autochthonous sedimentary cover (Fig. 2.2), and are common to both Mamonia and Troodos basement terranes and related fragments (Figs 2.1,4).

2.3.1 Sediments associated with the Troodos basement terrane and fragments

The associated sediments of the Troodos basement terrane and fragments are the umbers and radiolarites of the Perapedhi Formation, and overlying volcaniclastic sediments and bentonitic clays of the Kannaviou Formation (Fig. 2.2).

2.3.1.1 Perapedhi Formation

The Perapedhi Formation was named by Wilson (1959) with its type locality situated east of Perapedhi (Fig. 2.1), defined by Swarbrick and Robertson (1980). The umbers and radiolarites immediately overlie Troodos pillow lavas unconformably, to form the basal component of the sedimentary succession, and are overlain conformably in places by the bentonitic clays of the Kannaviou Formation, and elsewhere unconformably by chalks of the Lefkara and Pakhna Formations (Gass, 1960). Urquhart and Banner (1994) proposed that the Perapedhi Formation should be restricted to the umber sediments only, with the overlying non-calcareous radiolarian shales assigned to the Kannaviou Formation. The Author disagrees with the proposal and side with Gass *et al.* (1994) who argue, that the umbers and radiolarites are an integral part of the

ophiolite setting, due to their association with hydrothermal activity resulting in chemical and biological precipitation respectively. In contrast, the Kannaviou Formation is primarily calc-alkaline volcanic in origin (Robertson, 1977b).

The Perapedhi Formation is preserved in depressions on the pillow lava surface and has a discontinuous outcrop pattern around the margin of the Troodos Massif (Robertson and Hudson, 1973) and the Troulli Inlier (Lilljequist, 1969) (Fig. 2.1). They are also seen as small outcrops in the Akamas and Mavrokolymbus areas (Fig. 2.4) of S.W. Cyprus (Swarbrick, 1979).

The umbers are rich in iron and manganese oxides (Robertson and Hudson, 1974), may either be massive or well bedded and in places, have interbedded silicified layers and pale, radiolarian-rich bands, grading upwards into manganiferous and umberiferous shales. The shales are succeeded by and grade into radiolarites and radiolarian mudstones (Robertson and Hudson, 1974; Robertson, 1975).

The age of the Perapedhi Formation is constrained by the age of the underlying Troodos pillow lavas (c. 91 Ma., Mukasa and Ludden, 1987 for the plagiogranites of the Troodos ophiolite sequence) and in places the sediments of the overlying Kannaviou Formation (upper Campanian, Urquhart and Banner, 1994). Research carried out by Urquhart and Banner (1994) suggested an age range for the formation, based on radiolarian evidence, to the equivalent calcareous nannofossil zones of CC21 - CC23a (Campanian). However, there is biostratigraphically evidence by past researchers to suggest that the Perapedhi Formation could be episodic or diachronous, due to the varying age dates (Blome and Irwin, 1985, Turonian; Bragin and Bragina, 1991, Santonian; Thurow, 1991, Cenomanian-Turonian and Campanian) from various localities based on radiolarians recovered. The research carried out by Urquhart and Banner (1994) suggested the incompatibility between their findings and past workers could be caused by contamination, reworking or the age ranges of radiolarians recovered, being not well enough established to permit accurate dating.

2.3.1.2 Kannaviou Formation

The Kannaviou Formation was defined by Lapiérre (1968), with its type section in the Paleomylon valley near Kannaviou (Fig. 2.4), S.W. Cyprus. The formation unconformably overlies the Troodos pillow lavas and conformably in places the Perapedhi Formation (Bear, 1960; Bear and Morel, 1960; Pantazis, 1967; Lilljequist,

1969), which these early workers had assigned the capping bentonitic clays to the Perapedhi Formation. The only exception to this is at Petra-tou-Romiou (Fig. 2.4,5) in S.W. Cyprus, where they unconformably (?reworked) overlie the Dhiarizos Group (Swarbrick, 1979).

The major exposures of the Kannaviou Formation are seen in southern and S.W. Cyprus (Robertson 1977b) (Fig. 2.4). It is possible that the formation continues beneath the neo-autochthonous sedimentary cover from the southern exposures towards the east, where exposures of bentonitic clays are seen in the Paralimini (Follows and Robertson, 1990; Urquhart and Banner, 1994) and Troulli Inliers (Lilljequist, 1969) (Figs 2.1). On the northern slopes of the Troodos Massif (Bear, 1960), and in the Troulli Inlier the bentonitic clays conformably overlie the Perapedhi Formation. In S.W. Cyprus the volcaniclastic sediments and bentonitic clays of the Kannaviou Formation outcrop in two main areas, with the western outcrop seen in a series of tectonic windows arcing from Arkhimandrita village in the south to the Akamas peninsula in the north and the second area to the east, seen against the updoming Troodos Massif (Robertson, 1977b). The Kannaviou Formation outcrops to the north and east of Limassol (Fig. 2.1), underlying and initially assigned to the Moni Formation (Pantazis, 1967). The Kannaviou Formation is overlain by in places by the tectonically emplaced sedimentary melange deposits of the Kathikas and Moni (which includes the Paralimini and Dhrousha Melanges) Formations, and overlain by calcareous sediments of the Lefkara, Pakhna and Myrtou-Nicosia Formations, conformably by the marls of the Lefkara Formation, Lower Member (Pantazis, 1967; Lilljequist, 1969; Robertson 1977b; Krasheninnikov and Kaleda, 1994), but unconformably by stratigraphically higher sediments.

Robertson (1977b) provided detailed descriptions of the Kannaviou Formation in S.W. Cyprus and only an outline is presented here, the lower part of the formation comprises predominantly non-calcareous bentonitic clays and radiolarian mudstones, indicating slow deposition below the calcite compensation depth. The upper part contains calcareous bentonitic clays, volcaniclastic siltstones and sandstones, indicating a more rapid deposition close to or above the calcite compensation depth.

Based on planktonic foraminiferal data, Mantis (1970) and Ealey and Knox (1975), dated the Kannaviou Formation as lower Campanian to middle Maastrichtian. Urquhart and Banner (1994), suggested that the Kannaviou Formation was deposited within the Campanian based upon radiolarian, planktonic foraminiferal and calcareous

nannofossil data, with no exclusive microfossil data to suggest that the upper horizons were deposited in the early Maastrichtian. A further constraint for the onset of deposition is supplied by Urquhart and Banner (1994), by the age of the Perapedhi Formation which the Kannaviou Formation conformably overlies (calcareous nannofossil zones CC21-CC23a, Campanian).

2.3.2 Neo-autochthonous sedimentary cover

The neo-autochthonous sedimentary cover unconformably overlies the Mamonia (Fig. 2.5), Troodos and Anti-Troodos (Fig. 2.2) basement terranes and related fragments. The sedimentation commenced during the late stages of the juxtapositioning event of the Mamonia and Troodos basement terranes, during the late Campanian to early Maastrichtian, which produced the emplacement of localised melanges of the Moni (including the Paralimini and Dhrousha Melanges) and Kathikas Formations near to source. During the emplacement of the melanges, calcareous sedimentation of the Lefkara Formation, Lower Member, occurred distally, intercalating with the proximal Dhrousha Melange and Kathikas Formation, producing pelagic chalk interbeds, representing pauses in debris flow. After the juxtapositioning event, the area around the Troodos Massif and S.W. Cyprus became tectonically quiescent, with the deposition of the predominantly calcareous sediments continuing through to the alluvium deposits of the Holocene, with ?periodic tectonic interruptions, seen as unconformities representing gaps in the sedimentary succession.

2.3.2.1 Sedimentary melange deposits

Four sedimentary melange deposits occur on Cyprus (Figs 2.1,4). In the south-east the Paralimini Melange (Follows and Robertson, 1990), in the south the Moni Formation (Pantazis, 1967), in the central part of S.W. Cyprus the Kathikas Formation (Swarbrick and Robertson, 1980) and in the northern part of S.W. Cyprus the newly recognised Dhrousha Melange (this thesis). All were tectonically emplaced and are proximal to source areas. Research carried out by Urquhart and Banner (1994), in part on the former three and this account in part on the latter two, suggest these melange deposits are coeval. They all unconformably overlie the Kannaviou Formation, and are conformably overlain by Lefkara Formation, Lower Member chalks (Pantazis 1967; Swarbrick and Naylor, 1980), apart from the Parlimini Melange which is unconformably overlain by Lefkara Formation, Upper Member chalks (Follows and Robertson, 1990). The Paralimini and Dhrousha Melanges appear lithologically similar to the upper unit of

the Moni Formation, which was described by Robertson (1977c) and contains smaller clasts. The Dhrousha Melange contains a number of pelagic chalk interbeds, similar to those seen in the Kathikas Formation.

2.3.2.1.1 Moni Formation

The Moni Formation outcrops in southern Cyprus, to the south and north of Limassol (Fig. 2.1). Pantazis (1967) originally defined and described the formation, which included a basal horizon of undisturbed bentonitic clay and radiolarian siltstones. Research carried out by Robertson (1977c), recognised the formation to be a melange, with the matrix of the melange and the undisturbed basal horizon to be contemporaneous with the Kannaviou Formation, which is seen further west in the Paphos district and east near Paralimini, and for that reason, assigned the entire Moni Formation to the Kannaviou Formation. For the purposes of this thesis the author, sides with Gass *et al.* (1994) by assigning the basal unit to the Kannaviou Formation and the stratigraphically higher sedimentary melange deposits to remain as part of the Moni Formation, based on the evidence that the melange has been tectonically emplaced.

The allochthonous components of the melange consists of exotic sedimentary and igneous blocks and olistoliths set in a matrix of bentonitic clay, similar to that seen in the Kannaviou Formation. Through detailed mapping of the melange, Robertson (1977c) grouped the components into four categories.

i). Exotic units that can be assigned to the Mamonia Complex of the Paphos district, and they tend to be the more resistant lithologies (Akamas sandstone, Petra-tou-Romiou limestone and Mamonia volcanics).
ii). Exotic units that cannot be assigned to the Mamonia Complex (Pareklisha sandstone and Monagroulli siltstone).
iii). Serpentinite sheets.
iv). A discontinuous, stratigraphically higher second melange, consisting of smaller fragments, with all lithologies represented, set in a bentonitic clay matrix.

Detailed fieldwork by Robertson (1977c), proposed that the dip and strike evidence from the olistoliths, suggested the emplacement of the Mamonia olistoliths were from the south to south-west with the serpentinites sourced from the STTFZ to the north. It is not known, if the exotic blocks or olistoliths collapsed into a structural low

filled with bentonitic clay, was either associated with a north dipping subduction zone (Moores *et al.*, 1984; Malpas *et al.*, 1992) or into an intra plate trough parallel to the plate boundary. However, Gass *et al.* (1994) postulates that all the blocks and olistoliths were derived from the south or south-west and were tectonically emplaced with the bentonitic clays to form the Moni Melange. Cyprus at the time of melange emplacement, was in a region of transpression oriented south-west to the north-east (Gass *et al.*, 1994), with the Mamonia basement terrane, south of present day Limassol, forming a structural high and the Anti-Troodos basement terrane and STTFZ forming a structural low (Fig. 2.1).

Research carried out by Urquhart and Banner (1994) on the matrix of the melange, yielding an assemblage of Campanian radiolaria which includes the species *Amphipyndax tylotus* Foreman *in* Petrushevskaya and Kozlova, 1972, *A. pseudocomulus* (Pessagno, 1963) and *Archaeodictyomitra lamellicostata* (Foreman, 1968), confirming Robertson and Woodcock's (1985) assessment of a possible age of emplacement to be a brief period in the Maastrichtian. The evidence being the age of the matrix (Kannaviou Formation - late Campanian) and the overlying Maastrichtian Lefkara Formation, Lower Member chalks.

2.3.2.1.2 Paralimini Melange

The Paralimini Melange was originally recognised as part of the Moni Formation (Pantazis, 1967, 1979; Robertson, 1977c), but considered as a separate unit by Follows and Robertson (1990), with its type locality south of Paralimini (Fig. 2.1). According to Follows and Robertson (1990) most of the area to the south of Paralimini is underlain by debris flows of the melange.

The Paralimini Melange consist of exotic blocks consisting of Mamonia and Troodos lithologies (including serpentinite) up to 1.5m in size, set in a matrix of pale pink bentonite clay of reworked Kannaviou Formation (Follows and Robertson, 1990).

Follows and Robertson (1990, p209) interpreted the origin of emplacement for the Paralimini Melange "as fragments of Mamonia terrane and ophiolitic slivers that were incorporated into deep sea volcanogenic sediments", and is comparable with the Moni Formation (Robertson, 1977c). It is likely that the Paralimini Melange was emplaced during the period of south-west to north-east transpression (during the late Campanian to early Maastrichtian), with the source area for the exotic fragments being to the south

of present day Paralimini, this ?transpressional event possibly generated the emplacement of the Moni Foramation (see Gass *et al.*, 1994).

Research carried out on the underlying Kannaviou Formation at Paralimini by Urquhart and Banner (1994), yielded species of radiolaria *Diacanthocapsa acanthica* Dumitrica, 1970, *Orbiculiforma sacramentoensis* Pessagno, 1976 and *A. tylotus* which is consistent with a Campanian age, therefore the emplacement of the melange post dates the Campanian deposition of the Kannaviou Formation. There are two pieces of evidence to suggest a possible upper age limit for emplacement. Firstly the melange does not contain any clasts of the overlying calcareous sediments (Follows and Robertson, 1990), suggesting emplacement prior to any calcareous sedimentation. Secondly if the Paralimini Melange and Moni Formation can be correlated then the latter which is capped by chalks of the Maastrichtian Lefkara Formation, Lower Member (Pantazis, 1967; Gass *et al.*, 1994), then this would suggest a ?late Campanian to early Maastrichtian age for the emplacement of the Paralimini Melange.

2.3.2.1.3 Dhrousha Melange

The Dhrousha Melange outcrops on the east side of a road cutting, 2km north of Dhrousha (Fig. 2.4), on the Polis road. The distribution of the melange coupled with the overlying Lefkara Formation, Lower Member (Maastrichtian) pelagic chalks, is limited to this single exposure underlying a west and south facing scarp of Terra Limestone (basal Miocene), with the melange dipping (50°, 072°N) towards the axis of the Polis Graben, and straddles the contact between the northern Mamonia basement fragment and the Troodos basement terrane to the east (Fig. 2.4).

The melange consists of alternating layers of reworked bentonitic clay and sand- to pebble-grained size clasts of predominantly Mamonia basement terrane origins, supported in a matrix of reworked bentonitic clay. The melange can be divided into three depositional units by the presence of two pelagic chalk interbeds.

Due to the Dhrousha Melange's association with Mamonia type rocks and coupled with the presence of pelagic chalk interbeds, it would appear the Dhrousha Melange and Kathikas Formation share the same mode of emplacement (discussed below), with the source area for the Mamonia clastic material coming from the ?west.

Like the Kathikas Formation the Dhrousha Melange contains pelagic chalk interbeds, containing calcareous nannofossils, which age dates the melange, to be ?late Campanian to early Maastrichtian (this study).

2.3.2.1.4 Kathikas Formation

The Kathikas Formation was formally defined and interpreted by Swarbrick and Robertson (1980), with its type section reported as a composite, based on localities to the west of Kathikas village. There are two large outcropping areas seen in S.W. Cyprus (Fig. 2.4), both straddle the contacts between the Mamonia basement fragments and Troodos basement terrane in the east and the Mamonia and Troodos southern basement fragments in the west.

The succession comprises multiple undeformed, submarine, matrix-supported debris flows (Swarbrick and Robertson, 1980). These multiple debris flows represent periods of rapid deposition, were the beds are defined by colour variations, from grey to purple and crude stratification marked by changes in size and fabric of clasts (Swarbrick and Naylor, 1980). Pelagic chalk interbeds provide the evidence for pauses in deposition between flow events. The debris was sourced locally from the southern Mamonia basement fragment, with volumetrically fewer clasts of serpentinite and Troodos ophiolite material (Gass *et al.*, 1994). The debris flows are texturally immature, with poor sorting of angular clasts, ranging from sand size to 2.5m, averaging 20 to 30cm (Gass *et al.*, 1994). The fine-grained matrix (<1mm) which can represent up to 70% of the deposit, has a clay content in the order of 70 to 80%. X-ray defraction analysis shows peaks of calcite, quartz, hematite, kalonite, illite and montmorillonite mixed layer clay (Swarbrick and Naylor, 1980).

The emplacement of the Kathikas Formation (including the Dhrousha Melange) occurred during the late stages (transpressional) of the juxtapositioning event of the Mamonia and Troodos basement terranes and their related fragments, separated by screens of serpentinite (Swarbrick, 1993). This resulted in the Mamonia basement fragments to 'flower' forming structural highs, bounded by fault scarps, these being the source areas for the debris flows, to be deposited into the structural lows.

Biostratigraphical research carried out by Urquhart and Banner (1994) on the matrix of the Kathikas Formation, observed benthonic (*Bathysiphon* spp.; *Glomospira* spp.) and rare planktonic foraminifera (*Globotruncanita stuartiformis* (Dalbiez, 1955);

Spiroplecta striata (Ehrenberg, 1840)), and radiolaria (*Gongylothorax* spp.; *A. tylotus*), which were in a poor state of preservation. Urquhart and Banner (1994), also dated the pelagic chalk interbeds by referring to previous research (unpublished report, University College London, 1992), which observed planktonic foraminifera and calcareous nannofossils, indicating a late Maastrichtian age (calcareous nannofossil zones CC25c - CC26).

2.3.2.2 Calcareous and evaporite sediments

The lithostratigraphic classification employed within the thesis for the calcareous neo-autochthonous cover sediments, is noted in Fig. 2.6 and is correlated with lithostratigraphic classifications of past researchers (Gass, 1960; Pantazis, 1967; Turner, 1971; Krasheninnikov and Kaleda, 1994). The lithostratigraphical boundaries in the main, follow those proposed by Gass (1960) and Pantazis (1967) for the Lefkara and Pakhna Formations, with modifications, especially at the unconformable boundary between the Lefkara and Pakhna Formations. The stratigraphic classifications proposed by Turner (1971), for research carried out between Polis and Kathikas, which forms the northern section of the study area, and Krasheninnikov and Kaleda (1994), for research carried out on the Perapedhi section, located to the south of the study area, are included for the boundaries of the overlying Kalavasos and Pissouri Formations. The reason for not employing one of the more recent lithostratigraphic classifications, with respect to the Lefkara and Pakhna Formations, is because Turner (1971) has been taken from unpublished research and Krasheninnikov and Kaleda (1994) is based on a localised measured section, and both are not representative of what is observed overall in S.W. Cyprus.

2.3.2.2.1 Lefkara Formation

Initially the formation was named the Lapithos Group (Henson *et al.*, 1949; Wilson, 1959; Gass, 1960), based on the "Lapithos Beds" of Bellamy and Jukes-Brown (1905), in the Kyrenia Range, northern Cyprus. This group was renamed the Lefkara Group (Pantazis, 1967), due to the validity of the type locality, (see Gass 1960 and Ducloz 1964). Gass (1960) subdivided the Lapithos Group into Lower, Middle and Upper Lapithos, with the Middle Lapithos being further subdivided into the "Chalk and Chert Member" and "Massive Chalk Member", these divisions are based on partial unconformities, lithological differences and palaeontological evidence (Cockburn *in*

AGE		GROUPS, FORMATIONS AND MEMBERS				
		Gass 1960	Pantazis 1967	Turner 1971	Krasheninnikov & Kaleda 1994	Morse (this thesis)
Plio	Piacenzian	Nicosia-Athalassa Fm.	Athalassa Formation	Pissouri Formation	Pissouri Formation	Pissouri Formation (Mrytou Marls)
	Zanclean	Pliocene Marls				
Miocene	Messinian	Hiatus	Dahli Gp: Koronia/Kalavasos	Dahli Gp: Yiolou Formation	Kalavasos Formation	Kalavasos Formation
	Tortonian	Dahli Gp: Pakhna Formation	Dahli Gp: Pakhna Formation	Dahli Gp: Pakhna Formation	Pakhna Formation	Pakhna Fm: Koronia Lst.
	Serravallian					Pakhna Fm: Calc. sediments
	Langhian					Pakhna Fm: Terra Lst.
	Burdigalian	Lapithos Group: Upper	Lefkara Group: Upper Chalks: Bedded	Terra Formation	Arsos Formation	
	Aquitanian					
Oligo	Chattian			Lapithos Group: Mavroli Formation	Kilani Formation	Lefkara Formation: Hiatus
	Rupelian					
Eocene	Priabonian	Lapithos Group: Middle: Massive Chalk	Lefkara Group: Upper Chalks: Massive		Upper Lefkara Formation	Lefkara Formation: Middle: Massive Chalks
	Bartonian					
	Lutetian	Lapithos Group: Middle: Chalk and Chert	Lefkara Group: Chalk with Chert	Lapithos Group: Pano-Lefkara Formation	Middle Lefkara Fm.	Lefkara Formation: Middle: Chalk with Chert
	Ypresian					
Palaeo	Thanetian	Lapithos Group: Hiatus			Lower Lefkara Formation	Lefkara Formation: Hiatus
	Danian					
L Cret	Maastrichtian	Lapithos Group: Lower	Lefkara Group: Lower Chalks	Lapithos Group: Simou Formation		Lefkara Formation: Lower Member
	Campanian					

Fig. 2.6. The lithostratigraphic classification of different authors for the Late Cretaceous and Tertiary calcareous sediments of the neo-autochthonous sedimentary cover, which overlie the Mamonia and Troodos basement terranes and fragments.

Gass, 1960). Pantazis (1967) recognised similar lithological divisions of the newly named Lefkara Group, which he elevated to formation status, the Lower Marl Formation (equivalent to Lower Lapithos), the Chalk and Chert Formation (equivalent to Chalk and Chert Member of the Middle Lapithos), and the Upper Chalk Formation (equivalent to Massive Chalk Member of the Middle Lapithos plus the Upper Lapithos). Research carried out on the Late Cretaceous and Tertiary calcareous deposits of the Perapedhi section by Krasheninnikov and Kaleda (1994), subdivided the Lefkara Group of Pantazis (1967) into five formations and are correlated in Fig. 2.6. However, due to many facies variations within the upper units throughout Cyprus, this account will follow Robertson and Hudson (1974) in referring to all these essentially calcareous pelagic sediments (Upper Cretaceous to ?Lower Miocene) as the Lefkara Formation and the traditional divisions proposed by Gass (1960), to member status (Lower, Middle and Upper).

Lefkara Formation, Lower Member

The chalks of the Lower Member form a thin (<12m) continuous out crop against the south-west margin of the Troodos Massif between Ayios Nikolaos and Apsiou villages (Fig. 2.1) (Wilson, 1959; Bear and Morel, 1960; Krasheninnikov and Kaleda, 1994). From Apsiou in an anti-clockwise direction around the margin of the Troodos Massif the Lower Member thins and becomes progressively more discontinuous until west of Lymbia village (Fig. 2.1) on the northern margin the Troodos Massif where finally it is no longer seen (Bagnall, 1960; Bear and Morel, 1960; Gass, 1960; Pantazis, 1967). Against the south-west margin, north-west of Ayios Nikolaos village (Fig. 2.1) the Lower Member again thins and becomes discontinuous (Gass *et al.*, 1994). In S.W. Cyprus the Lower Member is seen as a continuous outcrop from Lara to Tala village (Fig. 2.4) (Turner, 1971), following and straddling the lineament between the Mamonia and Troodos southern basement fragments, north and north-east of Paphos (Fig. 2.4) with a regional dip to the west. The Lower Member is also seen to the east of the Troodos Massif around the margin of the Troulli Inlier (Lilljequist, 1969).

At Perapedhi (Fig. 2.1) the Lower Member comprises fine-grained, finely laminated marls, with intercalations of marly chalk, nodular cherts (bedded cherts are rare to absent) and rare calcarenites (Gass *et al.*, 1994). Bagnall (1960) reported the presence of tuffaceous siltstones, vitric tuffs, agglomerates and isolated volcanic bombs in the Pano Lefkara - Larnaca area (Fig. 2.1), suggesting a brief period of localised

vulcanicity during the Maastrichtian. Krasheninnikov and Kaleda (1994) subdivided their Lower Lefkara Formation into two members (unnamed), the lower 28m being composed of soft conchoidally jointed marls and clayey limestones, with the first bed of 12m forming the Lefkara Formation, Lower Member of this study.

Due to the absence of benthonic foraminifera, clastic material and macro fossils, with the exception of fish teeth. The evidence suggest that the pelagic chalks of the Lefkara Formation, Lower Member to be a deep water carbonate sequence, deposited close to the calcite compensation depth (Pantazis, 1967; Gass *et al.*, 1994).

The chalks of the Lower Member unconformably overlie the Mamonia and Troodos basement terranes and fragments (Wilson, 1959; Bagnall, 1960; Pantazis, 1967; Gass *et al.*, 1994), and the Perapedhi Formation, where the capping Kannaviou Formation is not present (Gass, 1960; Gass *et al.*, 1994). It conformably overlies the Kannaviou (Lilljequist, 1969; Robertson, 1977c), Kathikas (Swarbrick and Naylor, 1980) and Moni (Pantazis, 1967; Robertson, 1977a) Formations. North of the Troodos Massif (Gass, 1960), and in the Troulli Inlier (Lilljequist, 1969), and the Pano Lefkara - Larnaca area (Bagnall, 1960), the chalks of the Lower Member are unconformably overlain by sediments of the Middle and Upper Members of the Lefkara Formation, and the Pakhna Formation. South of the Troodos Massif, between Ayios Nikolaos and Kalavasos (Fig. 2.1), the Lower Member passes up conformably into the Chalk and Chert unit of the Middle Member (Wilson, 1959; Pantazis, 1967; Gass *et al.*, 1994; Krasheninnikov and Kaleda, 1994). However it must be noted the Chalk and Chert unit overlaps the Lower Member north-west of the Perapedhi and makes unconformable contact with the Troodos pillow lavas, indicating a ?partial unconformity. Further to the north-west the chalks of the Lower Member are seen in several localised areas, along the Troodos Massif margin, unconformably overlain by sediments of the Lefkara (Middle Member) and Pakhna Formations.

Research carried out by Krasheninnikov and Kaleda (1994) and Khokhlova, Bragina and Krasheninnikov (1994), on the calcareous sediments of the Perapedhi section, confirmed and refined the biostratigraphical work of A. G. Davis (*in* Wilson, 1959), which suggested the age of their Lower Lefkara Formation sediments to be, Late Cretaceous (upper Campanian) to Early Eocene (Ypresian), based on radiolarian and foraminiferal zonal evidence. The two unnamed members of the Lower Lefkara Formation of Krasheninnikov and Kaleda (1994) have been separately dated, the first 12m of the lower member to be upper Campanian to Maastrichtian, with the remaining

16m to be Early Palaeocene and the upper member (82m thick) to be Late Palaeocene to Early Eocene. Pervious researchers (e.g. Gass, 1960; Pantazis, 1967; Lilljequist, 1969; Gass *et al.*, 1994 etc.) have considered the pelagic chalks of the Lower Member to be entirely of Maastrichtian age, with the overlying chalks ?conformably (Pantazis, 1967) or unconformably (Gass, 1960; Bagnall, 1960; Lilljequist, 1969) to be the basal unit of the Lefkara Formation, Middle Member.

Lefkara Formation, Middle Member (Chalk and Chert unit)

The Middle Member (Chalk and Chert unit), forms a thick (150-200m) continuous outcrop around the margin of the Troodos Massif, in a clockwise direction between Lymbia and Ayios Nikolaos villages (Fig. 2.1) on the northern and south western margins respectively (Wilson, 1959; Bagnall 1960; Bear and Morel, 1960; Gass, 1960; Pantazis, 1967). Along the northern margin of the Troodos Massif the unit thins in a westerly direction (Bear, 1960; Gass, 1960), after overstepping the Lefkara Formation, Lower Member onto the Troodos basement terrane at Lymbia Village (Fig. 2.1), and is not seen west of Eliophotes village (Fig. 2.1). Along the south western margin, after Ayios Nikolaos village (Fig. 2.1) the unit thins and becomes discontinuous (Gass *et al.*, 1994), and is not seen north-west of Pano-Panayia (Fig. 2.4). The unit is also seen to the east of the Troodos Massif exposed around the Troulli Inlier (Lilljequist, 1969).

The Chalk and Chert unit succession at Perapedhi is described in detail lithologically by Krasheninnikov and Kaleda (1994) and is representative of the unit seen throughout Cyprus, which they assigned to their Lower and Middle Lefkara Formations, with their basal 12m belonging to the Lefkara Formation, Lower Member of this study. The remaining basal horizon (100m) of the Chalk and Chert unit consists of calcarenites and cherts (even though rare are a distinctive part of the sequence), and are present along with marls, marly chalks and limestones. The bulk of the upper horizon (80m) consists of rhythmic alternation of light grey to white, calciturbidite chalks with bioturbation and chert bands to give the strata a well bedded appearance, including nodular bone cherts and calcarenites. Gass (1960), reported numerous thin bands (<10cm) of volcanic tuff throughout the Chalk and Chert unit, but becoming progressively rarer towards the top and can be seen exposed within the Tremithios river section, east of Ayia Anna village (Fig. 2.1). The tuffs consist of altered basic rock and glassy shards, indicating the Troodos Massif may have been exposed during deposition. Gass *et al.* (1994), reported well rounded Mamonia clast up to 2cm diameter to be

present, within the Chalk and Chert unit and are concentrated at the base of individual beds, and can be seen in a north-east facing exposure, south-east of Pano-Panayia (Fig. 2.4). This suggests, like the Troodos Massif, the Mamonia rocks were also exposed during the deposition of the unit.

The non-turbidite chalks and marls of the Chalk and Chert unit have all the features of deep-water calcareous pelagic sedimentation (Gass *et al.*, 1994), whereas the calciturbidites contain clastic grains, benthonic foraminifera and bioturbation, indicating deposition in relatively shallower waters with bottom circulation (Robertson, 1976). Gass (1960), reported current bedding present throughout the unit, indicating that deposition had taken place in a shallow water environment in the Dhali area (Fig. 2.1). Pantazis (1967), reported from the Kalavasos area (Fig. 2.1), that the transgressive event from the ?south was more widespread than that of the Lefkara Formation, Lower Member, due to the Chalk and Chert unit overstepping the Lower Member pelagic chalks, onto the basement, and the absence of coarse fractions of clastic material and the presence of foraminiferal oozes, suggest deposition occurred in warm seas of moderate depth.

The Chalk and Chert unit oversteps older calcareous units to rest unconformably on the Mamonia and Troodos (including associated sediments) basement terranes and fragments (e.g. Wilson, 1959; Pantazis, 1967; Gass *et al.*, 1994; this study, etc.), in S.W. Cyprus. The unit also overlies the Lefkara Formation, Lower Member unconformably, against the northern and eastern margins of the Troodos Massif and around the Troulli Inlier (Bagnall, 1960; Gass, 1960; Lilljequist, 1969), and conformably, against the southern and south western margins of the Troodos Massif (Wilson, 1959; Bear and Morel, 1960; Pantazis, 1967; Gass *et al.*, 1994). The unit is conformably overlain by the Massive Chalk unit (Wilson, 1959; Bagnall, 1960; Bear and Morel, 1960; Gass, 1960; Pantazis, 1967; Lilljequist, 1969; Gass *et al.*, 1994) and unconformably by stratigraphically higher units of the neo-autochthonous sedimentary cover.

Biostratigraphical studies with respect to the Chalk and Chert unit are of limited value, apart from research on the calcareous sediments of the Perapedhi section by Krasheninnikov and Kaleda (1994) and Khokhlova, Bragina and Krasheninnikov (1994), which confirmed and refined the biostratigraphical work of A. G. Davis (*in* Wilson, 1959), suggesting the age of their Lower and Middle Lefkara Formation sediments to be, Late Cretaceous (upper Campanian) to Mid Eocene, based on radiolarian and foraminiferal zonal evidence. The two unnamed members of the Lower

Lefkara Formation of Krasheninnikov and Kaleda (1994) have been separately dated, the first 12m of the lower member to be upper Campanian to Maastrichtian and assigned to the Lefkara Formation, Lower Member of this study, with the remaining 16m to be Early Palaeocene and the upper member (82m thick) to be Late Palaeocene to Early Eocene. Their overlying Middle Lefkara Formation is dated Early to Mid Eocene. This gives the Chalk and Chert unit of the Perapedhi section a relative biostratigraphical (calcareous nannofossil) zonal range of NP1 to NP16. It must be noted that Krasheninnikov and Kaleda (1994) did not find any basal layers of the Lower Palaeocene due to sparse sampling.

Research carried out by Baroz and Bizon (1977), on the neo-autochthonous sediments deposited against the northern margin of the Troodos Massif, confirmed and refined the biostratigraphical research of Cockbain (*in* Bear, 1960; *in* Gass, 1960), in suggesting the age of isolated outcrops of the Chalk and Chert unit which overlie the basement, to have an overall range of Palaeocene to Mid Eocene, based on foraminiferal zonal evidence. Against the southern margin of the Troodos Massif in the Kalavasos area (Fig. 2.1), Mantis (*in* Pantazis, 1967) also gave an overall range for the Chalk and Chert unit a Palaeocene to Eocene age.

Lefkara Formation, Middle Member (Massive Chalk unit)

The Middle Member (Massive Chalk unit), forms a thick (120-200m) continuous outcrop, against the south and south-west margin of the Troodos Massif, between Kalavasos and Ayios Nikolaos villages (Fig. 2.1) (Wilson, 1959; Bear and Morel, 1960; Pantazis, 1967). From Kalavasos village in an anti-clockwise direction around the margin of the Troodos Massif, the outcrop thins and becomes progressively more discontinuous, until it is not seen west of Alambia village (Fig. 2.1) on the northern margin of the Troodos Massif (Bagnall; 1960; Gass, 1960), where it is overstepped unconformably by the chalks of the Lefkara Formation, Upper Member (Gass, 1960). The unit north-west of Ayios Nikolaos village thins and becomes discontinuous until it is not seen north-west of Lyso (Fig. 2.4), against the south western margin of the Troodos Massif. The unit is also seen to the east of the Troodos Massif exposed around the Troulli Inlier (Lilljequist, 1969).

At the Perapedhi section, Krasheninnikov and Kaleda (1994), described in detail the Massive Chalk unit (80m) and is representative of the unit seen throughout Cyprus, which they assigned to their Upper Lefkara Formation. The unit consists of a lower

(35m) section of massive thick-bedded chalks and an upper (45m) section of distinctly-layered marly chalks.

The chalks and marls of the Massive Chalk unit, consists of abundant foraminifera with subordinate radiolarian shells, with a low (7-15%) non-biogenic component, suggesting deposition in clear warm seas of moderate depth (Gass *et al.*, 1994).

The Massive Chalk unit oversteps older calcareous sediments to rest unconformably (this study) on the Mamonia and Troodos (including associated sediments) basement terranes and fragments in S.W. Cyprus (this study). The unit conformably overlies the Lefkara Formation, Middle Member (Chalk and Chert unit) (Wilson, 1959; Bagnall, 1960; Bear and Morel, 1960; Gass, 1960; Pantazis, 1967; Lilljequist, 1969; Gass *et al.*, 1994). The unit is overlain by the Lefkara Formation, Upper Member, unconformably against the northern margin of the Troodos Massif and around the Troulli Inlier (Gass, 1960; Lilljequist, 1967), and conformably against the southern margin of the Troodos Massif (Wilson, 1959; Bagnall, 1960; Bear and Morel, 1960; Pantazis, 1967; Gass *et al.*, 1994), and is also unconformably overlain by the Pakhna Formation and other stratigraphically higher formations of the neo-autochthonous sedimentary cover.

Biostratigraphical studies with respect to the Massive Chalk unit are of limited value, apart from research on the calcareous sediments of the Perapedhi section by Krasheninnikov and Kaleda (1994) and Khokhlova, Bragina and Krasheninnikov (1994), which confirmed and refined the biostratigraphical work of A. G. Davis (*in* Wilson, 1959), suggesting the age of their Upper Lefkara Formation to be Mid to Late Eocene age (calcareous nannofossil biostratigraphical zonal range of NP16 to NP20), based on radiolarian and foraminiferal zonal evidence.

Early researchers Cockbain (*in* Gass, 1960), Mantis (*in* Pantazis, 1967) and Baroz and Bizon (1977) gave an overall range for the Massive Chalk unit outcrops against the northern and southern margins of the Troodos Massif a Mid to Late Eocene age.

Lefkara Formation, Upper Member

The Upper Member forms a thick (50-180m) continuous outcrop around the margin of the Troodos Massif, in an anti-clockwise direction between the villages of Ayios Nikoloas and Alambia (Fig. 2.1), against the south western and northern margins respectively (Wilson, 1959; Bagnall 1960; Bear, 1960; Bear and Morel, 1960; Gass, 1960; Pantazis, 1967). Along the northern margin the member thins in a westerly direction (Bear, 1960) between the villages of Alambia and Eliophotes (Fig. 2.1), where it is unconformably overstepped by the Pakhna Formation. The member is not present north-west of Ayios Nikoloas, against the south western margin of the Troodos Massif (Gass *et al.*, 1994). The member is also seen to the east of the Troodos Massif exposed in the Troulli Inlier (Lilljequist, 1969) and south of Paralimini (Follows and Robertson, 1990).

The Upper Member succession (200m) at Perapedhi (Fig. 2.1) is described in detail lithologically by Krasheninnikov and Kaleda (1994), which they assign to their Kilani Formation, Members I and II. It is representive of the member seen against the southern margin of the Troodos Massif, mostly composed of marls and marly and clayey limestones, with the grey marls containing a uniform fine-grained clay-carbonate mass which accounts for 75% of the volume. Against the northern (Bear, 1960), north eastern (Gass, 1960) and south eastern (Bagnall, 1960) margins of the Troodos Massif, the member is composed of white flaggy, massive and cleaved foraminiferal chalks and marls, with the upper part of the succession also consisting of thin black shales, pyritic nodules and chalks and marls with a red colouration.

The depositional environment for the Upper Member against the southern margin, can be interpreted by the presence of carbonate clayey sediments with abundant planktonic foraminifera, coccoliths and rare radiolaria, to suggest an upper bathyal zone (Krasheninnikov and Kaleda, 1994). Against the northern (Bear, 1960), north eastern (Gass, 1960) and south eastern (Bagnall, 1960) margins of the Troodos Massif, the increasing presence of benthonic fauna throughout the member, and black shales indicating anaerobic conditions, red colouration indicating nearby lateritized land surface, current bedding and washout structures seen in the upper part of the member, suggests a shallowing upwards from the upper bathyal zone, to a near shore, lagoonal environment. The slumping and highly contorted units seen within the upper part of the

member (Bagnall, 1960; Gass, 1960), separated by relatively undisturbed strata, suggests differential uplift of the Troodos Massif, during the late deposition of the member and not compressional activity.

The Upper Member unconformably oversteps in a westerly direction from the Troulli Inlier, older sediments to rest on the Troodos basement terrane against the northern margin of the Troodos Massif (Bear, 1960; Gass, 1960; Lilljequist, 1969). Against the southern margin, the member conformable overlies the Middle Member, Massive Chalk unit (Wilson, 1959; Bagnall, 1960; Bear and Morel, 1960; Pantazis, 1967; Gass *et al.*, 1994). The member is unconformably overlain by all stratigraphically higher units of the neo-autochthonous sedimentary cover. However, south of Paralimini, Follows and Robertson (1990) reported the member unconformably overlies lithologies of the basement and Paralimini Melange and is conformably overlain by the Pakhna Formation, Terra Limestone Member.

Biostratigraphical studies by Krasheninnikov and Kaleda (1994) and Khokhlova, Bragina and Krasheninnikov (1994), confirmed and refined the biostratigraphical work of A. G. Davis (*in* Wilson, 1959), suggesting the age of the Upper Member (their Kilani Formation, Members I and II) as Oligocene in age, based on radiolarian and foraminiferal zonal evidence (calcareous nannofossil biostratigraphical zonal range of NP21 to NP24).

2.3.2.2.2 Pakhna Formation

The Pakhna Formation essentially consists of chalks, marls, limestones, gypsum lenses and calcareous sandstones. The limestones of the Terra and Koronia (Eaton, 1987) Members are prominent horizons, at or near to the base and top of the formation respectively, which Follows and Robertson (1990, 1996), demonstrated to be intimately associated with and designated them as formal members of the Pakhna Formation, and discussed the tectonic controls during their deposition.

Pakhna Formation chalks

The Pakhna Formation chalks have a variable thickness (<60-500m) at outcrop, thickening northwards into the Mesaoria basin away from the northern margin of the Troodos Massif (Cleintaur et al., 1977) and south westwards away from the southern margin (Wilson, 1959). The formation forms a discontinuous outcrop pattern, in an anti-clockwise direction between Kalavasos and Pano-Koutraphas villages, against the

southern (Pantazis, 1967), eastern (Bagnall, 1960) and northern (Bear, 1960; Carr and Bear, 1960; Gass, 1960) margins of the Troodos Massif, with isolated outcrops east of the Troulli Inlier (Lilljequist, 1969; Follows and Robertson, 1990). In southern Cyprus, north-west of Limassol, the outcrop of the Pakhna chalks are extensive (Pantazis, 1979) and outcrop continuously against the southern and south western margins of the Troodos Massif, until Ayios Nikolaos village (Wilson, 1959; Bagnall and Morel, 1960), where the outcrop becomes discontinuous until north-west of Kannaviou village (Pantazis, 1979; Kluyver, 1969; Gass *et al.*, 1994). The formation chalks also form an extensive outcrop between Marathounda and Dhrousha villages (Fig. 2.4), against the western flank of the Polis graben (Pantazis, 1969; Turner 1969).

The sediments of the Pakhna Formation other than the Terra and Koronia Limestone Members, are cream to buff-coloured marls, chalks, calcarenites, gypsum lentils and polymictic conglomerates. Against the south and south-west margins of the Troodos Massif, Gass *et al.* (1994) noted the polymictic conglomerates near to the base of the formation, containing clasts derived from Mamonia lithologies, whereas, those located higher in the sequence contained Troodos lithologies. There are lateral facies variations within the formation, which makes it difficult for any formal stratigraphy to be formulated, which had been attempted by earlier researchers (Bagnall, 1960; Pantazis, 1967) resulting in contradictory interpretations.

The Pakhna Formation chalks unconformably oversteps all older sedimentary formations to rest on Mamonia and Troodos basement lithologies (Wilson, 1959; Bagnall, 1960; Bear, 1960; Carr and Bear, 1960; Gass, 1960; Pantazis, 1967; Lilljequist, 1969; Gass *et al.*, 1994), and conformably overlain by sediments of the localised Kalavasos Formation (Pantazis, 1967; Eaton, 1987; Follows and Robertson, 1990), where the Koronia Limestone Member is missing, and unconformably by stratigraphically younger formations. However, in the areas of Perapedhi village (Krasheninnikov and Kaleda, 1994; Gass *et al.*, 1994), Kalavasos village (Eaton, 1987) and Paralimini (Follows and Robertson, 1990), the formation chalks conformably overlie the Lefkara Formation, Upper Member.

The sediments of the Pakhna Formation have a composition, texture and faunal assemblage which is indicative of been deposited in an open marine to hemi-pelagic environment (Gass *et al.*, 1994). The alternating relative rise and fall of sea level during the formations deposition, may be responsible for the irregular cyclic sequence of chalk, marl and limestone (Gass *et al.*, 1994; Pantazis, 1967). By the end of the cycle of

sedimentation, the marine environment was shallow enough for the localised development of the Koronia Limestone Member. Gass *et al.* (1994), reported the presence of rudites outcropping near Pano-Panayia, forming the unconformable base of the Pakhna Formation overlying the Lefkara Formation, Middle Member (Massive Chalk unit). These rudites are comprised of a disorganised, matrix-supported, polymictic conglomerate. Shallow-water carbonate material is dominant, with non-carbonate material consisting of chert and sandstone fragments derived from Mamonia rocks. The presence of Mamonia rocks and the lack of Troodos derived material, would indicate a source area to the west of Pano-Panayia, where shallow-water carbonates would develop over elevated Mamonia basement fragment.

Biostratigraphical research carried out for Gass *et al.* (1994), on samples collected from a borehole near Ayios Nikolaos (Fig. 2.1), suggest an Aquitanian age (basal Miocene; calcareous nannofossil zonal range of NN1-part NN2), for the base of the Pakhna Formation. Research carried out by Krasheninnikov and Kaleda (1994), suggest a relative planktonic foraminiferal biostratigraphical zonal range of P22 *Turborotalia kugleri* (Oligo-Miocene boundary; calcareous nannofossil zonal range of NP25-NN1), for the base of the Pakhna Formation (their Kilani Formation, Member III). Also Krasheninnikov and Kaleda (1994), suggest a relative planktonic foraminiferal biostratigraphical zonal range of P22-N16 (calcareous nannofossil zonal range of NP25-part NN11) for the entire Pakhna Formation (their Kilani (Member III), Arsos and Pakhna Formations) sedimentary sequence, at the Perapedhi section. Earlier research by Baroz and Bizon (1977), suggest a relative planktonic foraminiferal biostratigraphical zonal range of N5-N16 (calcareous nannofossil zonal range of part NN2-part NN11), for the Pakhna Formation sedimentary sequence, against the northern margin of the Troodos Massif.

Terra Limestone Member

The Terra Limestone Member is predominantly seen in S.W. Cyprus (Turner, 1969, 1971; Pantazis, 1979) and S.E. Cyprus (Follows and Robertson, 1990), as localised outcrops, the largest being situated against the western flank of the Polis graben (Fig. 2.4). In S.E. Cyprus the member is defined as a coral framestone, with red algae- and benthonic foraminiferal dominated facies, this diverse fauna and the presence of corals, suggest deposition had occurred in shallow marine conditions with normal salinity (Follows and Robertson, 1990). Stratigraphically the member is seen at or near to the base of the Pakhna Formation.

Allen (1967), dated the Terra Limestone Member as Late Oligocene to Early Miocene, based on the presence of benthonic foraminifera *Loxostomum delicatum* and on reef dwelling *Lepidocyclinia* sp. and *Miocypsina* sp. Mantis (1970), dated the member Early Miocene (Burdigalian) based on the recognition of planktonic foraminiferal zones *Globigerinita dissimilis*, *Globoquadrina dehiscens* and *Globigerinoides glomerosa* (calcareous nannofossil zones NN2-NN5). Follows and Robertson (1990), summarised and gave an Aquitanian to Burdigalian (calcareous nannofossil zones NN1-NN4) age for the member in S.E. Cyprus, based on the presence of corals *Favia aquitainensis, Favites neugeboreni var. Burdigalensis* and *Hydnophora (Monticulastraea) provincialis.*

Koronia Limestone Member

The Koronia Limestone Member is seen as discontinuous outcrops against all margins of the Troodos Massif, including the Akamas peninsula (northern Troodos basement fragment; Fig. 2.4). At the northern margin the member is designated as facies dominated by Poritid corals, with less abundant benthonic foraminifera than that seen in the Terra Limestone Member of S.E. Cyprus, indicating deposition had occurred in a more turbulent and shallow marine environment (Follows and Robertson, 1990). Stratigraphically, the member is seen at the top of the Pakhna Formation. The member is reported to overlie and overstep the Pakhna Formation chalks, unconformably against the northern margin (Zomenis, 1972; Baroz and Bizon, 1977) and southern margin (Gass *et al.*, 1994), and conformably against the northern margin (Bear, 1960; Carr and Bear, 1960), and southern margin (Bagnall, 1960; Pantazis, 1967; Gass *et al.*, 1994), to rest unconformably on Troodos basement lithologies, against the northern margin (Wilson, 1959; Bear, 1960; Carr and Bear, 1960), southern margin (Pantazis, 1967; Gass *et al.*, 1994) and in S.W. Cyprus (Turner, 1971; Kluyver, 1969).

Allen (1967) and Mantis (1968), dated the upper part of the Koronia Limestone Member as Mid Miocene age, based on the benthonic foraminifera *Borelis melo melo.* Mantis (1970) correlated the member with the upper part of the Pakhna Formation chalks, based on the upper Mid Miocene planktonic foraminifera zone *Globorotalia margaritae - Sphaeroidineua grimsdallei.* Baroz and Bizon (1977) identified *Globorotalia acostaensis* and *Globorotalia humerosa* in overlying marls and limestones respectively, near Eliophotes village, suggesting a Tortonian and Messinian age respectively, however, Follows and Robertson (1990) suggest these foraminifera were sampled from reworked successions. Follows and Robertson (1990), summarised and

inferred the member, located against the northern margin of the Troodos Massif, as Tortonian to ?early Messinian age, based on calcareous nannofossil dating of the underlying marls of the Pakhna Formation chalks as Late Miocene and the overlying marls of the Pissouri (their Nicosia) Formation as Early Pliocene.

2.3.2.2.3 Kalavasos Formation (evaporites)

The Kalavasos Formation outcrop is represented mostly by evaporites and is located within three synclinal structures: south-west of the Troodos Massif, with its centre located east of Kathikas village (Fig. 2.4), the Polemi basin; south of the massif near Pissouri village (Fig. 2.1), the Pissouri basin; and south-east of the massif near Kalavasos village (Fig. 2.1), the Psematismenos basin (Orszag-Sperber *et al.*, 1989). Also the formation is seen as discontinuous outcrops along the northern margin of the massif (Pantazis 1967), initially reported as local lenses within the Pakhna Formation (Bear, 1960; Carr and Bear, 1960; Gass, 1960).

Krasheninnikov and Kaleda (1994), noted the Kalavasos Formation evaporite sequence near Pissouri village, which is typical of other Cyprus localities and also the Mediterranean region, to consist of three distinct members: a lower member composed of marls and diatomites, with beds of limestones; a middle member composed of fine-grained bedded to coarse crystalline gypsums, with a polygenetic breccia at the base and a gypsiferous breccia within the member; and an upper member composed of intercalated conglo-breccias, limestone and marls, in lens-shaped layers of variable thickness.

The presence of gypsum, indicates the depositional environment of the Kalavasos Formation, as shallow water conditions in closed or semi-closed basins, with abnormal salinity. The formation is associated with the salinity crisis of the Mediterranean region during the Messinian (Hsü, 1972; Hsü *et al.*, 1978; Robertson *et al.*, 1995a).

The Kalavasos Formation conformably overlies the Pakhna Formation (Pantazis, 1967; Eaton, 1987; Follows and Robertson, 1990) and is unconformably overlain by all stratigraphically higher formations (e.g. Pantazis, 1967; Follows and Robertson, 1990; Krasheninnikov and Kaleda, 1994 etc.).

2.3.2.2.4 Pissouri Formation (Myrtou Marls)

The Myrtou Marls forms the base of the Pissouri Formation, which is of variable thickness (30-120m at outcrop; >600m in borehole, Mesaoria basin), seen as a discontinuous outcrop pattern around the Troodos Massif, in an anti-clockwise direction it is located, within the Polis graben structure (Fig. 2.4), along the coast north of Paphos, centred around Pissouri village, south of the Troulli Inlier, centred around Paralimini, within the Mesaoria basin and against the northern margin of the massif (Pantazis, 1979).

Against the northern margin of the Troodos Massif and northwards into the Mesaoria basin, the Pissouri Formation (Myrtou Marls) is a homogeneous grey sediment, but locally contains thin limestone bands and sandy layers which shows a brown or buff colouration (Wilson, 1959; Bear, 1960; Carr and Bear, 1960; Gass, 1960). South of the massif the formation comprises interclated clayey-carbonate and sandy rocks (Krasheninnikov and Kaleda, 1994).

The different lithologies noted within the Pissouri Formation (Myrtou Marls), against the northern margin of the Troodos Massif, may represent facies variations, between deep water (marls) and near shore (limestones and sandy layers) environments (Wilson, 1959; Bear, 1960). However, the lithologies noted by Krasheninnikov and Kaleda (1994) from the outcrop centred around Pissouri village, indicate a shallow water outer shelf environment.

The Pissouri Formation unconformable oversteps all older sedimentary formations to rest on Mamonia and Troodos basement lithologies and is unconformably overlain by stratigraphically higher formations.

Biostratigraphical studies carried out by Krasheninnikov and Kaleda (1994), on the Perapedhi section, suggest a relative biostratigraphical age of basal Pliocene (their planktonic foraminiferal *Sphaeroidinellopsis* Acme-Zone), for the base of the Pissouri Formation (calcareous nannofossil zonal range of NN12).

2.4 Major Tectonic Events

The major tectonic events covered below are in historical order, with the earliest first, and all have affected the depositional history of the formations which make up the

neo-autochthonous sedimentary cover, during the Late Cretaceous (Campanian-Masstrichtian) to Holocene.

2.4.1 The Mamonia Complex (Mamonia basement fragments)

A number of mechanisms have been proposed to explain the style of disruption displayed within the Mamonia Complex (Fig. 2.4) of S.W. Cyprus. Lapierre (1972, 1975), considered the Mamonia Complex had been emplaced across the Troodos Massif from the north-east, during the collision between the African and European plates, as a duplex of alpine-style thrusts and nappes. Turner (1973), suggested that the field evidence was consistent with a gravity slide emplacement, southwards across the Troodos Massif from Turkey, to form the nappe stack. Both Lapierre and Turner considered the serpentinites to be the detachment horizon, for their models. Robertson and Woodcock (1979) and Swarbrick (1980), showed the highly disrupted Ayios Photios Group to be separated from the underlying Dhiarizos Group by a low angle tectonic contact. Robertson and Woodcock (1979), followed Turner in suggesting a gravity slide, but proposed emplacement to be from the south-west, directly onto the Troodos basement terrane. Swarbrick (1980), proposed through field evidence, the Mamonia Complex was separated from the Troodos basement terrane, by high angle to vertical faults, and the lower Dhiarizos Group of lithologies to be the Mamonia basement. The date of the event is poorly constrained between the age of the youngest sediments of the Ayios Photios and Dhiarizos Groups, probably Berriasian/Hauterivian, of the Early Cretaceous (Ealey and Knox, 1975) and to be earlier than the juxtapositioning event (section 2.4.2) of the Mamonia and Troodos basement terranes. Evidence to suggest the latter, is the sub-vertical serpentinite screens that separate the two basement terranes, have been seen to cross-cut the contact between the Ayios Photios and Dhiarizos Groups (Swarbrick, 1980, 1993), and the contact between Kannaviou Formation (late Campanian) and its associated Troodos basement terrane or fragments.

2.4.2 Juxtapositioning of the Mamonia and Troodos basement terranes

A number of mechanisms have been proposed to explain the juxtapositioning event between the Mamonia and Troodos basement terranes and associated fragments. They involve a strike slip (e.g. Swarbrick, 1980; Clube and Robertson, 1986; Swarbrick, 1993) or subduction (e.g. Moores *et al.*, 1984; Murton, 1990; Malpas *et al.*, 1992; Malpas *et al.*, 1993) related scenario, with or without the anticlockwise rotation of the Troodos micro plate being involved. What is accepted by all models is that two dissimilar

basement terranes have been brought together side by side. Where the contact is exposed the two terranes are separated by high angle to vertical faults containing screens of serpentinite. Straddling the contact between the Mamonia and Troodos basement terranes and fragments, is the melange of the Kathikas Formation, which is thought to be the product produced by the late stages of docking (Swarbrick, 1993). Therefore the date for the cessation of the event is based on the age of the chalk interbeds found within the Kathikas Formation, which are early Maastrichtian in age (this study).

2.4.3 Rotation of the Troodos micro plate

It is thought by some researchers (e.g. Moores *et al.*, 1984; Clube and Robertson, 1986; Murton, 1990; Swarbrick, 1993 etc.), the first phase of anticlockwise rotation (<60°) of the Troodos micro plate, is coeval with the juxtapositioning event of the Mamonia and Troodos basement terranes and fragments, and therefore is related to the proposed mechanisms of that event.

Moores and Vine (1971) reported palaeomagnetic vectors with a westerly declination indicating an anticlockwise rotation of 90° for the Troodos micro plate, since the Campanian. Later it was suggested the rotation had occurred during the Miocene, based on relative plate motions between the African and Euro-Asian plates (Shelton and Gass, 1980). However, after extensive sampling of the ophiolite and Turonian to Recent sedimentary cover, it was reported the rotation event consisting 90° of anticlockwise movement, had occurred during the Late Cretaceous to early Tertiary (Clube *et al.*, 1985). Studies carried out on the umbers and radiolarites of the Perapedhi Formation, indicate an anticlockwise rotation of 45° out of the 90° had taken place during the Campanian (Morris *et al.*, 1990).

2.4.4 Kyrenia - D1 Tectonic Event

The deformation of metamorphism, uplift, brecciation and erosion, which took place during the D1 tectonic event, was caused by pervasive ?dextral strike slip at a closing northward dipping subduction zone, south of the present day Kyrenia basement terrane (Robertson and Woodcock, 1986). The event is reliably dated as pre-Maastrichtian by the unconformable overlying basal breccias of the Lapithos Group onto sediments of the Trypa Group (Fig. 2.7).

The event is associated with the rotation of the Troodos micro plate, due to the ?dextral strike slip motion (Robertson and Woodcock, 1986), the effect would give an anticlockwise sense of movement to the Troodos micro plate, which is situated to the south of the Kyrenia Lineament.

2.4.5 Kyrenia - D2 Tectonic Event

The deformation of localised metamorphism, flysch and olistostrome deposition within the Kyrenia basement terrane, took place during the D2 tectonic event (Fig. 2.7), and was caused by a southward thrusting event, during the Mid to Late Eocene. This is thought to be related to the final closure of the Neo-Tethyan oceanic strands within the Taurides, Turkey (Robertson and Woodcock, 1986).

2.4.6 Polis Graben

The major north to south trending extensional structures recorded in the asymmetrical Polis graben structure (Fig. 2.5) of S.W. Cyprus, are thought to be the result of extension generated above a subduction zone, located to the south of Cyprus, driven by subduction roll-back and trench migration, during the Late Miocene. (Payne and Robertson, 1995)

2.4.7 Yerasa Fold Belt

The narrow Yerasa fold belt, trending north-west to south-east is located against the south western edge of the Southern Troodos Transform Fault Zone (STTFZ), near the village of Apsiou (Fig. 2.1). The fold deformation has affected the melange deposits of the Moni Formation and the calcareous deposits of the Lefkara and Pakhna Formations (Bear and Morel, 1960; Robertson, 1977a; Murton, 1986), with the overlying Late Miocene Koronia Limestone unaffected. Also associated with the fold belt is the late stage thrusting of mantle sequence rocks. The cause for the formation of the fold belt, has been tentatively suggested to be attributed to late stage serpentinisation of the mantle sequence peridotites (MacLeod, 1988), located at the western edge of the STTFZ, during the Mid to Late Miocene.

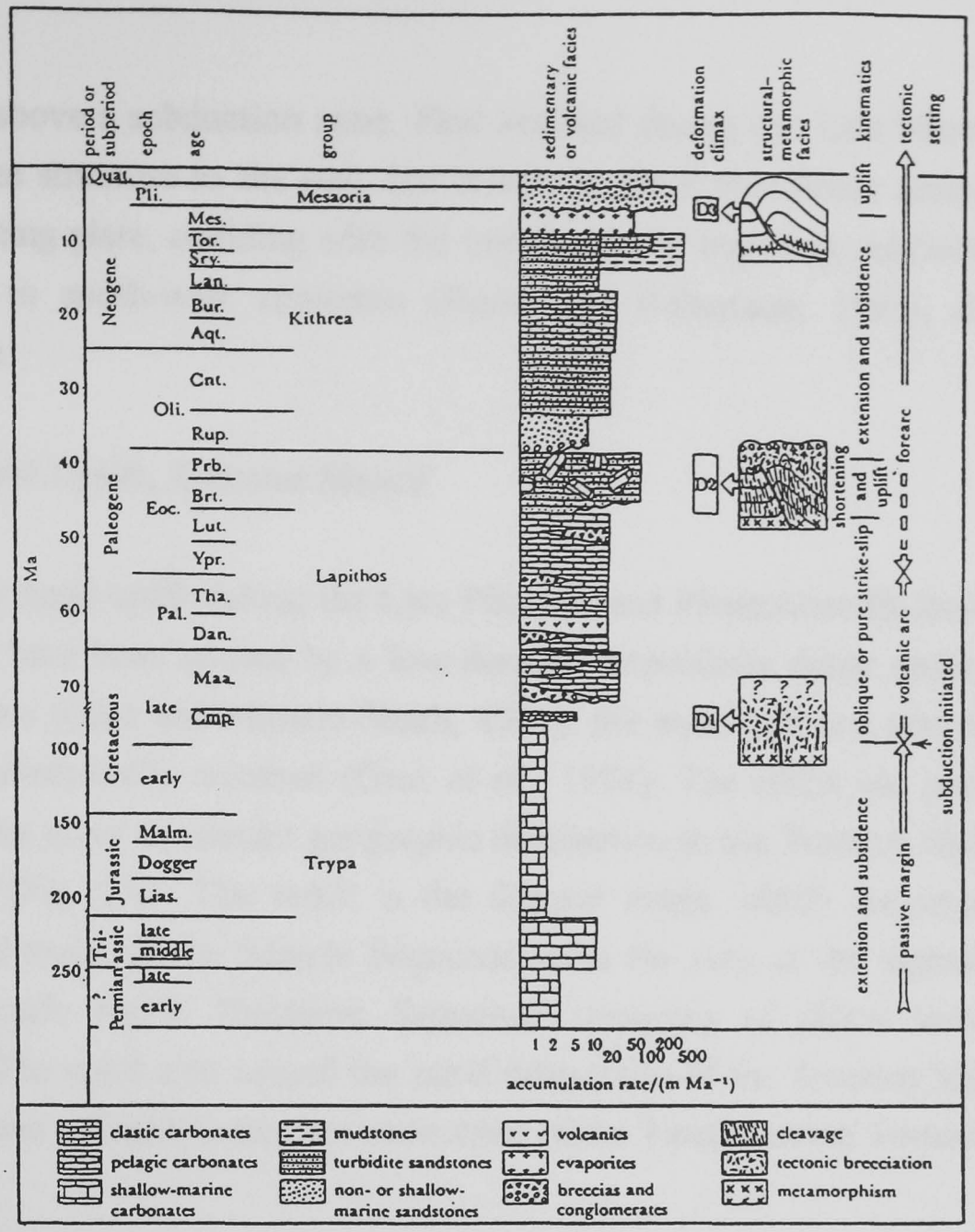

Fig. 2.7. Stratigraphic summary of the Kyrenia terrane with relation to the deformation events D1, D2, and D3. Vertical scale is true time but with a scale change at 75 Ma (modified from Robertson and Woodcock, 1986).

2.4.8 Kyrenia - D3 Tectonic Event

The deformation of south-vergent folding of the Kithrea Group and the already deformed Troodos and Lapithos sheets onto Kithrea Group along the southern Kyrenia basement terrane front, which took place during the D3 tectonic event (Fig. 2.7), was caused by another southward thrusting event, which is thought to be related to the northward under-thrusting of African crustal elements (Robertson and Woodcock, 1986), during the Late Miocene to mid Pliocene.

2.4.9 Peyia Half Graben

The major north-west to south-east extensional structures recorded in the Peyia half graben structure, located to the west of the Polis graben (Fig. 2.5), running parallel to the coastline of S.W. Cyprus, are thought to be the result of continued extension

generated above a subduction zone. First initiated during the Late Miocene to form the Polis graben structure to the east, but driven by the Eratosthenes seamount located on the subducting plate, colliding with the trench, locally impeding subduction, resulting in north-east to south-west extension (Payne and Robertson, 1995), during the Plio-Pleistocene.

2.4.10 Rapid Uplift, Troodos Massif

The rapid uplift during the Late Pliocene and Pleistocene (Robertson, 1977a), is thought to have been caused by a low-density, serpentinite diapir under the summit of Mt. Olympus (Gass and Masson-Smith, 1963), the style, age and rate of uplift has not yet been satisfactorily resolved (Gass *et al.*, 1994). The effect has produced a domal structure that gives an annular geographic distribution to the Troodos Ophiolite Complex Sequences (Fig. 2.3). The result is the deepest rocks, which are situated below the petrological moho of the 'Mantle Sequence' form the core at the highest point and the stratigraphically higher 'Extrusive Sequence' consisting of pillow lava, occur at the periphery. The uplift also caused the rapid denudation of the Troodos Massif, producing vast quantities of highly immature sediments, of the 'Fanglomerate' Formation.

2.4.11 Subduction

Subduction has played an important part in the geological evolution of Cyprus, since the Late Cretaceous. There is geochemical evidence to suggest the Troodos micro plate was formed by sea floor spreading above a subduction zone (Pearce, 1975, 1980; Smewing *et al.*, 1975), with some workers (e.g. Moores *et al.*, 1984; Robertson and Dixon, 1984) favouring a northward dipping zone and others (e.g. Dilek *et al.*, 1990; Taylor *et al.*, 1991) favouring a southward dipping zone. Robertson and Woodcock (1986) and Kempler and Ben-Avraham (1987) proposed that a northward dipping subduction zone existed to the south of the Kyrenia Lineament between the ?Santonian and Campanian. Currently there is a subduction zone to the south of Cyprus, where the north eastern edge of the African plate dips northwards under the Turkish plate. Research by Robertson et al. (1995b, 1996a), suggests the Eratosthenes seamount, which is situated to the south of Cyprus on the subducting plate, is breaking up and being thrust under Cyprus, and could be responsible for the Late Pliocene to mid Quaternary uplift of southern Cyprus. The onset of subduction to the south of Cyprus is uncertain, but is thought to have been present during the Oligocene and Miocene (Eaton and Robertson, 1993). The Late Tertiary to Recent tectonic and palaeo-environmental development of the Mediterranean region is extensively covered by Robertson and Grasso (1995), and Robertson et al. (1996b).

CHAPTER 3

INTRODUCTION TO CALCAREOUS NANNOFOSSILS AND SYSTEMATICS

3.1 Introduction

With reference to chapters relating to calcareous nannofossils (Appendix C), of Initial Reports of the Deep Sea Drilling Project and Scientific Reports of the Ocean Drilling Project, one cannot fail to be aware of the importance of this group of microfossils in providing a standard biozonation for the world-wide correlation of Cretaceous and Tertiary calcareous sediments.

Calcareous nannofossils can be split into two distinct groups, coccoliths and nannoliths. Coccoliths are the minute skeletal plates (1-25μm in diameter), produced by marine golden-brown unicellular photosynthetic algae termed a coccolithophore. These skeletal plates in an interlocking arrangement, form a coccosphere on the external surface of the coccolithophore cell. The coccolithophorid is the most abundant organism in the marine environment and generally less than 50μm in diameter. Other minute calcareous skeletal remains found in the same sample fraction and considered to be organic, are termed nannoliths. However, these skeletal remains are of uncertain biological origin.

Present day coccolithophores live in the top 200m of the marine water column and play an important role in the food chain. After death, either by natural causes or digestion by predators, individual coccoliths separate from the coccolithosphere or form part of a faecal pellet respectively, and sink to the sea floor. These skeletal remains along with nannoliths become part of the sedimentary record, to provide a high resolution biostratigraphy for many pelagic deposits of Jurassic to Holocene in age, which is reviewed in Young *et al.* (1994).

The biology of calcareous nannoplankton is extensively covered in Haq (1978) and most recently in Siesser (1993).

3.2 History of Research

In 1836 the German biologist, C. G. Ehrenberg made the first reference to nannofossils after observing very small flat circular and elliptical discs, in the chalks from the Island of Rügen in the Baltic Sea. He figured discoasters and coccoliths, but termed them 'Kalkerigie crystalldrusen' and 'Morpholite' respectively and considered them to be inorganic. It was not until 1858 when the term 'coccolith' was proposed by T. M. Huxley after reporting the presence of Ehrenberg type crystalliods in deep sea oozes and also like Ehrenberg considered them to be inorganic. G. C. Wallich and H. C. Sorby came to the same conclusion independently in 1861, that the calcareous nannofossils were parts of larger spherical objects, to which the former termed them as coccospheres. Through a series of short papers between 1863 and 1877, Wallich clarified the true nature of the coccospheres and in 1865 reported the discovery of living coccospheres.

In the latter part of the 19th century, J. Murray and A. F. Renard carried out research on deep sea sediments collected during the H.M.S. Challenger expedition. It resulted in the publication of their report in 1891, which was the first reported attempt to understand life in the oceanic realm. In the early part of this century, the importance of calcareous nannoplankton as a primary link in the marine food chain was realised. It provided the impetus for pioneers such as H. Lohmann, J. Schiller, F. Bernard, G. Deflandre and E. Kamptner to publish extensively on the biological, structural and stratigraphical nature of nannoplankton in general.

3.3 Systematic Palaeontology

3.3.1 Construction

Based on their calcite element construction, calcareous nannofossils are subdivided into two groups, holococcoliths and heterococcoliths. Holococcoliths comprise calcite elements of identical shape and size, whilst in heterococcoliths the calcite elements are of differing shapes and sizes.

3.3.2 Classification and definitions

Calcareous nannofossils are classified according to the International Code of Botanical Nomenclature (ICBN). However, there is no general agreement on the higher levels of classification relating to calcareous nannofossils, particularly the extinct group, the nannoliths, which is reviewed in Green and Jordan (1994). Consequently the thesis

follows many authors (e.g. Bukry, 1969; Thierstein, 1973; Perch-Nielsen, 1985a,b etc.) in arranging families (defined in Appendix B) and taxa in alphabetical order. Therefore the classification philosophy followed in this thesis, will follow the morphological definitions provided by Bown (1987, p12), expanded herein to include nannoliths (see below). The philosophy allows all species of calcareous nannofossils observed during the project to be classified based on easily recognisable morphological characters.

Definitions

Family	Coccoliths	Generalised overall morphology of the rim, including the general organisation and width of the elements that make up the rim, plus the nature of the central area.
	Nannoliths	Generalised overall morphology of shape. NB. Many nannolith families are monogeneric.
Genus	Coccoliths	Detailed rim features and general central area structures.
	Nannoliths	General organisation of elements within the shape.
Species	Coccoliths	Detailed central area structures.
	Nannoliths	Detailed organisation of elements or distinguishing features.

Systematic descriptions follow the format required by the Journal of Micropalaeontology and are split stratigraphically into three separate sections, and form parts of chapters 4, 5 and 6. The plates and their descriptions relating to the systematics, are located to the rear of their respective chapters. These chapters relate to the age of the sediments under investigation, Late Cretaceous, Palaeogene and Neogene.

3.3.3 Biostratigraphical zonal schemes

Until 1954 the usefulness of calcareous nannofossils as a biostratigraphical tool was poorly known, until M. N. Bramlette and W. R. Riedel noted the distinctiveness of Mesozoic and Tertiary assemblages and suggested they might be useful as biostratigraphical indicators for the world-wide correlation of pelagic sediments. By the late 1960's the vertical ranges for species of fossil nannoflora from the Tertiary had reached the stage were biostratigraphical zonations could be erected.

The history of development for biostratigraphical zonal schemes for the Mesozoic and Cenozoic, with respect to calcareous nannofossils, is extensively covered in Perch-Nielsen (1985a,b).

Currently the world-wide zonal scheme erected to subdivide the Jurassic, is still poorly established, with no world-wide subdivision for the pre-Jurassic. The world-wide zonal subdivision for the Cretaceous is well established, especially for the Late Cretaceous, whereas, the Early Cretaceous subdivisions within the zonal schemes have in the main, larger time spans. The reason for the differences between the Jurassic and Cretaceous is that more zonal schemes have been erected for the Cretaceous. This is largely due to the globally widespread Cretaceous marine deposits, both on the continents and in the oceans, and in part to the greater abundance and diversity of calcareous nannofossils during the Cretaceous, and therefore greater potential for a more refined subdivision of the Cretaceous. Cenozoic zonal schemes are even more refined than those of the Cretaceous for the same reasons. The erection of calcareous nannofossil biostratigraphical zonal schemes, usually use first occurrences of the species, which in the main, should be abundant, cosmopolitan and solution-resistant, to subdivide the scheme accurately. This is because first occurrences (FO's) will be more accurate than last occurrences (LO's) for defining zonal boundaries, since LO's can be distorted by reworking. However, biostratigraphers working with borehole material use LO's, because of the problems with downhole contamination (Perch-Nielsen, 1985a,b; Siesser, 1993).

The thesis employs the biostratigraphical zonal scheme erected by Sissingh (1977), with the modifications and refinement by Perch-Nielsen (1979, 1983; Fig. 3.1). The zonal scheme proposed for the Late Cretaceous was developed for the eastern Mediterranean and is based on range data obtained from Europe and Tunisia, areas located on the opposite margins of the Tethys Ocean. The refinements made by Perch-Nielsen (1979, 1983), were based on range data obtained from the Mediterranean and

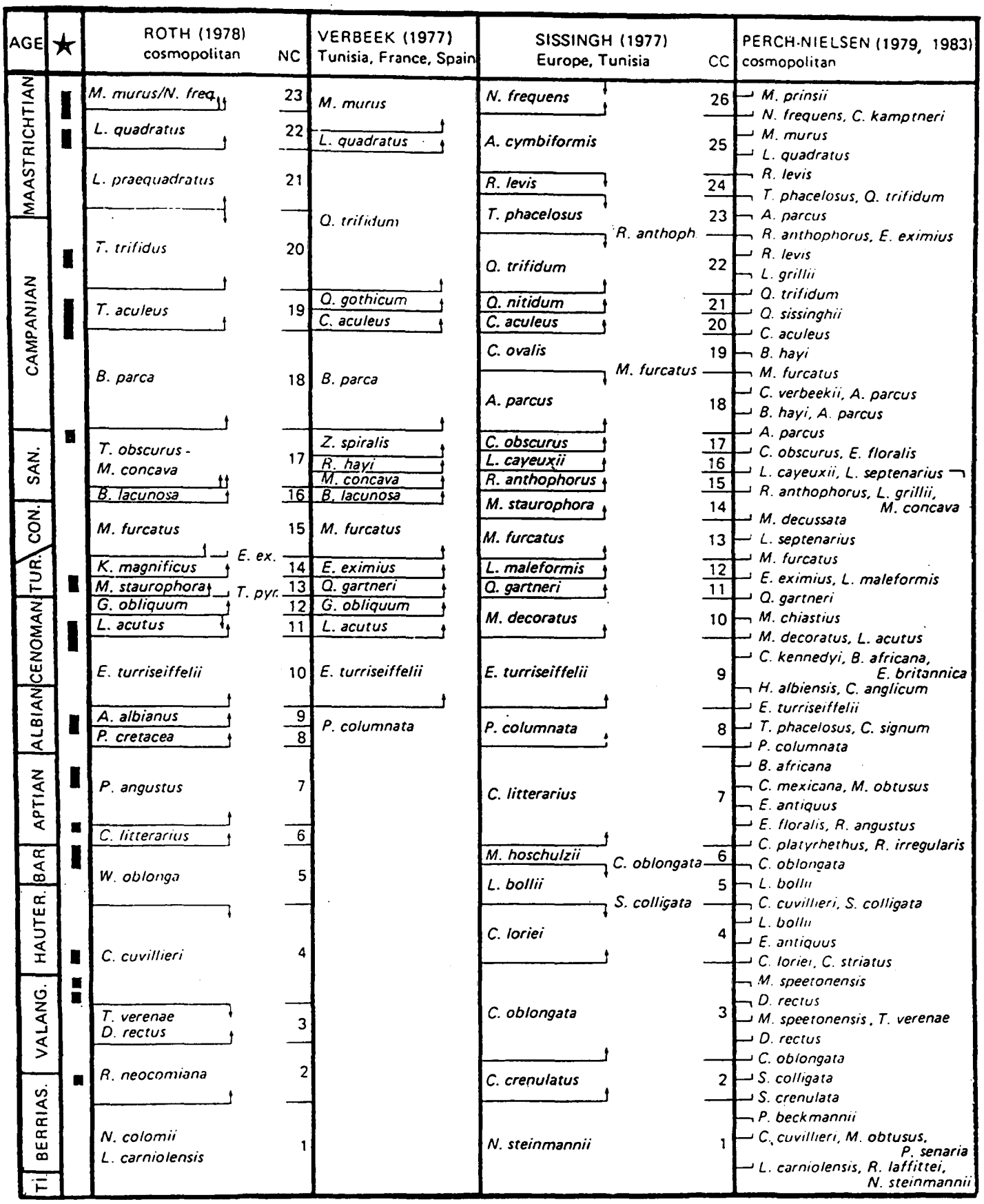

Fig. 3.1. Correlation of Cretaceous zonal schemes and their correlation with stratotypes (*) of the stages (modified from Perch-Nielsen, 1985b).

North Sea. Also the Sissingh (1977) zonal scheme has a higher resolution, especially during the Late Cretaceous, than the scheme proposed by Verbeek (1977) (Fig. 3.1) based on range data obtained from the same region (France, Spain and Tunisia) and the cosmopolitan derived scheme proposed by Roth (1978) (Fig. 3.1). The correlation of the Cretaceous biostratigraphical zonal scheme for calcareous nannofossils employed in this thesis, with palaeomagnetic data is displayed in Fig. 3.2, along with zonal schemes proposed for planktonic foraminifera and radiolaria.

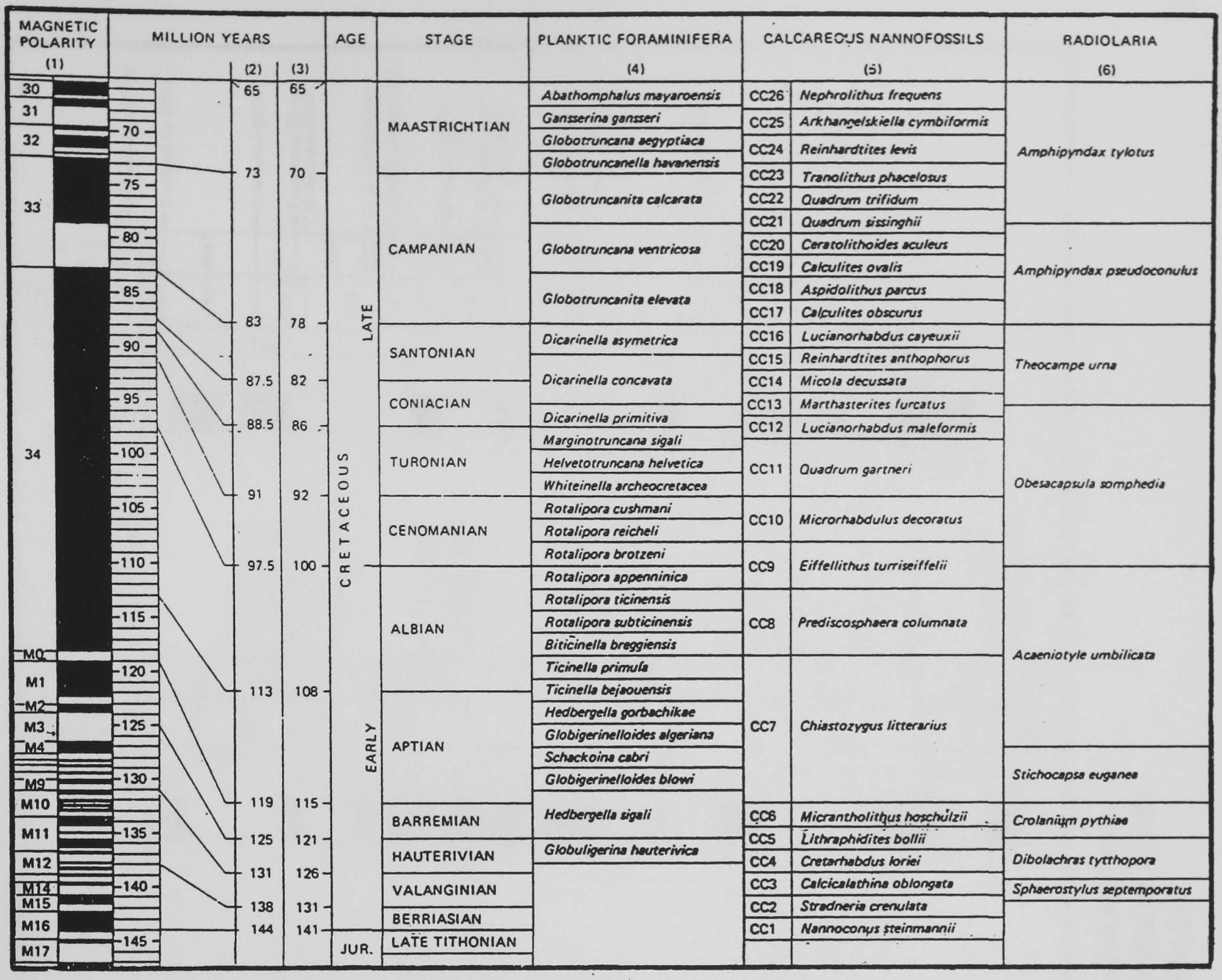

Fig. 3.2. Correlation of the biostratigraphic zonal schemes for the Late Jurassic and Cretaceous, relating to planktonic foraminifera, calcareous nannofossils and radiolaria (modified from Bolli *et al.*, 1985). 1. Harland *et al.*, 1982 (black = normal, white = reverse); 2. Harland *et al.*, 1982; 3. van Hinte, 1976; 4. Caron, 1985; 5. Sissingh, 1977; 6. Sanfilippo and Riedel, 1985.

The biostratigraphical zonal scheme proposed by Martini (1971), will be employed in the thesis for the subdivision of the Tertiary (Fig. 3.3). This is because the scheme is more suited to a restricted oceanic environment, similar to the depositional environment for the Late Cretaceous to Holocene sediments of Cyprus, rather than the zonal scheme erected by Okada and Bukry (1980) (Fig. 3.3), which is more suited to an open oceanic environment (Perch-Nielsen, 1985b). Both the zonal schemes of Martini (1971) and Okada and Bukry (1980), have been used successfully for more than a decade, for the use in correlation between globally separated areas and used locally as a framework for high resolution biostratigraphy (Perch-Nielsen, 1985b). The correlation of Tertiary biostratigraphical zonal scheme for calcareous nannofossils employed in this thesis, with palaeomagnetic data is displayed in Fig. 3.3, and with planktonic foraminifera in Fig. 3.4.

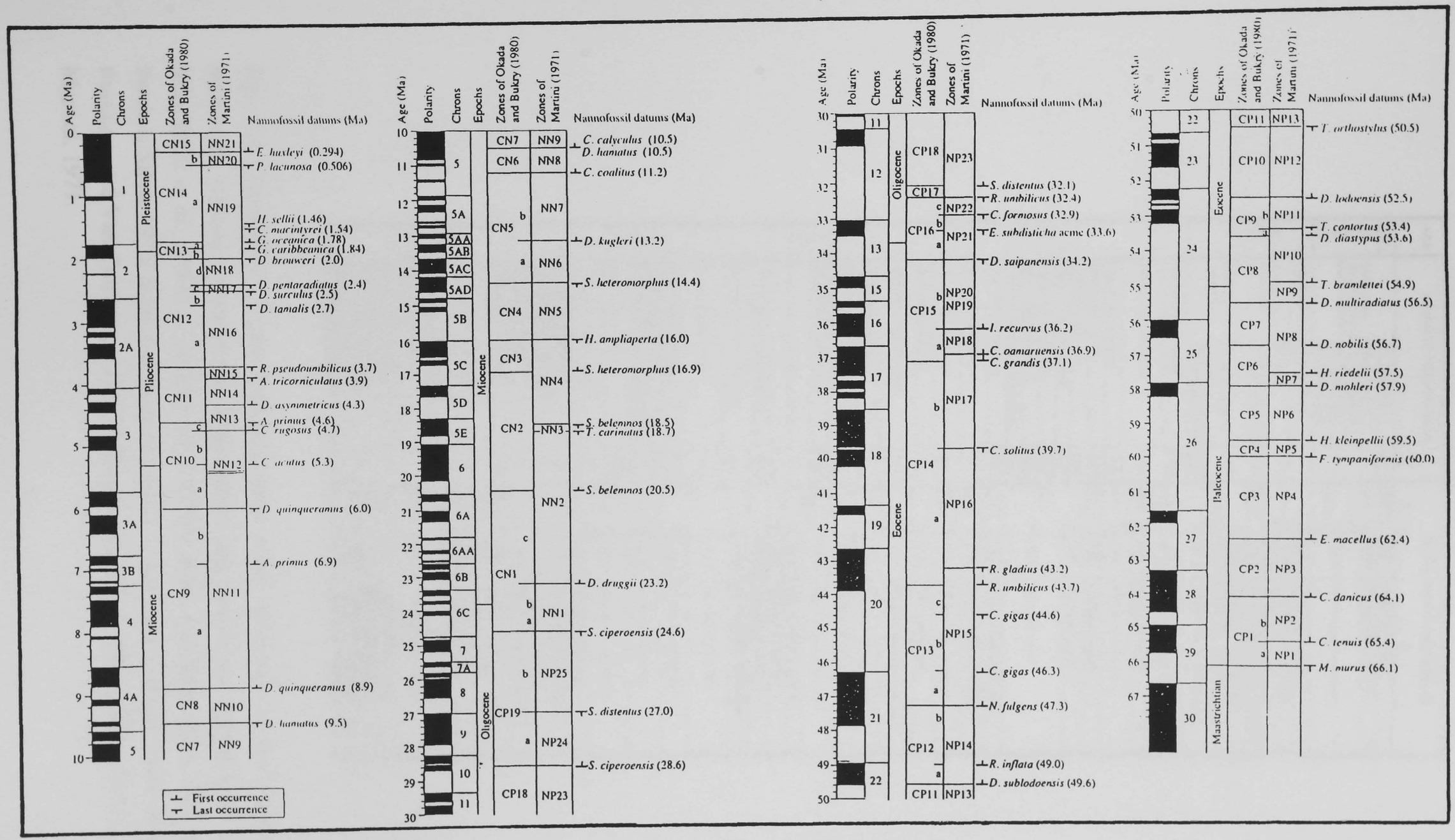

Fig. 3.3. Tertiary nannofossil magnetobiochronology and correlation of zonal schemes (after Wei and Peleo-Alampay, 1993). The magnetic polarity time scale is that of Cande and Kent (1992). The datum ages are converted from Berggren *et al.* (1985a,b).

AGE		PLANKTIC FORAMINIFERA 1		2	CALCAREOUS NANNOFOSSILS 3		4	
HOL.		*Globorotalia truncatulinoides truncatulinoides*	*Gr. fimbriata*	N23	CN15		NN21	*Emiliania huxleyi*
PLEISTOC.			*Gg. bermudezi*		CN14	b	NN20	*Gephyrocapsa oceanica*
			Gg. calida calida			a		
			Gr. crassaf. hessi	N22	CN13	b	NN19	*Pseudoemiliania lacunosa*
			Gr. crassaf. viola			a		
PLIOCENE	L	*Globorotalia tosaensis tosaensis*		N21	CN12	d	NN18	*Discoaster brouweri*
	M	*Globorotalia miocenica*	*Gr. exilis*			c	NN17	*Discoaster pentaradiatus*
						b	NN16	*Discoaster surculus*
			Gs. trilob. fistulosus	N20		a		
	E	*Globorotalia margaritae*	*Gr. marg. evoluta*	N19	CN11		NN15	*Reticulofenestra pseudoumbilica*
					CN10	c	NN14	*Discoaster asymmetricus*
							NN13	*Ceratolithus rugosus*
			Gr. marg. margaritae	N18		b	NN12	*Amaurolithus tricorniculatus*
						a		
MIOCENE	L	*Globorotalia humerosa*		N17	CN9	b	NN11	*Discoaster quinqueramus*
		Globorotalia acostaensis		N16		a		
	M	*Globorotalia menardii*		N15	CN8	b	NN10	*Discocaster calcaris*
		Globorotalia mayeri		N14		a		
		Globigerinoides ruber		N13	CN7	b	NN9	*Discoaster hamatus*
		Globorotalia fohsi robusta		N12		a		
		Globorotalia fohsi lobata		N11	CN6		NN8	*Catinaster coalitus*
		Globorotalia fohsi fohsi		N10	CN5	b	NN7	*Discoaster kugleri*
		Globorotalia fohsi peripheroronda		N9		a	NN6	*Discoaster exilis*
	E	*Praeorbulina glomerosa*		N8	CN4		NN5	*Sphenolithus heteromorph*
		Globigerinatella insueta		N7	CN3		NN4	*Helicosphaera ampliaperta*
		Catapsydrax stainforthi		N6	CN2		NN3	*Sphenolithus belemnos*
		Catapsydrax dissimilis		N5	CN1	c	NN2	*Discoaster druggii*
		Globigerinoides primordius		N4		b	NN1	*Triquetrorhabdulus carinatus*
						a		
OLIGOCENE	L	*Globorotalia kugleri*		P22	CP19	b	NP25	*Sphenolithus ciperoensis*
		Globigerina ciperoensis ciperoensis				a	NP24	*Sphenolithus distentus*
	M	*Globorotalia opima opima*		P21	CP18		NP23	*Sphenolithus predistentus*
		Globigerina ampliapertura		P19/20	CP17			
	E	*Cassig. chipolensis/Pseudohast. micra*		P18	CP16	c	NP22	*Helicosphaera reticulata*
				P17		b	NP21	*Ericsonia subdisticha*
				P16	CP15	b	NP19/20	*Isthmolithus recurvus*
EOCENE	L	*Turborotalia cerroazulensis s.l.*		P15		a	NP18	*Chiasmolithus oamaruensis*
		Globigerinatheka semiinvoluta			CP14	b	NP17	*Discoaster saipanensis*
		Truncorotaloides rohri		P14		a	NP16	*Discoaster tani nodifer*
	M	*Orbulinoides beckmanni*		P13	CP13	c	NP15	*Nannotetrina fulgens*
		Morozovella lehneri		P12		b		
		Globigerinatheka s. subconglobata		P11		a		
		Hantkenina nuttalli		P10	CP12	b	NP14	*Discoaster sublodoensis*
	E	*Acarinina pentacamerata*		P9		a		
		Morozovella aragonensis		P8	CP11		NP13	*Discoaster lodoensis*
		Morozovella formosa formosa		P7	CP10		NP12	*Tribrachiatus orthostylus*
		Morozovella subbotinae		P6	CP9	b	NP11	*Discoaster binodosus*
		Morozovella edgari				a	NP10	*Tribrachiatus contortus*
PALEOCENE		*Morozovella velascoensis*		P5	CP8	b	NP9	*Discoaster multiradiatus*
	L	*Planorotalites pseudomenardii*		P4		a		
					CP7		NP8	*Heliolithus riedelii*
					CP6		NP7	*Discoaster mohleri*
					CP5		NP6	*Heliolithus kleinpellii*
	M	*Planorotalites pusilla pusilla*		P3	CP4		NP5	*Fasciculithus tympaniformis*
		Morozovella angulata						
		Morozovella uncinata		P2	CP3		NP4	*Ellipsolithus macellus*
	E	*Morozovella trinidadensis*		P1 c	CP2		NP3	*Chiasmolithus danicus*
		Morozovella pseudobulloides		P1 b	CP1	b	NP2	*Cruciplacolithus tenuis*
		Globigerina eugubina		P1 a		a	NP1	*Markalius inversus*

Fig. 3.4. Correlation of the biostratigraphic zonal schemes for the Palaeocene to Holocene, relating to planktonic foraminifera and calcareous nannofossils (modified from Bolli *et al.*, 1985). 1. Bolli *et al.*, 1957a,b; Bolli and Bermudez, 1965; Bolli and Premoli Silva, 1973; Bolli and Saunders, 1985; 2. Banner and Blow, 1965; Blow, 1969; Berggren and Van Couvering, 1974; 3. Okada and Bukry, 1980 (Bukry, 1973c, 1975); 4. Martini, 1971.

CHAPTER 4

BIOSTRATIGRAPHY OF THE LATE CRETACEOUS (CAMPANIAN TO MAASTRICHTIAN) SEDIMENTARY COVER OF S. W. CYPRUS:

4.1 Introduction

The study reported here involves the micropalaeontological analyses (calcareous nannofossils), of 41 samples from 24 localities (Figs 4.1,2). It also forms part of an overall review of the biostratigraphy of the neo-autochthonous sedimentary cover of S.W. Cyprus and concentrates on the sedimentary melange units of the Moni (Dhrousha Melange) and Kathikas Formations and the overlying pelagic chalks of the Lefkara Formation, Lower Member (Fig. 4.3).

The aim of this study is: 1. to date the Kannaviou Formation where contact is made with the overlying neo-autochthonous sedimentary cover; 2. to date the sedimentary melange deposits of the Moni (Dhrousha Melange) and Kathikas Formations; 3. to date the base of the Lefkara Formation, Lower Member, where it makes conformable or unconformable contact with the underlying rocks.

4.2 Sampling Strategy and Localities

The sampling of the Kannaviou (KN), Kathikas (KT), Moni (MN) and Lefkara (Lower Member, LL) Formations (Figs 4.1,2), forms part of a wider biostratigraphical study on the Late Cretaceous (late Campanian) to Late Miocene sediments of S.W. Cyprus, involving 372 samples from 100 localities. Samples were collected as near as possible to the contact (conformable or unconformable) with the underlying Mamonia and Troodos basement terranes and their related fragments or sedimentary formations, apart from the Kannaviou Formation were sampling was restricted to the top, were contact is made with the overlying sediments. Also samples were collected at measured intervals at several localities (Figs 4.4,5,6).

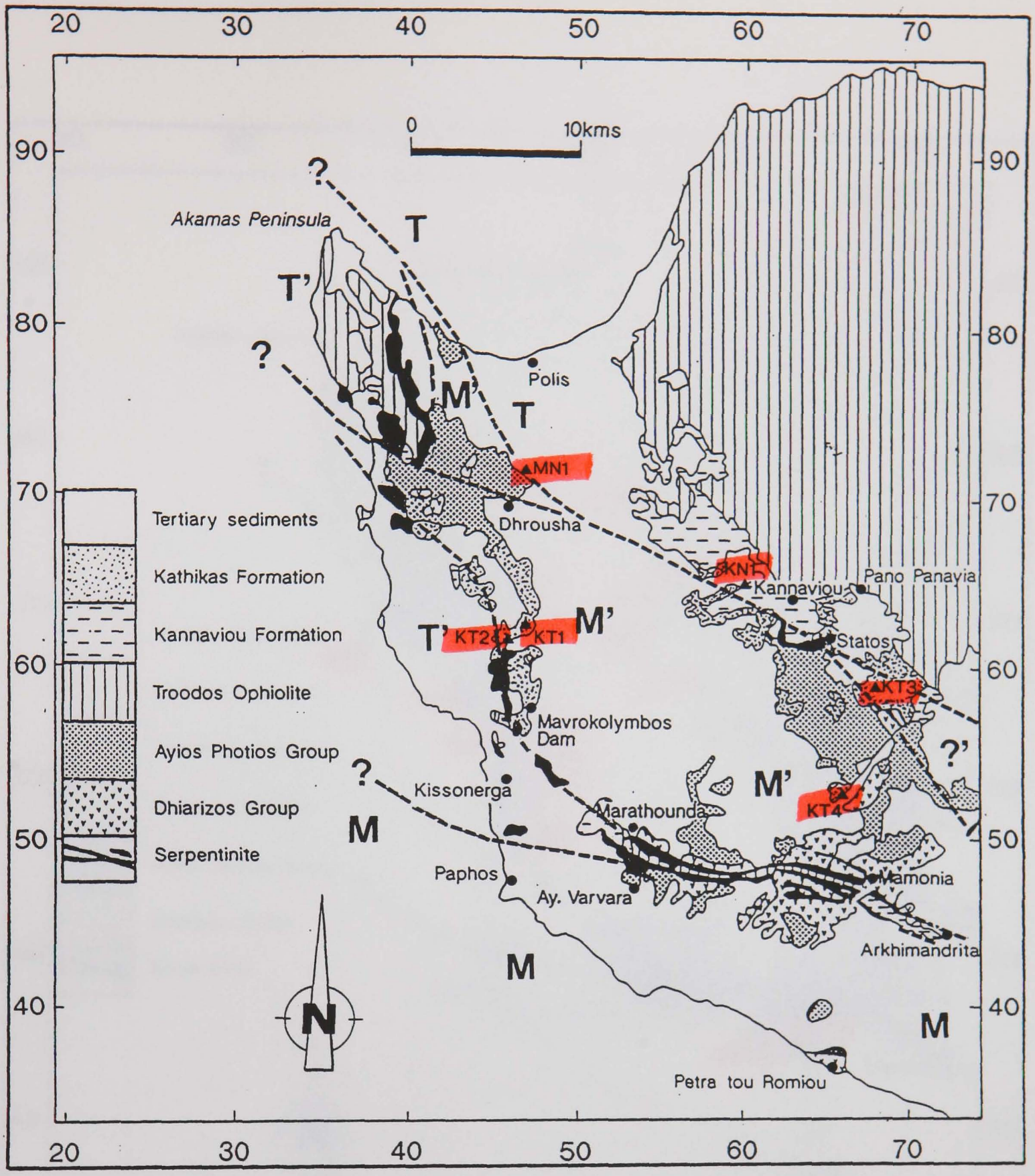

Fig. 4.1. General geological map of S.W. Cyprus, displaying the relationship between the Mamonia and Troodos (including the associated sediment, the Kannaviou Formation) basement terranes (M and T respectively), including their related terrane fragments (M', T' respectively and ?' uncertain) and the overlying Kathikas Formation and Tertiary sediments (modified from Swarbrick, 1980). Sample localities: KN = Kannaviou Formation; KT = Kathikas Formation; MN = The newly recognised Dhrousha Melange (Moni Formation).

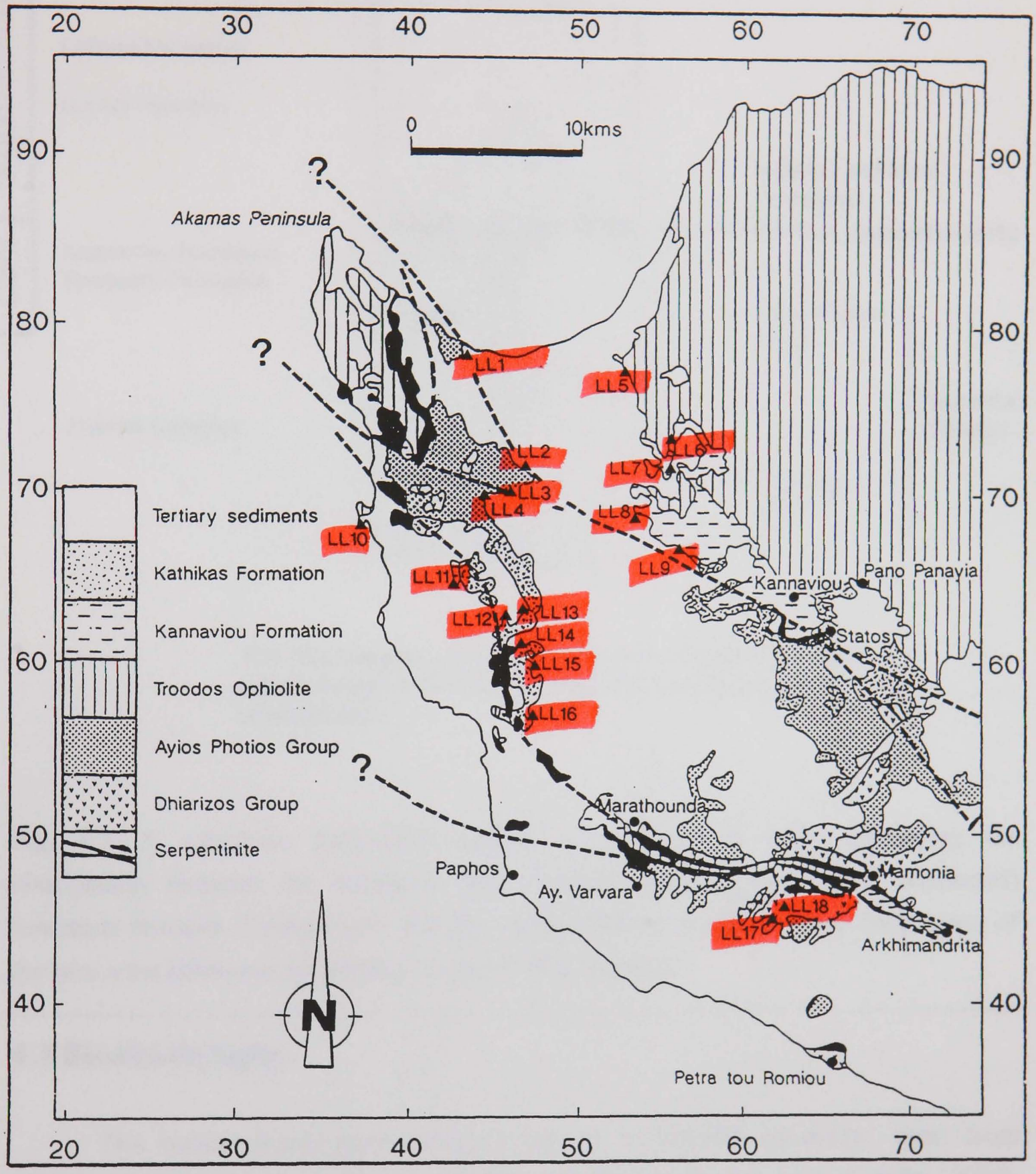

Fig. 4.2. General geological map of S.W. Cyprus, displaying the relationship between the Mamonia and Troodos basement terranes and related fragments and the sample localities (LL), associated with the outcrop of the overlying Lefkara Formation, Lower Member (modified from Swarbrick, 1980).

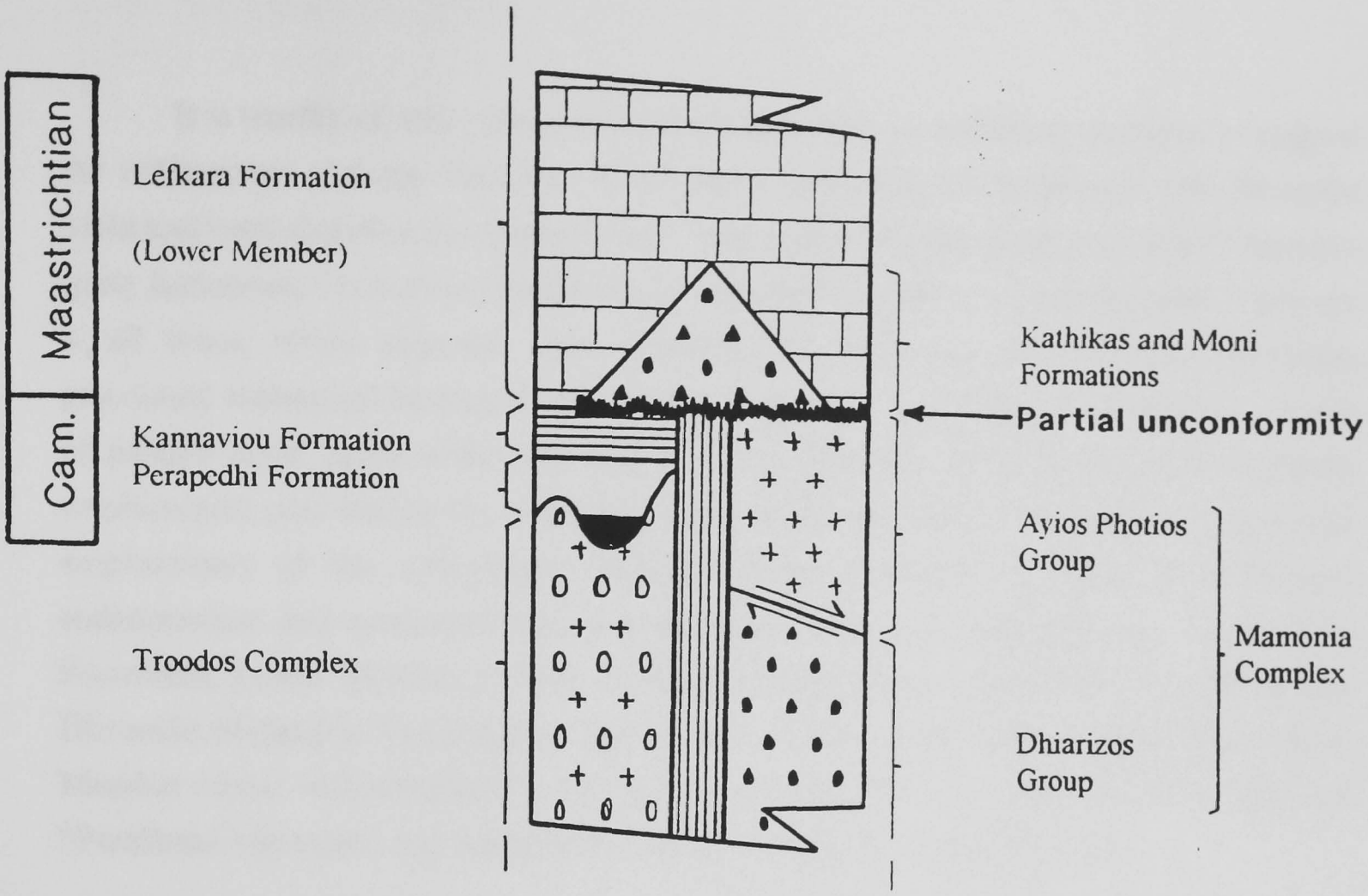

N.B. The Mamonia and Troodos Complexes are separated from one another by vertical to high angle faults containing screens of serpentinite.

Fig. 4.3. A schematic geological vertical section (not to scale) displaying the relationship between the Mamonia and Troodos (including associated sediments) basement terranes (Complexes), and the unconformably overlying basal formations of the neo-autochthonous sedimentary cover of S.W. Cyprus.

4.3 Biostratigraphy

The earlier micropalaeontological data is of limited reliability, apart from research by Urquhart and Banner (1994) and Krasheninnikov and Kaleda (1994). Therefore this study attempts to develop the application of micropalaeontology, to the Kannaviou Formation and basal formations of the neo-autochthonous sedimentary cover (Fig. 4.3) of S.W. Cyprus. The study reviews the micropalaeontological data, with respect to the biostratigraphical significance of calcareous nannofossil species observed, to confirm earlier findings and also provide new or refined age information for the formations studied. This is based on samples collected from localities (Figs 4.1,2) in S.W. Cyprus, which are discussed below.

It is worthy of note, that to date there has been no published evidence to suggest the sedimentary melange deposits of the Moni (including the Paralimini and Dhrousha Melanges) and Kathikas Formations, have been seen to be emplaced over late Campanian (post Kannaviou Formation) chalks of the Lefkara Formation, Lower Member. They are at all times, where exposed, seen overlying the Mamonia and Troodos (including associated sediments) basement terranes and fragments. Also there have been no reports of pelagic chalk clasts within the matrix of the melange units which could represent emplacement post-dating the onset of pelagic chalk deposition. Therefore the localised emplacement of the sedimentary melange units pre-date the onset of calcareous sedimentation and continued after the onset of calcareous sedimentation, the Lefkara Formation, Lower Member (pelagic chalk interbeds, seen in the Kathikas Formation and Dhrousha Melange). This suggests the lower horizons of the Lefkara Formation, Lower Member (distal sedimentation) to be coeval with the Moni (including the Dhrousha and ?Paralimini Melanges) and Kathikas Formations (proximal sedimentation).

The species distribution tables for the Kannaviou (KN), Moni (MN), Kathikas (KT) and Lefkara (Lower Member, LL) Formations (Figs 4.7,8), display the species observed within each sample, their state of preservation and overall content. The biostratigraphical ranges of individual species observed are displayed in Fig. 4.9, which have been determined from various published sources (4.5 Systematics) and are correlated with the calcareous nannofossil zonal scheme erected by Sissingh (1977). All localities are given a six figure Cyprus Grid Reference (CGR).

4.3.1 Kannaviou Formation

Though samples were collected from a number of localities throughout S.W. Cyprus, only a single locality north of Kannaviou village (Fig. 4.1, KN1), yielded a microfossil assemblage with an abundance of calcareous nannofossil species for biostratigraphical studies.

KN1 (CGR 598 650). Sample **D277**, was collected from the top of the exposure at the contact with overlying Kathikas Formation. Seventeen species were observed (Fig. 4.7), including the presence of the biostatigraphically useful of *Ellipsagelosphaera fossacincta* Black, 1971a (Bajocian to Campanian; Taylor, 1982), *Sollasites horticus* (Stradner *et al. in* Stradner and Adamiker, 1966) (Oxfordian to Campanian; Grün *in*

Grün and Allemann, 1975) and *Prediscosphaera cretacea* (Arkhangelsky, 1912) (CC18b-CC26; Perch-Nielsen, 1985a), indicating a zonal range of CC18b-CC23a (Fig. 4.9), for the assemblage.

The horizon studied, which does not contain any Maastrichtian-restricted species, is dated as Campanian. This concurs with research carried out by Urquhart and Banner (1994).

4.3.2 Moni Formation (Dhrousha Melange)

Previous research has not been able constrain the age of the Moni Formation within a biostratigraphical zonal scheme, or with any great accuracy, other than its field relationship with the under and overlying sediments. This is due to the matrix of the formation being made up entirely of derived bentonitic clay of the Kannaviou Formation, with no post Campanian-restricted micro fauna or flora being present (Urquhart and Banner, 1994). However, the Dhrousha Melange first reported here, with its type section seen north of Dhrousha, in a road cutting on the Polis road, shares similarities with the upper melange unit (Robertson, 1977c) of the Moni Formation but differs by containing pelagic chalk interbeds and calcareous nannofossils within the matrix of the derived Kannaviou Formation material, making it possible to age date the Moni Formation via this outcrop.

The samples were collected from the matrix of the melange and pelagic chalk interbeds (discussed separately, below), of the newly recognised outcrop, the Dhrousha Melange, (Fig. 4.1, MN1), and form part of a measured section (Fig. 4.4, Plate 4.1).

MN1 (CGR 455 713)

The matrix, in the main, contains a moderate to well preserved assemblage of calcareous nannofossils (Fig 4.7). Sample **D329**, contains a sparse population with three species observed (Fig. 4.7). The presence of *P. cretacea* indicates a zonal range of CC18b-CC26 (Perch-Nielsen, 1985a) for this small assemblage (Fig. 4.9). Sample **D164**, contains a common population, with eleven species observed (Fig. 4.7) The presence of *Eiffellithus gorkae* Reinhardt, 1965, indicates a more restrictive zonal range of CC23-CC26 (Perch-Nielsen, 1985a) for the assemblage (Fig. 4.9). Sample **D165**, contains a common population, with eight species observed (Fig. 4.7). The presence of *Arkhangelskiella cymbiformis* Vekshina, 1959, indicates a zonal range of CC21-CC26

(Perch-Nielsen, 1985a) for the assemblage (Fig. 4.9). Sample **D332**, contains a sparse population, with two species observed (Fig. 4.7). The presence of *Eiffellithus turriseffelii* (Deflandre *in* Deflandre and Fert, 1954), indicates a broad zonal range of CC8-CC26 (Fig. 4.9).

The chalk interbeds, contain a well preserved assemblage of calcareous nannofossils (Fig. 4.7). Sample **D167**, contains a common population, with seven species observed (Fig. 4.7). the presence of *Calculites obscurus* (Deflandre, 1959) indicates a zonal range of CC17-CC25a (Prins and Sissingh *in* Sissingh, 1977) for the assemblage (Fig. 4.9). Sample **D336**, contains a common population, with fourteen species observed (Fig. 4.7). The presence of *A. cymbiformis* (CC21-CC26; Perch-Nielsen, 1985a) and *C. obscurus* (CC17-CC25a; Prins and Sissingh *in* Sissingh, 1977) indicates a restricted zonal range of CC21-CC25a (Fig. 4.9) for the assemblage.

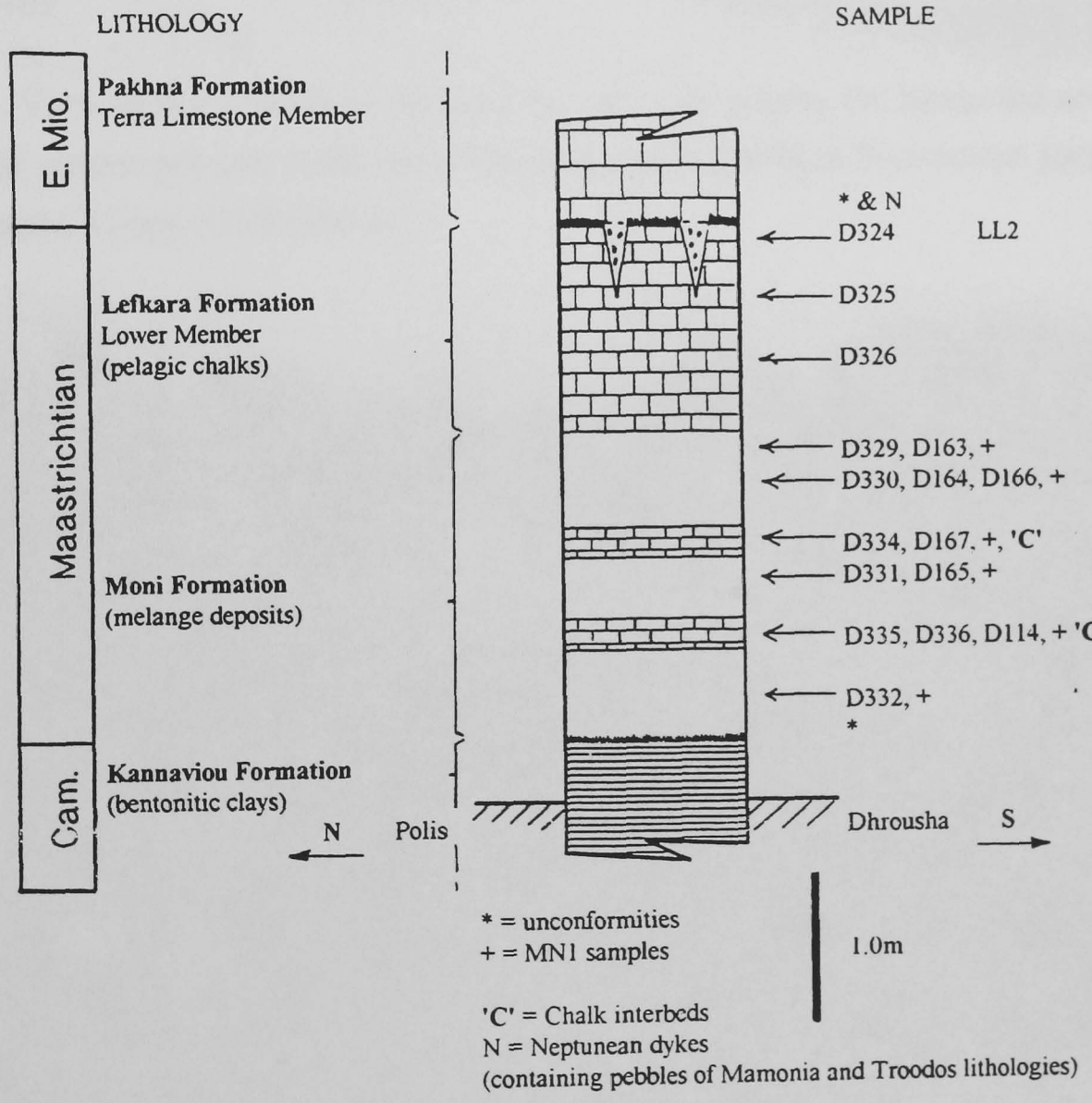

Fig. 4.4. Geological measured vertical section, containing the newly recognised Dhrousha Melange (Moni Formation, Fig. 4.1, MN1, CGR 455713), overlying unconformably the Kannaviou Formation and underlying the pelagic chalks of the Lefkara Formation, Lower Member, with its type section exposed on the east side of a new road cut, north of Dhrousha, on the Polis road.

Plate 4.1. View of the south-east facing river cliff, containing the measured section (Fig. 4.5) of the eleven pelagic chalk interbeds within the Kathikas Formation, located in the Xeropotamos valley (CGR 655 531)

Plate 4.2. View of the west facing scarp, containing the measured section (Fig. 4.4 of the newly recognised Dhrousha Melange (Moni Formation)), located 2kms north of Dhrousha in a road cut on the Polis road (CGR 455 713).

Plate 4.3. View of locality LL11 (CGR 422 641) showing the Pakhna Formation (basal Miocene) unconformably overlying the Lefkara Formation, Lower Member (late Maastrichtian), with the Kannaviou Formation (late Campanian) forming the base of the exposure.

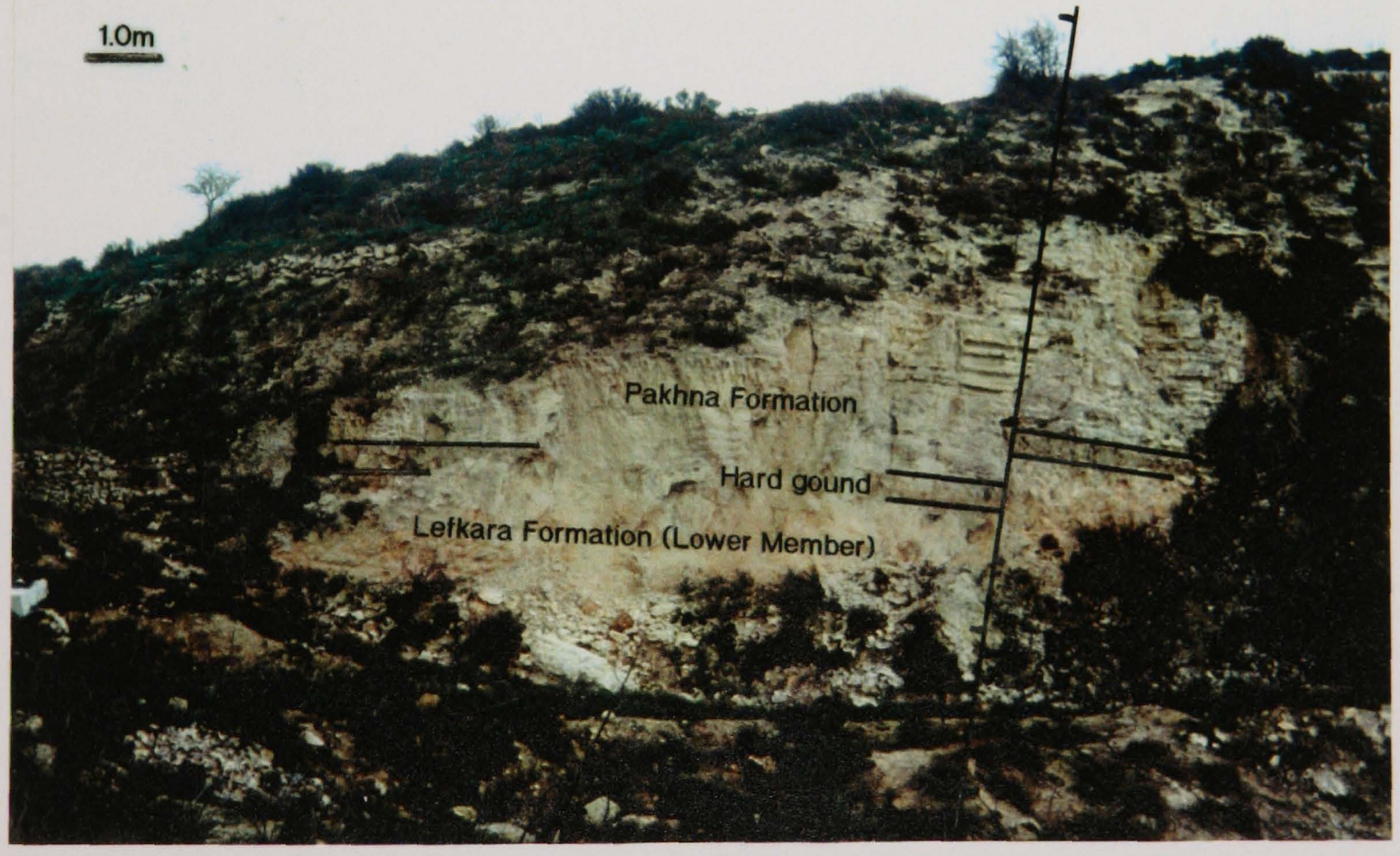

Plate 4.4. View of a west facing scarp, containing the measured section (Fig. 4.6) of the Pakhna Formation (basal Miocene) unconformably overlying the Lefkara (Lower Member) and Kathikas Formations (Maastrichtian), separated by a hard ground, located 4kms to the west of Kathikas, on the north side of the Kathikas valley (CGR 461 629).

From the samples studied above and with no late Maastrichtian-restricted species observed, the Dhrousha Melange is dated late Campanian to early Maastrichtian. This is based on the combined presence of *C. obscurus* (CC17-CC25a; Prins and Sissingh *in* Sissingh, 1977) observed in samples **D167** and **D336** (Fig. 4.7), and *E. gorkae* (CC23-CC26; Perch-Nielsen, 1985a) observed in sample **D164** (Fig. 4.7), to support an overall zonal range of CC23-CC25a (Fig. 4.9).

Discussion. Research carried out on the matrix of the Moni Formation by Urquhart and Banner (1994), recovered radiolaria specimens to suggest the matrix is the same age as the lithologically similar sediments of the underlying Kannaviou Formation, but differ by containing fragments and olistoliths of predominantly Mamonia basement terrane lithologies (Robertson, 1977c). However, the field evidence for emplacement of the Moni Formation suggest the melange post dates the Kannaviou Formation (late Campanian), with the lithologically similar sediments being reworked, and pre-dates the chalks of the Lefkara Formation, Lower Member of Maastrichtian age (Pantazis, 1967; Robertson and Woodcock, 1985). Therefore, the research carried out during this study on the calcareous nannofossil rich matrix and pelagic chalk interbeds of the recently discovered Dhrousha Melange, supports the assessment made by Robertson and Woodcock (1985), that the emplacement of the Moni Formation to be 'a brief period in the Maastrichtian'.

4.3.3 Kathikas Formation

Biostratigraphical research for the Kathikas Formation is of limited value. Early research by Swarbrick and Naylor (1980), suggested an age for the formation by its field relationships of being 'bracketed by the underlying Campanian/early Maastrichtian Kannaviou Formation (Mantis, 1970; Ealey and Knox, 1975) and the overlying Maastrichtian and Cenozoic chalk sequence'.

Samples were collected from several localities, situated in the type area south-west of Kathikas village (Fig. 4.1, KT1,2) and the Xeropotamos valley (Fig. 4.1, KT3,4), from the matrix of the melange and pelagic chalk interbeds, of the Kathikas Formation. The matrix proved to be barren of calcareous nannofossils, with the pelagic chalk interbeds each containing in the main, a moderate to well preserved assemblage of calcareous nannofossils.

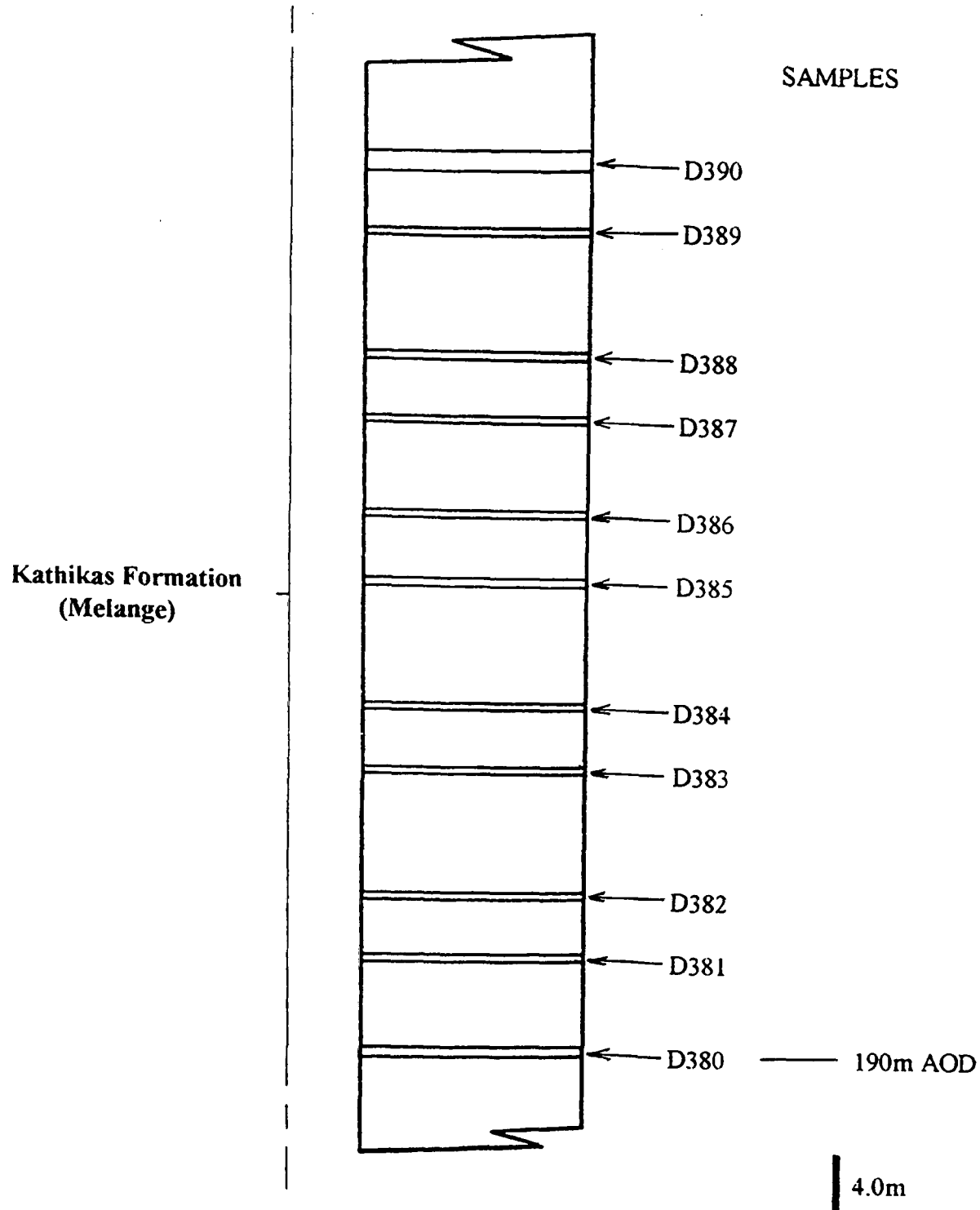

Fig. 4.5. Geological measured section, containing eleven pelagic chalk interbeds within the melange of the Kathikas Formation, located in a south-east facing river cliff in the Xeropotamos valley (CGR 655 531).

KT1 (CGR 470 627). Two samples were collected from the pelagic chalk interbeds situated west of Kathikas (Fig. 4.1). Sample **D448**, contains a sparse population, with nine species observed and sample **D449**, contains a common population, with seven species observed (Fig. 4.7). The presence of *A. cymbiformis* indicates a zonal range of CC21-CC26 (Perch-Nielsen, 1985a), for both assemblages (Fig. 4.9).

KT2 (CGR 450 610). Sample **D485**, was collected from a pelagic chalk interbed situated east of Peyia and contains an abundant population, with twelve species observed (Fig. 4.7). The presence of *Prediscosphaera grandis* Perch-Nielsen, 1979, indicates a zonal range of CC23b-CC26 (Perch-Nielsen, 1979) for the assemblage (Fig. 4.9).

KT3 (CGR 668 601). Two samples were collected from pelagic chalk interbeds situated west of Kilinia (Fig. 4.1). Sample **D379**, contains a common population, with ten species observed (Fig. 4.7), The combined presence of *C. obscurus* (CC17-CC25a; Prins and Sissingh *in* Sissingh, 1977) and *P. grandis* (CC23b-CC26; Perch-Nielsen, 1979), indicates a restricted zonal range of CC23b-CC25a for the assemblage (Fig. 4.9). Sample **D378**, contains a common population, with nine species observed (Fig. 4.7). The presence of *A. cymbiformis* indicates a zonal range of CC21-CC26 (Perch-Nielsen, 1985a) for the assemblage (Fig. 4.9).

KT4 (CGR 655 531). The samples were collected from eleven pelagic chalk interbeds, which form a measured section (Fig. 4.5, Plate 4.1), located within a south-east facing river cliff in the Xeropotamos valley (Fig. 4.1). Samples **D380** to **D390** inclusive, contain in the main, a common to abundant populations, with a poor to moderately diverse species content (Fig. 4.7). The age diagnostic species of *C. obscurus* (CC17-CC25a; Prins and Sissingh *in* Sissingh, 1977), *E. gorkae* (CC23-CC26; Perch-Nielsen, 1985a) and *P. grandis* (CC23b-CC26; Perch-Nielsen, 1979), occur in samples **D380**, **D383**, **D384** and **D386** (Fig. 4.7), indicate a restricted zonal range of CC23b-CC25a (Fig. 4.9) for the Kathikas Formation at this locality.

From the samples studied above (localities KT1-KT4) and with no late Maastrichtian-restricted species observed, the Kathikas Formation is dated early Maastrichtian. This is based on the combined presence of the biostratigraphically useful species of *C. obscurus* (CC17-CC25a; Prins and Sissingh *in* Sissingh, 1977) observed in samples **D379**, **D380** and **D384** (Fig. 4.7), *E. gorkae* (CC23-CC26; Perch-Nielsen, 1985a) observed in samples **D383**, **D387**, **D389** and **D485** (Fig. 4.7) and *P. grandis* (CC23b-CC26; Perch-Nielsen, 1979) observed in samples **D379**, **D386** and **D485** (Fig. 4.7), to support an overall zonal range of CC23b-CC25a (Fig. 4.9).

Discussion. Research by Urquhart and Banner (1994), found the matrix of the Kathikas Formation to be poorly microfossiliferous and offered an unpublished report, University College London (1992), based on biostratigraphical research carried out on three Pelagic chalk interbeds, located west of Kathikas village in the Kathikas valley, to age date the Kathikas Formation as CC25-CC26, suggesting the formation was emplaced entirely within the mid to late Maastrichtian. By contrast the data reported here is based on the analyses of sixteen pelagic chalk interbeds and age dated the Kathikas Formation to be CC23b-CC25a, suggesting the formation was emplaced during the early to mid Maastrichtian. The combined evidence from this study and the

UCL report, suggests the emplacement for the Kathikas Formation took place during most of the Maastrichtian, terminating with the deposition of the upper horizons of the Lefkara Formation, Lower Member pelagic chalks.

4.3.4 Lefkara Formation (Lower Member)

To date there has been little published biostratigraphical research relating to the Lefkara Formation, Lower Member, and is of limited value, apart from research carried out by Krasheninnikov and Kaleda (1994), on the Late Cretaceous (Campanian) to Pliocene sediments of the Perapedhi section, situated north of Limassol against the south western margin of the Troodos Massif. The age for the base of the Lefkara Formation, Lower Member is important, as it marks the start of calcareous sedimentation overlying the Kathikas Formation and represents the end of the juxtapositioning event between the Mamonia and Troodos basement terranes.

Throughout Cyprus, the Lefkara Formation, Lower Member terminates at an unconformity, apart from the Perapedhi section and the southern outcrop (A. G. Davis *in* Wilson, 1959; Mantis *in* Pantazis, 1967; Krasheninnikov and Kaleda, 1994), where the sedimentary succession appears to continue without break, at the Cretaceous/Tertiary boundary. However, Krasheninnikov and Kaleda (1994) during their biostratigraphical study of the Perapedhi section, noted the basal layers of the Danian stage could be missing, and suggested this could be down to sparse sampling during their study. Like other outcrops, this could represent an unconformity.

The pelagic chalk samples of the Lefkara Formation, Lower Member of S.W. Cyprus, were collected from 18 localities, located as near as possible to the contact with the underlying basement and formations. These samples contain in the main (Fig. 4.8), moderate to well preserved assemblages of calcareous nannofossils (Fig. 4.8), and have been assigned to three distinctive geographical areas: The northern area (Figs 4.2, LL1-LL9) is associated with the Polis graben and lineament trending north-west to south-east, separating the Mamonia basement fragments from the Troodos basement terrane. The western area (Figs 4.2, LL10-LL16) is associated with the lineament arcing in a clockwise direction north-east of Paphos, separating the Mamonia and Troodos southern basement fragments. The southern area (Figs 4.2, LL17,18) is not associated with any major lineaments and overlies the Mamonia basement terrane. The latter two areas have a regional dip towards the west, whereas the former is seen as isolated outcrops with no overall measurable dip.

The following summaries give the Locality number (LL), Cyprus Grid Reference (CGR), Sample number (D), underlying formation or basement and zonal range (CC) which is discussed below, in biostratigraphical order.

Northern area

LL1 (CGR 422 782), **D312**, Mamonia basement, CC21-CC26.
LL2 (CGR 455 713), **D324**, Moni Formation CC23-CC26
(forms part of a measured section, Fig. 4.4, Plate 4.2).
LL3 (CGR 451 696), **D116**, Mamonia basement, CC23-CC25a.
LL4 (CGR 438 695), **D117**, Mamonia basement, CC23b.
LL5 (CGR 528 760), **D254**, Troodos basement, CC26.
LL6 (CGR 550 740), **D261**, Kannaviou Formation, CC23-CC26.
LL7 (CGR 545 718), **D215**, Kannaviou Formation, CC23-CC26.
LL8 (CGR 536 678), **D531**, Kannaviou Formation, CC21-CC26.
LL9 (CGR 546 670), **D272**, Kathikas Formation, CC21-CC26.

Western area

LL10 (CGR 368 677), **D538**, Kathikas Formation, CC17-CC26.
LL11 (CGR 422 641), **D125**, Kannaviou Formation, CC26 (Plate 4.3).
LL12 (CGR 461 629), **D197**, Kathikas Formation, CC26
(forms part of a measured section, Fig. 4.6, Plate 4.4).
LL13 (CGR 462 629), **D437**, Kathikas Formation, CC21-CC26.
LL14 (CGR 461 609) **D482**, Kathikas Formation, CC21-CC26.
LL15 (CGR 468 601), **D207**, Kathikas Formation, CC12-CC26.
LL16 (CGR 457 563), **D486**, Kathikas Formation, CC21-CC26.

Southern area

LL17 (CGR 617 455), **D520**, ?bentonitic clay/?Mamonia, CC18b-CC25a.
LL18 (CGR 630 458), **D248**, Mamonia basement, Late Cretaceous.

Sample **D248 (LL18),** contains a sparse population, with a low diverse species content (Fig. 4.8). The presence of *Placozygus fibuliformis* (Reinhardt, 1964), indicates a broad zonal range of CC8-CC26 (Perch-Nielsen, 1985a) for the assemblage (Fig.4.9).

Sample **D207 (LL15),** contains a sparse population, with a low diverse species content (Fig. 4.8). The presence of *Micula staurophora* (Gardet, 1955), indicates a broad zonal range of CC12-CC26 (Stradner, 1963) for the assemblage (Fig.4.9).

Sample **D538 (LL10),** contains a sparse population, with a low diverse species content (Fig. 4.8). The presence of *Cribrosphaerella ehrenbergii* (Arkhangelsky, 1912), indicates a broad zonal range of CC17-CC26 (Stradner, 1963) for the assemblage (Fig.4.9).

Sample **D520 (LL17),** contains a sparse population, with a moderately diverse species content (Fig. 4.8). The combined presence of *C. obscurus* (CC17-CC25a; Prins and Sissingh *in* Sissingh, 1977) and *P. cretacea* (CC18b-CC26; Perch-Nielsen, 1985a), indicates a zonal range of CC18b-CC25a, for the assemblage (Fig.4.9).

Samples **D215 (LL7), D272 (LL9), D312 (LL1), D437 (LL13), D482(LL14) D486 (LL16)** and **D531 (LL8),** contain in the main, sparse to common populations, with a moderately diverse species content (Fig. 4.8). The presence of *A. cymbiformis,* indicates a zonal range of CC21-CC26 (Perch-Nielsen, 1985a), for the assemblages (Fig. 4.9).

Sample **D116 (LL3),** contains a common population, with a moderately diverse species content (Fig. 4.8). The combined presence of *C. obscurus* (CC17-CC25a; Prins and Sissingh *in* Sissingh, 1977) and *E. gorkae* (CC23-CC26; Perch-Nielsen, 1985a), indicates a restricted zonal range of CC23-CC25a, for the assemblage (Fig.4.9).

Samples **D261 (LL6)** and **D324 (LL2),** contain a sparse and abundant population respectively, both with a moderately diverse species content (Fig. 4.8). The presence of *E. gorkae*, indicates a zonal range of CC23-CC26 (Perch-Nielsen, 1985a), for the assemblages (Fig.4.9).

Sample **D117 (LL4),** contains an abundant population, with a moderately diverse species content (Fig. 4.8). The combined presence of *Vagalapillia compacta* Bukry, 1969 (Santonian to Campanian and rare in the Masstrichtian; Bukry, 1969) and *P. grandis* (CC23b-CC26; Perch-Nielsen, 1979), indicates a restricted zonal range of CC23b (Campanian-Maastrichtian boundary), for the assemblage (Fig.4.9).

Samples **D125 (LL11), D197 (LL12)** and **D254 (LL5),** contain a sparse to common population, with a moderately diverse species content (Fig. 4.8). The presence of either species of *Micula mura* (Martini, 1961) (CC26; Perch-Nielsen, 1985a) or *Micula swastica* Stradner and Steinmetz, 1984 (CC26; Stradner and Steinmetz, 1984), indicates a restricted zonal range of CC26, for the assemblages (Fig.4.9).

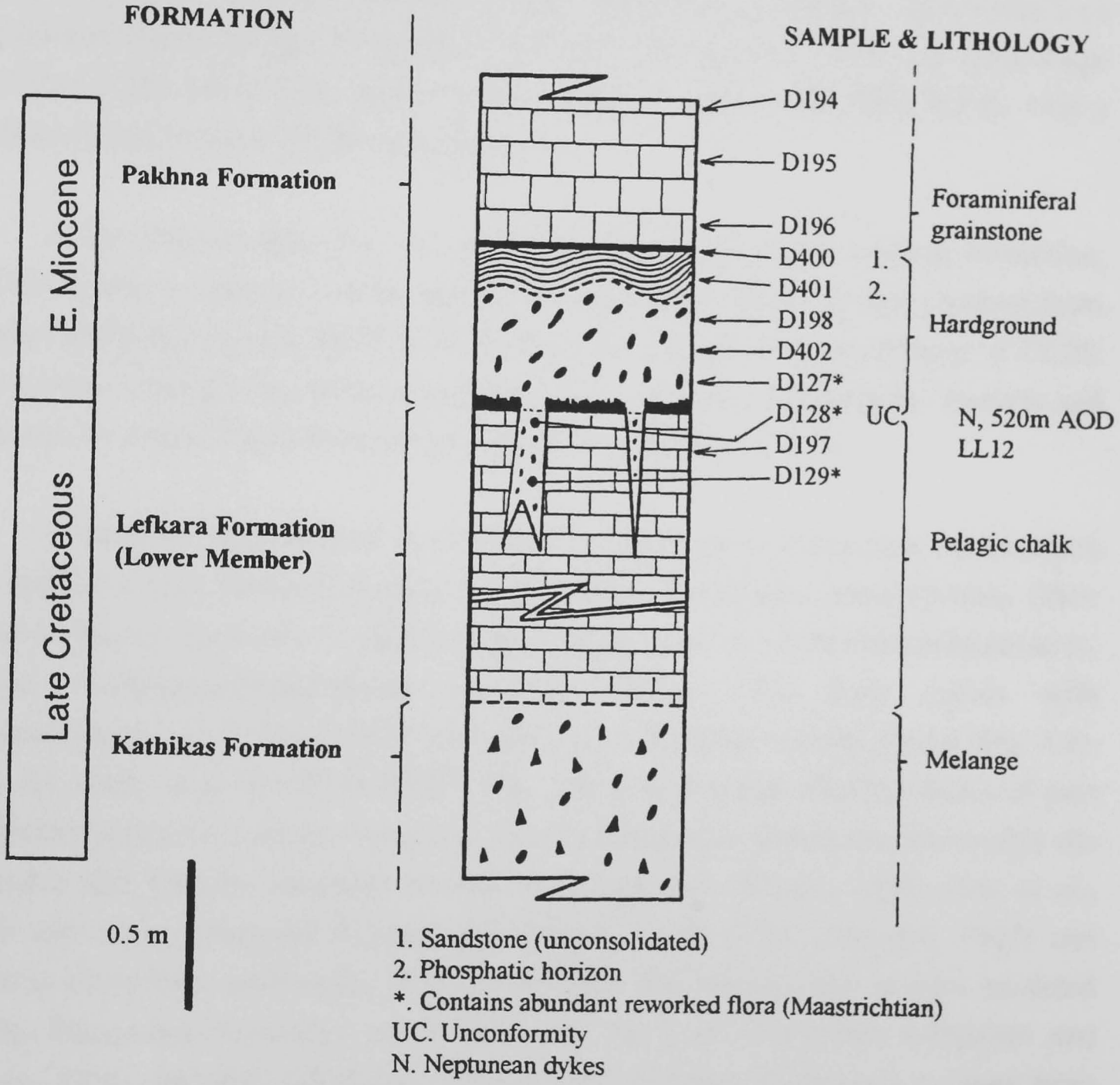

Fig. 4.6. Geological measured vertical section, containing the Pakhna Formation (basal Miocene), unconformably overlying the Lefkara (Lower Member) and Kathikas Formations (Maastrichtian), separated by a hard ground, located in a west facing scarp, 4kms west of Kathikas, on the north side of the Kathikas valley (CGR 461 629).

The data obtained from sample **D117 (LL4),** with a restricted zonal range of CC23b (Campanian-Maastrichtian boundary) and samples **D125 (LL11), D197 (LL12)** and **D254 (LL5),** with a restricted zonal range of CC26, suggest the Lefkara Formation, Lower Member was continuously deposited throughout the entire Maastrichtian.

In the northern area (Fig. 4.2, LL1-LL9), there is a biostratigraphical zonal range pattern for the Lefkara Formation, Lower Member, to suggest the basal horizon is diachronous from west to east, overstepping both Mamonia basement fragments and Troodos Basement terrane, including the separating major lineament. This is based on data obtained from samples **D116 (LL3)** and **D117 (LL4)**, with a restricted zonal range of CC23-CC25a and CC23b respectively in the west, and sample **D254 (LL5)**, with a restrictive zonal range of CC26 in the east.

In the western area (Fig. 4.2, LL10-LL16), the age of the Lefkara Formation, Lower Member at contact with the underlying basement, is based on data obtained from samples **D125 (LL11)** and **D197 (LL12)**, which have a restricted zonal range of CC26. The outcrop oversteps the major lineament, which separates the southern Troodos and Mamonia basement fragments between Lara (LL10) and Tala (LL16).

Discussion. Krasheninnikov and Kaleda (1994), recovered benthic foraminifera and radiolaria from the basal horizon of the Lefkara Formation, Lower Member (their Lower Lefkara Formation), to suggest a date for the onset of calcareous sedimentation, at the Campanian-Maastrichtian boundary (CC23). This study agrees with Krasheninnikov and Kaleda (1994), with data from a localised outcrop at LL4 (Fig. 4.2), were the zonal range of CC23b (**D117,** Fig. 4.8) was obtained. Field evidence of past researchers noted the Lefkara Formation, Lower Member to overlie unconformably the Mamonia and Troodos basement terranes and fragments (Wilson, 1959; Gass *et al.*, 1994) and conformably the Kannaviou (Pantazis, 1967), Moni (Pantazis, 1967) and Kathikas (Swarbrick and Naylor, 1980) Formations. The conformable contacts are dated for the Kannaviou Formation, as no later than the latest Campanian (Urquhart and Banner, 1994), the Moni (Dhrousha Melange) and Kathikas Formations to range from the latest Campanian to early Maastrichtian (this study). The data obtained during this study suggests the deposition of the Lefkara Formation, Lower Member, to be continuous from its onset at the Campanian-Maastrichtian boundary, post-dating the onset of the emplacement of the Moni and Kathikas Formations and to continue distally during proximal emplacement of the Moni and Kathikas Formations, through to the Cretaceous-Tertiary boundary. This is supported by the presence of Lefkara Formation, Lower Member pelagic chalks seen as interbeds within the Moni (Dhrousha Melange) and Kathikas Formations.

LOCALITY	SAMPLE	PRESERVATION	NANNOFOSSIL CONTENT	*Ellipsagelosphaera fossacincta*	*Sollasites horticus*	*Watznaueria barnesae*	*Biscutum constans*	*Discorhadus ignotus*	*Lithraphidites carniolensis*	*Stradneria crenulata*	*Glaukolithus compactus*	*Vekshinella stradneri*	*Placozygus fibuliformis*	*Corollithion signum*	*Eiffellithus turriseiffelii*	*Microrhabdulus decoratus*	*Cribrosphaerella ehrenbergii*	*Quadrum gartneri*	*Eiffellithus eximius*	*Micula staurophora*	*Micula decussata*	*Calculites obscurus*	*Lithraphidites praequadratus*	*Microrhabdulus attenuatus*	*Retecapsa neocomiana*	*Prediscosphaera cretacea*	*Arkhangelskiella cymbiformis*	*Eiffellithus gorkae*	*Prediscosphaera grandis*
KT1	D448	M	S			x				x			x		x	x	x			x						x	x		
	D449	G	C			x		x								x	x							x		x	x		
KT2	D485	G	A			x			x	x			x			x	x			x	x					x	x	x	x
KT3	D379	G	C			x				x			x			x	x			x		x				x	x		x
	D378	G	C			x			x	x						x	x			x				x		x	x		
KT4	D390	P	S			x			x							x	x						x			x			
.	D389	G	A			x			x	x			x		x	x	x				x			x		x	x	x	
	D388	M	A			x				x			x			x	x				x					x	x		
	D387	G	A			x			x	x			x			x	x				x		x	x		x	x	x	
	D386	G	A			x			x	x			x			x	x						x			x	x		x
	D385	P	S			x							x			x	x				x					x	x		
	D384	P	S			x				x			x		x	x	x				x	x	x			x			
	D383	M	C			x				x			x			x	x				x					x		x	
	D382	P	S			x				x			x			x	x										x		
	D381	M	C			x			x	x			x			x	x							x					
	D380	M	C			x				x			x		x	x	x			x		x				x	x		x
MN1	D329	P	S			x				x																x			
	D164	G	C			x			x	x			x		x	x	x				x			x				x	x
	D167	G	C			x			x	x						x	x				x	x							
	D165	G	C			x										x	x				x		x		x	x	x		
	D336	G	C			x			x	x	x		x			x	x			x	x	x	x	x		x	x		
	D332	M	S			x									x														
KN1	D277	G	A	x	x	x	x	x	x		x	x	x	x		x	x	x	x					x	x	x			

Preservation of calcareous nannofossils.
G = GOOD (little or no alteration).
M = MODERATE (50% showing some form of alteration).
P = POOR (all showing some form of alteration).

Calcareous nannofossil content (field of view = 390μm).
A = ABUNDANT (>5 individuals per field of view).
C = COMMON (<5 individuals per field of view).
S = SPARSE (isolated occurrences).

LOCALITY (Fig. 4.1)
KT = Kathikas Formation (chalk interbeds only), the matrix of the melange unit is barren.
MN = Moni Formation, samples form part of a measured section (Fig. 4.4).
KN = Kannaviou Formation, sample taken from a calcareous rich horizon, near to the contact with the overlying Kathikas Formation

Notes
i) Kathikas and Moni Formations are coeval, in that they are both located stratigraphically between the underlying Kannaviou and overlying Lefkara Formations.

Fig. 4.7. Distribution of calcareous nannofossils observed in samples collected from the Kannaviou, Moni and Kathikas Formations of S.W. Cyprus.

LOCALITY	SAMPLE	PRESERVATION	NANNOFOSSIL CONTENT	Watznaueria barnesae	Discorhadus ignotus	Lithraphidites carniolensis	Stradneria crenulata	Glaukolithus compactus	Vekshinella stradneri	Placozygus fibuliformis	Eiffellithus turriseiffelii	Microrhabdulus decoratus	Cribrosphaerella ehrenbergii	Micula staurophora	Vagalapilla compacta	Micula decussata	Calculites obscurus	Lithraphidites praequadratus	Microrhabdulus attenuatus	Prediscosphaera cretacea	Arkhangelskiella cymbiformis	Eiffellithus gorkae	Prediscosphaera grandis	Micula mura	Micula swastica
LL1	D312	M	S	x			x				x	x	x			x				x	x				x
LL2	D324	M	A	x						x		x	x	x		x				x	x	x			
LL3	D116	G	C	x			x	x				x	x			x	x			x	x	x			
LL4	D117	G	A	x	x				x	x		x	x	x	x			x	x		x		x		
LL5	D254	M	S	x			x			x	x	x		x							x				x
LL6	D261	M	S	x			x					x		x		x					x	x			
LL7	D215	G	C	x						x		x	x			x			x	x	x				
LL8	D531	M	S	x			x			x			x			x					x				
LL9	D272	G	C	x			x			x		x	x			x				x	x				
LL10	D538	P	S	x						x			x												
LL11	D125	G	C	x			x		x	x		x	x	x					x		x			x	x
LL12	D197	M	C	x					x	x		x	x	x		x					x			x	
LL13	D437	M	S	x						x	x		x								x				
LL14	D482	M	C	x							x	x	x	x		x			x		x				
LL15	D207	P	S	x							x		x												
LL16	D486	M	A	x		x	x			x		x	x								x				
LL17	D520	M	S	x			x			x			x			x	x			x					
LL18	D248	P	S	x			x			x															

Preservation of calcareous nannofossils.
G = GOOD (little or no alteration).
M = MODERATE (50% showing some form of alteration).
P = POOR (all showing some form of alteration).

Calcareous nannofossil content (field of view = 390μm).
A = ABUNDANT (>5 individuals per field of view).
C = COMMON (<5 individuals per field of view).
S = SPARSE (isolated occurrences).

LOCALITY (Fig. 4.2)
LL = Lefkara Formation (Lower Member).

Note
i) All chalk samples were collected as near as possible to the contact with the underlying rocks.

Fig. 4.8. Distribution of calcareous nannofossils observed in samples collected from the Lefkara Formation (Lower Member), of S.W. Cyprus.

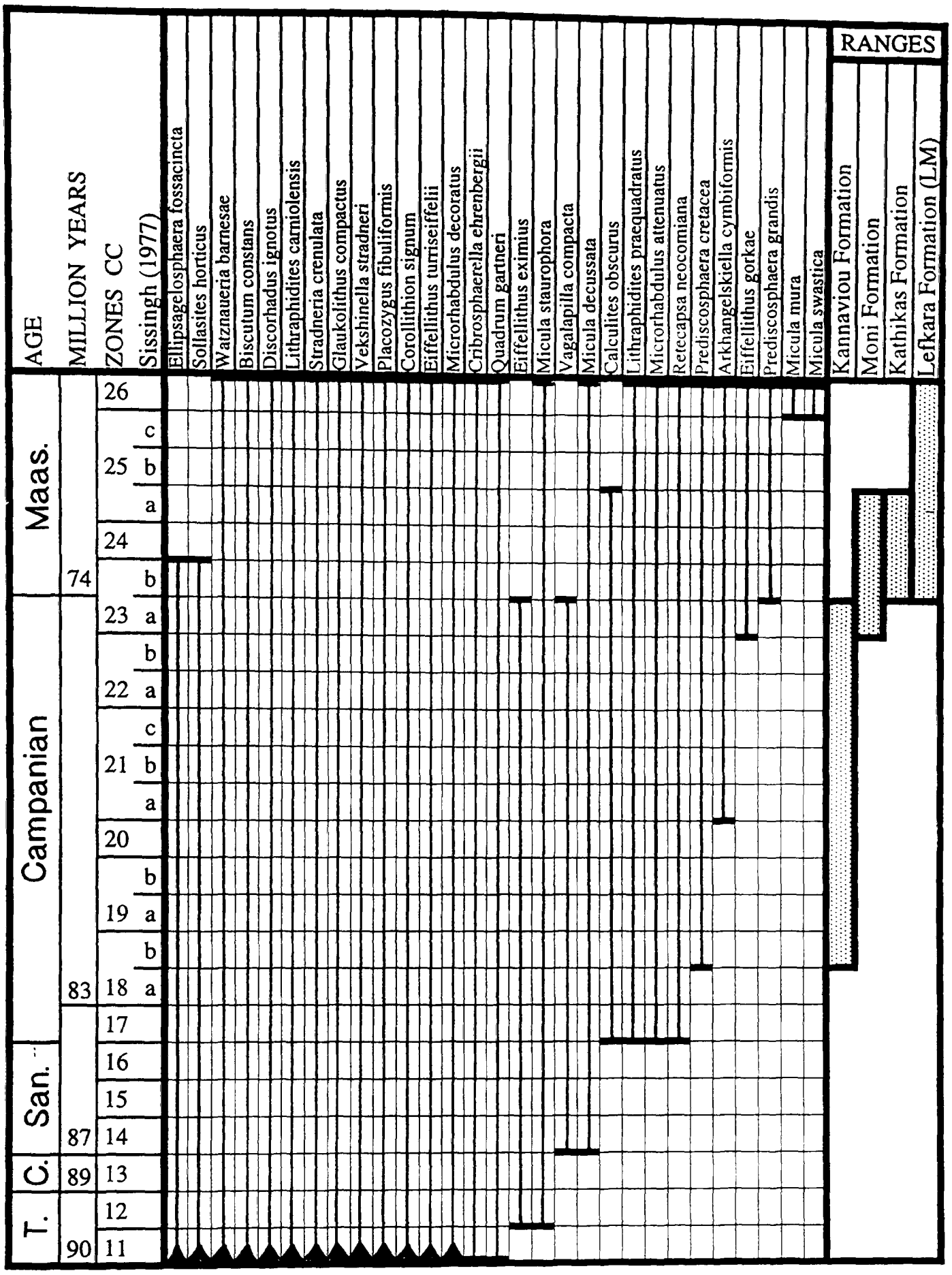

Maa. = Maastrichtian
San. = Santonian
C. = Coniacian
T. = Turonian

Notes

i) Dates have been rounded to nearest Ma (Harland et al., 1989).

ii) Ranges, see relevant text (4.3 Biostratigraphy).

iii) The biostratigraphical ranges of individual species have been determined from various published sources (4.5. Systematics).

Fig. 4.9. The ranges of calcareous nannofossil species observed in samples collected from the Upper Cretaceous rocks, and the overall ranges of the Kannaviou, Moni, Kathikas and Lefkara (Lower Member, [LM]) Formations of S.W. Cyprus.

The current outcrop pattern displayed (Fig. 4.10) for the Lefkara Formation. Lower Member, suggests the southern Mamonia basement fragment has acted as a structural high during deposition and/or post-depositional erosion. This outcrop pattern also displays similarities to the outcrop pattern of the underlying Kathikas Formation (Swarbrick, 1993).

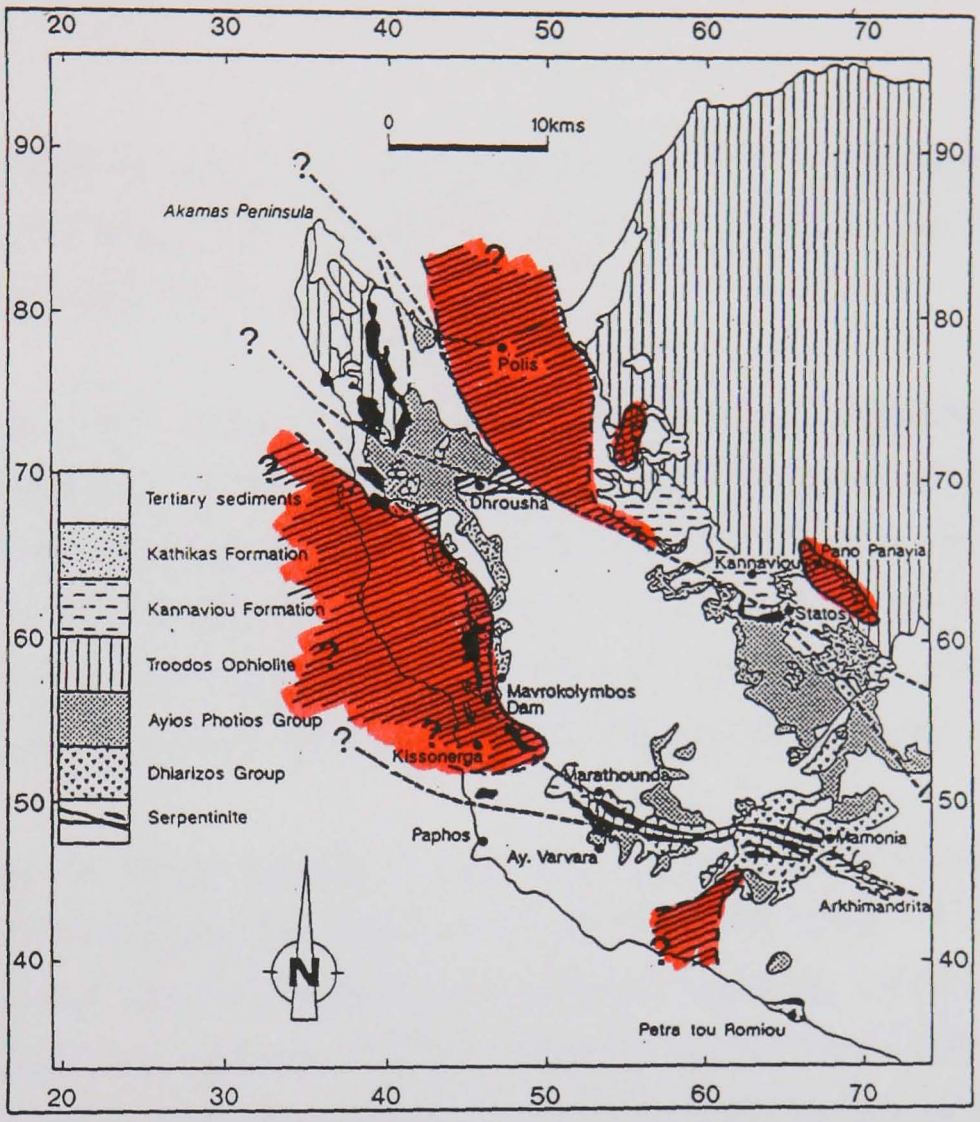

Fig. 4.10. General geological map of S.W. Cyprus, displaying the relationship between the major lineaments and the current outcrop pattern (cross-hatched) of the Lefkara Formation, Lower Member (modified from Swarbrick, 1980). N.B. Information obtained from Turner (1971), Gass *et al.* (1994) and this study.

4.4 Summary

The summary below is based on biostratigraphical data (calcareous nannofossils) obtained during this study, on the Late Cretaceous (Campanian-Maastrichtian) sedimentary cover of S.W. Cyprus.

1). The top of the Kannaviou Formation (cover to the Troodos basement terrane and fragments) making contact with the overlying sediments, has a zonal range of CC18-CC23a (Campanian).

2). The Moni Formation, based on data obtained from the Dhrousha Melange, has a restricted zonal range of CC23-CC25a (late Campanian to early Maastrichtian).

3). The Kathikas Formation, based on data obtained from 16 pelagic chalk interbeds from localities (KT1-KT4), has a zonal range of CC23b-CC25a (early Maastrichtian).

4). The basal horizon of the Lefkara Formation, Lower Member, making conformable and unconformable contact with the underlying rocks, has a zonal range of CC23b-CC26 (Maastrichtian).

5). Based on field and biostratigraphical data, the Moni (including the Paralimini and Dhrousha Melanges) and Kathikas Formations, share the same field relationships of being bracketed by the underlying Kannaviou and overlying Lefkara (Lower Member) Formations, and also similar age constraints of CC23-CC25a and CC23b- CC25a respectively, and are therefore considered to be coeval within a zonal range band (CC23-CC25a), sharing the same compressional tectonic event for emplacement.

6). Based on biostratigraphical data, the proximal Moni (Dhrousha Melange, zonal range of CC23-CC25a) and Kathikas (zonal range of CC23b- CC25a) Formations along with the lower horizons of the distal Lefkara Formation, Lower Member (zonal range of CC23b-CC26), suggest the chalk interbeds of the Moni (Dhrousha Melange) and Kathikas Formations are intercalations of the Lefkara Formation, Lower Member.

7). There is biostratigraphical data to suggest the onset of deposition of the Lefkara Formation, Lower Member, may be diachronous from west (CC23b) to east (CC26), within the northern area (Fig. 4.2, LL1-LL9).

8). The biostratigraphical data from the chalk interbeds of the Kathikas Formation, which have a zonal range of CC25b-CC25a and overlies the major lineaments east and west of the southern Mamonia basement fragment, suggest there has been no major lateral movement along these lineaments since the early Maastrichtian.

9). The current outcrop pattern displayed by the Lefkara Formation, Lower Member, suggest the southern Mamonia basement fragment may have been a structural high during the deposition and/or post-depositional erosion event(s).

4.5 Systematic Descriptions

Family **Ahmuellerellaceae** Reinhardt, 1965

Genus ***Vagalapilla*** Bukry, 1969

Type species. *Vekshinella imbricata* Gartner, 1968.

Remarks. Includes species of elliptical coccoliths with a rim of one cycle of 20 to 50 elements, which imbricate dextrally in distal view. In proximal view, a secondary cycle of elements is present in the rim, at the distal margin of central area. The distal surface is slightly abcentral, proximal surface is more strongly adcentral. Open central area bridged by cross aligned to axes of ellipse and stem or spine may extend from distal surface. Bukry (1969), felt that *Vekshinella* nor *Staurolithites* was a satisfactory designation for a number of species that fitted the above definition of *Vagalapilla*, as described above.

Vagalapilla compacta Bukry, 1969

(Pl. 1, fig. 11)

1969 *Vagalapilla compacta* Bukry: 56, pl. 31, figs 10,11.

Holotype. Bukry, pl. 31, fig. 11, UI-H-3470, sample PSA-3, horizon lower Austin Chalk, locality South Dallas County, Texas.

Description. Elliptical coccoliths (ellipticity of 1.3) with narrow outer rim cycle composed of dextrally imbricated elements. In distal view the outer margin is inclined abcentraly and outline slightly serrated. Inner rim comprises a narrow cycle of elongate elements which line distal margin of central area. Central area bridged by a cross with broad flanking elements which have recessed median sutures aligned to the axes of the ellipse.

Dimensions. Length 4.3µm: Width 3.3µm.

Remarks. Bukry (1969), considered a number of characters, such as the inner cycle of elements at the distal margin of central area, and broad stemless crossbars composed of few elements, to distinguish the species from others placed in *Vagalapilla.*

Occurrence. *Vagalapilla compacta* is rare in Maastrichtian sediments (Bukry, 1969) and during this study was found at only one locality, north-west of Inia, S.W. Cyprus, in the Lefkara Formation (Lower Member).

Range. Santonian to Campanian (CC14 to CC23), Bukry (1969).

Genus ***Vekshinella*** Loeblich & Tappan, 1963

Type species. *Ephippium acutiferrus* Vekshina, 1959.
Description. *Vekshinella* differs from *Vagalapilla* in lacking the secondary cycle of rim elements seen in proximal view. Due to the name *Ephippium* being already occupied, Loeblich & Tappan (1963), transferred *E. acutiferrus* to *Vekshinella.*

Vekshinella stradneri Rood *et al.*, 1971
(Pl. 2, fig. 10; Pl. 3, fig. 1)

1971 *Vekshinella stradneri* Rood *et al.*: 249, pl. 1, fig. 2.

1977 *Vekshinella stradneri* Rood *et al.*; Wise & Wind: 308, pl. 83, fig. 6; pl. 84, figs 1,3,5,6; pl. 89, fig. 7.

Holotype. Rood *et al.*, pl. 1, fig. 2, 34.5.1, sample 4971, horizon Ampthill Clay, locality Millbrook, Bedfordshire.
Description. Elongated elliptical coccoliths with narrow outer rim. Open central area bridged by cross aligned to the axes of ellipse, short arms of cross are slightly offset at centre, and are slightly enlarged at contact with rim. Between crossed polars the curvature of the extinction line across the rim is sinistral in distal view.
Dimensions. Length 5.0μm: Width 3.5μm.
Remarks. At the centre of the cross the short arms are offset and is considered diagnostic of the species (Rood *et al.*, 1971).
Occurrence. Found in the Kannaviou Formation, upper part, at Kritou Marottou and two localities north and north-west of Kathikas in the Lefkara Formation, (Lower Member), S.W. Cyprus.
Range. Aptian to Maastrichtian (CC7 to CC26), Wise & Wind (1977).

Family **Arkhangelskiellaceae** Bukry, 1969

Genus ***Arkhangelskiella*** (Vekshina) Bramlette & Martini, 1964

Type species. *Arkhangelskiella cymibiformis* Vekshina, 1959.
Remarks. Includes species of elliptical coccoliths, characterised by a rim consisting of three to five tiers composed of numerous joint elements, distal tiers are slightly larger than proximal tiers. Central area divided into quadrants aligned to the axes of the ellipse, each quadrant shows a less conspicuous radial subdivision and each subdivision

shows a stronger birefringence between crossed polars from the other, giving the appearance of a windmill, (Bramlette & Martini 1964). Pores or deep pits may be present in well preserved specimens. No central stem or boss is present.

Arkhangelskiella cymibiformis Vekshina, 1959
(Pl. 2, fig. 3; Pl. 3, figs 2,3)

1959 *Arkhangelskiella cymibiformis* Vekshina: 66, pl. 2, figs 3a-b.

1964 *Arkhangelskiella cymibiformis* Vekshina; Bramlette & Martini: 297, pl. 1, figs 3-9.

1973 *Arkhangelskiella cymibiformis* Vekshina; Roth: 715, pl. 19 figs 1,3,5,7.

1990a *Arkhangelskiella cymibiformis* Vekshina; Pospichal & Wise: pl. 5, fig. 2.

Holotype. Vekshina, pl. 2, figs 3a-b (line illustration).

Description. Between crossed polars, large elliptical coccoliths with narrow outer rim enclosing a closed central area, which has a distinctive 'windmill' cross. Pores/deep pits not present, possibly due to overgrowths.

Dimensions. Overall, length 9.6µm, width 7.2µm: Central area, length 8.0µm, width 5.6µm.

Remarks. Many authors consider *Arkhangelskiella cymibiformis* and *A. specillata* (Vekshina, 1959) to be cospecific with two different preservational states, the former develops overgrowths which mask the central area. Between crossed polars, specimens observed from the Cyprus material, did not display the characteristic pores or deep pits, that may have allowed differentiation between *A. cymibiformis* and *A. specillata*. The narrow rim in relation to its large size is diagnostic of the species (Bramlette & Martini, 1964).

Occurrence. *Arkhangelskiella cymibiformis* is well documented with a world wide occurrence in Upper Cretaceous sediments and is used as a zonal marker in the upper Maastrichtian. The short vertical range of *A. cymibiformis,* makes this species stratigraphically important. It is common in the chalk inter beds of the Moni (Dhrousha Melange) and Kathikas Formations and the Lefkara Formation (Lower Member), of the studied localities in S.W. Cyprus. It is also found in middle and Late Palaeocene, and Mid Eocene sediments of S.W. Cyprus and is considered to be reworked.

Range. Late Campanian to Maastrichtian (CC21 to CC26), Perch-Nielsen (1985a).

Family **Biscutaceae** Black, 1971

Genus ***Biscutum*** Black *in* Black & Barnes, 1959

Type species. *Biscutum testudinarium* Black *in* Black & Barnes, 1959.
Remarks. Includes species of elliptical coccoliths consisting of two appressed shields, made up of radial, non-imbricated petaloid elements. Central area open or closed with various constructions.

Biscutum constans (Gorka) Black, 1967
(Pl. 2 figs 11,12)

1957 *Discolithus constans* Gorka: 257, 279, pl. 4, fig. 7.

1959 *Biscutum testudinarium* Black *in* Black & Barnes: 325, pl. 10, fig. 1.

1967 *Biscutum constans* (Gorka); Black: 139.

1969 *Biscutum testudinarium* Black *in* Black & Barnes; Bukry: 28, pl. 8, figs 7-12.

1973 *Biscutum constans* (Gorka); Thierstein: 41.

1985a *Biscutum constans* (Gorka); Perch-Nielsen: 357, 502, fig. 19.6,7,22; fig. 57.3,4.

Holotype. Gorka, pl. 4, fig. 7 (line illustration).
Description. Elliptical coccoliths consisting of a broad outer rim of elements, enclosing a small closed central area, occupied by an irregular group of granules.
Dimensions. Overall, length 5.3µm, width 4.0µm: Central area, length 1.5µm, width 1.0µm
Remarks. *Biscutum constans* and *Discorhabdus ignotus* are distinguished on shape, elliptical and circular respectively (Perch-Nielsen, 1985a).
Occurrence. *Biscutum constans* is a common species documented within Cretaceous sediments world wide and is found only in the Kannaviou Formation, upper part, at Kritou Marottou, S.W. Cyprus.
Range. Cretaceous (CC1 to CC26), Thierstein (1973).

Genus ***Discorhabdus*** Noël, 1965

Type species. *Rhabdolithus patulus* Deflandre & Fert, 1954.
Remarks. Includes species of circular coccoliths consisting of two appressed shields, made up of radial, non-imbricated petaloid elements. Whole of central area may contain a distal stem.

Discorhabdus ignotus (Gorka) Perch-Nielsen, 1968
(Pl. 1, fig. 10)

1957 *Tremalithus ignotus* Gorka: 248, pl. 2, fig. 9.

1968 *Discorhabdus ignotus* (Gorka); Perch-Nielsen: 81, figs 41,42, pl. 28, figs 6-8.

Holotype. Gorka, pl. 2, fig. 9 (line illustration).

Description. Circular coccoliths consisting of petaloid rim elements, with central area open, central stem absent, in all specimens.

Dimensions. Diameter 2.5μm.

Remarks. Similar to *Biscutum constans* but circular in shape with large central distal stem, which rarely remains attached (Perch-Nielsen, 1985a).

Occurrence. Found in the Kannaviou Formation. Also in two isolated localities, a chalk inter bed of the Kathikas Formation, west of Kathikas and the Lefkara Formation, (Lower Member), north-west of Inia, S.W. Cyprus.

Range. Maastrichtian (CC1 to CC26), Perch-Nielsen (1985a).

Family **Calyptroshaeraceae** Boudreaux & Hay, 1969

Genus ***Calculites*** Prins & Sissingh *in* Sissingh, 1977

Type species. *Tetralithus obscurus* Deflandre, 1959.

Remarks. Including species of elliptical coccoliths, composed of a narrow rim and broad wall consisting of a limited number of blocks. A plate structure is absent.

Calculites obscurus (Deflandre) Prins & Sissingh *in* Sissingh, 1977
(Pl. 3, fig. 4)

1959 *Tetralithus obscurus* Deflandre: 138, pl. 3, figs 26-29.

1977 *Calculites obscurus* (Deflandre); Prins & Sissingh *in* Sissingh: 60.

Holotype. Deflandre, pl. 3, figs 26-29, sample BG5, locality Craie de Vanves, France.

Description. Between crossed polars, elliptical coccoliths with a very narrow rim. Central area divided into four segments by extinction lines forming a cross 45° to the axes of the ellipse.

Dimensions. Length 8.2μm: Width 7.2μm.

Remarks. *Calculites obscurus* can be distinguished from *C. ovalis* (Stradner, 1963) between crossed polars. The extinction lines are offset to the axes of the ellipse and is diagnostic of the species (Perch-Nielsen, 1985a). Plus the elements forming the distal central surface are virtually smooth (Prins & Sissingh *in* Sissingh, 1977).

Occurrence. Found at several localities, within the Kannaviou, chalk inter beds of the Moni (Dhrousha Melange) and Kathikas Formations and the Lefkara Formation (Lower Member), S.W. Cyprus.

Range. Santonian to Maastrichtian (CC14 to CC26), Deflandre (1959). Campanian to Maastrichtian (CC17 to CC25a), Prins & Sissingh *in* Sissingh (1977).

Family **Eiffellithaceae** Reinhardt, 1965

Genus ***Eiffellithus*** Reinhardt, 1965

Type species. *Zygolithus turriseiffelii* Deflandre *in* Deflandre & Fert, 1954.

Remarks. Includes species of elliptical coccoliths, with narrow outer rim, composed of inclined, imbricated elements and inner cycle of plate elements. Central area bridged by elements to form a cross and supports a stem or boss.

Eiffellithus eximius (Stover) Perch-Nielsen, 1968

(Pl. 1, fig. 2; Pl. 3, fig. 5)

1966 *Clinorhabdus eximius* Stover: 138, pl. 2, figs 15,16; pl. 8, fig. 15.

1968 *Eiffellithus eximius* (Stover); Perch-Nielsen: 30, pl. 3, figs 8-10.

1973 *Eiffellithus eximius* (Stover); Roth: 726, pl. 18, fig. 1.

Holotype. Stover, pl. 2, fig. 15, USMN 41472, sample 2, locality Sens, France.

Description. Between crossed polars, elliptical coccoliths, with outer rim composed of inclined, dextrally imbricated elements. The inner rim of elements which supports a cross with central boss, is aligned to the axes of the ellipse.

Dimensions. Length 4.2μm: Width 3.2μm.

Remarks. *Eiffellithus eximius* differs from *E. turriseiffelii,* in having an axial cross aligned to the axes of the ellipse, which Stover (1966), considered as a diagnostic feature of the species. The specimens seen in S.W. Cyprus are much smaller than those described by Stover (1966); length 10 to 12μm, width 7 to 9μm.

Occurrence. Found only in the Kannaviou Formation, at Kritou Marottou, near Kannaviou, S.W. Cyprus.

Range. Turonian to Campanian (CC12 to CC23), Stover (1966).

Eiffellithus gorkae Reinhardt, 1965

(Pl. 3, fig. 6)

1965 *Eiffellithus gorkae* Reinhardt: 36, fig. 6, pl. 2, fig. 2.

Holotype. Reinhardt, pl. 2, fig. 2, sample 78/19, locality Rugen, Maastricht, Netherlands.

Description. Between crossed polars, elliptical coccoliths with narrow outer rim. Central area covered by plate elements, supporting a cross with short arms offset from the axes of the ellipse by 45° and is more stub like in appearance.

Dimensions. Length 8.8µm: Width 7.2µm.

Remarks. *Eiffellithus gorkae* differs from *E. turriseiffelii* by the full covering of the central area of plate elements which Perch-Nielsen (1985a) considered to be a diagnostic feature of the species and a stub like boss.

Occurrence. Found at several localities in S.W. Cyprus, within the chalk inter beds of the Moni (Dhrousha Melange) and Kathikas Formations and the Lefkara Formation, (Lower Member). The short vertical range of *Eiffellithus gorkae* makes this species stratigraphically important.

Range. Maastrichtian (CC23 to CC26), Reinhardt (1965) and Perch-Nielsen (1985a).

Eiffellithus turriseiffelii (Deflandre *in* Deflandre & Fert), Reinhardt, 1965

(Pl. 3, fig. 7)

1954 *Zygolithus turriseiffelii* Deflandre *in* Deflandre & Fert: 149, fig. 65, pl. 13, figs 15,16.

1965 *Eiffellithus turriseiffelii* (Deflandre *in* Deflandre & Fert); Reinhardt: 36, fig. 5, pl. 2, fig. 3.

1966 *Clinorhabdulus turriseiffelii* Deflandre *in* Deflandre & Fert; Stover: n. comb. 138, pl. 3, figs 7-9.

1969 *Eiffellithus turriseiffelii* (Deflandre *in* Deflandre & Fert); Bukry: 52, pl. 29, figs 2-5.

1972 *Eiffellithus turriseiffelii* (Deflandre *in* Deflandre & Fert); Roth & Thierstein: pl. 4, figs 1-6,9.

Holotype. Deflandre, pl. 13, figs 15,16, sample BG75, locality Burham, Kent.

Description. The stems taper inwards to a point from the distal surface. Between crossed polars the outer surface displays a checker-board effect about a median line or central cavity.

Dimensions. Length of central stem 11.2μm.

Remarks. Perch-Nielsen (1985a), considered the long central stem supported by elements in the form of a cross, offset to axis of ellipse, to be diagnostic of the species. Central stem rarely remains attached to the distal surface.

Occurrence. *Eiffellithus turriseiffelii* has a world wide geographic distribution throughout the Late Cretaceous. It is found at several localities throughout S.W. Cyprus. The chalk inter beds of the Moni (Dhrousha Melange) and Kathikas Formations and also the Lefkara Formation, (Lower Member).

Range. Upper Albian to Maastrichtian (CC8 to CC26), Perch-Nielsen (1985a).

Family **Ellipsagelosphaeracae** Noël, 1965

Genus **Ellipsagelosphaera** Noël, 1965

Type species. *Ellipsagelosphaera britannica* Stradner, 1963.

Remarks. Includes species of elliptical coccoliths with a distinct central tube between the two shields. Distal shield has slight clockwise overlapping elements, whereas the proximal shield has radial elements. Central area can be closed or open (with or without a bridge).

Ellipsagelosphaera fossacincta Black, 1971a

(Pl. 2, fig. 9)

1971a *Ellipsagelosphaera fossacincta* Black: 399, pl. 30, fig. 8.

1975 *Ellipsagelosphaera keftalrempti* Grün *in* Grün & Allemann: 161, fig. 7 pl. 11, figs 5,6.

1985a *Ellipsagelosphaera fossacincta* Black; Perch-Nielsen: 371, fig. 37; fig. 40.12,13,31.

Holotype. Black, pl. 30, fig. 8, sample H.710/23927, horizon Speeton Clay, locality Speeton.

Description. Elliptical coccoliths, with the distal shield comprising of an outer cycle of slightly overlapping (clockwise) elements and sitting flush with the distal surface a smaller inner cycle of elements. The distal shield encloses a slightly inset elongated tube to form the open central area.

Dimensions. Length 6.7μm: Width 5.2μm.
Remarks. Black (1971a) considered the unbridged small open central area and narrow groove at distal margin of central area to be distinguishing features of the species. *Ellipsagelosphaera keftalrempti* lacks a bridge and Perch-Nielsen (1985a) considered it a junior synonym of *E. fossacincta.*
Occurrence. Found only in the Kannaviou Formation, upper part, at Kritou Marottou, near Kannaviou, S.W. Cyprus.
Range. Bajocian (Mid Jurassic) to Campanian (Late Cretaceous), Taylor (1982).

Genus ***Watznaueria*** Reinhardt, 1964

Type species. *Watznaueria angustoralis* Reinhardt, 1964.
Remarks. *Watznaueria* is similar in construction to *Ellipsagelosphaera,* but species differ in lacking a central tube. Central area is therefore partially or wholly blocked by elements of the proximal shield.

Watznaueria barnesae (Black *in* Black & Barnes) Perch-Nielsen, 1968
(Pl. 1, fig. 3; Pl. 2, fig. 4; Pl. 3, fig. 8)

1959 *Tremalithus barnesae* Black *in* Black & Barnes: 325, pl. 9, figs 1,2.

1968 *Watznaueria barnesae* (Black *in* Black & Barnes); Perch-Nielsen: 69, fig. 32, pl. 22, figs 1-7; pl. 23, figs 1,4,5,16.

1975 *Watznaueria barnesae* (Black *in* Black & Barnes); Grun & Allemann: 162, fig. 8, pl. 2, fig. 10.

Holotype. Black, pl. 9, fig. 2, sample 3068, locality Weston Colville, Cambridgeshire.
Description. Elliptical coccoliths, with distal shield which slope steeply away from closed central area, giving central area elevation. Central area formed by elements of the proximal shield, that forms a slit oriented to long axis of the ellipse. Proximal shield with serrated outline and similar number of elements is slightly smaller than distal shield.
Dimensions. Length 9.3μm: Width 7.2μm.
Remarks. The elements of the smaller proximal shield fill the central area, and is a distinguishing feature of the species (Black in black & Barnes, 1959).*Watznaueria barnesae* has a high resistance to dissolution and is therefore the most common Cretaceous coccolith in poorly preserved assemblages (Perch-Nielsen, 1985a). *W.*

barnesae with a single perforation or elongated slit like opening, differs from *W. biporta* Bukry, 1969, which has two perforations. Both arrangements are oriented to the long axis of the ellipse.

Occurrence. *Watznaueria barnesae* has a well documented world wide occurrence, throughout the Late Cretaceous and is found in all the Late Cretaceous localities studied in S.W. Cyprus. It is also found in middle and Late Palaeocene, Mid Eocene and Miocene calcareous sediments of S.W. Cyprus and is considered to be reworked.

Range. Mid Jurassic to Late Cretaceous, Perch-Nielsen (1985a).

Family **Microrhabdulaceae** Deflandre, 1963

Genus ***Lithraphidites*** Deflandre, 1963

Type species. *Lithraphidites carniolensis* Deflandre, 1963.

Remarks. The genus includes rod-shaped calcareous nannofossil with tapering ends. Constructed of four keels about a central channel forming a cross in cross-section. Keels made up of two appressed blade like elements. Between crossed polars, elements have identical optical orientation.

Lithraphidites carniolensis Deflandre, 1963

(Pl. 2, fig. 5)

1963 *Lithraphidites carniolensis* Deflandre: 3486, figs-8.

1968 *Lithraphidites carniolensis* Deflandre; Gartner: 43, pl. 5, fig. 4; pl. 6, fig. 8; pl. 10, figs 16,17; pl. 12, fig. 8; pl. 22, figs 24,25; pl. 25, fig. 9.

1969 *Lithraphidites carniolensis* Deflandre; Bukry: 66, *non,* pl. 39, fig. 12; pl. 40, figs 1,2.

1977 *Lithraphidites carniolensis* Deflandre; Wise & Wind: pl. 74, fig. 6.

Holotype. Deflandre, figs 2-4, (LN, C Ph), locality Gargasien de Carniol, France.

Description. Blades maintain constant width, until the distal 2µm of each end which taper to a blunt end.

Dimensions. Length 10µm.

Remarks. Perch-Nielsen (1985a), considered the four long straight, smooth and slender blades to be diagnostic of the species.

Occurrence. *Lithraphidites carniolensis* is common to the Kannaviou Formation and the chalk inter beds of the Moni (Dhrousha Melange) and Kathikas Formations. But is

only found at an isolated locality of the Lefkara Formation, (Lower Member), at Tala, north of Paphos, S.W. Cyprus.

Range. Berriasian to Maastrichtian (CC1 to CC26), Perch-Nielsen (1985a)

Lithraphidites praequadratus Roth, 1978
(Pl. 3, fig. 9)

1969 *Lithraphidites carniolensis* Deflandre; Bukry: 66, pl. 39, fig. 12; *non* pl. 40, figs 1,2.

1978 *Lithraphidites praequadratus* Roth: 749, pl. 3, figs 1-3.

1992 *Lithraphidites praequadratus* Roth; Bralower & Siesser: pl. 4, fig. 12; pl. 8, figs 7-10.

Holotype. Roth, pl. 3, fig. 1, sample 44-390A-13-3 (DSDP), negative UUMM 55.

Description. Comprises four broad keels of constant width, which have a distinctive taper at each end, finishing at a point.

Dimensions. Length 7.6μm.

Remarks. *Lithraphidites praequadratus* differs from *L. quadratus* Bramlette & Martini, 1964, and *L. carniolensis,* by having wider keels which are more blade-like in appearance. *L. carniolensis* has a more gradual distal taper.

Occurrence. Of the localities studied, *Lithraphidites praequadratus* is found in several localities in S.W. Cyprus. The chalk inter beds of the Moni (Dhrousha Melange) and Kathikas Formations and also found at an isolated locality in the Lefkara Formation, (Lower Member), north-west of Inia. The species appears to be more common in mid to high latitudes and rare to absent in equatorial regions (Roth, 1978).

Range. Campanian to Maastrichtian (CC17 to CC26), Perch-Nielsen (1985a).

Genus *Microrhabdulus* Deflandre, 1959

Type species. *Microrhabdulus decoratus* Deflandre, 1959.

Remarks. The genus includes straight rod-shaped calcareous nannofossil, composed of small elongate elements, whose cross-section can be circular, oval, square or sub circular.

Microrhabdulus attenuatus (Deflandre) Deflandre, 1963
(Pl. 2, fig. 6; Pl. 3, fig. 10)

1959 *Microrhabdulus decoratus* var. *attenuatus* Deflandre: 141, pl. 4, figs 6-8.

1963 *Microrhabdulus attenuatus* Deflandre; Deflandre: 3486, fig. 11.

1964 *Microrhabdulus stradneri* Bramlette & Martini: 316, pl. 6, figs 3,4.

1968 *Microrhabdulus stradneri* Bramlette & Martini; Gartner: 44, pl. 12, fig. 14.

1985a *Microrhabdulus attenuatus* (Deflandre); Perch-Nielsen: 374, fig. 43.10-14.

Holotype. Deflandre, pl. 4, fig. 6, sample BZ 24, locality Detroit, Texas.

Description. Nannofossils of constant diameter, apart from the distal 2μm of each end, which gently taper to a blunt end. The elements form a low angle spiral about the central axis. Both ends are normally damaged.

Dimensions. Length 13.3μm.

Remarks. *Microrhabdulus attenuatus* differs from other members of the genus, by the low angle spiral of the individual elements about the central axis, plus tapered ends (Bramlette & Martini, 1964). Perch-Nielsen (1985a) considers *M. stradneri* to be a junior synonym of *M. attenuatus*.

Occurrence. Found at several localities in S.W. Cyprus, within the Kannaviou, Moni (Dhrousha Melange), Kathikas and Lefkara (Lower Member) Formations.

Range. Campanian to Maastrichtian (CC17 to CC26), Perch-Nielsen (1985a).

Microrhabdulus decoratus Deflandre, 1959

(Pl. 1, fig. 12; Pl. 3, fig. 11)

1959 *Microrhabdulus decoratus* Deflandre: 140, pl. 4, figs 1-5.

1964 *Microrhabdulus decoratus* Deflandre; Bramlette & Martini: 314, pl. 6, figs 1,2.

1966 *Microrhabdulus decoratus* Deflandre; Stover: 152, pl. 7, figs 15,16.

1992 *Microrhabdulus decoratus* Deflandre; Bralower & Siesser: pl. 8, figs 17,18.

Holotype. Deflandre, pl. 4, figs 1,2, sample BG 38, locality Siene, France.

Description. Nannofossil of constant diameter throughout their length. Between crossed polars and the addition of a sensitive tint (quartz red I plate), a distinctive alternating blue and yellow rectangular appearance is seen.

Dimensions. Length 22.4μm.

Remarks. The species takes the form of small straight elongated elements of equal length, formed into a series of stacked bundles (Deflandre, 1959). Specimens viewed from the Cyprus material, comprise on average 10 stacked bundles (17max).

Occurrence. *Microrhabdulus decoratus* is found in almost all of the Late Cretaceous localities studied in S.W. Cyprus. It is also found in middle and Late Palaeocene, and Mid Eocene calcareous sediments of S.W. Cyprus and is considered to be reworked.

Range. Cenomanian to Maastrichtian (CC10 to CC26), Perch-Nielsen (1985a).

Family **Podorhabdaceae** Noël, 1965

Genus ***Cribrosphaerella*** Deflandre *in* Piveteau, 1952

Type species. *Cribrosphaera ehrenbergii* Arkhangelsky, 1912.
Remarks. The genus includes elliptical coccoliths, with narrow rim enclosing large central area comprising a gridwork pattern. In distal view, the rim is comprised of a large outer and small inner cycle of block-shaped elements.

Cribrosphaerella ehrenbergii (Arkhangelsky) Deflandre *in* Piveteau, 1952
(Pl. 1, figs 4,5; Pl. 3, fig. 12)

1912 *Cribrosphaera ehrenbergii* Arkhangelsky: 412, pl. 6, figs 19,20.

1952 *Cribrosphaerella ehrenbergii* (Arkhangelsky); Deflandre *in* Piveteau: 111, fig. 54.

1964 *Favocentrum laughtoni* Black: 313, pl. 53, figs 1,2.

1968 *Cretadiscus colatus* Gartner: 36, pl. 10, figs 7,8; pl. 12, figs 5,6; pl. 19, fig. 10.

1968 *Cretadiscus polyporus* Gartner: 36, pl. 1, figs 17,19; pl. 4, fig. 13; pl. 25, fig. 5.

1969 *Cribrosphaera ehrenbergii* Arkhangelsky; Bukry: 44, pl. 22, figs 7-12.

1973 *Cribrosphaera ehrenbergii* Arkhangelsky; Roth: 725, pl. 20, fig. 3.

1992 *Cribrosphaerella ehrenbergii* (Arkhangelsky); Bralower & Siesser: figs 3,4; pl. 4, figs 5-7.

Holotype. Arkhangelsky, pl. 6, figs 1,2 (line illustration).
Description. Elliptical coccoliths, when seen in distal view, comprising narrow outer rim cycle of large elements and inner cycle of smaller elements, both non-imbricate and block-shaped in appearance. Central area closed with perforations/depressions in a gridwork pattern.
Dimensions. Length 7.3μm: Width 6.0μm.
Remarks. Bukry(1969), considers the large non-imbricate outer rim elements to be diagnostic of the species.
Occurrence. *Cribrosphaerella ehrenbergii* is found at almost all of the Late Cretaceous localities studied in S.W. Cyprus. It is also found in middle and Late Palaeocene, and Mid Eocene calcareous sediments of S.W. Cyprus and is considered to be reworked.
Range. Turonian to Maastrichtian (CC11 to CC26), Roth (1973).

Genus *Retecapsa* Black, 1971a

Type species. *Retecapsa brightoni* Black, 1971a.

Remarks. The genus includes elliptical coccolith, with distal shield consisting of two cycles of elements and proximal shield with one cycle. The genus is restricted to forms with eight openings situated at the distal margin of central area. These are separated by a cross aligned to the axes of the ellipse and each quadrant subdivided by a lateral bar. The cross and lateral bars buttress a short central boss/spine.

Retecapsa neocomiana Black, 1971a

(Pl. 1, fig. 1)

1971a *Retecapsa neocomiana* Black: 410, pl. 33, fig. 2.

Holotype. Black, pl. 33, fig. 2, sample H.710/25109, horizon Compound Nodular Bed, locality Speeton.

Description. Elliptical coccoliths, with distal shield consisting of two cycles, containing petaloid elements in each cycle. Central area contains eight angular openings situated round the distal margin, separated by lateral bars supporting a central boss.

Dimensions. Overall length 6.7μm, and width 6.0μm: Central area, length 3.0μm and width 2.7μm.

Remarks. *Retecapsa neocomiana* differs from other species of *Retecapsa* by the angular shape of the openings, between the buttresses and lateral bars (Black, 1971a). Dissolution of the outer rim elements, can give the impression that it is comprised of several tiers.

Occurrence. Found in the Kannaviou Formation, and a single chalk inter bed of the Moni Formation (Dhrousha Melange), S.W. Cyprus.

Range. Campanian to Maastrichtian (CC17 to CC26), Black (1971a).

Genus *Stradneria* Reinhardt, 1964

Type species. *Stradneri limbicrassa* Reinhardt, 1964.

Remarks. The genus includes elliptical coccolith, comprising a distal shield of two cycles and proximal shield of one cycle. In distal view, upper cycle is smaller than lower cycle. A small conical central area contains a crown of large elements buttressing the

central structure and stem. *Stradneria* differs from other genera of the Podorhabdaceae, in having more than eight openings surrounding the distal margin of the central area (Grun and Allemann, 1975, fig. 19a).

Stradneria crenulata (Bramlette & Martini) Noël, 1970
(Pl. 3, fig. 16)

1964 *Cretarhabdulus crenulata* Bramlette & Martini: 300, pl. 2, figs 21-24.

1970 *Stradneri crenulata* (Bramlette & Martini); Noël: pl. 13, fig. 5; pl. 17, fig. 3a-b.

1975 *Retecapsa crenulata* Bramlette & Martini; Grun & Allemann: 175, fig. 19a, pl. 4, figs 4-6.

1985a *Stradneri crenulata* (Bramlette & Martini); Perch-Nielsen: 386, fig. 8.88,89; fig. 43.1.

Holotype. Bramlette & Martini, pl. 2, figs 21,22, sample USNM 648200, locality Bellocq, Southwest France.

Description. Between crossed polars, elliptical coccoliths with a broad outer rim. Small central area shows strong suture lines (crenulate) in the form of a cross aligned to the axes of the ellipse, plus laterals.

Dimensions. Length 7.2μm: Width 5.6μm.

Remarks. Between crossed polars the small central area appears perforate, resulting in a crenulate appearance (Bramlette and Martini, 1964).

Occurrence. Found in almost all localities studied, in the Moni (Dhrousha Member), Kathikas and Lefkara (Lower Member) Formations, of S.W. Cyprus.

Range. Cretaceous (CC2 to CC26), Perch-Nielsen (1985a).

Family **Polcyclolithaceae** Forchheimer, 1972

Genus ***Micula*** Vekshina, 1959

Type species. *Micula decussata* Vekshina, 1959.

Remarks. The genus includes nannofossils in the shape of a cube, normally with concave faces, however, later forms include flat or conical types.

Micula decussata Vekshina, 1959
(Pl. 1, fig. 9)

1959 *Micula decussata* Vekshina: 71, pl. 1, fig. 6; pl. 2, fig. 11.

1968 *Micula decussata* Vekshina; Gartner: *partim* , 47, pl. 2, figs 5,8; pl. 4 fig. 17; pl. 9, fig. 18; pl. 14, fig. 13; pl. 18, fig. 7; pl. 20, fig. 15.

1969 *Micula decussata* Vekshina; Bukry: 67, pl. 40, figs 5,6.

Holotype. Vekshina, pl. 1, fig. 6 (line illustration).

Description. Cube-shaped nannofossils, with central depression in each face. Between crossed polars, crystal boundaries are seen as curving suture lines forming a diagonal cross.

Dimensions. Cube 6μm.

Remarks. The diagonal suture lines on each cube face distinguishes the species from others (Gartner, 1968). The species is resistant to erosion and is found in Tertiary deposits due to reworking.

Occurrence. Found in almost all localities studied, in the Moni (Dhrousha Melange), Kathikas and Lefkara (Lower Member) Formations, of S.W. Cyprus. It is also found in middle and Late Palaeocene, and Mid Eocene calcareous sediments of S.W. Cyprus and is considered to be reworked.

Range. Santonian to Maastrichtian (CC14 to CC26), Perch-Nielsen (1985a).

Micula mura (Martini) Bukry, 1973b
(Pl. 3, fig. 14)

1961 *Tetralithus murus* Martini: 4, pl. 1, fig. 6; pl. 4, fig. 42.

1973b *Micula mura* (Martini); Bukry: 679.

1992 *Micula murus* (Martini); Bralower & Siesser: pl. 7, figs 1,2.

Holotype. Martini, pl. 1, fig. 6 (line illustration).

Description. Between crossed polars, cube-shaped nannofossils, with straight extinction lines perpendicular from the cube sides, forming off-centre cross, producing a dark square in the centre, sides parallel to the margin.

Dimensions. Cube 6.4μm.

Remarks. Bukry (1973b), considered the elements extending from the central structure forming a cube shape to be diagnostic of the species.

Occurrence. Found at two localities west of Kathikas, S.W. Cyprus in the Lefkara Formation, (Lower Member).The species is well documented and is a zonal marker of the late Maastrichtian, and common to sub-tropical to equatorial environments. The short vertical range of *Micula mura* makes this species stratigraphically important.
Range. Maastrichtian (CC26), Perch-Nielsen (1985a).

Micula staurophora (Gardet) Stradner, 1963
(Pl. 3, fig. 15)

1955 *Discoaster staurophorus* Gardet: 534, pl. 10, fig. 96.

1963 *Micula staurophora* (Gardet); Stradner: 170, pl. 4, figs 12a-c.

1974 *Micula staurophora* (Gardet); Thierstein: *partim*, pl. 12, figs 1-3,9-11. *non*, pl. 12, figs 4-8,

1984 *Micula staurophora* (Gardet); Stradner & Steinmetz: pl. 31, figs 1,2.

Holotype. Gardet, pl. 10, fig. 96.
Description. Between crossed polars, cube-shaped nannofossils, with concave faces and a 'petaloid effect' forming diagonal cross.
Dimensions. Cube 8.0μm.
Remarks. Identical to that displayed in Thierstein (1974), cube-shaped, with elongated corners of the cube, giving a petaloid effect, between crossed polars.
Occurrence. Found in several localities in the Moni (Dhrousha Melange), Kathikas and Lefkara (Lower Member) Formations, S.W. Cyprus.
Range. Turonian to Maastrichtian (CC12 to CC26), ?early Tertiary, Stradner (1963).

Micula swastica Stradner & Steinmetz, 1984
(Pl. 3, fig. 18)

1984 *Micula swastica* Stradner & Steinmetz: 595, pl. 31, figs 3,5,6.

Holotype. Stradner & Steinmetz, pl. fig. 6, sample DSDP 530A-50-2.
Description. Between crossed polars, cube-shaped nannofossils, with internal sutures forming a 'swastica' effect, caused by four central interlocking square 'hook-shaped' elements, radiating inwardly perpendicular from the external elements.
Dimensions. Cube 2.8μm.
Remarks. The Internal suture lines have a 'swastica' form and is a diagnostic feature of the species (Stradner & Steinmetz, 1984).

Occurrence. Found at two localities, west of Kathikas and east of Pelathousa in the Lefkara Formation, (Lower Member), of S.W. Cyprus. The short vertical range of *Micula swastica* makes this species stratigraphically important.
Range. Maastrichtian (CC26), Stradner & Steinmetz (1984).

Genus ***Quadrum*** Prins & Perch-Nielsen *in* Manivit *et al.*, 1977

Type species. *Quadrum gartneri* Prins & Perch-Nielsen *in* Manivit *et al.*, 1977.
Remarks. The genus includes cube-shaped nannofossils, composed of four large calcite elements in plan view, with the sutures generally perpendicular to the margins, forming a cross.

Quadrum gartneri Prins & Perch-Nielsen *in* Manivit *et al.*, 1977
(Pl. 3, fig. 19)

1974 *Micula staurophora* (Gardet); Stradner; Thierstein: *partim,* pl. 12, figs 4-8, *non,* pl. 12, figs 1-3,9-11.

1977 *Quadrum gartneri* Prins & Perch-Nielsen *in* Manivit *et al.*: 177, pl. 1. figs 9,10.

1991 *Quadrum gartneri* Prins & Perch-Nielsen *in* Manivit *et al.*; Resiwati: pl. 8, fig. 3.

Holotype. The specimen illustrated by Thierstein (1974), pl. 12, figs 4-8, sample DSDP 258-10-1.
Description. Between crossed polars, cube-shaped nannofossils, constructed from four calcite blocks showing curved suture lines in the form of a cross. Suture lines are perpendicular to the margins, making quadrants appear petaloid.
Dimensions. Cube 4.0μm.
Remarks. The species is distinguished by the four large/high calcite units, formed by one or two layers. these are separated by sutures that run perpendicular to the margin on both distal and proximal surfaces (Prins & Perch-Nielsen *in* Manivit *et al.,* 1977). Crux (1982), split *Quadrum gartneri* into two subspecies. Subspecies 1, ranges Turonian to Santonian (CC11 to CC16), with elements orthogonally arranged. Subspecies 2, Coniacian to Maastrichtian (CC13 to CC26), with elements slightly offset and elongate.
Occurrence. Found only in the Kannaviou Formation, at Armou, east of Paphos, S.W. Cyprus.
Range. Turonian to Maastrichtian (CC11 to CC26), Crux (1982).

Family **Prediscosphaeraceae** Rood, Hay & Barnard, 1971

Genus ***Prediscosphaera*** Vekshina, 1959
1964 *Deflandrius* Bramlette & Martini

Type species. *Prediscosphaera decoratus* Vekshina, 1959.
Remarks. Contains species with elliptical or circular coccoliths and constructed of two marginal shields. Each shield is composed of sixteen petaloid, non-imbricated elements. Central area is open with a distal marginal cycle of thin elements and bridged by a cross, which is oriented diagonally or aligned to the axes of the ellipse and supports a distal stem.

Prediscosphaera cretacea (Arkhangelsky) Gartner, 1968
(Pl. 1, fig. 7; Pl. 3, fig. 13)

1912 *Coccolithophora cretacea* Arkhangelsky: 410, pl. 6, figs 12,13.

1964 *Deflandrius cretacea* Arkhangelsky; Bramlette & Martini: 301, pl. 2, figs 11,12.

1968 *Prediscosphaera cretacea* (Arkhangelsky); Gartner: 19, *partim*, pl. 2, figs 10-14; pl. 3, figs 8a-c; pl. 4, figs 19-24; pl. 6, figs 14,15; pl. 9, figs 1-4; pl. 12, fig. 1; pl. 14, figs 20-22; pl. 18, fig. 8; pl. 22, figs 1-3; pl. 23, fig. 4; pl. 25, figs 12-14; pl. 26, figs 2a-c; *non,* pl. 23, figs 5,6.

1970 *Prediscosphaera cretacea* (Arkhangelsky); Noël: 64, fig. 16, pl. 15, figs 3-6,9,11; pl. 16, figs 2,3,7,8.

1982 *Prediscosphaera cretacea* (Arkhangelsky); Crux: pl. 5.5, figs 9,10, pl. 5.8, fig. 6.

1992 *Prediscosphaera cretacea* (Arkhangelsky); Bralower & Siesser: 547, pl. 3, figs 27,28; pl. 4, fig. 2.

Holotype. Arkhangelsky, pl. 6, figs 12,13 (line illustration).
Description. Elliptical coccoliths, consisting of two closely appressed narrow shields, comprising sixteen petaloid, non-imbricate elements. Cycle of broad elements form distal margin of open central area, bridged by double oblique cross, slightly offset from one another.
Dimensions. Length 8.8μm: Width 6.4μm.
Remarks. The slightly offset double crossbar consisting of a distal and proximal set and the broad inner cycle of elements surrounding the distal margin of the central area. is diagnostic of the species (Gartner, 1968).
Occurrence. *Prediscosphaera cretacea* appears to be more common to the chalk inter beds of the Moni (Dhrousha Melange) and Kathikas Formations. However, it is also

found in the Kannaviou Formation, and several localities of the Lefkara Formation, (Lower Member), of S.W. Cyprus.

Range. Campanian to Maastrichtian (CC18b to CC26), Perch-Nielsen (1985a).

Prediscosphaera grandis Perch-Nielsen, 1979
(Pl. 3, fig. 17)

1968 *Deflandrius cretaceus* (Arkhangelsky); Bramlette & Martini; Perch-Nielsen: 62, pl. 13, figs 1,5,6; pl. 14, fig. 2.

1979 *Prediscosphaera grandis* Perch-Nielsen: 267, pl. 2, fig. 8.

1992 *Prediscosphaera grandis* Perch-Nielsen; Bralower & Siesser: 547, pl. 3, figs 23,24.

Holotype. Perch-Nielsen (1968), *Deflandrius cretaceus,* pl. 13, fig. 1. locality Mon's Klint, Denmark.

Description. Between crossed polars, large elliptical coccoliths, with a narrow outer rim which comprises sixteen petaloid, non-imbricate elements, with weak birefringence. A cycle of broad elements showing strong birefringence form the distal margin of open central area, bridged by double oblique cross, slightly offset from one another.

Dimensions. Length 12.8μm: Width 10.4μm.

Remarks. Perch-Nielsen (1979) considered the size (10 to 15μm long) to be the diagnostic feature of the very large, broad elliptical species, which is similar in form to the smaller *P. cretacea* (6 to 8μm long).

Occurrence. *Prediscosphaera grandis* is found in several localities of the Kathikas (chalk inter beds) Formation and an isolated locality in the Lefkara Formation, (Lower Member), north-west of Inia S.W. Cyprus. The short vertical range of *P. grandis* makes this species stratigraphically important.

Range. Maastrichtian (CC23b to CC26), Perch-Nielsen (1979).

Family **Sollasitaceae** Black, 1971a

Genus ***Sollasites*** Black, 1967
1969 *Costacentrum* Bukry.

Type species. *Sollasites barringtonensis* Black, 1967.

Remarks. The genus includes elliptical coccoliths, with two shields of dextrally imbricated elements enclosing open central area. Central area has a cycle of sub vertical elements at its distal margin and bridged by crossbar aligned to short axis. Differing

configurations of crossbars aligned to long axis, are species diagnostic. A partial covering of elements may be present within centre.

Sollasites horticus (Stradner *et al. in* Stradner & Adamiker) Black, 1968
(Pl. 2, fig. 7)

1966 *Coccolithus horticus* Stradner *et al. in* Stradner & Adamiker: 337, figs 1,2, pl. 2, fig. 4.

1967 *Sollasites barringtonensis* Black: 144, fig. 4.

1968 *Sollasites horticus* (Stradner *et al.*); Black: pl. 144, figs 1,2.

1969 *Costacentrum horticus* Stradner *et al.*; Bukry: 44, pl. 21, fig. 12; pl. 22, figs 1-3.

1975 *Sollasites horticus* (Stradner *et al.*); Grün *in* Grün & Allemann: 189, fig. 28, pl. 7, figs 5,6.

1990 *Sollasites horticus* (Stradner *et al.*); Mutterlose & Wise: pl. 4, fig. 3.

Holotype. Stradner *et al. in* Stradner & Adamiker, pl. 2, fig. 4.
Description. In distal view, elliptical coccoliths, with distal shield composed of dextrally imbricate elements. A cycle of sub vertical elements form distal margin of open central area, bridged by lateral bar oriented to short axis. Aligned to long axis three sub parallel bars intersect lateral bar.
Dimensions. Length 6μm: Width 4.5μm.
Remarks. The diagnostic feature of the species is the three crossbars aligned to long axis of the ellipse, crossing lateral bar aligned to short axis (Grün *in* Grün and Allemann, 1975).
Occurrence. Found only in the Kannaviou Formation, at Kritou Marottou, near Kannaviou, S.W. Cyprus.
Range. Lower Oxfordian to Campanian, Grün in Grün & Allemann (1975).

Family **Stephanolithiaceae** Black, 1968

Genus ***Corollithion*** Stradner, 1961

Type species. *Corollithion exiguum* Stradner, 1961.
Remarks. Includes rhomboidal- or polygonal-shaped coccoliths, distal shield comprised of sub vertical prismatic elements, inclined slightly distally and proximal shield made up of small blocky elements. Central area open and bridged by four or six radial to sub radial bars.

Corollithion signum Stradner, 1963
(Pl. 2, figs 1,2)

1963 *Corollithion signum* Stradner: 177, pl. 1, fig. 13.

1969 *Corollithion signum* Stradner; Bukry: 41, pl. 19, figs 5-8.

1984 *Corollithion signum* Stradner; Stradner & Steinmetz: pl. 7 figs 6,7.

Holotype. Stradner, pl. 1, fig. 13, sample KLB/4A, locality Klafterbrunn, Austria.
Description. The polygonal-shaped coccoliths, when seen in distal view comprise a narrow rim margin of dextrally imbricate (sub vertical) elements. A cycle of narrow elongate elements form the distal margin of the open central area, bridged by a cross of broad plate-like elements with enlarged tips.
Dimensions. Maximum 4μm.
Remarks. The four radial bars present within the central area is diagnostic of the species (Stradner, 1963).
Occurrence. Found only in the Kannaviou Formation, Kritou Marottou, near Kannaviou, S.W. Cyprus.
Range. Upper Albian to Maastrichtian (CC9 to CC26), Perch-Nielsen (1985a).

Family **Zygodiscaceae** Hay & Mohler, 1967

Genus *Glaukolithus* Reinhardt, 1964

Type species. *Zygolithus diplogrammus* Deflandre *in* Deflandre & Fert, 1954.
Remarks. Includes elliptical coccoliths with two cycles of elements. Broad elements of the distal cycle are inclined and slightly dextrally imbricated. Central area bridged by two crossbars aligned to short axis.

Glaukolithus compactus (Bukry) Perch-Nielsen, 1984
(Pl. 1, fig. 6; Pl. 2, fig. 8)

1969 *Zygodiscus compactus* Bukry: 59, pl. 34, figs 1,2.

1970 *Zygodiscus compactus* Bukry; Noël: 26, figs 2,3, pl. 2, figs 2-8; pl. 3, figs 1-3.

1982 *Zygodiscus compactus* Bukry; Crux: pl. 5.1, figs 13-15.

1984 *Glaukolithus compactus* (Bukry); Perch-Nielsen: 43.

Holotype. Bukry, pl. 34, fig. 2, sample UI-H-3333, locality Meudon, France.

Description. Elliptical coccoliths, with distal shield composed of slightly dextrally imbricate elements and central area almost covered with irregular ordered rhomb-shaped elements.

Dimensions. Length 6.7μm: Width 4.6μm.

Remarks. The broad crossbars aligned to short axis, consisting of inter fingering elements, that may cover entire central area is considered to be diagnostic of the species (Perch-Nielsen, 1985a).

Occurrence. Found in the Kannaviou Formation and the chalk inter beds of the Moni Formation (Dhrousha Melange). Also found at an isolated locality in the Lefkara Formation, (Lower Member), of S.W. Cyprus.

Range. Barremian to Maastrichtian (CC6 to CC26), Crux (1982).

Genus ***Placozygus*** Hoffmann, 1970b

Type species. *Glaukolithus fibuliformis* Reinhardt, 1964.

Remarks. Genus includes elliptical coccoliths, characterised by rim comprising of a single wall, constructed of inclined to vertical, block-shaped elements. Open central area bridged by I-shaped crossbar aligned to short axis.

Placozygus fibuliformis (Reinhardt) Hoffmann, 1970b
(Pl. 1, fig. 8; Pl. 3, fig. 20)

1964 *Glaukolithus ?fibuliformis* Reinhardt: 758, pl. 1, fig. 4.

1964 *Zygodiscus spiralis* Bramlette & Martini: 303, pl. 4, figs 6-8.

1969 *Zygodiscus fibuliformis* (Reinhardt); Bukry: 59, pl. 34, figs 9,10.

1970b *Placozygus fibuliformis* (Reinhardt); Hoffmann: 1004, pl. 1, figs 1-4.

Holotype. Reinhardt, pl. 1, fig. 4, 78-11, locality Rügen, Maastricht.

Description. Elliptical coccoliths. In proximal view, outer rim cycle comprised of vertical, block-shaped elements. An inner rim cycle of inclined elements forms the distal margin of an open central area, which is bridged by several elements aligned to short axis of ellipse.

Dimensions. Length 5.6μm: Width 3.2μm.

Remarks. Bukry (1969), considered the secondary inner cycle of the outer rim on the proximal surface to be a diagnostic feature of the species. *Placozygus fibuliformis* is distinguished from *Glaukolithus compactus* in side view, by having a distal cycle of sub

vertical elements, but inclined in the latter. Also the central I-shaped bridging structure is thinner in construction.

Occurrence. Found at almost all Late Cretaceous localities studied in S.W. Cyprus.

Range. Albian to Maastrichtian (CC8 to CC26), Perch-Nielsen (1985a).

PLATE 1.

SEM photomicrographs

Fig. 1. *Retecapsa neocomiana* Black, 1971, distal view, UD609 14A, D277-1113, X4320.

Fig. 2. *Eiffellithus eximius* (Stover, 1966), distal view, UD609 18A, D277-1113, X9050.

Fig. 3. *Watznaueria barnesae* (Black *in* Black and Barnes, 1959), proximal view, UD609 32A, D277-1113, X4720.

Figs 4,5. *Cribrosphaerella ehrenbergii* (Arkhangelsky, 1912): Fig. 4, distal view, UD619 41A, D277-1113, X4659; Fig. 5, distal view, UD618 26A, D336-1419, X4670.

Fig. 6. *Glaukolithus compactus* (Bukry, 1969), distal view, UD618 23A, D277-1113, X3880.

Fig. 7. *Prediscosphaera cretacea* (Arkhangelsky, 1912), distal view, UD618 41A, D336-1419, X3290.

Fig. 8. *Placozygus fibuliformis* (Rienhardt, 1964), proximal view, UD619 35A, D277-1113, X6070.

Fig. 9. *Micula decussata* Vekshina, 1959, side view, UD618 6A, D336-1419, X4830.

Fig. 10. *Discorhadus ignotus* (Gorka, 1957), distal view, UD596 3, D117-1180, X9600.

Fig. 11. *Vagalapilla compacta* Bukry, 1969, distal view, UD595 1, D117-1180, X4880.

Fig. 12. *Microrhabdulus decoratus* Deflandre, 1959, side view, UD596 1, D117-1180, X2510.

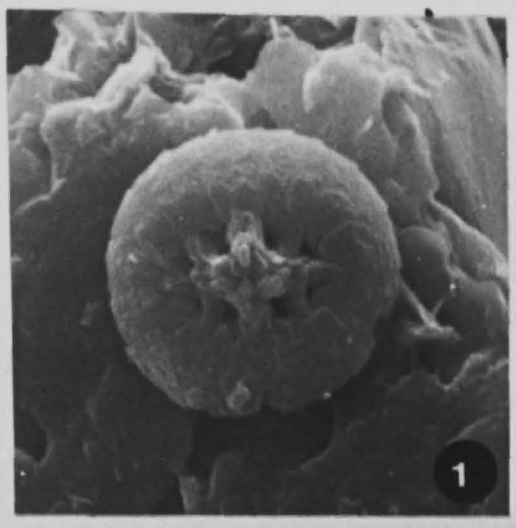
1

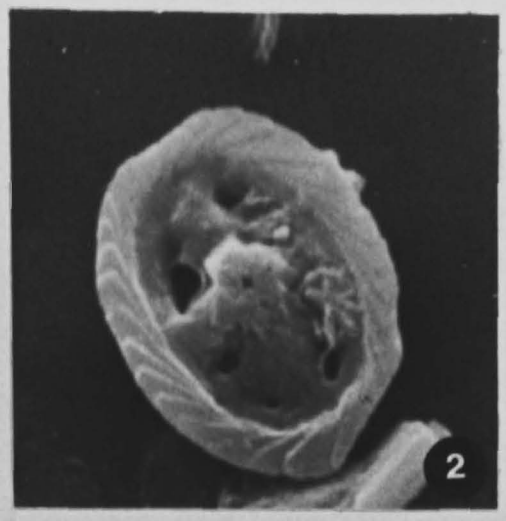
2

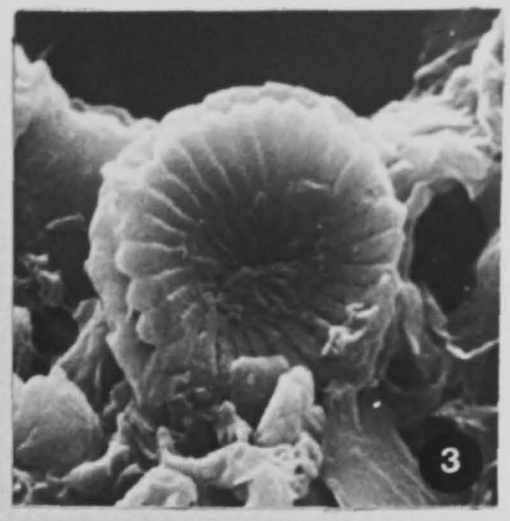
3

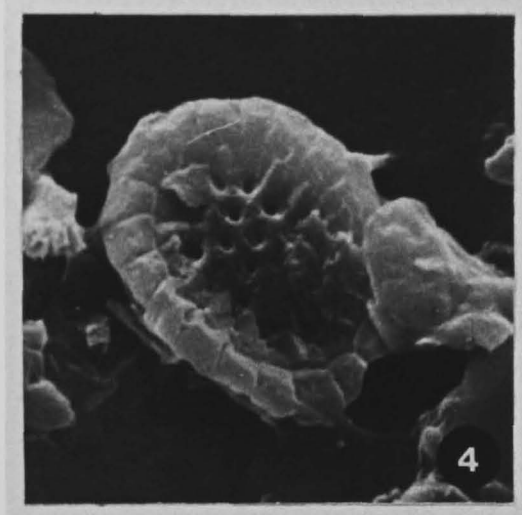
4

5

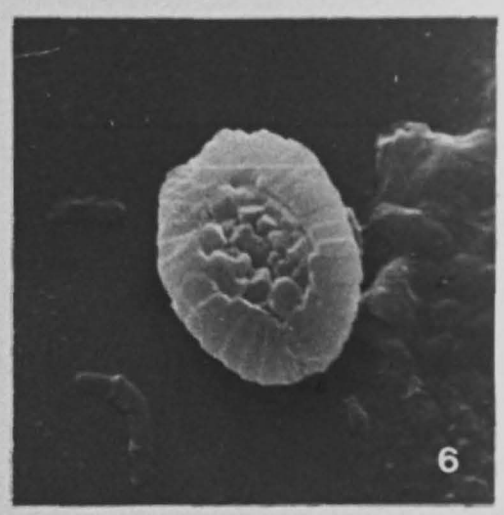
6

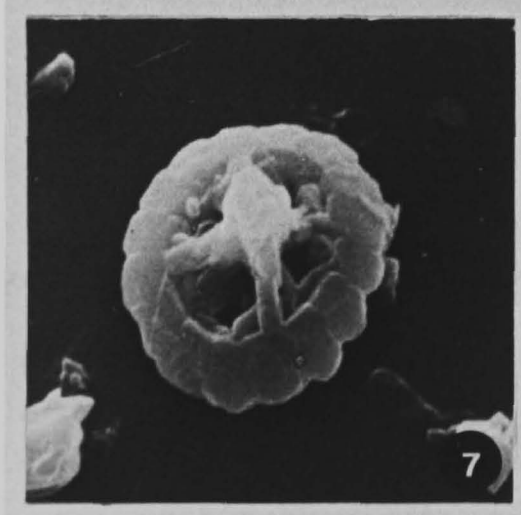
7

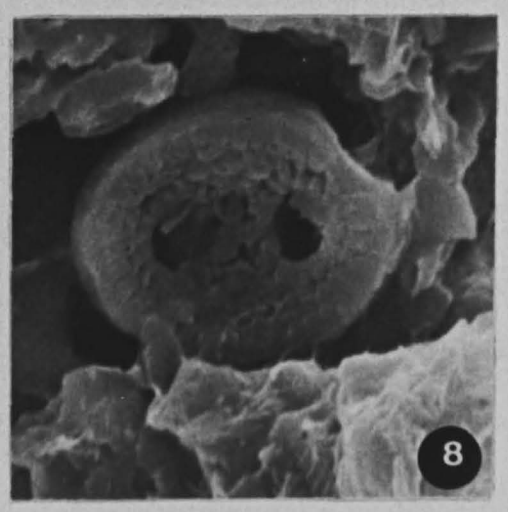
8

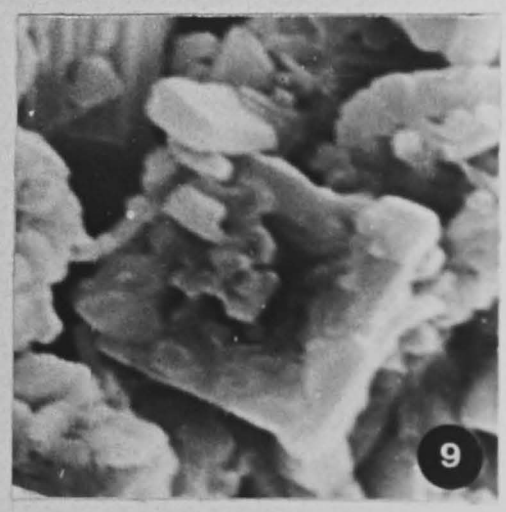
9

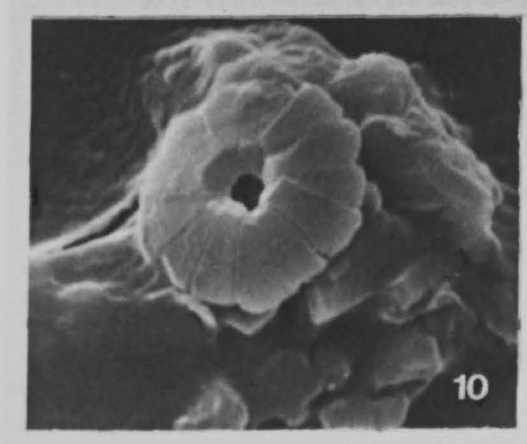
10

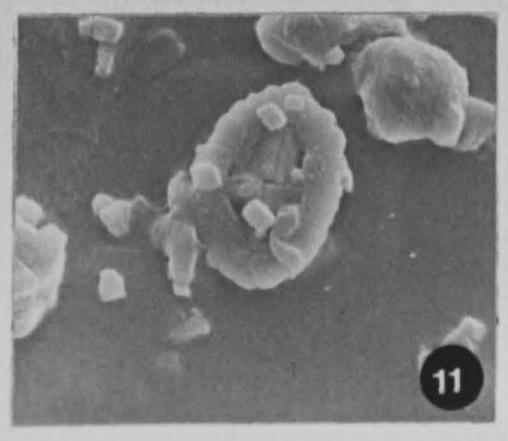
11

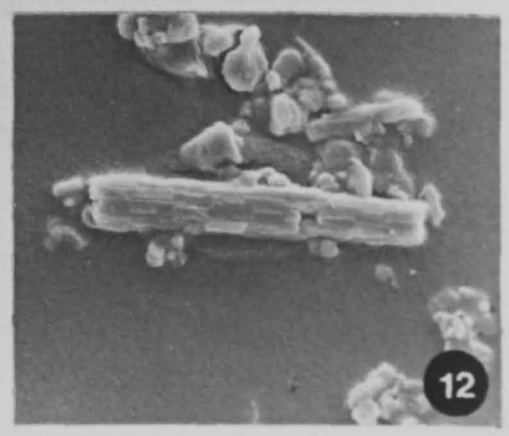
12

PLATE 2.

SEM photomicrographs

Figs 1,2. *Corollithion signum* Stradner, 1963, D277-1113: Fig. 1, distal view, UD619 4A, X8750; Fig. 2, distal view, UD619 44A, X9550.

Fig. 3. *Arkhangelskiella cymbiformis* Vekshina, 1959, distal view, UD618 17A, D336-1419, X4600.

Fig. 4. *Watznaueria barnesae* (Black *in* Black and Barnes, 1959), distal view, UD609 27A, D277-1113, X4510.

Fig. 5. *Lithraphidites carniolensis* Deflandre, 1963, side view, UD618 35A, D336-1419, X5000.

Fig. 6. *Microrhabdulus attenuatus* (Deflandre, 1959), side view, UD619 39A, D277-1113, X4510.

Fig. 7. *Sollasites horticus* (Stradner, Adamiker and Maresch *in* Stradner and Adamiker, 1966), distal view, UD609 19A, D277-1113, X9160.

Fig. 8. *Glaukolithus compactus* (Bukry, 1969), distal view, UD609 35A, D277-1113, X8650.

Fig. 9. *Ellipsagelosphaera fossacincta* Black, 1971, coccolithophore, UD609 33A, D277-1113, X3730.

Fig. 10. *Vekshinella stradneri* Rood *et al.*, 1971, distal view, UD609 26A, D277-1113, X7540.

Figs 11, 12. *Biscutum constans* (Gorka1957), D277-1113: Fig. 11, distal view, UD609 40A, X 7540; Fig. 12, coccolithophore, UD609 39A, X4200.

1

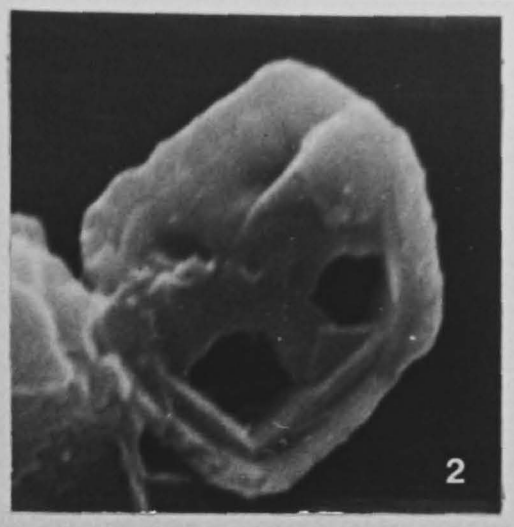
2

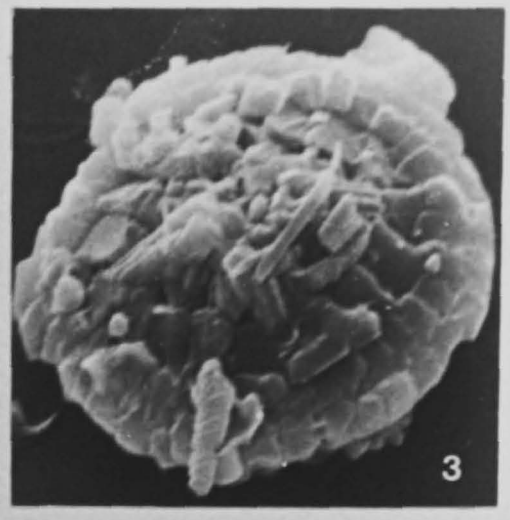
3

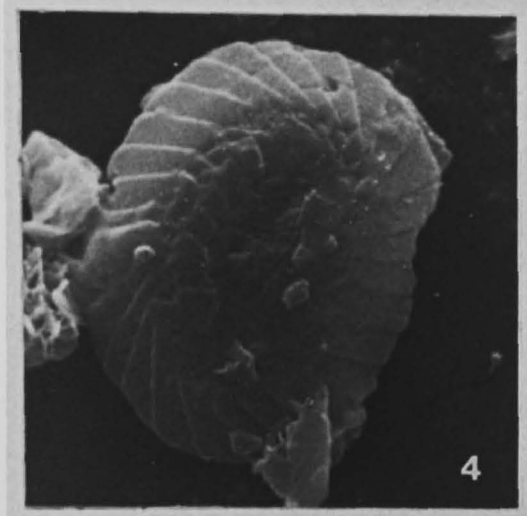
4

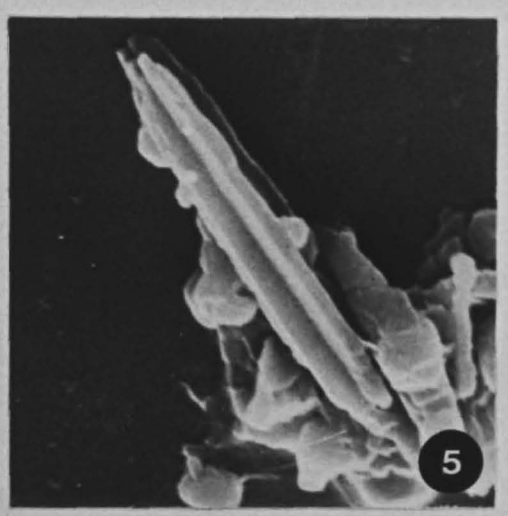
5

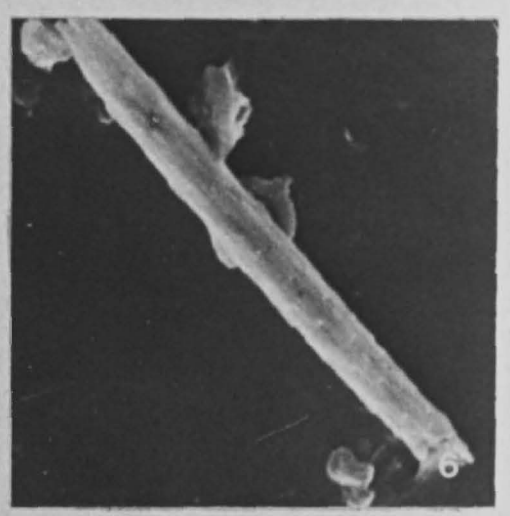
6

7

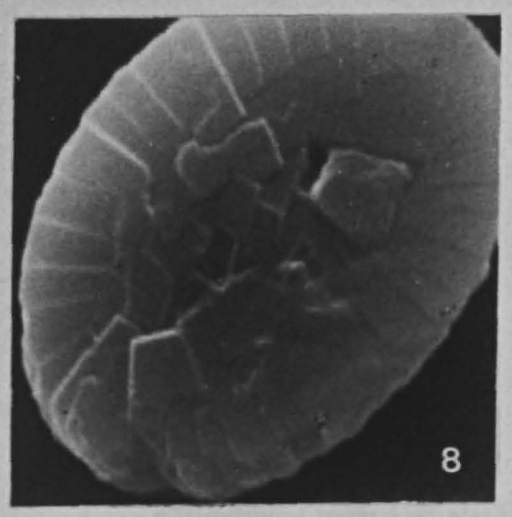
8

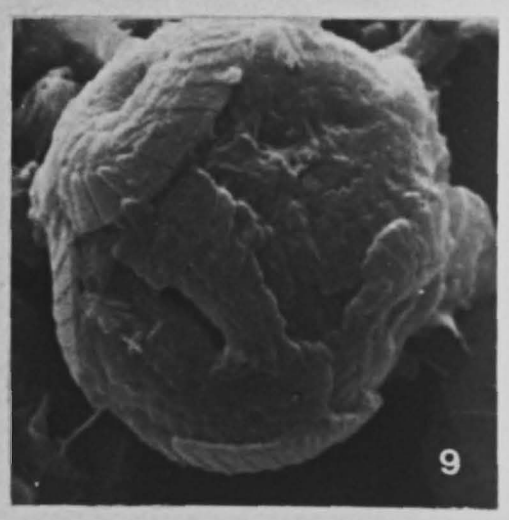
9

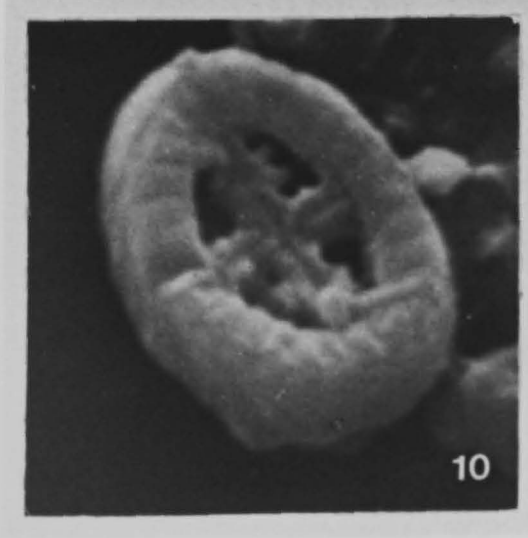
10

11

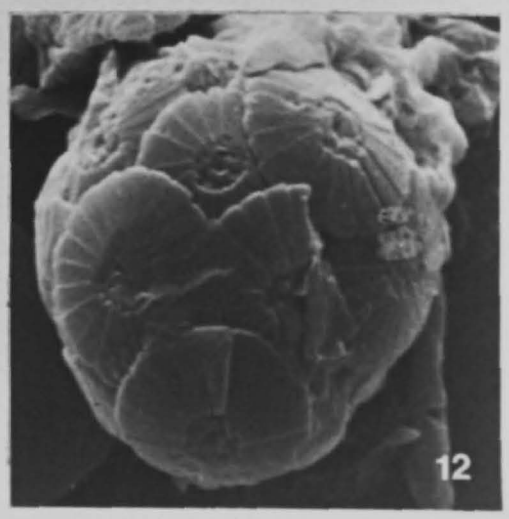
12

UNIV DUNELM

PLATE 3.

Light photomicrographs

XPL = Crossed Polarised Light
PC = Phase Contrast Scale Bar = 5μm

Fig. 1. *Vekshinella stradneri* Rood *et al.*, 1971, plan view, PC, UD617 15A, D125-1216.

Figs 2,3. *Arkhangelskiella cymbiformis* Vekshina, 1959: Fig. 2, plan view, XPL, UD621 26A, D261-1405; Fig. 3, plan view, PC, UD586 3, D115-1213.

Fig. 4. *Caculites obscurus* (Deflandre, 1959), distal view, XPL, UD617 34A, D115-1213.

Fig. 5. *Eiffellithus eximius* (Stover, 1966), distal view, XPL, UD614 19, D277-1113.

Fig. 6. *Eiffellithus gorkae* Reinhardt, 1965, distal view, XPL, UD621 25A, D261-1405.

Fig. 7. *Eiffellithus turriseiffelii* (Deflandre *in* Deflandre and Fert, 1954), side view, XPL, UD617 39A, D197-1038.

Fig. 8. *Watznaueria barnesae* (Black *in* Black and Barnes, 1959), plan view, XPL, UD612 23A, D115-1213.

Fig. 9. *Lithraphidites praequadratus* Roth, 1978, side view, XPL, UD617 41A, D117-1180.

Fig. 10. *Microrhabdulus attenuatus* (Deflandre, 1959), side view, XPL, UD617 1A, D125-1216.

Fig. 11. *Microrhabdulus decoratus* Deflandre, 1959, side view, XPL, UD617 3A, D277-1113.

Fig. 12. *Cribrosphaerella ehrenbergii* (Arkhangelsky, 1912), distal view, XPL, UD613 36A, D277-1113.

Fig. 13. *Prediscosphaera cretacea* (Arkhangelsky, 1912), distal view, XPL, UD613 31A, D272-1105.

Fig. 14. *Micula mura* (Martini, 1961), side view, XPL, UD617 35A, D125-1216.

Fig. 15. *Micula staurophora* (Gardet, 1955), side view, XPL, UD617 7A, D125-1216.

Fig. 16. *Stradneria crenulata* (Bramlette and Martini, 1964), distal view, XPL, UD612 22A, D115-1213.

Fig. 17. *Prediscosphaera grandis* Perch-Nielsen, 1979, distal view, XPL, UD617 12A, D117-1180.

Fig. 18. *Micula swastica* Stradner and Steinmetz, 1984, side view, XPL, UD599 26A, D125-1216.

Fig. 19. *Quadrum gartneri* Prins and Perch-Nielsen *in* Manivit *et al.*, 1977, side view, XPL, UD613 37A, D277-1113.

Fig. 20. *Placozygus fibuliformis* (Rienhardt, 1964), plan view, XPL, UD617 9A, D336-1419.

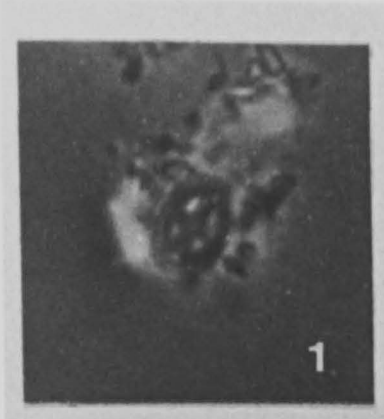
1

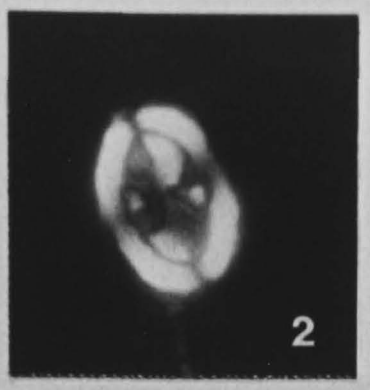
2

3

4

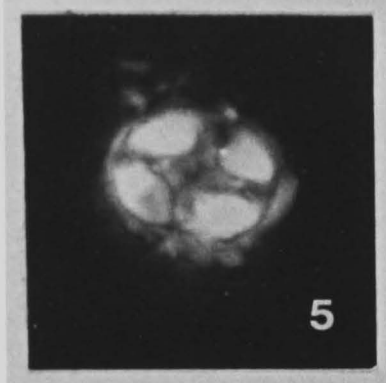
5

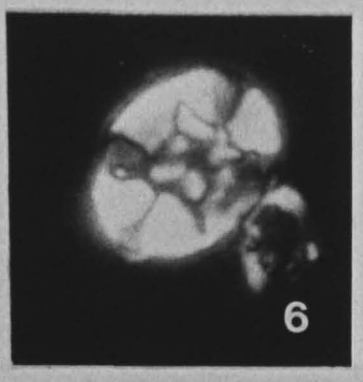
6

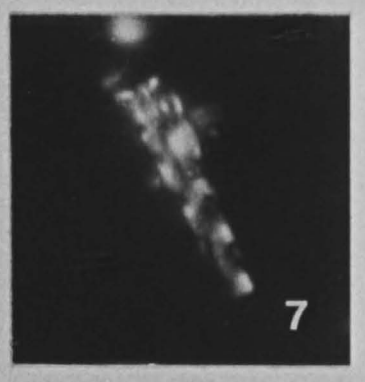
7

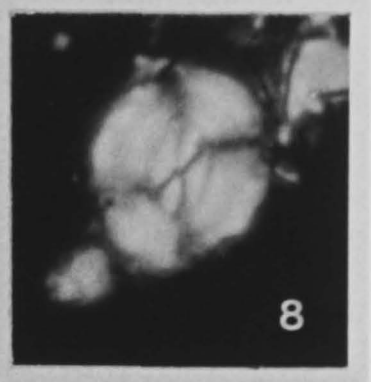
8

9

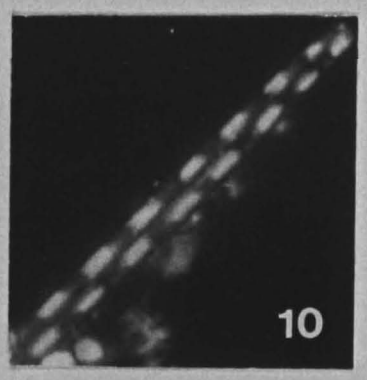
10

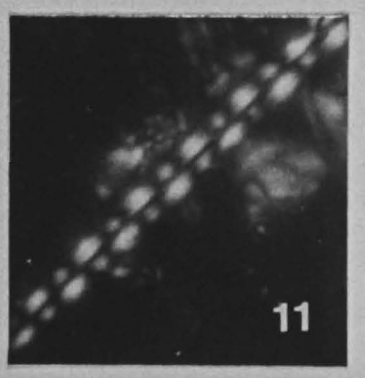
11

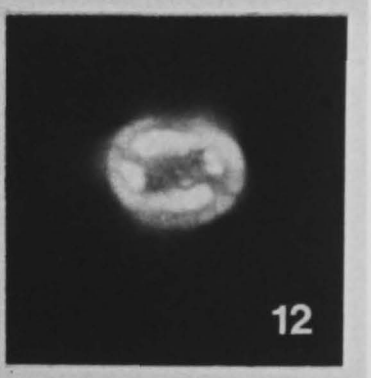
12

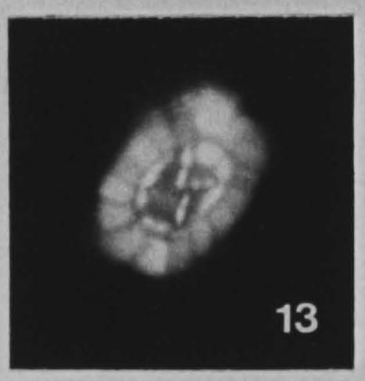
13

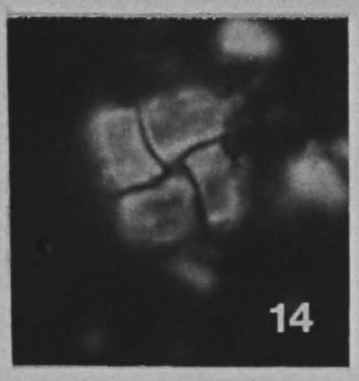
14

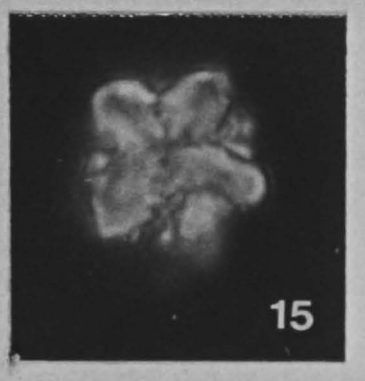
15

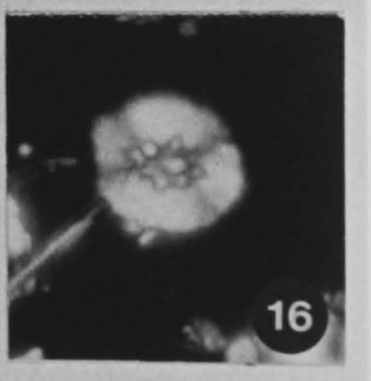
16

17

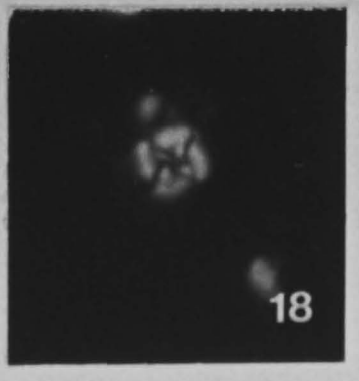
18

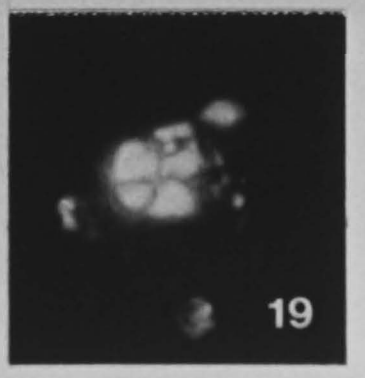
19

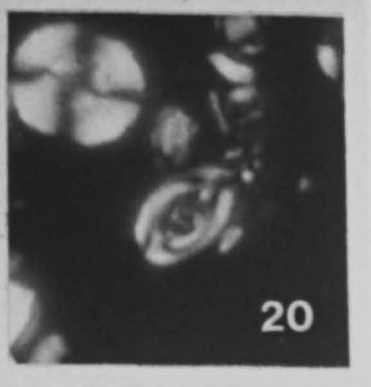
20

CHAPTER 5

BIOSTRATIGRAPHY OF THE PALAEOCENE AND EOCENE NEO-AUTOCHTHONOUS SEDIMENTARY COVER OF S. W. CYPRUS:

5.1 Introduction

The study reported here involves micropalaeontological analyses (calcareous nannofossils), of 34 samples from 30 localities (Figs 5.1,2,3). It also forms part of an overall review of the biostratigraphy of the neo-autochthonous sedimentary cover of S.W. Cyprus and concentrates on the calcareous sediments of the Lefkara Formation, Middle Member (Chalk and Chert and Massive Chalk units).

The aim of this study is to date the age of the Lefkara Formation, Middle Member (Chalk and Chert and Massive Chalk units), where the basal horizon makes unconformable contact with the underlying sedimentary members and formations of the neo-autochthonous sedimentary cover, and the Mamonia and Troodos (including the Kannaviou Formation) basement terranes and fragments (Fig. 5.4).

5.2 Sampling Strategy and Localities

The sampling of the Lefkara Formation (Figs 5.1,2,3), Middle Member (Chalk and Chert and Massive Chalk units [ML]), forms part of a wider biostratigraphical study on the Late Cretaceous (late Campanian) to Late Miocene sediments of S.W. Cyprus, involving 372 samples from 100 localities. Samples were collected as near as possible to the unconformable contact with the underlying basement terranes or sedimentary formations. Also samples were collected at measured intervals from one locality at Petra-tou-Romiou (Figs 5.5).

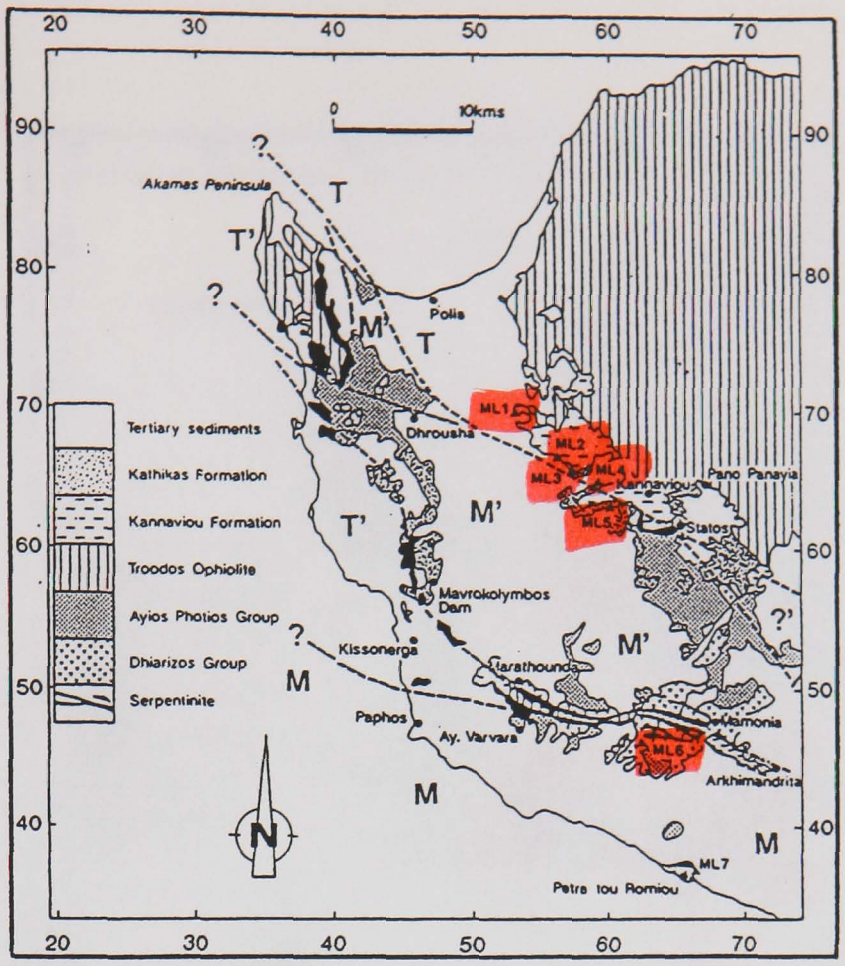

Fig. 5.1. General geological map of S.W. Cyprus, displaying the relationship between the Mamonia and Troodos basement terranes (M and T respectively) and their associated fragments (M', T' respectively and ?' uncertain). Also displaying the Late Palaeocene sample localities (ML1-ML7) of the Lefkara Formation, Middle Member (Chalk and Chert unit) (modified from Swarbrick 1980).

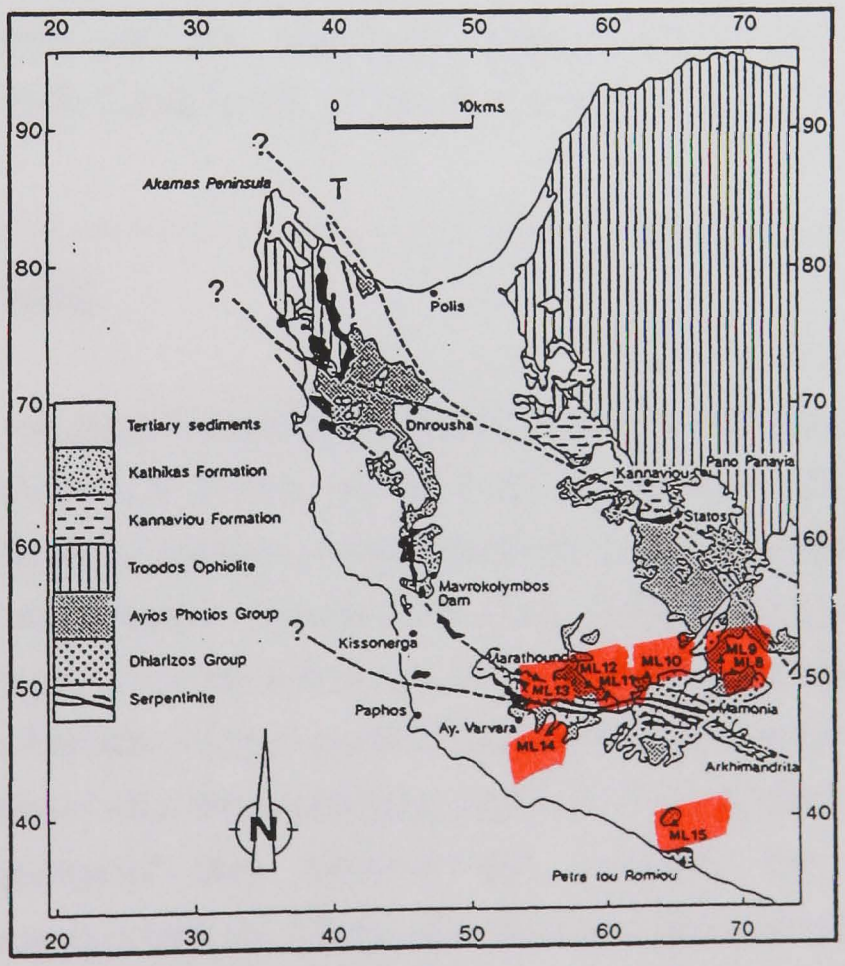

Fig. 5.2. General geological map of S.W. Cyprus, displaying the relationship between the Eocene sample localities (ML8-ML15) of the Lefkara Formation, Middle Member (Chalk and Chert unit) and the underlying groups and formations (modified from Swarbrick, 1980).

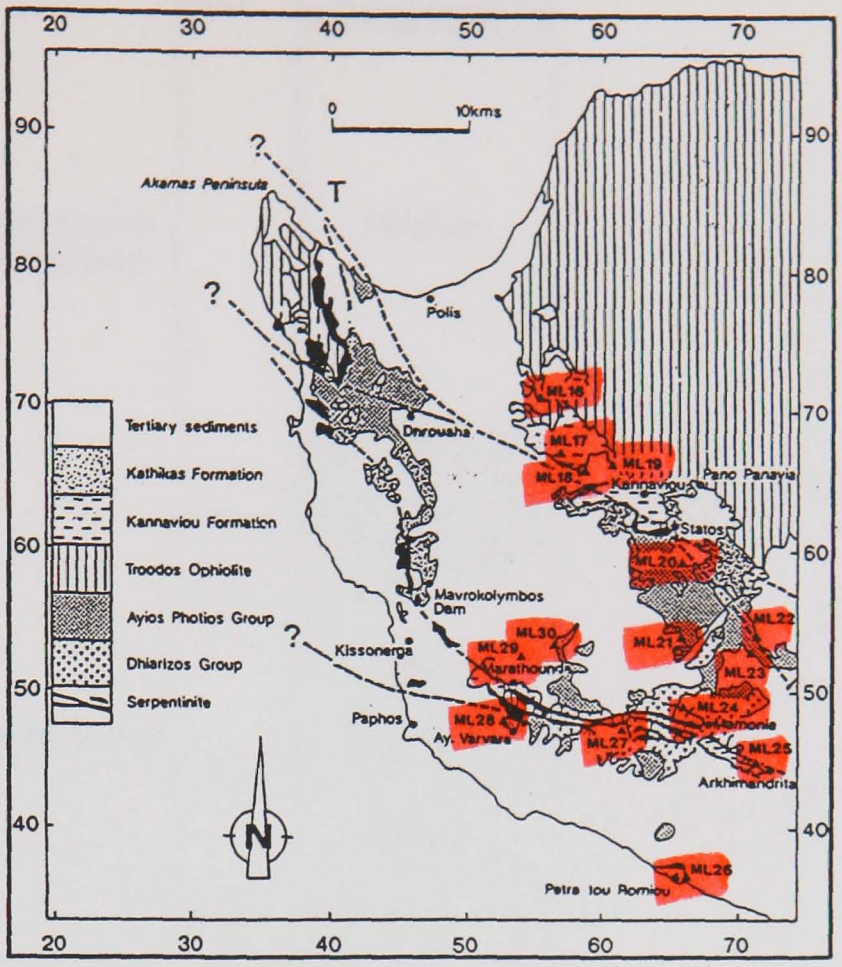

Fig. 5.3. General geological map of S.W. Cyprus, displaying the relationship between the Eocene sample localities (ML16-ML30) of the Lefkara Formation, Middle Member (Massive Chalk unit) and the underlying groups and formations (modified from Swarbrick, 1980). N.B. Locality ML16 overlies unconformably the Lefkara Formation, Lower Member.

5.3 Biostratigraphy

The earlier micropalaeontological data is of limited value, apart from research by Krasheninnikov and Kaleda (1994), on the Late Cretaceous (Campanian) to Pliocene sediments of the Perapedhi section, situated north of Limassol against the south western margin of the Troodos Massif. Therefore the study attempts to develop the application of micropalaeontology, to the basal horizons of the chalk outcrop, relating to the Lefkara Formation, Middle Member of the neo-autochthonous sedimentary cover, which makes unconformable contact with the underlying rocks, in S.W. Cyprus. The study reviews the micropalaeontological data obtained and confirms the presence of three unconformable contacts within the Chalk and Chert unit and a fourth located at the base of the overlying Massive Chalk unit (Fig. 5.4).

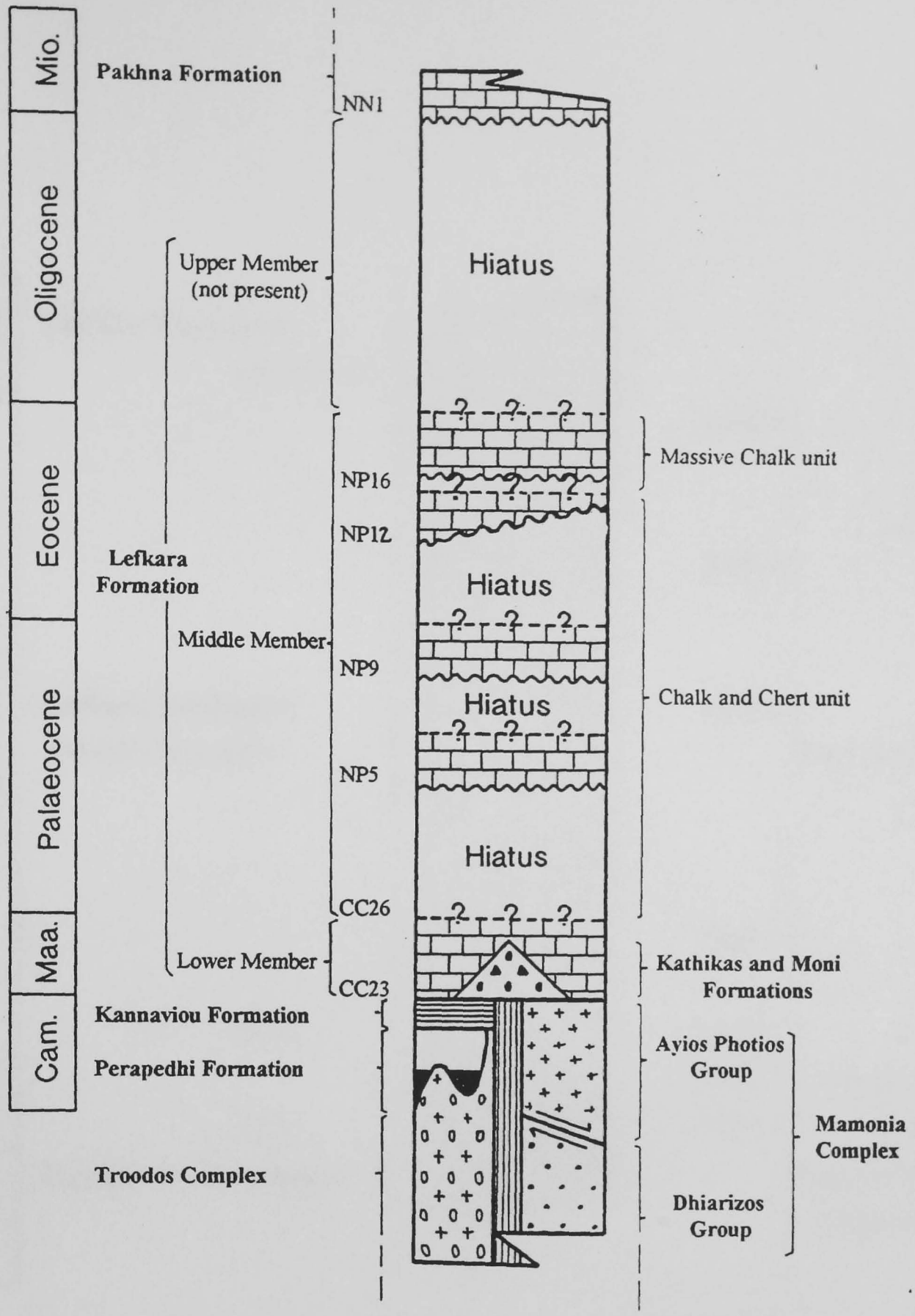

Notes.

1). CC (Sissingh, 1977), NP and NN (Martini, 1971) calcareous nannofossil biostratigraphical zonal schemes, indicating the relative ages of the unconformable contacts

2). Unconformable contacts made with:

CC23 Mamonia Complex only.

NP5 Kannaviou and Kathikas Formations.

NP9 Mamonia Complex, Kannaviou (?reworked) and Kathikas Formations.

NP13 Mamonia Complex, Kannaviou Formation and serpentinites.

NP16 Mamonia and Troodos Complexes, Kannaviou, Kathikas and Lefkara (Lower Member) Formations.

Fig. 5.4. A schematic geological vertical section (not to scale), displaying the relationship between the Mamonia and Troodos (including associated formations) basement terranes (Complexes) and the overlying neo-autochthonous sedimentary cover of S.W. Cyprus (north-west of the line formed by the Dhiarizos valley).

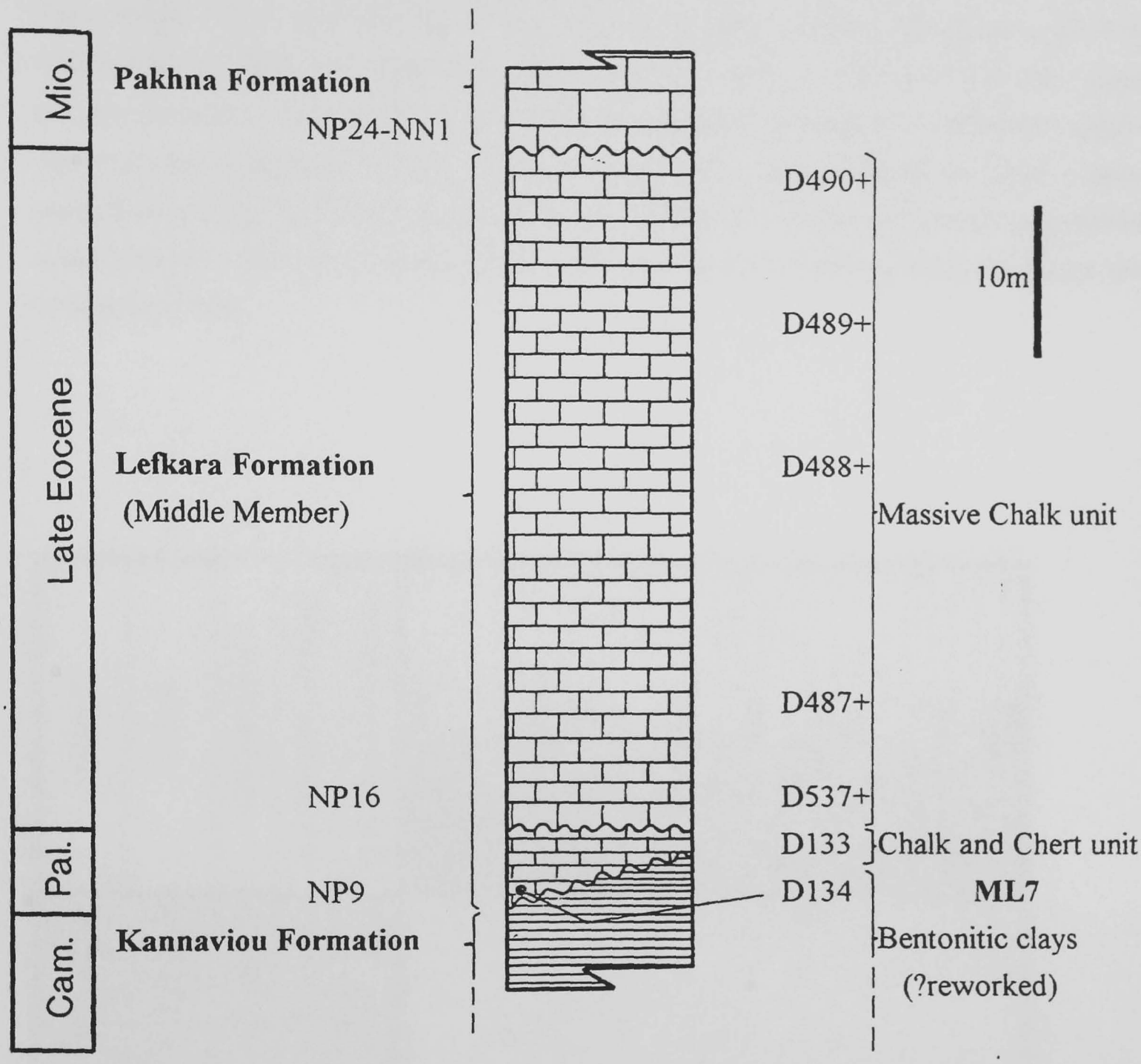

Notes.

1). D numbers = sample processing number.

2). + = ML26 samples,

3). NP and NN (Martini, 1971) calcareous nannofossil biostratigraphical zonal scheme, indicating the relative ages of the unconformable contacts.

Fig. 5.5. Geological composite measured vertical section at Petra-tou-Romiou, containing unconformities between: 1). The Pakhna and Lefkara (Middle Member, Massive Chalk) Formations; 2). The Massive Chalk and Chalk and Chert units of Lefkara Formation, Middle Member; 3). The Lefkara (Middle Member, Chalk and Chert unit) and Kannaviou (?reworked) Formations

The biostratigraphical significance of calcareous nannofossils observed, within the samples collected from localities (Figs 5.1,2,3) in S.W. Cyprus, are discussed below. The species distribution tables for the Lefkara Formation, Middle Member, Chalk and Chert (Figs 5.6,7) and Massive Chalk (Fig. 5.8) units, display the species observed within each sample, including state of preservation, overall content of the assemblage and the presence of derived species. The biostratigraphical ranges of individual species observed are displayed in Figs 5.9,10,11, which have been determined from various published sources (5.5 Systematics), and are correlated with the calcareous nannofossil zonal scheme erected by Martini (1971). All localities have been given a six figure grid reference (CGR).

LOCALITY	SAMPLE	PRESERVATION	NANNOFOSSIL CONTENT	DERIVED NANNOFOSSILS	Thoracosphaera operculata	Biscutum castrorum	Coccolithus pelagicus	Ericsonia cava	Ericsonia subpertusa	Neochiastozygus modestus	Cruciplacolithus tenuis	Neochiastozygus perfectus	Ericsonia robusta	Ellipsolithus macellus	Fasciculithus pileatus	Fasciculithus tympaniformis	Zygodiscus bramlettei	Sphenolithus primus	Cruciplacolithus frequens	Heliolithus cantabriate	Heliolithus kleinpelli	Sphenolithus anarrhopus	Chiasmolithus consuetus	Discoaster mohleri	Fasciculithus climatus	Heliolithus reidelli	Neochiastozygus distentus	Fasciculithus alanii	Discoaster multiradiatus	Cruciplacolithus cribellum
ML7	D134	G	A	X			x		x		x		x	x		x	x	x	x	x	x	x	x	x	x		x	x	x	
ML6	D246	M	C	X	x		x	x	x				x		x	x		x					x		x	x	x	x	x	x
ML5	D535	M	S				x				x		x	x		x		x						x			x		x	
ML4	D276	G	A	X		x		x	x	x	x	x	x				x	x													
ML3	D534	G	A	X				x	x	x	x		x				x														
ML2	D217	M	A	X	x		x		x		x		x				x														
ML1	D532	G	C	X	x		x	x			x	x			x	x	x	x													

Preservation of calcareous nannofossils.
G = GOOD (little or no alteration).
M = MODERATE (50% showing some form of alteration).
P = POOR (all showing some form of alteration).

Calcareous nannofossil content (field of view = 390μm).
A = ABUNDANT (>5 individuals per field of view).
C = COMMON (<5 individuals per field of view).
S = SPARSE (isolated occurrences).

LOCALITY (Fig. 5.1)
ML = Lefkara Formation (Middle Member, Chalk and Chert unit).
X = Derived nannofossils present from Cretaceous sediments.

Note
i) All chalk samples were collected as near as possible to the contact with the underlying lithologies.

Fig. 5.6. Distribution of calcareous nannofossils observed in samples collected from the Lefkara Formation, Middle Member, Chalk and Chert unit of Palaeocene age, of S.W. Cyprus.

LOCALITY	SAMPLE	PRESERVATION	NANNOFOSSIL CONTENT	DERIVED NANNOFOSSILS	Coccolithus pelagicus	Chiasmolithus californicus	Chiasmolithus solitus	Discoaster barbadiensis	Toweius gammation	Chiasmolithus grandis	Sphenolithus radians	Discoaster lodoensis	Chiasmolithus expansus	Ericsonia formosa	Sphenolithus moriformis	Reticulofenestra dictyoda	Sphenolithus spiniger	Discoaster wemmelensis	Thoracosphaera tuberosa	Coccolithus eopelagicus	Chiasmolithus medius	Cruciplacolithus vanheckae	Sphenolithus furcatolithoides	Sphenolithus pseudoradians	Cyclicargolithus marismontium
ML8	D365	M	C	X"	x		x	x						x	x			x		x				x	
ML9	D366	M	S		x				x			x	x	x	x	x				x					
ML10	D237	M	A	X'		x		x					x		x										
ML11	D235	M	S	X'	x			x	x			x		x		x		x		x					
ML12	D371	G	A	X'	x			x	x		x		x	x		x				x					x
ML13	D576	P	S	X	x															x			x	x	
ML14	D231	M	C	X'	x			x	x	x				x	x	x	x		x		x	x			
ML15	D240	M	S	X'	x					x	x			x	x	x	x						x		

Preservation of calcareous nannofossils.

G = GOOD (little or no alteration).

M = MODERATE (50% showing some form of alteration).

P = POOR (all showing some form of alteration).

Calcareous nannofossil content (field of view = 390μm).

A = ABUNDANT (>5 individuals per field of view).

C = COMMON (<5 individuals per field of view).

S = SPARSE (isolated occurrences).

Derived nannofossils present from:-

X = Cretaceous sediments.

X' = Palaeocene sediments.

X" = Cretaceous and Palaeocene sediments

LOCALITY (Fig. 5.2)

ML = Lefkara Formation (Middle Member, Chalk and Chert unit)

Notes

i) All chalk samples were collected as near as possible to the contact with the underlying lithologies.

Fig. 5.7. Distribution of calcareous nannofossils observed in samples collected from the Lefkara Formation, Middle Member, Chalk and Chert unit, of Eocene age, in S.W. Cyprus.

The following summary, gives the Locality number (ML), Cyprus Grid Reference (CGR), Sample number (D), underlying formation or basement and zonal range (NP) which is discussed in detail below.

ML1 (CGR 528 688), **D532,** Kannaviou Formation, NP5-NP6.

ML2 (CGR 554 666), **D217,** Kannaviou Formation, NP5-NP9.

ML3 (CGR 555 665), **D534,** Kathikas Formation, NP5.

ML4 (CGR 575 643), **D276,** Kathikas Formation, NP5.

ML5 (CGR 600 632), **D535,** Kathikas Formation, NP9.

ML6 (CGR 619 449), **D246,** Mamonia, NP8/NP9.

LOCALITY	SAMPLE	PRESERVATION	NANNOFOSSIL CONTENT	DERIVED NANNOFOSSILS	Coccolithus pelagicus	Chiasmolithus consuetus	Discoaster barbadiensis	Chiasmolithus grandis	Sphenolithus radians	Chiasmolithus expansus	Ericsonia formosa	Sphenolithus moriformis	Reticulofenestra dictyoda	Calcidiscus protoannula	Thoracosphaera tuberosa	Coccolithus eopelagicus	Cruciplacolithus vanheckae	Reticulofenestra reticulata	Sphenolithus pseudoradians	Chiasmolithus modestus	Chiasmolithus nitidus	Cyclicargolithus marismontium	Reticulofenestra umbilica	Dictyococcites scrippsae	Dictyococcites bisectus
ML16	D264	P	S									x			x	x		x	x					x	
ML17	D266	P	S	X'	x							x	x	x		x								x	
ML18	D273	P	S	X'					x				x			x		x						x	
ML19	D274	P	S		x		x				x	x				x						x	x	x	
ML20	D219	P	S		x				x	x	x	x	x			x								x	
ML21	D224	P	S	X'	x				x		x	x				x								x	x
ML22	D368	M	C		x						x				x	x		x					x	x	x
ML23	D367	M	C						x		x	x				x							x	x	x
ML24	D364	M	C	X"	x				x	x	x		x		x	x						x	x		
ML25	D244	M	S		x					x	x	x	x	x	x									x	x
ML26	D490	M	C		x						x	x						x				x		x	x
	D489	M	S		x						x	x													
	D488	M	S		x						x												x	x	
	D487	M	C		x				x	x		x	x			x						x	x	x	
	D537	M	S	X'	x				x		x	x	x			x					x		x	x	
ML27	D236	M	S	X'	x		x	x	x		x		x	x		x								x	x
ML28	D351	G	C	X"	x		x			x	x		x			x	x	x	x	x	x	x			
ML29	D226	M	S		x				x		x	x	x							x		x			
ML30	D227	M	S		x	x					x	x	x			x				x					x

Preservation of calcareous nannofossils.

G = GOOD (little or no alteration).

M = MODERATE (50% showing some form of alteration).

P = POOR (all showing some form of alteration).

Calcareous nannofossil content (field of view = 390μm).

A = ABUNDANT (>5 individuals per field of view).

C = COMMON (<5 individuals per field of view).

S = SPARSE (isolated occurrences).

Derived nannofossils present from:-

X' = Palaeocene sediments.

X" = Cretaceous and Palaeocene sediments

LOCALITY (Fig. 5.3)

ML = Lefkara Formation (Middle Member, Massive Chalks)

ML26 = Samples represent part of a measured section (see Fig. 5.5).

Note

i) All chalk samples were collected as near as possible to the contact with the underlying lithologies.

Fig. 5.8. Distribution of calcareous nannofossils observed in samples collected from the Lefkara Formation, Middle Member, Massive Chalk unit, of Eocene age, in S.W. Cyprus.

ML7 (CGR 662 366), **D134,** Kannaviou Formation, NP9
(forms part of measured section, Fig. 5.5).

ML8 (CGR 682 505), **D365,** Mamonia, NP15-NP16.
ML9 (CGR 682 523), **D366,** Mamonia, NP14.
ML10 (CGR 630 513), **D237,** Mamonia, NP12-NP13.
ML11 (CGR 588 490), **D235,** Kannaviou Formation, NP14.
ML12 (CGR 588 495), **D371,** serpentinite, NP14-NP16.
ML13 (CGR 539 502), **D576,** Kannaviou Formation, NP15-NP16.
ML14 (CGR 555 461), **D231,** Mamonia, NP15.
ML15 (CGR 650 390), **D240,** Mamonia, NP15.

ML16 (CGR 545 718), **D264,** Lefkara Formation, NP16-NP18.
ML17 (CGR 545 674), **D266,** Kannaviou Formation, NP16.
ML18 (CGR 575 652), **D273,** Kathikas Formation, NP16.
ML19 (CGR 596 660), **D274,** Kannaviou Formation, NP16-NP19.
ML20 (CGR 653 395), **D219,** Mamonia, NP16.
ML21 (CGR 648 547), **D224,** Mamonia, NP17-NP19.
ML22 (CGR 713 543), **D368,** Mamonia, NP17-NP18.
ML23 (CGR 698 592), **D367,** Mamonia NP17-NP19.
ML24 (CGR 657 496), **D364,** Mamonia, NP16.
ML25 (CGR 701 458), **D244,** Kannaviou Formation, NP16/NP17 boundary.
ML26 (CGR 661 369), **D490** (NP17-NP18), **D489** (NP12-NP21), **D488** (NP16-NP21), **D487** (NP16), **D537** (NP16), these samples form part of a measured section (Fig. 5.5), Kannaviou Formation, overall NP16-NP18.
ML27 (CGR 602 478), **D236,** Mamonia, NP16.
ML28 (CGR 525 475), **D351,** Kannaviou Formation, N16.
ML29 (CGR 541 512), **D226,** Troodos, NP16.
ML30 (CGR 565 525), **D227,** Mamonia, NP16.

5.3.1 Lefkara Formation, Middle Member, Chalk and Chert unit (Palaeocene)

Based on the micropalaeontological data discussed below, the Palaeocene dated horizons of the Chalk and Chert samples studied from S.W. Cyprus, which make unconformable contact with the underlying rocks, fall into two groups. Firstly a mid Palaeocene localised outcrop between the villages of Evretou and Dhrina (ML1 to ML4; Fig. 5.2), and secondly, several Late Palaeocene localised outcrops situated either side

of the southern Mamonia basement fragment (ML7 to ML9, Fig. 5.2). The samples contain a moderate to well preserved assemblage of calcareous nannofossils.

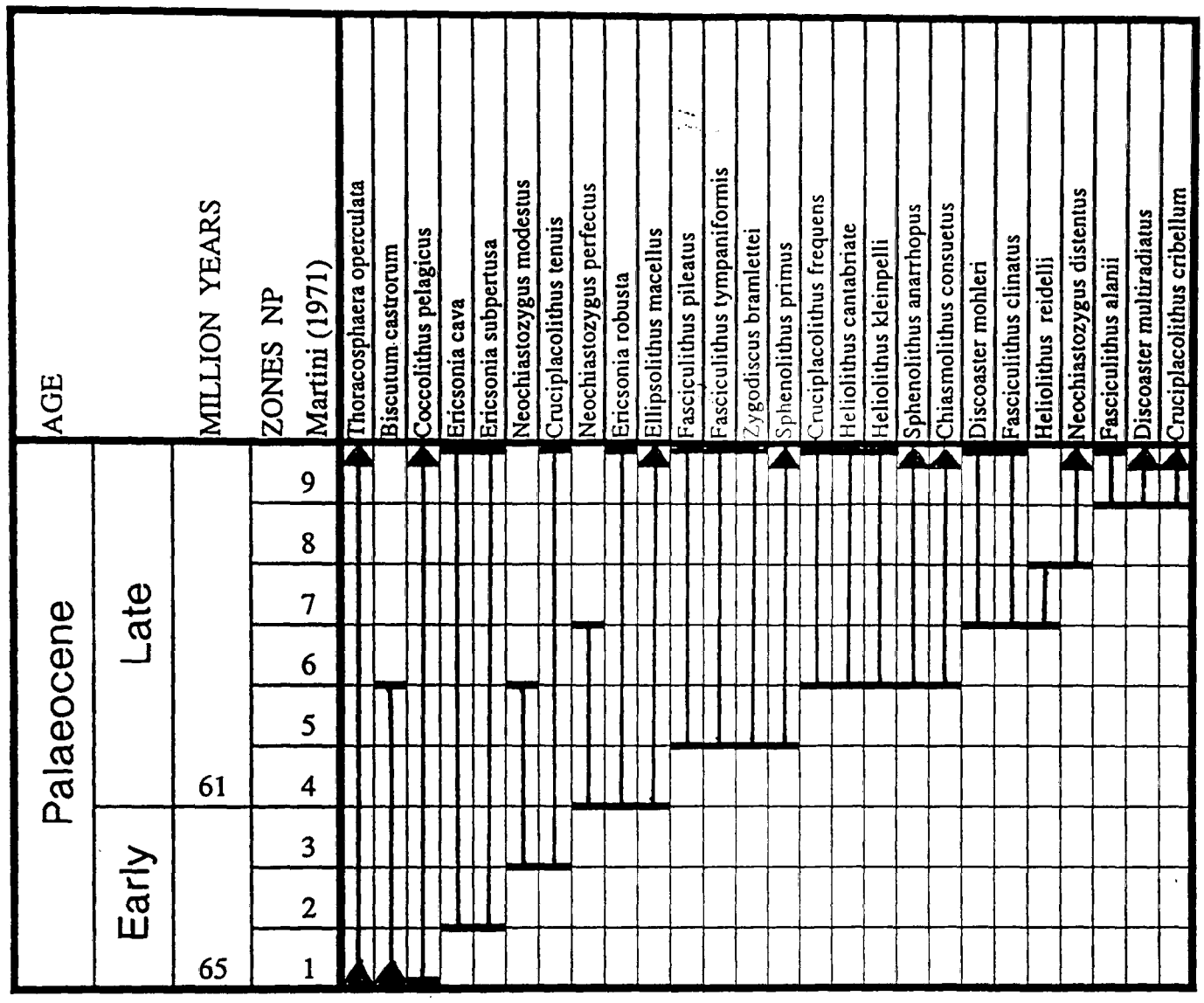

Notes
Dates have been rounded to nearest Ma (Harland et al., 1989).
The biostratigraphical ranges of individual species have been determined from various published sources (5.5. Systematics).

Fig. 5.9. The ranges of calcareous nannofossil species observed in samples collected from the Late Palaeocene chalks of the Lefkara Formation, Middle Member, Chalk and Chert unit, of S.W. Cyprus.

5.3.1.1 Mid Palaeocene

Samples **D534 (ML3)** and **D276 (ML4)**, contain a common and abundant population, with a poor and moderately diverse species content respectively (Fig. 5.6). The combined presence of *Neochiastozygus modestus* Perch-Nielsen, 1971a (NP3-NP5; Perch-Nielsen, 1985b) and *Zygodiscus bramlettei* Perch-Nielsen, 1981 (NP5-NP9; Perch-Nielsen, 1985b), indicates a zonal range of NP5 (Fig. 5.9) for both assemblages.

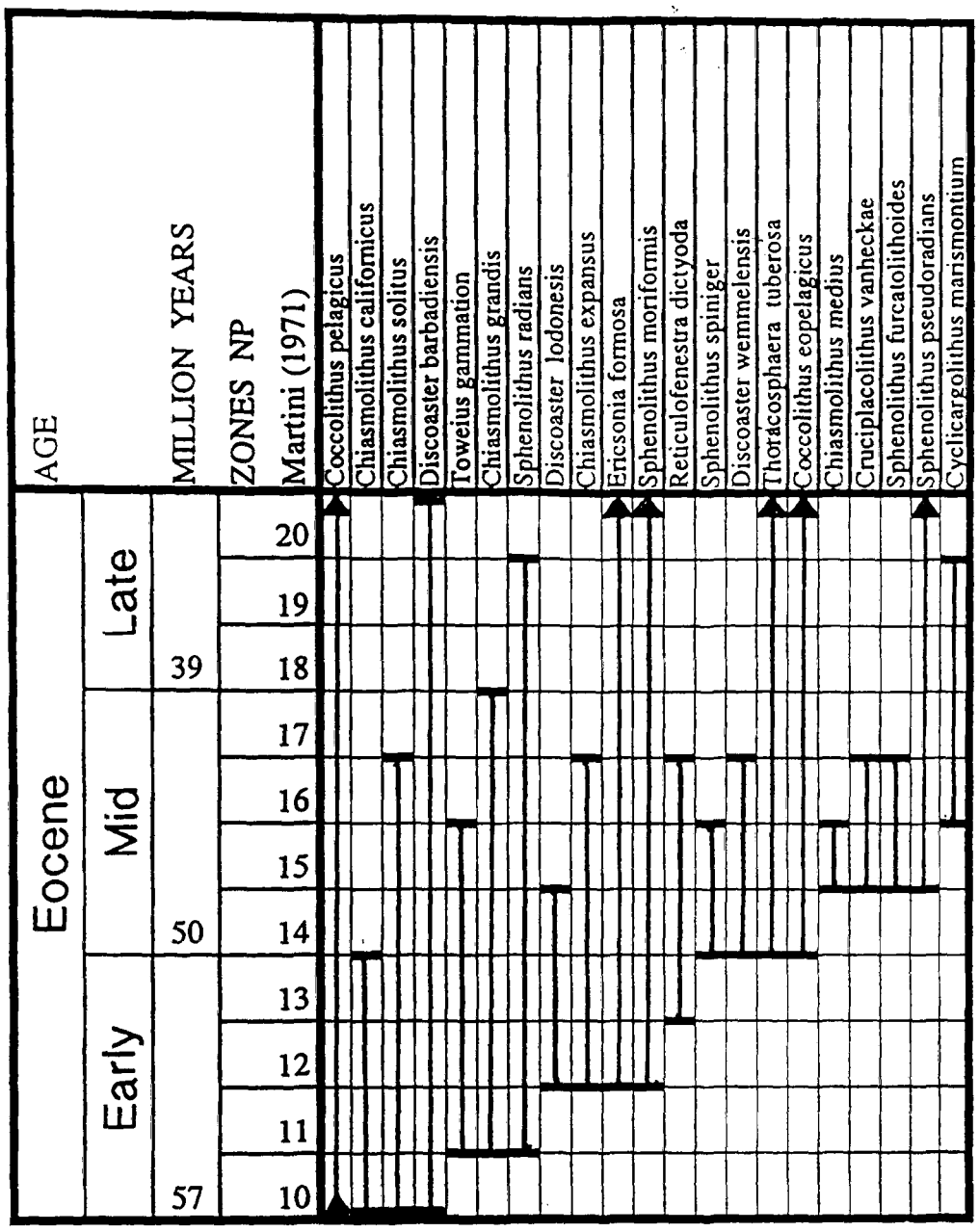

Notes
Dates have been rounded to nearest Ma (Harland et al., 1989).
The biostratigraphical ranges of individual species have been determined from various published sources (5.5. Systematics).

Fig. 5.10. The ranges of calcareous nannofossils observed in samples collected from the Eocene chalks of the Lefkara Formation, Middle Member, Chalk and Chert unit, of S.W. Cyprus.

Sample **D532 (ML1),** contains a common population, with a moderately diverse species content (Fig. 5.6). The combined presence of *Neochiastozygus perfectus* Perch-Nielsen, 1971a (NP4-NP6; Perch-Nielsen, 1985b), *Fasciculithus pileatus* Bukry, 1973a (NP5-NP9; Haq and Aubry, 1981) and *Fasciculithus tympaniformis* Hay and Mohler *in* Hay *et al.*, 1967 (NP5-NP9; Perch-Nielsen, 1985b), indicates a zonal range of NP5-NP6 (Fig. 5.9) for the assemblage.

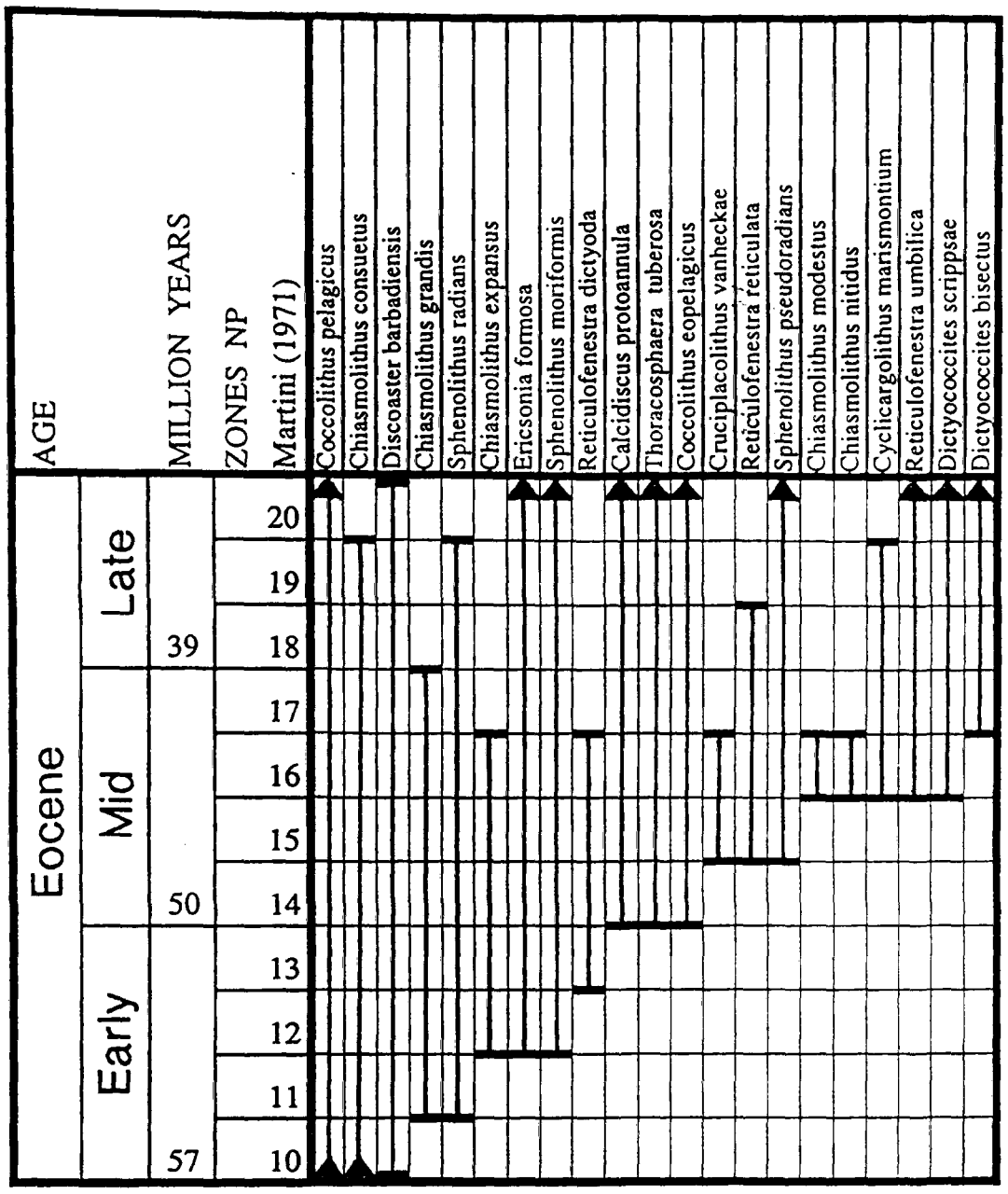

Notes
Dates have been rounded to nearest Ma (Harland et al., 1989).
The biostratigraphical ranges of individual species have been determined from various published sources (5.5. Systematics).

Fig. 5.11. The ranges of calcareous nannofossil species observed in samples collected from the Eocene chalks of the Lefkara Formation, Middle Member, Massive Chalk unit, in S.W. Cyprus.

Sample **D217 (ML2),** contains an abundant population, with a poor diverse species content (Fig. 5.6). The presence of *Z. bramlettei* indicates a zonal range of NP5-NP9 (Perch-Nielsen, 1985b) for the assemblage.

Based on above samples, the basal horizon of the mid Palaeocene Chalk and Chert unit, making unconformable contact with the underlying rocks, has an overall zonal range of NP5.

Discussion. The unconformity which is first reported here in S.W. Cyprus, with a biostratigraphical zonal range within NP5, corresponds with the conformable base of the Lower Lefkara Formation, Member II (planktonic foraminiferal zone P3a *Morozovella angulata;* Fig. 3.4) at Perapedhi (Krasheninnikov and Kaleda 1994; Fig. 12.1, p199), which is the lithological change from the underlying marls and clayey limestones of Member I to the calcarenites and rare cherts. It also corresponds with a similar unconformity reported by Baroz and Bizon (1977), between the base of the Chalk and Chert unit and the basement (planktonic foraminiferal zone P2 *Morozovella uncinata,* Fig. 3.4), seen against the northern margin of the Troodos Massif, near Aradiou village (Fig. 2.1).

5.3.1.2 Late Palaeocene

Sample **D246 (ML6),** contains a common population, with a high diversity of species content (Fig. 5.6). The presence of *Heliolithus riedelii* Bramlette and Sullivan, 1961 (NP8; Perch-Nielsen, 1985b) and *Fasciculithus alanii* Perch-Nielsen, 1971b (NP9; Perch-Nielsen, 1985b), indicates a zonal range at the NP8/NP9 boundary, for the assemblage (Fig. 5.9).

Sample **D535 (ML5),** has a sparse population of moderate diversity but sample **D134 (ML7),** has an abundant population with a high species diversity (Fig. 5.6). The combined presence of *Discoaster mohleri* Bukry and Percival, 1971 (NP7-NP9; Perch-Nielsen, 1985b) and *Discoaster multiradiatus* Bramlette and Riedel, 1954 (NP9-NP11; Perch-Nielsen 1985b), indicates a zonal range of NP9 (Fig. 5.9) for the assemblage.

Based on above samples, the basal horizon of the Late Palaeocene Chalk and Chert unit, making unconformable contact with the underlying rocks, has an overall zonal range at the NP8/NP9 boundary.

Discussion. The unconformity which is first reported here in S.W. Cyprus, with a biostratigraphical zonal range at the NP8/NP9 boundary, corresponds with the conformable base of the Lower Lefkara Formation, Member II, Bed 5 (planktonic foraminiferal zone, P5 *Morozovella velascoensis;* Fig. 3.4) at Perapedhi (Krasheninnikov and Kaleda 1994, Fig. 12.1, p199), this is the lithological change from the underlying grey marly limestone with layers of silicified white biomicritic limestones of Member II, Bed 4 to conchoidal and coarse-grained, biomicritic marls with silicified layers.

5.3.1.3 Outcrop pattern

The current outcrop pattern displayed (Fig. 5.1) for the individually dated Palaeocene unconformities, with a zonal range of NP5 and NP8/NP9, suggests that the southern Mamonia basement fragment continued to act as a structural high during deposition and/or post-depositional erosion of the Lefkara Formation, Middle Member. This pattern is similar to the pattern displayed by the emplacement of the Kathikas Formation (Swarbrick, 1993) and the overlying conformable Lefkara Formation Lower Member (chapter 4).

5.3.2 Lefkara Formation, Middle Member, Chalk and Chert unit (Eocene)

The samples collected from the Lefkara Formation, Middle Member (Chalk and Chert unit), contain in the main, a moderate to well preserved assemblages of calcareous nannofossils.

Sample **D237 (ML10),** contains an abundant population with a low diversity of species content (Fig. 5.7). The combined presence of *Chiasmolithus californicus* (Sullivan, 1961) (NP10-NP13; Perch-Nielsen, 1985b) and *Chiasmolithus expansus* (Bramlette and Sullivan, 1961) (NP12-NP13; Perch-Nielsen, 1985b), indicates a zonal range of NP12-NP13 (Fig. 5.10), for the assemblage.

Samples **D366 (ML9)** and **D235 (ML11),** contain a common population, with a moderately diverse species content (Fig. 5.7). The combined presence of *Discoaster lodoensis* Bramlette and Riedel, 1954 (NP12-NP14; Perch-Nielsen, 1985b) observed in both samples, *Coccolithus eopelagicus* (Bramlette and Riedel, 1954) (NP14-NP22; Bramlette and Riedel, 1954) observed in sample **D366** and *Discoaster wemmelensis* Achuthan and Stradner, 1969 (NP14-NP16; Perch-Nielsen, 1985b) observed in sample **D235,** indicate a zonal range of NP14 (Fig. 5.10), for both assemblages.

Sample **D371 (ML12),** contains an abundant population, with a moderately diverse species content (Fig. 5.7). The combined presence of *C. expansus* (NP10-NP13; Perch-Nielsen, 1985b) and *C. eopelagicus* (NP14-NP22; Bramlette and Riedel, 1954), indicates a zonal range of NP14-NP16 (Fig. 5.10), for the assemblage.

Samples **D240 (ML15)** and **D231 (ML14),** contain a sparse and common population respectively, with a moderately diverse species content (Fig. 5.7). The combined presence of *Sphenolithus furcatolithoides* Locker, 1967 (NP15-NP16; Perch-Nielsen, 1985b) and *Sphenolithus spiniger* Bukry, 1971 (NP14-NP15; Perch-Nielsen, 1985b) observed in sample **D240,** and the presence of *Chiasmolithus medius* Perch-Nielsen, 1971c (NP15; Perch-Nielsen, 1985b) observed in sample **D231,** indicates a zonal range of NP15 (Fig. 5.10), for both assemblages.

Samples **D576 (ML13)** and **D365 (ML8),** contain a sparse and common population, with a low and moderately diverse species content respectively (Fig. 5.7). The presence of *S. furcatolithoides* (NP15-NP16; Perch-Nielsen, 1985b) observed in sample **D576,** and the combined presence of *D. wemmelensis* (NP14-NP16; Perch-Nielsen, 1985b) and *Sphenolithus pseudoradians* Bramlette and Wilcoxon, 1967 (NP15-NP24; Perch-Nielsen, 1985b) observed in sample **D365,** indicates a zonal range of NP15-NP16, (Fig. 5.10), for both assemblages.

The basal horizon of the Eocene dated Chalk and Chert unit samples studied, from S.W. Cyprus, which make unconformable contact with the underlying rocks, are based on micropalaeontological data discussed above, and collectively have a zonal range of NP12 to NP15.

The current outcrop pattern for the Eocene dated Chalk and Chert unit unconformity, suggest there has been a structural low located in the south (Fig. 5.12), associated with the Mamonia basement terrane and southern fragment. Also coupled with the ?conformable Chalk and Chert unit, with the underlying Lefkara Formation, Lower Member reported by Gass *et al.* (1994), south-east of Pano-Panayia against the Troodos Massif, suggest that the bulk (northern portion) of the southern Mamonia basement fragment has again continued to act as a structural high, during deposition and/or post-depositional erosion.

When viewing the zonal ranges for the individual sample localities (Fig. 5.2,13), they appear to indicate the base of the Eocene dated Chalk and Chert unit is diachronous, from the centre (ML8; NP12-NP13) located at the northern edge of the outcrop, infilling a ?semi-circular structure from the north.

Discussion. Based on the biostratigraphical data above, the Eocene (zonal range NP12 to NP16) Chalk and Chert unit outcrop corresponds with the Middle Lefkara Formation sediments at Perapedhi (Krasheninnikov and Kaleda 1994, Fig. 12.1, p199). These sediments have a planktonic foraminifera zonal range of P9 to P11 and when correlated with the calcareous nannofossil zonal scheme (Fig. 3.4), the sediments have a zonal range of part NP13 to part NP15. This corresponds with the findings of Cockbain (*in* Bear, 1960; *in* Gass, 1960), relating to the Chalk and Chert unit which overlies the basement unconformably, against the northern margin of the Troodos Massif, and is Early to Mid Eocene.

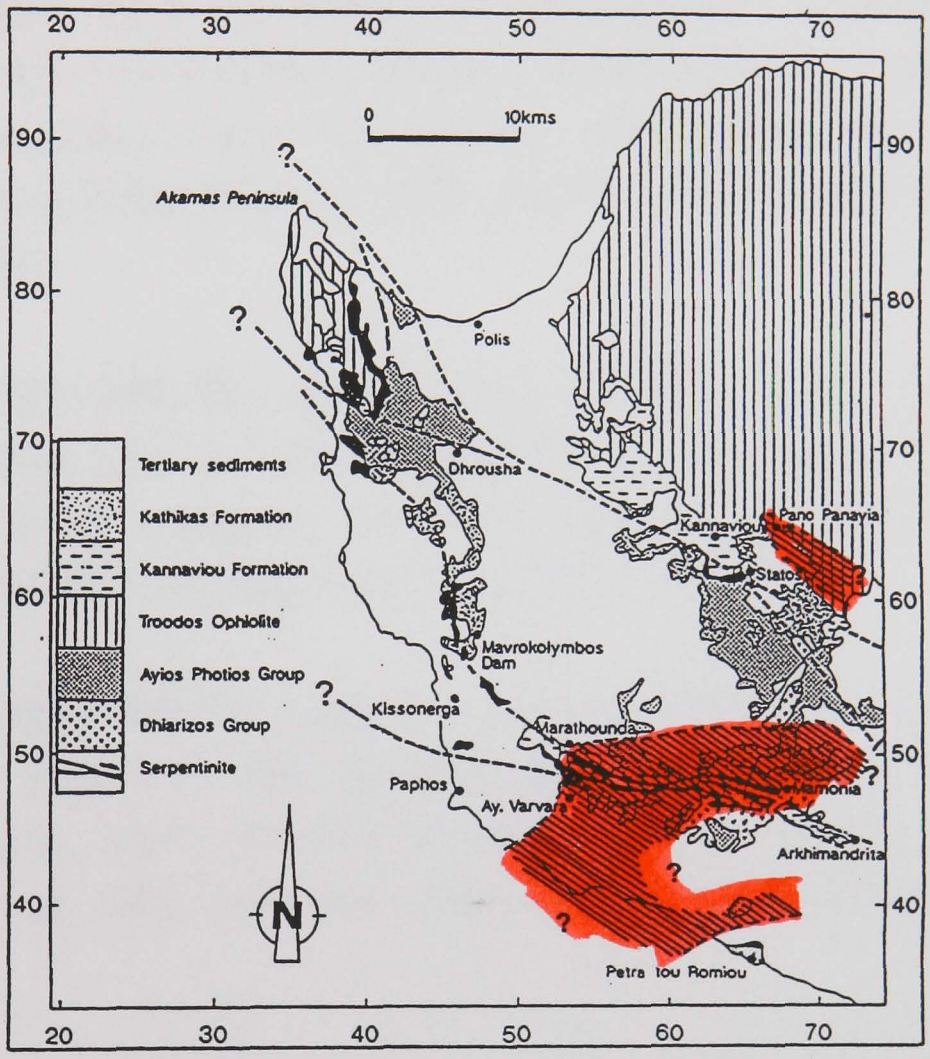

Fig. 5.12. General geological map of S.W. Cyprus, displaying the relationship between the major lineaments and the current outcrop pattern (cross-hatched area) of the Lefkara Formation, Middle Member, Chalk and Chert unit (Eocene) (modified from Swarbrick, 1980). N.B. Information obtained from Gass *et al.* (1994) and this study.

5.3.3 Lefkara Formation, Middle Member, Massive Chalk unit (Eocene)

The samples collected from the Lefkara Formation, Middle Member (Massive Chalk unit), contain poor to moderate preserved assemblages of calcareous nannofossils.

Samples **D219 (ML20), D226 (ML29), D227 (ML30), D236 (ML27), D266 (ML17), D273 (ML18), D351 (ML28), D368 (ML22)** and **D537 (ML26),** contain a sparse to common population, with a low to moderately diverse species content (Fig. 5.8). The combined presence of *Reticulofenestra dictyoda* (Deflandre *in* Deflandre and Fert, 1954) (NP13-NP16; Perch-Nielsen, 1985b) observed in samples **D236, D266** and **D273,** *Dictyococcites scrippsae* Bukry and Percival, 1971 (NP16-NN1; Lazarus *et al.*, 1995) observed in samples **D219, D266** and **D273,** *Chiasmolithus expansus* (Bramlette and Sullivan, 1961) (NP12-NP16; Perch-Nielsen, 1985b) observed in samples **D219** and **D364,** *Reticulofenestra umbilica* (Levin, 1965) (NP16-NP22; Perch-Nielsen, 1985b) observed in samples **D236** and **D364,** also the presence of *Chiasmolithus modestus* Perch-Nielsen, 1971c (NP16; Perch-Nielsen, 1985b) observed in samples **D351** and **D537** and *Chiasmolithus nitidus* Perch-Nielsen, 1971c (NP16; Perch-Nielsen, 1985b) observed in samples **D226, D227** and **D351,** indicate a zonal range of NP16 (Fig 5.11), for the assemblages.

Sample **D244 (ML25),** contains a sparse population, with a moderately diverse species content (Fig. 5.8). The combined presence of *C. expansus* (NP12-NP16; Perch-Nielsen, 1985b) and *D. scrippsae* (NP16-NN1; Lazarus *et al.*, 1995), indicates a zonal range at the NP16/NP17 boundary (Fig. 5.11), for the assemblage.

Sample **D264 (ML16),** contains a sparse population, with a low diversity of species content (Fig. 5.8). The combined presence of *Reticulofenestra reticulata* (Gartner and Smith, 1967) (NP15-NP18; Gallagher, 1989) and *D. scrippsae* (NP16-NN1; Lazarus *et al.*, 1995), indicates a zonal range of NP16-NP18 (Fig. 5.11), for the assemblage.

Sample **D274 (ML19),** contains a sparse population, with a moderately diverse species content (Fig. 5. 8). The presence of *Cyclicargolithus marismontium* (Black, 1964), indicates a zonal range of NP16-NP19 (Perch-Nielsen, 1985b), for the assemblage (Fig. 5.11).

Sample **D368 (ML22),** contains a common population, with a moderately diverse species content (Fig. 5.8). The combined presence of *R. reticulata* (NP15-NP18; Gallagher, 1989) and *Dictyococcites bisectus* (Hay, Mohler and Wade, 1966) (NP17-NN1; Lazarus *et al.*, 1995), indicates a zonal range of NP17-NP18 (Fig. 5.11), for the assemblage.

Samples **D224 (ML21)** and **D367 (ML23),** contain a sparse and common population respectively, with a moderately diverse species content (Fig. 5.8). The combined presence of *Sphenolithus radians* Deflandre in Grassé, 1952 (NP11-NP19, Perch-Nielsen, 1985b) and *D. bisectus* (NP17-NN1; Lazarus *et al.*, 1995), indicates a zonal range of NP17-NP19 (Fig. 5.11), for the assemblage.

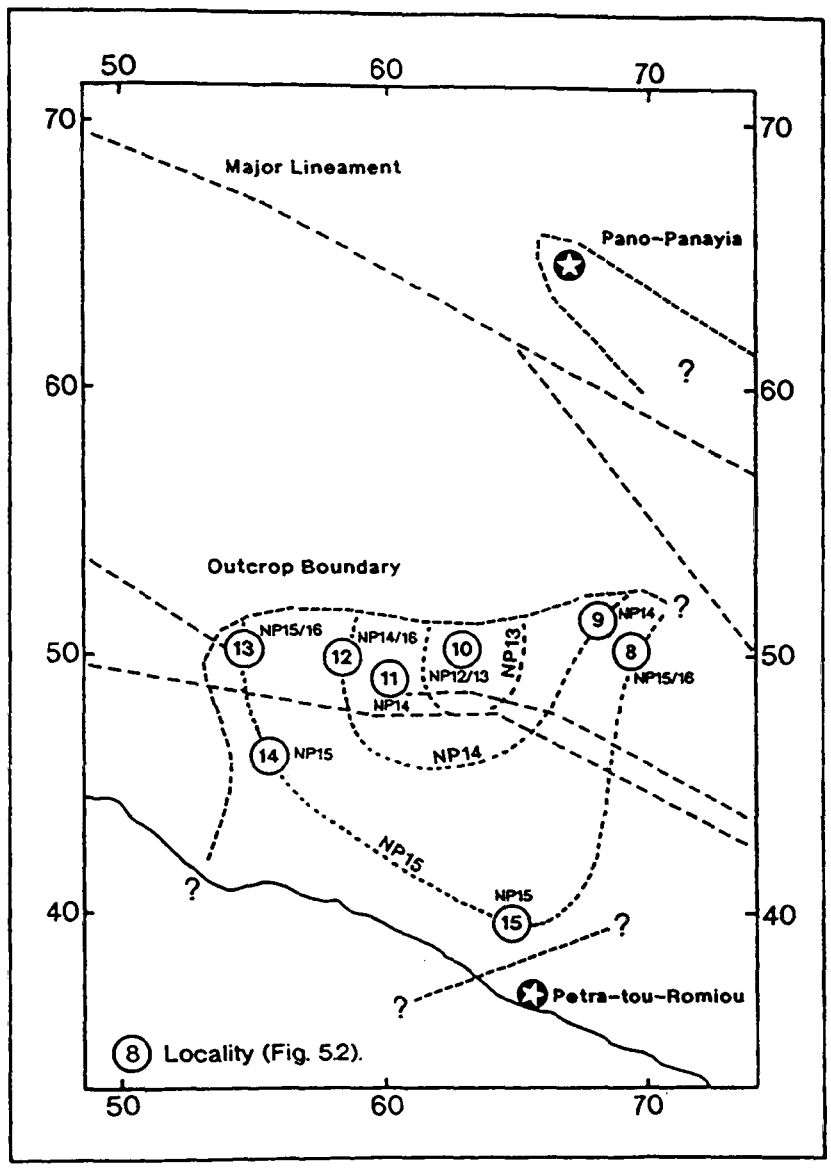

Fig. 5.13. A zonal range isopleth map (dotted lines), displaying the relationship with the outcrop pattern and the major lineaments, for the Lefkara Formation, Middle Member, Chalk and Chert unit (Early Eocene outcrop).

The samples studied from the basal horizon of the Eocene dated Massive Chalk unit, from S.W. Cyprus, which make ?conformable and unconformable contact with the underlying rocks, are based on micropalaeontological data discussed above, and collectively have a zonal range of NP16. However, samples **D224, D368** and **D367** have a collective zonal range of NP17-NP18, for a small localised outcrop (ML21, ML22 and ML23; Fig. 5.3), suggesting a localised structural high associated with the near by lineament, may have been present during deposition of the Massive chalk unit, or due to the presence of chalk talus masking the exposures, the localities may have been sampled further up the sedimentary sequence, from the contact.

The current outcrop pattern for the base of the Massive Chalk unit (Fig. 5.14), suggest there has been a structural low associated with the Mamonia and Troodos basement terranes and the southern portion of the southern Mamonia basement fragment, with the bulk of the fragment (northern portion), acting as a structural high, during deposition and/or post-depositional erosion.

ML26 (CGR 661 369). The samples were collected from the Massive Chalk unit, which forms part of a measured section (Fig. 5.5) at Petra-tou-Romiou (Fig. 5.3), unconformably overlying the Kannaviou Formation (?reworked) and terminating at the unconformable contact with the Pakhna Formation (basal Miocene). Samples **D487, D488, D489, D490** and **D537,** contain a sparse to common population, with a low to moderately diverse species content (Fig. 5.8). The age diagnostic species of *C. nitidus* (NP16; Perch-Nielsen, 1985b) observed in sample **D537** (Fig. 5.8), *R reticulata* (NP15-NP18; Gallagher, 1989) and *D. bisectus* (NP17-NN1; Lazarus *et al.*, 1995) observed in sample **D490,** indicate an overall zonal range of NP16-NP18 for the Massive Chalk unit at this locality.

Discussion. Based on the biostratigraphical data above, the Eocene (overall zonal range of NP16 to NP18) Massive Chalk unit outcrop corresponds with the Krasheninnikov and Kaleda (1994, Fig. 12.1, p199) Upper Lefkara Formation sediments. These sediments have a planktonic foraminifera zonal range of P12 to P17 and when correlated with the calcareous nannofossil zonal scheme (Fig. 3.4), the sediments have a zonal range of part NP15 to part NP21. Also the data corresponds with the findings of Cockbain (*in* Gass, 1960) and Mantis (*in* Pantazis, 1967), Late Eocene.

5.4 Summary

1). Age dated, the two newly recognised unconformable contacts in S.W. Cyprus, between the Lefkara Formation, Middle Member (Chalk and Chert unit) and the underlying rocks, with a relative biostratigraphical zonal range of NP5 and at the NP8/NP9 boundary, and can be correlated with the conformable boundaries reported by Krasheninnikov and Kaleda (1994) at Perapedhi.

2). Age dated the newly recognised diachronous unconformable contact in S.W. Cyprus, between the Lefkara Formation, Middle Member (Chalk and Chert unit) and the underlying rocks, with a relative biostratigraphical zonal range of NP12 to NP15,

infilling a ?semi-circular structural low, and the unit can be correlated with the conformable Middle Lefkara Formation of Krasheninnikov and Kaleda (1994) at Perapedhi.

3). Age dated, the unconformable contact in S.W. Cyprus, between the base of the Lefkara Formation, Middle Member (Massive Chalk unit) and the underlying rocks, with a relative biostratigraphical zonal range of NP16, and the unit can be correlated with the conformable Upper Lefkara Formation of Krasheninnikov and Kaleda (1994) at Perapedhi.

4). The Lefkara Formation, Middle Member (Massive Chalk unit) straddles the major lineaments (Fig. 5.14) and suggests there has been no major lateral movements along these lineaments since the onset of deposition (NP16).

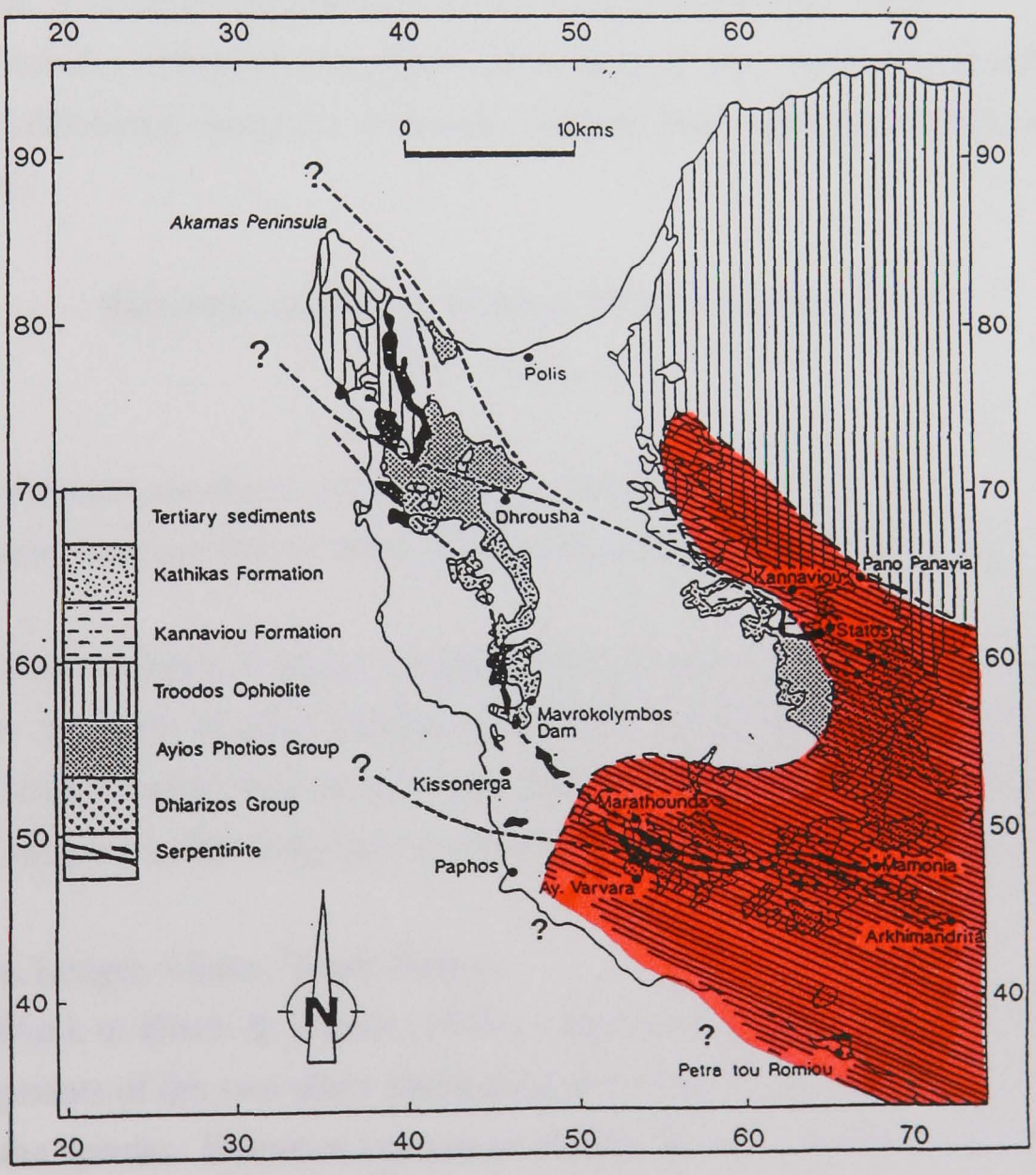

Fig. 5.14. General geological map of S.W. Cyprus, displaying the relationship between the major lineaments and the current outcrop pattern (cross-hatched area) of the Lefkara Formation, Middle Member, Massive Chalk unit (modified from Swarbrick, 1980).

5). The current outcrop patterns displayed in Figs 5.1,12,14 of the individual Lefkara Formation, Middle Member outcrops, suggest the southern Mamonia basement fragment has acted as a structural high during deposition and/or post-depositional erosion. The outcrop patterns also display similarity to the outcrop patterns of the Lefkara Formation, Lower Member (chapter 4) and also the Kathikas Formation (Swarbrick, 1993), by being restricted to the structural lows around the southern Mamonia basement fragment.

5.5 Systematic Descriptions

Family **Biscutaceae** Black, 1971a

Genus ***Biscutum*** Black *in* Black & Barnes, 1959

Type species. *Biscutum testudinarium* Black *in* Black & Barnes, 1959.
Remarks. Includes elliptical coccoliths, consisting of two appressed shields, made of radial, non-imbricated, petaloid elements. Central area open or closed with various constructions.

Biscutum castrorum Black *in* Black & Barnes, 1959
(Pl. 4, fig. 1)

1959 *Biscutum castrorum* Black *in* Black & Barnes: 326, pl. 10, fig. 2.

1990a *Biscutum castrorum* Black *in* Black & Barnes; Pospichal & Wise: 519, pl. 3, figs 1a-d.

Holotype. Black *in* Black & Barnes, sample 2833, locality Shudy Camp, Cambridge.
Description. Between crossed polars, with distal shield composed of radial petaloid elements. Closed central area with suture lines forms two inward pointing tooth-like projections, aligned to the long axis of ellipse and connected by the median extinction line.
Dimensions. Length 9.6μm: Width 8.0μm.
Remarks. Black *in* Black & Barnes (1959), considered the two unequal elliptical discs, with the segments of the two discs alternating and closely moulded, to be distinguishing features of the species. *Biscutum castrorum* differs from *B. constans* (Gorka, 1957), by having two inward pointing tooth-like projections, aligned to the long axis of the ellipse, between crossed polars.

Occurrence. During the project, the species is found at one locality in the Lefkara Formation (Middle Member, Chalk and Chert unit), at a quarry north of Dhrymou, near Kannaviou, S.W. Cyprus.
Range. Late Cretaceous, Black *in* Black & Barnes (1959). Upper Maastrichtian to Early Palaeocene, Pospichal & Wise (1990a).

Family **Coccolithaceae** Poche (1913)

Genus ***Calcidiscus*** Kamptner, 1950

Type species. *Calcidiscus quadriforatus* Kamptner, 1950.
Remarks. The genus includes circular coccoliths, with distal shield composed of single cycle of elements and larger than the simple proximal shield. Central area open or closed. Refer to Loeblich & Tappan (1978), who have provided a detailed review of the genus.

Calcidiscus protoannula (Gartner) Loeblich & Tappan, 1978
(Pl. 4, figs 2,3)

1971 *Cyclococcolithina protoannula* Gartner: 109, pl. 5, figs 1a-c,2.
1978 *Calcidiscus protoannula* (Gartner); Loeblich & Tappan: 1392.

Holotype. Gartner, pl. 5, figs 1a-c, JOIDES core J-6B, 251'.
Description. Between crossed polars, circular coccoliths, with a rim consisting of two cycles of elements. Inner cycle forms collar enclosing the large open central area, shows good birefringence. Outer rim cycle is less distinct.
Dimensions. Overall diameter 6.4μm: Central area 2.4μm diameter.
Remarks. Perch-Nielsen (1985b), considered the large central opening to be a distinguishing feature of the species. *Calcidiscus protoannula* is distinguished from *C. kingi* (Roth, 1970) by the central opening being greater than half the diameter of the whole coccolith.
Occurrence. The species is found at several localities, in the Lefkara Formation (Middle Member, Massive Chalk unit), in S.W Cyprus.
Range. Mid to Late Eocene (NP14 to NP20), Gartner (1971) and Perch-Nielsen (1985b).

Genus ***Chiasmolithus*** Hay, Mohler & Wade, 1966

Type species. *Tremalithus oamaruensis* Deflandre *in* Deflandre & Fert, 1954.

Remarks. The genus Includes elliptical coccoliths, whose distal shield is larger than proximal shield. The latter comprises two cycles of elements. Open central area bridged by a cross offset to the axes of the ellipse. In distal view, elements at distal margin of central area normally forms a crest and partially covers distal shield, in most species of the genus (Perch-Nielsen, 1985b).

Chiasmolithus californicus (Sullivan) Hay & Mohler, 1967
(Pl. 4, fig. 4)

1961 *Coccolithus* aff. *C. gigas* Bramlette & Sullivan: 140, pl. 1, figs 7a-d.

1964 *Coccolithus californicus* Sullivan: 180, pl. 2, figs 3a-b,4a-b.

1967 *Chiasmolithus californicus* (Sullivan); Hay & Molher: 1527, pl. 196, figs 18-20; pl. 198, fig. 5.

1978 *Chiasmolithus californicus* (Sullivan); Decima *et al.*: pl. 10, fig. 7.

Holotype. Sullivan, pl. 2, figs 3a-b, specimen 44411, slide A-7079, locality Media Agua Creek, California.

Description. Between crossed polars, large elliptical coccoliths, with broad distal outer rim. In distal view, elements forming distal margin to open central area do not form a crest. Central area bridged by oblique cross offset to axes of ellipse.

Dimensions. Length 14.4μm: Width 12.0μm.

Remarks. Perch-Nielsen (1985b), considered size (>12μm) and the elements that surround open central area that do not form a crest, plus the oblique bridging central cross, to be distinguishing features of the species. Between crossed polars, *Chiasmolithus californicus* is larger than *C. consuetus*, and differs from *C. medius* in lacking a crest.

Occurrence. During the project, the species is found at one locality in the Lefkara Formation (Middle Member, Chalk and Chert unit), at the base of a river section (Xeropotamos), east of Nata, S.W. Cyprus.

Range. Late Palaeocene to Early Eocene, Gartner (1970). Eocene (NP10 to NP13), Perch-Nielsen (1985b).

Chiasmolithus consuetus (Bramlette & Sullivan) Hay & Mohler, 1967
(Pl. 4, figs 5,6)

1961 *Coccolithus consuetus* Bramlette & Sullivan: 139, pl. 1, figs 2a-c.

1967 *Chiasmolithus consuetus* (Bramlette & Sullivan); Hay & Mohler: 1526, pl. 196, figs 23-25; pl. 198, fig. 16.

1992 *Chiasmolithus consuetus* (Bramlette & Sullivan); Siesser & Bralower: pl. 2, fig. 2.

Holotype. Bramlette & Sullivan, pl. 1, figs 2a-c (USNM 564178), sample 73, horizon Lodo formation, locality Frenso County, California.

Description. Between crossed polars, elliptical coccoliths, with broad distal outer rim. In distal view, elements forming distal margin to small open central area that do not form a crest. Central area bridged by oblique cross offset to axes of ellipse.

Dimensions. Length 9.6µm: Width 8.0µm.

Remarks. Perch-Nielsen (1985b) considered size (<12µm) and the elements surrounding open central area that do not form a crest, plus oblique central cross to be distinguishing features of *Chiasmolithus consuetus.*

Occurrence. The species is found at several localities in S.W. Cyprus, in the Lefkara Formation (Middle Member).

Range. Late Palaeocene to Mid Eocene (NP6 to NP19), Perch-Nielsen (1985b).

Chiasmolithus expansus (Bramlette & Sullivan) Gartner, 1970
(Pl. 4, fig. 17)

1961 *Coccolithus expansus* Bramlette & Sullivan: 139, pl. 1, figs 5a-d.

1970 *Chiasmolithus expansus* (Bramlette & Sullivan); Gartner: 943, pl. 11, figs 1,2a-b.

1992 *Chiasmolithus expansus* (Bramlette & Sullivan); Siesser & Bralower: pl. 2, fig. 18.

Holotype. Bramlette & Sullivan, pl. 1, figs 5a-d (USNM 564181), horizon Canoas Member, Kreyenhagen Formation, locality Oil City, California.

Description. Between crossed polars, large elliptical coccoliths with narrow distal shield. Elements forming distal margin of large central opening, form a crest that partially covers distal shield. Central area bridged by arching cross of thin construction, offset to axes of ellipse.

Dimensions. Overall, length 19.2µm, width 16.0µm: Central area, length 12.0µm, width 8.0µm.

Remarks. Perch-Nielsen (1985b), considered size (>17μm) and the elements surrounding open central area that form a crest, plus the arching central cross to be distinguishing features of the species. Between crossed polars, *Chiasmolithus expansus* differs from *C. grandis*, by the absence of four teeth located at the distal margin of the central area, oriented to the axes of the ellipse.

Occurrence. The species is found at several localities in S.W. Cyprus, in the Lefkara Formation (Middle Member Massive Chalk unit). The short vertical range of *Chiasmolithus expansus*, makes the species stratigraphically important.

Range. Early to Mid Eocene (NP12 to NP16), Perch-Nielsen (1985b).

Chiasmolithus grandis (Bramlette & Riedel) Radomski, 1968
(Pl. 4, fig. 18)

1954 *Coccolithus grandis* Bramlette & Riedel: 391, pl. 38, figs 1a-b.

1968 *Chiasmolithus grandis* (Bramlette & Riedel); Radomski: 560, pl. 44, figs 3,4.

1970 *Chiasmolithus grandis* (Bramlette & Riedel); Gartner: 944, pl. 11, fig. 3: pl. 14, figs 1-3.

1992 *Chiasmolithus grandis* (Bramlette & Riedel); Siesser & Bralower: pl. 3, fig. 2.

Holotype. Bramlette & Riedel, pl. 38, fig. 1a, locality Scripps Mid-Pacific Core No. 25 E-1

Description. Between crossed polars, large elliptical coccoliths with narrow distal shield. Elements forming distal margin of large central opening, form a crest that partially covers distal shield. Central area bridged by arching cross, offset to axes of ellipse and four teeth-like projections in inter-area between bridging cross.

Dimensions. Overall, length 23.2μm, width 20.0μm: Central area, length 14.4μm, width 10.4μm.

Remarks. Perch-Nielsen (1985b) considered size (>17μm), and four teeth-like projections located on the distal margin of central area, aligned to axes of ellipse to be distinguishing features of the species.

Occurrence. The species appears to be restricted to several localities in the south-west of the area, in the Lefkara Formation (Middle Member), in S.W Cyprus.

Range. Early to Mid Eocene (NP11 to NP17), Perch-Nielsen (1985b).

Chiasmolithus medius Perch-Nielsen, 1971c

(Pl. 4, figs 7,8)

1971c *Chiasmolithus medius* Perch-Nielsen: 18, pl. 11, fig. 4; pl. 12, fig. 7; pl. 14, fig. 10; pl. 60, figs 7,8.

Holotype. Perch-Nielsen, pl. 12, fig. 7 (KPN 2815), sample MMH 11532, locality Ørby, Denmark.

Description. Between crossed polars, elliptical coccoliths, with elements forming distal margin of central opening, that forms a crest that partially covers distal shield. Central area bridged by cross, offset to axes of ellipse.

Dimensions. Length 10.4μm: Width 8.0μm.

Remarks. Perch-Nielsen (1985b), considered the elements that surround open central area that form a crest, with oblique bridging cross, to be distinguishing features of the species.

Occurrence. The species appears to be restricted to several localities west of Nata in the Lefkara Formation (Middle Member, Chalk and Chert unit), in S.W Cyprus. The short vertical range of *Chiasmolithus medius*, makes the species stratigraphically important.

Range. Mid Eocene (NP15), Perch-Nielsen (1985b).

Chiasmolithus modestus Perch-Nielsen, 1971c

(Pl. 4, fig. 9)

1971c *Chiasmolithus modestus* Perch-Nielsen: 20, pl. 8, figs 1,2; pl. 11, figs 2,3; pl. 12, fig. 6; pl. 60, figs 21,22.

Holotype. Perch-Nielsen, pl. 8, fig. 1 (KPN 3538), sample MMH 11506, locality Ørby, Denmark.

Description. Between crossed polars, elliptical coccoliths, with elements forming distal margin of central opening, that form a crest that partially covers distal shield. Central area bridged by cross with perpendicular arms, offset to axes of ellipse.

Dimensions. Length 8.8μm: Width 7.2μm.

Remarks. Perch-Nielsen (1985b), considered elements that surround open central area, to form a narrow crest and the bridging cross with perpendicular arms, to be distinguishing features of the species. Between crossed polars *Chiasmolithus modestus* is distinguished from *C. altus* Bukry & Percival, 1971, by having a narrower crest.

Occurrence. The species is found at several localities in S.W. Cyprus, in the Lefkara Formation (Middle Member, Massive Chalk unit). The short vertical range of *Chiasmolithus modestus*, makes the species stratigraphically important.
Range. Mid Eocene (NP16), Perch-Nielsen (1985b).

Chiasmolithus nitidus Perch-Nielsen, 1971c
(Pl. 4, figs 10,11)

1971c *Chiasmolithus nitidus* Perch-Nielsen: 20, pl. 13, figs 5,6; pl. 60, figs 13,14.

1989 *Chiasmolithus nitidus* Perch-Nielsen; Firth: pl. 1, fig. 8.

Holotype. Perch-Nielsen, pl. 13, fig. 6 (KPN 4601), sample MMH 11538, locality Søvind, Denmark.
Description. Between crossed polars, elliptical coccoliths, with elements forming distal margin of large central opening, that do not form a crest. Central area bridged by cross with enlarged tips making contact with distal margin, offset to axes of ellipse. Two arms of the cross are offset at the centre and curve away towards the distal margin.
Dimensions. Length 6.8μm: Width 4.8μm.
Remarks. *Chiasmolithus nitidus* differs from *C. titus* Gartner, 1970, by having enlarged tips of central cross making contact with its distal margin. Perch-Nielsen (1985b), considered that the central area bridged by oblique cross, with enlarged tips making contact with distal central margin and two arms of the cross are offset at the centre and curve towards the distal margin, to be distinguishing features of the species.
Occurrence. The species appears to be restricted to several localities in the south-west of the area, in the Lefkara Formation (Middle Member, Massive Chalk unit), in S.W Cyprus. The short vertical range of *Chiasmolithus nitidus*, makes the species stratigraphically important.
Range. Mid Eocene (NP16), Perch-Nielsen (1985b).

Chiasmolithus solitus (Bramlette & Sullivan) Locker, 1968
(Pl. 4, figs 13,14)

1961 *Coccolithus solitus* Bramlette & Sullivan: 140, pl. 2, figs 4a-c.

1968 *Chiasmolithus solitus* (Bramlette & Sullivan); Locker: 222, pl. 1, figs 5,6.

1970 *Chiasmolithus solitus* (Bramlette & Sullivan); Gartner: 945, pl. 16, figs 1a-c,2.

1992 *Chiasmolithus solitus* (Bramlette & Sullivan); Siesser & Bralower: pl. 4, fig. 25.

Holotype. Bramlette & Sullivan, pl. 2, figs 4a-c (USNM 564187), sample 62, type horizon Lodo formation, locality Frenso County, California.

Description. Between crossed polars, elliptical coccoliths, with elements forming distal margin of large central opening, that form a crest. Central area bridged by cross offset to axes of ellipse. Two arms of the cross are offset at the centre and curve away towards distal margin.

Dimensions. Length 10.4μm: Width 8.8μm.

Remarks. *Chiasmolithus solitus* differs from *C. bidens* (Bramlette & Sullivan, 1961) by not having two teeth-like projections aligned to the short axis, projecting inwards from the distal margin of central area. However, this is not normally evident between crossed polars (Gartner, 1970), but the larger central opening and the more delicate nature of the oblique central cross make it easily distinguishable. Also differs from *C. titus* Gartner, 1970, by having a crest formed by elements surrounding open central area.

Occurrence. The species is restricted to only two localities in the south-west of the area, in the Lefkara Formation (Middle Member), in S.W Cyprus.

Range. Early to Mid Eocene (NP10 to NP16), Perch-Nielsen (1985b).

Genus ***Coccolithus*** Schwarz, 1894

Type species. *Coccosphaera pelagica* Wallich, 1877.

Remarks. Includes elliptical coccoliths, with distal shield comprising single cycle of elements. Elements at distal margin of open central area are radially oriented and do not form a crest above the distal surface. Bridging may be present, aligned to short axis. The genus tends to be used more in the Neogene, rather than in the Palaeogene were the genus *Ericsonia* is used (Perch- Nielsen, 1985b).

Coccolithus eopelagicus (Bramlette & Riedel) Bramlette & Sullivan, 1961

(Pl. 4, fig. 19)

1954 *Tremalithus eopelagicus* Bramlette & Riedel: 392, pl. 38, figs 2a-b.

1961 *Coccolithus eopelagicus* (Bramlette & Riedel); Bramlette & Sullivan: 139.

1966 *Coccolithus eopelagicus* (Bramlette & Riedel); Hay, Mohler & Wade: 385, pl. 1, fig. 1.

1992 *Coccolithus eopelagicus* (Bramlette & Riedel); Siesser & Bralower: pl. 2, fig. 16.

Holotype. Bramlette & Riedel, pl. 38, figs 2a-b, horizon Oceanic Formation, locality Bath, Barbados.

Description. Between crossed polars, large elliptical coccoliths, with a broad distal rim enclosing cycle of inclined irregular granules, forming distal margin of open central area. Central area in relation to overall size, long axis 56% and short axis 50% of total length, on average.

Dimensions. Overall length 18.4µm, width 10.4µm: Central area, length 16.0µm, width 8.0µm.

Remarks. *Coccolithus eopelagicus* in plane polarised light, is similar in appearance to *C. miopelagicus* Bukry, 1971, and *C. pliopelagicus* Wise, 1973, but can be distinguished in the former by the size of the central area in relation to its overall size (long axis 59% [50%], short axis 50% [42%] of total length, maximum) and in the latter by the overall size (>13µm). *C. eopelagicus* differs from *Toweius ?magnicrassus* (Bukry, 1971), by the elements at the distal margin of the open central area not forming a crest.

Occurrence. The species is found at almost all of the Eocene localities studied, in S.W. Cyprus, in the Lefkara Formation (Middle Member).

Range. Mid Eocene to Early Oligocene, Bramlette & Riedel (1954).

Coccolithus pelagicus (Wallich) Schiller, 1930

(Pl. 4, fig. 15; Pl. 8, fig. 1)

1877 *Coccosphaera pelagica* Wallich: 348, pl. 17, figs 1,2,5,11,12.

1930 *Coccolithus pelagicus* (Wallich); Schiller: 246, figs 123,124.

1973 *Coccolithus pelagicus* (Wallich); Roth: 730, pl. 1, fig. 1; pl. 4, figs 3,6.

Holotype. Wallich, pl. 17, figs 1,2,5,11,12 (line illustrations).

Description. Elliptical coccoliths, with distal shield of slightly dextral imbricating elements and inner cycle composed of irregular granules inclined inwards to small open central area.

Dimensions. Length 10.7µm: Width 8.7µm.

Remarks. *Coccolithus pelagicus* is similar in appearance to *C. eopelagicus* and *C. miopelagicus* Bukry, 1971, but is much smaller in size (<13µm). The species tends to used as a 'waste basket' for simple elliptical coccoliths of the Coccolithaceae.

Occurrence. The species is found at almost all of the Tertiary localities studied, in S.W. Cyprus, in the Lefkara, Pakhna and Nicosia (Myrtou Marls) Formations.

Range. Palaeocene to Holocene, Perch-Nielsen (1985b).

Genus ***Cruciplacolithus*** Hay & Mohler *in* Hay *et al.*, 1967

Type species. *Heliorthus tenuis* Stradner, 1961.

Remarks. *Cruciplacolithus* differs from *Chiasmolithus*, by having the orientation of the central cross or elements covering central area, whose extinction lines (between crossed polars) form a cross, are both aligned to axes of ellipse. In distal view, elements at the distal margin of the central area normally do not build a crest in most species of the genus, (Perch-Nielsen, 1985b).

Cruciplacolithus cribellum (Bramlette & Sullivan) Romein, 1979
(Pl. 4, fig. 12,16)

1961 *Coccolithites cribellum* Bramlette & Sullivan: 151, pl. 7, figs 5a-b,6a-b.

1979 *Cruciplacolithus cribellum* (Bramlette & Sullivan); Romein: 103.

1986 *Cruciplacolithus cribellum* (Bramlette & Sullivan); Perch-Nielsen: pl. 1, figs 9-11.

Holotype. Bramlette & Sullivan, pl. 7, 5a-b (USNM 564268), sample 46, horizon Lodo formation, locality Frenso County, California.

Description. Between crossed polars, all specimens display weak birefringence. Narrow outer rim enclosing closed (perforate) central area, with weak extinction lines visible forming cross aligned to axes of ellipse.

Dimensions. Length 8.8μm: Width 6.4μm.

Remarks. Bramlette & Sullivan (1961), considered the closed central area with several rows of perforations and the cross-shaped extinction lines between crossed polars to be distinguishing features of the species.

Occurrence. The species is restricted to three localities in the south-west of the area. Two localities north of Nikoklia in the Lefkara Formation (Middle Member, Chalk and Chert unit) and an unnamed horizon of locally reworked sediments (Miocene), in S.W Cyprus. The short vertical range of *Cruciplacolithus cribellum*, makes the species stratigraphically important.

Range. Early Eocene, Bramlette & Sullivan (1961). Late Palaeocene to Early Eocene (NP9 to NP11), Perch-Nielsen (1985b).

Cruciplacolithus frequens (Perch-Nielsen) Romein, 1979
(Pl. 5, fig. 1)

1977 *Chiasmolithus frequens* Perch-Nielsen: 746, pl. 18, figs 2,4; pl. 19, figs 1,3,5; pl. 50, figs 5,6.

1979 *Cruciplacolithus frequens* (Perch-Nielsen); Romein: 103, pl. 9, fig. 6.

Holotype. Perch-Nielsen, pl. 19, fig 3, sample 354-16-6, locality Ceará Rise, DSDP Site 354, South Atlantic Ocean.

Description. Between crossed polars, elliptical coccoliths, with distal shield of very weak birefringence, inner cycle of elements at distal margin of open central area having strong birefringence and not forming crest above distal shield. Central area bridged by cross slightly offset from axes of ellipse, having feet-like appendages with counter-clockwise orientation at tips of cross at distal margin of open central area.

Dimensions. Length 9.6μm: Width 7.2μm.

Remarks. *Cruciplacolithus frequens* is distinguished from *C. tenuis* by having the central cross slightly offset from axes of ellipse of up to 15° in counter-clockwise direction (Perch-Nielsen, 1977).

Occurrence. The species is restricted to one locality in the south-west of the area, at Petra-tou-Romiou, in the Lefkara Formation (Middle Member, Chalk and Chert unit), in S.W Cyprus. The short vertical range of *Cruciplacolithus frequens*, makes the species stratigraphically important.

Range. Late Palaeocene (NP6 to NP9), Perch-Nielsen (1985b).

Cruciplacolithus tenuis (Stradner) Hay & Mohler, 1967
(Pl. 5, fig. 2)

1961 *Heliorthus tenuis* Stradner: 84, figs 64,65.

1967 *Cruciplacolithus tenuis* (Stradner); Hay & Mohler: 1527, pl. 196, figs 29-31; pl. 198, figs 1,17.

1979 *Cruciplacolithus tenuis* (Stradner); Romein: 101.

Holotype. Stradner, sample HA 101/1/C, horizon Oberste Kreide (Danian), locality Haidhof bei Ernstbrunn, Niederösterreich, Häufig.

Description. Between crossed polars, elliptical coccoliths, with distal shield of very weak birefringence, inner cycle of elements at distal margin of open central area having strong birefringence and not forming crest above distal shield. Central area bridged by cross aligned to axes of ellipse, having feet-like appendages with counter-clockwise orientation at tips of cross.

Dimensions. Length 12.0μm: Width 10.4μm.

Remarks. Romein (1979), considered the central bridging cross aligned to axes of ellipse, with feet-like appendages at distal margin of open central area oriented counter-clockwise, to be distinguishing features of the species.

Occurrence. The species is found at almost all of the Palaeocene localities studied, in S.W. Cyprus, in the Lefkara Formation (Middle Member, Chalk and Chert unit).

Range. Mid to Late Palaeocene (NP3 to NP9) Perch-Nielsen (1985b).

Cruciplacolithus vanheckae Perch-Nielsen, 1986
(Pl. 5, fig. 3,4)

1986 *Cruciplacolithus vanheckae* Perch-Nielsen: 835, pl. 1, figs 1-8.

Holotype. Perch-Nielsen, pl. 1, figs 1,2, sample 356-9-2, locality DSDP Site 356, São Paulo Plateau, South Atlantic.

Description. Between crossed polars, elliptical coccoliths, with narrow outer rim of elements displaying weak birefringence with inner cycle of elements of strong birefringence and serrated appearance at distal margin of large closed central area.

Dimensions. Overall, length 9.6μm, width 7.2μm: Central area, length 7.2μ, width 4.8μm.

Remarks. Between crossed polars *Cruciplacolithus vanheckae* is distinguished from *C. cribellum* by having an inner cycle of elements with a serrated outline facing the centre (Perch-Nielsen, 1986).

Occurrence. The species is restricted to several localities in the south-west of the area, around Marathounda, in the Lefkara Formation (Middle Member), in S.W Cyprus. The short vertical range of *Cruciplacolithus vanheckae*, makes the species stratigraphically important.

Range. Mid Eocene (NP15 to NP16), Perch-Nielsen (1986).

Genus *Ericsonia* Black, 1964

Type species. *Ericsonia occidentalis* Black, 1964.

Remarks. *Ericsonia* differs from *Coccolithus* by having a proximal shield of two to three cycles of elements of different size, whereas in *Coccolithus* they are nearly of equal size. Open central area without distal margin of elements. The genus tends to be used more in the Palaeogene, rather than in the Neogene were the genus *Coccolithus* is used (Perch-Nielsen 1985b).

Ericsonia cava (Hay & Mohler) Perch-Nielsen, 1969
(Pl. 5, figs 5,6; Pl. 8, fig. 3)

1967 *Coccolithus cavus* Hay & Mohler: 1524, pl. 196, figs 1-3; pl. 197, figs 5,7,10,12.

1969 *Ericsonia cava* (Hay & Mohler); Perch-Nielsen: 61, pl. 2, figs 7,8.

1979 *Ericsonia cava* (Hay & Mohler);; Romein: 106, pl. 2, figs 4,5.

1992 *Ericsonia cava* (Hay & Mohler);; Siesser & Bralower: pl. 1, fig. 21.

Holotype. Hay & Mohler, pl. 197, fig. 12 (UI-N-2585), sample GAN 795, locality Pont Labau, near Pau, Basses Pyrenees, France.

Description. Between crossed polars, sub circular coccoliths with narrow distal shield of weak birefringence. Inner cycle of elements of strong birefringence at distal margin of open central area, forming slight crest covering distal shield.

Dimensions. Overall, length 8.8µm, width 8.0µm: Central area, length 5.6µm, width 4.8µm.

Remarks. Hay & Molher (1967), considered the unusually large central area and the 40-64 elements within the distal shield, to be distinguishing features of the species.

Occurrence. The species is found at almost all of the Palaeocene localities studied, in S.W. Cyprus, in the Lefkara Formation (Middle Member, Chalk and Chert unit).

Range. Palaeocene (NP2 to NP9), Hay & Mohler (1967).

Ericsonia formosa (Kamptner) Haq, 1971
(Pl. 5, figs 7,8)

1963 *Cyclococcolithus formosa* Kamptner: 163, fig. 20, pl. 2, fig. 8.

1971 *Ericsonia formosa* (Kamptner); Haq: 17, pl. 4, figs 7,8.

1992 *Ericsonia formosa* (Kamptner); Siesser & Bralower: pl. 20, fig. 20.

Holotype. Kamptner, pl. 2, fig. 8, sample 163, locality MP25-c (19°40'N, 174°16'W), Pacific Ocean.

Description. Between crossed polars, circular coccoliths with distal shield displaying weak birefringence and inner cycle of elements of similar width showing strong birefringence, forms distal margin of open central area and does not overlap the distal shield.

Dimensions. Diameter 9.6µm.

Remarks. Haq (1971), considered the open central area of circular coccolith lined on distal side by cycle of flat elements, to be distinguishing features of the species.

Occurrence. The species is found at almost all of the Eocene localities studied, in S.W. Cyprus, in the Lefkara Formation (Middle Member).
Range. Eocene to Early Oligocene (NP12 to NP21), Perch-Nielsen (1985b).

Ericsonia robusta (Bramlette & Sullivan) Perch-Nielsen, 1977
(Pl. 5, fig. 9)

1961 *Cyclolithus ?robustus* Bramlette & Sullivan: 141, pl. 2, figs 7a-c.

1977 *Ericsonia* cf. *E. robusta* (Bramlette & Sullivan); Perch-Nielsen: *partim,* pl. 16, figs 1,4,5; *non,* pl. 16, fig. 6; pl. 50, figs 34-35.

1977 *Ericsonia robusta* (Bramlette & Sullivan); Perch-Nielsen: *non,* pl. 16, figs 2,7; pl. 50, fig. 23.

1979 *Ericsonia robusta* (Bramlette & Sullivan); Romein: 108.

Holotype. Bramlette & Sullivan, pl. 2, 7a-c (USNM 564190), sample 7, type horizon Lodo formation, locality Frenso County, California.
Description. Between crossed polars, circular coccoliths with narrow distal shield in relation to broad inner cycle of flat elements forming margin to open central area, that almost cover the distal shield.
Dimensions. Overall diameter 6.4µm: Inner cycle diameter 4.0µm: Open central area 1.6µm.
Remarks. *Ericsonia robusta* is distinguished from *E. formosa* between crossed polars by the narrow distal shield and straight isogyrs displayed by the inner cycle of elements. Romein (1979), considered the inner cycle of elements that almost cover the distal shield to be a distinguishing feature of the species.
Occurrence. The species is found at almost all of the Palaeocene localities studied, in S.W. Cyprus, in the Lefkara Formation (Middle Member, Chalk and Chert unit).
Range. Mid to Late Palaeocene, Perch-Nielsen (1985b).

Ericsonia subpertusa Hay & Mohler, 1967
(Pl. 5, figs 10,11; Pl. 8, fig. 7)

1967 *Ericsonia subpertusa* Hay & Mohler: 1531, pl. 198, figs 11,15,18; pl. 199, figs 1-3.

1979 *Ericsonia subpertusa* Hay & Mohler; Romein: 106, pl. 2, fig. 6.

1992 *Ericsonia subpertusa* Hay & Mohler; Siesser & Bralower: pl. 5, fig 3.

Holotype. Hay & Mohler, pl. 198, fig. 18 (UI-H-2657), sample GAN 834, locality Pont Labau, near Pau, Basses Pyrenees, France.

Description. Between crossed polars, sub circular coccoliths with distal shield having weak birefringence, composed of elements inclined clockwise. Inner cycle having strong birefringence, appears to overlap the proximal margin of distal shield and enclosing open central area.

Dimensions. Diameter 8.0μm.

Remarks. Between crossed polars, *Ericsonia subpertusa* is similar to *E. formosa* and *E. robusta* but can be distinguished in the former by the inner cycle overlapping the proximal margin of the distal shield and in the latter, by not almost covering the distal shield.

Occurrence. The species is found at almost all of the Palaeocene localities studied, in S.W. Cyprus, in the Lefkara Formation (Middle Member, Chalk and Chert unit).

Range. Palaeocene (NP2 to NP9), Hay & Mohler (1967).

Family **Discoasteraceae** Tan Sin Hok, 1927

Genus ***Discoaster*** Tan Sin Hok, 1927

Type species. *Discoaster pentaradiatus* Tan Sin Hok, 1927.

Remarks. The genus includes rosette- or star-shaped nannoliths in plan view. In side view species can be either bi-convex, concavo-convex or plano-convex and all species show radial symmetry. Central boss and/or stem may be present on distal and/or proximal surface.

Discoaster barbadiensis Tan Sin Hok, 1927

(Pl. 5, fig. 8)

1927 *Discoaster barbadiensis* Tan Sin Hok: 415.

1954 *Discoaster barbadiensis* Tan Sin Hok; sens. *emend.* Bramlette & Riedel: 398, pl. 39, figs 5a-b.

1971c *Discoaster barbadiensis* Tan Sin Hok; Perch-Nielsen: 61, pl. 51, fig. 5.

1992 *Discoaster barbadiensis* Tan Sin Hok; Siesser & Bralower: pl. 1, fig. 7.

Description. In plane polarised light, rosette-shaped nannolith composed of normally eleven pointed rays joined along almost their length. In central area, rays bend in proximal direction and dextrally to form a stem.

Dimensions. Overall diameter 16μm.

Remarks. *Discoaster barbadiensis* is distinguished from *D. multiradiatus* by having less rays and the consistent presence of a stem. Bramlette & Riedel (1954), considered the concavo-convex disc with central stem on its concave surface, to be distinguishing features of the species.

Occurrence. The species is found at several localities in S.W. Cyprus, in the Lefkara Formation (Middle Member).

Range. Eocene (NP10 to NP20), Perch-Nielsen, (1985b).

Discoaster lodoensis Bramlette & Riedel, 1954
(Pl. 7, fig. 14)

1954 *Discoaster lodoensis* Bramlette & Riedel: 398, pl. 39, fig. 3.

1961 *Discoaster lodoensis* Bramlette & Riedel; Bramlette & Sullivan: 161, pl. 12, figs 4,5.

1971c *Discoaster lodoensis* Bramlette & Riedel; Perch-Nielsen: 64, pl. 52, fig. 2.

1990b *Discoaster lodoensis* Bramlette & Riedel; Pospichal & Wise: pl. 2, fig. 7.

Holotype. Bramlette & Riedel, pl. 39, fig. 3, horizon Lodo Formation, locality Lodo Gulch, Fresno County, California.

Description. In plane polarised light, star-shaped nannoliths, composed of normally six pointed rays which are free for two-thirds of their length and curving anticlockwise. The right side of each ray is thickened and continues as a curving suture line into central area.

Dimensions. Overall diameter 25.6μm.

Remarks. In poor specimens it is still possible to distinguish *Discoaster lodoensis* from *D. strictus* (Stradner, 1961) by the curved and offset thickness of the rays. The Six, rarely 5 or 7 curved rays tapering to points that have raised ridges offset from the median line, are considered by Bramlette & Riedel (1954), to be distinguishing features.

Occurrence. The species is restricted to several localities in the south-west of the area, in the Lefkara Formation (Middle Member, Chalk and Chert unit), in S.W Cyprus. The short vertical range of *Discoaster lodoensis*, makes the species stratigraphically important.

Range. Early to Mid Eocene, Bramlette & Sullivan (1961). Early Eocene (NP12 to NP14), Perch-Nielsen (1985b).

Discoaster mohleri Bukry & Percival, 1971
(Pl. 5, fig. 16; Pl. 8, fig. 2)

1971 *Discoaster mohleri* Bukry & Percival: 128, pl. 3, figs 3-5.

1979 *Discoaster mohleri* Bukry & Percival; Romein: 160, pl. 5, fig. 9.

1992 *Discoaster mohleri* Bukry & Percival; Siesser & Bralower: pl. 3, fig. 17.

Holotype. Bukry & Percival, pl. 3, fig. 3 (USNM 169192), locality DSDP core 47.2-9-6, Shatsky Rise, Pacific Ocean.

Description. In plane polarised light, rosette-shaped nannoliths, composed of normally 13 rays joined along their entire length, with broad rounded tips. No distinct central area or structure present.

Dimensions. Diameter 7.2μm to 14.0μm.

Remarks. *Discoaster mohleri* is distinguished from *D. gemmeus* Stradner, 1959, by having less imbrication of the rays and the presence of a median ridge. Bukry & Percival (1971), considered the straight rays with median ridge, no central structure and no free ray length to be distinguishing features of the species.

Occurrence. The species is found at almost all of the Late Palaeocene localities studied, in S.W. Cyprus, in the Lefkara Formation (Middle Member, Chalk and Chert unit). The short vertical range of *Discoaster mohleri*, makes the species stratigraphically important. It is also found in Mid Eocene chalks of the Lefkara Formation (Middle Member) and is considered to be reworked.

Range. Late Palaeocene (NP7 to NP9), Perch-Nielsen (1985b).

Discoaster multiradiatus Bramlette & Riedel, 1954
(Pl. 5, fig. 19)

1954 *Discoaster multiradiatus* Bramlette & Riedel: 396, pl. 38, fig. 10.

1992 *Discoaster multiradiatus* Bramlette & Riedel; Siesser & Bralower: pl. 3, fig. 19.

Holotype. Bramlette & Riedel, pl. 38, fig. 10, horizon Velasco shale, locality Estacion Velasco, nr. Tampico, Mexico.

Description. In plane polarised light, rosette-shaped nannoliths, composed of normally 28 rays joined along their entire length, with broad rounded tips. No distinct central area or structure present.

Dimensions. Diameter 16μm.

Remarks. In plane polarised light *Discoaster multiradiatus* can be distinguished from the morphologically similar upper Palaeocene *D. mohleri* by the greater number of rays present (>16). Bramlette & Riedel (1954), considered the large number of bluntly pointed rays producing a serrated margin and slightly depressed central surfaces, to be distinguishing features of the species.

Occurrence. The species is found at almost all of the Late Palaeocene localities studied, in S.W. Cyprus, in the Lefkara Formation (Middle Member, Chalk and Chert unit). The short vertical range of *Discoaster multiradiatus*, makes the species stratigraphically important. It is also found in Mid Eocene chalks of the Lefkara Formation (Middle Member) and is considered to be reworked.

Range. Late Palaeocene to Early Eocene (NP9 to NP11), Perch-Nielsen (1985b).

Discoaster wemmelensis Achuthan & Stradner, 1969
(Pl. 5, fig. 12)

1969 *Discoaster wemmelensis* Achuthan & Stradner: 5, fig. 2, pl. 4, figs 3,4.

Holotype. Achuthan & Stradner, pl. 4, figs 3,4, sample/preparation 26a, locality Wemmel, Belgium.

Description. In plane polarised light, small rosette-shaped nannoliths, composed of normally 24 rays, with rounded tips giving serrated outline and joined throughout their length. The central area contains a second cycle of elements, appressed to the proximal surface of the distal cycle with same number of elements.

Dimensions. Diameter 5.0μm.

Remarks. *Discoaster wemmelensis* closely resembles the form *D. lenticularis* Bramlette & Sullivan, 1961, in plane polarised light, however, the latter has a smaller cycle of elements appressed to the distal surface (Perch-Nielsen, 1985b). Achuthan & Stradner (1969), considered the 20-30 wedge-shaped rays that form a circular serrated outline, with slightly depressed central faces, to be distinguishing features of the species.

Occurrence. The species is found at several localities in S.W. Cyprus, in the Lefkara Formation (Middle Member, Massive Chalk unit). The short vertical range of *Discoaster wemmelensis*, makes the species stratigraphically important.

Range. Mid Eocene (NP14 to NP16) Perch-Nielsen (1985b).

Family **Fasciculithaceae** Hay & Mohler, 1967

Genus ***Fasciculithus*** Bramlette & Sullivan, 1961

Type species. *Fasciculithus involutus* Bramlette & Sullivan, 1961.

Remarks. The genus includes short cylinder-like nannoliths with proximal column composed of short rods, forming a concave proximal surface. A disc or lateral elements separate the column from distal cone. In end view, shows radial symmetry.

Fasciculithus alanii Perch-Nielsen, 1971b
(Pl. 5, fig. 13)

1971b *Fasciculithus alanii* Perch-Nielsen: 355, pl. 7, figs 1-3; pl. 9, fig. 4; pl. 14, figs 13,14.

1971b *Fasciculithus lillianae* Perch-Nielsen: *partim,* 353, pl. 6, fig 3, *non* pl. 6, fig. 1; pl. 14, figs 40-42.

1979 *Fasciculithus alanii* Perch-Nielsen; Romein: 153.

Holotype. Perch-Nielsen, pl. 9, fig. 4 (KPN 5309), MMH 11098, sample DSDP 119-27, locality Cantabria Seamount, Bay of Biscay.

Description. Between crossed polars, lateral view, long conical-shaped nannoliths with slightly concave outline and median extinction line present. Double convex proximal surface separated by extinction line.

Dimensions. Diameter 4.8μm: Length 5.6μm.

Remarks. *Fasciculithus alanii* can be distinguished from *F. lillianae* Perch-Nielsen, 1971b, which is smaller and the proximal part of the column is sub-parallel. Perch-Nielsen (1985b), considered the high conical shape with slightly concave sides to be distinguishing features of the species.

Occurrence. The species is found at almost all of the Late Palaeocene localities studied, in S.W. Cyprus, in the Lefkara Formation (Middle Member, Chalk and Chert unit). The short vertical range of *Fasciculithus alanii*, makes the species stratigraphically important. It is also found in Mid Eocene chalks of the Lefkara Formation (Middle Member) and is considered to be reworked.

Range. Late Palaeocene (NP9), Perch-Nielsen (1985b).

Fasciculithus clinatus Bukry, 1971

(Pl. 5, fig. 14)

1971 *Fasciculithus clinatus* Bukry: 318, pl. 4, figs 8,9.

Holotype. Bukry, pl. 4, figs 8,9 (USNM 176906), locality Shatsky Rise (DSDP 47.2-9-5), Pacific Ocean.

Description. Between crossed polars, lateral view, short conical-shaped nannoliths. Straight sides slightly convex, base line straight and top rounded to produce triangular outline bisected by a median extinction line.

Dimensions. Diameter 4.0μm: Length 4.0μm.

Remarks. *Fasciculithus clinatus* is distinguished from other species of *Fasciculithus* by its smallness in size and triangular outline. (Bukry, 1971).

Occurrence. The species is found at almost all of the Late Palaeocene localities studied, in S.W. Cyprus, in the Lefkara Formation (Middle Member, Chalk and Chert unit). The short vertical range of *Fasciculithus clinatus*, makes the species stratigraphically important. It is also found in Mid Eocene chalks of the Lefkara Formation (Middle Member) and is considered to be reworked.

Range. Late Palaeocene (NP7 to NP9), Perch-Nielsen (1985b).

Fasciculithus pileatus Bukry, 1973a

(Pl. 5, fig. 15)

1973a *Fasciculithus pileatus* Bukry: 307, pl. 1, figs 7-9; pl. 2, figs 1-5.

1981 *Fasciculithus stonehengei* Haq & Aubry: 301, pl. 1, figs 11-13.

1992 *Fasciculithus pileatus* Bukry; Siesser & Bralower: pl. 4, fig. 7.

Holotype. Bukry, pl. 2, figs 2-5 (USNM 188514), locality Caroline Abyssal Plain (DSDP199-10-2), western Pacific Ocean.

Description. Between crossed polars, lateral view, the nannoliths are composed of two slightly tapering columns proximally. Distally a curved rectangular (in outline) disc caps and slightly overlaps the proximal columns.

Dimensions. Diameter 7.2μm: Length 5.6μm.

Remarks. *Fasciculithus stonehengei* Haq and Aubry, 1981, and *F. merloti* Pavsic, 1977, are considered junior synonyms of *F. pileatus,* which differs from *F. janii* Perch-Nielsen, 1971b, a similar form by the apical disc not greatly overlapping the proximal column.

Occurrence. The species is found at almost all of the Palaeocene localities studied in S.W. Cyprus, in the Lefkara Formation (Middle Member, Chalk and Chert unit). It is also found in Mid Eocene chalks of the Lefkara Formation (Middle Member) and is considered to be reworked.

Range. Late Palaeocene (NP5 to NP9), Bukry (1973a); Haq & Aubry (1981).

Fasciculithus tympaniformis Hay & Mohler *in* Hay *et al.*, 1967
(Pl. 5, fig. 17)

1967 *Fasciculithus tympaniformis* Hay & Mohler *in* Hay *et al.*: 447, pl. 8, figs 1-5; pl. 9, figs 1-5.

1992 *Fasciculithus tympaniformis* Hay & Mohler *in* Hay *et al.*; Siesser & Bralower: pl. 5, fig. 10.

Holotype. Hay & Mohler, pl. 8, fig. 1 (UI-H-3731), sample GAN 822, locality Gan, Basses Pyrenees, France.

Description. Between crossed polars, in lateral view, the nannoliths are composed of two parallel columns, separated by median extinction line which bends to the right near the slightly domed distal surface. Proximal surface slightly concave

Dimensions. Diameter 8.0μm: Length 6.4μm.

Remarks. In phase contrast *Fasciculithus tympaniformis* is distinguished from *F. involutus* Bramlette & Sullivan, 1961, by its smooth finish (lacking depressions).

Occurrence. The species is found at almost all of the Late Palaeocene localities studied, in S.W. Cyprus, in the Lefkara Formation (Middle Member, Chalk and Chert unit). It is also found in Mid Eocene chalks of the Lefkara Formation (Middle Member) and is considered to be reworked.

Range. Late Palaeocene (NP5 to NP9), Perch-Nielsen (1985b).

Family **Heliolithaceae** Hay & Mohler, 1967

Genus ***Heliolithus*** Bramlette & Sullivan, 1961

Type species. *Heliolithus riedelii* Bramlette & Sullivan, 1961.

Remarks. The genus includes in plan view, circular coccoliths composed of two or three appressed discs, with same number of elements in each disc. Forming a cylindrical structure in side view, with the distal disc being the largest. Between crossed polars the whole of the structure is bright, whereas, in the genus *Bomolithus* Roth, 1973, only the central area appears bright.

Heliolithus cantabriate Perch-Nielsen, 1971a

(Pl. 6, fig. 1)

1971a *Heliolithus cantabriate* Perch-Nielsen: 55, pl. 2, figs 1,3,5,7; pl. 7, figs 33-36.

1979 *Heliolithus cantabriate* Perch-Nielsen; Romein: 156.

Holotype. Perch-Nielsen, pl. 2, fig. 1 (KPN 5080), sample MMH 11399, locality DSDP 119-32-2, Bay of Biscay.

Description. Between crossed polars, circular coccoliths of strong birefringence, with distal disc composed of radiating petaloid elements, with serrated edge. Normally the proximal column/disc is visible through the thin distal disc.

Dimensions. Distal diameter 7.2μm: Proximal diameter 5.6μm.

Remarks. *Heliolithus cantabriate* is distinguished from *H. kleinpelli* by having a proximal disc forming a column. Perch-Nielsen (1985b), considered the composition of three discs, with the proximal disc forming a column structure of perpendicular oriented elements to be distinguishing features of the species.

Occurrence. During the project, the species is found at one locality in the Lefkara Formation (Middle Member, Chalk and Chert unit), at Petra-tou-Romiou, S.W. Cyprus. The short vertical range of *Heliolithus cantabriate*, makes the species stratigraphically important.

Range. Late Palaeocene (NP6 to NP9), Perch-Nielsen (1985b).

Heliolithus kleinpelli Sullivan, 1964

(Pl. 6, fig. 17)

1964 *Heliolithus kleinpelli* Sullivan: 193, pl. 12, figs 5a-b.

1992 *Heliolithus kleinpelli* Sullivan; Siesser & Bralower: pl. 3, fig. 10.

Holotype. Sullivan, pl. 12, figs 5a-b, 44522, slide/sample A-7616, locality Simi Valley, California.

Description. Between crossed polars, large circular coccoliths of strong birefringence. Distal disc composed on average of 40 elements and proximal disc visible through thin distal disc. Extinction cross, straight arms, thin at centre but curve and flare distally.

Dimensions. Distal disc 15.2μm: Proximal disc 10.4μm.

Remarks. *Heliolithus kleinpelli* is distinguished from *H. cantabriae* and *H. riedelii* by having three discs of approximately the same thickness, but of different diameters. (Perch-Nielsen, 1985b).

Occurrence. During the project, the species is found at only one locality in the Lefkara Formation (Middle Member, Chalk and Chert unit), at Petra-tou-Romiou, S.W. Cyprus. The short vertical range of *Heliolithus kleinpelli*, makes the species stratigraphically important. It is also found in Mid Eocene chalks of the Lefkara Formation (Middle Member) and is considered to be reworked.

Range. Late Palaeocene (NP6 to NP9), Perch-Nielsen (1985b).

Heliolithus riedelii Bramlette & Sullivan, 1961

(Pl. 6, fig. 2)

1961 *Heliolithus riedelii* Bramlette & Sullivan: 164, pl. 14, figs 9a-c,10,11.

Holotype. Bramlette & Sullivan, pl. 14, figs 9a-c, 564380, sample 6+1", horizon Lodo Formation, locality Fresno County, California.

Description. Between crossed polars, circular coccoliths of strong birefringence, with distal disc of rough serrated outline, composed of on average 24 elements and proximal disc just visible through thinner distal disc.

Dimensions. Distal diameter 8.8μm: Proximal diameter 8.0μm.

Remarks. *Heliolithus riedelii* is distinguished from other members of the genus by having a rough serrated outline, with distal disc being slightly larger and thinner than proximal disc (Perch-Nielsen 1985b).

Occurrence. During the project, the species is found at one locality in the Lefkara Formation (Middle Member, Chalk and Chert unit), at Petra-tou-Romiou, S.W. Cyprus. The short vertical range of *Heliolithus riedelii*, makes the species stratigraphically important.

Range. Late Palaeocene (NP8), Perch-Nielsen (1985b).

Family **Prinsiaceae** Hay & Mohler, 1967

Genus ***Cyclicargolithus*** Bukry, 1971

Type species. *Coccolithus floridanus* Roth & Hay *in* Hay *et al.,* 1967.

Remarks. The genus includes circular to sub circular coccoliths, with distal shield slightly larger than proximal shield, joined by central tube. The Inner wall at distal

margin of open (not spanned by grid) or closed central area, does not rise above distal surface.

Cyclicargolithus floridanus (Roth & Hay *in* Hay *et al.*) Bukry, 1971
(Pl. 8, fig. 6)

1967 *Coccolithus floridanus* Roth & Hay *in* Hay *et al.*: 445, pl. 6, figs 1-4.

1970 *Cyclococcolithus floridanus* (Roth & Hay *in* Hay *et al.*); Roth: 854, pl. 5, fig. 6.

1971 *Cyclicargolithus floridanus* (Roth & Hay *in* Hay *et al.*); Bukry: 312.

1973 *Cyclicargolithus floridanus* (Roth & Hay *in* Hay *et al.*); Roth: 731, pl. 6, figs 2-4.

Holotype. Roth & Hay, pl. 6, fig. 1, sample IMS-J501-164, locality Blake Plateau, western Atlantic.

Description. Sub circular coccoliths, with distal shield composed of slightly dextrally imbricate elements, forming broad rim enclosing small open central area. Proximal margin of distal shield forms a depression, within lies a ring of disorientated, broad, irregularly shaped elements, surrounding central area.

Dimensions. Overall diameter 6.7μm: Central area 2.0μm.

Remarks. *Cyclicargolithus floridanus* is distinguished from *C. abisectus* (Müller, 1970), which is larger and the partial covering of elements surrounding central area are oriented more regularly. *C. marismontium* is elliptical and has larger central opening (Roth & Hay *in* Hay *et al.*, 1967).

Occurrence. During the project, the species is found at one locality in the Lefkara Formation (Middle Member, Massive Chalk unit), at Ayia Varvara, S.W. Cyprus.

Range. Late Eocene to Oligocene, Roth (1970). Late Eocene to Mid Miocene (NP20 to NN7), Lazarus, *et al.* (1995).

Cyclicargolithus marismontium (Black) Perch-Nielsen, 1985b
(Pl. 8, fig. 4)

1964 *Coccolithus marismontium* Black: 309, pl. 51, figs 1-4; pl. 52, fig. 3.

1985b *Cyclicargolithus marismontium* (Black); Perch-Nielsen: 539.

Holotype. Black, pl. 51, fig. 3, sample 11048, locality Muir Seamount, north-east of Bermuda.

Description. Elliptical coccoliths, composed of slightly dextrally imbricate elements, forming broad rim enclosing large elliptical open central area. Proximal margin of distal

shield forms a depression, within lies a ring of broad, radially arranged, polygonal elements.

Dimensions. Overall, length 6.0µm, width 5.3µm: Central area, length 2.0µm, width 1.0µm.

Remarks. Due to similarities between *Cyclicargolithus marismontium* (elliptical) and *C. floridanus* (sub-circular) it is probable that *C. marismontium* has been included in range charts as *C. floridanus* (Perch-Nielsen, 1985b).

Occurrence. The species is found at several localities in S.W. Cyprus, in the Lefkara Formation (Middle Member). The short vertical range of *Cyclicargolithus marismontium*, makes the species stratigraphically important.

Range. Mid Eocene (NP16 to NP19), Perch-Nielsen (1985b).

Genus ***Dictyococcites*** Black, 1967

Type species. *Dictyococcites danicus* Black, 1967.

Remarks. The genus includes elliptical to sub circular coccoliths, with distal shield slightly larger than proximal shield, joined at margin of large central area. The central area is spanned proximally by a grid and distally by elements radially arranged on inner wall, at distal margin of central area to form a crest, and the elements meet along the major axis of ellipse to form a slit.

Dictyococcites bisectus (Hay, Mohler & Wade) Bukry & Percival, 1971
(Pl. 6, figs 18,19; Pl. 8, fig. 5)

1966 *Syracosphaera bisecta* Hay, Mohler & Wade: *partim,* 393, pl. 10, figs 4-6.

1971 *Dictyococcites bisectus* (Hay, Mohler & Wade); Bukry & Percival: 127, pl. 2, figs 12,13.

Holotype. Hay, Mohler & Wade, pl. 10, fig. 4, sample U1-H-2094, horizon Nal 11, locality north-east of Nal' chik, north-west Caucasus.

Description. Large elliptical coccoliths, with distal shield composed of dextrally imbricate elements, forming broad rim. Central area covered with broad imbricate elements within multiple cycles, forming dome structure, elements meet at the centre to form a slit oriented to the major axis of ellipse.

Dimensions. Length 11.3µm: Width 9.3µm.

Remarks. *Dictyococcites bisectus* is the largest species of the genus (Perch-Nielsen, 1985b).

Occurrence. The species is found at several localities in S.W. Cyprus, in the Lefkara Formation (Middle Member, Massive Chalk unit).
Range. Late Eocene to Early Miocene (NP17 to NN1), Lazarus *et al.* (1995).

Dictyococcites scrippsae Bukry & Percival, 1971
(Pl. 6 fig. 3)

1971 *Dictyococcites scrippsae* Bukry & Percival: 128, pl. 2, figs 7,8.

Holotype. Bukry & Percival, pl. 2, figs 7,8 (USNM 169185), horizon Red Bluff Clay, locality Chickasawhay River, Shubuta, Mississippi.
Description. Between crossed polars, elliptical coccoliths, with serrated outline caused by blunt pointed elements of distal shield. Continuous extinction lines from outer rim to closed central area, where it bends sharply. In plane polarised light the elements sitting on distal surface, bridge the central area and meet along major axis to form a slit.
Dimensions. Length 8.0μm: Width 7.2μm.
Remarks. Between crossed polars *Dictyococcites scrippsae* is distinguished from *D. bisectus* by having a continuous extinction line from outer rim to central area and being smaller (Bukry & Percival, 1971).
Occurrence. The species is found at almost all of the Eocene localities studied, in S.W. Cyprus, in the Lefkara Formation (Middle Member).
Range. Late Eocene to Early Miocene (NP16 to NN1), Lazarus *et al.* (1995).

Genus *Reticulofenestra* Hay, Mohler & Wade, 1966

Type species. *Reticulofenestra caucasica* Hay, Mohler & Wade, 1966.
Remarks. The genus includes elliptical to sub circular coccoliths, with distal shield slightly larger than proximal shield, joined at margin of open central area. Inner wall at distal margin of central area does not rise above the distal surface, with central area spanned by a lacy network.

Reticulofenestra dictyoda (Deflandre *in* Deflandre & Fert) Stradner *in* Stradner & Edwards, 1968
(Pl. 6, figs 4,8)

1954 *Discolithus dictyodus* Deflandre *in* Deflandre & Fert: 140, *partim*, fig. 15, *non*, fig. 16.

1968 Non *Reticulofenestra dictyoda* (Deflandre *in* Deflandre & Fert); Stradner *in* Stradner & Edwards: 19, fig. 2c, pl. 12-14; pl. 22, fig. 4.

1989 *Reticulofenestra dictyoda* (Deflandre *in* Deflandre & Fert); Gallagher: 53, pl. 3.1, fig. 5.

1992 *Reticulofenestra dictyoda* (Deflandre *in* Deflandre & Fert); Siesser & Bralower: pl. 2, fig. 9.

Holotype. Deflandre *in* Deflandre & Fert, fig. 15, locality Donzacq, France.

Description. Between crossed polars, elliptical coccoliths, distal shield larger than proximal shield, composed of elements with blunt marginal points forming a serrated outline and broad rim enclosing small open central area.

Dimensions. Overall, length 8.8µm, width 8.0µm: Central area, length 2.4µm, width 1.6µm.

Remarks. Stradner *in* Stradner & Edwards (1968), describes the species in detail. However the illustrations are not of the species. Gallagher (1989), considered the size of the central area (25% of whole coccolith) that contains a grill which has long holes at the margin and irregular holes in the centre, to be distinguishing features of the species.

Occurrence. The species is found at almost all of the Eocene localities studied, in S.W. Cyprus, in the Lefkara Formation (Middle Member). The short vertical range of *Reticulofenestra dictyoda*, makes the species stratigraphically important.

Range. Mid Eocene (NP13 to NP16), Perch-Nielsen (1985b).

Reticulofenestra hillae Bukry & Percival, 1971

(Pl. 6, fig. 7)

1971 *Reticulofenestra hillae* Bukry & Percival: 136, pl. 6, figs 1-3.

1989 *Reticulofenestra hillae* Bukry & Percival; Gallagher: 57.

Holotype. Bukry & Percival, pl. 6, figs 1,2 (USNM 169215), horizon Shubuta Member of Yazoo Clay, locality Chickasawhay River, Shubuta, Mississippi USA.

Description. Between crossed polars, large elliptical coccoliths, with distal shield composed of many thin radial elements with marginal blunt points that form slight serrated outline, surrounding a large central opening.

Dimensions. Overall, length 12.8µm, width 9.8µm: Central area, length 4.8µm, width 4.0µm.

Remarks. *Reticulofenestra hillae* is smaller than (<14µm) *R. umbilicus* (Gallagher, 1989).

Occurrence. The species is restricted to several localities in the south-west of the area, in the Lefkara Formation (Middle Member, Massive Chalk unit), in S.W Cyprus.
Range. Late Eocene to Early Oligocene (NP17 to NP22), Perch-Nielsen (1985b).

Reticulofenestra reticulata (Gartner & Smith, 1967) Roth & Thierstein, 1972
(Pl. 6, figs 5,6)

1967 *Cyclococcolithus reticulatus* Gartner & Smith: 4, pl. 5, figs 1-4a-d.

1971c *Cribrocentrum reticulata* (Gartner & Smith); Perch-Nielsen: 28, pl. 25, figs 4-9.

1972 *Reticulofenestra reticulata* (Gartner & Smith); Roth & Thierstein: 436.

1989 *Reticulofenestra reticulata* (Gartner & Smith); Gallagher: 63, pl. 3.3, figs 7-11.

1991 *Reticulofenestra reticulata* (Gartner & Smith); Wei & Thierstein: pl. 5, figs 2-4.

Holotype. Gartner & Smith, pl. 5, fig. 2, horizon Yazoo Formation, locality Louisiana, USA.
Description. Between crossed polars, circular coccoliths, with distal shield showing strong birefringence, composed of radial elements that terminate at distal margin with rounded points and forms broad rim. Open central area is rectangular in shape with distinctive diagonal extinction cross, caused by the thin lacy network covering.
Dimensions. Overall diameter 6.4μm: Central area 2.0μm square.
Remarks. Between crossed polars, *Reticulofenestra reticulata* is distinguished from a similar form *R. dictyoda* by being circular and having a diagonal extinction cross in central area (Gallagher, 1989).
Occurrence. The species is found at several localities in S.W. Cyprus, in the Lefkara Formation (Middle Member, Massive Chalk unit). The short vertical range of *Reticulofenestra reticulata* makes the species stratigraphically important.
Range. Mid to Late Eocene, (NP15 to NP18), Gallagher (1989).

Reticulofenestra umbilica (Levin) Martini & Ritzkowski, 1968
(Pl. 6, fig. 20)

1965 *Coccolithus umbilicus* Levin: 265, pl. 41, fig. 2.

1968 *Reticulofenestra umbilica* (Levin); Martini & Ritzkowski: 245, pl. 1, figs 11,12.

1989 *Reticulofenestra umbilicus* (Levin); Gallagher: 66, pl. 3.1, figs 1,3,4; pl. 3.3, figs 2,5,9.

1992 *Reticulofenestra umbilica* (Levin); Siesser & Bralower: pl. 5, fig. 11.

Holotype. Levin, pl. 41, fig. 2, sample 27-A, 42.6-109.5, WUMC 000023, horizon Yazoo Formation, locality Yazoo City, Mississippi, USA.

Description. Between crossed polars, large elliptical coccoliths, with distal shield composed of many thin radial elements with marginal blunt points that form a slight serrated outline. Large open central area.

Dimensions. Overall, length 16.0μm, width 14.4μm: Central area, length 6.4μm, width 4.8μm.

Remarks. Gallagher (1989), considered the size of the area spanned by lacy network, of 70% of the total coccolith area, to be a distinguishing feature of the species.

Occurrence. The species is found at several localities in S.W. Cyprus, in the Lefkara Formation (Middle Member, Massive Chalk unit).

Range. Mid Eocene to Early Oligocene (NP16 to NP22), Perch-Nielsen (1985b).

Genus ***Toweius*** Hay & Mohler, 1967

Type species. *Toweius craticulus* Hay & Mohler, 1967.

Remarks. The genus includes circular to sub circular coccoliths, with distal shield slightly larger than the double proximal shield, joined at open central area. Inner double wall of elements at distal margin of open central area forms a large crest that part covers distal surface. Central area may be bridged by coarse grid. Between crossed polars, proximal shield displays good birefringence, whereas, distal shield is slightly indistinct.

Toweius gammation (Bramlette & Sullivan) Romein, 1979
(Pl. 6, fig. 9)

1961 *Coccolithus gammation* Bramlette & Sullivan: 152, pl. 7, figs 7a-c,14a-b.

1979 *Toweius gammation* (Bramlette & Sullivan); Romein: 126, pl. 4, figs 4,5.

1992 *Toweius gammation* (Bramlette & Sullivan); Siesser & Bralower: pl. 2, fig. 23.

Holotype. Bramlette & Sullivan, pl. 7, figs 7a-c (USNM 564271), sample 46, horizon Lodo formation, locality Frenso County, California.

Description. Between crossed polars, both shields are indistinct with central area showing stronger birefringence and extinction cross in shape of a swastika. Distal shield and central wall cycle composed of on average 56 elements, with the central area closed.

Dimensions. Overall diameter 11.2μm: Central area (inner wall) diameter 8.0μm.

Remarks. Perch-Nielsen (1985b), suggested that there is some doubt as to the generic assignment of the species which could belong to *Cyclagelosphaera*. Romein, (1979)

considered the absence of upper centro-distal cycle and proximal cycle of distal shield in recognising the species.

Occurrence. The species is found at several localities in S.W. Cyprus, in the Lefkara Formation (Middle Member, Chalk and Chert unit).

Range. Early to Mid Eocene (NP11 to NP15), Perch-Nielsen (1985b).

Family **Sphenolithaceae** Deflandre, 1952

Genus ***Sphenolithus*** Deflandre *in* Grassé, 1952

Type species. *Sphenolithus radians* Deflandre *in* Grassé, 1952

Remarks. The genus includes Nannoliths which have the form of a distal dome or cone/spine and proximal column with concave base. Proximal column/shield composed of radial arranged elements with triangular cross-section, capped distally by one or more cycles of lateral elements, radially arranged. Distally a dome structure of laterally arranged elements or apical spine of blade type elements that might bifurcate, is present.

Sphenolithus anarrhopus Bukry & Bramlette, 1969

(Pl. 6, fig. 10)

1969 *Sphenolithus anarrhopus* Bukry & Bramlette: 140, pl. 3, figs 5-8.

1979 *Sphenolithus anarrhopus* Bukry & Bramlette; Romein: 145.

Holotype. Bukry & Bramlette, pl. 3, figs 5-8 (USNM 651429), horizon JOIDES core 4, 150 to 153m, locality Blake Plateau, Atlantic Ocean.

Description. Between crossed polars, cone-shaped nannoliths. Proximally, composed of compact non-flaring column of elements. Distally the apical spine (not visible when viewed at 0°) is asymmetric when viewed at 45°

Dimensions. Diameter 4.8μm: Height 5.2μm.

Remarks. The only other Palaeocene species *S. primus* lacks the apical spine. Perch-Nielsen (1985b), considered the large asymmetrical apical spine to a distinguishing feature of the species.

Occurrence. The species is found at several localities in S.W. Cyprus, in the Lefkara Formation (Middle Member, Chalk and Chert unit).

Range. Late Palaeocene to Early Eocene (NP6 to NP10), Perch-Nielsen (1985b).

Sphenolithus furcatolithoides Locker, 1967
(Pl. 6, fig. 11)

1967 *Sphenolithus furcatolithoides* Locker: 363, figs 7,8, pl. 1, figs 14-16.

1979 *Sphenolithus furcatolithoides* Locker; Romein: 146.

1992 *Sphenolithus furcatolithoides* Locker; Siesser & Bralower: pl. 2, fig. 22.

Holotype. Locker, pl. 1, fig. 14.

Description. Between crossed polars, cone-shaped nannoliths in side view. Proximally, composed of compact non-flaring short column of elements. Distally the apical spine with median extinction line starts to bifurcate. However, due to delicate construction of the diverging arms they tend to be missing.

Dimensions. Diameter 4.8μm: Length 5.2μm (diverging portion missing).

Remarks. *Sphenolithus furcatolithoides* is distinguished from other Eocene species by having a bifurcating apical spine, and is distinguished from the Late Oligocene to Early Miocene form *S. capricornutus* Bukry & Percival, 1971, by having a smaller angle between the diverging spines, Perch-Nielsen (1985b).

Occurrence. The species is restricted to several localities in the south-west of the area, in the Lefkara Formation (Middle Member, Chalk and Chert unit), in S.W Cyprus. The short vertical range of *Sphenolithus furcatolithoides*, makes the species stratigraphically important.

Range. Mid Eocene (NP15 to NP16), Perch-Nielsen (1985b).

Sphenolithus moriformis (Bronnimann & Stradner) Bramlette & Wilcoxon, 1967
(Pl. 6, fig. 12)

1960 *Nannoturbella moriformis* Bronnimann & Stradner: 368, figs 11-16.

1967 *Sphenolithus moriformis* (Bronnimann & Stradner); Bramlette & Wilcoxon: 124, pl. 3, figs 1-6.

1992 *Sphenolithus moriformis* (Bronnimann & Stradner); Siesser & Bralower: pl. 3, fig. 18.

Holotype. Bronnimann & Stradner, figs 11-13,16, sample Präp, BR/538/1 T, horizon Alkazar Formation, locality Reporto Capri, near Arroyo Naraujo, Cuba.

Description. Between crossed polars, dome-shaped nannoliths in side view. Proximally, comprising a slightly flaring column of radial arranged elements, and distally a dome structure is present, both having median extinction lines and separated by a median extinction line, forming a cross.

Dimensions. Maximum overall length 4.8μm.

Remarks. Between crossed polars, it is sometimes difficult to distinguish several Palaeogene and Neogene dome-shaped sphenoliths from one another.

Occurrence. The species is found at almost all of the Eocene localities studied, in S.W. Cyprus, in the Lefkara (Middle Member) and Pakhna Formations.

Range. Mid Eocene to Mid Miocene (NP12 to NN9), Perch-Nielsen (1985b).

Sphenolithus primus Perch-Nielsen, 1971a
(Pl. 6, fig. 13)

1971a *Sphenolithus primus* Perch-Nielsen: 357, pl. 11, fig. 4; pl. 12, figs 4,5,7-12; pl. 14, figs 22-24.

1979 *Sphenolithus primus* Perch-Nielsen; Romein: 145.

Holotype. Perch-Nielsen, pl. 12, fig. 7 (KPN 5277), MMH 11124, locality DSDP 119-37, Bay of Biscay.

Description. Between crossed polars, dome-shaped nannoliths. Proximally, comprising a column of radial arranged elements, and distally a dome structure is present, both having median extinction line and separated by a median extinction line, forming a cross.

Dimensions. Maximum overall length 4.8μm.

Remarks. Between crossed polars *Sphenolithus primus* is distinguished from *S. moriformis* by having a more cylindrical proximal column.

Occurrence. The species is found at almost all of the Palaeocene localities studied, in S.W. Cyprus, in the Lefkara Formation (Middle Member, Chalk and Chert unit).

Range. Late Palaeocene to Early Eocene (NP5 to NP11), Perch-Nielsen (1985b).

Sphenolithus pseudoradians Bramlette & Wilcoxon, 1967
(Pl. 6, figs 14,15)

1967 *Sphenolithus pseudoradians* Bramlette & Wilcoxon: 126, pl. 2, figs 12-14.

1992 *Sphenolithus pseudoradians* Bramlette & Wilcoxon; Xu & Wise: pl. 2, fig. 3.

Holotype. Bramlette & Wilcoxon, pl. 2, figs 12-14 (USNM 650671), sample TT193785 (Bolli material), locality Cipero section, Trinidad, West Indies.

Description. Between crossed polars, cone-shaped nannoliths. Proximally, comprising of low cylindrical column of radially arranged elements, capped distally by lateral elements. Distally, long broad apical spine with median extinction line.

Dimensions. Diameter 4.8μm: Length 8.8μm.

Remarks. *Sphenolithus pseudoradians* is distinguished from *S. radians* in having broader blades forming the apical spine.

Occurrence. The species is found at several localities in S.W. Cyprus, in the Lefkara Formation (Middle Member), in S.W Cyprus.

Range. Mid Eocene to Early Oligocene (NP15 to NP24), Perch-Nielsen (1985b).

Sphenolithus radians Deflandre *in* Grassé, 1952

(Pl. 6, fig. 16)

1952 *Sphenolithus radians* Deflandre *in* Grassé: 466, fig. 343, J-K; fig. 363, A-G.

1979 *Sphenolithus radians* Deflandre *in* Grassé; Romein: 146, pl. 7, fig. 9.

1992 *Sphenolithus radians* Deflandre *in* Grassé; Siesser & Bralower: pl. 4, fig. 16.

Holotype. Deflandre *in* Grassé, fig. 363, F-G, locality Donzacq, France.

Description. Between crossed polars, cone-shaped nannoliths. Proximally, comprising of low cylindrical column of radially arranged elements, capped distally by lateral elements. Distally, long thin apical spine with median extinction line.

Dimensions. Diameter 4.0μm: Length 8.0μm.

Occurrence. The species is found at almost all of the Eocene localities studied, in S.W. Cyprus, in the Lefkara Formation (Middle Member).

Range. Eocene (NP11 to NP19), Perch-Nielsen (1985b).

Sphenolithus spiniger Bukry, 1971

(Pl. 7, figs 9,13)

1971 *Sphenolithus spiniger* Bukry: 321, pl. 6, figs 10-12; pl. 7, figs 1,2.

1979 *Sphenolithus spiniger* Bukry; Romein: 146.

Holotype. Bukry, pl. 6, figs 10-12 (USNM 176916), locality DSDP 44.0-4-6, horizon Horizon Ridge, Pacific Ocean

Description. Between crossed polars, cone-shaped nannoliths. Proximally, comprising a high slightly flaring column of radial arranged elements, and distally a shorter apical spine, both having median extinction lines and separated by a extinction line, forming a cross; proximal quadrants taller than distal quadrants.

Dimensions. Diameter 4.0μm: Length 4.4μm.

Remarks. Between crossed polars *Sphenolithus spiniger* can be distinguished from *S. orphankollensis* Perch-Nielsen, 1971a, by a more rounded outline.
Occurrence. The species is found at several localities in S.W. Cyprus, in the Lefkara Formation (Middle Member, Chalk and Chert unit). The short vertical range of *Sphenolithus spiniger*, makes the species stratigraphically important.
Range. Mid Eocene (NP14 to NP15), Perch-Nielsen (1985b).

Family **Thoracosphaeraceae** Schiller, 1930

Genus ***Thoracosphaera*** Kamptner, 1927

Type species. *Syracosphaera heimii* Lohmann, 1920.
Remarks. Thoracosphaerids are considered to be a calcareous dinoflagellates (Romein, 1979). They include hollow spherical and ovoid calcareous forms, composed of interlocking polygonal elements. An archaeopyle and operculum may be present.

Thoracosphaera operculata Bramlette & Martini, 1964
(Pl. 7, fig. 1)

1964 *Thoracosphaera operculata* Bramlette & Martini: 305, pl. 5, figs 3-7.
1979 *Thoracosphaera operculata* Bramlette & Martini; Romein: 182, pl. 1, fig. 1.
1984 *Thoracosphaera operculata* Bramlette & Martini; Steinmetz & Stradner: pl. 45, figs 7,8.

Holotype. Bramlette & Martini, pl. 5, 4,5 (USNM 648204), Alabama 2A, horizon McBryde Member, Clayton Formation, locality Livingston, Alabama, USA.
Description. Between crossed polars, spherical shells comprising elements of good birefringence, making irregular wall pattern. In some specimens an archaeopyle was observed but they all lacked an operculum.
Dimensions. Diameter 23.2μm.
Remarks. Due to the overall size of the spherical shells, there is insufficient resolution caused by the lack of depth of field, when viewing between crossed polars. However, the irregular wall pattern and good birefringence distinguishes the species.
Occurrence. The species is found at several localities in S.W. Cyprus, in the Lefkara Formation (Middle Member, Chalk and Chert unit).
Range. Late Cretaceous to Early Eocene, Perch-Nielsen (1985b).

Thoracosphaera tuberosa Kamptner, 1963
(Pl. 7, figs 2,3)

1963 *Thoracosphaera tuberosa* Kamptner: 179, pl. 4, fig. 26.

Holotype. Kamptner, pl. 4, fig. 26, sample 179, locality ST 61 (0° 6'S, 135° 58'W), Pacific Ocean.

Description. Between crossed polars, spherical shells comprising elements of poor birefringence, making an irregular wall pattern, archaeopyle or operculum were not observed in any of the specimens.

Dimensions. Diameter 20.0μm.

Remarks. Between crossed polars *Thoracosphaera tuberosa* is distinguished by the 'halo' effect, when the spherical outline is brought into focus.

Occurrence. The species is found at several localities in S.W. Cyprus, in the Lefkara Formation (Middle Member).

Range. Mid Eocene and Pliocene to Holocene, Perch-Nielsen (1985b).

Family **Zygodiscaceae** Hay & Mohler, 1967

Genus ***Neochiastozygus*** Perch-Nielsen, 1971a

Type species. *Neochiastozygus perfectus* Perch-Nielsen, 1971a.

Remarks. The genus includes elliptical coccoliths, characterised by rim comprised of two thin walls, constructed from inclined to vertical elements. Open central area bridged by cross offset to axes of ellipse.

Neochiastozygus distentus (Bramlette & Sullivan) Perch-Nielsen, 1971a
(Pl. 7, fig. 4)

1961 *Zygolithus distentus* Bramlette & Sullivan: 150, pl. 6, figs 4-7.

1971a *Neochiastozygus distentus* (Bramlette & Sullivan); Perch-Nielsen: 61, pl. 4, figs 1-4; pl. 7, figs 1-3.

Holotype. Bramlette & Sullivan, pl. 6, fig. 6a-d (USNM 564248), sample 22, horizon Lodo formation, locality Frenso County, California.

Description. Between crossed polars, elliptical coccoliths of high ellipticity, with broad rim enclosing small open central area, bridged by small cross, with arms formed of parallel blocks, offset to axes of ellipse.

Dimensions. Length 8.8μm: Width 5.6μm.

Remarks. Between crossed polars *Neochiastozygus distentus* differs from *N. perfectus* and *N. concinnus* (Martini, 1961) by having a broader rim, and central cross, and in the latter, the tips of the cross do not bifurcate. (Perch-Nielsen, 1985b).

Occurrence. The species is found at almost all of the Late Palaeocene localities in S.W. Cyprus, in the Lefkara Formation (Middle Member, Chalk and Chert unit). The short vertical range of *Neochiastozygus distentus*, makes the species stratigraphically important.

Range. Late Palaeocene to Early Eocene (NP8 to NP11), Perch-Nielsen (1985b).

Neochiastozygus modestus Perch-Nielsen, 1971a
(Pl. 7, figs 5,6)

1971a *Neochiastozygus modestus* Perch-Nielsen: 62, pl. 5, figs 5-8; pl. 7, figs 22,23.

1979 *Neochiastozygus modestus* Perch-Nielsen; Romein: 134.

Holotype. Perch-Nielsen, pl. 5, fig. 6 (KPN 6668), sample MMH 11425, locality Havalløse, Dänemark.

Description. Between crossed polars, elliptical coccoliths, with rim comprising of outer and inner wall, with the inner wall showing stronger birefringence. Open central area, bridged by cross, with arms formed of parallel blocks, offset to axes of ellipse.

Dimensions. Length 4.8μm: Width 4.0μm.

Remarks. Between crossed polars *Neochiastozygus modestus* is distinguished from *N. perfectus* by being smaller and coarser in appearence. (Perch-Nielsen, 1985b).

Occurrence. The species is found at several localities in S.W. Cyprus, in the Lefkara Formation (Middle Member, Chalk and Chert unit). The short vertical range of *Neochiastozygus modestus*, makes the species stratigraphically important.

Range. Early Palaeocene (NP3 to NP5), Perch-Nielsen (1985b).

Neochiastozygus perfectus Perch-Nielsen, 1971a
(Pl. 7, figs 7,11)

1971a *Neochiastozygus perfectus* Perch-Nielsen: 63, pl. 6, figs 1,2; pl. 7, figs 24,25.

1979 *Neochiastozygus perfectus* Perch-Nielsen; Romein: 135.

Holotype. Perch-Nielsen, pl. 6, fig. 2 (KPN 6681), sample MMH 11429, locality Sundkrogen, Hafen von Kopenhagen, Dänemark.

Description. Between crossed polars, elliptical coccoliths of high ellipticity, with rim comprising outer and inner wall, with the inner wall showing stronger birefringence. Open central area bridged by slender cross, offset to axes of ellipse and its acute angle aligned to short axis.

Dimensions. Length 7.2μm: Width 4.8μm.

Remarks. Perch-Nielsen (1985b), considered the central cross with acute angle aligned to the short axis of the ellipse, to be a distinguishing feature of the species.

Occurrence. The species is found at several localities in S.W. Cyprus, in the Lefkara Formation (Middle Member, Chalk and Chert unit). The short vertical range of *Neochiastozygus perfectus*, makes the species stratigraphically important.

Range. Mid Palaeocene (NP4 to NP6), Perch-Nielsen (1985b).

Genus ***Zygodiscus*** Bramlette & Sullivan, 1961

Type species. *Zygodiscus adamas* Bramlette & Sullivan, 1961.

Remarks. The genus includes elliptical coccoliths, characterised by rim comprised of two thin walls, constructed of inclined to vertical elements. Open central area bridged by I-shape crossbar aligned to short axis.

Zygodiscus bramlettei Perch-Nielsen, 1981

(Pl. 7, figs 8,12)

1981 *Zygodiscus bramlettei* Perch-Nielsen: 843, pl. 7, fig. 6.

Holotype. Perch-Nielsen, pl. 7, fig. 6 (KPN 6703), sample 6+1', horizon Lodo Formation, locality Frenso County, California, USA.

Description. Between crossed polars, elliptical coccoliths, with rim comprising outer and inner wall, the inner wall shows stronger birefringence. Open central area bridged by I- shape crossbar aligned to short axis.

Dimensions. Length 9.6μm: Width 7.2μm.

Remarks. Between crossed polars *Zygodiscus bramlettei* is distinguished from *Placozygus sigmoides* (Bramlette and Sullivan, 1961) by the I-shape crossbar not being sigmoidal in shape. (Perch-Nielsen, 1981).

Occurrence. The species is found at several localities in S.W. Cyprus, in the Lefkara Formation (Middle Member, Chalk and Chert unit).
Range. Mid to Late Palaeocene (NP5 to NP9), Perch-Nielsen (1985b).

Incertae sedis

Genus *Ellipsolithus* Sullivan, 1964

Type species. *Coccolithites macellus* Bramlette & Sullivan, 1961.
Remarks. The genus includes elliptical coccoliths with high ellipticity, with raised rim at proximal margin of thin distal shield, bordering open or closed central area.

Ellipsolithus macellus (Bramlette & Sullivan) Sullivan, 1964
(Pl. 7, fig. 10)

1961 *Coccolithites macellus* Bramlette &. Sullivan: 152, pl. 7, figs 11,12,13a-d.

1964 *Ellipsolithus macellus* (Bramlette & Sullivan); Sullivan: 184, pl. 5, figs 3a-b.

1979 *Ellipsolithus macellus* (Bramlette & Sullivan); Romein: 188.

1989 *Ellipsolithus macellus* (Bramlette & Sullivan); Firth: pl. 1, fig. 14.

Holotype. Bramlette & Sullivan, pl. 7, figs 13a-d (USNM 564273), sample 33, horizon Lodo formation, locality Frenso County, California.
Description. Between crossed polars, elliptical coccoliths of high ellipticity and good birefringence. Closed central area with narrow slit oriented to long axis of ellipse.
Dimensions. Length 11.2μm: Width 7.2μm.
Remarks. Due to the delicate nature of the specimens, the proximal shield is rarely preserved, also it is difficult to view in normal transmitted light. Bramlette & Sullivan (1961), considered the central area which is bisected by a narrow slit oriented to long axis of ellipse, to be a distinguishing feature of the species.
Occurrence. The species is found at several localities in S.W. Cyprus, in the Lefkara Formation (Middle Member, Chalk and Chert unit).
Range. Palaeocene to Early Eocene (NP4 to NP12), Perch-Nielsen (1985b).

PLATE 4.

Light photomicrographs

XPL = Crossed Polarised Light
PC = Phase Contrast Scale Bar = 5μm

Fig. 1. *Biscutum castrorum* Black *in* Black & Barnes, 1959, distal view, XPL, UD614-31, D276-1454.

Figs 2,3. *Calcidiscus protoannula* (Gartner, 1971), D229-1148: Fig. 2, distal view, XPL, UD615-23; Fig. 3. distal view, PC, UD615-22.

Fig. 4. *Chiasmolithus californicus* (Sullivan, 1964), distal view, XPL, UD624-25, D237-1052.

Figs 5,6. *Chiasmolithus consuetus* (Bramlette & Sullivan, 1961), D246-1179: Fig. 5, distal view, XPL, UD621-41A; Fig. 6, distal view, PC, UD621-0.

Figs 7,8. *Chiasmolithus medius* Perch-Nielsen, 1971c, D231-1153: Fig. 7, distal view, XPL, UD624-27; Fig. 8, distal view, PC, UD624-28.

Fig. 9. *Chiasmolithus modestus* Perch-Nielsen, 1971c, distal view, XPL, UD621-31A, D226-1143.

Figs 10,11. *Chiasmolithus nitidus* Perch-Nielsen, 1971c, D351-1050: Fig. 10, distal view, PC, UD615-40; Fig. 11, distal view, XPL, UD615-41.

Figs 12,16. *Cruciplacolithus cribellum* (Bramlette & Sullivan, 1961), D352-1429: Fig. 12, distal view, PC, UD614-41; Fig. 16, distal view, XPL, UD614-42.

Figs 13,14. *Chiasmolithus solitus* (Bramlette & Sullivan, 1961), D228-1141: Fig. 13, distal view, PC, UD624-30; Fig. 14, distal view, XPL, UD624-31.

Fig. 15. *Coccolithus pelagicus* (Wallich, 1877), distal view, XPL, UD613-16A, D226-1141.

Fig. 17. *Chiasmolithus expansus* (Bramlette & Sullivan, 1961), distal view, XPL, UD624-22A, D349-1433.

Fig. 18. *Chiasmolithus grandis* (Bramlette & Reidel, 1954), distal view, XPL, UD631-38, D229-1148.

Fig. 19. *Coccolithus eopelagicus* (Bramlette & Reidel, 1954), distal view, XPL, UD614-40, D348-1432 (ML26).

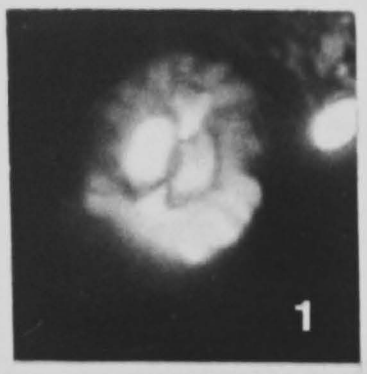
1

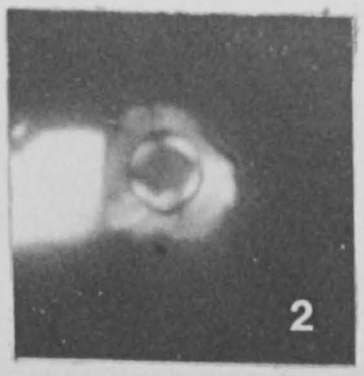
2

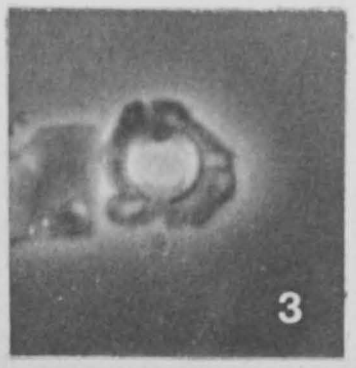
3

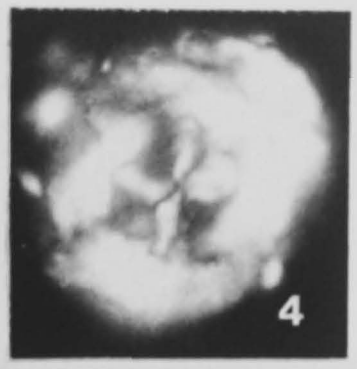
4

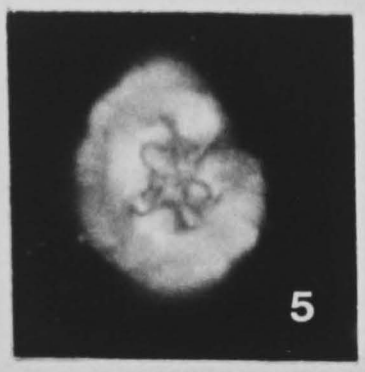
5

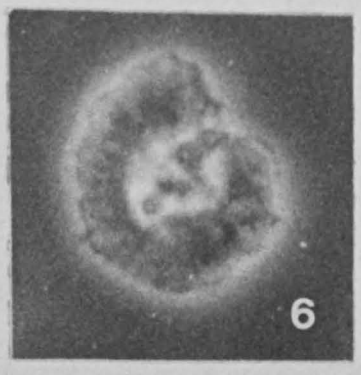
6

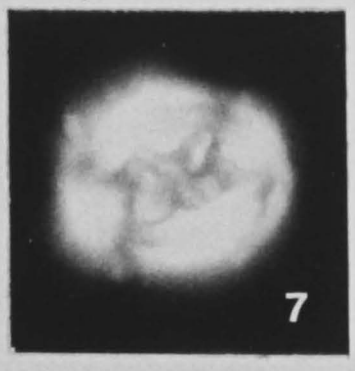
7

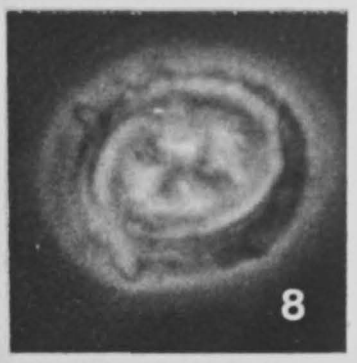
8

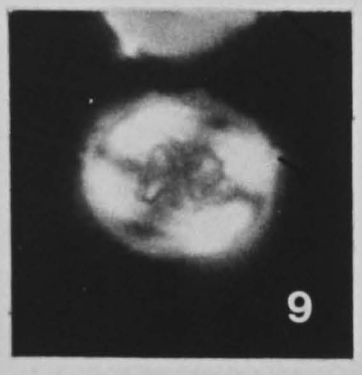
9

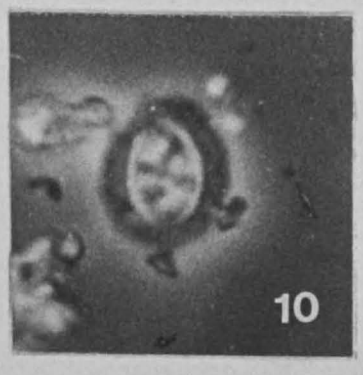
10

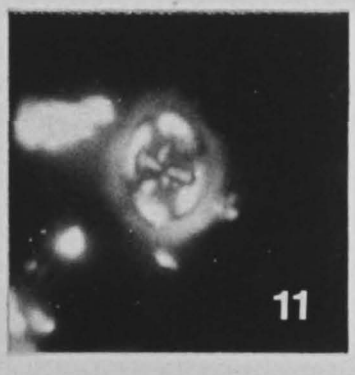
11

12

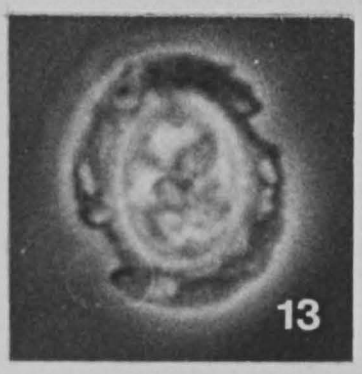
13

14

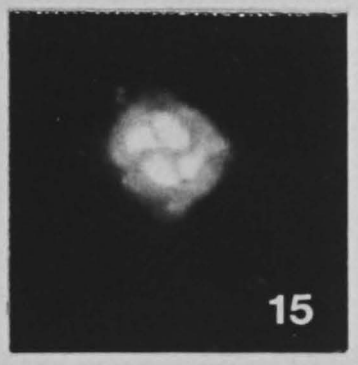
15

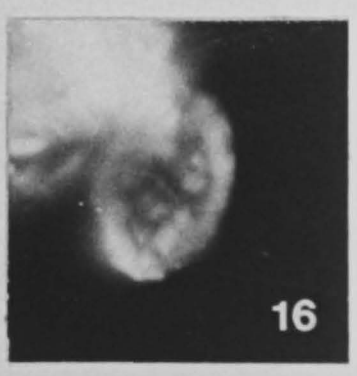
16

17

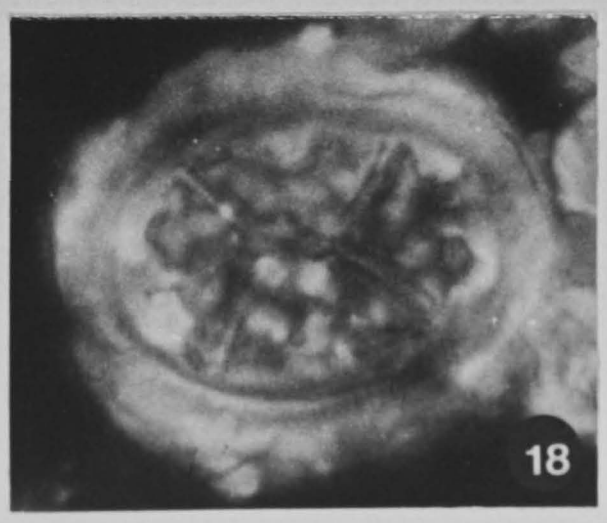
18

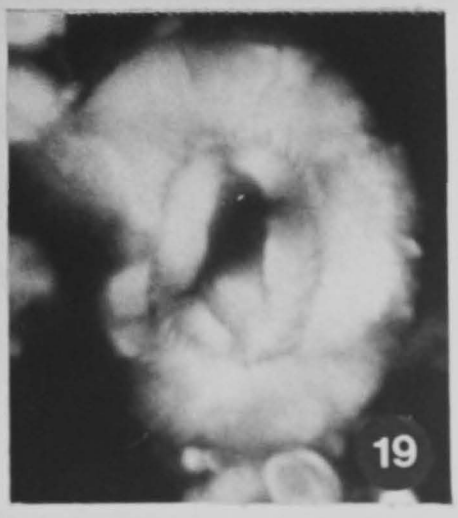
19

PLATE 5.

Light photomicrographs

XPL = Crossed Polarised Light
PC = Phase Contrast
PPL = Plane Polarised Light
Scale Bar = 5μm

Fig. 1. *Cruciplacolithus frequens* (Perch-Nielsen, 1977), distal view, XPL, UD615-5, D134-1003.

Fig. 2. *Cruciplacolithus tenuis* (Stradner, 1961), distal view, XPL, UD615-2, D134-1003.

Figs 3,4. *Cruciplacolithus vanheckae* Perch-Nielsen, 1986, D476-1477: Fig. 3, distal view, XPL, UD613-34A; Fig. 4, distal view, PC, UD613-35A.

Figs 5,6. *Ericsonia cava* (Hay & Mohler, 1967), D246-1179: Fig. 5, distal view, XPL, UD621-34A; Fig. 6, distal view, PC, UD621-35A.

Figs 7,8. *Ericsonia formosa* (Kamptner, 1963), D351-1050: Fig. 7, distal view, PC, UD625-3; Fig. 8, distal view, XPL, UD614-21.

Fig. 9. *Ericsonia robusta* (Bramlette & Sullivan, 1961), distal view, XPL, UD614-20, D246-1179.

Figs 10,11. *Ericsonia subpertusa* Hay & Mohler, 1967, D134-1003: Fig. 10, distal view, XPL, UD629-35A; Fig. 11, distal view, PC, UD629-36A.

Fig. 12. *Discoaster wemmelensis* Achuthan & Stradner, 1969, plan view, PC, UD621-1A, D349-1433.

Fig. 13. *Fasciculithus alanii* Perch-Nielsen, 1971a, side view, XPL, UD625-22A, D246-1179.

Fig. 14. *Fasciculithus clinatus* Bukry, 1971, side view, XPL, UD621-3A, D133-1004.

Fig. 15. *Fasciculithus pileatus* Bukry, 1973, side view, XPL, UD616-17A, D246-1179.

Fig. 16. *Discoaster mohleri* Bukry & Percival, 1971, plan view, PC, UD629-41A, D133-1004.

Fig. 17. *Fasciculithus tympaniformis* Hay & Mohler *in* Hay *et al.*, 1967, side view, XPL, UD624-14A, D134-1003.

Fig. 18. *Discoaster barbadiensis* Tan, 1927, plan view, PPL, UD625-29A, D351-1050.

Fig. 19. *Discoaster multiradiatus* Bramlette & Reidel, 1954, plan view, PC, UD629-42A, D133-1004.

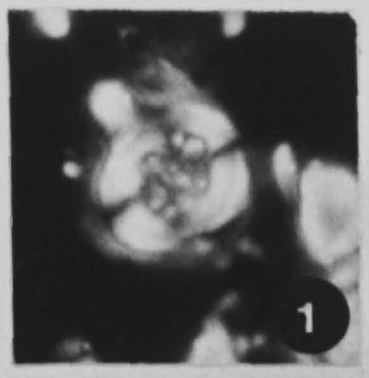
1

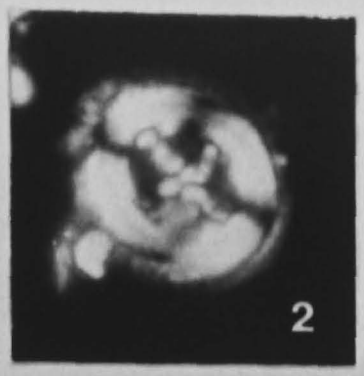
2

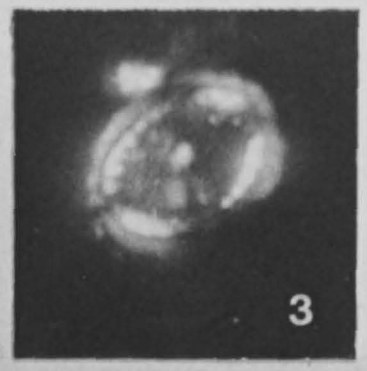
3

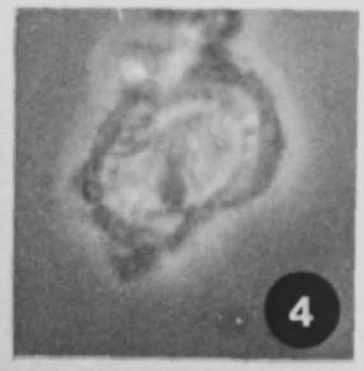
4

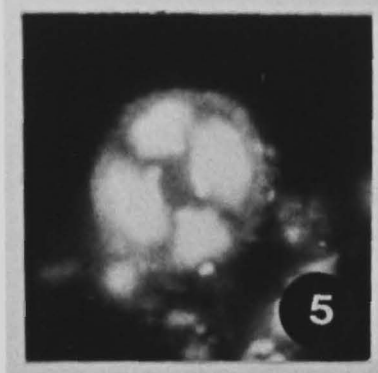
5

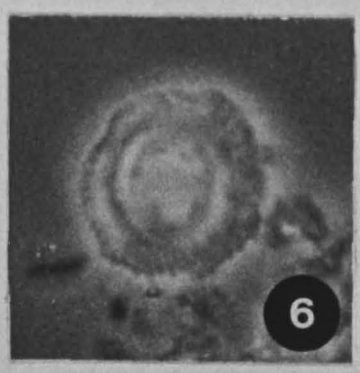
6

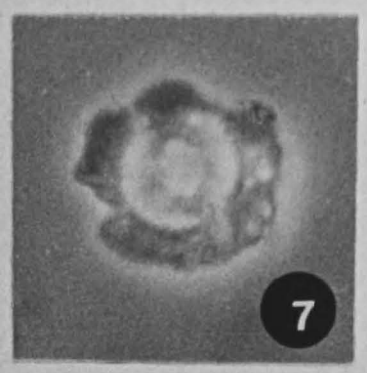
7

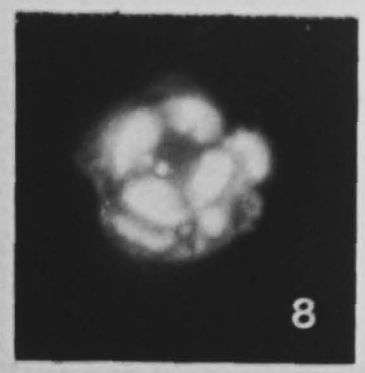
8

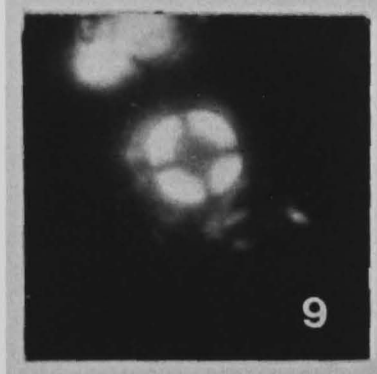
9

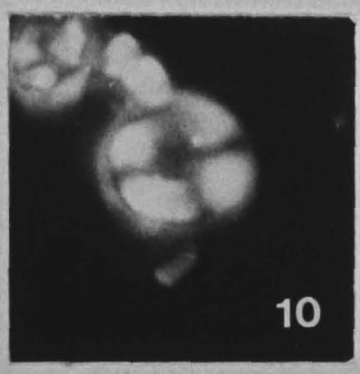
10

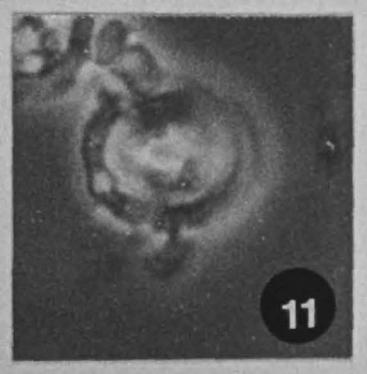
11

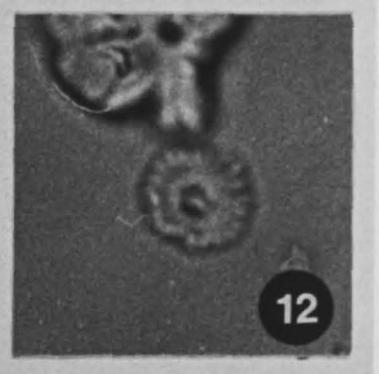
12

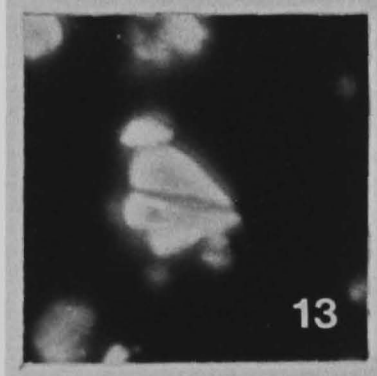
13

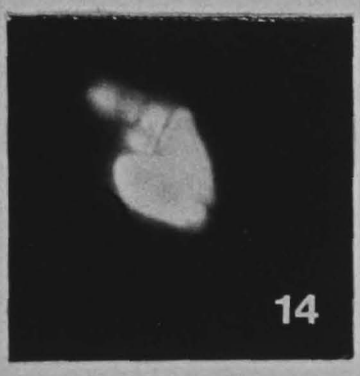
14

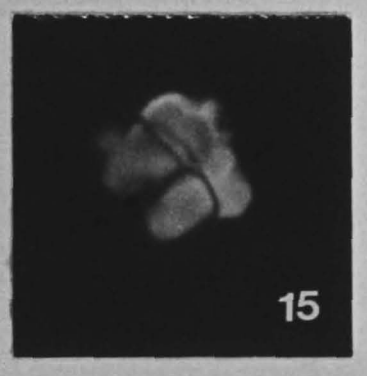
15

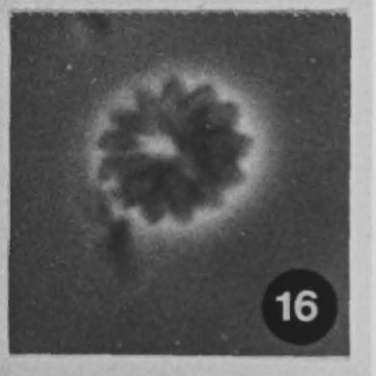
16

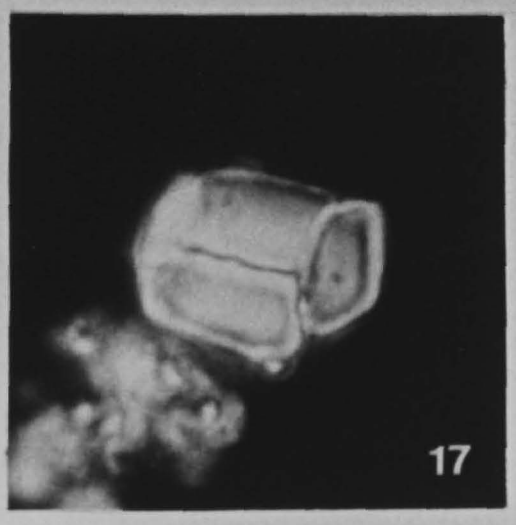
17

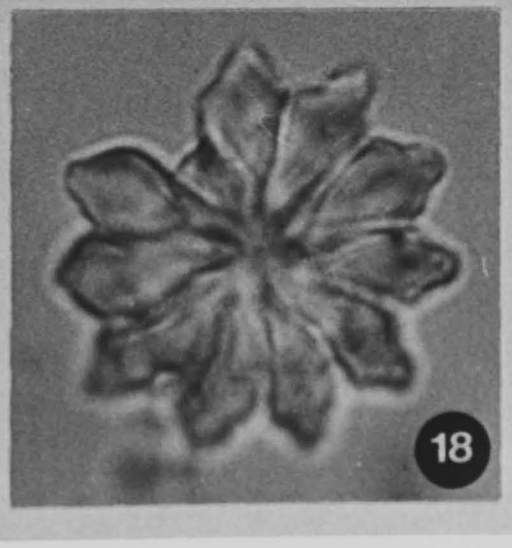
18

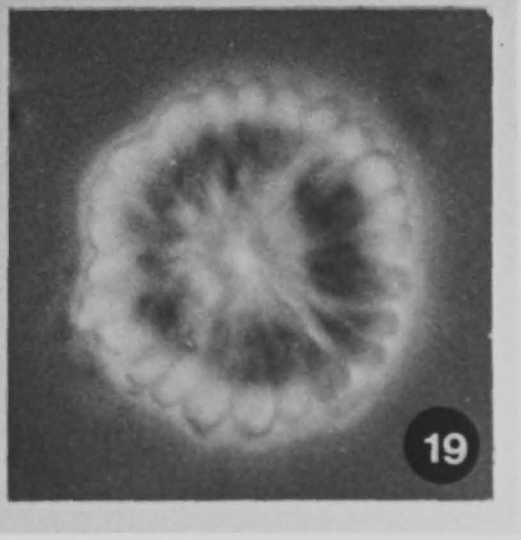
19

PLATE 6.

Light photomicrographs

XPL = Crossed Polarised Light
PC = Phase Contrast Scale Bar = 5μm

Fig. 1. *Heliolithus cantabriae* Perch-Nielsen, 1971a, distal view, XPL, UD615-8, D134-1003.

Fig. 2. *Heliolithus reidelli* Bramlette & Sullivan, 1961, distal view, XPL, UD616-15A, D246-1179.

Fig. 3. *Dictyococcites scrippsae* (Hay, Mohler & Wade, 1966), distal view, XPL, UD631-31, D234-1156.

Figs 4,8. *Reticulofenestra dictyoda* (Deflandre *in* Deflandre & Fert, 1954), D351-1050: Fig. 4, proximal view, XPL, UD625-6A; Fig. 8, proximal view, PC, UD625-7A.

Figs 5,6. *Reticulofenestra reticulata* (Gartner & Smith, 1967), D351-1050: Fig. 5, distal view, XPL, UD629-1A; Fig. 6, distal view, PC, UD629-2A.

Fig. 7. *Reticulofenestra hillae* Bukry & Percival, 1971, distal view, XPL, UD625-14A, D229-1148.

Fig. 9. *Toweius gammation* (Bramlette & Sullivan, 1961), distal view, XPL, UD629-3A, D366-1448.

Fig. 10. *Sphenolithus anarrhopus* Bukry & Bramlette,1969, side view, XPL, UD624-17, D133-1004.

Fig. 11. *Sphenolithus furcatolithoides* Locker, 1967, side view, XPL, UD626-40A, D350-1434.

Fig. 12, *Sphenolithus moriformis* (Bronnimann & Stradner, 1960), side view, XPL, UD624-24, D237-1052.

Fig. 13. *Sphenolithus primus* Perch-Nielsen, 1971a, side view, XPL, UD624-14, D133-1004.

Figs 14,15. *Sphenolithus pseudoradians* Bramlette & Willcoxon, 1967: Fig. 14, side view, XPL, UD614-29, D351-1050; Fig. 15, side view, XPL, UD615-32, D349-1433.

Fig. 16. *Sphenolithus radians* Deflandre *in* Grasse, 1952, side view, XPL, UD615-27, D229-1148.

Fig. 17. *Heliolithus kleinpelli* Sullivan, 1964, distal view, XPL, UD624-19A, D133-1004.

Figs 18,19. *Dictyococcites bisectus* (Hay, Mohler & Wade, 1966), D234-1156: Fig. 18, distal view, PC, UD625-8A; Fig. 19, distal view, XPL, UD625-9A.

Fig. 20. *Reticulofenestra umbilicus* (Levin, 1965), distal view, XPL, UD631-39, D229-1148.

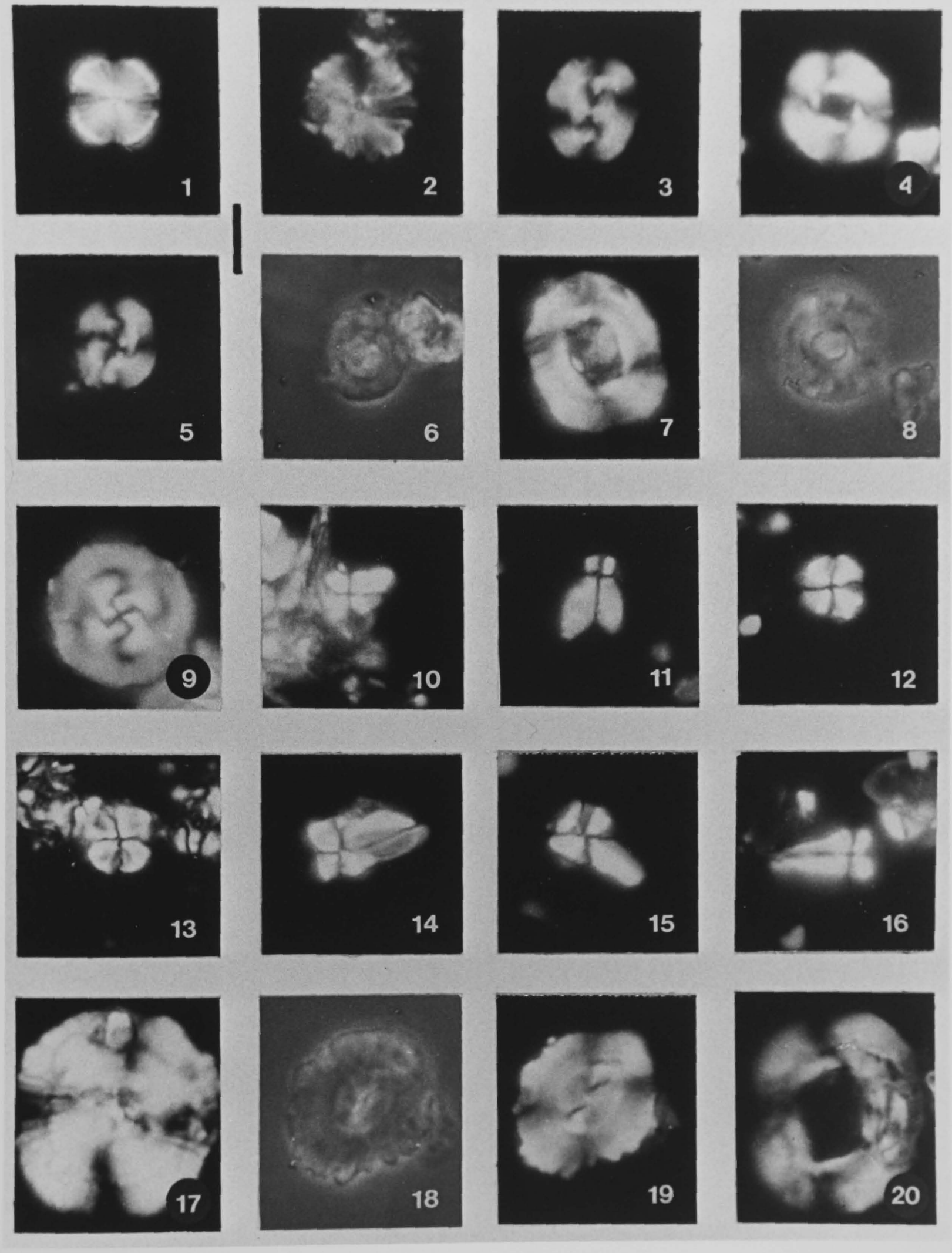
1
2
3
4
5
6
7
8
9
10
11
12
13
14
15
16
17
18
19
20

PLATE 7.

Light photomicrographs

XPL = Crossed Polarised Light
PC = Phase Contrast
PPL = Plane Polarised Light
Scale Bar = 5μm

Fig. 1. *Thoracosphaera operculata* Bramlette & Martini, 1964, sphere, XPL, UD616-10A, D246-1179.

Figs 2,3. *Thoracosphaera tuberosa* Kamptner, 1963, D229-1148: Fig. 2, sphere, XPL, UD615-25; Fig. 3, sphere, UD615-24.

Fig. 4. *Neochiastozygus distentus* (Bramlette & Sullivan, 1961), plan view, XPL, UD621-8A, D246-1179.

Figs 5,6. *Neochiastozygus modestus* Perch-Nielsen, 1971a, D276-1454: Fig. 5, plan view, XPL, UD621-12A; Fig. 6, plan view, PC, UD621-13A.

Figs 7,11. *Neochiastozygus perfectus* Perch-Nielsen, 1971a, D276-1454: Fig. 7, plan view, PC, UD621-10A; Fig. 11, plan view, XPL, UD621-11A.

Figs 8,12. *Zygodiscus bramlettei* Perch-Nielsen, 1981: Fig. 8, plan view, PC, UD624-2, D276-1454; Fig. 12, plan view, XPL, UD624-10, D133-1004.

Figs 9,13. *Sphenolithus spriniger* Bukry, 1971: Fig. 9, side view, XPL, UD615-21, D349-1433; Fig. 13, side view, XPL, UD615-36, D348-1432.

Fig. 10. *Ellipsolithus macellus* Sullivan, 1964, plan view, XPL, UD615-9, D134-1003.

Fig. 14. *Discoaster lodenesis* Bramlette & Reidel, 1954, plan view, PPL, UD613-32A, D476-1477.

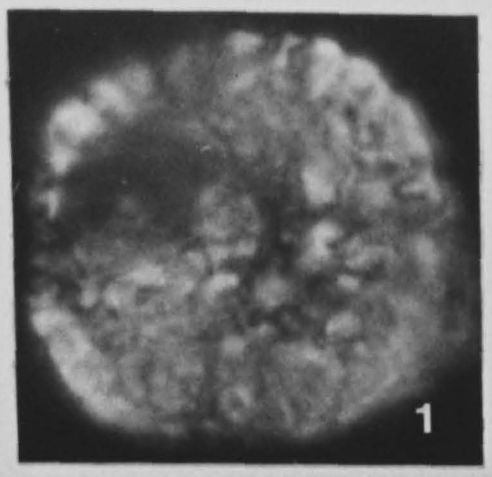
1

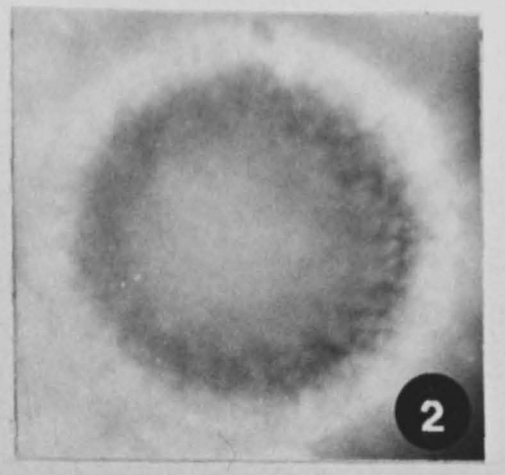
2

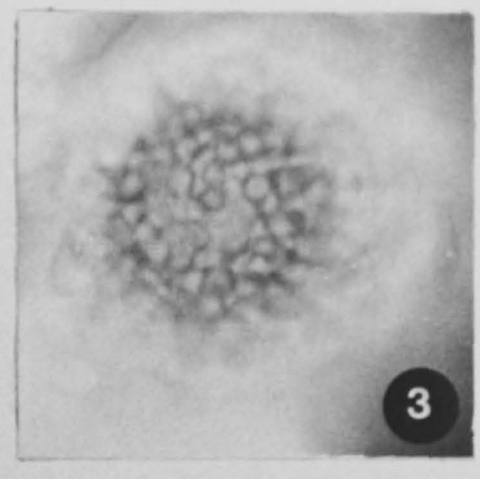
3

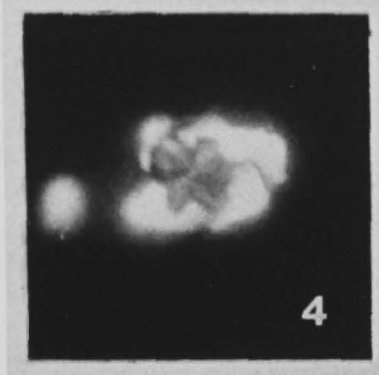
4

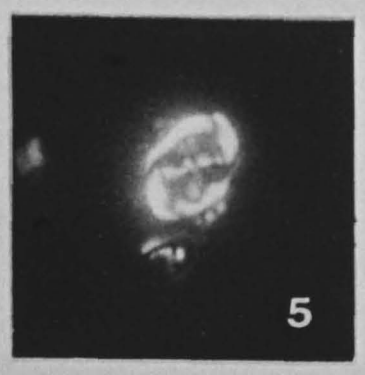
5

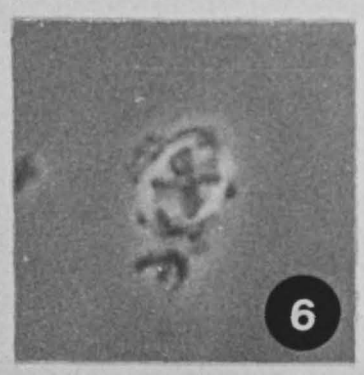
6

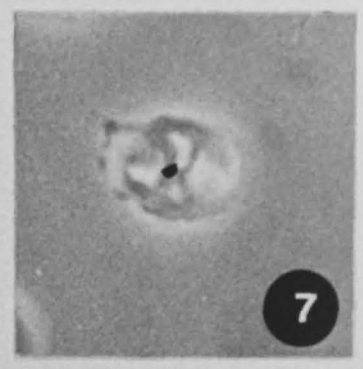
7

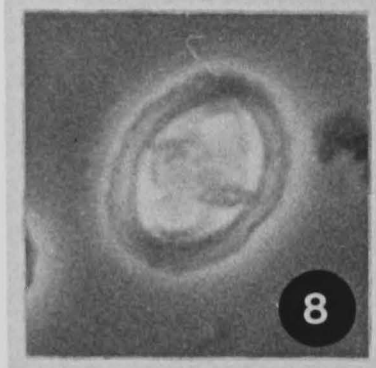
8

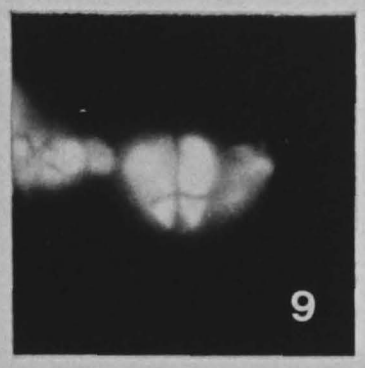
9

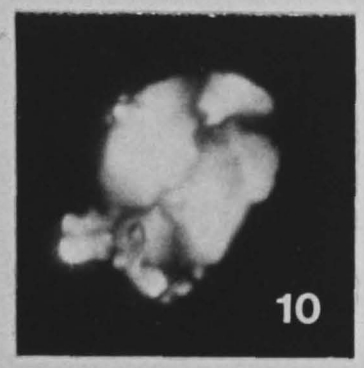
10

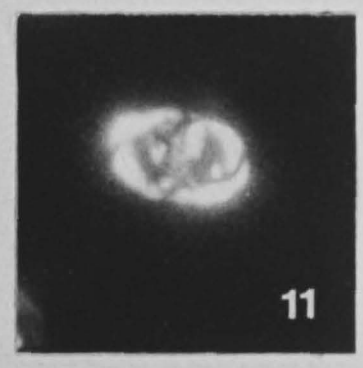
11

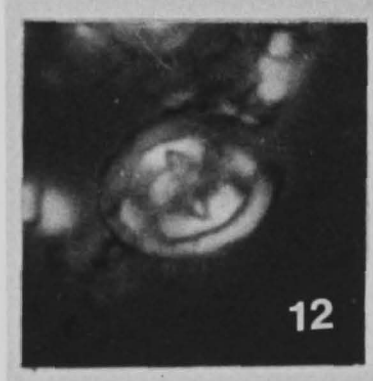
12

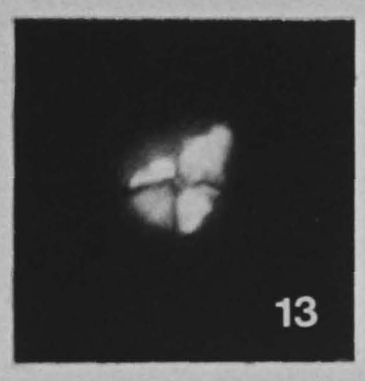
13

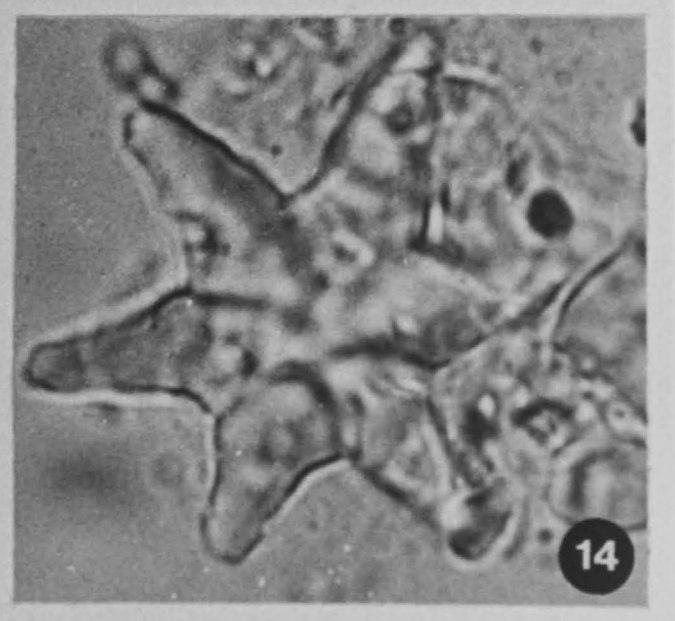
14

PLATE 8.

SEM photomicrographs

Fig. 1. *Coccolithus pelagicus* (Wallich, 1877), distal view, UD601-2, D130-1152, X4250.

Fig. 2. *Discoaster mohleri* Bukry & Percival, 1971, plan view, UD601-22, D134-1003, X3750.

Fig. 3. *Ericsonia cava* (Hay & Mohler, 1967), distal view, UD620-21, D276-1454, X4780.

Fig. 4. *Cyclicargolithus marismontium* (Black, 1964), distal view, UD620-30, D371-1470, X5500.

Fig. 5. *Dictyococcites bisectus* (Hay, Mohler & Wade, 1966), distal view, UD620-39, D234-1156, X4600.

Fig. 6. *Cyclicargolithus floridanus* (Roth & Hay *in* Hay *et al.*, 1967), distal view, UD620-37, D234-1156, X9120.

Fig. 7. *Ericsonia subpertusus* Hay & Mohler, 1967, distal view, UD620-10, D133-1004, X9600.

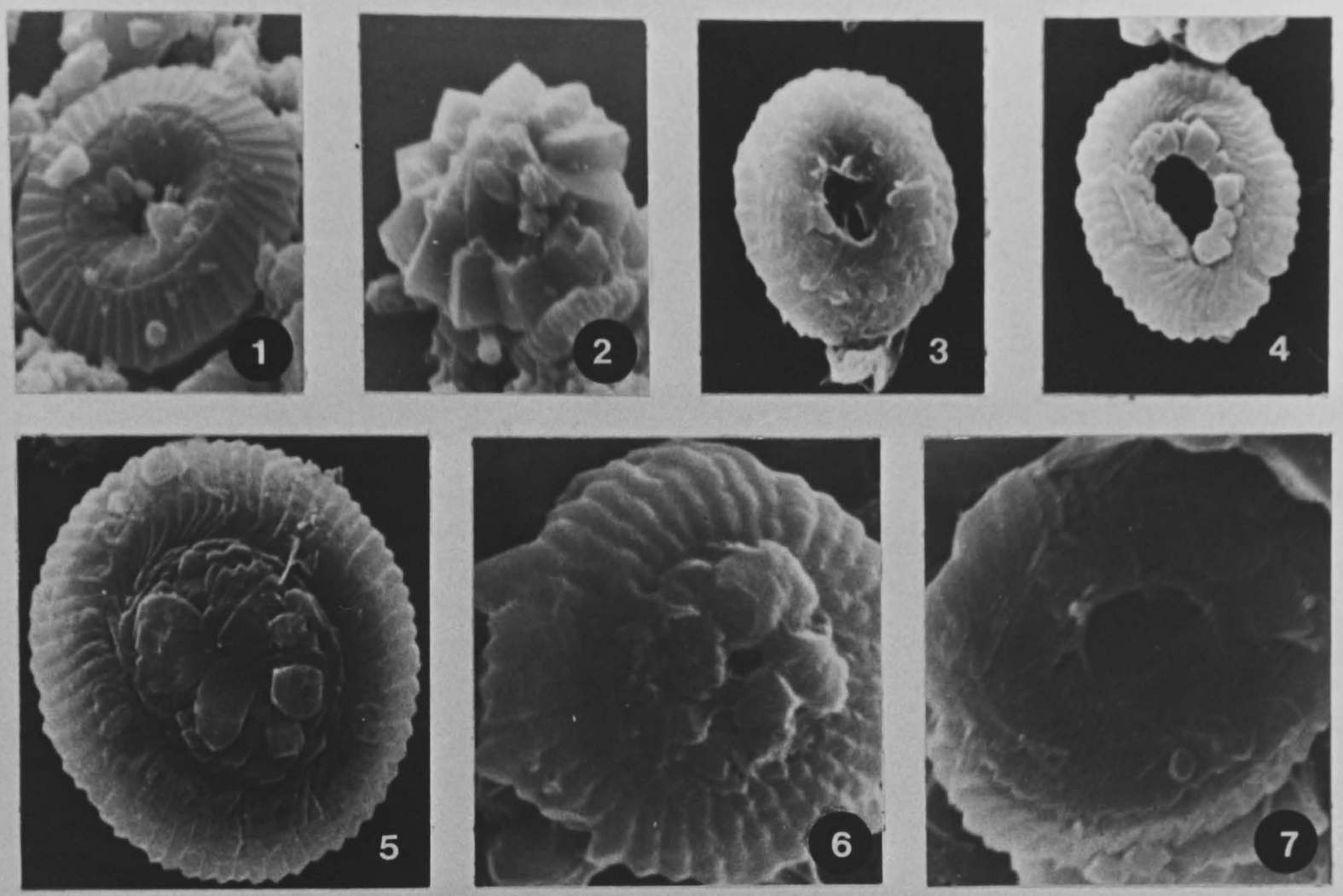
1
2
3
4
5
6
7

CHAPTER 6

BIOSTRATIGRAPHY OF THE MIOCENE NEO-AUTOCHTHONOUS SEDIMENTARY COVER OF S. W. CYPRUS

6.1 Introduction

The study reported here involves the micropalaeontological analyses, of 57 samples from 19 localities (Fig. 6.1), including Kottaphi Hill located near Agrokipia village (Fig. 2.1), against the northern margin of the Troodos Massif. It also forms part of an overall review of the biostratigraphy of the neo-autochthonous sedimentary cover of S.W. Cyprus and concentrates on the calcareous sediments of the Pakhna and Pissouri Formations, which underlie and overlie the evaporite sequence of the Kalavasos Formation respectively.

The aim of this study is to date the Pakhna, Kalavasos and Pissouri (Myrtou Marls) Formations, where the basal horizon of the Pakhna and Pissouri Formations makes unconformable contact with the underlying older sedimentary formations of the neo-autochthonous sedimentary cover, and the Mamonia and Troodos basement terranes and fragments (Fig. 6.2).

6.2 Sampling Strategy and Localities

The sampling of the Pakhna (P) and Pissouri (MM; Myrtou Marls) Formations (Fig. 6.1), forms part of a wider biostratigraphical study, involving 372 samples from 100 localities, on the Late Cretaceous (late Campanian) to Late Miocene sediments of S.W. Cyprus. The samples were collected as near as possible to the unconformable contact with the underlying rocks. Samples were collected from several localities, which form part of four measured sections (Figs 6.3,4,5,6) from S.W. Cyprus and Kottaphi Hill (K; Fig. 6.7), against the northern margin of the Troodos Massif.

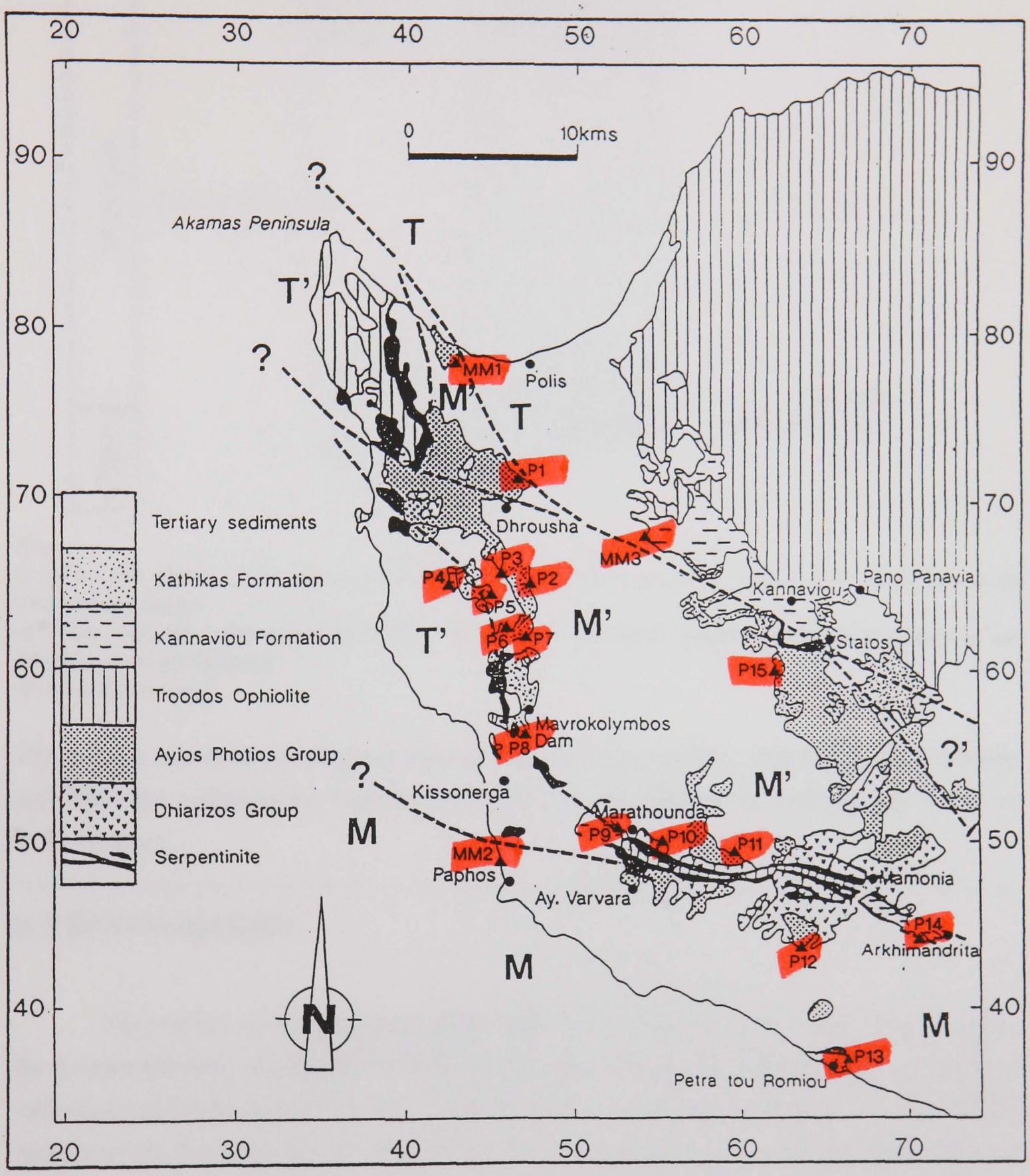

Fig. 6.1. General geological map of S.W. Cyprus, displaying the relationship between the Mamonia and Troodos basement terranes (M and T respectively) and their associated fragments (M', T' respectively and ?' uncertain). Also displaying the sample localities of the Pakhna (P1-P15) and Pissouri (Myrtou Marls; MM1-MM3) Formations (modified from Swarbrick 1980).

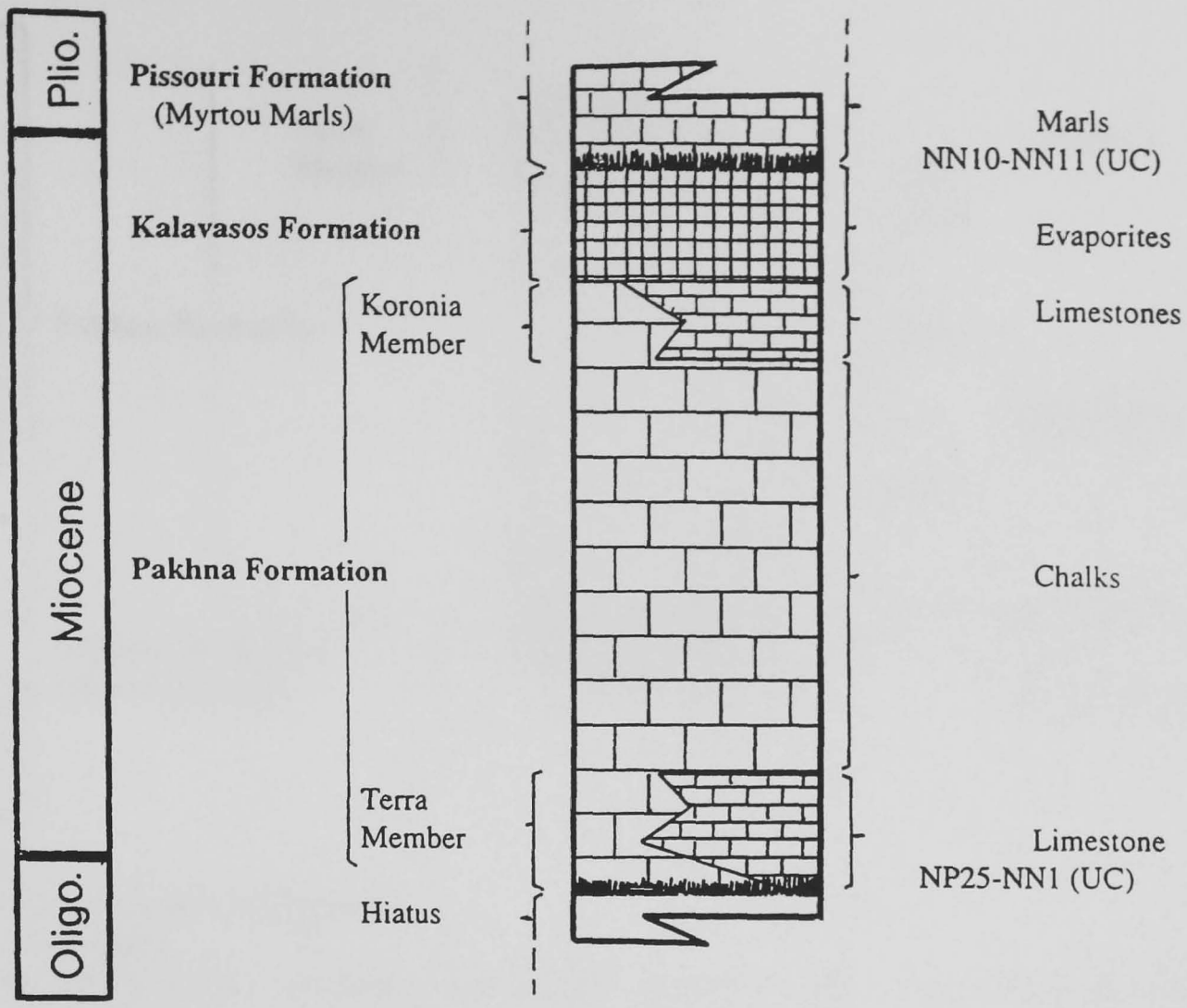

Notes.

i). NP and NN (Martini, 1971) calcareous nannofossil biostratigraphical zonal scheme, relating to the relative ages of the unconformable contacts.

ii). Pakhna Formation makes unconformable (NP25-NN1) contact with Lefkara, Kathikas and Kannaviou Formations, and basement terranes and fragments.

iii). UC = Unconformity

Fig. 6.2. A schematic geological vertical section (not to scale), displaying the Miocene and Pliocene sedimentary formations of the neo-autochthonous sedimentary cover of S.W. Cyprus.

6.3 Biostratigraphy

The earlier micropalaeontological data are of limited value, apart from research by Krasheninnikov and Kaleda (1994), on the Late Cretaceous (Campanian) to Pliocene sediments of the Perapedhi section, situated north of Limassol against the south western margin of the Troodos Massif. Therefore the study attempts to develop the application of micropalaeontology, to the basal horizons of the chalk outcrop, relating to the Pakhna and Pissouri Formations of the neo-autochthonous sedimentary cover, which both formations make unconformable contact with the underlying rocks, in S.W. Cyprus. The study reviews the micropalaeontological data obtained, to provide new or refined age information for the unconformable contacts (Fig. 6.2), and in turn constrain the age of the Kalavasos Formation.

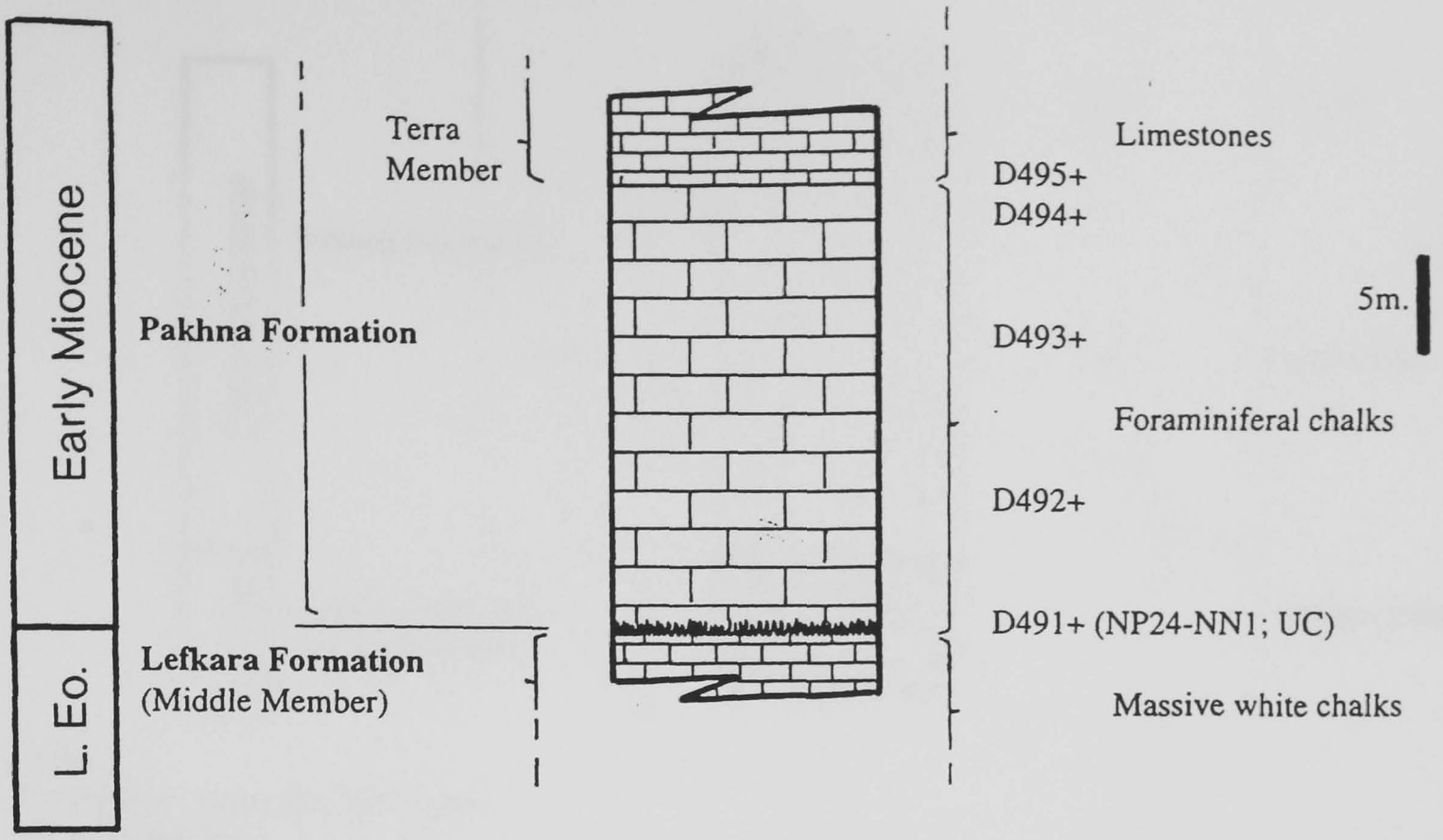

Notes

i). D number = Sample processing number.

ii). + = P13 samples.

iii). NP and NN (Martini, 1971) calcareous nannofossil biostratigraphical zonal scheme indicating the relative age of the unconformable contact.

iv). UC = unconformity.

Fig. 6.3. Geological measured vertical section from Petra-tou-Romiou (CGR 670 367), displaying the unconformity between the Pakhna and underlying Lefkara (Middle Member , Massive Chalk unit) Formation.

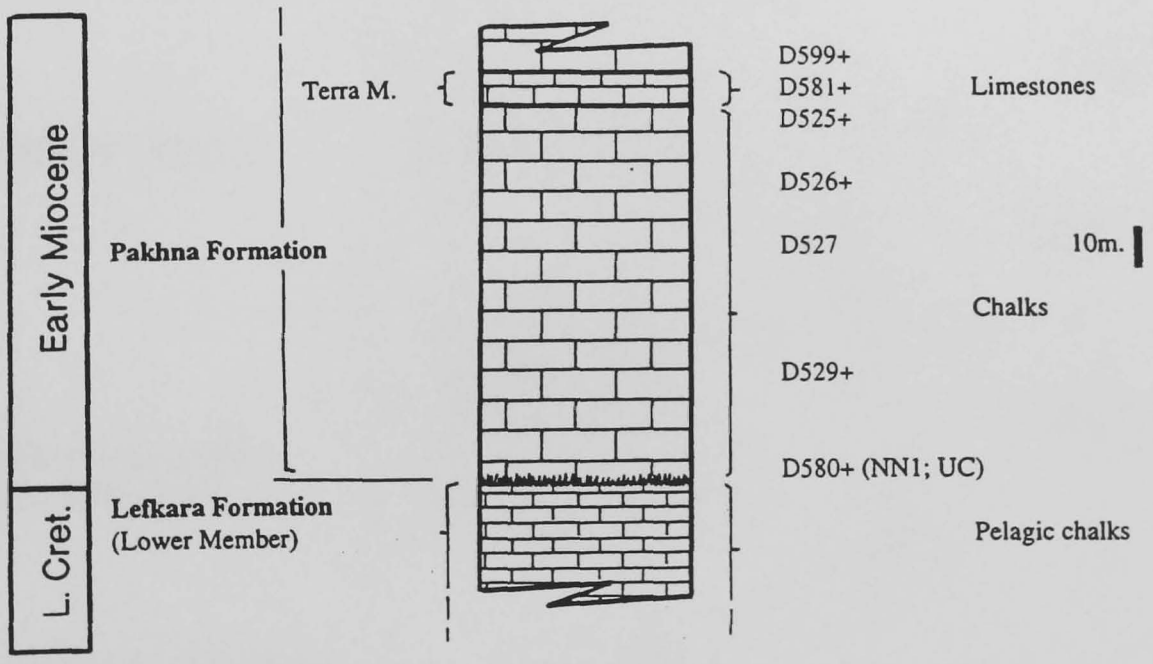

Notes

i). D number = Sample processing number.

ii). + = P8 samples.

iii). NN (Martini, 1971) calcareous nannofossil biostratigraphical zonal scheme indicating the relative age of the unconformable contact.

iv). UC = unconformity.

Fig. 6.4. Geological measured vertical section from Tala (CGR 482 571), displaying the unconformity between the Pakhna and underlying Lefkara (Lower Member) Formation.

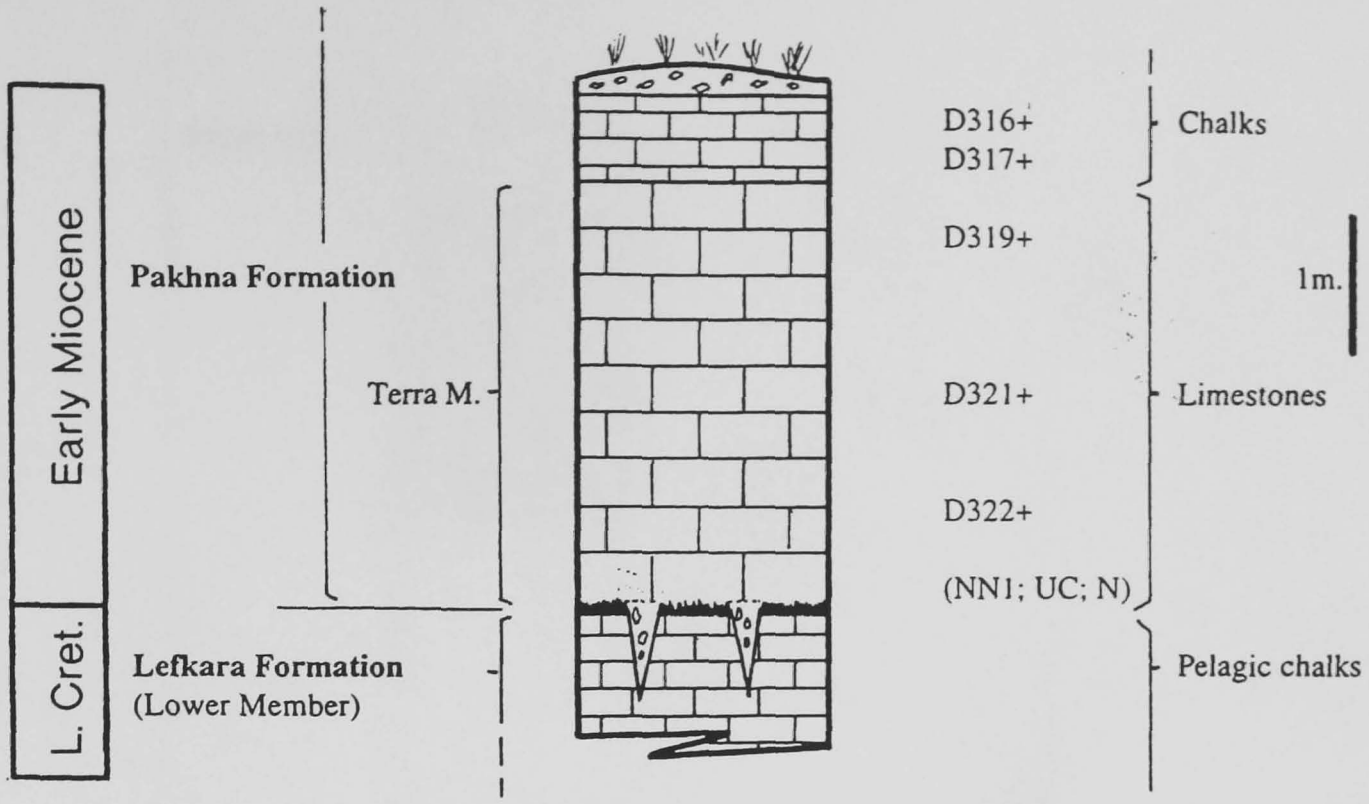

Notes

i). D number = Sample processing number.

ii). + = P1 samples.

iii). NN (Martini, 1971) calcareous nannofossil biostratigraphical zonal scheme indicating the relative age of the unconformable contact.

iv). UC = unconformity.

v). N = Neptunean dykes (containing pebbles of Mamonia and Troodos basement lithologies).

Fig. 6.5. Geological measured vertical section from Dhrousha (CGR 455 713), displaying the unconformity between the Pakhna (Terra Limestone Member) and underlying Lefkara (Lower Member) Formations.

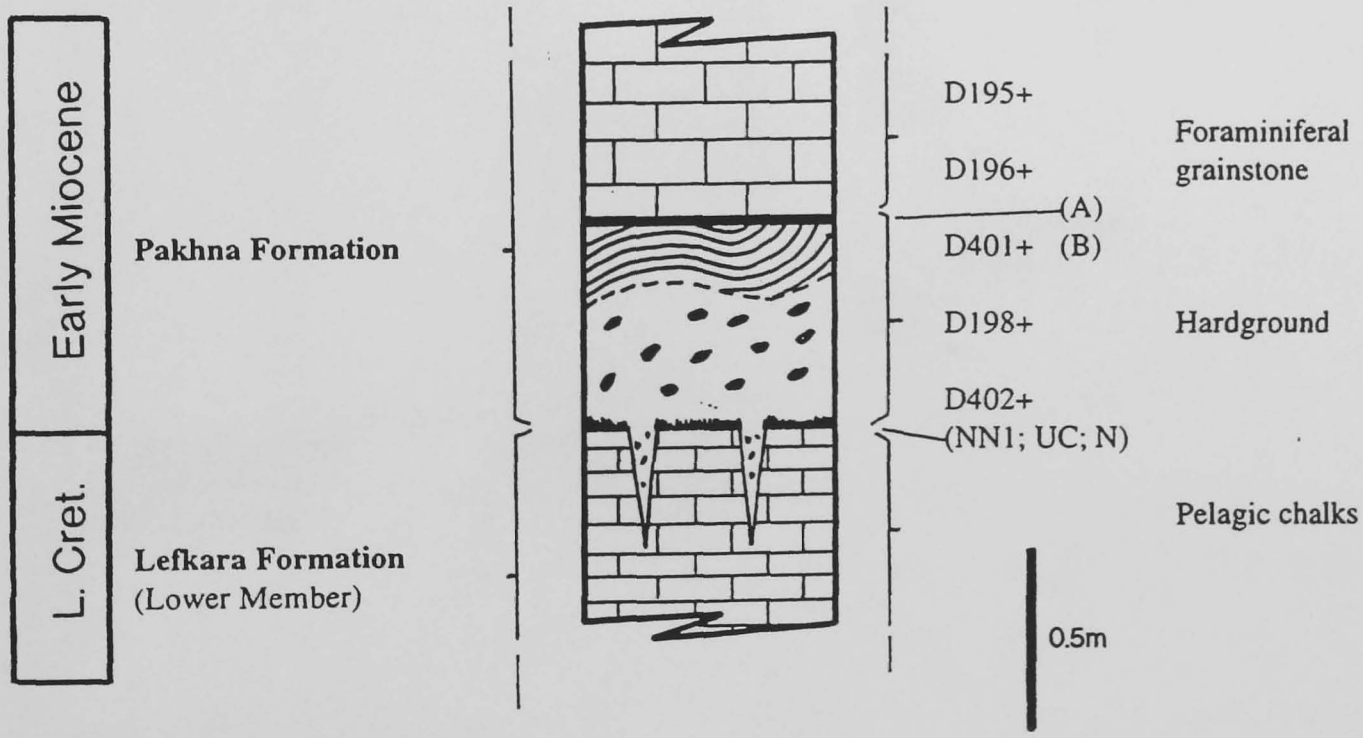

i). D number = Sample processing number.

ii). + = P6 samples.

iii). NN (Martini, 1971) calcareous nannofossil biostratigraphical zonal scheme indicating the relative age of the unconformable contact.

iv). A = Sandstone (unconsolidated).

v). B = Phosphatic horizon.

vi). UC = Unconformity.

vii). N = Neptunean dykes.

Fig. 6.6. Geological measured vertical section from Kathikas valley (CGR 461 629), displaying the unconformity between the Pakhna and underlying Lefkara (Lower Member) Formations.

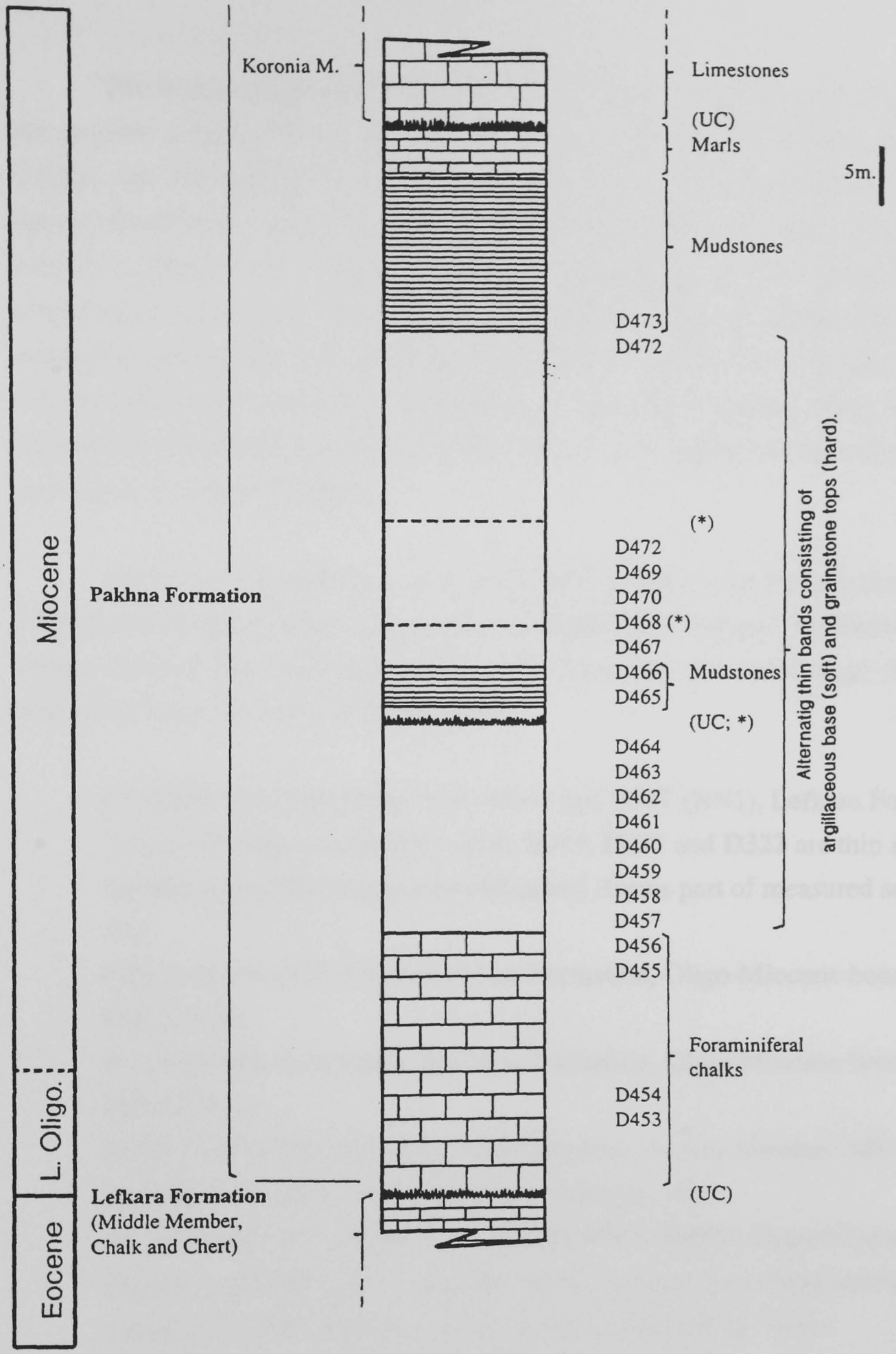

Notes

i). D number = Sample processing number.

ii). UC = Unconformity.

iii). * = Hard grounds.

Fig. 6.7. Geological measured vertical section from Kottaphi Hill (CGR 142 785), displaying the major unconformities between the Pakhna and underlying Lefkara (Middle Member, Chalk and Chert unit) Formations, and the overlying Koronia Limestone Member.

The biostratigraphical significance of calcareous nannofossils observed, within the samples collected from the localities (Figs 6.1; P1-P15 and MM1-MM3) in S.W. Cyprus and Kottaphi Hill (K) near Agrokipia (Fig. 2.1), are discussed below. The species distribution tables for the Pakhna and Pissouri (Myrtou Marls) Formations (Figs 6.8,9,10), display the species observed within each sample, including state of preservation and overall content of the assemblage. The biostratigraphical ranges of individual species observed are displayed in Fig 6.11, which have been determined from various published sources (6.5 Systematics), and are correlated with the calcareous nannofossil zonal scheme erected by Martini (1971). All localities have been given a six figure grid reference (CGR).

The following summary, gives the Locality number (P = Pakhna Formation; MM = Pissouri Formation, Myrtou Marls; K = Kottaphi Hill), Cyprus Grid Reference (CGR), Sample number (D), underlying formation or basement and zonal range (NP and NN), with all samples discussed in detail below.

P1 (CGR 455 713), **D316** (NN1-NN4) and **D317** (NN1), Lefkara Formation, Lower Member, overall NN1 (N.B. **D319, D321** and **D322** are thin sections of the underlying Terra Limestone Member) (forms part of measured section, Fig. 6.5).

P2 (CGR 465 655), **D122,** Kathikas Formation, Oligo-Miocene boundary (NP25/NN1).

P3 (CGR 453 653), **D119,** Kathikas Formation, Oligo-Miocene boundary (NP25/NN1).

P4 (CGR 422 641), **D124,** Lefkara Formation, Lower Member, NN1.

P5 (CGR 446 642), **D187,** Kathikas Formation, NN1.

P6 (CGR 461 629), **D195** (NN1), **D196** (NN1), **D401** (Oligo-Miocene boundary), **D198** (NN1) and **D402** (NN1), Lefkara Formation Lower Member, overall NP25/NN1 (forms part of measured section, Fig. 6.6).

P7 (CGR 470 627), **D404,** Kathikas Formation, NN1.

P8 (CGR 482 571), **D599** (NN1), **D581** (Oligo-Miocene boundary; thin section produced - Terra Limestone Member), **D525** (NP24-NN1), **D526** (NN1), **D527** (Oligo-Miocene boundary), **D529** (NN1) and **D580** (NN1), Lefkara Formation, Lower Member, overall NP25/NN1 (forms part of measured section, Fig. 6. 4).

P9 (CGR 522 509), **D344,** Kathikas Formation, NN1-NN7.

P10 (CGR 539 502), **D582,** Lefkara Formation, Middle Member, NN1.

P11 (CGR 588 505), **D373,** Lefkara Formation, Middle Member, NN1-NN4.

LOCALITY	SAMPLE	PRESERVATION	NANNOFOSSIL CONTENT	Coccolithus pelagicus	Pontosphaera mulipora	Sphenolithus moriformis	Dictyococcites scrippsae	Dictyococcites bisectus	Cyclicargolithus floridanus	Cyclicargolithus abisectus	Dictyococcites antarcticus	Coccolithus miopelagicus	Helicosphaera sissura	Thoracosphaera fossata	Helicosphaera kamptneri	Helicosphaera granulata	Umbilicosphaera sibogae
P1	D316	M	C	x					x		x	x	x	x	x		
	D317	M	C	x			x		x		x	x		x	x		
P2	D122	M	A	x			x	x	x	x		x					
P3	D119	M	A	x			x	x	x	x		x					
P4	D124	M	A	x	x		x		x	x	x	x	x				
P5	D187	M	C	x	x		x		x		x	x	x		x		
P6	D195	M	C	x	x				x	x	x	x			x		
	D196	M	C	x			x		x	x	x	x			x		
	D401	P	S	x			x	x	x			x					
	D198	M	C	x			x		x		x	x			x		
	D402	M	C	x			x		x		x	x			x		
P7	D404	M	A	x		x	x	x	x	x		x	x				
P8	D599	M	C	x			x		x	x	x	x	x				
	D581	P	S				x				x	x					
	D525	P	S	x				x		x		x					
	D526	M	S	x					x	x	x	x			x		
	D527	M	S	x			x	x	x		x	x					
	D529	M	S	x		x	x			x		x	x		x		
	D580	P	A	x			x	x	x	x		x			x		
P9	D344	P	S	x					x		x	x			x		
P10	D582	M	C	x				x	x	x	x	x	x		x		
P11	D373	G	A	x	x	x			x		x	x	x		x		
P12	D65	M	S	x	x		x	x	x	x	x	x			x		
P13	D494	M	C	x	x		x		x	x	x	x			x		
	D493	M	C	x	x		x	x	x	x		x			x		
	D492	M	C	x	x		x			x	x	x		x	x		
	D491	M	C	x	x	x	x	x		x	x	x					
P14	D252	M	C	x	x	x	x	x	x	x	x	x	x		x	x	x
P15	D583	G	A	x	x		x		x		x	x	x		x		

Preservation of calcareous nannofossils.

G = GOOD (little or no alteration).

M = MODERATE (50% showing some form of alteration).

P = POOR (all showing some form of alteration).

Calcareous nannofossil content (field of view = 390μm).

A = ABUNDANT (>5 individuals per field of view).

C = COMMON (<5 individuals per field of view).

S = SPARSE (isolated occurrences).

Notes

1) All chalk samples were collected as near as possible to the contact with the underlying lithologies.

2) P = Pakhna Formation

Fig. 6.8. Distribution of calcareous nannofossils observed in the basal horizon of the Pakhna Formation (Late Oligocene to Early Miocene).

***P12 (CGR 630 437),* D65,** Mamonia, NN1.

***P13 (CGR 670 367),* D494** (NN1), **D493** (NN1), **D492** (NN1) and **D491** (NP24-NN1), Lefkara Formation, Middle Member, overall NP24-NN1 (N.B. **D495** is a thin section of the overlying Terra Limestone Member) (forms part of measured section, Fig. 6.3).

***P14 (CGR 694 448),* D252**, Kannaviou Formation, NN1/NN2 boundary.

***P15 (CGR 620 594),* D583,** Kathikas Formation, NN1.

LOCALITY	SAMPLE	PRESERVATION	NANNOFOSSIL CONTENT	Pontosphaera multipora	Thoracosphaera fossata	Reticulofenestra minuta	Reticulofenestra haqii	Helicosphaera kamptneri	Umbilicosphaera sibogae	Hayaster perplexus	Reticulofenestra pseudoumbilicus	Calcidiscus macintyrei	Calcidiscus leptoporus	Scyphosphaera apsteini	Scyphosphaera canescens	Scyphosphaera conica	Scyphosphaera recta	Scyphosphaera recurvata	Scyphosphaera turris	Coccolithus pliopelagicus	Catinaster coalitus	Rhabdosphaera procera	Sphenolithus abies	Discoaster pentaradiatus	Discoaster bellus	Helicosphaera selli	Discoaster neorectus	Amaurolithus amplificus	Sphenolithus verensis	Amaurolithus delicatus
MM1	D311	G	A	x		x	x	x			x	x	x		x	x			x				x	x	x		x			
MM2	D565	G	A		x			x	x	x	x	x		x	x	x	x	x	x	x		x	x	x		x	x	x	x	x
MM3	D267	M	A	x				x				x	x		x						x		x				x			

Preservation of calcareous nannofossils.

G = GOOD (little or no alteration).

M = MODERATE (50% showing some form of alteration).

P = POOR (all showing some form of alteration).

Calcareous nannofossil content (field of view = 390μm).

A = ABUNDANT (>5 individuals per field of view).

C = COMMON (<5 individuals per field of view).

S = SPARSE (isolated occurrences).

Notes

1) All chalk samples were collected as near as possible to the contact with the underlying lithologies.

2) MM = Pissour Formation (Myrtou Marls).

Fig. 6.9. Distribution of calcareous nannofossils observed in the basal horizon of the Pissouri (Myrtou Marls) Formation (Late Miocene) of S.W. Cyprus.

***MM1 (CGR 423 773),* D311,** Mamonia, NN10.

***MM2 (CGR 510 447),* D565,** Kannaviou Formation, NN11.

***MM3 (CGR 536 678),* D267,** Kannaviou Formation, NN10.

***K1 (CGR 142 785),* D473** (NN9-NN15), **D472** (barren) **D471** (NN8-NN18), **D469** (NN8-NN18), **D470** (NN4-NN11), **D468** (NN4-NN7), **D467** (NN4-NN5), **D466** (NN4-NN5), **D465** (NN4-NN5), **D464** (NN4-NN7), **D463** (NN1-NN8), **D462** (NN1-NN4) **D461** (NN1-NN4), **D460** (NN1-NN7), **D459** (NN1), **D458** (NP24-NN1), **D457** (NP24-NN1), **D456** (NN1), **D455** (NN1), **D454** (NN1) and **D453** (NP24-NN1), Lefkara Formation, Middle Member, overall NP24-NN9.

6.3.1 Pakhna Formation chalks

The samples collected from the base of the Pakhna Formation (chalks) of S.W. Cyprus, contain in the main, a poor to moderately preserved assemblage of calcareous nannofossils.

Sample **D119 (P3),** contains an abundant population, with a low diverse species content (Fig. 6.8). The combined presence of *Dictyococcites bisectus* (Hay, Mohler and Wade, 1966) (NP17-NN1; Lazarus *et al.*, 1995) and *Coccolithus miopelagicus* Bukry,1971 (Late Oligocene-Mid Miocene; Perch-Nielsen, 1985b), Indicates a range at the Oligo-Miocene boundary (Fig. 6.11), for the assemblage.

Samples **D122 (P2)** and **D494 (P13),** contain a common to abundant population, with a low to moderately diverse species content (Fig. 6.8). The presence of *Cyclicargolithus abisectus* (Müller, 1970) (NP24-NN1; Lazarus *et al.*, 1995), indicate a zonal range of NP24-NN1 (Fig. 6.11), for the assemblages.

Samples **D65 (P12), D124 (P4), D187 (P5), D317 (P1), D402 (P6), D404 (P7), D580 (P8), D582 (P10)** and **D583 (P15),** contain in the main, a common to abundant population, with a low to moderately diverse species content (Fig. 6.8). The combined presence of *Dictyococcites scrippsae* Bukry and Percival, 1971 (NP16-NN1; Lazarus *et al.*, 1995) observed in samples **D124, D187, D317, D402** and **D583,** *Helicosphaera kamptneri* Hay and Mohler *in* Hay *et al.*, 1967 (NN1-NN21; Perch-Nielsen, 1985b) observed in samples **D65, D317, D402, D582** and **D583,** *Helicosphaera sissura* Miller, 1981 (NN1-NN4; Perch-Nielsen, 1985b) observed in samples **D124, D187** and **D404,** and *C. abisectus* (NP24-NN1; Lazarus *et al.*, 1995) observed in samples **D65, D404, D580** and **D582,** indicates a zonal range of NN1 (Fig. 6.11), for the assemblages.

Sample **D373 (P11),** contains an abundant population, with a moderately diverse species content (Fig. 6.8). The presence of *H. sissura* indicates a zonal range of NN1-NN4 (Perch-Nielsen, 1985b), for the assemblage (Fig. 6.11).

Sample **D344 (P9),** contains a sparse population, with a low diverse species content (Fig. 6.8). The combined presence of *H. kamptneri* (NN1-NN21; Perch-Nielsen, 1985b) and Cyclicargolithus floridanus (Roth and Hay *in* Hay *et al.*, 1967) (NP20-NN7; Lazarus *et al.*, 1995), indicates a zonal range of NN1-NN7 (Fig. 6.11), for the assemblage.

LOCALITY	SAMPLE	PRESERVATION	NANNOFOSSIL CONTENT	Coccolithus pelagicus	Pontosphaera multipora	Dictyococcites scrippsae	Dictyococcites bisectus	Cyclicargolithus floridanus	Cyclicargolithus abisectus	Dictyococcites antarcticus	Coccolithus miopelagicus	Helicosphaera sissura	Thoracosphaera fossata	Helicosphaera kamptneri	Umbilicosphaera sibogae	Discoaster variabilis	Sphenolithus heteromorphis	Reticulofenestra pseudoumbilicus	Calcidiscus macintyrei	Calcidiscus leptoporus	Rhabdosphaera procera	Sphenolithus abies
K1	D473	P	S											x	x			x			x	x
	D472		N																			
	D471	P	S											x	x			x			x	
	D469	M	C							x				x	x			x		x	x	
	D470	M	C							x				x	x			x	x	x		
	D468	M	C					x		x				x	x			x				
	D467	P	S	x				x		x				x			x			x		
	D466	M	A	x						x	x		x	x		x	x					
	D465	P	A	x	x						x			x		x	x			x		
	D464	P	C	x	x			x		x	x	x		x		x		x				
	D463	P	C	x						x	x			x								
	D462	M	C	x				x		x	x	x	x	x								
	D461	P	C	x				x		x	x	x		x								
	D460	M	C	x				x		x	x			x								
	D459	M	C	x		x		x	x	x	x		x	x								
	D458	P	S	x				x	x		x											
	D457	P	S	x				x	x	x	x											
	D456	M	C	x			x	x	x	x	x	x										
	D455	P	S	x				x	x		x			x								
	D454	P	S	x				x	x		x			x								
	D453	P	S	x		x		x	x		x											

Preservation of calcareous nannofossils.

G = GOOD (little or no alteration).

M = MODERATE (50% showing some form of alteration).

P = POOR (all showing some form of alteration).

Calcareous nannofossil content (field of view = 390μm).

A = ABUNDANT (>5 individuals per field of view).

C = COMMON (<5 individuals per field of view).

S = SPARSE (isolated occurrences).

N = BARREN

Fig. 6.10. Distribution of calcareous nannofossils observed in the measured section at Kottaphi Hill (K) (CGR 145 785), near Agrokipia village, against the northern margin of the Troodos Massif.

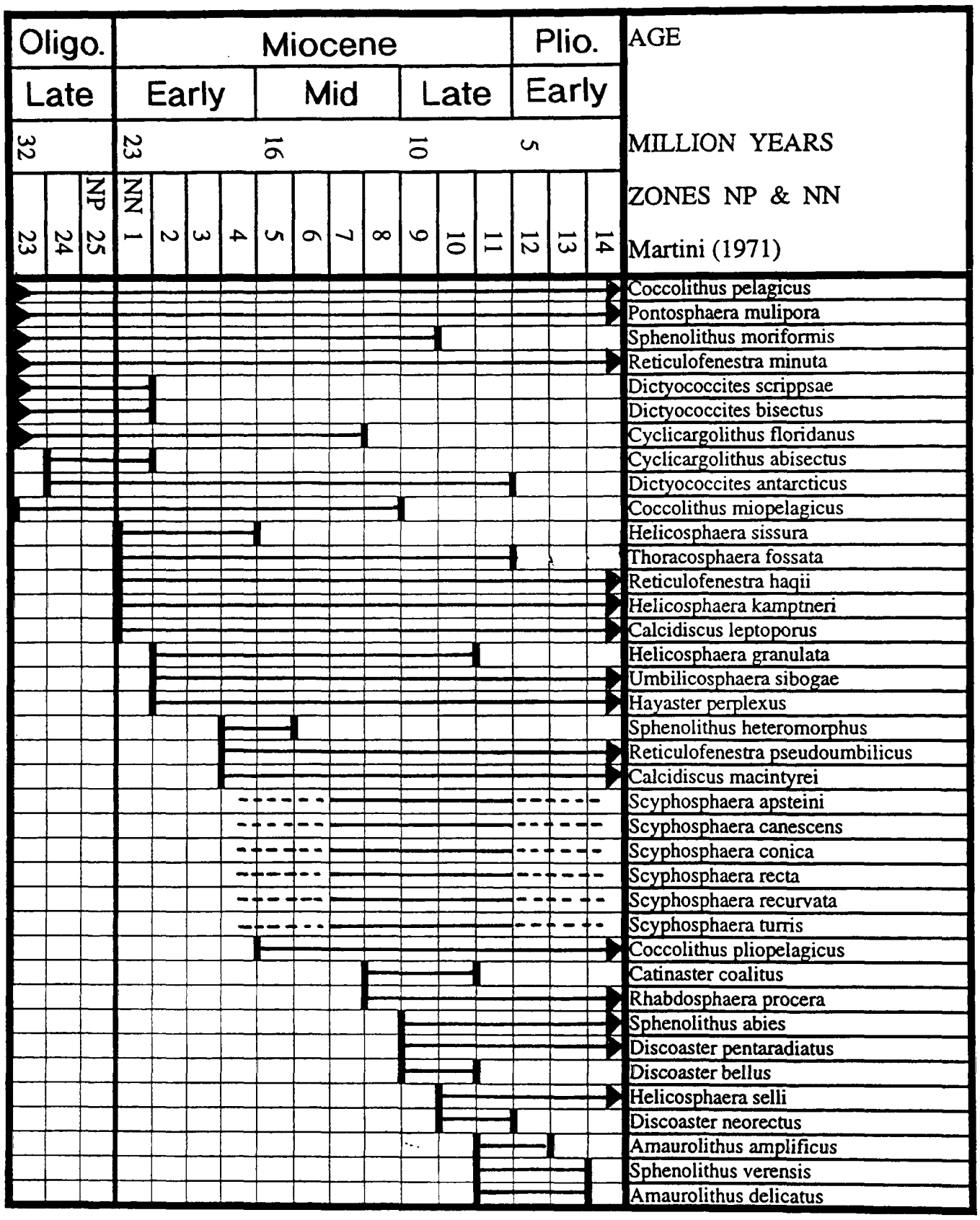

Notes.

Dates have been rounded to nearest Ma. (Harland et at., 1989).

The biostratigraphical ranges of individual species have been determined from various published sources (6.5 Systematics).

Fig. 6.11. The ranges of calcareous nannofossil species observed in the Miocene chalks of the Pakhna and Pissouri (Myrtou Marls) Formations of S.W. Cyprus.

Sample **D252 (P14),** contains a common population, with a high diverse species content (Fig. 6.8). The combined presence of *C. abisectus* (NP24-NN1; Lazarus *et al.*, 1995) and Helicosphaera granulata Bukry and Percival, 1971 (NN2-NN10; Perch-Nielsen, 1985b), indicates a zonal range at the NN1/NN2 boundary (Fig. 6.11), for the assemblage.

The samples studied from the basal horizon of the Pakhna Formation, which make unconformable contact with the underlying rocks, are age dated on the micropalaeontological data discussed above and collectively have a zonal range of NP25-NN1 (Oligo-Miocene boundary). However, sample **D252** indicates a younger age, with a zonal range at the NN1/NN2 boundary, this anomaly is possibly due to chalk talus masking the contact and the sample was collected further up the sedimentary sequence at outcrop.

The outcrop pattern displayed by the base of the Pakhna Formation, which makes direct unconformable contact with the southern Mamonia basement fragment, suggest the fragment continued to act as a structural high, surrounded by structural lows. These lows contain older sediments of the neo-autochthonous sedimentary cover, overlying in the main, sediments associated with the Troodos basement terrane and fragments (Perapedhi and Kannaviou Formations), this ensured their preservation during the erosional event(s), prior to the onset of deposition - the Pakhna ?transgressive event, trending south-east to north-west from a deep structural low centred to the east of Petra-tou-Romiou.

P1 (CGR 455 713). The remaining sample **D316** collected from the top of the Dhrousha measured section (Fig. 6.5), contains a common population, with a moderately diverse species content (Fig. 6.8). The presence of *H. sissura* indicates a zonal range of NN1-NN4 (Perch-Nielsen, 1985b), for the assemblage (Fig. 6.11) and the outcrop of the Pakhna Formation at this locality, when including the zonal range (NN1) for the basal sample **D317**.

P6 (CGR 461 629). Samples were collected from the Pakhna Formation (basal hard ground and chalks), which form part of the Kathikas measured section (Fig. 6.6), unconformably overlying the Lefkara Formation, Lower Member. Samples **D195, D196, D198, D401** and **D402,** contain in the main, a common population, with a low to moderately diverse species content (Fig. 6.8). The age diagnostic species of *C. abisectus* (NP24-NN1; Lazarus *et al.*, 1995) observed in samples **D195** and **D196,** *D. scrippsae*

(NP16-NN1; Lazarus *et al.*, 1995) observed in samples **D198** and **D402,** and *H. sissura* (NN1-NN4; Perch-Nielsen, 1985b) observed in samples **D195, D196, D198** and **D402** indicate an overall zonal range of NN1 for the Pakhna Formation at this locality.

P8 (CGR 482 571). Samples were collected from the Pakhna Formation, which form part of the Tala measured section (Fig. 6.4), unconformably overlying the Lefkara Formation, Lower Member. Samples **D525, D526, D527, D529, D580, D581** and **D599,** contain in the main a sparse population, with a low to moderately diverse species content (Fig. 6.8). The age diagnostic species of *C. abisectus* (NP24-NN1; Lazarus *et al.*, 1995) observed in samples **D525, D526, D529, D580** and **D599,** *H. sissura* (NN1-NN4; Perch-Nielsen, 1985b) observed in samples **D529** and **D599,** and *H. kamptneri* (NN1-NN21; Perch-Nielsen, 1985b) observed in samples **D526** and **D580,** indicate an overall zonal range of NN1 for the Pakhna Formation chalks at this locality.

P13 (CGR 670 367). Samples were collected from the Pakhna Formation chalks, which form part of the Petra-tou-Romiou measured section (Fig. 6.3), unconformably overlying the Lefkara Formation, Middle Member, Massive Chalk unit. Samples **D491, D492, D493** and **D494,** contain a common population, with a moderately diverse species content (Fig. 6.8). The age diagnostic species of *C. abisectus* (NP24-NN1; Lazarus *et al.*, 1995) observed in all samples and *H. kamptneri* (NN1-NN21; Perch-Nielsen, 1985b) observed in all samples apart from **D491,** indicate a zonal range of NP24-NN1 for the Pakhna Formation chalks at this locality.

Discussion. Based on the biostratigraphical data above, the unconformable base of the Pakhna Formation of S.W. Cyprus, which has a zonal range of NP25-NN1 (Oligo-Miocene boundary), can be loosely correlated with research carried out by Krasheninnikov and Kaleda (1994) on the Perapedhi section and corresponds with the conformable base of the Member III of their Kilani Formation (planktonic foraminiferal zone P22 *Turborotalia kugleri,* Fig. 3.4).

6.3.2 Pakhna Formation, Terra Limestone Member

The samples were collected from three localities of the Pakhna Formation, Terra Limestone Member, and all form part of measured sections (Figs 6.3,4,5) located in S.W. Cyprus. The Tala locality (P8; CGR 482 571) with sample **D581,** which is sandwiched within the basal horizon of the Pakhna Formation chalks, with a zonal range of NN1 and the Dhrousha locality (P1; CGR 455 713), with samples **D319, D322** and

D321, underlying the Pakhna Formation chalks again with a zonal range of NN1 and unconformably overlying the Lefkara Formation, Lower Member, and are both recognised localities of the Terra Limestone Member (Pantazis, 1979; Turner, 1971 respectively). The remaining locality is the newly recognised outcrop, first reported here, from Petra-tou-Romiou (P13; CGR 482 571) with sample **D495,** overlying the Pakhna Formation chalks with a zonal range of NN1. Thin sections were produced for all samples, and using the known locality of the Terra Limestone Member at Tala (sample **D581**) as a datum and along with published research (Follows and Robertson, 1990), the newly recognised locality was verified as a Terra Limestone Member locality, other than by its field relationship of being located at or near to the base of the Pakhna Formation.

The Terra Limestone Member was initially dated by Allen (1967) as Late Oligocene - Early Miocene, based on the presence of Benthonic foraminifera *Loxostomum delicatum* and the reef dwelling *Lepidocyclina sp.* and *Miogypsina sp.* Mantis (1970) also dated the member as Burdigalian, based on the presence of planktonic foraminiferal zones *Globigerinita dissimilis*, *Globoquadrina dehiscens* and *Globigerinoides glomerosa.*

The presence of the reef dwelling benthonic foraminifera *Lepidocyclina sp.* and *Miogypsina sp.* observed in all thin sections, indicates all samples were collected from the Terra Limestone Member.

6.3.3 Pakhna Formation, Kottaphi Hill measured section

K1 (CGR 142 785). The samples were collected from the Pakhna Formation chalks, which form part of a measured section at Kottaphi Hill (Fig. 6.7), near Agrokipia village, against the northern margin of the Troodos Massif. The section unconformably overlies the Lefkara Formation, Middle Member, Chalk and Chert unit, and is unconformably overlain by the Koronia Limestone Member of the Pakhna Formation (Zomenis, 1972).

Samples **D453 - D473** inclusive, contain a poor to moderately preserved assemblage of calcareous nannofossils, with a sparse to common population and a low to moderately diverse species content (Fig. 6.10). The age diagnostic species of *C. abisectus* (NP24-NN1; Lazarus *et al.*, 1995) observed in samples **D453 - D456** inclusive, *H. kamptneri* (NN1-NN21; Perch-Nielsen, 1985b) observed in samples **D454**

and **D450,** and *H. sissura* (NN1-NN4; Perch-Nielsen, 1985b) observed in sample **D456,** indicates a zonal range of NP24-NN1 (Fig. 6.11) for the base of the section (**D453**) and NN1 (Fig. 6.11) for the remaining units of the basal horizon. The presence of *Sphenolithus abies* Deflandre *in* Deflandre and Fert, 1954 (NN9-NN15; Perch-Nielsen, 1985b), observed in sample **D473,** indicates the top of the section to be no older than NN9 (Fig. 6.11). This gives an overall zonal range of NP24-NN9 for the measured section at Kottaphi Hill.

Discussion. The base of the Pakhna Formation chalks at Kottaphi Hill measured section, with a zonal range of NP24-NN1, is similar in age to the base of the formation seen in S.W. Cyprus, with a zonal range of NP25-NN1 (Oligo-Miocene boundary). Research carried out by Bear (1960) during the initial survey, mapped the area around Agrokipia and noted the unconformity between the basement and Lefkara Formation (Lapithos Group), Middle Member (Middle Lapithos), Chalk and Chert unit, followed by the unconformable overlying Pakhna Formation chalks and unconformable Koronia Limestone Member of the Pakhna Formation. Research by Mantis *in* Zomenis (1972), placed his lower units 1 and 2, which unconformably overlie the Lefkara Formation, Middle Member, Chalk and Chert unit into The Lefkara Formation, Upper Member (Upper Lefkara), with an age range of Late Oligocene to Early Miocene and the remaining higher units into the Pakhna Formation. Later research by Baroz and Bizon (1977) followed Bear (1960), by placing all the chalks between the Lefkara Formation and Koronia Limestone Member into the Pakhna Formation chalks, with an age range of Burdigalian to lower Messinian. Therefore the study agrees with Bear (1960) and Baroz and Bizon (1977), by placing all the chalks above the unconformity with the Lefkara Formation, Middle Member, Chalk and Chert unit, which represents the Pakhna ?transgressive event and below the unconformity with the Koronia Limestone Member, into the Pakhna Formation chalks at Kottaphi Hill.

6.3.4 Pissouri Formation (Myrtou Marls)

The samples collected from the Pissouri Formation (Myrtou Marls) of S.W. Cyprus, contain a moderate to well preserved assemblage of calcareous nannofossils.

Samples **D267 (MM3)** and **D311 (MM1),** contain an abundant population, with a high diversity of species content (Fig. 6.9). The combined presence of *Discoaster neorectus* Bukry, 1971 (NN10-NN11; Perch-Nielsen, 1985b) observed in both samples, *Discoaster bellus* Bukry and Percival, 1971 (NN9-NN10; Perch-Nielsen, 1985b)

observed in sample **D311** and *Catinaster coalitus* Martini and Bramlette, 1963 (NN8-NN10; Perch-Nielsen, 1985b) observed in sample **D267,** indicates a zonal range of NN10 for both assemblages.

Sample **D565 (MM2),** contains an abundant population, with a high diversity of species content (Fig. 6.9). The combined presence of *D. neorectus* (NN10-NN11; Perch-Nielsen, 1985b) and *Amaurolithus amplificus* (Bukry and Percival, 1971) (NN11-NN12; Perch-Nielsen, 1985b), indicates a zonal range of NN11 (Fig. 6.11), for the assemblage.

The outcrop pattern displayed by the limited sampling of the Pissouri Formation (Myrtou Marls), basal horizon in S.W. Cyprus, which makes unconformable contact with the underlying rocks, is diachronous from the north (NN10; MM1 and MM3; Fig. 6.1) to south (NN11; MM2; Fig. 6.1), and suggest the underlying Kalavasos Formation (evaporites), located south-east of Dhrousha village (Polemi basin), to older (Tortonian) than initially reported as Messinian (Pantazis, 1978; Orszag-Sperber et al., 1989).

Discussion. Based on the biostratigraphical data above, the north to south diachronous (NN10 to NN11) unconformable contact of the Pissouri Formation (Myrtou Marls), continues southwards and can be correlated with the research carried out by Krasheninnikov and Kaleda (1994), on the Perapedhi section and corresponds with their unconformable contact of basal Pliocene (calcareous nannofossil zonal range of NN12).

6.4 Summary

1). The unconformable contact between the basal horizon of the Pakhna Formation chalks (Pakhna transgressive event) and the underlying rocks has been dated, with a relative biostratigraphical zonal range of NP25-NN1 (Oligo-Miocene boundary) for S.W. Cyprus.

2). The outcrop pattern displayed by the Pakhna Formation, where it makes direct contact with the southern Mamonia basement fragment, suggest the fragment continued to act as a structural high, during an erosional event prior to the onset of the Pakhna transgressive event

3). A newly recognised outcrop of the Pakhna Formation, Terra Limestone Member has been located at Petra-tou-Romiou, conformably overlying the Pakhna Formation chalks, with a relative biostratigraphical zonal range of NN1.

4).The study of the Pakhna Formation basal horizon, from the Kottaphi Hill measured section, near Agrokipia village, against the northern margin of the Troodos Massif, confirms the onset of the Pakhna transgressive event at this locality, with a relative biostratigraphical zonal range of NP24-NN1, which is similar to the zonal range of NP25-NN1 (Oligo-Miocene boundary), recorded for the ?transgressive event in S.W. Cyprus.

5). Age dated the north to south trending diachronous unconformable contact between the basal horizon of the Pissouri Formation (Myrtou Marls) and the underlying rocks, with a relative biostratigraphical zonal range of NN10 west of Polis, NN11 north of Paphos and NN12 east of Petra-tou-Romiou (Perapedhi section of Krasheninnikov and Kaleda, 1994) for S.W. Cyprus.

6). Age dated the Kalavasos Formation of S.W. Cyprus (Polemi basin) as Tortonian, older than initially thought (Messinian).

6.5 Systematic Descriptions

Family **Ceratolithaceae** Norris, 1965

Genus ***Amaurolithus*** Gartner & Bukry, 1975

Type species. *Ceratolithus tricorniculatus* Gartner, 1967.

Remarks. The horseshoe-shaped genus *Amaurolithus* differs from the similar form *Ceratolithus* (Kamptner, 1950), by only showing weak birefringence between crossed polars.

Amaurolithus amplificus (Bukry & Percival) Gartner & Bukry, 1975

(Pl. 10, fig. 1)

1971 *Ceratolithus amplificus* Bukry & Percival: 125, pl. 1, figs 9-11.

1975 *Amaurolithus amplificus* (Bukry & Percival); Gartner & Bukry: 454, pl. 6, figs g-l.

1994 *Amaurolithus amplificus* (Bukry & Percival); Staerker: pl. 1, figs 13a-b.

Holotype. Bukry & Percival, pl. 1, figs 9,10, USNM 169176, sample V3-153, 531cm, locality Lamont core , Atlantic Ocean.

Description. Between crossed polars, horseshoe-shaped nannoliths of robust construction. Asymmetrical outline with one arm straighter and shorter than the other and displays a central ridge (overgrowths commonly cover node-like projections to form the ridge). Short apical spine on outer part of arch located above shorter arm.
Dimensions. Length 14.4μm: Width 8.0μm.
Remarks. Normally viewed in plane polarised light, due to weak birefringence. Gartner & Bukry (1975), considered the robust arms, asymmetrical outline and small broad apical spine above the straight arm, to be distinguishing features of the species.
Occurrence. The species is observed in the basal section of the Myrtou Marls, Pissouri Formation of S.W. Cyprus, which makes contact with the underlying rocks unconformably. The short vertical range of *Amaurolithus amplificus*, makes the species stratigraphically important.
Range. Late Miocene (NN11 to NN12), Perch-Nielsen (1985b).

Amaurolithus delicatus Gartner & Bukry, 1975
(Pl. 10, fig. 2)

1975 *Amaurolithus delicatus* Gartner & Bukry: 456, pl. 7, figs a-f.

1992 *Amaurolithus delicatus* Gartner & Bukry; Xu & Wise: pl. 5, figs 3,4.

Holotype. Gartner & Bukry, pl. 7, fig. e, sample DSDP 22-214-9, 22-23cm, locality Indian Ocean (lat 11°20' S.; long 88°43' E.).
Description. In plane polarised light, horseshoe-shaped nannoliths of delicate construction. Slightly asymmetrical, with sub equal arms of equal thickness tapering to points and pointing inwards to indicate closure of open end of horseshoe.
Dimensions. Length 12.8μm: Width 9.6μm.
Remarks. *Amaurolithus delicatus* is distinguished from *A. primus* (Bukry & Percival, 1971) and *A. tricorniculatus* (Gartner, 1967) by being longer than the width in the former and in the latter by not having apical spine on outer part of the arch. Gartner & Bukry (1975), considered the delicate construction and lacking an apical spine, to be distinguishing features of the species.
Occurrence. The species is observed in the basal section of the Myrtou Marls, Pissouri Formation of S.W. Cyprus, which makes contact with the underlying rocks unconformably. The short vertical range of *Amaurolithus delicatus*, makes the species stratigraphically important.
Range. Late Miocene to Early Pliocene (NN11 to NN13), Perch-Nielsen (1985b).

Family **Coccolithaceae** Poche, 1913

Genus ***Calcidiscus*** Kamptner, 1950

Type species. *Calcidiscus quadriforatus* Kamptner, 1950.

Remarks. The genus includes circular coccoliths, with distal shield composed of a single cycle of elements and larger than simple proximal shield. Central area open or closed. Refer to Loeblich and Tappan (1978), who have provided a detailed review of the genus.

Calcidiscus leptoporus (Murray & Blackman) Loeblich & Tappan, 1978
(Pl. 10, fig. 3; Pl. 11, fig. 5)

1898 *Coccosphaera leptoporus* Murray & Blackman: 430, 439, pl. 15, figs 1-7.

1978 *Calcidiscus leptoporus* (Murray & Blackman); Loeblich & Tappan: 1391.

1994 *Calcidiscus leptoporus* (Murray & Blackman); Staerker: pl. 3, fig. 2.

Holotype. Murray & Blackman, pl. 15, figs 1-7 (line illustrations).

Description. Circular coccoliths, with distal shield comprising a single cycle of on average 28 overlapping elements. Central area formed by depression with small central opening.

Dimensions. Diameter 9.3μm.

Remarks. *Calcidiscus leptoporus* is distinguished from *C. macintyrei* by having less elements in distal shield (<34) and being smaller (<10μm), (Perch-Nielsen, 1985b).

Occurrence. The species observed at several Early and Late Miocene localities, in the Pakhna and Pissouri (Myrtou Marls) Formations, of S.W. Cyprus.

Range. Miocene to Holocene, Perch-Nielsen (1985b).

Calcidiscus macintyrei (Bukry & Bramlette) Loeblich & Tappan, 1978
(Pl. 10, fig. 4; Pl. 11, fig. 8)

1969 *Cyclococcolithus macintyrei* Bukry & Bramlette: 132, pl. 1, figs 1-3.

1978 *Calcidiscus macintyrei* (Bukry & Bramlette); Loeblich & Tappan: 1392.

1992 *Calcidiscus macintyrei* (Bukry & Bramlette); Wei & Wise: pl. 1, figs 1,2.

Holotype. Bukry & Bramlette, pl. 1, fig. 1, USNM 651407, locality south of Lugagnano, Torrente Arda, south of Piacenza, Po Valley, Italy.

Description. Circular coccoliths, with distal shield composed of on average 40 overlapping elements. Small central opening.
Dimensions. Diameter 10.4μm.
Remarks. Perch-Nielsen (1985b), considered the distal shield comprising not less than 40 elements and small central opening, to be distinguishing features of the species.
Occurrence. The species observed at several Early and Late Miocene localities, in the Pakhna and Pissouri (Myrtou Marls) Formations, of S.W. Cyprus.
Range. Miocene to Pliocene (NN4 to NN18), Perch-Nielsen (1985b).

Genus ***Coccolithus*** Schwarz, 1984

Type species. *Coccosphaera pelagica* Wallich, 1877.
Remarks. The genus includes elliptical coccoliths, with distal shield comprising a single cycle of elements. Elements at distal margin of open central area are radially oriented and do not form a crest above distal surface. A bridge may be present, aligned to the short axis.

Coccolithus miopelagicus Bukry, 1971
(Pl. 10 fig. 7)

1971 *Coccolithus miopelagicus* Bukry: 1971: 310, pl. 2, figs 6-9.
1973 *Coccolithus miopelagicus* Bukry; Wise: *emend* 593, pl. 8, figs 9-11.

Holotype. Bukry, pl. 2, figs 7,8, USNM 176888, sample DSDP 63.0-3-4, 80-81cm, locality East Caroline Basin, western equatorial Pacific Ocean.
Description. In plane polarised light, large elliptical coccoliths. In distal view, broad rim enclosing cycle of inclined irregular granules, forming distal margin of open central area. Central area in relation to overall size, long axis 47% and short axis 35% of total length, on average.
Dimensions. Overall length 15.2μm, width 13.6μm: Central area, length 7.2μm, width 4.8μm.
Remarks. In plane polarised light, *Coccolithus miopelagicus* is similar in appearance to *C. eopelagicus* (Bramlette & Riedel, 1954) and *C. pliopelagicus*, but can be distinguished in the former by size of central area in relation to its overall size (Bukry, 1971), with the long axis at 50% [59%], and the short axis at 42% [50%] of total length, maximum (Wise (1973), emended the short axis measurement to include down to 30%), and in the latter by overall size (>13μm).

Occurrence. The species is observed at almost all of the Early Miocene localities, in the Pakhna Formation, of S.W. Cyprus.
Range. Late Oligocene to Mid Miocene, Perch-Nielsen (1985b).

Coccolithus pelagicus (Wallich) Schiller, 1930
(Pl. 10, fig. 5)

1877 *Coccosphaera pelagica* Wallich: 348, pl. 17, figs 1,2,5,11,12.

1930 *Coccolithus pelagicus* (Wallich); Schiller: 246, figs 123,124.

1973 *Coccolithus pelagicus* (Wallich); Roth: 730, pl. 1, fig. 1; pl. 4, figs 3,6.

Holotype. Wallich, pl. 17, figs 1,2,5,11,12 (line illustrations).
Description. Between crossed polars and plane polarised light, elliptical coccoliths, with a distal shield of weak birefringence, composed of slightly dextral imbricating elements and inner cycle with stronger birefringence forming distal margin to small open central area, sometimes bridged by a crossbar aligned to short axis of the ellipse.
Dimensions. Length 8.0μm: Width 6.4μm.
Remarks. *Coccolithus pelagicus* is similar in appearance to *C. eopelagicus* (Bramlette & Riedel, 1954), *C. miopelagicus* and *C. pliopelagicus* but is much smaller in size (<13μm) and lacks an elongate central area. Tends to be used as a 'waste basket' for simple elliptical coccoliths of the Coccolithaceae family(Perch-Nielsen, 1985b).
Occurrence. The species is observed at almost all of the Tertiary localities, of S.W. Cyprus, in the Lefkara, Pakhna and Pissouri (Myrtou Marls) Formations.
Range. Palaeocene to Holocene, Perch-Nielsen (1985b).

Coccolithus pliopelagicus Wise, 1973
(Pl. 10, fig. 6)

1973 *Coccolithus pliopelagicus* Wise: 593, pl. 8, figs 1-6.

Holotype. Wise, pl. 8, figs 1-3, USNM 186174, sample DSDP 176-5, (120cm), locality Oregon continental shelf, Pacific Ocean.
Description. In plane polarised light, large elliptical coccoliths, with a broad rim enclosing cycle of inclined irregular granules, forming distal margin of open elongate central area. Central area in relation to overall size, long axis 53% and short axis 46% of total length.

Dimensions. Overall length 12.0μm, width 10.4μm: Central area, length 6.4μm, width 4.8μm.

Remarks. The central area of specimen described, on average has a short axis length greater than 40% of total length. However, Wise (1973) noted forms from the Miocene, that resemble the specimens described, by having central area less elongate and more oval in shape and suggests that those forms may be ancestor to *Coccolithus pliopelagicus*.

Occurrence. The species is observed in the basal section of the Myrtou Marls, Pissouri Formation of S.W. Cyprus, which makes contact with the underlying rocks unconformably.

Range. Mid Miocene to Pliocene (NN5 to NN18), Wise (1973).

Genus ***Umbilicosphaera*** Lohmann, 1902

Type species. *Coccosphaera sibogae* Weber-van Bosse, 1901.

Remarks. The genus includes elliptical or circular coccoliths, with distal shield comprising a single cycle of radially arranged elements. Between crossed polars, central tube or inner cycle of elements shows strong birefringence, giving a collar appearance at distal margin of open central area.

Umbilicosphaera sibogae (Weber-van Bosse) Gaarder, 1970
(Pl. 10, fig. 7,8)

1901 *Coccosphaera sibogae* Weber-van Bosse: 137, 140, pl. 17, figs 1,2.

1902 *Umbilicosphaera mirabilis* Lohmann: 139, pl. 5, figs 66,66a.

1970 *Umbilicosphaera sibogae* (Weber-van Bosse); Gaarder: 126. figs 8e,9c-d.

1991 *Umbilicosphaera sibogae* (Weber-van Bosse); Shyu & Müller: pl. 3, fig. 10.

Holotype. Weber-van Bosse, pl. 17, figs 1,2 (line illustrations).

Description. Circular coccoliths, with distal shield composed of on average 40 radial elements. At distal margin of open central area, elements of central tube form a collar, showing good birefringence when seen between crossed polars.

Dimensions. Overall diameter 8.0μm: Central area 2.4μm.

Remarks. Perch-Nielsen (1985b), considered the circular shape and the relatively large central opening to be distinguishing features of the species.

Occurrence. The species observed at several Early and Late Miocene localities, in the Pakhna and Pissouri (Myrtou Marls) Formations, of S.W. Cyprus.
Range. Mid Miocene to Holocene, Perch-Nielsen (1985b).

Family **Discoasteraceae** Tan Sin Hok, 1927

Genus ***Catinaster*** Martini & Bramlette, 1963

Type species. *Catinaster coalitus* Martini & Bramlette, 1963.
Remarks. The genus includes basket-shaped nannoliths, composed of rays that may extend beyond the central section. The inter areas between the rays may be thin or partially open.

Catinaster coalitus Martini & Bramlette, 1963
(Pl. 11, fig. 5)

1963 *Catinaster coalitus* Martini & Bramlette: 851, pl. 103, figs 7-10.

1975a *Catinaster coalitus* Martini & Bramlette; Jafar: 53, pl. 6, figs 13-16.

1992 *Catinaster coalitus* Martini & Bramlette; Xu & Wise: pl. 5, figs 9,10,17.

Holotype. Martini & Bramlette, pl. 103, fig. 7, USNM 647856, horizon Lengue Formation, locality Lengue Settlement, Trinidad.
Description. Basket-shaped nannoliths, sub circular- to hexagonal-shaped in plan view, formed by six bent rays that appear to bifurcate perpendicular to the ray at the tips, to form outer rim. The inter areas between rays are partially open.
Dimensions. Diameter 12μm.
Remarks. *Catinaster coalitus* differs from *C. calyculus* Martini & Bramlette, 1963, by the rays not extending beyond the basket. The species is distinguished by the form of six rays that bifurcate at right angles at the tips, to form distal outer rim (Martini & Bramlette, 1963).
Occurrence. The species is observed in the basal section of the Myrtou Marls, Pissouri Formation of S.W. Cyprus, which makes contact with the underlying rocks unconformably. The short vertical range of *Catinaster coalitus*, makes the species stratigraphically important.
Range. Late Miocene (NN8 to NN10), Perch-Nielsen (1985b).

Genus *Discoaster* Tan Sin Hok, 1927

Type species. *Discoaster pentaradiatus* Tan Sin Hok, 1927.

Remarks. The genus includes rosette- or star-shaped nannoliths in plan view. In side view, species can be either bi-convex, concavo-convex or plano-convex and all species show radial symmetry. Central boss and/or stem may be present on distal and/or proximal surface.

Discoaster cf *bellus* Bukry & Percival, 1971

(Pl. 10, fig. 9)

1971 *Discoaster bellus* Bukry & Percival: 128, pl. 3, figs 1,2.

Holotype. Bukry & Percival, pl. 3, fig. 1, USNM 169189, sample DSDP core 55.0-4-1, 130-131cm, locality Caroline Rise, Pacific Ocean.

Description. In plane polarised light, star-shaped nannoliths, all showing dissolution. Composed of five slightly tapering arms that terminate as blunt points. Suture lines visible between crossed polars from centre to inter-areas between arms, no central structure present.

Dimensions. Diameter 10.4μm.

Remarks. *Discoaster bellus* is distinguished from *D. hamatus* Martini & Bramlette, 1963, by being consistently smaller in size, broader rays and lacking ray-tip spur. Bukry & Percival (1971), considered the simple five rays with no central structure, to be distinguishing features of the species.

Occurrence. The species is observed in the basal section of the Myrtou Marls, Pissouri Formation of S.W. Cyprus, which makes contact with the underlying rocks unconformably. The short vertical range of *Discoaster bellus*, makes the species stratigraphically important.

Range. Late Miocene (NN9 to NN10), Perch-Nielsen (1985b).

Discoaster pentaradiatus (Tan Sin Hok) *emend* Bramlette & Riedel, 1954

(Pl. 10, fig. 18)

1927 *Discoaster pentaradiatus* Tan Sin Hok: 416, fig. 14.

1954 *Discoaster pentaradiatus* (Tan Sin Hok); *emend* Bramlette & Riedel: 401, figs 2a-b, pl. 39, fig. 11.

1991 *Discoaster pentaradiatus* (Tan Sin Hok); Spaulding: pl. 3, figs 7,8.

Holotype. Tan, 416, fig. 14 (line illustration).

Description. In plane polarised light, star-shaped nannoliths. Composed of five thin tapering arms with terminal bifurcation that is thin and delicate.

Dimensions. Diameter 16μm.

Remarks. Bramlette & Riedel (1954), considered the five thin tapering arms with delicate terminal bifurcation to be distinguishing features of the species.

Occurrence. The species is observed in the basal section of the Myrtou Marls, Pissouri Formation of S.W. Cyprus, which makes contact with the underlying rocks unconformably.

Range. Late Miocene to Pliocene (NN9 to NN17), Perch-Nielsen (1985b).

Discoaster cf *neorectus* Bukry, 1971

(Pl. 10, fig. 19)

1971 *Discoaster neorectus* Bukry: 316, pl. 4, figs 6,7.

Holotype. Bukry, pl. 4, fig. 7, USNM 176905, sample DSDP 72.0-3-4, 63-64cm, locality western flank East Pacific Rise, Equatorial Pacific Ocean.

Description. In plane polarised light, large star-shaped nannoliths, composed of six long straight to slightly convex arms, that terminate in simple points.

Dimensions. Diameter 17.0μm.

Remarks. Possible due to dissolution, specimens described are smaller than that described by Bukry (1971),which are >20.0μm in diameter.

Occurrence. The species is observed in the basal section of the Myrtou Marls, Pissouri Formation of S.W. Cyprus, which makes contact with the underlying rocks unconformably. The short vertical range of *Discoaster neorectus*, makes the species stratigraphically important.

Range. Late Miocene (NN10 to NN11), Perch-Nielsen (1985b).

Discoaster variabilis Martini & Bramlette, 1963

(Pl. 10 fig. 13)

1963 *Discoaster variabilis* Martini & Bramlette: 854, pl. 104, figs 4-9.

1992 *Discoaster variabilis* Martini & Bramlette; Siesser & Bralower: pl. 5, fig. 12.

Holotype. Martini & Bramlette, pl. 104, figs 4,5, USNM 647860, horizon Tortonian type locality, locality Rio Mazzapiedi-Castellania, near Tortona, Italy.

Description. In plane polarised light, star-shaped nannoliths, comprising six broad slightly tapered arms, thinning distally and terminate with bifurcation to form angle of approximately 90°. Centrally, stellate knob is present, with tips extending into median line of the arms.

Dimensions. Diameter 12μm.

Remarks. *Discoaster variabilis* is distinguished from *D. exilis* Martini & Bramlette, 1963, by having more robust/broad rays and *D. challengeri* (Bramlette & Riedel, 1954) by having smaller central area.

Occurrence. The species is observed at several Mid Miocene localities, in the Pakhna Formation, of S.W. Cyprus..

Range. Mid Miocene to Early Pliocene (NN3 to NN16), Perch-Nielsen (1985b).

Family **Helicosphaeraceae** Black, 1971b

Genus ***Helicosphaera*** Kamptner, 1954

Synonym: *Helicopontosphaera* Hay & Mohler *in* Hay *et al.* (1967).

Type species. *Coccosphaera carteri* Wallich, 1877.

Remarks. The genus includes helical-rimmed, elliptical coccoliths, usually with an asymmetrical flange, constructed of radial elements. Central area, open with or without bridge or closed and may display median slit oriented to long axis.

Helicosphaera granulata Bukry & Percival, 1971

(Pl. 10, figs 10,14)

1971 *Helicopontosphaera granulata* Bukry & Percival: 132, pl. 5, figs 1,2.

1991 *Helicosphaera granulata* Bukry & Percival; Shyu & Müller: pl. 2, fig. 3.

Holotype. Bukry & Percival, pl. 5, figs 1,2, USNM 169208, sample DSDP core 15-3-2, 78-79cm, locality Mid-Atlantic Ridge, Atlantic Ocean.

Description. Between crossed polars, elliptical coccoliths, with distal shield forming helix about central shield and terminal flange protrudes below base-line. In plane polarised light central area displays a granular texture.

Dimensions. Overall length 13.6μm, width 10.0μm: Central area, length 6.4μm, width 4.8μm: Flange protrudes below the base-line by 2.5μm.

Remarks. Between crossed polars *Helicosphaera granulata* is distinguished from *H. burkei* Black, 1971b, by the terminal flange protruding below base-line (Perch-Nielsen, 1985b).

Occurrence. The species is observed at a single locality in the Pakhna Formation (Early Miocene), south of Arkhimandrita, S.W. Cyprus.

Range. Miocene (NN2 to NN10), Perch-Nielsen (1985b).

Helicosphaera kamptneri Hay & Mohler *in* Hay *et al.*, 1967
(Pl. 10, fig. 12; Pl. 11, fig. 7)

1967 *Helicopontosphaera kamptneri* Hay & Mohler *in* Hay *et al.*: 448, pl. 10, fig. 5; pl. 11, fig. 5.

1992 *Helicosphaera kamptneri* Hay & Mohler *in* Hay *et al.*; Xu & Wise: pl. 4, figs 6,7.

Holotype. Hay & Mohler, pl. 10, fig. 5; pl. 11, fig. 5, sample UI-H-3730, locality Core CG-9, Lat. 17°12' N, Long. 65°45' W, eastern Venezuelan Basin.

Description. Between crossed polars, elliptical coccoliths, with distal shield forming helix about central shield with small terminal flange. Closed central area, with median slit oriented to long axis and both ends terminating at a small perforation.

Dimensions. Overall length 12.0μm, width 7.2μm: Central area, length 7.2μm, width 4.8μm.

Remarks. Between crossed polars *Helicosphaera kamptneri* is distinguished from *H. orientalis* Black, 1971b, by its size (>5μm).

Occurrence. The species is observed at almost all of the Early and Late Miocene localities, in the Pakhna and Pissouri (Myrtou Marls) Formations, of S.W. Cyprus.

Range. Miocene to Pleistocene (NN1 to NN21), Perch-Nielsen (1985).

Helicosphaera selli Bukry & Bramlette, 1969
(Pl. 10 figs 11,15)

1969 *Helicopontosphaera selli* Bukry & Bramlette: 134, pl. 2, figs 3-7.

1991 *Helicosphaera selli* Bukry & Bramlette; Spaulding: pl. 1, figs 15-17.

Holotype. Bukry & Bramlette, pl. 2, figs 3,4, USNM 651416, locality Le Castella 81, Calabria, southern Italy.

Description. Between crossed polars, elliptical coccoliths, with distal shield forming helix about central shield with terminal flange. Open central area, bridged by continuos oblique (leaning towards terminal flange in relation to base-line) crossbar, aligned to short axis.

Dimensions. Overall length 13.6μm, width 8.8μm: Central area, length 7.2μm, width 4.0μm.

Remarks. Between crossed polars, *Helicosphaera selli* differs from *H. kamptneri* by having an oblique central crossbar. in poorly preserved specimens, calcite overgrowth reduces the central opening and enlarges the central crossbar.

Occurrence. The species is observed in the basal section of the Myrtou Marls, Pissouri Formation of S.W. Cyprus, which makes contact with the underlying rocks unconformably.

Range. Late Miocene to Pliocene (NN10 to NN19), Perch-Nielsen (1985b).

Helicosphaera sissura Miller, 1981

(Pl. 10, fig. 16)

1981 *Helicosphaera sissura* Miller: 433, pl. 3, figs 10a-c,11a-c.

Holotype. Miller, pl. 3, figs 10a-c, sample Chevron CN02B, 513-94 horizon Galloway Formation, locality Galloway Creek, Point Arena, California.

Description. Between crossed polars, long elliptical coccoliths, with distal shield which displays a small rounded terminal flange. Central area with narrow elongate opening oriented to long axis.

Dimensions. Length 11.2μm: Width 7.2μm.

Remarks. Between crossed polars *Helicosphaera sissura* is distinguished from *H. ampliaperata* Bramlette & Wilcoxon, 1967, and *H. californiana* Bukry, 1981, by its moderate size and the elongate central opening.

Occurrence. The species is observed at several Lower Miocene localities, in the Pakhna Formation, of S.W. Cyprus. The short vertical range of *Helicosphaera sissura*, makes the species stratigraphically important.

Range. Early Miocene (NN1 to NN4), Perch-Nielsen (1985b).

Family **Pontosphaeraceae** Lemmermann, 1908

Genus ***Pontosphaera*** Lohmann, 1902

Type species. *Pontosphaera syracusana* Lohmann, 1902.
Remarks. The genus includes elliptical coccoliths, composed of two concavo-convex appressed plates, forming low to medium high walls in side view, the distal shield being the convex surface. Distally a flange cycle may be present. Central area may have one large opening or completely covered, few or many perforations/depressions may be present.

Pontosphaera multipora (Kamptner) Roth, 1970
(Pl. 9, fig. 18)

1948 *Discolithus multipora* Kamptner: 5, pl. 1, fig. 9.

1970 *Pontosphaera multipora* (Kamptner); Roth: 860.

1979 *Pontosphaera multipora* (Kamptner); Romein: 177.

1982 *Pontosphaera multipora* (Kamptner); Hamilton & Hojjatzadak: pl. 6.3, figs 5,6; pl. 6, figs 20-23.

Holotype. Kamptner, pl. 1, fig. 9 (line illustration).
Description. Between crossed polars, large elliptical coccoliths. When seen in distal view, a narrow rim surrounds a large closed central area containing >20 pores.
Dimensions. Length 10.0μm: Width 6.7μm.
Occurrence. The species is observed at almost all of the Early and Late Miocene localities, of S.W. Cyprus, in the Pakhna and Pissouri (Myrtou Marls) Formations.
Range. Palaeocene to Pleistocene, Hamilton and Hojjatzadak (1982).

Genus ***Scyphosphaera*** Lohmann, 1902

Type species. *Scyphosphaera apsteini* Lohmann, 1902.
Remarks. The genus includes large, high barrel-shaped coccoliths, with a proximal plate, similar to that seen in the central area of the genus *Pontosphaera*.

Scyphosphaera apsteini Lohmann, 1902

(Pl. 9, figs 1,2)

1902 *Scyphosphaera apsteini* Lohmann: 132, pl. 4, figs 26-30.

1955 *Scyphosphaera apsteini* Lohmann; Kamptner: 22, pl. 8, figs 109-112.

1975a *Scyphosphaera apsteini* Lohmann; Jafar: 27, pl. 1, figs 1,4-7,9.

Holotype. Lohmann, pl. 4, figs 26-30 (line illustrations).

Description. Between crossed polars, barrel-shaped coccoliths, in side view, with proximal surface slightly concave, side wall slightly convex and side wall terminating simply at distal opening.

Dimensions. Height 12.0μm: Diameter 10.0μm.

Remarks. A simple barrel-shaped coccolith, were height is slightly smaller or greater than the maximum width and is considered by Jafar (1975a), to be a distinguishing feature of the species.

Occurrence. The species is observed in the basal section of the Myrtou Marls, Pissouri Formation of S.W. Cyprus, which makes contact with the underlying rocks unconformably.

Range. Mid Miocene to Early Pliocene, Perch-Nielsen (1985b).

Scyphosphaera canescens Kamptner, 1955

(Pl. 9, fig. 3)

1955 *Scyphosphaera canescens* Kamptner: 24, pl. 9, fig. 120.

1975b *Scyphosphaera canescens* Kamptner; Jafar: 370, pl. 1, fig. 2.

Holotype. Kamptner, pl. 9, fig. 120 (line illustration).

Description. Between crossed polars, cylindrical-shaped coccoliths, in side view, with concave proximal surface and side wall more or less vertical.

Dimensions. Height 16μm: Diameter 7.2μm.

Remarks. Between crossed polars *Scyphosphaera canescens* differs from *S. conica* by having more or less parallel sides, with apical opening and proximal base of similar size, which is considered a distinguishing feature of the species by Jafar (1975b).

Occurrence. The species is observed in the basal section of the Myrtou Marls, Pissouri Formation of S.W. Cyprus, which makes contact with the underlying rocks unconformably.

Range. Mid Miocene to Early Pliocene, Perch-Nielsen (1985b).

Scyphosphaera conica Kamptner, 1955
(Pl. 9, fig. 5)

1955 *Scyphosphaera conica* Kamptner: 26, pl. 9, figs 130,131.

1975b *Scyphosphaera conica* Kamptner; Jafar: 370. pl. 2, fig. 8.

Holotype. Kamptner, pl. 9, figs 130,131 (line illustrations).

Description. Between crossed polars, cylindrical-shaped coccoliths, in side view. Flat proximal surface, with converging side wall, terminating simply at apical opening, which is smaller than the proximal base.

Dimensions. Height 16.0μm: Proximal base 6.4μm: Apical opening 4.8μm.

Remarks. The Large cylindrical-shaped coccolith, with converging side wall is considered to be a distinguishing feature of the species, by Jafar (1975b).

Occurrence. The species is observed in the basal section of the Myrtou Marls, Pissouri Formation of S.W. Cyprus, which makes contact with the underlying rocks unconformably.

Range. Mid Miocene to Early Pliocene, Perch-Nielsen (1985b).

Scyphosphaera recta (Deflandre) Kamptner, 1955
(Pl. 9, fig. 4)

1942 *Scyphosphaera apsteini* Deflandre: 131, fig. 16.

1955 *Scyphosphaera recta* (Deflandre); Kamptner: 23, pl. 8, figs 115,116.

1975a *Scyphosphaera recta* (Deflandre); Jafar: 30, pl. 2, figs 5,6.

Holotype. Deflandre, fig. 16 (line illustration).

Description. Between crossed polars, barrel-shaped coccoliths, in side view. Broad proximal surface slightly concave, wall rises from proximal surface and diverges distally, then terminates with inward curve to form apical opening of similar dimensions to proximal surface. Position of maximum width just below apical opening.

Dimensions. Height 16μm: Diameter 11.2μm.

Remarks. Between crossed polars *Scyphosphaera recta* is distinguished from *S. recurvata* and *S. piriformis* Kamptner, 1955, by having in the former an apical opening and proximal base of similar size, and in latter by being smaller in overall size.

Occurrence. The species is observed in the basal section of the Myrtou Marls, Pissouri Formation of S.W. Cyprus, which makes contact with the underlying rocks unconformably.

Range. Mid Miocene to Early Pliocene, Perch-Nielsen (1985b).

Scyphosphaera recurvata Deflandre, 1942
(Pl. 9, fig. 6)

1942 *Scyphosphaera recurvata* Deflandre: 132, figs 17-20.

1955 *Scyphosphaera recurvata* Deflandre; Kamptner: 24, fig. 121.

1975a *Scyphosphaera recurvata* Deflandre; Jafar: 31, pl. 3, figs 4-7.

Holotype. Deflandre, figs 17-20.

Description. Between crossed polars, pear-shaped coccoliths, in side view. Proximal surface slightly concave, wall rises from proximal surface diverging with slight concavity, becoming convex distally, then terminates with inward and downward curve to form apical opening smaller than proximal base. Position of maximum width just below apical opening.

Dimensions. Length 16.0µm: Diameter 12.0µm: Proximal surface 6.4µm: Apical opening 4.8µm.

Remarks. The pear-shaped coccolith with apical opening formed by inward and downward curve of side wall, is considered to be a distinguishing feature of the species, by Jafar (1975a).

Occurrence. The species is observed in the basal section of the Myrtou Marls, Pissouri Formation of S.W. Cyprus, which makes contact with the underlying rocks unconformably.

Range. Mid Miocene to Early Pliocene, Perch-Nielsen (1985b).

Scyphosphaera turris Kamptner, 1955
(Pl. 9, fig. 7)

1955 *Scyphosphaera turris* Kamptner: 26, pl. 9, fig. 132.

1975a *Scyphosphaera turris* Kamptner; Jafar: 35, pl. 3, figs 2,3.

Holotype. Kamptner, pl. 9, fig. 132 (line illustration).

Description. Between crossed polars, flask-shaped coccoliths. In side view, concave proximal surface, with side wall diverging slightly outwards from base and then

converges sharply and forms a gentle concave profile. The wall terminates simply at apical opening. Position of maximum width, just above base.

Dimensions. Height 14.4µm: Diameter 8.4µm: Proximal base 6.4µm: Apical opening 4.0µm.

Remarks. Between crossed polars *Scyphosphaera turris* differs from *S. intermedia* Deflandre, 1942, and *S. lagena* Kamptner, 1955, by having in the former, less concave walls and not having divergent bend at apical opening, and in the latter, by having less parallel sides terminating at apical opening.

Occurrence. The species is observed in the basal section of the Myrtou Marls, Pissouri Formation of S.W. Cyprus, which makes contact with the underlying rocks unconformably.

Range. Mid Miocene to Early Pliocene, Perch-Nielsen (1985b).

Family **Prinsiaceae** Hay & Mohler, 1967

Genus ***Cyclicargolithus*** Bukry, 1971

Type species. *Coccolithus floridanus* Roth & Hay *in* Hay *et al.* (1967).

Remarks. The genus includes circular to sub circular coccoliths, with distal shield slightly larger than proximal shield, joined by central tube. Inner wall at distal margin of open (not spanned by grid) or closed central area, does not rise above distal surface.

Cyclicargolithus abisectus (Müller) Wise, 1973
(Pl. 9, figs 8,12)

1970 *Coccolithus abisectus* Müller: 112, pl. 9, figs 1,2.

1973 *Cyclicargolithus abisectus* (Müller); Wise: 594.

1980 *Cyclicargolithus abisectus* (Müller); Backman: pl. 1, figs 8,9.

Holotype. Muller, pl. 9, figs 1,2.

Description. Between crossed polars, sub circular coccoliths, with distal shield composed of on average 48 radial elements, forming broad rim. At distal margin of central area with small opening, wall/tube displays extinction lines which forms a square structure.

Dimensions. Diameter 10.4µm: Central area 4.8µm.

Remarks. *Cyclicargolithus abisectus* is distinguished from *C. floridanus,* by the partial covering of regularly arranged elements surrounding central area, size (>9µm) and

between crossed polars, extinction lines of central tube are disjunct (Perch-Nielsen, 1985b).

Occurrence. The species is observed at almost all of the Early Miocene localities, in the Pakhna Formation, of S.W. Cyprus. The short vertical range of *Cyclicargolithus abisectus*, makes the species stratigraphically important.

Range. Oligocene/Miocene boundary (NP24 to NN1), Lazarus *et al.* (1995).

Cyclicargolithus floridanus (Roth & Hay *in* Hay *et al.*) Bukry, 1971
(Pl. 11, fig. 1)

1967 *Coccolithus floridanus* Roth & Hay *in* Hay *et al.*: 445, pl. 6, figs 1-4.

1970 *Cyclococcolithus floridanus* (Roth & Hay *in* Hay *et al.*) Roth: 854, pl. 5, fig. 6.

1971 *Cyclicargolithus floridanus* (Roth & Hay *in* Hay *et al.*) Bukry: 312.

Holotype. Roth & Hay, pl. 6, fig. 1, sample IMS-J501-164, locality Blake Plateau, western Atlantic.

Description. Sub circular coccoliths, with distal shield composed of slightly dextrally imbricate elements, forming broad rim enclosing small open central area, partially covered by irregular shaped and oriented elements attached to proximal margin of distal shield.

Dimensions. Overall diameter 6.7μm: Central area 2.0μm.

Remarks. *Cyclicargolithus floridanus* is distinguished from similar form *C. marismontium* (Black, 1964) which is elliptical and has larger central opening.

Occurrence. The species is observed at almost all of the Early Miocene localities, in the Pakhna Formation, of S.W. Cyprus.

Range. Late Eocene to Oligocene, Roth (1970). Late Eocene to Mid Miocene (NP20 to NN7), Lazarus *et al.* (1995).

Genus ***Dictyococcites*** Black, 1967

Type species. *Dictyococcites danicus* Black, 1967.

Remarks. The genus includes elliptical to sub circular coccoliths, with distal shield slightly larger than proximal shield, joined at margin of large central area. Central area is spanned proximally by a grid and distally by elements radially arranged on inner wall, at distal margin of central area to form a crest, and meet along the major axis of ellipse to form a slit.

Dictyococcites antarcticus Haq, 1976
(Pl. 9, fig. 11)

1976 *Dictyococcites antarcticus* Haq: 561, pl. 3, figs 1-5,7,8.

Holotype. Haq, pl. 3, fig. 3, sample DSDP site 325, core 8, section 2, interval 132-134cm. locality Antarctica Continental Rise, west of Antarctica Peninsula.

Description. Between crossed polars, elliptical coccoliths, with distal shield with serrated outline caused by blunt pointed elements. Continuous extinction lines from closed central area to outer rim, where it bends sharply, curving anti-clockwise. In plane polarised light the elements of central area meet along major axis to form a long furrow/slit.

Dimensions. Length 6.0μm: Width 4.0μm.

Remarks. In plane polarised light *Dictyococcites antarcticus* differs from the older form *D. scrippsae* by the longer furrow/slit and generally smaller size, which Haq (1976) considered to be a distinguishing feature of the species.

Occurrence. The species is observed at almost all of the Early Miocene localities, in the Pakhna Formation, of S.W. Cyprus.

Range. Late Oligocene to Mid Miocene, Haq (1976). Miocene, Perch-Nielsen, (1985b).

Dictyococcites bisectus (Hay, Mohler & Wade) Bukry & Percival, 1971
(Pl. 11, fig. 4)

1966 *Syracosphaera bisecta* Hay, Mohler & Wade: *partim,* 393, pl. 10, figs 4-6.

1971 *Dictyococcites bisectus* (Hay, Mohler & Wade); Bukry & Percival: 127, pl. 2, figs 12,13.

Holotype. Hay, Mohler & Wade, pl. 10, fig. 4, sample U1-H-2094, horizon Nal 11, locality north-east of Nal' chik, north-west Caucasus.

Description. Large elliptical coccoliths, with distal shield composed of dextrally imbricate elements, forming a broad rim. Central area covered with broad imbricate elements within multiple cycles, forming dome structure and meet at the centre to form a slit oriented to the major axis of the ellipse.

Dimensions. Length 11.3μm: Width 9.3μm.

Remarks. *Dictyococcites bisectus* is the largest species of the genus (Perch-Nielsen, 1985b).

Occurrence. The species is observed at almost all of the Early Miocene localities, in the Pakhna Formation, of S.W. Cyprus.
Range. Late Eocene to Early Miocene (NP17 to NN1), Lazarus *et al.* (1995).

Dictyococcites scrippsae Bukry & Percival, 1971
(Pl. 9, fig. 10)

1971 *Dictyococcites scrippsae* Bukry & Percival: 128, pl. 2, figs 7<8.

Holotype. Bukry & Percival, pl. 2, figs 7,8, USNM 169185, horizon Red Bluff Clay, locality Chickasawhay River, Shubuta, Mississippi.
Description. Between crossed polars, elliptical coccoliths with distal shield, of serrated outline caused by blunt pointed elements. Continuous extinction lines from outer rim to closed central area, where it bends sharply. In plane polarised light the elements of central area meet along major axis to form a slit.
Dimensions. Length 8.0μm: Width 6.4μm.
Remarks. Between crossed polars *Dictyococcites scrippsae* is distinguished from *D. bisectus* by having a continuous extinction line from outer rim to central area and being smaller (Bukry & Percival, 1971).
Occurrence. The species is observed at almost all of the Early Miocene localities, in the Pakhna Formation, of S.W. Cyprus.
Range. Late Eocene to Early Miocene (NP16 to NN1), Lazarus *et al.* (1995).

Genus ***Reticulofenestra*** Hay, Mohler & Wade, 1966

Type species. *Reticulofenestra caucasica* Hay, Mohler & Wade, 1966.
Remarks. The genus includes elliptical to sub circular coccoliths, with distal shield slightly larger than proximal shield, joined at margin of open central area. Inner wall at distal margin of central area does not rise above the distal surface, with central area spanned by a lacy network.

Reticulofenestra haqii Backman, 1978
(Pl. 11, fig. 2)

1978 *Reticulofenestra haqii* Backman: 110, pl. 1, figs 1-4; pl. 2, fig. 10.

1989 *Reticulofenestra haqii* Backman; Gallagher: 56.

Holotype. Backman, pl. 1, figs 1-4, sample 11, locality Vera Basin, Spain, Atlantic Ocean.

Description. Small elliptical coccoliths, with distal shield composed of slightly dextrally imbricate elements. Distal margin of open central area consists of coarse radiating elements that do not form a crest above the distal surface.

Dimensions. Overall length 4.0µm, width 3.0µm: Central area, length 1.0µm, width 0.3µm.

Remarks. *Reticulofenestra haqii* is distinguished from *R. minuta* and R. *minutula* (Gartner, 1967), by being larger in former (>3.0µm) and in latter, a central opening longer than 1.5µm (Gallagher, 1989).

Occurrence. The species is observed in the basal section of the Myrtou Marls, Pissouri Formation of S.W. Cyprus, which makes contact with the underlying rocks unconformably.

Range. Miocene to Pliocene (NN1 to NN18), Gallagher (1989).

Reticulofenestra minuta Roth, 1970

(Pl. 11, fig. 3)

1970 *Reticulofenestra minuta* Roth: 850, pl. 5, figs 3,4.

1989 *Reticulofenestra minuta* Roth; Gallagher: 59, pl. 3.1, fig. 7.

Holotype. Roth, pl. 5, fig. 3, sample IMS-A 610130 (A833), horizon Red Bluff Formation, locality The Lone Star Cement Quarry, St. Stephens, Alabama, USA.

Description. Small elliptical coccoliths, with distal shield composed of on average 24 slightly dextrally imbricate elements. Distal margin of open central area consists of coarse radiating elements that do not form a crest above the distal surface.

Dimensions. Overall Length 2.5µm, width 2.0µm: Central area, length 0.83µm, width 0.30µm.

Remarks. *Reticulofenestra minuta* is distinguished from *R. minutula* (Gartner, 1967), by being smaller (<3.0µm) in size (Gallagher, 1989).

Occurrence. The species is observed in the basal section of the Myrtou Marls, Pissouri Formation of S.W. Cyprus, which makes contact with the underlying rocks unconformably.

Range. early Eocene to Pliocene (NP13 to NN18), Gallagher (1989).

Reticulofenestra pseudoumbilicus (Gartner) Gartner, 1969
(Pl. 9, fig. 9)

1967 *Coccolithus pseudoumbilicus* Gartner: 4, pl. 6, figs 1-4.

1969 *Reticulofenestra pseudoumbilica* (Gartner); Gartner: 587-589.

1989 *Reticulofenestra pseudoumbilicus* (Gartner); Gallagher: 63, pl. 3.2, fig. 6.

Holotype. Gartner (1967), pl. 6, fig. 3, sample core 64-A-9-5E, 250cm, locality Sigsbee knolls, Gulf of Mexico.

Description. Between crossed polars, elliptical coccoliths, with distal shield composed of many thin radial elements, forming slight serrated outline. Large open central area.

Dimensions. Overall diameter 6.4μm: Central area, diameter 2.4μm.

Remarks. The large central opening is normally spanned by a lacy network, which rarely survives, and therefore between crossed polars is seen dark. The large central area/opening (<50% of total coccolith area) distinguishes the species (Gallagher, 1989).

Occurrence. The species is observed at several Early and Late Miocene localities in the Pakhna and Pissouri (Myrtou Marls) Formations, of S.W. Cyprus.

Range. Mid Miocene to Pliocene (NN4 to NN18), Gallagher (1989).

Family **Rhabdosphaeraceae** Lemmermann, 1908

Genus ***Rhabdosphaera*** Haeckel, 1894

Type species. *Rhabdosphaera claviger* Murray & Blackman, 1898.

Remarks. The genus includes coccoliths with a relatively high central process which may or may not be hollow, attached to distal surface of basal plate, with or with out collar. Basal plate composed of one or more cycle of elements, with concave proximal surface.

Rhabdosphaera procera Martini, 1969
(Pl. 9, fig. 13)

1969 *Rhabdosphaera procera* Martini: 289, pl. 26, figs 10,11.

1975a *Rhabdosphaera procera* Martini; Jafar: 59, pl. 7, figs 3,4,23,24.

1992 *Rhabdosphaera procera* Martini; Siesser & Bralower: pl. 4, fig. 11.

Holotype. Martini, pl. 26, figs 10-11, sample SMB 10701, locality YB-1, near Port Gentil, Gabon, West Africa.

Description. Between crossed polars, coccoliths seen in side view. Comprising a small simple sub circular basal plate, with concave proximal surface. Long hollow slender central process attached to distal surface of basal plate, with parallel sides.

Dimensions. Basal plate, diameter 5.2μm: Central Process, length 11.6μm.

Remarks. The species is distinguished by the slender hollow process, with parallel sides that display a gradual thickening towards the distal end (Jafar, 1975a).

Occurrence. The species is observed in the basal section of the Myrtou Marls, Pissouri Formation of S.W. Cyprus, which makes contact with the underlying rocks unconformably.

Range. Mid Miocene to Early Pliocene (NN8 to NN15), Jafar (1975a).

Family **Sphenolithaceae** Deflandre, 1952

Genus ***Sphenolithus*** Deflandre *in* Grassé, 1952

Type species. *Sphenolithus radians* Deflandre *in* Grassé, 1952

Remarks. The genus includes nannoliths having the form of a distal dome or cone/spine and proximal column with concave base. Proximal column/shield composed of radial arranged elements with triangular cross-section, capped distally by one or more cycles of lateral elements, radially arranged. Distally a dome structure of laterally arranged elements or apical spine of blade type elements that might bifurcate is present.

Sphenolithus abies Deflandre *in* Deflandre & Fert, 1954
(Pl. 9, fig. 15)

1954 *Sphenolithus abies* Deflandre *in* Deflandre & Fert: 50, pl. 10, figs 1-4.

1975a *Sphenolithus abies* Deflandre *in* Deflandre & Fert; Jafar: 62, pl. 7, figs 17,18.

1991 *Sphenolithus abies* Deflandre *in* Deflandre & Fert; Spaulding: pl. 2, figs 7-9.

Holotype. Deflandre *in* Deflandre & Fert, pl. 10, figs 1-4.

Description. Between crossed polars, dome-shaped nannoliths, normally seen in side view. Proximally, comprising flaring column of radially arranged elements, with an inter-angle slightly greater than 90°. Distally a dome structure is present. Column and dome structures both having median extinction line and separated by a median extinction line, forming a cross.

Dimensions. Height 4.8μm: Width 4.0μm.

Remarks. Between crossed polars *Sphenolithus abies* is distinguished from *S. verensis* by being more uniformly bright and not having a broad proximal base.

Occurrence. The species is observed in the basal section of the Myrtou Marls, Pissouri Formation of S.W. Cyprus, which makes contact with the underlying rocks unconformably.

Range. Late Miocene to Early Pliocene (NN9 to NN15), Perch-Nielsen (1985b).

Sphenolithus heteromorphus Deflandre, 1953
(Pl. 9, fig. 16)

1953 *Sphenolithus heteromorphus* Deflandre: 1786, figs 1,2,

1967 *Sphenolithus heteromorphus* Deflandre; Bramlette & Wilcoxon: 122, pl. 2, figs 6-9.

1992 *Sphenolithus heteromorphus* Deflandre; Siesser & Bralower: pl. 3, fig. 4.

Holotype. Deflandre, figs 1,2 (line illustrations).

Description. Between crossed polars, cone-shaped nannoliths, normally seen in side view. Proximally, a compact column of slightly flaring radially arranged elements, capped distally by lateral elements of equal thickness and robust apical spine.

Dimensions. Length 7.2μm: Diameter 5.6μm.

Remarks. *Sphenolithus heteromorphus* differs from *S. conicus* (Bukry, 1971) and *S. belemnos* (Bramlette & Wilcoxon, 1967) by having a more robust apical spine.

Occurrence. The species is observed at several Early to Mid Miocene localities, in the Pakhna Formation, of S.W. Cyprus. The short vertical range of *Sphenolithus heteromorphus*, makes the species stratigraphically important.

Range. Early to Mid Miocene (NN4 to NN5), Perch-Nielsen (1985b).

Sphenolithus moriformis (Bronnimann & Stradner) Bramlette & Wilcoxon, 1967
(Pl. 9 fig. 19)

1960 *Nannoturbella moriformis* Bronnimann & Stradner: 368, figs 11-16.

1967 *Sphenolithus moriformis* (Bronnimann & Stradner); Bramlette & Wilcoxon: 124, pl. 3, figs 1-6.

1992 *Sphenolithus moriformis* (Bronnimann & Stradner); Siesser & Bralower: pl. 3, fig. 18.

Holotype. Bronnimann & Stradner, figs 11-13,16, sample Präp, BR/538/1 T, horizon Alkazar Formation, locality Reporto Capri, near Arroyo Naraujo, Cuba.

Description. Between crossed polars, dome-shaped nannoliths, normally seen in side view. Proximally, comprising a slightly flaring column of radial arranged elements, and distally a dome structure is present, both having median extinction line and separated by a median extinction line, forming a cross.

Dimensions. Maximum overall length 4.8μm.

Remarks. Between crossed polars, sometimes it is difficult to distinguish several Palaeogene and Neogene dome-shaped sphenoliths from one another.

Occurrence. The species is observed at almost all of the Early Miocene localities, in the Pakhna Formation, of S.W. Cyprus.

Range. Mid Eocene to Mid Miocene (NP12 to NN9), Perch-Nielsen(1985b).

Sphenolithus verensis Backman, 1978

(Pl. 9, fig. 20)

1978 *Sphenolithus verensis* Backman: 111, pl. 2, figs 4-6,11,12.

Holotype. Backman, pl. 2, figs 4-6, sample 11, locality Vera basin, Spain, Atlantic Ocean.

Description. Between crossed polars, dome-shaped nannoliths, normally seen in side view. Proximally, comprising a pronounced flaring column of radially arranged elements, with an inter-angle greater than 90°. Distally a dome structure is present. Column and dome structures both having median extinction line and separated by a median extinction line, forming a cross.

Dimensions. Length 8μm: Diameter 6.4μm.

Remarks. Between crossed polars *Sphenolithus verensis* can be distinguished from *S. abies* by the pronounced flaring of the proximal elements.

Occurrence. The species is observed in the basal section of the Myrtou Marls, Pissouri Formation of S.W. Cyprus, which makes contact with the underlying rocks unconformably. The short vertical range of *Sphenolithus verensis*, makes the species stratigraphically important.

Range. Late Miocene to Early Pliocene (NN11 to NN13), Perch-Nielsen (1985b).

Family **Thoracosphaeraceae** Schiller, 1930

Genus ***Thoracosphaera*** Kamptner, 1927

Type species. *Syracosphaera heimii* Lohmann, 1920.
Remarks. Thoracosphaerids are considered to be a calcareous dinoflagellates (Romein, 1979). They include hollow spherical and ovoid calcareous forms, composed of interlocking polygonal elements. Anarchaeopyle and operculum may be present.

Thoracosphaera fossata Jafar, 1975a
(Pl. 9, fig. 14)

1975a *Thoracosphaera fossata* Jafar: 83, pl. 11, figs 1,2.

Holotype. Jafar, pl. 11, figs 1,2, sample 168, SM.B 125 93 16, locality Bebalain, Rotti, Indonesia.
Description. Between crossed polars, slightly ovoid shells comprising finger-like elements of good birefringence, interwoven in complex manner producing irregular wall pattern. Anarchaeopyle and operculum was not observed in any of the specimens.
Dimensions. Diameter 20.8μm.
Remarks. Normally when viewing with light microscope, there is insufficient resolution across the whole specimen due to problems with depth of field. However, when focused centrally on the specimen it is possible to recognise the wall pattern, which is a distinguishing feature of the species (Jafar, 1975a).
Occurrence. The species is observed at several of all the Early and Late Miocene localities, in the Pakhna and Pissouri (Myrtou Marls) Formations, of S.W. Cyprus.
Range. Miocene (NN1 to NN11), Perch-Nielsen (1985b).

Incertae sedis

Genus ***Hayaster*** Bukry, 1973a

Type species. *Discoaster perplexus* Bramlette & Riedel, 1954.
Remarks. The genus includes sub circular nannoliths, in the form of a flat disc. Composed of several radiating arms from simple central area. The inter-areas between the arms are uniform and closed with straight peripheral edges. Small proximal shield present, with both shields remaining dark between crossed polars.

Hayaster perplexus (Bramlette & Riedel) Bukry, 1973a
(Pl. 9, fig. 17)

1954 *Discoaster perplexus* Bramlette & Riedel: 400, pl. 39, fig. 9.

1973a *Hayaster perplexus* (Bramlette & Riedel); Bukry: 308.

Holotype. Bramlette & Riedel, pl. 39, fig. 9, sample 555, horizon Cipero Formation, locality Retrench Quarry, Trinidad.

Description. In plane polarised light, sub circular nannoliths, in the form of a flat disc. Composed of ten thin radiating arms from central point. The inter-areas between the arms are uniform and closed with straight peripheral edges. The disc is non-birefringent and is dark between crossed polars.

Dimensions. Diameter 9.6μm.

Remarks. Originally described as a Discoaster species, however, SEM investigations revealed a small proximal shield (Bukry, 1973a).

Occurrence. The species is observed in the basal section of the Myrtou Marls, Pissouri Formation, of S.W. Cyprus.

Range. Miocene to Pleistocene (NN2 to NN21), Perch-Nielsen (1985b).

PLATE 9.

Light photomicrographs

XPL = Crossed Polarised Light
PC = Phase Contrast Scale Bar = 5μm

Figs 1,2. *Syphosphaera apsteini* Lohmann, 1902, D565-1801: Fig. 1, side view, XPL, UD630-4; Fig. 2, side view, XPL, UD630-11.

Fig. 3. *Syphosphaera canescens* Kamptner, 1955, side view, XPL, UD630-37, D565-1801.

Fig. 4. *Syphosphaera recta* (Deflandre, 1942), side view, XPL, UD630-37, D565-1801.

Fig. 5. *Syphosphaera conica* Kamptner, 1955, side view, XPL, UD630-35, D565-1801.

Fig. 6. *Syphosphaera recuvata* Deflandre, 1942, side view, XPL, UD630-42, D565-1801.

Fig. 7. *Syphosphaera turris* Kamptner, 1955, side view, XPL, UD630-7, D565-1801.

Figs 8,12. *Cyclicargolithus abisectus* (Müller, 1970), D252-1165: Fig. 8, distal view, XPL, UD632-24; Fig. 12, distal view, PC, UD632-23.

Fig. 9. *Reticulofenestra pseudoumbilicus* (Gartner, 1967), proximal view, XPL, UD631-10, D565-1801.

Fig.10. *Dictyococcites scrippsae* Bukry & Percival, 1971, distal view, XPL, UD632-26, D252-1165.

Fig. 11. *Dictyococcites antarcticus* Haq, 1976, proximal view, XPL, UD630-1, D565-1801.

Fig. 13. *Rhabdosphaera procera* Martini, 1969, side view, XPL, UD629-18A, D565-1801.

Fig. 14. *Thoracosphaera fossata* Jafar, 1975a, sphere, XPL, UD630-2, D565-1801.

Fig. 15. *Sphenolithus abies* Deflandre *in* Deflandre & Fert, 1954, side view, XPL, UD629-6A, D565-1801.

Fig. 16. *Sphenolithus heteromorphus* Deflandre, 1953, side view, XPL, UD614-32, D353-1431.

Fig. 17. *Hayaster perplexus* (Bramlette & Reidel, 1954), plan view, PC, UD629-19A, D565-1801.

Fig. 18. *Pontosphaera multipora* (Kamptner, 1948), distal view, XPL, UD625-18A, D343-1442.

Fig. 19. *Sphenolithus moriformis* (Bronnimann & Stradner, 1960), side view, XPL, UD613-29A, D373-1474.

Fig. 20. *Sphenolithus verensis* Backman, 1978, side view, XPL, UD630-17, D565-1801.

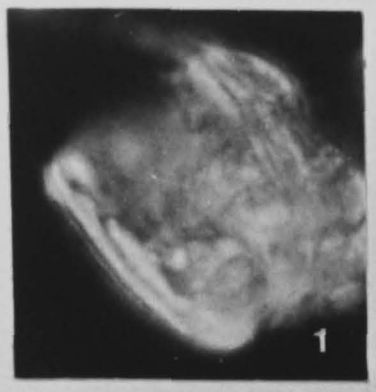
1

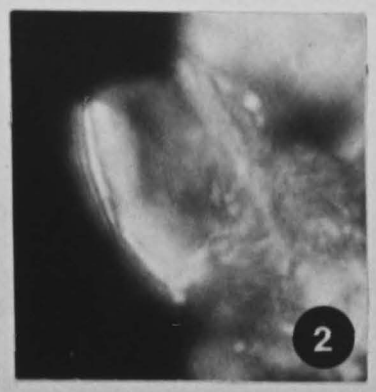
2

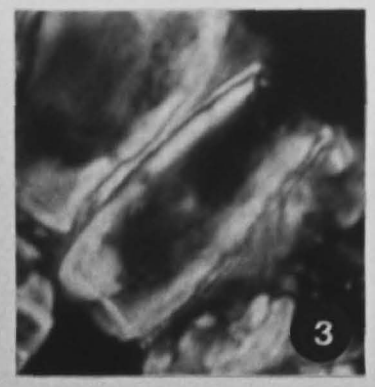
3

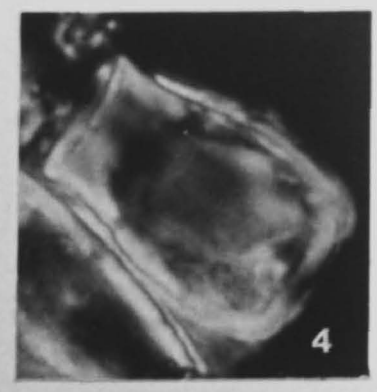
4

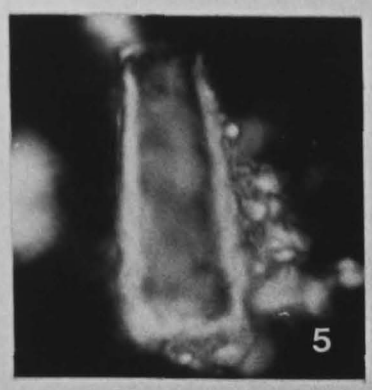
5

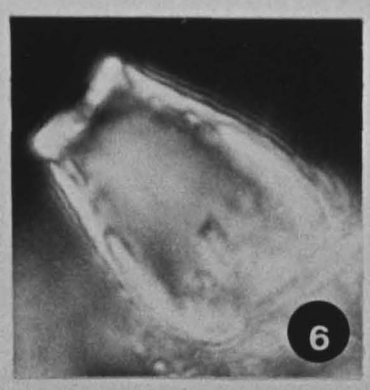
6

7

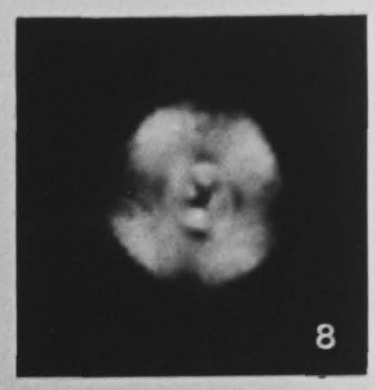
8

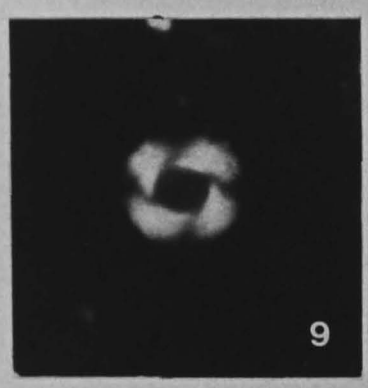
9

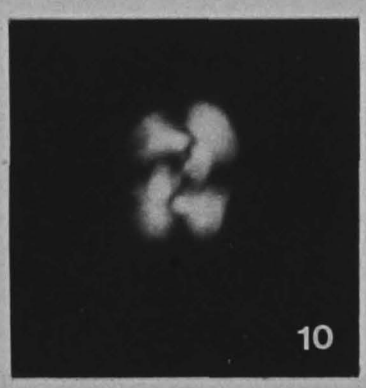
10

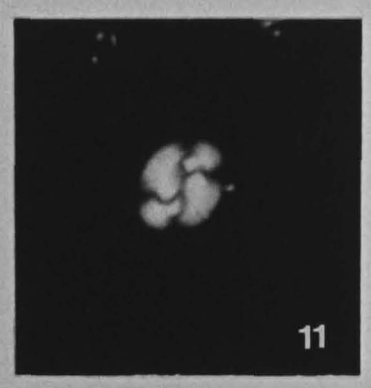
11

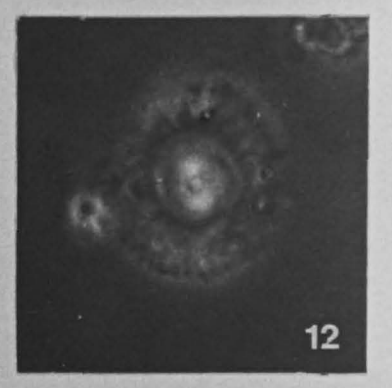
12

13

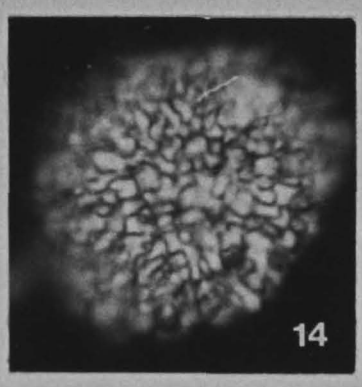
14

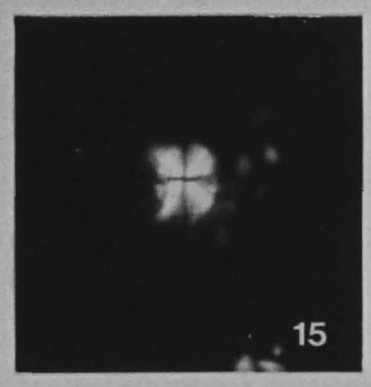
15

16

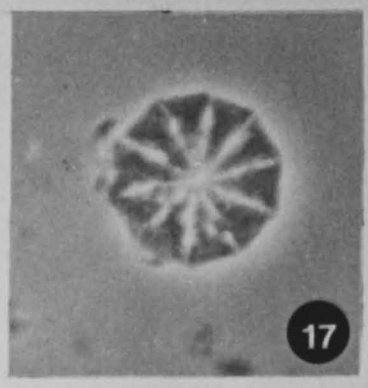
17

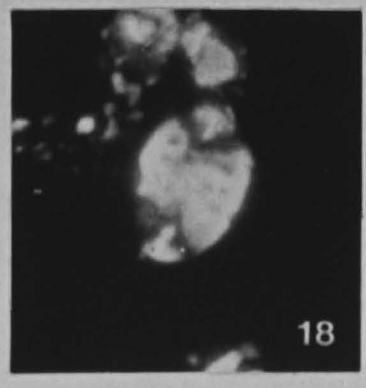
18

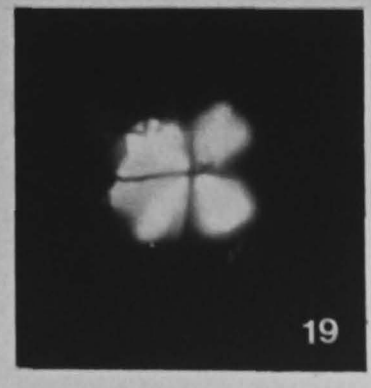
19

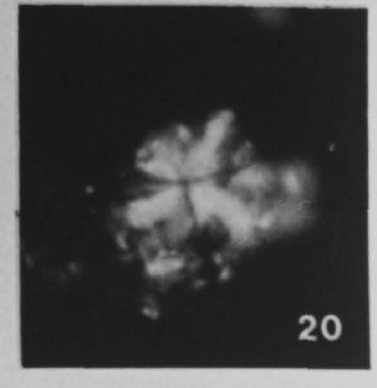
20

PLATE 10.

Light photomicrographs

XPL = Crossed Polarised Light
PPL = Plane Polarised Light
PC = Phase Contrast
Scale Bar = 5μm

Fig. 1. *Amaurolithus amplificus* (Bukry & Percival, 1971), side view, XPL, UD631-13, D565-1801.

Fig. 2. *Amaurolithus delicatus* Gartner & Bukry, 1975, side view, PPL, UD630-38, D565-1801.

Fig. 3. *Calcidiscus leptoporous* (Murray & Blackman, 1898), distal view, PC, UD626-4A, D311-1437.

Fig. 4. *Calcidiscus macintyrei* (Bukry & Bramlette, 1969), proximal view, PC, UD631-14, D565-1801.

Fig. 5. *Coccolithus pelagicus* (Wallich, 1877), distal view, PPL, UD613-22A, D225-1145.

Fig. 6. *Coccolithus pliopelagicus* Wise, 1973, distal view, PPL, UD631-11, D565-1801.

Figs 7,8. *Umbilicosphaera sibogae* (Weber-van-Bosse, 1901), D252-1165: Fig. 7, distal view, PC, UD626-23A; Fig. 8, distal view, XPL, UD626-21A.

Fig. 9. *Discoaster bellus* Bukry & Percival, 1971, plan view, PPL, UD626-8A, D311-1437.

Figs 10,14. *Helicosphaera granulata* Bukry & Percival, 1971, D252-1165: Fig. 10, proximal view, XPL, UD631-1; Fig. 14, proximal view, PC, UD631-2.

Figs 11,15. *Helicosphaera selli* Bukry & Bramlette, 1969, D565-1801: Fig. 11, proximal view, PC, UD630-14; Fig. 15, proximal view, XPL, UD630-15.

Fig. 12. *Helicosphaera kamptneri* Hay & Mohler *in* Hay *et al.*, 1967, proximal view, XPL, UD630-12, D565-1801.

Fig. 13. *Discoaster variabilis* Martini & Bramlette, 1963, plan view, PPL, UD614-23, D360-1147.

Fig. 16. *Helicosphaera sissura* Miller, 1981, distal view, XPL, UD631-17, D252-1165.

Fig. 17. *Coccolithus miopelagicus* Bukry, 1971, distal view, PC, UD631-7, D252-1165.

Fig. 18. *Discoaster pentaradiatus* (Tan, 1927), plan view, PPL, UD629-14A, D565-1801.

Fig. 19. *Discoaster neorectus* Bukry, 1971, plan view, PPL, UD631-19, D565-1801.

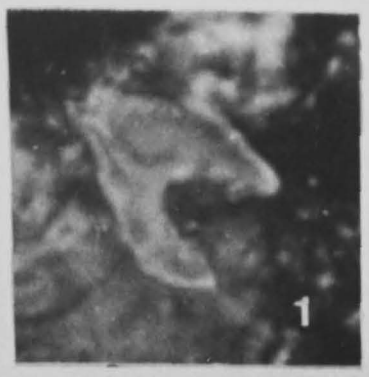
1

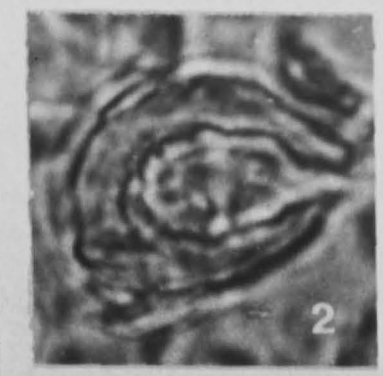
2

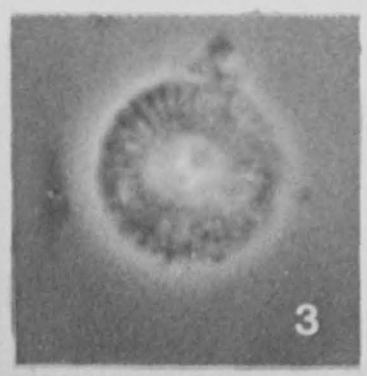
3

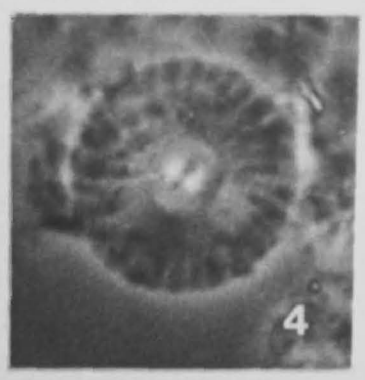
4

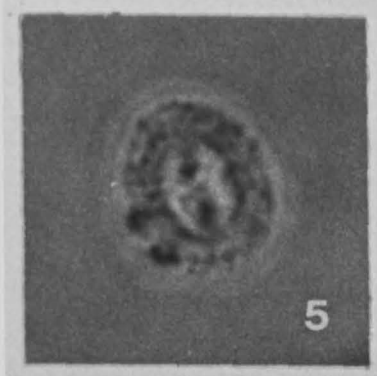
5

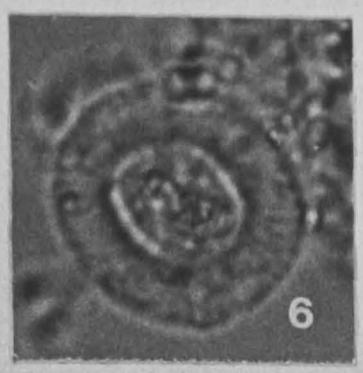
6

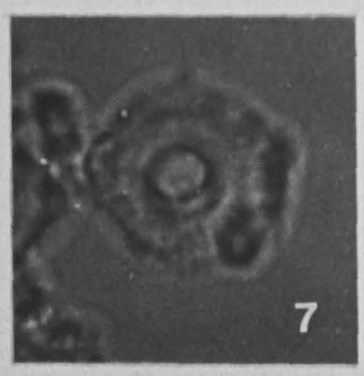
7

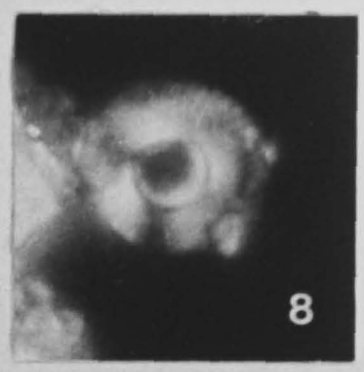
8

9

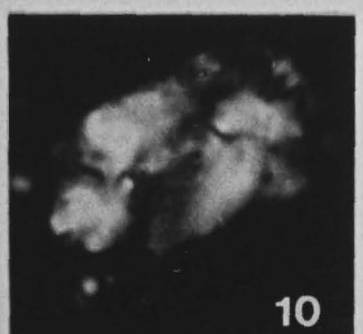
10

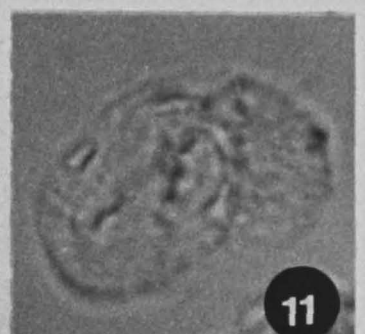
11

12

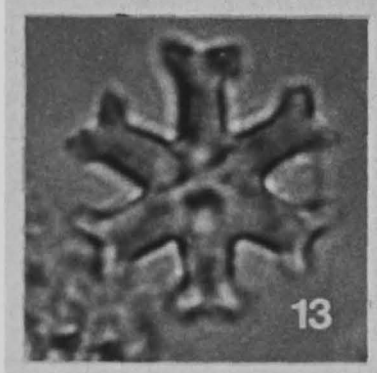
13

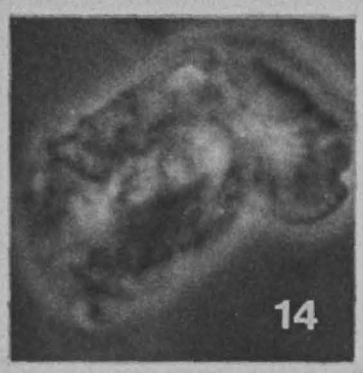
14

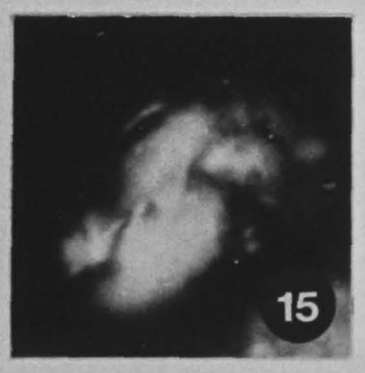
15

16

17

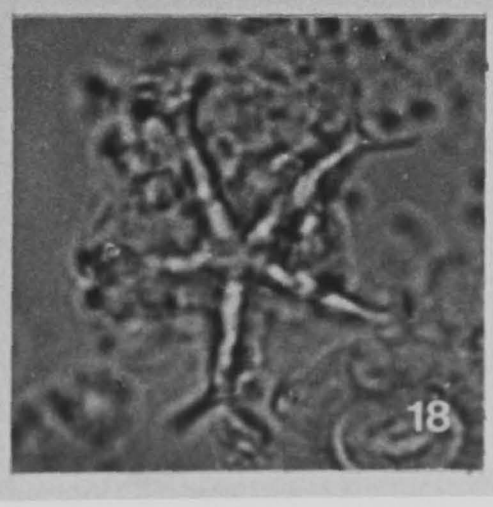
18

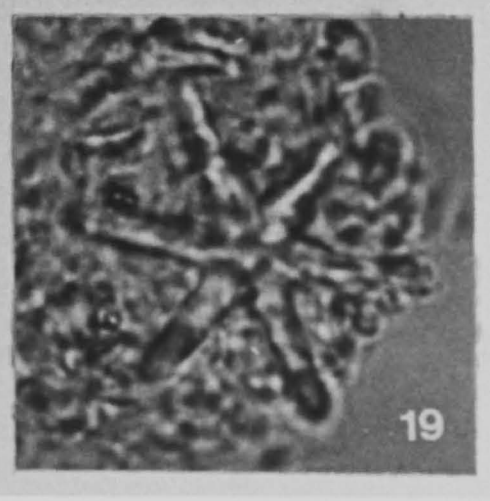
19

PLATE 11.

SEM photomicrographs

Fig. 1. *Cyclicargolithus floridanus* (Roth & Hay *in* Hay *et al.*, 1967), distal view, UD603-12A, D124-1217, X5220.

Fig. 2. *Reticulofenestra haqii* (bottom) Backman, 1978; *Coccolithus pelagicus* (top) (Wallich, 1877), distal view, UD627-5A, D311-1437, X4750.

Fig. 3. *Reticulofenestra minuta* Roth, 1970, distal view, UD627-8A, D311-1437, X11200.

Fig. 4. *Dictyococcites bisectus* (Hay, Mohler & Wade, 1966), distal view, UD628-4A, D252-1165, X4400.

Fig. 5. *Calcidiscus leptoporus* (Murray & Black, 1898), distal view, UD627-41A, D311-1437, X4630.

Fig. 6. *Cantinaster coalitus* Martini & Bramlette, plan view, UD622-29, D267-1410, X2420.

Fig. 7. *Helicosphaera burkei* Black, 1971b, proximal view, UD628-8A, D252-1165, X3920.

Fig. 8. *Calcidiscus macintyrei* (Bukry & Bramlette, 1969), proximal view, UD627-15A, D311-1437, X4330.

1

2

3

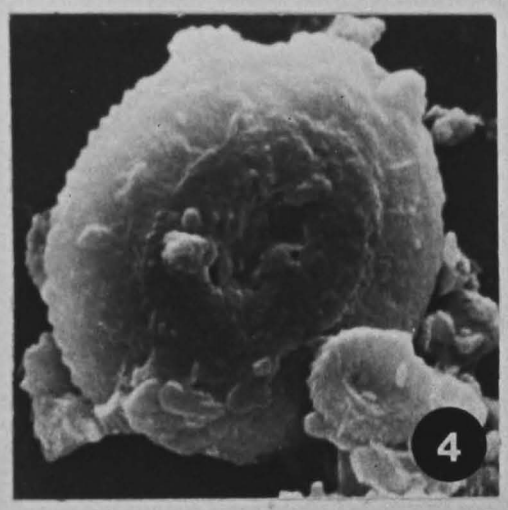
4

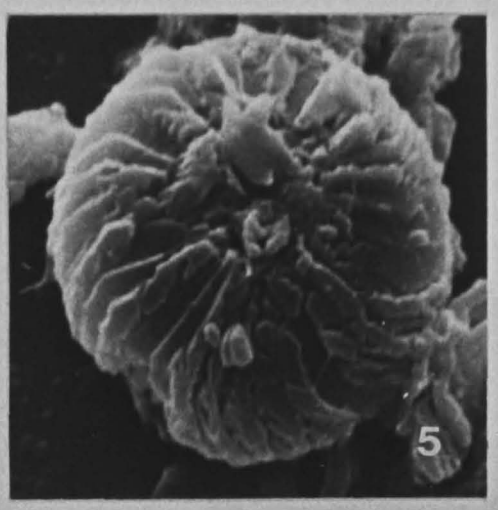
5

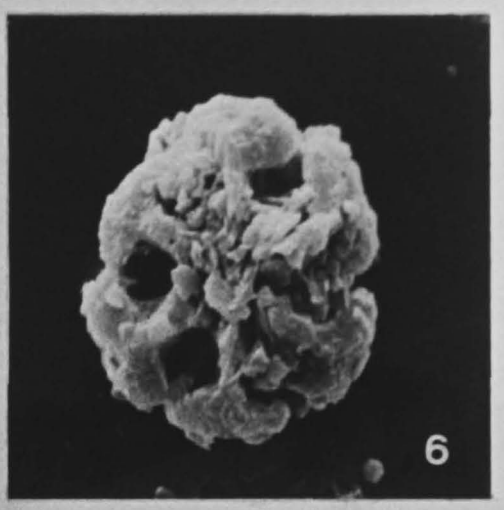
6

7

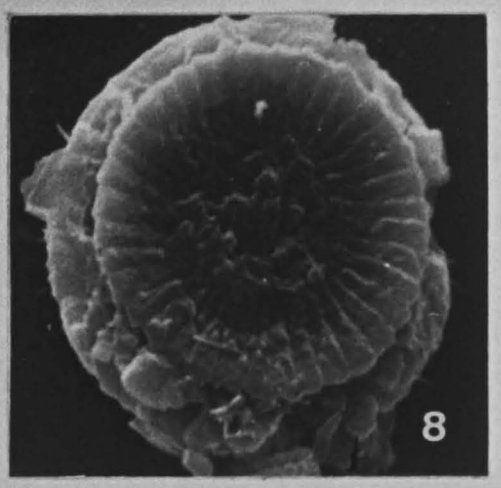
8

CHAPTER 7

DISCUSSION AND IMPLICATIONS

7.1 Introduction

The data obtained during the project and reported in this thesis (chapters 4, 5 and 6), provide a number of relative biostratigraphical (calcareous nannofossils) age dates, for the conformable (Kannaviou Formation only) and unconformable lithological contacts seen in S.W. Cyprus, between the Late Cretaceous (late Campanian) and Late Miocene. These contacts are between the juxtaposed Mamonia and Troodos (including the associated sediments of the Perapedhi and Kannaviou Formations) basement terranes, plus related fragments and the overlying basal horizon of the Late Cretaceous (late Campanian) to Late Miocene sedimentary formations, which in part, make up the neo-autochthonous sedimentary cover. Also included are the unconformable contacts between the older and younger formations of the neo-autochthonous sedimentary cover.

The biostratigraphically (i.e. relative) dated unconformities, which indicate gaps in the sedimentary succession and the outcrop patterns produced by the surviving sedimentary packages bounded by these unconformities, can show that differential uplift and subsidence, including ?lateral movement, has occurred between the individual terranes and fragments of S.W. Cyprus, with the tectonic movement taking place at their boundaries (major lineaments), and are related to a subduction zone located to the south of Cyprus. Hence the tectonic events which have occurred between the Late Cretaceous (late Campanian) to Late Miocene in S.W. Cyprus, can be constrained and related to the overall geological evolution of Cyprus and offshore area.

7.2 Conformable and Unconformable Contacts

The conformable (between the Kannaviou and Lefkara [Lower Member] Formations only) and unconformable contacts are summarised in Fig. 7.1, and are correlated with their respective biostratigraphical (calcareous nannofossil) age-dates. Each contact has been designated by a letter, in ascending order from A (Campanian) to G (Late Miocene), to avoid descriptive repetition and for ease of comparison between diagrams. A cycle length between the start of each ?transgressive event (contacts B, C,

D, E, F and G) and the onset of calcareous sedimentation (contact A), is given in Ma. All cycles include an erosional/nondepositional event of unknown time span.

The ?transgressive and erosional/nondepositional events, may represent a tectonic release or compressional event (isostatic sea level rise and fall), eustatic sea level rise and fall, or a combination of both respectively.

The cycle lengths (Fig. 7.1) between the start of each ?transgressive event, suggest the relative rise and fall of sea level, was tectonically driven. The evidence for this suggestion is where the overlying chalks are seen to make unconformable contact with the older sediments of the neo-autochthonous sedimentary cover and/or basement (Chapter 4, loclities LL2, LL11 and LL17; Chapter 5, localities ML7, ML21 and ML28; Chapter 6, localities P4, P6, P10, P13, P15 and MM2), the contacts are sharp and without a reworked basal conglomerate/breccia horizon, suggesting rapid subsidence (tectonic release event) had taken place, resulting in isostatic sea level rise. In turn this would suggest a compressive event is responsible for isostatic sea level fall, for the period (unknown time span) of erosion/nondeposition. However, it must be noted that microscopal studies did detect derived calcareous nannofossils (Figs 5.6,7,8), indicating older chalks were available for reworking, during the deposition of the Lefkara Formation, Middle Member (Chalk and Chert and Massive Chalk units).

A possible cause for the driving force behind these tectonic release and compressional events noted in S.W. Cyprus, is the interaction between the African and European plates in the eastern Mediterranean. Where Cyprus is situated at or near to the plate boundary, by subjecting the individual allochthonous basement terranes and fragments to tensional and compressional forces, involving subduction, local (Cyprus) and/or regional (eastern Mediterranean) movement along one or more of the major lineaments (Kempler, 1994), or a combination of both, during the ?Late Cretaceous to Holocene.

When correlating the schematic geological vertical section (Fig. 7.1) of this study, with past research (Fig. 7.2), the overall observation of the outcrop pattern is that the succession of the neo-autochthonous sedimentary cover of S.W. Cyprus, becomes progressively less and less complete in a north westerly direction, with the younger formations and their members overstepping one another (Figs 4.10, 5.1,12,14) to rest unconformably on the basement (Fig. 7.3) from the Perapedhi section (Krasheninnikov and Kaleda, 1994) to the Polis/Kathikas area (Turner, 1969).

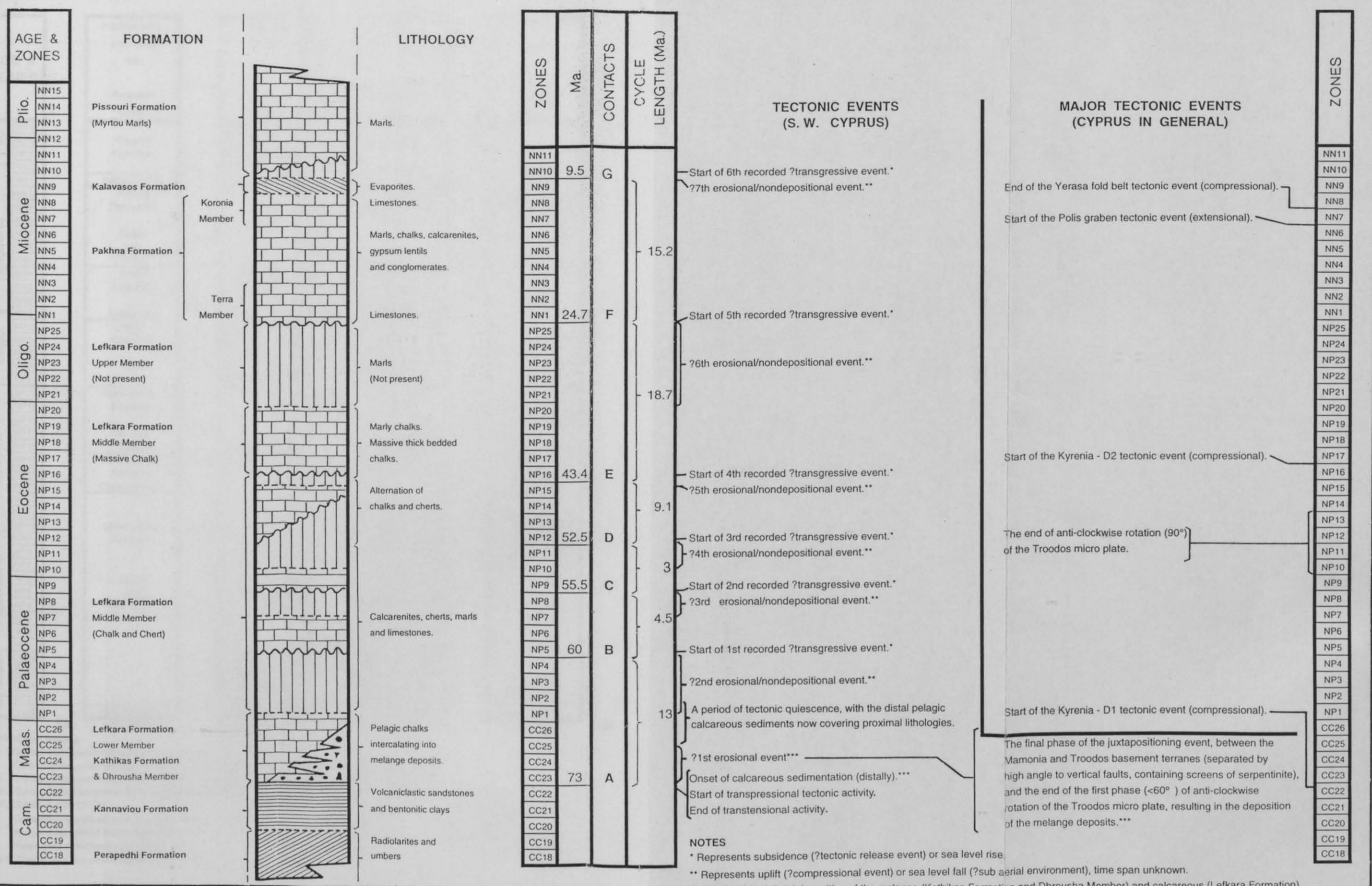

Fig. 7.1. A schematic geological vertical section (not to scale), displaying the relative biostratigraphical ages of the unconformities and hiatuses (vertical lines; time span unknown), located during the project, suggesting possible tectonic events and their correlation with the major tectonic events of Cyprus (chapter 2, section 2.4).

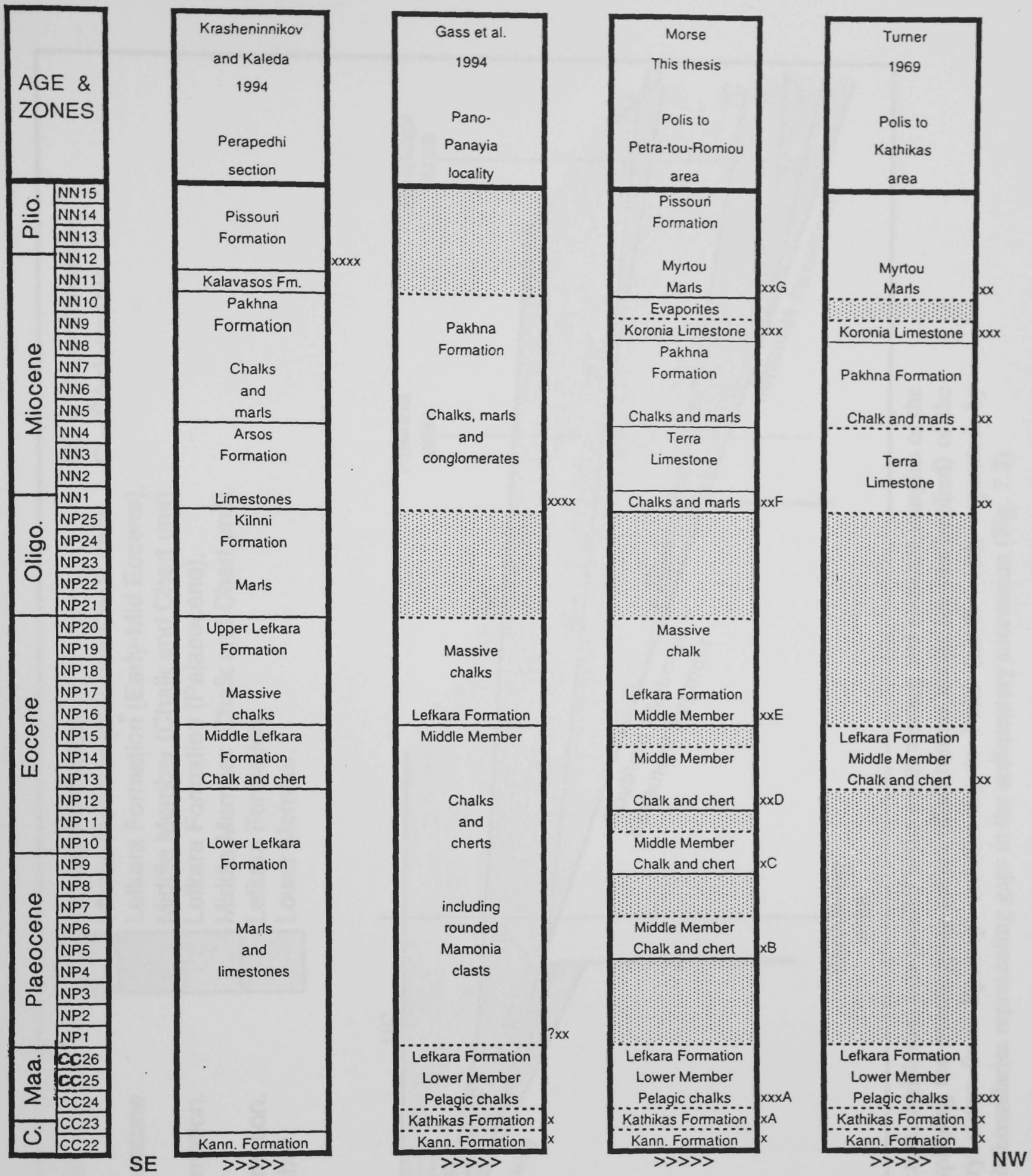

Contact relationships

x Contact resting unconformably on the basement.

xx Contact resting unconformably (? inferred) on underlying sediments and overstepping onto the basement.

xxx Contact resting conformably on underlying sediments and overstepping onto the basement unconformably.

xxxx Contact resting unconformably on underlying sediments, but no evidence to suggest that it overstepped onto the basement.

AGE, ZONES & CONTACTS

CC Cretaceous nannofossil zone (Sissingh, 1977).

NN Neogene nannofossil zone (Martini, 1971).

NP Palaeogene nannofossil zone (Martini,1971).

A to G Conformable and unconformable contacts (Fig. 7.1)

C = Campanian.

Maa = Maastrichtian.

Oligo = Oligocene.

Plio = Pliocene.

Vertical columns

Kann = Kannaviou.

Broken line = Inferred age.

Fine line = Inferred boundary.

Fig. 7.2. Composite geological vertical sections modified from Cyprus Memoirs, publications and this thesis, which relate to the south western margin of the Troodos Massif and Mamonia Complex, showing the contact relationship between the individual sedimentary formations and their overstepping nature onto the basement (for localities see Fig.7.6).

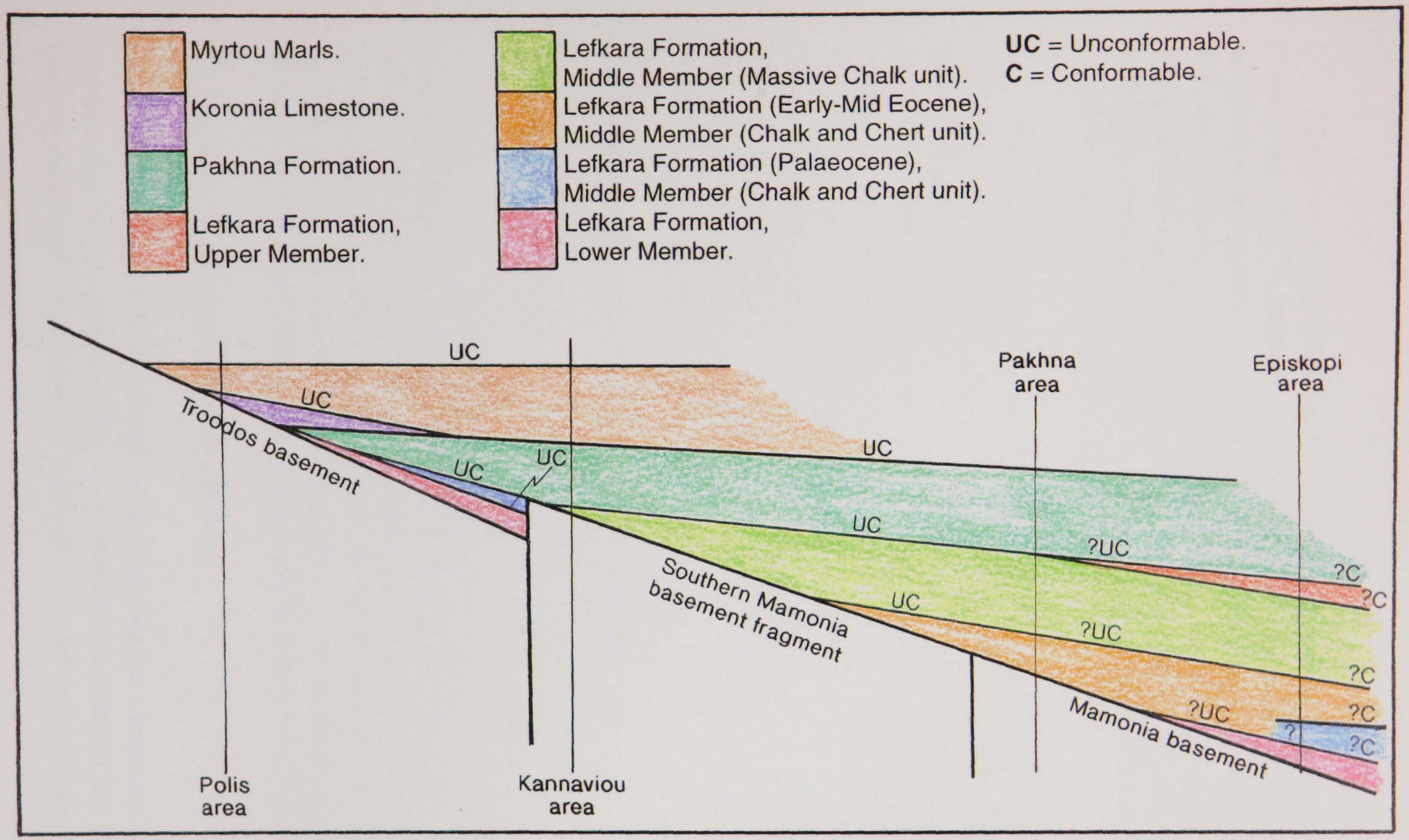

Fig. 7.3. A schematic cross-section, which runs sub-parallel to the south western and southern margins of the Troodos Massif (Fig. 7.6), displaying the overstepping nature (diachronous trends are not implied) of the neo-autochthonous sedimentary cover from Episkopi (south-east) to Polis (north-west), separated by conformable and unconformable boundaries representing gaps in the sedimentary succession (Fig. 7.2).

The pattern of deposition displayed by the sedimentary succession seen in S.W. Cyprus (Figs 7.2,3), is similar to that displayed by the sedimentary succession seen against the northern margin of the Troodos Massif and including the Troulli Inlier (Fig. 7.4), with the neo-autochthonous sedimentary cover again becoming progressively less and less complete in a westerly direction, with the younger formations and their members in the main, overstepping one another to rest unconformably onto the basement (Fig. 7.5), from Troulli (Lilljequist, 1969) to Xeros (Wilson, 1959).

The major difference between the two cross-sections (figs 7.3,5), is that the cross-section of S.W. Cyprus (Fig. 7.3), has been complicated by the presence of basement fragments reacting differentially to the tectonic events, especially the southern Mamonia basement fragment. It has remained structurally high, preserving the older sediments of the neo-autochthonous sedimentary cover (Kathikas Formation; Lefkara Formation, Lower and Middle [Chalk and Chert and Massive Chalk units] Members) within the surrounding structural lows. Whereas the cross-section of the northern margin of the Troodos Massif (Fig. 7.5), which overlies the southern margin of the Mesaoria Basin basement (Troodos basement lithologies), has reacted to the ?same tectonic events as one whole unit, resulting in a more simplified outcrop pattern.

7.3 Sedimentary Outcrop Patterns of S.W. Cyprus

7.3.1 Kannaviou Formation

Apart from the basement rocks, the Kannaviou Formation forms part of the underlying sediment of contact A (Fig. 7.1), and is thought to be exclusively associated with the Troodos basement terrane and fragments, with the outcrop pattern (Fig. 7.7) based on field evidence, displaying this trend in S.W. Cyprus. However, there is a small localised outcrop, unconformably overlying pillow lavas of the Mamonia basement terrane (Dhiarizos Group) which may be reworked, located at Petra-tou-Romiou.

7.3.2 Kathikas Formation and Dhrousha Melange

With the onset of transpressional activity during the late Campanian, involving the final phase of the juxtapositioning event, between the Mamonia and Troodos basement terranes and related fragments (Swarbrick, 1993), the southern Mamonia

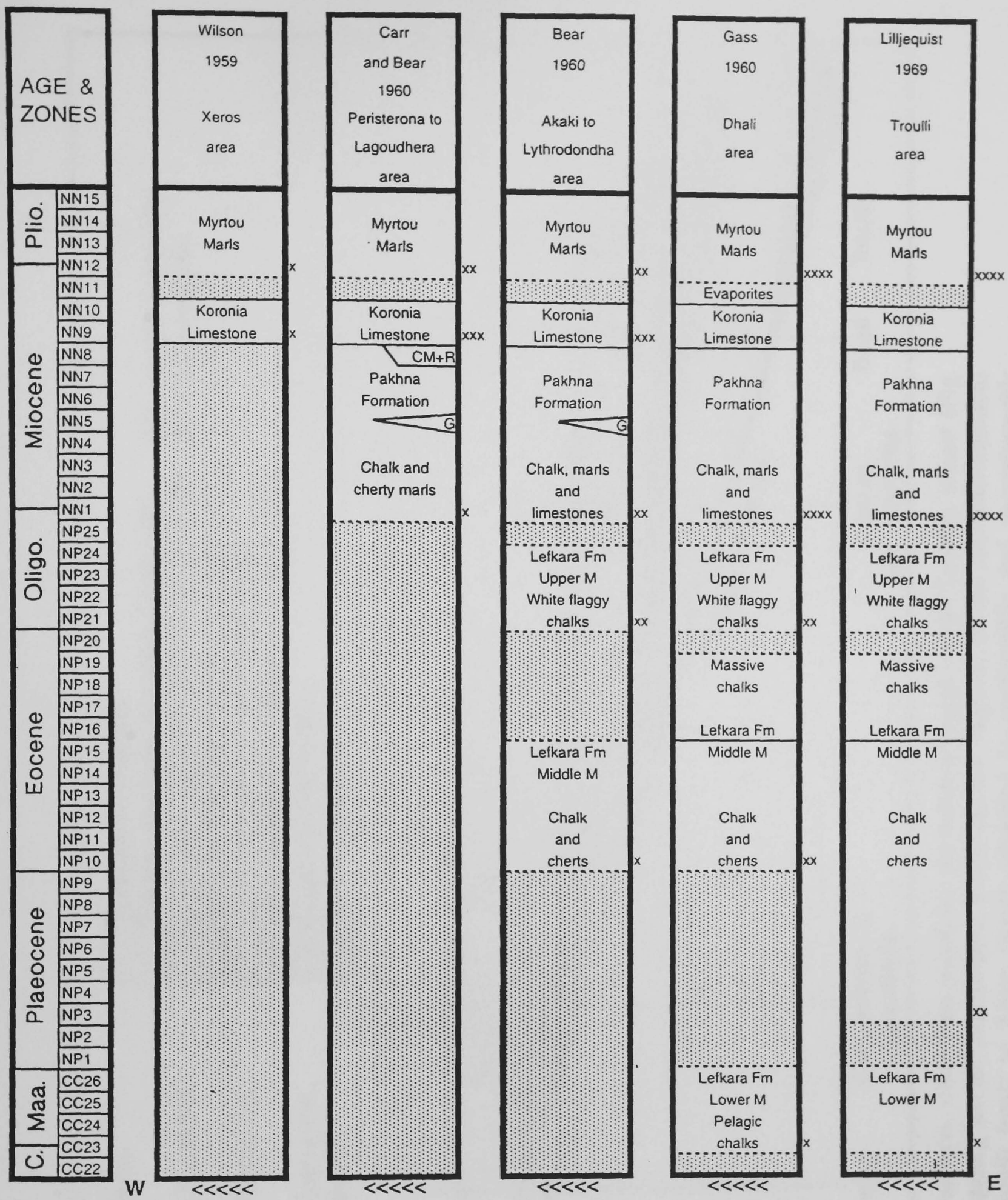

Contact relationships

x Contact resting unconformably on the basement.

xx Contact resting unconformably on underlying sediments and overstepping onto the basement.

xxx Contact resting conformably on underlying sediments and overstepping onto the basement unconformably.

xxxx Contact resting unconformably on underlying sediments, but no evidence to suggest that it overstepped onto the basement.

AGE & ZONES

CC Cretaceous nannofossil zone (Sissingh, 1977).

NN Neogene nannofossil zone (Martini, 1971).

NP Palaeogene nannofossil zone (Martini,1971).

C = Campanian.

Maa = Maastrichtian.

Oligo = Oligocene.

Plio = Pliocene.

Vertical columns

CM+R = Chalk, marls and reef limestones.

Fm = Formation.

G = Gypsum.

M = Member.

Broken line = Inferred age.

Fig. 7.4. Composite geological vertical sections modified from Cyprus Memoirs and Bulletins, which relate to the northern margin of the Troodos Massif and Troulli Inlier, showing the contact relationship between the individual sedimentary formations and their overstepping nature onto the basement (for localities see Fig. 7.6).

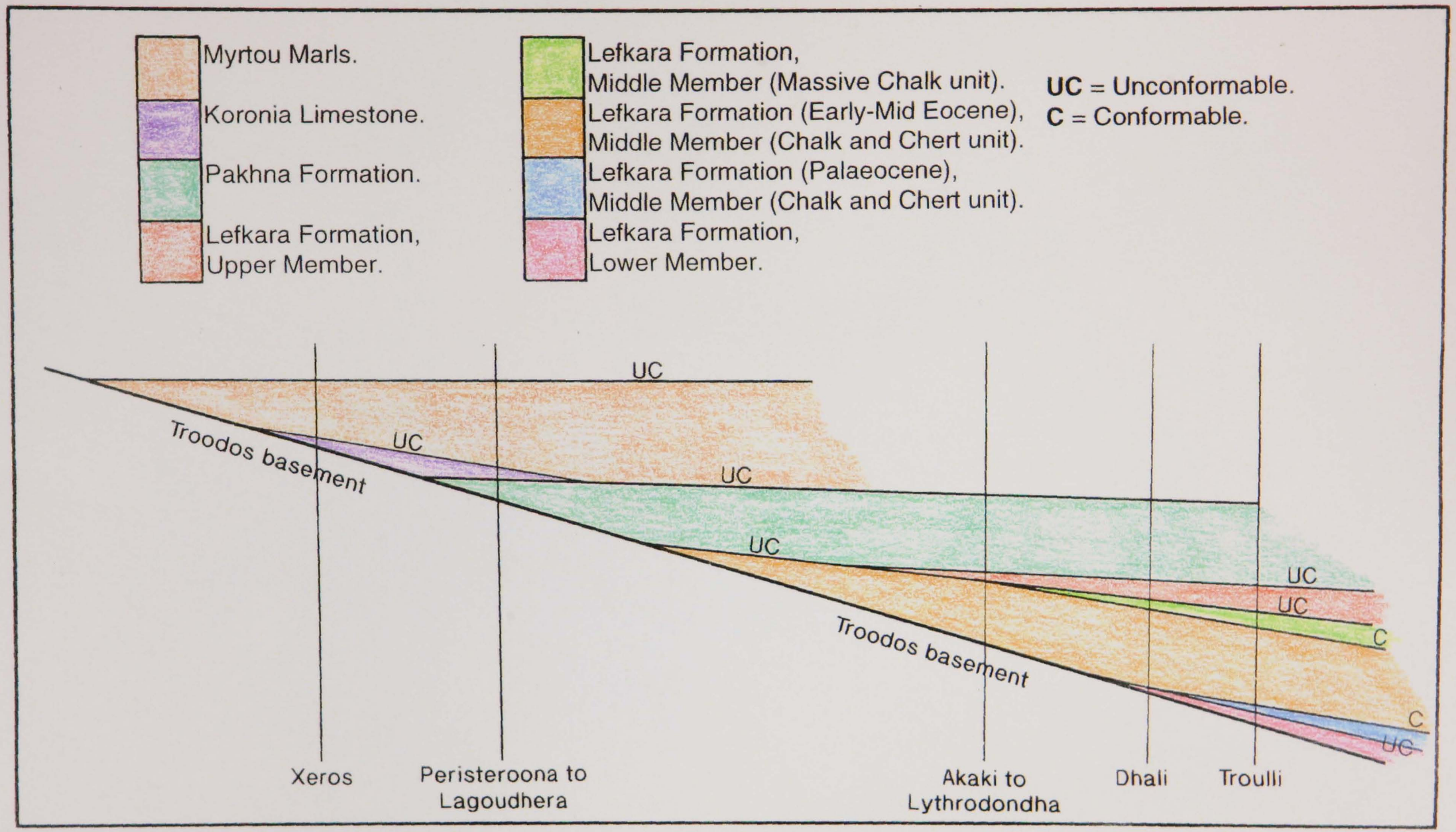

Fig. 7.5. A schematic cross-section, which runs parallel to the northern margin of the Troodos Massif (Fig. 7.6), displaying the overstepping nature (diachronous trends are not implied) of the neo-autochthonous sedimentary cover from Troulli (east) to Xeros (west), separated by conformable and unconformable boundaries representing gaps in the sedimentary succession (Fig. 7.4).

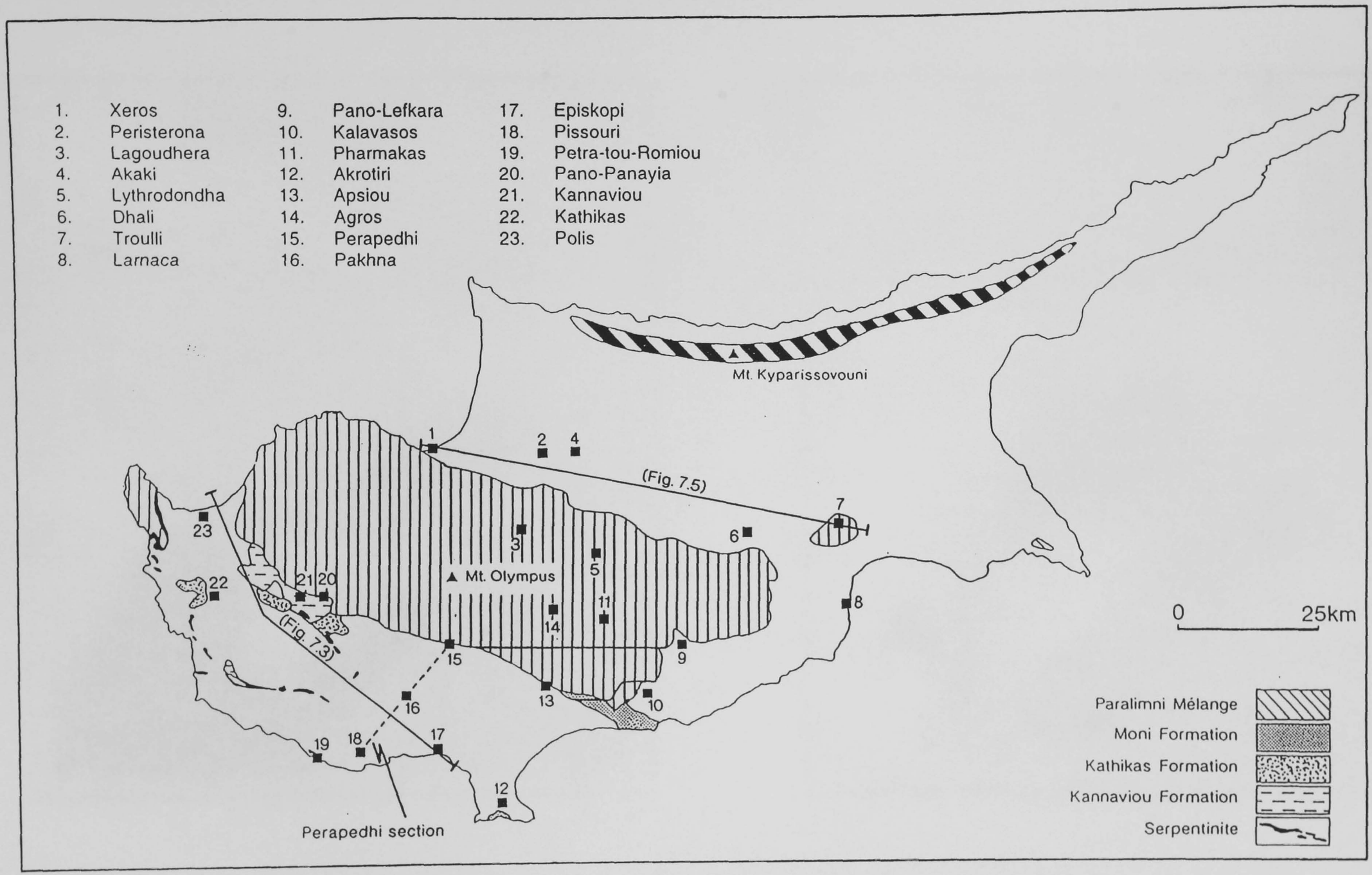

Fig. 7.6. Simplified geological map of Cyprus, displaying the localities of place names employed in Chapter 7, cross-section lines (Figs 7.3,5) and the position of the Perapedhi section (Krasheninnikov and Kaleda, 1994).

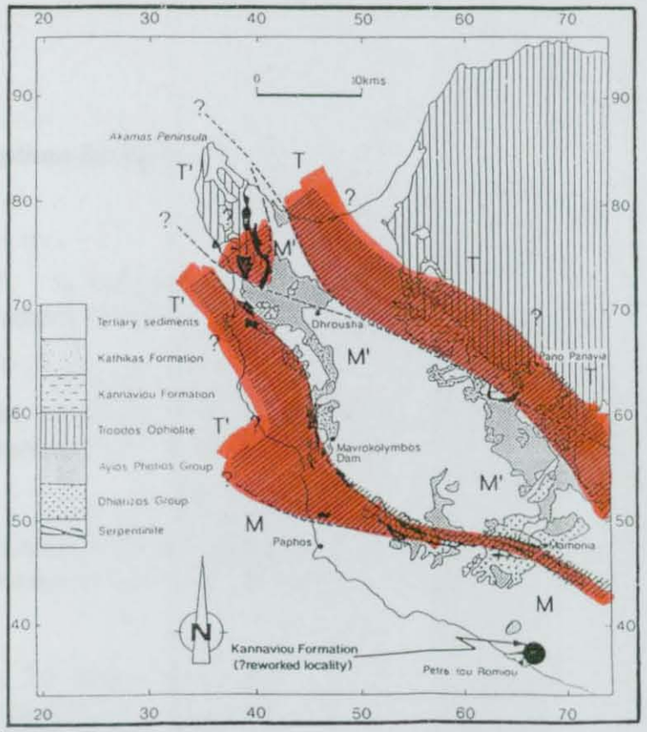

Fig. 7.7.

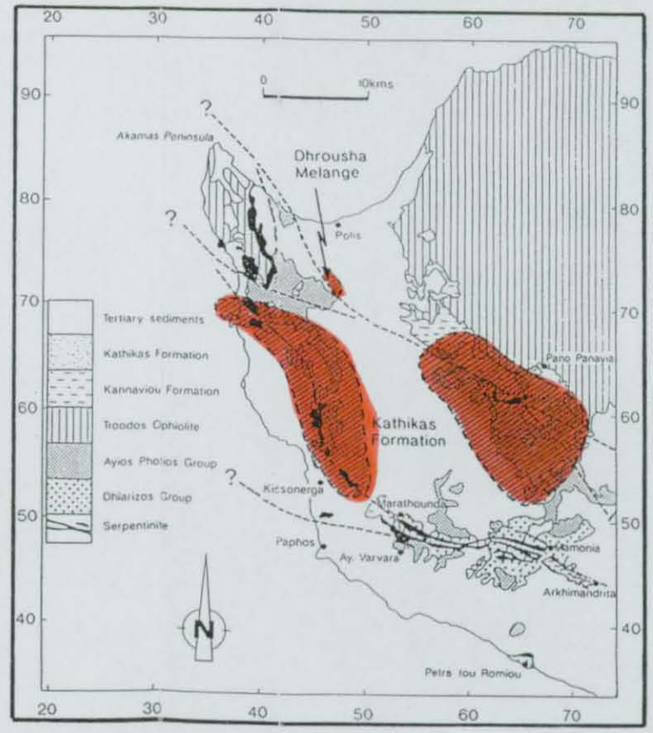

Fig. 7.8.

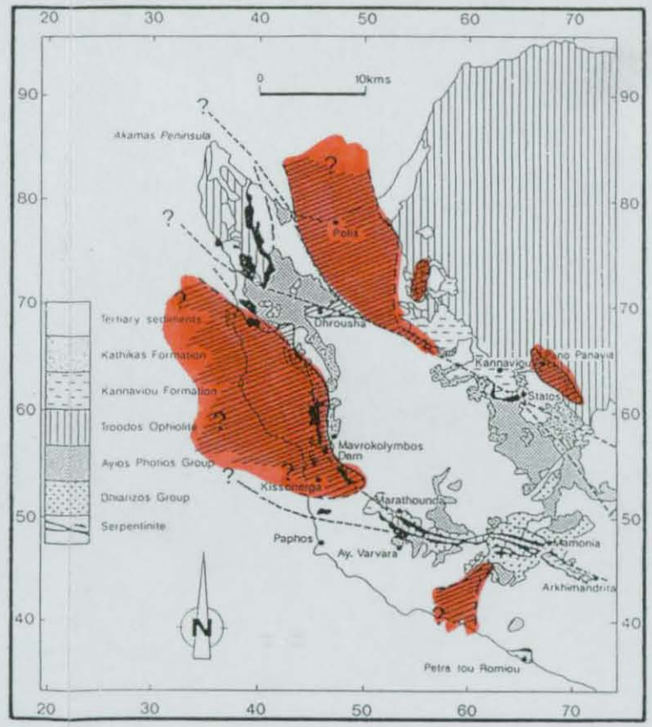

Fig. 7.9.

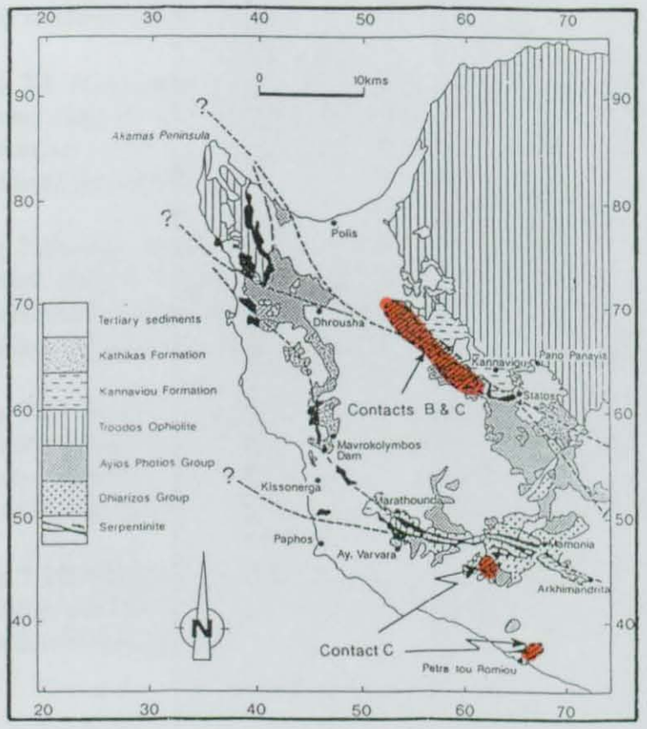

Fig. 7.10.

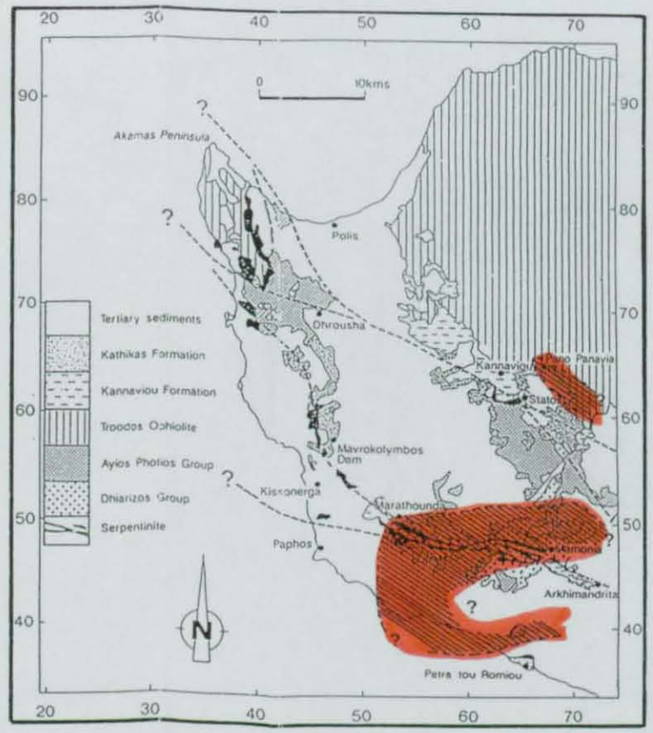

Fig. 7.11.

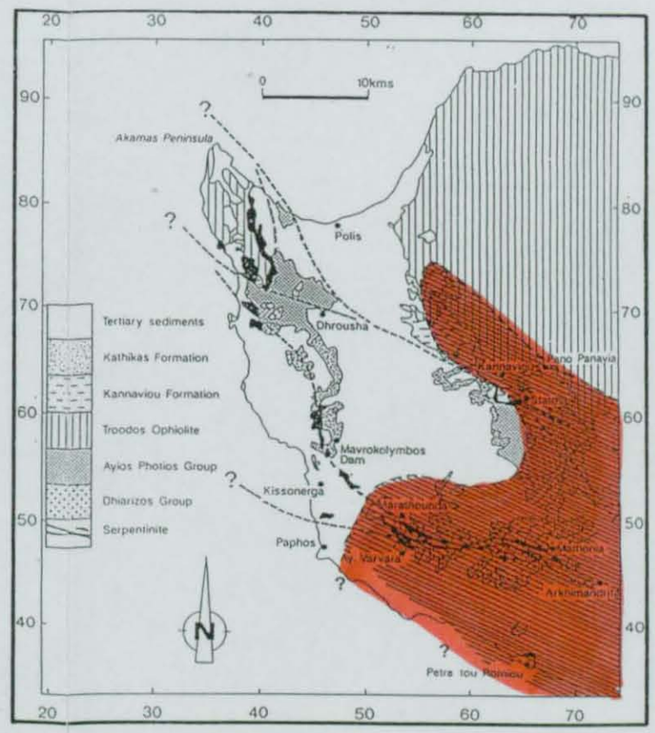

Fig. 7.12.

For figure captions see over--->

Captions for figures 7.7 to 7.12.

N.B. 1). The base map is a simplified geological map of S.W. Cyprus, modified from Swarbrick (1980).

2). Figs 7.7,8. The cross-hatched areas represent inferred maximum depositional areas, which have been subjected to erosional events, resulting in localised outcrops observed in S.W. Cyprus.

3). Figs 7.9,10,11,12. The boundaries of the cross-hatched areas represent the maximum possible regression line, based on the current preserved localised outcrops, observed during the project and research by Turner (1971) and Gass *et al.* (1994).

Fig. 7.7. Map displaying the inferred major depositional areas (cross-hatched), of the Kannaviou Formation (part of contact A), including its relationship with the Mamonia and Troodos basement terranes (M and T respectively) and their related fragments (M' and T' respectively).

Fig. 7.8. Map displaying the inferred major depositional areas (cross-hatched), of the Dhrousha Melange (Moni Formation) and Kathikas Formation (part of contact A), and their relationship to the major lineaments.

Fig. 7.9. Map displaying the relationship between the major lineaments and the inferred current outcrop pattern (cross-hatched), of the Lefkara Formation, Lower Member (part of contact A). N.B. Information is based on research by Turner (1971), Gass *et al.* (1994) and from this project.

Fig. 7.10. Map displaying the relationship between the major lineaments and the inferred current outcrop patterns (cross-hatched), of the Lefkara Formation, Middle Member, Chalk and Chert unit of Palaeocene age (contacts B and C). N.B. Consult Fig 7.1 for the relationship between the sediments above the contacts B and C.

Fig. 7.11. Map displaying the relationship between the major lineaments and the current outcrop pattern (cross-hatched), of the Lefkara Formation, Middle Member, Chalk and Chert unit of Eocene age (contact D). N.B. Information is based on research by Gass *et al.* (1994) and from this project.

Fig. 7.12. Map displaying the relationship between the major lineaments and the current outcrop pattern (cross-hatched), of the Lefkara Formation, Middle Member, Massive Chalk unit (contact E).

basement fragment 'flowered'. It formed a structural high bounded by fault scarps, these being the source areas for the debris flows of the Kathikas Formation, to be deposited into the structural lows, formed on either side of the fragment and straddling the contacts (Fig. 7.8), to rest unconformably on the underlying basements and sediments.

The Dhrousha Melange (Moni Formation) is associated with the 'flowering' of the northern Mamonia basement fragment, with the debris flows of the Dhrousha Melange being sourced from the northern fragment and deposited into a localised structural low (Fig. 7.8), to the east of the fragment, unconformably overlying the Kannaviou Formation. The 'flowering' of the northern fragment appears to be less pronounced than that of the southern Mamonia basement fragment, with little or no evidence of large scale debris flows.

Both the Kathikas Formation and the Dhrousha Melange form the proximal sediments of contact A (Fig. 7.1), which unconformably overlie the Kannaviou Formation and basements.

7.3.3 Lefkara Formation, Lower Member

The preserved outcrop pattern displayed by the Lefkara Formation, Lower Member (Fig. 7.9), suggest the Mamonia basement fragments have continued to act as structural highs, during its deposition and/or post-depositional erosion event(s).

During the early Maastrichtian, the chalks of the Lower Member form the distal depositional portion of contact A, overlying conformably the Kannaviou Formation and unconformably the basement. The lower horizon of the Lower Member is coeval with the proximal deposition of the debris flows of the Kathikas Formation and Dhrousha Melange (Lower Member intercalating to form chalk interbeds). When the area became tectonically quiescent, during the latter part of the Maastrichtian, the debris flows (proximal) ceased, with the chalks of the Lower Member continuing to be deposited across the entire area.

7.3.4 Lefkara Formation, Middle Member, Chalk and Chert unit

The preserved outcrop patterns of the chalks unconformably overlying contacts B, C and D (Fig. 7.1), of the Lefkara Formation, Middle Member, Chalk and Chert unit (Figs 7. 10,11), suggest the whole of the southern Mamonia basement fragment again

continued to act as a structural high, during its deposition and/or post-depositional erosion event(s), with respect to the chalks overlying contacts B and C, which are located in structural lows either side of the southern fragment (Fig. 7.10). The chalks which overlie contact D (Fig. 7.11), are seen to carpet the southern portion of the southern Mamonia fragment, with only the northern and central portions of the fragment remaining as a structural high, during its deposition and/or post-depositional erosion event(s).

7.3.5 Lefkara Formation, Middle Member, Massive Chalk unit

The preserved outcrop pattern displayed by the chalks of the Lefkara Formation, Middle Member, Massive Chalk unit, unconformably overlying contact E (Fig. 7.1), suggest again that only the northern and central portions of the southern Mamonia basement fragment acted as a structural high, during its the deposition and/or post-depositional erosion event(s). The outcrop carpets a greater part of the southern portion of the fragment (Fig. 7.12), than that of the chalks above contact D (Fig. 7.11).

7.3.6 Lefkara Formation, Upper Member

The Lefkara Formation, Upper Member, was not seen/present north-west of a line trending SW-NE, from the coast to the Troodos Massif through the village of Mamonia, approximately following the Dhiarizos valley. Any marls which were sampled above the contact F (Pakhna Transgressive event), which may have been attributed to the Upper Member by other researchers, are considered to be part of the Pakhna Formation during this study.

7.3.7 Pakhna Formation

The Pakhna Formation (Figs 7.13A,B) blankets the entire area of S.W. Cyprus, unconformably (Fig. 7.1; contact F) overlying all older sediments and basement rocks. After the start of the Pakhna transgressive event, the southern Mamonia basement fragment no longer played an active role, relating to the depositional history of the neo-autochthonous sedimentary cover. By Late Miocene the northern and central portions of S.W. Cyprus (Figs 7.13B,C) were in a tensional environment (Chapter 2 section 2.4.6) to form the north - south asymmetrical Polis graben structure (Payne and Robertson, 1995).

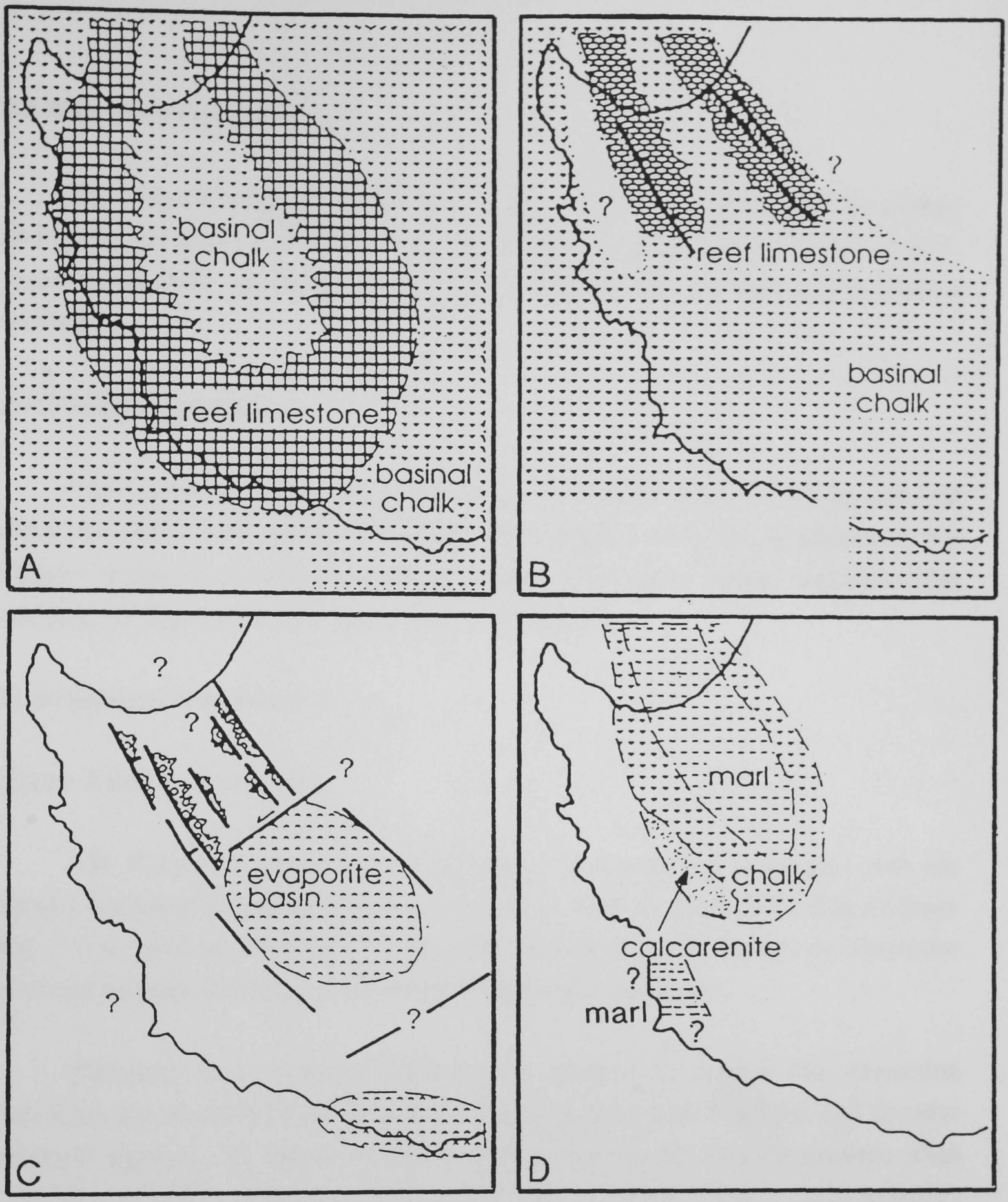

A). Early Miocene. The outcrop pattern for the Terra Limestone Member of the Pakhna Formation, in relation to the formation chalks (contact F).

B). Late Miocene. The outcrop pattern for the Koronia Limestone Member of the Pakhna Formation in relation to the formation chalks.

C) Late Miocene. The outcrop pattern of the Kalavasos Formation (evaporites).

D) Mio/Pliocene. The outcrop pattern displayed by the marls, chalks and calcarenites of the Pissouri Formation (contact G).

N.B. 1). The areas free of ornamentation are subaerially exposed.
2). Scale, 10km = 25mm

Fig. 7.13. Palaeogeographic reconstruction of the Miocene formations and related members of S.W. Cyprus (modified from Payne and Robertson, 1995).

7.3.8 Kalavasos Formation

The evaporite deposits of the Kalavasos Formation are situated in the Polemi and Pissouri sub basins, located in the central and southern areas (Fig. 7.13C) of S.W. Cyprus respectively, and both outcrops conformably overlie sediments of the Pakhna Formation.

7.3.9 Pissouri Formation

The calcareous sediments of the Pissouri Formation (Fig. 7.13D) are situated within the infant Polis graben structure, unconformably overlying sediments of the Pakhna Formation and located north of Paphos of unknown extent, unconformably overlying the Kannaviou Formation (Fig. 7.1; contact G).

7.3.10 General observations

7.3.10.1 Kannaviou Formation

The Kannaviou Formation is thought to be exclusively associated with the Troodos basement terrane and fragments, based on field evidence, with little evidence (Fig. 7.7 at Petra-tou-Romiou) to suggest the sediments of the Kannaviou Formation have ever overlain the Mamonia basement terranes and fragments.

However, there is much circumstantial evidence to suggest the Kannaviou Formation was deposited across the entire area, overlying both Mamonia and Troodos basement terranes and related fragments. When viewing the outcrop patterns (Figs 7.8,9,10,11,12) of the preserved neo-autochthonous sedimentary cover, with respect to the sediments overlying contacts A to E, the outcrops are found to be limited to the structural lows surrounding the Mamonia basement fragments and the sediments overlying contacts D and E are also carpeting the southern portion of the southern Mamonia basement fragment. Therefore the circumstantial field evidence would suggest that after six erosional events (Fig. 7.1), especially after the first, when the Mamonia basement fragments 'flowered', there would be little or no chance of any of the sediments relating to the Kannaviou Formation ever being preserved. Apart from the outcrop at Petra-tou-Romiou, which may have been reworked.

Other circumstantial evidence is the mixing of Mamonia related olistoliths and clasts with the bentonitic clays of the Kannaviou Formation, to form the sedimentary melanges of the Moni Formation, Dhrousha and Paralimini Melanges. If as suggested the Kannaviou Formation is exclusively associated with the Troodos basement terrane and fragments, the more complex situation of two separate source areas are required for the mixing event. Whereas if the Kannaviou Formation was also deposited over the Mamonia basement terranes and fragments, then the more simplified situation of a single source area would only be required.

Further circumstantial evidence is seen at locality LL17 (Chapter 4; CGR 617 455), where the Maastrichtian chalks of the Lefkara Formation. Lower Member are seen to overlie a bentonitic clay type material (further research required), which in turn overlies the Mamonia basement terrane.

To confirm the circumstantial evidence that the Kannaviou Formation has been deposited overlying the Mamonia basement terranes and fragments, is to locate outcrops of the Lefkara Formation, Lower Member (Maastrichtian) overlying Mamonia Basement, which may be sandwiching bentonitic clays or volcaniclastic sediments.

7.3.10.2 Southern Mamonia basement fragment

From the onset of the transpressional activity, during the late Campanian, which caused the Mamonia basement fragments to 'flower' and form structural highs, the southern basement fragment continued to remain structurally high until the ?Late Oligocene and played an important role in the depositional history of the neo-autochthonous sedimentary cover, in S.W. Cyprus. When viewing the preserved current outcrop patterns of the Lefkara Formation (Figs 7.9,10,11,12), the southern basement fragment is becoming more progressively less pronounced, during the deposition and/or post-depositional erosion event(s), which have affected the individual members and units of the Lefkara Formation.

7.3.10.3 Overall observation of the outcrop pattern

The surviving sedimentary packages (Figs 7.8,9,10,11,12,13) of the neo-autochthonous sedimentary cover, which are bounded by unconformities (Fig. 7.3) and overstep one another in the main, younging in a north westerly direction, to overlie unconformably the basement rocks of S.W. Cyprus, is generally correct. However, the

micro floral data (Chapter 6) for the base of the Pissouri Formation (Myrtou Marls), suggest contact G is diachronous, younging from north to south following the axis of the Polis graben (Fig 7.13D), which is opposite to the overall south-east to north-west trend.

7.4 Lateral Movement (Major Lineaments)

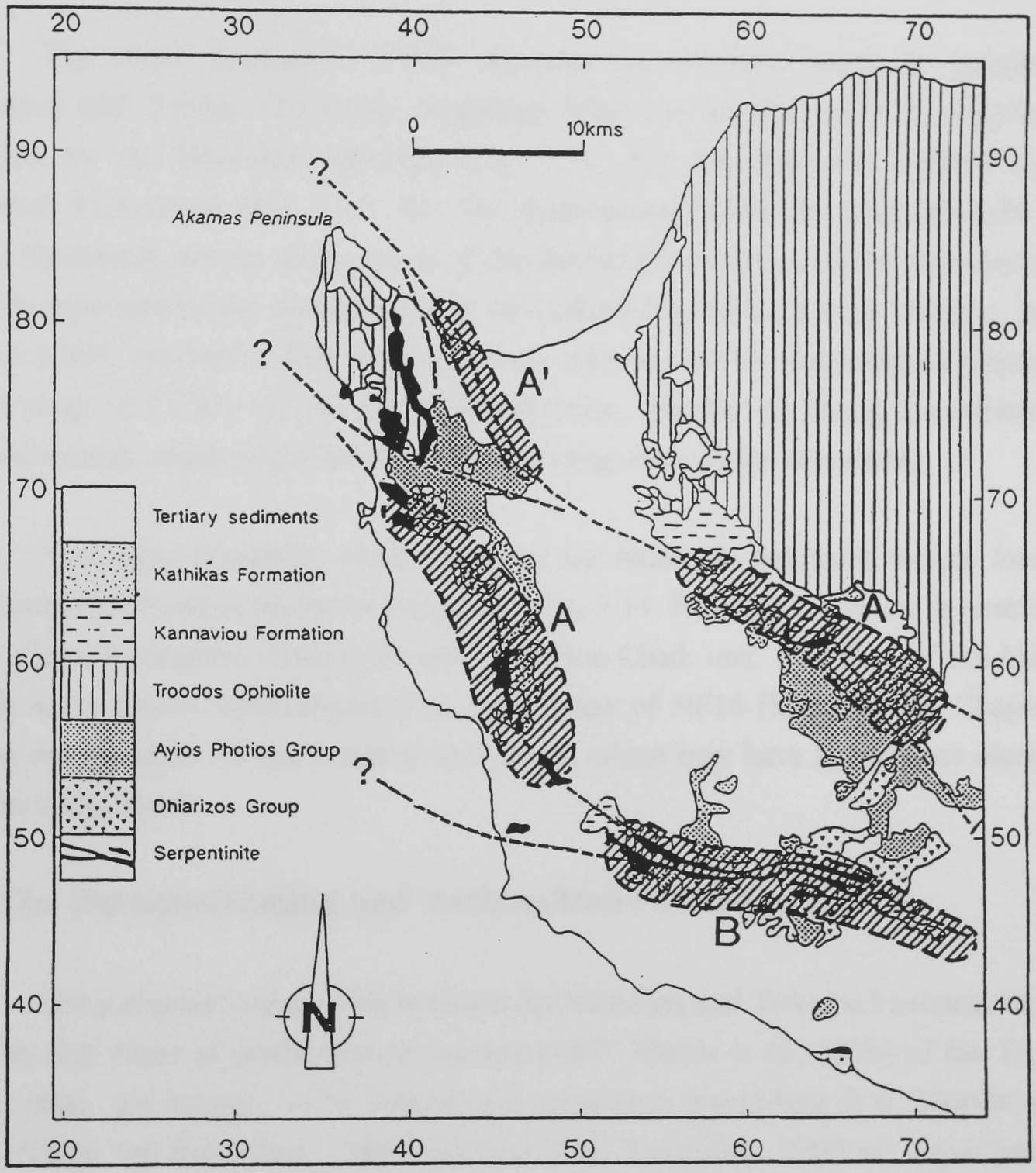

A = Lineaments overlain by relatively undisturbed sediments of the Kathikas (**A'** = Dhrousha Melange) and Lefkara (Lower Member) Formations, with a calcareous nannofossil zonal range of CC23b-CC25a (early Maastrichtian; Chapter 4).

B = Lineaments overlain by undisturbed sediments of the Lefkara Formation, Middle Member, Massive Chalk, with a calcareous nannofossil zonal range of NP16 (Mid Eocene; Chapter 5).

7.14. Simplified geological map of Cyprus, displaying the age of sediments which straddle the major lineaments

The micro floral data will give relative biostratigraphical (calcareous nannofossils) dates, for the sediments which immediately overlie the major lineaments. These dates could only infer the cessation of movements along these major lineaments. No inferences may be drawn as to the start of these movements, distance travelled or whether there was any movement along these lineaments. These problems were outside the bounds of the project.

The major lineaments which separates the Troodos basement terrane and Mamonia and Troodos basement fragments from one another in S.W. Cyprus, are overlain by the Dhrousha Melange (Fig. 7.14, A'), Kathikas and Lefkara (Lower Member) Formations (Fig. 7.14, A). The predominant sediments which straddle these major lineaments are the debris flows of the Kathikas Formation, which they themselves may be separated by the intercalation of the Lefkara Formation, Lower Member, pelagic chalks (chalk interbeds). The chalk interbeds have an overall relative biostratigraphical zonal range of CC23b-CC25a (early Maastrichtian; Chapter 4), dating the cessation of any movement, which might have taken place along these major lineaments.

The major lineament which separates the Mamonia basement terrane from the Mamonia and Troodos basement fragments (Fig. 7.14, B) in S.W. Cyprus, is overlain by the Lefkara Formation, Middle Member, Massive Chalk unit. The base of the Massive Chalk has a relative biostratigraphical zonal range of NP16 (Mid Eocene; Chapter 5), dating the cessation of any possible movement, which may have taken place along this southern lineament.

7.5 The Juxtapositioning and Anticlockwise Rotation Events

The juxtapositioning event between the Mamonia and Troodos basement terranes and the first phase of anticlockwise rotation (<60°, Morris *et al.*, 1990) of the Troodos micro plate, are thought to be interrelated by several researchers (e.g. Moores et al., 1984; Clube and Robertson, 1986; Murton, 1990; Swarbrick, 1993 etc.) and therefore are related to the many proposed mechanisms involving strike slip and subduction scenarios, which attempt to explain the juxtapositioning event.

What is generally accepted by most researchers is that: 1) Two dissimilar basement terranes have been brought together side by side; 2) where the contact is exposed, the two terranes are separated by high angle to vertical faults, containing screens of serpentinite; 3) 90° of anticlockwise rotation of the Troodos micro plate has

taken place between the Late Cretaceous (Campanian) to Early Eocene; 4) The first 60° of anticlockwise rotation had occurred by the Maastrichtian; 5) The size of the rotated unit is within the boundaries of Cyprus.

The micro floral data of the project infers that the juxtapositioning event had ended by the end of the early Maastrichtian, dated by the presence of chalk interbeds within the Kathikas Formation, overlying the major lineaments (Fig. 7.14, A, A').

If the anticlockwise rotation is related to the juxtapositioning event, then the rotation probably took place along all of the major lineaments, seen in S.W. Cyprus. The micro floral data could infer that the first phase of anticlockwise rotation (<60°, Morris *et al.*, 1990) and the juxtapositioning event had ended at the same time (early Maastrichtian), when all but one of the major lineaments (Fig. 7.14, A, A') became frozen. The remaining southern major lineament (Fig. 7.14, B) could be associated with the final phase (30°) of the anticlockwise rotation, were the micro floral data infers a Mid Eocene age for the ending of movement along this lineament, based on the presence of the Lefkara Formation. Middle Member, Massive Chalk unit overlying the major lineament.

The juxtapositioning and ?anticlockwise rotation events are related to the ?first erosional/compressional event (Fig. 7.1), which resulted in the Mamonia basement terranes and fragments (oceanic and continental margin lithologies) to be uplifted in relation to the Troodos basement terrane and fragments (oceanic lithologies). It resulted in the 'flowering' of the Mamonia basement fragments, to produce the melange units (debris flows) of the Kathikas and Moni (Dhrousha Melange) Formations (Fig. 7.8) and uplifting the Mamonia basement terranes (Fig. 1.1) to produce the Moni Formation located south-east of Apsiou village, and the Paralimini Melange of S.E. Cyprus (Fig. 7.6).

7.6 Subduction Zone History of Cyprus

The active plate margin between the African and European plates, have played an important role in the geological evolution of Cyprus, which is located at or near to the boundary. Subduction with respect to the area of Cyprus, was first noted when the geochemical signature of the Troodos ophiolite extrusives, suggested the Troodos oceanic micro plate had formed above a subduction zone (Pearce, 1975,1980; Smewing

et al., 1975), during the Late Cretaceous (Cenomanian-Turonian; 91.6 Ma, Mukasa and Ludden, 1987).

Robertson and Woodcock (1986), suggested from the field evidence relating to the Kyrenia - D1 tectonic event (Fig. 2.7), which includes metamorphism, uplift, brecciation and erosion, to represent pervasive ?dextral strike slip at a closing northward dipping subduction zone, within the Kyrenia lineament (Fig. 2.1), during the late Cretaceous (?Santonian-Campanain; ?>73 Ma., Fig. 3.2). Eaton and Robertson (1993), thought the present northward subduction zone south of Cyprus to have commenced during the Late Oligocene-Early Miocene (?NN1, ?>23 Ma., Fig. 3.3), when the convergent plate boundary migrated southwards from the Kyrenia lineament. Between the closing subduction event of the late Campanian (Robertson and Woodcock, 1986) and the commencement of the poorly constrained subduction event of the Late Oligocene-Early Miocene (Eaton and Robertson, 1993), there appears to be an hiatus of 50 Ma. in subduction zone activity, suggesting the African and European plates were passive, in the region of Cyprus.

However, there is circumstantial evidence obtained through this study, and past research (Fig. 7.4), to suggest that the African and European plates continued to be an active convergent margin in the region of Cyprus, resulting in the migration of the subduction zone from within the Kyrenia lineament to the south of Cyprus, during the Early Palaeocene (Fig. 7.1, calcareous nannofossil zonal range of NP1-NP4, tectonic release event resulting in calcareous sedimentation at NP5).

When viewing the composite geological vertical sections (Fig. 7.2), the schematic cross-section (Fig. 7.3) and the outcrop patterns (Figs 7.9,10,11,12), for S.W. Cyprus, the boundary lines of the outcrop patterns which make unconformable contact with the basement, are the 'maximum regression lines' for the individual sedimentary packages, which are bounded by unconformities. These 'maximum regression lines' overstep one another in the main (Fig. 7.3), younging in a north westerly direction, with each overlying sedimentary package preserving the last regression event. A similar simplified pattern occurs against the northern margin of the Troodos Massif (Figs 7.4,5).

The sedimentary package which shows evidence of the greatest amount of erosional activity during one event, is the Lefkara Formation, Lower Member (Fig. 7.1, Maastrichtian, calcareous nannofossil zonal range of CC23b-CC26). In S.W. Cyprus the 'maximum regression line' is inferred south of the Pakhna area (Fig. 7.3) and is seen

outcropping west of Perapedhi village (Fig. 7.6) against the Troodos Massif, and is protected from further erosional activity, by the sediments overlying contact D (Fig. 7.1,3). This excludes the Lefkara Formation, Lower Member outcrops seen to the north-west of the 'maximum regression line', because they have been preserved in structural lows surrounding the structural highs of the Mamonia basement fragments. Against the northern margin of the Troodos Massif, the 'maximum regression line' of the Lefkara Formation is seen to the south of Dhali village (Fig. 7.5) and again is protected by the sediments overlying a type D contact (Fig. 7.1,4,5; Gass, 1960).

Between the base of the preserving sedimentary package which overlies contact D and the underlying erosion surface (?Maastrichtian), of the outcrops seen in S.W Cyprus and against the northern margin of the Troodos Massif, an age of Early Palaeocene to Early Eocene (Fig.7.1, calcareous nannofossil zonal range of NP1-NP12), can be inferred for the migration of the subduction zone to the south of Cyprus. However, in S.W. Cyprus a sedimentary package unconformably overlying the basement at contact B (Fig. 7.1, calcareous nannofossil zonal range NP5), has been noted. Also around the margins of the Troulli Inlier, field work (Lilljequist, 1969) has located an unconformable contact between the Lower and Middle (Chalk and Chert unit) Members of the Lefkara Formation, which can be inferred as a type B contact. Therefore the evidence from the contact B localities, refines the initial date of Early Palaeocene to Early Eocene for the migration of the subduction zone to Early Palaeocene (Fig. 7.1, calcareous nannofossil zonal range of NP1-NP4) and represents the tectonic release event for the onset of calcareous sedimentation above contact B (Fig. 7.1).

The mechanics behind the migration of the subduction zone to the south of Cyprus, occurred after its closure at the Kyrenia lineament, during the late Campanian (Robertson and Woodcock, 1986). The African plate continued to exert northward pressure against the European plate in the region of Cyprus, causing the European plate to bulge ?north of the plate contact, uplifting the western edge of Cyprus into an erosional environment (?subaerially), subjecting the Lefkara Formation, Lower Member pelagic chalks to erosional forces, which was eroded back to the preserved 'maximum regression line'. The presence of Mamonia basement terranes and fragments (continental rocks), forming the south and south-west portion of the basement in Cyprus and the continued northward pressure of the African plate, caused the African plate (oceanic) to subduct, dipping northwards under Cyprus, causing a tectonic release event, resulting in

the subsidence of the European plate at the plate boundary, followed by a transgressive event at NP5 (Fig. 7.1).

After the migration of the subduction zone to the south of Cyprus, resulting in the first tectonic release and transgressive events, the African plate continued to exert a ?northward pressure against the western edge of Cyprus (European plate), resulting in eventual uplift at the overriding margin. However, the younging north westward and westward overstepping nature of the sedimentary packages, which overlie and protect the last erosional event ('maximum regression line'), in S.W. Cyprus and against the northern margin of the Troodos Massif respectively, suggest the uplifting effect of the subducting plate and its ability to stick, was becoming progressively less pronounced, between the Early Palaeocene to Late Oligocene-Early Miocene (?Late Miocene-Early Pliocene).

In the Late Miocene the subduction zone directly to the south of Cyprus may have undergone 'roll-back' caused by pulsed accelerated subduction, resulting in the subduction zone migrating further south and causing extensional forces in S.W. Cyprus, to form the Polis graben system (Payne and Robertson, 1995). The migration event is thought to be connected to a change in convergence direction between the African and European plates (Dewey *et al.*, 1989).

The micro floral data obtained through this study (Chapters 4, 5 and 6) and the fieldwork of past researchers, has adequately demonstrated that the differential uplift and subsidence history, experienced by the allochthonous basement terranes and fragments forming the western edge of Cyprus, was caused by a north dipping subduction zone to the south/south-west of Cyprus, being present since the Early Palaeocene. These tectonic events ultimately affected the depositional history of the neo-autochthonous sedimentary cover, between the Late Cretaceous (late Campanian) and Holocene. The subducting African plate continues at the present day to exert compressional forces, causing the overriding European plate to uplift at the western margin of Cyprus, with the arcuate allochthonous basement terranes having a regional dip towards the Levant coastline of northern Syria and south-east Turkey (Fig. 2.1). The overall picture is further complicated by the Rapid Plio-Pleistocene uplift, attributed to the progressive serpentinisation of the mantle sequence underlying the Troodos Massif in the region of Mt. Olympus (1951m), If the pillow lavas were at sea level at the start serpentinisation, the overall uplift to date would be ?>6 km.

7.7 Conclusions

The relative biostratigraphical data obtained during the project and reported in chapters 4, 5 and 6, have provided age dates (calcareous nannofossil zonal ranges) for the following sedimentary formations and members, and conformable and unconformable contacts.

1). The top of the Kannaviou Formation making contact with the overlying sediments, has a zonal range of CC18-CC23a (Campanian).

2). The newly recognised Dhrousha Melange, with its type locality situated to the north of Dhrousha, in a road cut on the Polis road, shows similarities to the upper melange unit of the Moni Formation and has a zonal range of CC23-CC25a (late Campanian to early Maastrichtian).

3). The Kathikas Formation based on data obtained from the pelagic chalk interbeds, has a zonal range of CC23b-CC25a (early Maastrichtian).

4). The basal horizon of the Lefkara Formation, Lower Member making conformable contact with the Kannaviou and Kathikas Formations and unconformable contact with the basement rocks, has a zonal range of CC23b-CC26 (Maastrichtian).

5). Three newly recognised unconformable contacts, between the basal horizon of the Lefkara Formation, Middle Member, Chalk and Chert unit and the underlying rocks, have a zonal range of NP5, NP8/NP9 boundary and NP12-NP15 (diachronous contact) (mid and Late Palaeocene and Early Eocene respectively).

6). The basal horizon of the Lefkara Formation, Middle Member, Massive Chalk unit making unconformable contact with the underlying rocks, has a zonal range of NP16 (early Late Eocene).

7). The basal horizon of the Pakhna Formation chalks making unconformable contact with the underlying rocks, has a zonal range of NP25-NN1 (Oligo-Miocene boundary).

8). A newly recognised outcrop of the Pakhna Formation Terra Limestone Member, has been located at Petra-tou-Romiou, conformably overlying Pakhna Formation chalks, with a zonal range of NN1 (Miocene).

9). A study of the basal horizon of the Pakhna Formation located at Kottaphi Hill on the northern side of the Troodos Massif, making unconformable contact with the Lefkara Formation, Middle Member, Chalk and Chert unit, was found to have a zonal range of NP24-NN1, which is similar in age to the basal horizon of S.W. Cyprus (NP25-NN1).

10). The basal horizon of the Pissouri Formation (Myrtou Marls), has made a north to south (Polis to Paphos), diachronous unconformable contact with the underlying rocks, with a zonal range of NN10 to NN11 (NN12 at the Perapedhi section of Krasheninnikov and Kaleda, 1994).

Based on the relative biostratigraphical age dates, obtained for the sedimentary formations and their members seen in S.W. Cyprus, a number of implications are noted.

1). The field and biostratigraphical data suggests the Moni (Dhrousha and ?Paralimini Melanges) and the Kathikas Formations are coeval within a zonal range band of CC23-CC25a, (late Campanian to early Maastrichtian), and therefore share the same compressive event.

2). The biostratigraphical data suggests the chalk interbeds of the proximal Moni (Dhrousha Melange) and Kathikas Formations (zonal range CC23-CC25a), are part of the intercalating distal Lefkara Formation, Lower Member (zonal range CC23b-CC26).

3). The sediments of the Kathikas Formation, with a zonal range of CC23b-CC25a (early Maastrichtian), overlie two major lineaments in S.W. Cyprus, suggesting if there was any lateral movement, little or no movement occurred after the onset of deposition.

4). The presence of the Kathikas Formation straddling the major lineaments, indicates a possible age (CC23b-cc25a), for the cessation of the juxtapositioning event between the Mamonia and Troodos basement terranes and their related fragments.

5). If the first phase of anticlockwise rotation of the Troodos micro plate is related to the juxtapositioning event, then it is possible that lateral movement may have occurred along all of the major lineaments, in S.W. Cyprus. This would imply the first 60° of anticlockwise rotation ended at the same time as the juxtapositioning event (CC23b-CC25a).

6). The basal horizon of the Lefkara Formation may be diachronous, from west (CC23b) to east (CC26) within the structural low, east of the northern Mamonia basement fragment.

7). The basal horizon of the Lefkara Formation, Middle Member, Massive Chalks, with a zonal range of NP16, overlies the southern major lineaments of S.W. Cyprus, suggesting that if there was any lateral movement, little or no movement occurred after the onset of deposition.

8). The presence of the Lefkara Formation, Middle Member, Massive Chalk unit straddling the southern major lineaments, indicates a possible age (NP16) for the cessation of the final phase (30°) of anticlockwise rotation of the Troodos micro plate, providing the lateral movement is associated with southern lineament.

9). Based on the age of the overlying Pissouri Formation (Myrtou Marls), the evaporites of the Kalavasos Formation in the Polomi basin are Tortonian, older than initially thought (Messinian, Late Miocene).

The outcrop patterns of the preserved neo-autochthonous sedimentary cover, suggest several tectonic implications, which may or may not include differential uplift and subsidence.

1). The onset of transpressional activity in the area of S.W. Cyprus, during the late Campanian, caused the Mamonia basement fragments to 'flower' and form structural highs. The southern fragment remained structurally high through to the Oligo-Miocene boundary and played an important role in the depositional history of the neo-autochthonous sedimentary cover. The outcrop patterns of the preserved sedimentary packages, show the southern fragment becoming less pronounced, during deposition and/or post-depositional erosion of the Lefkara Formation, until the Pakhna transgressive event, were it no longer plays a part in the depositional history.

2). The preserved sedimentary packages, bounded by unconformities, overstep one another in the main, younging in a north westerly direction, similar to that seen against the northern margin of the Troodos Massif, where the sediments overstep one another in a westerly direction.

3). The boundary lines of the preserved sedimentary packages are 'maximum regression lines', for the sediments which have survived the last erosional event. These regression lines are preserved by the next overstepping sedimentary package.

The biostratigraphical data, the implications derived from the data, the outcrop patterns of the preserved sedimentary packages and the fieldwork of past research, offers circumstantial evidence to suggest that the Kannaviou Formation was deposited across both Mamonia and Troodos basements in the region of S.W. Cyprus, and the migration of the subduction zone from the Kyrenia lineament to the south of Cyprus, occurred during the Early Palaeocene (pre-NP5).

REFERENCES

Achuthan, M. V. & Stradner, H. 1969. Calcareous Nannoplankton from the Wemmelian stratotype. *In*: Brönniman, P. & Renz, H. H. (eds), *Proceedings First International Conference on Planktonic Microfossils,* Geneva, vol. 1, pp. 1-13. E. Brill, Leiden

Allen, C. G. 1967. The micropalaeontology of Cyprus: *Unpublished report,* Cyprus Geological Survey Department, 21pp.

Arkhangelsky, A. D. 1912. Upper Cretaceous deposits of east European Russia. *Mater. Geol. Russ.*, **25,** 1-631.

Backman, J. 1978. Late Miocene-Early Pliocene nannofossil biochronology in the Vera Basin, SE Spain. *Acta Univ. Stockholm. Contrib. Geol.*, **32**(2), 93-114.

Backman, J. 1980. Miocene-Pliocene nannofossils and sedimentation rates in the Hatton -Rockall basin, NE Atlantic Ocean. *Acta Univ. Stockholm. Contrib. Geol.*, **36** (1), 1-91.

Backman, J. & Hermelin, J. O. R. 1986. Morphology of the Eocene nannofossil *Reticulofenestra umbilicus* lineage and its biochronological consequences. *Palaeogeogr., Palaeoclimatol., Palaeoecol.*, **57**, 103-116.

Bagnall, P. S. 1960. The geology and mineral resources of the Pano Lefkara-Lanrnca area *Cyprus Geol. Mem.*, **5,** 116pp.

Banner, F. T. & Blow, W. H. 1965. Progress in planktonic foraminiferal biostratigraphy of the Neogene. *Nature,* **208,** 1164-6.

Baroz, F. & Bizon, G. 1977. La couverture Tertiaire du flanc nord du massif du Troodos et de la partie meridionale de la Mesaoria: Etude stratigraphique et micropaleontologique: *Revue de l' Institut Francais du Petrole,* **32,** 719-759.

Bear, L. M. 1960. The geology and mineral resources of the Akaki-Lythrodondha area. *Cyprus Geol. Mem.*, **3,** 122pp.

Bear, L. M. & Morel, S. W. 1960. The geology and mineral resources of the Agros-Akrotiri area. *Cyprus Geol. Mem.*, **7,** 88pp.

Bellamy, C. V. & Jukes-Brown, A. J. 1905. The Geology of Cyprus. London.

Berggren, W. A. & Van Couvering, J. A. 1974. The Late Neogene. Biostratigraphy, geochronology and palaeoclimatology of the last 15 million years in marine and continental sequences. *Palaeogeogr. Palaeoclimatol. Palaeoecol.*, **16,** 1-215.

Berggren, W. A., Kent, D. V. & Flynn, J. J. 1985a. Palaeogene geochronology and chronostratigraphy. *In*: Snelling, N. J. (ed.), *The Chronology of the Geological Record,* Blackwell, 141-195.

Berggren, W. A., Kent, D. V. & Van Couvering, J. A. 1985b. Neogene geochronology and chronostratigraphy. *In*: Snelling, N. J. (ed.), *The Chronology of the Geological Record,* Blackwell, 211-260.

Black, M. 1964. Cretaceous and Tertiary coccoliths from Atlantic sea mounts. *Palaeontology,* **7,** 306-16.

Black, M. 1967. New names for some coccolith taxa. *Proc. geol. Soc. London,* **1640,** 139-45.

Black, M. 1968. Taxonomic problems in the study of coccoliths, *Palaeontology,* **11**(5), 793-813.

Black, M. 1971a. Coccoliths of the Speeton Clay and Sutterby Marl. *Proc. Yorkshire geol. Soc.*, **38**(3), 381-424.

Black, M. 1971b. The systematics of coccoliths in the relation to the palaeontological record. In: Funnell, B. M. & Riedel, W. R. (eds), *The Micropalaeontology of Oceans,* pp. 611-24. Cambridge University Press.

Black, M. & Barnes, B. 1959. The structure of coccoliths from the English Chalk. *Geol. Mag.*, **96,** 321-8.

Blome, C. & Irwin, W. 1985. Equivalent radiolarian ages from ophiolite terranes of Cyprus and Oman. *Geology* **13,** 401-4.

Blow, W. H. 1969. Late Middle Eocene to Recent planktonic foraminiferal biostratigraphy. *Proceedings First International Conference on Planktonic Microfossils, Geneva 1967,* **1,** 199-422.

Bolli, H. M. 1957a. Planktonic foraminifera from the Oligocene-Miocene Cipero and Lengya formations of Trinidad, B.W.I. *Bull. u.s. natl. Mus.*, **215,** 97-123.

Bolli, H. M. 1957b. Planktonic foraminifera from the Eocene Navet and San Fernando formations of Trinidad, B.W.I. *Bull. U.S. natl. Mus.*, **215,** 155-72.

Bolli, H. M. & Bermudez, P. J. 1965. Zonation based on planktonic foraminifera of Middle Miocene to Pliocene warm-water sediments. *Boletino Informativo, Asoc. Ven. Geol., Min. y Petr.*, **8,** 119-49.

Bolli, H. M. & Premoli Silva, I. 1973. Oligocene to Recent planktonic foraminifera and stratigraphy of the Leg 15 Sites in the Caribbean Sea. *Initial Rep. Deep Sea drill. Proj.*, **15,** 475-97.

Bolli, H. M. &. Saunders, J. 1985. Oligocene to Holocene low latitude planktic foraminifera. *In*: Bolli, H. M., Saunders, J. & Perch-Nielsen, K. (eds), *Plankton Stratigraphy.* Cambridge University Press, Cambridge, 155-262.

Bolli, H. M, Saunders, J. & Perch-Nielsen, K. (eds) 1985. *Plankton Stratigraphy.* Cambridge University Press, Cambridge, 1006pp.

Boudreaux, J. E. & Hay, W. W. 1969. Calcareous nannoplankton and biostratigraphy of the Late Pliocene-Pleistocene-Recent sediments of the Submarex cores. *Rev. Esp. Micropaleontol.*, **1,** 249-92.

Bown, P. 1987. The biostratigraphy, evolution and distribution of Early Mesozoic nannofossils. *unpublished PhD thesis,* University College London.

Bragin, N. Y. & Bragina, L. G. 1991. Radiolarian biostratigraphy of Troodos Upper Cretaceous sediments (Cyprus). *Abstracts volume, 6th meeting of the International Association of Radiolarlian Paleoontologists, Firenze 1991,* 17.

Bralower, T. J. & Siesser, W. G. 1992. Cretaceous calcareous nannofossil biostratigraphy of Sites 761, 762 and 763, Exmouth and Wombat plateaus, northwest Australia. *Proc. Ocean Drilling Program, Scientific Results,* **122,** 529-556.

Bramlette, M. N. & Martini, E. 1964. The great change in calcareous nannoplankton fossils between the Maestrichtian and Danian. *Micropaleontology,* **10,** 291-322.

Bramlette, M. N. & Riedel, W. R. 1954. Stratigraphic value of discoasters and some other microfossils related to recent coccolithophores. *J. Paleontol.*, **28,** 385-403.

Bramlette, M. N. & Sullivan, F. R. 1961. Coccolithophorids and related nannoplankton of the Early Tertiary in California. *Micropaleontology,* 7, 129-74.

Bramalette, M. N. & Wilcoxon, J. R. 1967. Middle Tertiary calcareous nannoplankton of the Cipero Section, Trinidad, W. I. *Tulane Stud. Geol.*, **5,** 93-131.

Brasier, M. D. 1980. *Microfossils.* George Allen and Unwin, London, 193pp.

Brönnimann, P. & Stradner, H. 1960. Die Foraminiferen und Discoasteridenzonen von Kuba und ihre interkontinentale Korrelation. *Erdoel-Z.*, **76,** 364-9.

Bukry, D. 1969. Upper Cretaceous coccoliths from Texas and Europe. *Univ. Kansas Paleontol. Contrib.*, **51** (Protista 2), 1-79.

Bukry, D. 1971. Cenozoic calcareous nannofossils from the Pacific Ocean. *Trans. San Diego Soc. nat. Hist.*, **16,** 303-27.

Bukry, D. 1973a. Phytoplankton stratigraphy, DSDP Leg 20, Western Pacific Ocean. *Initial Rep. Deep Sea drill. Proj.*, **20**, 307-17.

Bukry, D. 1973b. Coccolith stratigraphy, eastern equatorial Pacific, Leg 16, Deep Sea Drilling Project. *Initial Rep. Deep Sea drill. Proj.*, **16,** 653-711.

Bukry, D. 1973c. Low-Latitude coccolith biostratigraphic zonation. *Initial Rep. Deep Sea drill. Proj.*, **15,** 685-703.

Bukry, D. 1975. Coccolith and silicoflagellate stratigraphy, Northwestern Pacific Ocean, DSDP, Leg 32. *Initial Rep. Deep Sea drill. Proj.*, **32,** 677-701.

Bukry, D. 1981. Pacific Coast coccolith stratigraphy between Point Conception and Cabo Corrietes, Deep Sea Drilling Project, Leg 63. *Initial Rep. Deep Sea drill. Proj.*, **63,** 445-472.

Bukry, D. & Bramlette, M. N. 1969. Some new and stratigraphically useful calcareous nannofossils of the Cenozoic. *Tulane Stud. Geol. Paleontol.*, **7,** 131-42.

Bukry, D. & Percival, S. F. 1971. New Tertiary calcareous nannofossils. *Tulane Stud. Geol. Paleontol.*, **8,** 123-46.

Cameron, W. E. 1985. Petrology and origin of primative lavas from the Troodos ophiolite, Cyprus. *Contrib. Mineral. Petrol.*, **89,** 239-255.

Cande, S. & Kent, D. V. 1992. A new geomagnetic polarity time scale for the Late Cretaceous and Cenozoic. *J. Geophys. Res.*, **97,** 13917-13951.

Caron, M. 1985. Cretaceous planktic foraminifera. *In*: Bolli, H. M, Saunders, J. & Perch-Nielsen, K. (eds), *Plankton Stratigraphy.* Cambridge University Press, Cambridge, 17-86.

Carr, J. M. & Bear, L. M. 1960. The geology and mineral resources of the Peristerona-Lagoudhera area. *Cyprus Geol. Mem.*, **2,** 79pp.

Cleintuar, M. R., Knox, G. J. & Ealey, P. J. 1977. The geology of Cyprus and its place in the eastern Mediterranean framework. *Geologie en Mijnbow*, **56**(1), 66-82.

Clube, T. M. M., Creer, K. M. & Robertson A. H. F. 1985. Palaeorotation of the Troodos microplate, Cyprus. *Nature*, **317,** 522-525.

Clube, T. M. M. & Robertson, A. H. F. 1986. The palaeorotation of the Troodos microplate, Cyprus, in the Late Mesozoic-Early Cenozoic plate tectonic framework of the Eastern Mediterranean. *Surv. Geophys.*, **8,** 375-437.

Constantinou, G. 1980. Metallogenesis associated with Troodos Ophiolite. *In*: Panayiotou, A. (ed.), *Ophiolites, Proc. Inter. Oph. Symp.* Cyprus Geol. Surv. Dept., 663-674.

Crux, J. A. 1982. Upper Creataceous (Cenomanian to Campanian) calcareous nannofossils. *In*: Lord A. R. (ed.), *A Stratigraphical Index of Calcareous Nannofossils,* British Micropalaeontological Society, Ellis Horwood Press, Chichester, 81-135.

Dalbiez, F. 1955. The genus *Globotruncana* in Tunisia. *Micropaleontology,* **1,** 161-71.

Decima, F. P., Medizza, F. & Todesco, L. 1978. Southeastern Atlantic Leg 40 calcareous nannofossils. *Initial Rep. Deep Sea drill. Proj.*, **40**, 571-634.

Deflandre, G. 1942. Coccolithophoridées Fossiles d' Oranie. Genres *Scyphosphaera* Lohmann et *Thoracosphaera* Ostenfeld. *Bull. Soc. Hist. nat. Toulouse,* **77**, 125-37.

Deflandre, G. 1947. *Braarudosphaera* nov. gen., type d'une famille nouvelle de Coccolithophoridés actuels à éléments composites. *C. r. Seances Acad. Sci. Paris,* **225,** 439-41.

Deflandre, G. 1952. Classe des coccolithophoridés. In: P. P. Grassé (ed.), *Traité de Zoologie,* **1,** 439-70.

Deflandre, G. 1953. Hétérogénéité intrinsèque et pluralité des éléments dans les coccolithes actuels et fossiles. *C.r. Seances Acad. Sci. Paris,* **237,** 1785-7.

Deflandre, G. 1957. *Goniolithus* nov. gen., type d' une famille nouvelle de Coccolithophoridé fossiles, à éléments pentagonaux non composites. *C.r. Seavces Acad. Sci. Paris,* **244,** 2539-41.

Deflandre, G. 1959. Sur les nannofossils calcaires et leur systématique. *Rev. Micropaleontol.*, **2,** 127-52.

Deflandre, G. 1963. Sur les Microrhabdulidés, famille nouvelle de nannofossiles calcaires. *C.r. Seances Acad. Sci. Paris,* **256,** 3484-6.

Deflandre, G. & Fert, C. 1954. Observations sur les Coccolithophoridé actuels et fossiles, en microscopie ordinaire et électronique. *Ann. Paleontol.*, **40,** 115-76.

Dewey, J. F., Helmam, M. L., Turco, E., Hutton, D. H. W. & Nott, S.D. 1989. Kinematics of the western Mediterranean. *In*: Coward, M. P., Dietrich, D. & Park, R. G. (eds) *Alpine Tectonics.* Geological Society, London, Special Publication, **45,** 265-283.

Dilek, Y., Thy. P., Moores, E. M. & Ramsden, T. W. 1990. Tectonic evolution of the Troodos ophiolite within the Tethyan framework. *Tectonics,* **9**(4), 811-823.

Ducloz, C. H. 1964. Notes on the geology of the Kyrenia Range. *Cyprus Geol. Surv. Ann. Rept. 1963,* 57-67.

Dumitrica. P. 1970. Cryptocephalic and crytothoracic *Nassellaria* in some Mesozoic deposits of Romania. *Revue roumaine de Geologie, geophysique et geographie Serie de geologie,* **14,** 45-124.

Ealey, P. J. & Knox, G. J. 1975. The pre-Tertiary rocks of SW Cyprus. *Geol. Mijnbouw.,* **54,** 85-100.

Eaton, S., 1987, The sedimentology of Mid-Late Miocene carbonates and evaporites in southern Cyprus: *Unpublished Ph.D. thesis,* Edinburgh University, 259p.

Eaton, S. & Robertson, A. H. F. 1993. The Miocene Pakhna Formation and its relation to the Neogene tectonic evolution of the Eastern Mediterranean, *Sedimentary Geology,* **86,** 273-296.

Ehrenberg, C. G. 1840. Uber die Bilung der Kreidefelsen und des Kreidemergels durch unsichtbare Organismen. *Abhandlungen der K. Akademie der Wissenschaften Berlin, Physik.* (1838), p143.

Firth, J. V. 1989. Eocene and Oligocene calcareous nannofossils from the Labrador Sea, ODP Leg 105. *Proc. Ocean Drilling Program, Scientific Results,* **105**, 263-286.

Follows, E. J. & Robertson, A. H. F. 1990. Sedimentology and structural setting of Miocene reefal limestones in Cyprus. *In*: Malpas, J., Moores, E. M., Panayiotou, A. & Xenophontos, C. *(eds), Ophiolites. Oceanic Crustal Analogues,* Proc. 'Troodos 87' Symposium. Cyprus Geol. Surv. Dept., 207-215.

Follows, E. J. & Robertson, A. H. F. 1996. Tectonic controls on Miocene reefs and related carbonated facies in Cyprus. *In:* Franseen, E. K., Esteban, M., Ward, W. C. & Rouchy, J.-M. (eds), *Models for Carbonate Stratigraphy from Miocene Reef Complexes of Mediterranean Region.* SEPM Concepts in Sedimentology and Paleontology, Tulsa, Oklahoma, USA, **5,** 295-315.

Forchheimer, S. 1972. Scanning electron microscope studies of Cretaceous coccoliths from the Köpinsberg Borehole No. 1, SE Sweden. *Sver. geol. Unders.,* ser. C.668, **65**(14), 1-141.

Foreman, H. P. 1968. Upper Maestrichtian radiolaria of California. *Special Papers in Palaeontology,* **3,** iv and 1-82.

Gaarder, K. R. 1970. Three new taxa of Coccolihinae. *Nytt Mag. Bot.,* **17**, 113-26.

Gallagher, L. 1989. *Reticulofenestra*: a critical review of the taxonomy, structure and evolution. *In*: van Heck, S. E. and Crux, J. A. (eds), *Nannofossils and their Applications.* British Micropalaeontological Society, Ellis Horwood Press, Chichester, 41-75.

Gardet, M. 1955. Contribution à l' étude des coccolithes des terrains Mesogenes de l' Algerie. *Publ. Serv. Carte Geol. Algerie, ser.* 2, Bull. **5,** 477-550.

Gartner, S. Jr 1967. Calcareous nannofossils from Neogene of Trinidad, Jamaica and Gulf of Mexico. *Univ. Kansas, Paleontol. Contrib.*, **29**, 1-7.

Gartner, S. Jr 1968. Coccoliths and related calcareous nannofossils from Upper Cretaceous deposits of Texas and Arkansas. *Univ. Kansas paleontol. Contrib.*, **48**, 1-56.

Gartner, S. Jr 1969. Correlation of Neogene planktonic foraminifera and calcareous nannofossil zones. *Trans. Gulf Coast Assoc. geol. Soc.*, **19,** 585-99.

Gartner, S. Jr 1970. Phylogenic lineages in the Lower Tertiary coccolith genus *Chiasmolithus. North Am. Paleontol. Convention Sept.* 1969, *Proc. G.* 930-57.

Gartner, S. Jr 1971. Calcareous nannofossils from the JOIDES Blake Plateau cores and revision of Paleogene nannofossil zonation. *Tulane Stud. Geol.*, **8,** 101-21.

Gartner, S. Jr & Bukry, D. 1975. Morphology and phylogeny of the coccolithophylean family Ceratolithaceae. *J. Res. U.S. geol. Surv.*, **3,** 451-65.

Gartner, S. Jr & Smith, L. A. 1967. Coccoliths and related calcareous nannofossils from the Yazoo Formation (Jackson, late Eocene) of Louisiana. *Univ. Kansas Paleontol. Contrib.*, **20**, 1-7.

Gass, I. G. 1960. The geology and mineral resources of the Dhali area. *Cyprus Geol. Surv. Mem.*, **4,** 116pp.

Gass, I. G. 1968. Is the Troodos massif of Cyprus a fragment of Mesozoic ocean floor? *Nature*, **221,** 926-930.

Gass, I. G. & Masson-Smith, D. 1963. The geology and gravity anomalies of the Troodos massif, Cyprus. *Phil. Trans. Roy. Soc.*, **A255,** 417-467.

Gass, I. G., MacLeod, C. J., Murton, B. J., Panayiotou, A., Simonian, K. O. & Xenophontos, C. 1994. The geology of the Southern Troodos Transform Fault Zone. *Cyprus Geol. Surv. Mem.*, **9,** 218pp.

Gorka, H. 1957. Les coccolithophoridés du Maestrichien supérieur de Pologne. *Alta paleontol. Pol.*, **2**, 235-84.

Grassé, P. P. 1952. *Traité de Zoologie, Anatomie, Systématique, Biologie.* Vol. 1, fasc. 1: Phylogénie. Protozoaires: généralités. Flagellés. Masson, Paris, XII + 1071 pp., 830 figs.(Classe des Coccolithophoridés (Coccolithophoridae Lohmann, 1902), pp. 439-70, figs. 339-364 by G. Deflandre.)

Green, J. C. & Jordon, R. W. 1994. Systematic history and taxonomy. *In:* Green, J. C. & Leadbeater, B. S. C. (eds), *The Haptophyte Algae,* The Systematics Association Special Volume, Oxford Science Press, Oxford, **51,** 1-21.

Grün, W. & Allemann, F. 1975. The Lower Cretaceous of Caravaca (Spain): Berriasian calcareous nannoplankton of the Miravetes Section (Subbetic Zone, Prov. of Murcia). *Eclog. geol. Helv.*, **68**(1), 147-211.

Haeckl, E. 1894. *Systematische Phylogenie der Protisten und Pflanzen.* Reimer, Berlin, 400 pp.

Hamilton, G. B. & Hojjatzadak, M. 1982. Cenozoic nannofossils - A Reconnaissance. *In*: Lord A. R. (ed.), *A stratigraphical Index of Calcareous Nannofossils* British Micropalaeontological Society, Ellis Horwood Press, Chichester, 136-167.

Haq, B. U. 1971. Paleogene calcareous nannoflora Parts I-IV. *Stockholm Contrib. Geol.*, **25,** 1-158.

Haq, B. U. 1976. Coccoliths in cores from the Bellingham abyssal plain and Antarctic continental rise. *Initial Rep. Deep Sea drill. Proj.*, **35**, 577-67.

Haq, B. U. 1978. Calcareous nannoplankton. *In*: Haq, B. U. & Boersma, A. (eds), *Introduction to Marine Micropalaeontology,* Elsevier, 79-107.

Haq, B. U. & Aubry, M. -P. 1981. Early Cenozoic calcareous nannoplankton biostratigraphy and palaeobiogeography of North Africa and the Middle East and trans-Tethyan correlations. *In*: Salem M. J. & Busrewil M. T. (eds), *Geology of Libya,* vol. 1, pp. 271-304. Academic Press, London.

Haq, B. U. & Berggren, W. A. 1978. Late Neogene calcareous plankton biochronology of the Rio Grande Rise (South Atlantic Ocean). *J. Paleontol.*, **52**(6), 1167-94.

Harland, W. B., Cox, A. V., Llewellyn, P. G., Pikton, C. A. G., Smith, A. G. & Walters, R. 1982. *A Geologic Time Scale,* Cambridge University Press.

Harland, W. B., Armstrong, R. L., Cox, A. V., Craig, L. E., Smith, A. G. & Smith, D. G. 1989. *A Geologic Time Scale,* Cambridge University Press, 263pp.

Hay, W. W. 1977. Calcareous nannofossils. *In*: Ramsay A. T. S. (ed.), *Oceanic Micropalaeontology,* 1055-1200. Academic Press, London.

Hay, W. W. & Mohler, H. P. 1967. Calcareous nannoplankton from early Tertiary rocks at Pont Labau, France, and Paleocene-Eocene correlations. *J. Paleontol.*, **41,** 1505-41.

Hay, W. W., Mohler, H. P., Roth, P. H., Schmidt, R. R. & Boudreaux, J. E. 1967. Calcareous nannoplankton zonation of the Cenozoic of the Gulf Coast and Caribbean - Antillean area, and transoceanic correlation. *Trans. Gulf Coast Assoc. geol. Soc.*, **17,** 428-80.

Hay, W. W., Mohler, H. P. & Wade, M. E. 1966. Calcareous nannofossils from Nal'chik (northwest Caucasus). *Eclog. geol. Helv.*, **59,** 379-99.

Henson, F. R. S., Browne, R. V. & McGinty, J. 1949. A synopsis of the stratigraphy and geological history of Cyprus. *Quart. J. Geol. Soc. Lond.*, **105,** 1-41.

Hoffman, N. 1970b *Placozygus* n. gen. (Coccolithineen) aus der Oberkreide des nordlichen Mitteleuropas. *Geologie,* **19**, 1004-9.

Hsu, K. J. 1972. Origin of saline giants: a critical review after discovery of the Mediterranean evaporite. *Earth Sci. Rev.*, **8,** 371-396.

Hsu, K. J., Montadert, L., Bernoulli, D., Cita, M. B., Erickson, A., Garrison, R. E., Kidd, R. B., Melieres, F., Muller, C., and Wright, R. 1978. History of the Mediterranean salinity crisis, *Intial Reports of the Deep Sea Drilling Project,* **42**(1), 1053-1078.

Jafar, S. A. 1975a. Calcareous nannoplankton from the Miocene of Rotti, Indonesia. *Verh. Kon. Ned. Akad. Wetensch. afd. nat.*, **28,** 1-99.

Jafar, S. A. 1975b. Some comments on the calcareous nannoplankton genus *Scyphosphaera* and the neotypes of *Scyphosphaera* species from Rotti, Indonesia. *Senckenbergiana Lethaea,* **56**(4/5), 365-79.

Kamptner, E. 1927. Beitrag zur Kenntnis adriatischer Coccolithophoriden. *Arch. Protistenk.*, **58,** 173-84.

Kamptner, E. 1928. Über das System une die Phylogenie der Kalkflagellaten. *Arch. Protisenk.*, **64,** 19-43.

Kamptner, E. 1948. Coccolithen aus dem Torton des inneralpinen Wiener Beckens. *Sitz. Ber. Österr. Akad. Wiss., Math.-Naturw. Kl.*, Part 1, **157,** 1-16.

Kamptner, E. 1950. Über den submikroskopischen Aufbau der Coccolithen. *Anz. Österr. Akad. Wiss., Math.- Naturw. Kl.*, **87,** 152-86.

Kamptner, E. 1954. Untersuchungen über den Feinbau der Coccolithen. *Arch. Protistenk.*, **100,** 1-90.

Kamptner, E. 1955. Fossile Coccolithineen - Skelettreste aus Insulinde. *Verh. Ned. Akad, Wetensch. afd. nat.*, **50**(2), 1-105.

Kamptner, E. 1963. Coccolithineen-Skelettrests aus Tiefseeablagerungen des Pazifischen Ozeans. *Ann. Naturh. Mus. Wien,* **66,** 139-204.

Kempler, D. 1994. An Outline of Northeastern Mediterranean Tectonics in View of Cruise 5 of the Akademik Nikolaj Strakhov. *In*: Krasheninnikov, V. A. & Hall, J. K. (eds), *Geological Structure of the Northeastern Mediterranean,* Historical Productions-Hall Ltd. Jerusalem, Israel, 277-294.

Kempler, D. & Ben-Avraham, Z. 1987. The tectonic evolution of the Cyprean Arc. *Annales Tectonicae,* **1,** 58-71.

Khokhlova, I. Bragina, L.G. and E., Krasheninnikov, V. A. 1994. Zonal stratigraphy of the Upper Cretaceous and Palaeogene deposits of the key Perapedhi section (Southern Cyprus) by means of radiolarians and correlation with foraminiferal zones. *In*: Krasheninnikov, V. A. & Hall, J. K. (eds), *Geological Structure of the Northeastern Mediterranean,* Historical Productions-Hall Ltd. Jerusalem, Israel, 219-250.

Kluyver, H. M. 1969. Report on regional geologic mapping in Paphos District. *Bull. Geol. Surv. Dep. Cyprus,* **4,** 21-36.

Krasheninnikov, V. A. & Kaleda, K. G. 1994. Stratigraphy and Lithologhy of Upper Cretaceous and Cenozoic Deposits of the Key Perapedhi Section (Neoautochthon of southern Cyprus). *In*: Krasheninnikov, V. A. & Hall, J. K. (eds), *Geological Structure of the Northeastern Mediterranean,* Historical Productions-Hall Ltd. Jerusalem, Israel, 195-218.

Lapierre, H. 1968. Nouvelles observations sur le série sédimentaire de Mamonia (Chypre). *C. R. Acad. Sci. Paris,* **D267,** 32-35.

Lapierre, H. 1972. Les Formations Sediolentaires et Eruptives des Nappes de Maolonia et leurs Relations avec le Massif de Troodos (Chypre). *Doctorat d'etat,* Univ. Nancy, 420pp.

Lapierre, H. 1975. Les formations sédimentaires et éruptives des nappes de Mamonia et leurs avec le massif de Troodos (Chypre occidentale). *Mém. Soc. géol. Fr., Paris,* **123,** 420.

Lazarus, D., Spencer-Cervato, C., Pianka-Biolzi, M., Beckmann, J. P., Salis, K. von, Hilbrecht, H. & Thierstein, H. 1995. Revised Chronology of Neogene DSDP Holes from the World Ocean. *Ocean Drilling Program, Technical Note No. 24,* Texas A&M University.

Lemmermann, E. 1908. Flagellatae, Chlorophyceae, Coccosphaerales und Silicoflagellatae. In: K. Brandt & C. Apstein (eds.), *Nordisches Plankton,* pp. 1-40. Lipsius & Tischer, Kiel and Leipzig.

Leven, H. L. 1965. Coccolithophoridae and related microfossils from the Yazoo formation (Eocene) of Mississippi. *J. Paleontol.,* **39,** 265-72.

Lilljequist, R. 1969. The geology and Mineralisation of the Troulli Inlier. *Cyprus Geol. Surv. Bull.,* **4,** 45-87.

Lipps, J. H. 1969. *Triquetrorhabdulus* and similar calcareous nannoplankton. *J. Paleontol.,* **43,** 1029-32.

Locker, S. 1967. Neue Coccolithophoriden (Flagellata) aus dem Alttertiär Norddeutschlands. *Geologie* (Berlin), **16,** 361-4.

Locker, S. 1968. Biostratigraphie des Alttertiärs von Norddeutschland mit Coccolithophoriden. *Monatsber. Deutsch. Akad. Wiss. Berlin,* **10,** 220-9.

Loeblich, A. R. & Tappan, H. 1963 Type fixation and validation of certain calcareous nannoplankton genera. *Proc. Biol. Soc. Wash.,* **76,** 191-6.

Loeblich, A. R. & Tappan, H. 1978. The coccolithophorid genus *Calcidiscus* Kamptner and its synonyms. *J. Paleontol.,* **52**(6), 1390-2.

Lohmann, H. 1902. Die Coccolithophoridae, eine Monographie der Coccolithen bildenden Flagellaten, zugleich ein Beitrag zur Kenntnis des Mittelmeerauftriebs. *Arch. Protistenk.,* **1,** 89-165.

MacLeod, C. J. 1988. Tectonic evolution of the Eastern Limassol Forest Complex, Cyprus. *Unpublished PhD. thesis,* Open University, 231pp.

Malpas, J. & Xenophontos, C. 1987. The Mamonia Complex and its relation to the Troodos ophiolite. *In*: Xenophontos, C. & Malpas, J. (eds), *Troodos 87 Ophiolites and Oceanic Lithosphere. Field Excursion Guidebook.* Cyprus Geol. Surv. Dept., 234-259.

Malpas, J., Xenophontos, C. & Williams, D. 1992. The Ayia Varvara Formation of SW Cyprus: a product of complex collisional tectonics. *Tectonophysics,* **212,** 193-211.

Malpas, J., Calon, T. & Squires, G. 1993. The development of a late Cretaceous microplate suture zone in SW Cyprus. *In*: Prichard, H. M., Alabaster, T., Harris, N. B. W. & Neary, C. R. (eds), *Magmatic Processes and Plate Tectonics,* Geol. Soc. Sp. Publ., **76,** 177-195.

Manivit, H., Perch-Nielsen, K., Prins, B. & Verbeek, J. W. 1977. Mid Cretaceous calcareous nannofossil biostratigraphy. *Kon. Nederl. Akad. Wet.*, B **80,** (3), 169-81.

Mantis, M. 1968, Subsurface biostratigraphy of Western Mesaoria, Cyprus: *Unpublished report,* Cyprus Geological Survey Department, 13p.

Mantis, M. 1970. Upper Cretaceous - Tertiary foraminiferal zones in Cyprus. *Sci. Res. Centry, Cyprus, Epithris.* **3,** 227-241.

Martini, E. 1961. Nannoplankton aus dem Tertiär und der obersten Kreide von SW-Frankreich. *Notizbl. Hess. Landesamt. Bodenforsch.*, **42,** 1-32.

Martini, E. 1969. Nannoplankton aus dem Miozän von Gabon (Westafrika). *Neues Jahrb. Geol. Palaeontol. Abhandlungen,* **132,** 285-300.

Martini, E. 1971. Standard Tertiary and Quaternary calcareous nannoplankton zonation. *In*: Farinacci A. (ed.), *Proceedings II Planktonic Conference, Roma,* 1970, **2,** 739-85.

Martini, E. & Bramlette, M. N. 1963. Calcareous nannoplankton from the experimental Mohole drilling. *J. Paleontol.*, **37,** 845-56.

Martini, E. & Ritzkowski, S. 1968. Die Grenze Eozän/Oligozön in der Typus-Region des Unteroligozäns (Helmstedt-Egeln-Latdorf). *Mem. Bur. Rech. Geol. Mineral.*, **69** (Colloque sur l' Eocene, Paris, mai 1968), 233-7.

Miller, P. 1981.Tertiary calcareous nannoplankton and benthic foraminifera biostratigraphy of the Point Arena area, California. *Micropaleontology,* **27** (4), 419-43.

Moores, E. M. & Vine, F. J. 1971. The Troodos massif, Cyprus and other ophiolites as oceanic crust: evaluation and implications. *Phil. Trans. Roy. Soc. Lond.*, **A268,** 443-466.

Moores, E. M., Robinson, P. T., Malpas, J. & Xenophontos, C. 1984. Model for the origin of the Troodos massif, Cyprus, and other mideast ophiolites. *Geology,* **12,** 500-503.

Morris, A., Creer, K. M. & Robertson, A. H. F. 1990. Palaeomagnetic evidence for clockwise rotation related to dextral shear along the Southern Troodos Transform Fault (Cyprus). *Earth Planet. Sci. Lett.*, **99,** 250-262.

Mukasa, S. B. & Ludden, J. N. 1987. Uranium-Lead ages of plagiogranite from the Troodos ophiolite, Cyprus, and their tectonic significance. *Geology,* **15,** 825-828.

Müller, C. 1970. Nannoplankton-Zonen der Unteren Meeresmolasse Bayerns. *Geol. Bavar.*, **63,** 107-18.

Murray, G. & Blackman, V. H. 1898. On the nature of the coccospheare and rhabdospheares. *Philos. Trans. R. Soc. London,* **190B**, 427-41.

Murton, B. J. 1986. Tectonic evolution of the western Limassol Forest Complex, Cyprus. *Unpublished PhD. thesis,* Open University, 332pp.

Murton, B. J. 1990. Was the Southern Troodos Transform Fault a victim of microplate rotation? *In*: Malpas, J., Moores, E. M., Panayiotou, A. & Xenophontos, C. *(eds) Ophiolites. Oceanic Crustal Analogues,* Proc. 'Troodos 87' Symposium. Cyprus Geol. Surv. Dept., 214-233.

Mutterlose, J. & Wise, S. W. 1990. Lower Creataceous nannofossil biostratigraphy of ODP Leg 113 Holes 692B and 693A, continental slope off east Antarctica, Weddell Sea. *Proc. Ocean Drilling Program, Scientific Results,* **113**, 325-352.

Noël, D. 1965. *Sur les coccolithes du Jurassique Européen et d' Afrique du Nord.* Centre Nat. Rech. Sc., 209pp.

Noël, D. 1970. *Coccolithes Crétacés. La Craie Campanienne du Bassin de Paris.* CNRS, Paris, 129pp.

Noël, D. 1973. Nannofossiles calcaires de sédiments jurassiques finement laminés. *Bull. Mus. natl. Hist. nat.*, ser. 3, **75,** 95-156.

Norris, R. E. 1965. Living cells of *Ceratolithus cristatus* (Coccolithophorineae). *Arch. Protistenk.*, **108,** 19-24.

Okada, H. & Bukry, D. 1980. Supplementary modification and Introduction of code numbers to low-latitude coccolith biostratigraphic zonation (Bukry 1973,1975) *Mar. Micropalaeont.*, **5,** 321-5.

Orszag-Sperber, F., Rouchy, J. M. & Elion, P. 1989. The sedimentary expression of regional tectonic events during the Miocene-Pliocene transition in southern Cyprus basins. *Geol. Mag.*, **129**(3), 291-299.

Pantazis, P. D. 1979. Geological map of Cyprus, Geological Survey Department, Nicosia, Cyprus.

Pantazis, Th. M. 1967. The geology and mineral resources of the Pharmakas-Kalavasos area. *Cyprus Geol. Surv. Mem.*, **8,** 190pp.

Pantazis, Th. M. 1978. Cyprus evaporites. *Initial Reports of the Deep Sea Drilling Project,* **42**(2), 1185-1194.

Pavsic, J. 1977. Nannoplankton from the Upper Cretaceous and Paleocene beds in the Gorica Region. *Geol. Razprave in Porocila*, **20**, 33-83.

Payne, A. S. & Robertson, A. H. F. 1995. Neogene supra-subduction zone extension in the Polis graben system, west Cyprus. *J. Geol. Soc. Lond.*, **152**(4), 613-628.

Pearce, J. A. 1975. Basalt geochemistry used to investigate past tectonic environments in Cyprus. *Tectonophysics*, **25**, 41-67.

Pearce, A. S. 1980. Geochemical evidence for the genesis and setting of lavas from Tethyan ophiolites. *In*: Panayiotou, A. (ed.) *Ophiolites: Proceedings of the International Symposium, Cyprus*, 1979. Cyprus Geological Survey Department, 261-272.

Perch-Nielsen, K. 1968. Der Feinbau und die Klassifikation der Coccolithen aus dem Maastrichtien von Dänmark. *K. Dan. Vidensk. Selsk. Biol. Skr.*, **16**(1), 1-96.

Perch-Nielsen, K. 1969. Die Coccolithen einiger danischer Maastrichtien- und Danienlokalitäten. *Bull. geol. Soc. Denmark*. **19**, 51-66.

Perch-Nielsen, K. 1971a. Neue Coccolithen aus dem Paläozän von Dänemark der Bucht von Biskaya und dem Eozän der Labrador See.. *Bull. geol. Soc. Denmark*, **21**, 51-66.

Perch-Nielsen, K. 1971b. Einige neue Coccolithen aus dem Paläozän der Bucht von Biskaya. *Bull. geol. Soc. Denmark*, **20**, 347-361.

Perch-Nielsen, K. 1971c. Elektronenmikroskopische Untersuchungen an Coccolithen und verwandten Formen aus dem Eozän von Dänemark. *Det Kongelige Danske Videnskabernes Selskab Biol. Skrifter*, **18**(3), 1-76.

Perch-Nielsen, K. 1977. Albian to Pleistocene calcareous nannofossils from the western South Atlantic. *Initial Rep. Deep Sea drill. Proj.*, **39**, 699-823.

Perch-Nielsen, K. 1979. Calcareous nannofossils from the Cretaceous between the North Sea and the Mediterranean. *IUGS Series A*, **6**, 223-72.

Perch-Nielsen, K. 1981. New Maastrichtian and Paleocene calcareous nannofossils from Africa, Denmark, the USA and the Atlantic, and some Paleocene lineages. *Eclog. geol. Helv.*, **74**(3), 831-63.

Perch-Nielsen, K. 1983. Recognition of Cretaceous stage boundaries by means of calcareous nannofossils. In: T. Birkelund, *et al.* (eds), *Symposium on Cretaceous Stage Boundaries, Copenhagen, Abstracts*, 152-6.

Perch-Nielsen, K. 1984. Validation of new combinations. *INA Newsletter*, **6**(1), 42-6.

Perch-Nielsen, K. 1985a. Mesozoic calcareous nannofossils, *In*: Bolli, H. M., Saunders, J. & Perch-Nielsen, K. (eds), *Plankton Stratigraphy*. Cambridge University Press, Cambridge, 329-427.

Perch-Nielsen, K. 1985b. Cenozoic calcareous nannofossils. *In*: Bolli, H. M., Saunders, J. & Perch-Nielsen, K. (eds), *Plankton Stratigraphy*. Cambridge University Press, Cambridge, 428-554.

Perch-Nielsen, K. 1986. New Mesozoic and Palaeogene calcareous nannofossils. *Eclog. geol. Helv.* **79**(3), 835-47.

Pessagno, E. A. 1963. Upper Cretaceous Radiolaria from Puerto Rico. *Micropaleontology*, **9**, 197-214.

Pessagno, E. A. 1976. *Radiolarian Zonation and Stratigraphy of the Upper Cretaceous Portion of the Great Valley Sequence, California Coast Ranges.* Micropaleontology. Special Publication no, 2, 95pp.

Petrushevskaya, M. G. & Kozlova, G. E. 1972. Rodiolaria: Leg 14, Deep Sea Drilling Project. *Initial Reports of the Deep Drilling Project*, **14**, 495-648.

Piveteau, J. 1952. *Traité de Paléontologie*, vol. 1 pp. 107-15. Masson Paris.

Poche, F. 1913. Das System der Protozoa. *Arch. Protistenk.*, **30**, 125-321.

Pospichal, J. J. and Wise, S. W. 1990a Calcareous nannofossils across the K/T boundary, ODP Hole 690C, Maud Rise, Weddell Sea. *Proc. Ocean Drilling Program, Scientific Results*, **113**, 515-532.

Prins, B. 1979. Notes on nannology - 1. *Clausicoccus*, a new genus of fossil coccolithophorids. *INA Newsletter*, **1**(1), N-2-N-4.

Radomski, A. 1968. Calcareous nannoplankton zones in Palaeogene of the western Polish Carpathians. *Rocz. Pol. Tow. geol.*, **38**, 545-605.

Reinhardt, P. 1964. Einige Kalkflagellaten-Gattungen (Coccolithophoriden, Coccolithineen) aus dem Mesozoikum Deutschlands. *Monatsber. Dt. Akad. Wiss Berlin*, **6**, 749 - 59.

Reinhardt, P. 1965. Neue Familien für fossile Kalkflagellaten (Coccolithophriden, Coccolithineen). *Monatsber. Dt. Akad. Wiss. Berlin*, **7**, 30-40.

Remond, S. 1986. Diversité des cumulates ophiolitques du Massif du Limassol Forest (Chypre). *Unpupl. 3ème cycle doctorate thesis*, Université de Nancy.

Resiwati, P. 1991. Upper Cretaceous calcareous nannofossils from Broken Ridge and Ninetyeast Ridge, Indian Ocean. *Proc. Ocean Drilling Program, Scientific Results*, **121,** 141-170.

Robertson, A. H. F. 1975. Cyprus umbers: basalt-sediment relationships on a Mesozoic ocean ridge. *J. Geol. Soc. Lond.* **131,** 511-531.

Robertson, A. H. F. 1976. Pelagic chalks and calciturbidites from the Lower Tertiary of the Troodos Massif, Cyprus. *J. Sediment. Petrol.*, **46**(4), 1007-1016.

Robertson, A. H. F. 1977a. Tertiary uplift history of the Troodos massif, Cyprus. *Geol. Soc. Amer. Bull.* **88,** 1763-1772.

Robertson, A. H. F. 1977b. The Kannaviou Formation, Cyprus: volcaniclastic sedimentation of a probable late Cretaceous volcanic arc. *J. Geol. Soc. Lond.*, **133,** 447-466.

Robertson, A. H. F. 1977c. The Moni Melange, Cyprus: an olistostrome formed at a destructive plate margin. *J. Geol. Soc. Lond.* **133,** 447-66.

Robertson, A. H. F. & Hudson, J. D. 1973. Cyprus umbers: chemical precipitates on a Tethyan ocean ridge. *Earth and Planetary Science Letters* **18**, 93-101.

Robertson, A. H. F. & Hudson, J. D. 1974. Pelagic sediments in the Cretaceous and Tertiary history of the Troodos Massif, Cyprus. *Spec. Publ. Intenat. Assoc. Sediment.* **1,** 403-436.

Robertson A. H. F. & Woodcock, N. H. 1979. Mamonia Complex, southwest Cyprus: evolution and emplacement of a Mesozoic continental margin. *Geol. Soc. Amer. Bull.*, **90,** 651-665.

Robertson, A. H. F. & Dixon, J. E. 1984. Aspects of the geological evolution of the Eastern Mediterranean. *In*: Dixon. J. E. & Robertson A. H. F. (eds), *The Geological Evolution of the Eastern Mediterranean.* Geol. Soc. Lond. Spec. Public **17,** 1-74.

Robertson, A. H. F. & Woodcock, N. H. 1985. Evidence for the emplacement directions of allochthonous rocks in southern Cyprus. In *Sixth Colloquium on Geology of the Aegean Region* (eds E. Izdar and E. Nakoman) PIRI REIS International Contribution Series, Publication no. 2.

Robertson, A. H. F. & Woodcock, N. H. 1986. The role of the Kyrenia Range Lineament, Cyprus, in geological evolution of the eastern Mediterranean area. *Phil. Trans. Royal Soc. Lond.*, **317,** 141-177.

Robertson, A. H. F. & Xenophontos, C. 1993. Development of concepts concerning the Troodos ophiolite and adjacent units in Cyprus. *In*: Prichard, H. M., Alabaster, T., Harris, N. B. W. & Neary, C. R. (eds), *Magmatic Processes and Plate Tectonics,* Geol. Soc. Sp. Publ., **76,** 85-119.

Robertson, A. H. F. & Grasso, M. 1995. Overview of the Late Tertiary-Recent tectonic and palaeo-environmental development of the Mediterranean region. *Terra Nova,* **7,** 114-127.

Robertson, A. H. F., Eaton, S., Follows, E. J. & Payne, A. S. 1995a. Depositional processes and basin analysis of Messinian evaporites in Cyprus. *Terra Nova,* **7,** 233-253.

Robertson, A. H. F., Kidd, R. B., Ivanov, M. K., Limonov, A. F., Woodside, J. M., Galindo-Zaldivar, J., Nieto, L. & The Shipboard Party of the 1993 'TTR-3' Cruise. 1995b. Eratosthenes Seamount: collisional processes in the eastern most Mediterranean in relation to the Plio-Quaternary uplift of southern Cyprus. *Terra Nova,* **7,** 254-264.

Robertson, A. H. F. & Shipboard Scientific Party. 1996a. Role of the Eratosthenes seamount in collisional processesin the eastern Mediterranean. *Proc. Ocean Drilling Program, Initial Reports,* **160,** 513-520.

Robertson, A. H. F. & Shipboard Scientific Party. 1996b. Tectonic Introduction. *Proc. Ocean Drilling Program, Initial Reports,* **160,** 5-19.

Romein, A. J. T. 1979. Lineages in early Paleogene calcareous nannoplankton. *Utrecht Micropalaeontol. Bull.,* **22,** 1-231.

Rood, A. P., Hay, W. W. & Barnard, T. 1971. Electron microscope studies of Oxford clay coccoliths. *Eclog. geol. Helv.,* **64**(2), 245-72.

Roth, P. H. 1970. Oligocene calcareous nannoplankton biostratigraphy. *Eclog. geol. Helv.,* **63,** 799-881.

Roth, P. H. 1973. Calcareous nannofossils - Leg 17, Deep Sea Drilling Project. *Initial Rep. Deep Sea drill. Proj.,* **17**, 695-795.

Roth, P. H. 1978. Cretaceous nannoplankton biostratigraphy and oceanography of the Northwestern Atlantic Ocean. *Initial Rep. Deep Sea drill. Proj.,* **44**, 731-59.

Roth, P. H. & Thierstein, H. R. 1972. Calcareous nannoplankton: Leg 14 of the DSDP. *Initial Rep. Deep Sea drill. Proj.,* **14,** 421-85.

Sanfilippo, A. & Riedel, W. R. 1985. Cretaceous radiolaria. *In*: Bolli, H. M, Saunders, J. & Perch-Nielsen, K. (eds), *Plankton Stratigraphy.* Cambridge University Press, Cambridge, 573-630.

Schiller, J. 1930. Coccolithineae. *In: Dr. L. Rabenhorst's Kryptogamen-Flora von Deutschland, Österreich und der Schweiz.*, vol. 10, part 2, pp. 89-267. Akad. Verlagsges., Leipzig.

Schwarz, E. H. L. 1894. Coccoliths. *Ann. Mag. Nat. Hist.*, ser. 6, **14,** 341-6.

Shelton, A. W. & Gass, I. G. 1980. Rotation of the Cyprus microplate. *In*: Panayiotou, A. (ed.), *Ophiolites, Proc. Inter. Oph. Symp.* Cyprus Geol. Surv. Dept., 61-65.

Shyu, J. P. & Müller, C. M. 1991. Calcareous nannofossil biostratigraphy of the Celebes and Sulu Seas. *Proc. Ocean Drilling Program, Scientific Results,* **124**, 133-158.

Siesser, W. G. 1993. Calcareous nannoplankton. In J. H. Lipps (ed.), *Fossil Prokaryotes and Protists,* 169-201, Blackwell Scientific Publications.

Siesser, W. G. & Bralower, T. J. 1992. Cenozoic calcareous nannofossil biostratigraphy on the Exmouth Plateau, eastern Indian Ocean, *Proc. Ocean Drilling Program, Scientific Results,* **122**, 601-632.

Sissingh, W. 1977. Biostratigraphy of Cretaceous calcareous nannoplankton. *Geol. Mijnbouw.*, **56**(1), 37-65.

Smewing, J. D., Simonian, K. O. & Gass, I. G. 1975. Metabasalts from the Troodos Massif Cyprus: genetic implications deduced from petrography and trace element geochemistry. *Contrib, Mineral. Petrol.*, **51,** 49-64.

Spaulding, S. 1991. Neogene nannofossil biostratigraphy of Site 723 through to 730, Oman continental margin, northwestern Arabian Sea. *Proc. Ocean Drilling Program, Scientific Results,* **117**, 5-36.

Spray, J. G. & Roddick, J. C. 1981. Evidence for Upper Cretaceous transform fault metamorphism in West Cyprus. *Earth Planet. Sci. Lett.*, **55,** 273-291.

Staerker, T. S. 1994. Calcareous nannofossil biostratigraphy: Evidence for thrust faulting and sediment mixing in the accretionary complex of the central New Hebrides Island arc. *Proc. Ocean Drilling Program, Scientific Results,* **134**, 179-246.

Steinmetz, J. & Stradner, H. 1984. Cenozoic calcareous nannofossils from Deep Sea Drilling Project Leg 75, Southeast Atlantic Ocean. *Initial Rep. Deep Sea drill. Proj.*, **75**, 671-753.

Stover, L. E. 1966. Cretaceous coccoliths and associated nannofossils from France and the Netherlands. *Micropaleontology,* **12**, 133-67.

Stradner, H. 1959. Die fossilen Discoasterden Österreichs. II. *Erdöl-Z.*, **75,** 472-88.

Stradner, H. 1961. Vorkommen von Nannofossilien im Mesozoikum und Alttertiär. *Erdöl-Z.*, **77**, 77-88.

Stradner, H. 1963. New contributions to Mesozoic stratigraphy by means of nannofossils. *Proceedings of the 6th World Petrol. congr. Sect.* 1, paper 4 (preprint), 1-16.

Stradner, H. & Adamiker, D. 1966. Nannofossilien aus Bohrkernen und ihre electronenmikroskopische Bearbeitung. *Erdoel-Erdgas Z.*, **82,** 330-41.

Stradner, H. & Edwards, A. R. 1968. Electron microscope studies on Upper Eocene coccoliths from Oamaru Diatomite, New Zealand. *Jahrab. geol. Bundesanst. (Wien)*, special volume **13,** 1-66.

Stradner, H. & Steinmetz, J. 1984. Cretaceous calcareous nannofossils from the Angola Basin, Deep Sea Drilling Project Site 530. *Initial Rep. Deep Sea drill. Proj.*, **75**, 565-649.

Sullivan, F. R. 1964. Lower Tertiary nannoplankton from the California Coast Ranges. I. Paleocene. *Univ. Calif. Publ. Geol. Sci.*, **44,** 163-227.

Swarbrick, R. E. 1979. The Sedimentology and Structure of S.W. Cyprus and its Relationship to the Troodos Complex. *Unpublished Ph.D. thesis,* University of Cambridge. 277pp.

Swarbrick, R. E. 1980. The Mamonia Complex of SW Cyprus: a Mesozoic continental margin and its relationship to the Troodos Complex. *In*: Panayiotou, A. (ed.), *Ophiolites, Proc. Inter. Oph. Symp.* Cyprus Geol. Surv. Dept., 86-92.

Swarbrick, R. E. 1993. Sinistral strike-slip tectonics in an ancient oceanic setting: the Mamonia Complex, southwest Cyprus. *J. Geol. Soc. Lond.*, **150**(2), 381-392.

Swarbrick, R. E. & Naylor, M. A. 1980. The Kathikas melange, S.W. Cyprus: late Cretaceous submarine debris flows. *Sedimentology* **27,** 63-78.

Swarbrick, R. E. & Robertson, A. H. F. 1980. Revised stratigraphy of the Mesozoic rocks of southern Cyprus. *Geol. Mag.*, **117,** 547-563.

Tan, S. H. 1927. Discoasteridae incertae sedis. *Proc. Sect. Sc. K. Akad. Wet. Amsterdam,* **30**, 411-19.

Taylor, R. 1982. Lower Cretaceous (Ryazanian to Albian) calcareous nannofossils. *In*: Lord A.R. (ed.), *A Stratigraphical Index of Calcareous Nannofossils,* British Micropalaeontological Society, Ellis Horwood Press, Chichester, 40-80.

Taylor, R. N., Murton, B. J. & Nesbitt, R. W. 1991. Chemical transects across intra-oceanic arcs: Implications for the tectonic setting of ophiolites. *In*: Parson, L. & Murton, B. J. (eds), *Ophiolites and their modern oceanic analogues.* Geol. Soc. Lond. Spec. paper, **60,** 117-132.

Thierstein, H. R. 1973. Lower Cretaceous calcareous nannoplankton biostratigraphy. *Abh. Geol. Bundesanst. (Wien),* **29**, 52pp.

Thierstein, H. R. 1974. Calcareous nannoplankton: Leg26, Deep Sea Drilling Project. *Initial Rep. Deep Sea drill. Proj.,* **26**, 619-67.

Thurow, J. 1991. Upper Cretaceous radiolarians from Cyprus - evidence for increased productivity during paleoceanographic events. *Abstracts volume, 6th meeting of the International Association of Radiolarlian Paleoontologists, Firenze 1991,* 81.

Turner, W. M. 1969. Geological map of the Polis-Kathikas area, Geological Survey Department, Nicosia, Cyprus.

Turner, W. M. 1971. Geology of the Polis-Kathikes area. *Unpublished Doctoral dissertation.* Univ. New Mexico, Albiquerque.

Turner, W. M. 1973. The Cyprian Gravity Nappe and the Autochthonous Basement of Cyprus. *In: Gravity and Tectonics.* John Wiley & Sons, New York, 287-301.

Urquhart, E. & Banner, F. T. 1994. Biostratigraphy of the supra-ophiolite sediments of the Troodos Massif, Cyprus: the Cretaceous Perapedhi, Kannaviou, Moni and Kathikas formations. *Geol. Mag.,* **131**(4), 499-518.

van Hinte, J. E. 1976. A Cretaceous time scale. *Bull. Am. Assoc. Petrol. Geol.,* **60,** 498-516.

Verbeek, J. W. 1977. Calcareous nannoplankton biostratigraphy of Middle and Upper Cretaceous deposits in Tunisia, Southern Spain and France. *Utrecht Micropaleontol. Bull.,* **16,** 1-157.

Vekshina, V. N. 1959. Coccolithophoridae of the Maastichtian deposits of the west Siberian lowlands. *SNIIGGIMS,* **2,** 56-77.

Wallich, G. C. 1877. Observations on the coccosphere. *Ann. Mag. nat. Hist.,* ser. 4, **16,** 322-39.

Weber-van Bosse, A. 1901. Etudes sur les Algues de l' Archipel Malaisien. *Ann. Jard. Bot. Buitenzorgg,* **17** [ser. 2.2], 126-41.

Wei, W. & Thierstein, H. R. 1991. Upper Cretaceous and Cenozoic calcareous nannofossils of the Kerguelen Plateau (south Indian Ocean) and Prydz Bay (East Antartica). *Proc. Ocean Drilling Program, Scientific Results,* **119**, 467-493.

Wei, W. & Wise, S. W. 1992. Selected Neogene calcareous nannofossil index taxa of the Southern Ocean: Biochronology, Biometrics and Paleooceanography. *Proc. Ocean Drilling Program, Scientific Results,* **120**, 509-522.

Wei, W. & Peleo-Alampay, A. 1993. Updated Cenozoic Nannofossil Magneto-biochronology. *INA Newsletter,* **15**(1), 15-17.

Weiler, Y. 1965. The folded Kytherea Flysch in Cyprus. *Unpublished PhD. thesis,* The Hebrew University of Jerusalem, 70pp.

Wilson, R. A. M. 1959. The geology of the Xeros-Troodos area. *Cyprus Geol. Surv. Mem.*, **1,** 135pp.

Wise, S. W. 1973. Calcareous nannofossils from cores recovered during Leg18, Deep Sea Drilling Project: biostratigraphy and observations on diagenesis. *Initial Rep. Deep Sea drill. Proj.*, **18,** 569-615.

Wise, S. W. & Wind, F. H. 1977. Mesozoic and Cenozoic calcareous nannofossils recovered by DSDP Leg 36 drilling on the Falkland Plateau, southwest Atlantic sector of the Southern Ocean. *Initial Rep. Deep Sea drill Proj.*, **36**, 269-292.

Xu, Y. & Wise, S. W. 1992. Middle Eocene to Miocene calcareous nannofossils of Leg 125 from the Western Pacific Ocean. *Proc. Ocean Drilling Program, Scientific Results,* **125**, 43-70.

Young, J. R., Bown, P. R. & Burnett, J. A. 1994. Palaeontological perspectives. *In:* Green, J. C. & Leadbeater, B. S. C. (eds), *The Haptophyte Algae,* The Systematics Association Special Volume, Oxford Science Press, Oxford, **51,** 379-392.

Zomenis, S. L. 1972. Stratigraphy and hydrogeology of the Neogene rocks in the northern foothills of the Troodos Massif. *Bull. Geol. Surv. Dep. Cyprus,* **5,** 22-90.

BIOSTRATIGRAPHICAL CONSTRAINTS (CALCAREOUS NANNOFOSSILS) ON THE LATE CRETACEOUS TO LATE MIOCENE EVOLUTION OF S. W. CYPRUS.

Trevor John Morse BSc. Hons (Dunelm)

(St. Cuthbert's Society)

PART II
APPENDICES

A thesis submitted in part fulfillment
of the requirements for the degree of
Doctor of Philosophy.

Department of Geological Sciences
University of Durham
AUGUST 1996

Contents

A. Sampling and Processing. 3.

B. Calcareous Nannofossil Identification Key to Family Level. 8.

C. Deep Sea Drilling Project and Ocean Drilling Project Chapters Relating to Calcareous Nannofossils. 63.

D. Calcareous Nannofossil Glossary. 75.

E. Sample Data. 79.

APPENDIX A

Sampling and Processing

Purpose of the Investigation

The unconformable contact between the neo-autochthonous calcareous sedimentary cover and the basement lithologies of the Mamonia and Troodos Complexes in S.W. Cyprus is poorly constrained and understood. It is thought to be diachronous or consisting of a number of unconformities between the Late Cretaceous and Late Pliocene, younging or overstepping on to the basement respectively in a north-westerly direction away from a ?depositional basin centred south of Perapedhi village.

To solve the problem, it was decided to collect as many samples as possible, of the sedimentary cover, with the main criteria being that they were collected as close to the contact with the basement, throughout S.W. Cyprus (See locality map, Appendix E, Fig. E.1) and not collected for their abundance or high diversity of calcareous nannofossils.

At several measured sections located in S.W. Cyprus, samples were collected to search for breaks in the sedimentary record. Measured sections were also provided by Dr. R. E. Swarbrick (Petra-tou-Romiou, S.W. Cyprus) and Dr. H. A. Armstrong (Kottaphi Hill, Agrokipia, northern flank of the Troodos Massif). These localities were chosen because they were considered to be free of tectonic breaks.

The samples collected were processed so that the calcareous nannofossil evidence could be released from the rock and be recognised via light and scanning electron microscopy. Then using species of known range, the samples could be dated, so that a pattern may be determined for S.W. Cyprus and if possible be related to the rest of Cyprus.

Fieldwork

The Late Cretaceous to Late Miocene succession of S.W. Cyprus, which makes contact with the basement, outcrops along the south-westerly flank of the Troodos Massif, at the edge of several basement windows and were major drainage cuts the landscape. Sampling of these outcrops was carried out over several field seasons: 1992 based at Mamonia (8 weeks); 1993 based at Polis (2 weeks) and 1994 based at Paphos (2 weeks).

The samples were collected as near as possible to the contact with the basement or the underlying calcareous lithological unit, where it was thought there might be a break in the sedimentary record. When contact was actually seen, a second sample was collected 0.5 or 1.0m above the contact. All samples collected were fresh with unweathered surfaces, each sample, were possible was fist-sized (100gms).

To avoid major contamination during the collecting stage, the hammer head and chisel point was cleaned prior to the taking of each sample. The sample was double bagged for shipment.

A total of 372 samples were collected and processed during the project and information concerning these samples can be found in Appendix E.

Preparation of the Study Material

During the course of the project, two disaggregation techniques were employed. The crushing technique which was primarily used for reconnaissance work and the solvent soak technique, both techniques released the calcareous nannofossils from the sample. The resulting material was then mounted so that the calcareous nannofossils could be viewed under Light and Scanning Electron Microscopy (LM and SEM respectively) conditions. Prior to disaggregation the sample was washed, so as to remove any possible contamination, that may have occurred during collecting in the field.

Crushing Technique

1). Using a spatula, break off a few small fragments from the washed sample, then using an pestle and mortar, grind the small fragments into a fine powder.

NB. To avoid contamination from previous samples, wash and dry the spatula, pestle and mortar prior to use.

2). Add the fine powder to a disposable vial, containing distilled water and agitate, allow the heavies to settle out (60-90secs).

3). Using a glass pipette, extract the supernatant and place into a second disposable vial, then add cellosize and agitate. The cellosize breaks down the surface tension of the fluid, so that it can be more easily worked when transferring to the coverslips.

NB. To avoid contamination when using the pipette, wash the pipette out three times using distilled water prior to use.

4). Fluid is now ready to be mounted onto coverslips.

Solvent Soak Technique

1). Take three large clean polythene sample bags and triple bag the washed sample (100gms). Using a hammer and crushing surface, crush the sample into large fragments.

2). Place the crushed material into a clean beaker, then remove half of the sample (50gms) and bag ready for further possible investigations.

NB. Contamination during the first two stages of the technique can be avoided by washing and drying crushing surfaces and hands prior to handling the sample.

3). Cover the remaining sample in the beaker with fresh solvent and allow to soak into the sample for 60-120mins. Cover beaker with glass plate.

4). After soaking, decant and filter the excess solvent (not to be reused in further calcareous nannofossil work) from the beaker, then pour boiling water over the sample half filling the beaker. The boiling water makes the solvent within the sample expand

faster than the resulting pressure can be released through the pore spaces, causing minute explosions, which breakdown the sample and release the calcareous nannofossils into the water, allow the heavies to settle.

NB. Sections three and four must be carried out in a fume cupboard.

5). Using a glass pipette, extract the supernatant from the beaker and place into a disposable vial, then add cellosize and agitate.

NB. To avoid contamination when using the pipette, wash the pipette out three times using distilled water prior to use.

6). Fluid is now ready to be mounted onto coverslips.

Mounting coverslip for LM Investigation

1). From either the crushing or solvent soak disaggregation techniques, transfer the resulting fluid from the vial using a glass pipette and cover three coverslips (32x22mm), leaving to dry on hot plate.

NB. To avoid contamination when using the pipette, wash the pipette out three times using distilled water prior to use.

2). Using Canada balsam take two of the coverslips and fix onto two glass slides, to make permanent mounts. The coverslips are now ready for examination under LM conditions.

NB. The remaining coverslip is stored in readiness for examination under SEM conditions.

Mounting coverslip for SEM Investigations.

Due to financial constraints, not all coverslips were mounted onto an SEM stub. Only after examination under Light Microscopy conditions had taken place, and the abundance (Abundant) and preservation (Good to Moderate) of calcareous nannofossils had been noted, would a coverslip (if required) be examined under SEM conditions.

Preservation

Good (Little or no alteration).
Moderate (50% showing some form of alteration).
Poor (All showing some form of alteration).**

Calcareous nannofossil content.
(Field of view = 390μm)

Abundant (> 5 individuals per field of view).
Common (< 5 individuals per field of view).**
Sparse (Isolated occurrences).**

**Not considered good enough for SEM Investigations.

The coverslip is glued to an aluminium SEM stub, using a colloidal silver type conducting adhesive which allows the transmission of electrons. The surfaces of the coverslip and stub are then coated in a thin layer of gold, to make the specimen conductive.

Methods of Investigation

Two methods of investigation were employed during the course of the project LM and SEM techniques.

LM Technique

For the recognition of calcareous nannofossil species via the LM, the Olympus BH-2 biological microscope, fitted with analyser and port for sensitive tint was employed (maximum magnification x1250). Also fitted was a micrometer stage allowing specimens to be relocated, phase contrast condenser with associated objectives and a trinocular viewing head that sits on the analyser housing, allowing photomicrographs to be taken via Olympus OM4Ti camera with spot metering.

Plane polarised light, crossed polarised light with sensitive tint availability and phase contrast, allowed the maximum amount of information to be obtained. So via the two LM slides produced from each sample processed, it was possible to identify species, note occurrence, distribution and calcareous nannofossil content for each sample.

SEM Technique

Due to the inability of the SEM at the University of Durham to provide publication quality photomicrographs during the early stages of the project, the SEM at the Biomedical Electron Microscope Unit, University of Newcastle was used. During this period costs were minimal, with photographic charges only. However, during the latter part of the project, new costing arrangements at the University of Newcastle came into effect, coupled with a worsening financial environment for Universities in general, plus a lack of additional funding from NERC to cover the new costs, the use of the SEM was kept to a minimum, with costs borne by the Department of Geological Sciences, University of Durham.

The SEM employed was a Cambridge 600 Stereoscan, fitted with a 35mm Pentax camera. The technique gives high definition images of calcareous nannofossils and photomicrographs which assist in describing the species under examination with the minimum of misinterpretation of the morphological features. It also provided the opportunity to gain experience in the operation of the microscope to operator level.

APPENDIX B

Calcareous Nannofossil Identification Key to Family Level

HARD COVER

CALCAREOUS NANNOFOSSILS

IDENTIFICATION KEY

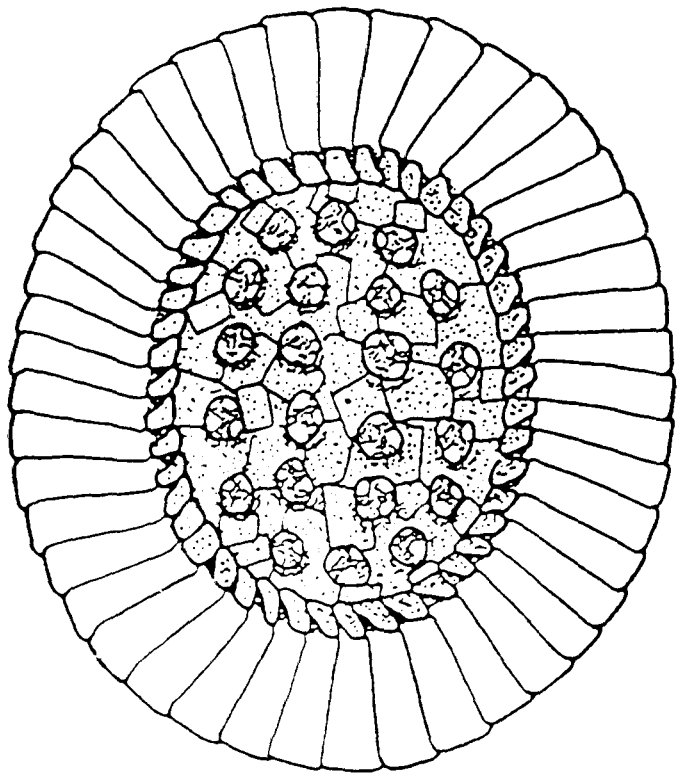

for use in

BIOSTRATIGRAPHY

T. J. MORSE BSc. HONS. (DUNELM)

DEPARTMENT OF GEOLOGICAL SCIENCES
UNIVERSITY OF DURHAM

APPENDIX B

CALCAREOUS NANNOFOSSIL

INDENTIFICATION KEY

for use in

BIOSTRATIGRAPHY

This appendix forms part of a thesis that
will be submitted in part fulfilment of
the requirements for the degree of
Doctor of Philosophy.

by

T. J. MORSE BSc. HONS. (DUNELM)
(ST. CUTHBERT'S SOCIETY)

DEPARTMENT OF GEOLOGICAL SCIENCES
UNIVERSITY OF DURHAM
AUGUST 1996

ACKNOWLEDGEMENTS

Thanks are given to the many researchers in the field of calcareous nannofossils and in particular to Drs. K. Perch-Nielsen and W. G. Siesser, whose work has formed the basis of this Identification Key.

The financial support by the Natural Environmental Research Council is acknowledged, with respect to the research studentship (GT4/91/GS/32). With reference to the project based in S.W. Cyprus titled; 'Biostratigraphical Constraints (calcareous nannofossils) on the Late Cretaceous to Late Miocene Geological Evolution of S.W. Cyprus'. The Identification Key forms part of the thesis as an appendix.

Special thanks are given to my supervisors Drs. R. E. Swarbrick and H. A. Armstrong for their assistance, patience and guidance throughout the length of the project.

Cover: Typical distal view of a coccolith, *Clausicoccus fenestratus* (modified after Prins, 1979).

CONTENTS

Introduction. 13.

First level search. 17.
Based on overall shape.

Second level search. 19.
Scanning Electron & Light Microscopy, based on distinguishing features.

Third level search. 26.
Detailed section in family alphabetical order.

Fourth level search. 57.
Calyptrosphaeraceae (holococcoliths of various constructions) and Incertae sedis.

Bibliography. 61.

ABBREVIATIONS

DSDP : Deep Sea Drilling Project.

K/T : Cretaceous/Tertiary Boundary.

LM : Light Microscopy.

ODP : Ocean Drilling Project.

SEM : Scanning Electron Microscopy.

INTRODUCTION

GENERAL INFORMATION

The calcareous nannofossil identification key for use in biostratigraphy, has been formulated to assist undergraduates and academics with little or no experience in identifying calcareous nannofossils. There are approximately 37 recognised calcareous nannofossil families, that are to varying degrees of suitability, biostratigraphically important (Perch-Nielsen, 1985 and Siesser, 1993). It is hoped that the identification key will assist the researcher in placing the specimen under examination into the correct family, in readiness for further identification to genus and species level.

The search pattern employed by the identification key is shown in Fig. B.1. This process takes the researcher through four levels of search, to identify the specimen under examination to family level. The first level of search is based on the overall shape, with the second level dealing with the distinguishing features. From the first and second levels of search, it should be possible to obtain a number of families that might make a near fit. All that remains, is to use the third level search section to make the final identification to family level. Within this section there are detailed descriptions of the 37 families, and it is in alphabetical order. If, after the first three levels of search, it has not been possible to make a satisfactory identification, a fourth level search section, covering the family **Calyptrosphaeraceae** (holococcoliths) and **Incertae sedis** can be utilised. It is worth noting at this point, that if there is difficulty in making a successful identification after use of the fourth level search section within the identification key, then it might be safe to assume that the specimen under examination is not biostratigraphically important, and that no further time should be taken up in attempting to identify the specimen.

Direction is given within the third level search section, for the identification of the specimen under examination to genus and species level, by making reference to page numbers from chapters 10 & 11 from the publication 'Plankton Stratigraphy' (Perch-Nielsen, 1985).

With reference to calcareous nannofossils, the publications 'Fossil Prokaryotes and Protists' (Siesser, 1993) and 'Plankton Stratigraphy' (Perch-Nielsen, 1985) make reference to many scientific papers, broad based publications and DSDP/ODP reports, which will further assist in making the identification to species level.

Fig. B.2. shows the range of the 37 calcareous nannofossil families mentioned in the identification key (Late Triassic to Holocene). If an approximate geological age is known of the horizon from which the specimen under examination has been extracted, it is possible to narrow the search to either side of the K/T extinction boundary event. Therefore some of the first and second level search figures have been ordered into Mesozoic, K/T (this includes families which exist either side of the boundary) and Cenozoic sections.

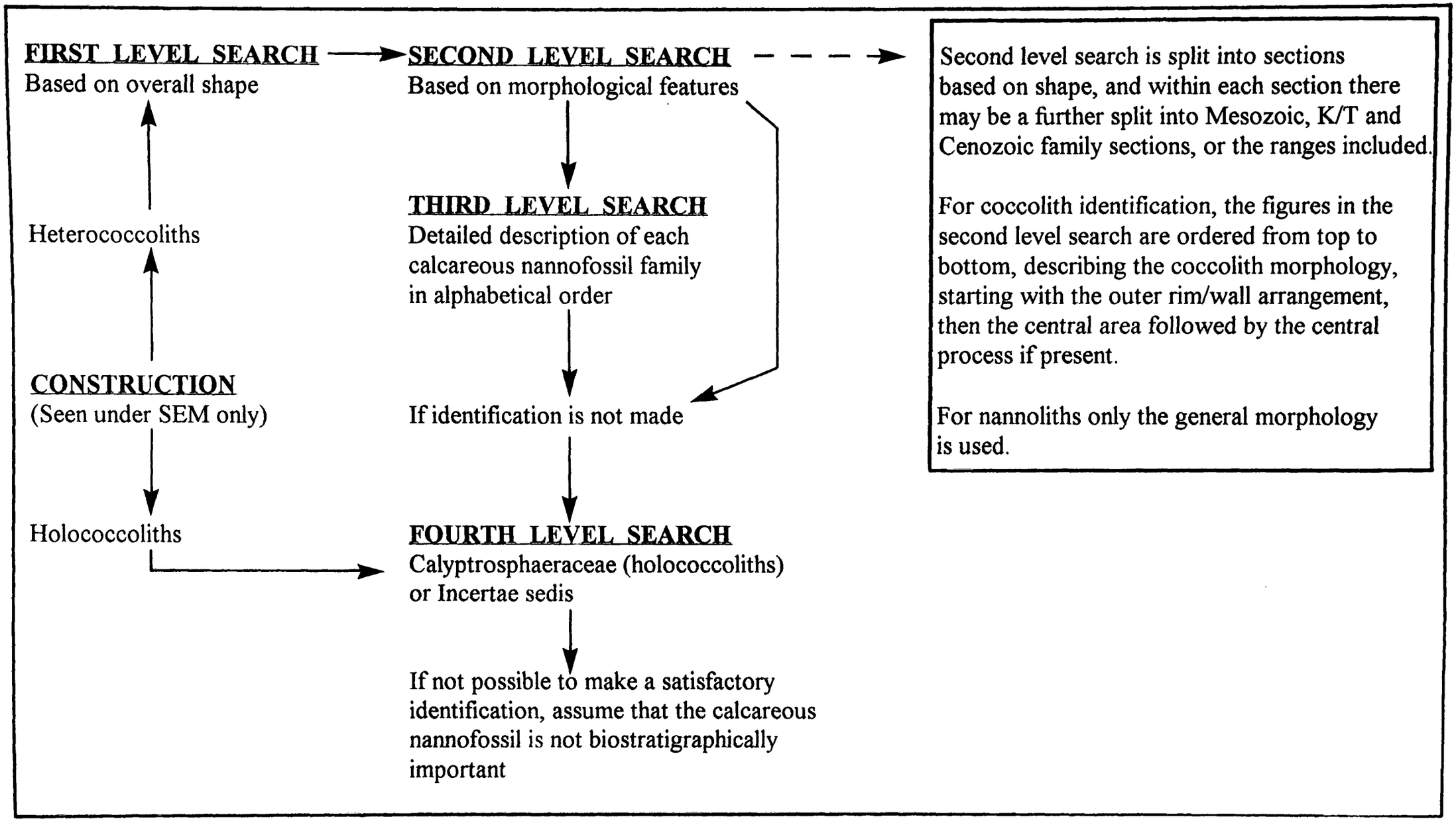

Fig. B.1. Search pattern employed within the Identification Key.

DISSOLUTION, OVERGROWTHS, DAMAGE and DEBRIS

It is important that the researcher should be aware that dissolution, overgrowths, damage and debris might have taken place and this will hinder the successful identification of the calcareous nannofossil under examination. Where possible whole and clean specimens in good condition should be used.

DERIVED, REWORKED and CAVING

Due to their size (<30μm), derived, reworked and caving within samples is a major problem with respect to calcareous nannofossil studies and the researcher should always be aware that the these major problems exist. This may cause inexperienced researchers to wrongly date the horizon under investigation.

FAMILY	Mesozoic									Palaeogene									Neogene						Quat.	
	Triassic			Jurassic			Cret.			Palaeo.			Eo.			Oligo.			Mio.			Plio.			Pl.	R.
	L	M	U	L	M	U	L	M	U	L	M	U	L	M	U	L	M	U	L	M	U	L	M	U		
Schizosphaerellaceae			X	X	X	X																				
Chiastozygaceae			X	X	X	X	X	X	X	X	X															
Calyculaceae				X	X	X																				
Podorhabdaceae				X	X	X	X	X	X																	
Stephenolithiaceae				X	X	X	X	X	X																	
Crepidolithaceae				X	X	X	X	X	X																	
Arkhangelskiellaceae				X	X	X	X	X	X																	
Ahmuellerellaceae				X	X	X	X	X	X																	
Biscutaceae				X	X	X	X	X	X	X																
Ellipsogelosphaeraceae				X	X	X	X	X	X	X																
Sollasitaceae				X	X	X	X	X	X	X	X															
Zygodiscaceae				X	X	X	X	X	X	X	X	X	X	X	X	X											
Nannoconaceae						X	X	X	X																	
Microrhabdulaceae						X	X	X	X																	
Calyptrosphaeraceae						X	X	X	X	X	X	X	X	X	X	X	X	X	X	X	X	X	X	X	X	X
Thoracosphaeraceae						X	X	X	X	X	X	X	X	X	X	X	X	X	X	X	X	X	X	X	X	X
Prediscosphaeraceae							X	X	X																	
Polycyclolithaceae							X	X	X																	
Rhagodiscaceae							X	X	X																	
Braarudosphaeraceae							X	X	X	X	X	X	X	X	X	X	X	X	X	X	X	X	X	X	X	X
Calciosoleniaceae							X	X	X	X	X	X	X	X	X	X	X	X	X	X	X	X	X	X	X	X
Eiffellithaceae								X	X																	
Goniolithaceae									X	X	X	X	X	X	X											
Coccolithaceae									X	X	X	X	X	X	X	X	X	X	X	X	X	X	X	X	X	X
Prinsiaceae									X	X	X	X	X	X	X	X	X	X	X	X	X	X	X	X	X	X
Pontosphaeraceae										X	X	X	X	X	X	X	X	X	X	X	X	X	X	X	X	X
Fasciculithaceae											X	X														
Heliolithaceae											X	X														
Discoasteraceae											X	X	X	X	X	X	X	X	X	X	X	X	X	X		
Sphenolithaceae											X	X	X	X	X	X	X	X	X	X	X	X	X	X		
Lithostromationaceae													X	X	X	X	X	X	X	X	X	X	X	X		
Helicosphaeraceae													X	X	X	X	X	X	X	X	X	X	X	X	X	X
Rhabdosphaeraceae													X	X	X	X	X	X	X	X	X	X	X	X	X	X
Triquetrorhabdulaceae														X	X	X	X	X	X	X	X					
Ceratolithaceae																		X	X	X	X	X	X	X	X	X
Syracosphaeraceae																		X	X	X	X	X	X	X	X	X
Deutschlandiaceae																						X	X	X	X	X

Fig. B.2. Ranges for the calcareous nannofossil families.

CONTAMINATION

Contamination is a separate problem to those mentioned above in the last section, but giving similar results. However, care taken during the collecting and processing stages can minimise its effects.

CONSTRUCTION

Calcareous nannofossils are generally divided into two groups based on their calcite construction, holococcoliths and heterococcoliths. Holococcoliths are constructed with calcite crystals of identical size and shape, whereas heterococcoliths are constructed with calcite crystals of differing shapes and sizes. It is easy to distinguish between the two under the SEM and for the holococcoliths (Fig. B.1), to be routed to the fourth level of search section. However, under the LM this is not possible and therefore the route to identification for holococcoliths, is the same as the heterococcoliths.

DIMORPHIC, DITHECATISM and PLEOMORPHIC

There are several miscellaneous problems which are defined below, but do not pose any biostratigraphical problems.

Dimorphic: possessing more than one kind of calcareous nannofossil shape.

Dithecatism: constructed of a double layer of coccoliths, each layer may contain different calcareous nannofossil shape.

Pleomorphic: calcareous nannofossil having both a holococcolith and heterococcolith stage throughout its life cycle.

NOTE

It is not the intention of the identification key to address any of the problems mentioned above, but merely to make the inexperienced researcher aware that they exist and that they will have to be addressed, if encountered during the course of their studies.

FIRST LEVEL SEARCH

(Based on overall shape)

FIRST LEVEL SEARCH (SHAPE)	SECOND LEVEL SEARCH fig.	THIRD LEVEL SEARCH FAMILY	REMARKS
ELLIPTICAL	B.5		
CIRCULAR	B.6		
SPHERICAL/OVOID	B.7		
ROD/SPINDLE	B.8		
CYLINDER	B.9		
CONE	B.10		
HELICAL/SPIRAL		Helicosphaeraceae	
PENTAGONAL		Braarudosphaeraceae	Central area nongranulated - made up of five plates
		Goniolithaceae	Central area granulated
HEXAGONAL		Lithostromationaceae	
TRIANGULAR		Lithostromationaceae	
RHOMBOIDAL		Calciosoleniaceae	
BLOCK		Polycyclolithaceae	Mesozoic species
		Sphenolithaceae	Cenozoic species
BASKET		Discoasteraceae	
HORSESHOE		Ceratolithaceae	
POLYGONAL		Stephenolithaceae	
VASE		Calyculaceae	Mesozoic species
		Pontosphaeraceae	Cenozoic species
ROETTE/STAR		Polycyclolithaceae	Mesozoic species
		Discoasteraceae	Cenozoic species

Fig. B.3. Primary search based on overall shape.

SECOND LEVEL SEARCH

SCANNING ELECTRON & LIGHT

MICROSCOPY

(Distinguishing Features)

NB.

Figure B.4. will assist in identification.

If identification is not made within this section, go to the Fourth Level Search section which includes the family Calyptrosphaeraceae and Incertae sedis.

RIM/OUTER WALL CONSTRUCTION

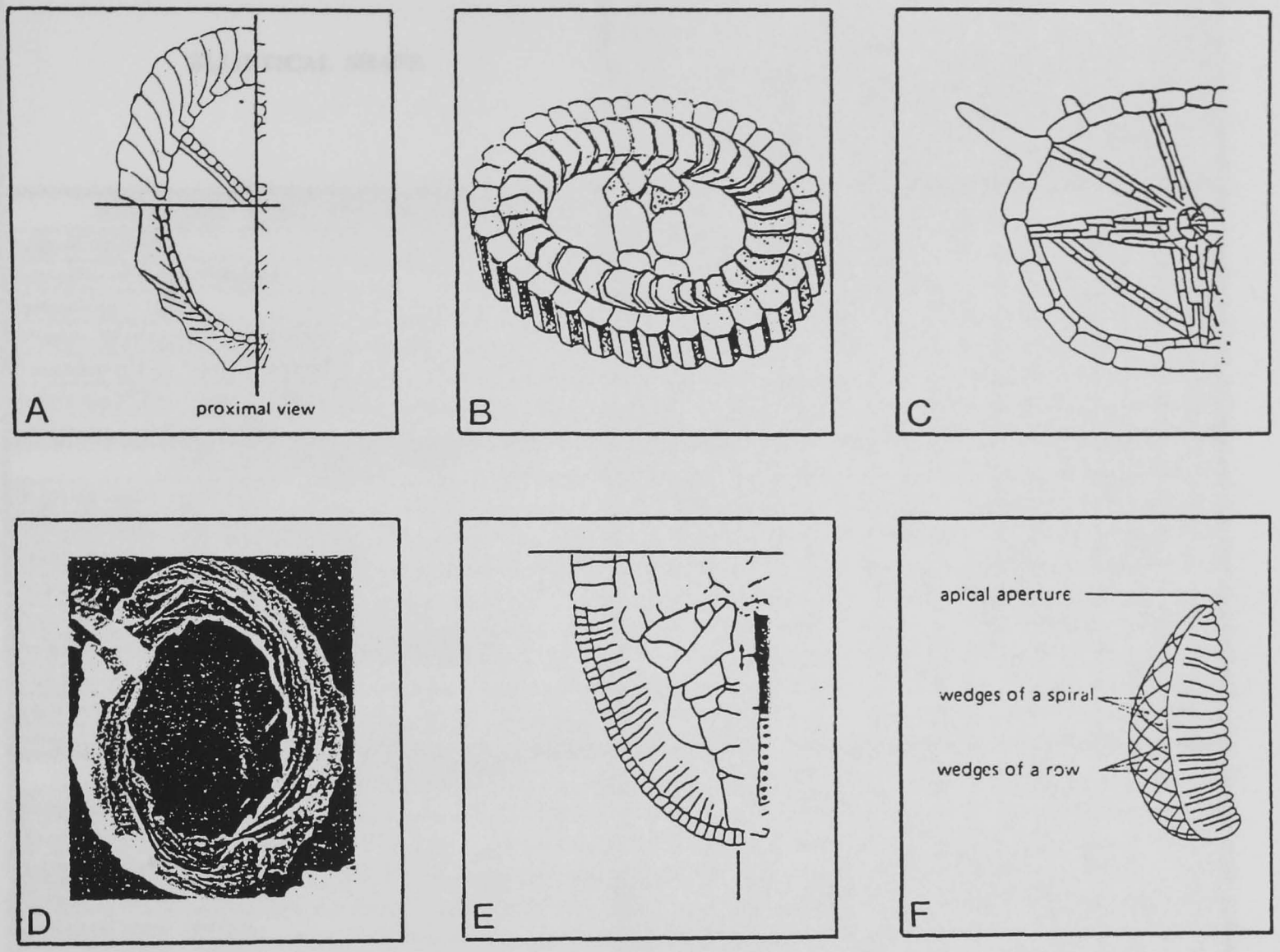

SHIELD CONSTRUCTION

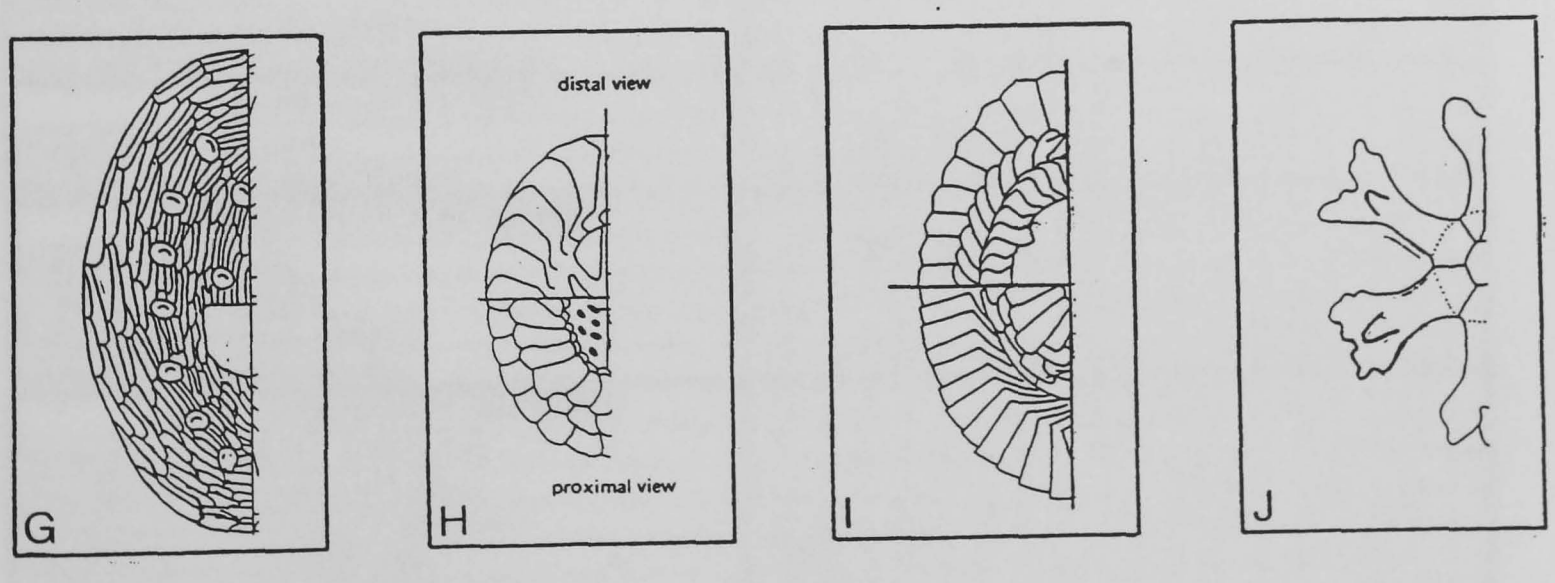

Fig. B.4. Sketches showing the typical types of rim/outer wall and shield constructions, with respect to the descriptive terms used in Figs B.5. and B.6. (modified from Perch-Nielsen, 1985a,b). **A.** inclined elements. **B.** vertically arranged elements. **C.** narrow rim. **D.** complex. **E.** tiers. **F.** wedge type plates. **G.** concentrically arranged elements. **H.** radiating petaloid elements. **I.** overlapping petaloid elements. **J.** rays.

ELLIPTICAL SHAPE	MESOZOIC									K/T						CENO.			
	Ahmuellerellaceae	Arkhangelskiellaceae	Calyculaceae	Crepidolithaceae	Eiffellithaceae	Podorhabdaceae	Prediscosphaeraceae	Rhagodiscaceae	Stephanolithiaceae	Biscutaceae	Chiastozygaceae	Coccolithaceae	Ellipsogelosphaeraceae	Sollasitaceae	Zygodiscaceae	Pontosphaeraceae	Prinsiaceae	Rhabdosphaeraceae	Syracosphaeraceae
RIM/OUTER WALL CONSTRUCTION																			
Inclined elements.	X				X			X			X				X				
Vertically arranged elements.			X						X										X
Narrow rim (<1 µm).	X	X	X		X	X	X	X	X		X				X				X
Complex arrangement of elements.																			X
Consisting of 3 to 5 tiers of elements.		X																	
Consisting of 2 to 3 tiers of elements.						X													
Containing 2 cycles of elements.																X			
SHIELD CONSTRUCTION																			
Distal elements, concentric.																X			
Distal elements, radiating petaloid.										X		X		X				X	
Distal elements, overlapping petaloid.													X				X		
Proximal elements, radiating petaloid.										X			X			X			
Proximal elements, overlapping petaloid.												X		X			X		
Proximal shield noticeably smaller than distal shield.												X							
2 closely appressed shields.										X									
Inner cycle of plate elements.					X														
Ring of calcite sectors without imbrication.				X															
CENTRAL AREA CONSTRUCTION																			
Bridging crossbar 'I' present.															X				
Bridging crossbars 'H' present.											X				X				
Bridging crossbars 'X' present.					X		X				X				X				
Bridging crossbars '+' present.	X				X		X												
Grid/mesh work covering.			X											X			X		
Granular surface covering.								X						X					
Perforations/holes.																X	X		
Thinned by depressions.																X			
Spanned by radially arranged elements.									X										
Several cycles of elements.																		X	
Partial cover of plates in distal view.																	X		
Closed with no process.		X																	
Partially closed by lath-shaped elements.																			X
Large central area (>75% of total surface area).						X								X		X			
CENTRAL STRUCTURE																			
Process present (if attached).				X		X												X	
May have a process (if present/attached).					X		X	X	X										X
MISCELLANEOUS FEATURES																			
Relatively thick (>3µm).				X															
16 elements in both shields.							X												
Radial spines may project from rim.									X										
Lacking a floor (open central area).															X				
LIGHT MICROSCOPY FEATURES																			
Whole of specimen has poor birefringence.										X									
Distal shield only, has poor birefringence.												X							
Dextrogyre interference figure in distal view.																	X		
Central area shows a 'windmill' effect.		X																	
Due to thickness, not all of specimen in focus.			X																

Fig. B.5. Distinguishing features of elliptical-shaped calcareous nannofossils.

CIRCULAR SHAPE	MESOZOIC					K/T			CENOZOIC					
	Calyculaceae	Crepidolithaceae	Nannoconaceae	Prediscosphaeraceae	Stephenolithiaceae	Biscutaceae	Coccolithaceae	Ellipsogelosphaeraceae	Deutschlandiaceae	Discoasteraceae	Heliolithaceae	Lithostromationaceae	Prinsiaceae	Rhabdosphaeraceae
RIM/OUTER WALL CONSTRUCTION														
Vertically arranged elements.	X				X									
Narrow rim (<1μm).	X			X	X									
Wedges/plates oriented perpendicular to axis.			X											
Wedges/plates spiral around axis.			X											
SHIELD CONSTRUCTION														
Distal elements, radiating petaloid.						X	X							X
Distal elements, overlapping petaloid.								X					X	
Proximal elements, radiating petaloid.						X		X						
Proximal elements, overlapping petaloid.							X						X	
Proximal shield noticeably smaller than the distal shield.							X							
3 closely appressed shields.											X			
2 closely appressed shields.						X					X			
Single shield made up of rays.									X	X				
Shields made up of thin elements.											X			
Ring of calcite sectors without imbrication.		X												
CENTRAL AREA CONSTRUCTION														
Bridging structure 'x' present.				X										
Bridging structure '+' present.				X										
Grid/mesh work present.	X												X	
Perforations/holes present.													X	
Spanned by radially arranged elements.					X									
Several cycles of elements.														X
Partial cover of plates in distal view.													X	
Inner cycle of elements.									X					
Symmetrically arranged depressions.												X		
Arrangement of ridges may be present.												X		
CENTRAL STRUCTURE														
Process present (if attached).		X												X
May have a process (if present/attached).				X	X									
Proximal knob may be present.										X				
Distal knob may be present.										X				
Cone will be present.									X					
Central cavity/canal present.			X											
MISCELLANEOUS FEATURES														
Relatively thick (>3μm).		X									X			
16 elements in both shields.				X										
Radial spines may project from rim.					X									
Shape due to dissolution.										X		X		
Can be relatively large (<30μm).			X									X		
LIGHT MICROSCOPY FEATURES														
Whole specimen has poor birefringence.						X								
Distal shield only, has poor birefringence.							X							
Dextrogyre interference figure in distal view.													X	
Due to thickness, not all of specimen in focus.	X											X		

Fig. B.6. Distinguishing features of circular-shaped calcareous nannofossils.

SPHERICAL/OVOID SHAPE	Schizosphaerellaceae	Thoracosphaeraceae	*Coccolithophores
OVERALL SHAPE			
Generally sub-spherical in shape.	X		
More spherical/ellipsoid in shape.		X	
Relatively large (>20μm).		X	X
Over-lapping/interlocking hemispheres.	X		
Bell- or cup-like in shape.	X		
MISCELLANEOUS FEATURES			
Large opening at the pole may be present.		X	
Lid may be present, covering the opening.		X	
Sub-peripheral groove.	X		
One or more keels may be present.		X	
External spines may be present.		X	
*Covered in shields (elliptical/circular).			X
RANGE			
Late Triassic to Late Jurassic.	X		
Late Jurassic to present day.		X	
LIGHT MICROSCOPY FEATURES			
Due to thickness, not all of specimen in focus.		X	X

* Return to second level search and make identification using a single shield

Fig. B.7. Distinguishing features of spherical/ovoid-shaped calcareous nannofossils, including range.

ROD/SPINDLE SHAPE	Microrhabdulaceae	Prediscosphaeraceae	Rhabdosphaeraceae	Triquetrorhabdulaceae
ONCE PART OF CENTRAL STRUCTURE				
Central process has separated from shield.		X	X	
Generally bulbous at distal end.			X	
At least one end may appear damaged.		X	X	
STRUCTURAL ARRANGEMENT				
Three concave blades.				X
Uniform arrangement about a central axis.	X	X	X	
Not uniform along length.			X	
Cruciform cross-section.	X			
Triradial cross-section.				X
MISCELLANEOUS FEATURES				
Ridges may be present on blade surfaces.				X
Simple arrangement of elements.	X			X
Complex arrangement of elements.		X	X	
RANGE				
Late Jurassic to Late Cretaceous.	X			
Early to Late Cretaceous.		X		
Early Eocene to present day.			X	
Middle Eocene to Late Miocene.				X
LIGHT MICROSCOPY FEATURES				
Central canal may be present.	X		X	
Complex extinction lines visible.		X		

Fig. B.8. Distinguishing features of rod/spindle-shaped calcareous nannofossils, including range.

CYLINDRICAL SHAPE	Calyculaceae	Crepidolithaceae	Microrhabdulaceae	Nannoconaceae	Polycyclolithaceae	Fasciculithaceae	Heliolithaceae
OVERALL SHAPE							
More squat than cylindrical.					X		X
Can be relatively large (<30µm).				X			
In side view only.	X						X
Could be described as a vase-like shape.	X						
Slightly tapered sides.		X					
Tapered sides.	X						
OUTER WALL							
Vertically arranged elements.			X				X
Vertical to slightly imbricated elements.					X		
Outer layer with vertically arranged thin elements.		X					
Wedges/plates orientated perpendicular to axial cavity.				X			
Wedges/plates spiral around the axial cavity.				X			
Ring of calcite sectors without imbrication.		X					
Distal cone or dome present.						X	
Disc of lateral elements may be present.						X	
Two to three cycles of elements.							X
Proximal column present.						X	
MISCELLANEOUS FEATURES							
Inner cycle of inclined elements.		X					
Axial cavity/canal present.				X			
Simple arrangement of elements.			X				
Lip may be present.	X						
RANGE							
Jurassic only.	X						
Jurassic to Late Cretaceous.		X	X	X			
Cretaceous only.					X		
Palaeocene only.						X	X
LIGHT MICROSCOPY FEATURES							
Due to thickness, not all of specimen in focus.	X	X					
Central canal may be visible.			X			X	

Fig. B.9. Distinguishing features of cylindrical-shaped calcareous nannofossils, including range.

CONE SHAPE	Nannoconaceae	Fasciculithaceae	Sphenolithaceae
GENERAL CONSTRUCTION			
Can be relatively large (<30μm).	X		
Wedges/plates orientated perpendicular to axial cavity.	X		
Wedges/plates spiral around the axial cavity.	X		
Distal cone present.		X	
Proximal shield of vertical elements.			X
Proximal column present.		X	
MISCELLANEOUS FEATURES			
Axial cavity/central canal present.	X		
Disc of lateral elements may be present.		X	X
Apical spine may be present.			X
RANGE			
Late Jurassic to Late Cretaceous.	X		
Palaeocene only.		X	
Middle Palaeocene to Upper Pliocene.			X
LIGHT MICROSCOPY FEATURES			
Central canal may be visible (median line).		X	X
Crucifix extinction line may be present.			X
'X' or '+' extinction line may be present.			X

Fig. B.10. Distinguishing features of cone-shaped calcareous nannofossils, including range.

THIRD LEVEL SEARCH

This section contains a detailed description of each calcareous nannofossil family in alphabetical order. However, if there is not a description that fits and therefore identification cannot be made within this section, go to the Fourth Level Search section which includes the family Calyptrosphaeraceae and Incertae sedis.

The page number is given for the publication 'Plankton Stratigraphy' (Perch-Nielsen, 1985) to aid possible identification to genus and species level.

SEM & LM distinguishing features is a breakdown of the initial overall description, to assist in making a correct identification.

Figures within this section are not intended to imply genera or species within a particular family, but to give an idea of shape and construction to aid with identification. Also scale is not shown. However, it can be assumed that size of the long axis does not exceed 15µm - remember there will be exceptions.

With reference to 'Shape', there will be at least one and may be more overall descriptive shapes mentioned. This indicates that the family is mentioned under that shape within the First or Second Level Search sections.

Additional information relating to the families biostratigraphical range and its importance to biostratigraphy is given.

Ahmuellerellaceae

Reinhardt (1965)

Description : The Ahmuellerellaceae include elliptical coccoliths, in which the narrow rim is formed by a wall of inclined elements, with the central area bridged by a cross (+) aligned with the axis of the ellipse or of composite construction (Fig. B.11).

Plankton Stratigraphy : page 349.

SEM Distinguishing features :
*elliptical.
*narrow wall/rim of inclined elements.
*central area bridged by a cross (+), aligned with the axis of the ellipse or of composite construction.

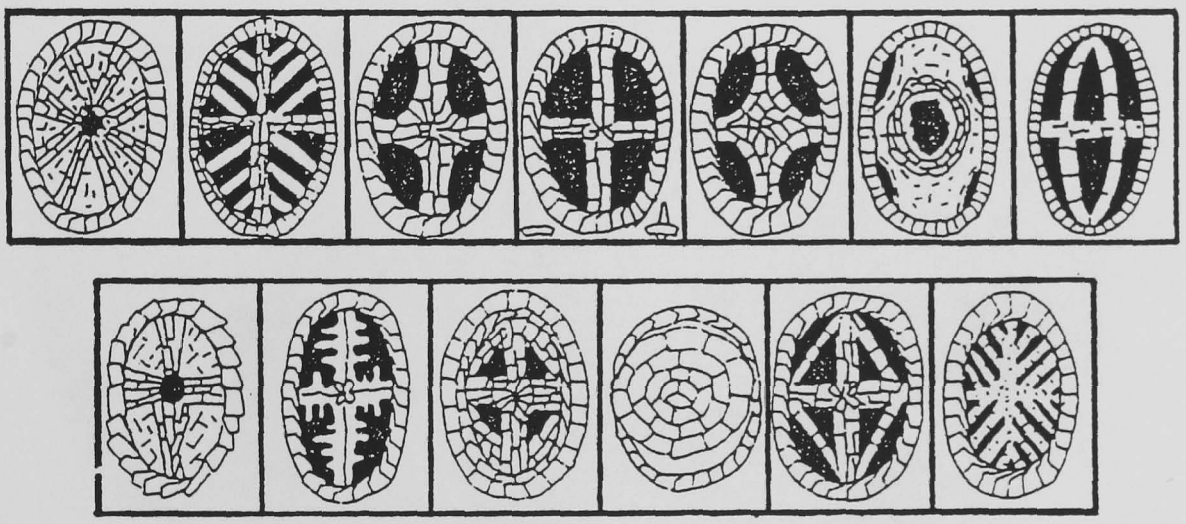

Fig. B.11. Typical Ahmuellerellace structural arrangements (modified from Perch-Nielsen, 1985a).

LM Distinguishing features : *similar to that seen under SEM conditions. However, it may be not possible to distinguish the inclined nature of wall/rim elements.

Shape : ELLIPTICAL

Range : Early Jurassic to Late Cretaceous.

Biostatigraphical : poor to moderate.

Arkhangelskiellaceae

Bukry (1969)

Description : The Arkhangelskiellaceae include elliptical coccoliths with a complex narrow rim consisting of 3 to 5 tiers. Two are visible in distal view with two to four being visible in

proximal view. The central area generally being enclosed by a variety of constructions, lacking a central process (Fig. B.12).

Plankton Stratigraphy : page 352.

SEM Distinguishing features :
*elliptical.
*narrow rim consisting of three to five tiers,
- two to four visible from proximal view,
- two visible from distal view.
*lacks a central process.
*central area closed with a few exceptions.

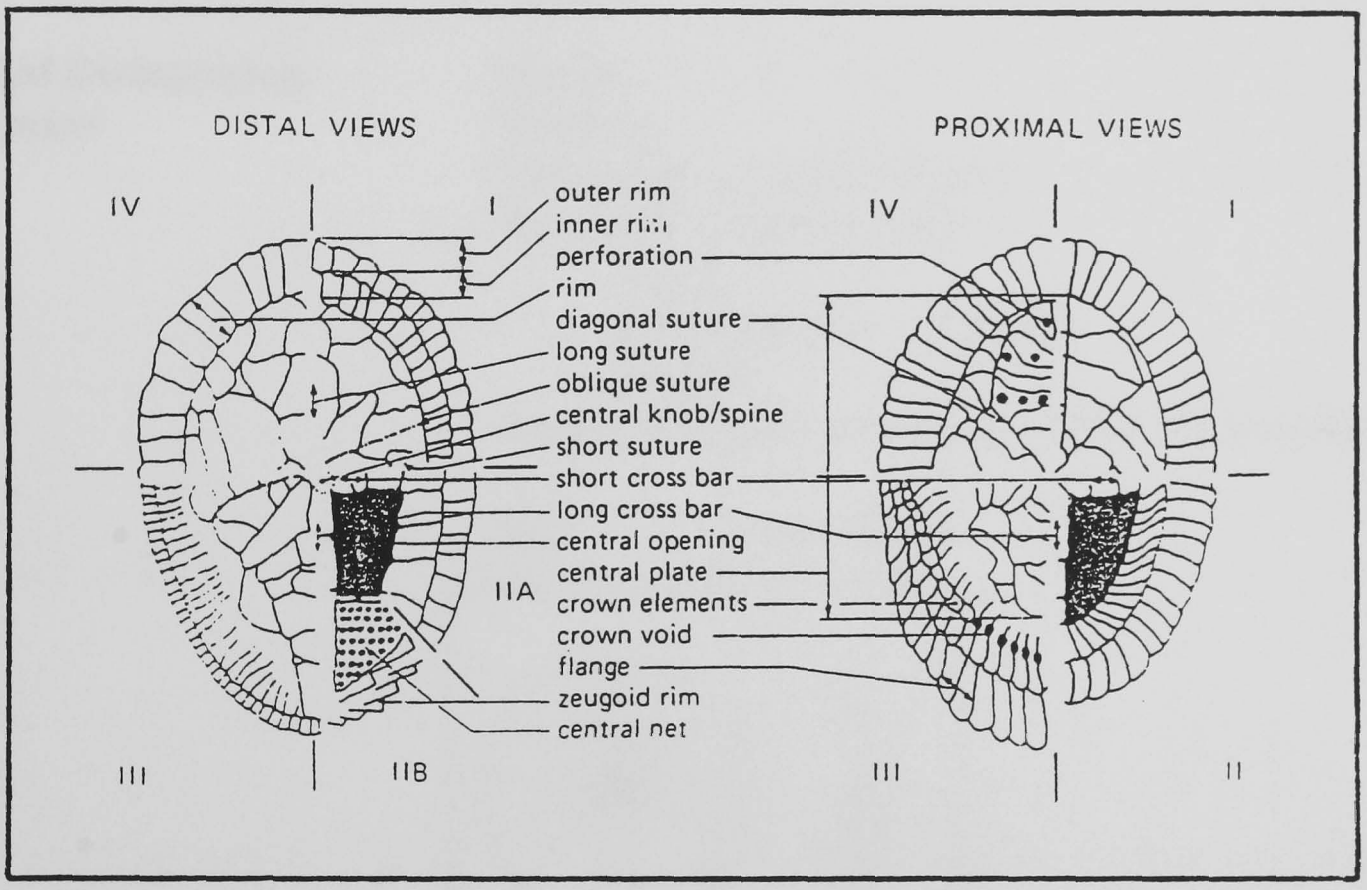

Fig. B.12. Terminology of the Arkhangelskiellaceae (after Perch-Nielsen, 1985a)

LM Distinguishing features :
*elliptical.
*narrow rim
*enclosed central area shows up as four equal quadrants with the cross (+) aligned to the axis of the ellipse, each quadrant is further divided in two, which are displayed by alternating good and poor birefringence to produce a 'windmill' effect.
*lacks a central process.
*central area closed with a few exceptions.

Shape : ELLIPTICAL

Range : Early to Late Cretaceous.

Biostratigraphical : moderate.

Biscutaceae

Black (1971)

Description : The Biscutaceae contain both circular and elliptical coccoliths and are constructed of two closely appressed shields. These are formed of radial, non-imbricate and petaloid elements. Both shields usually remain dark between crossed polars, with the central area sometimes birefringent. Central process may be present, attached to the distal surface (Fig. B.13).

Plankton Stratigraphy : page 356.

SEM Distinguishing features :

*circular.
*elliptical.
*two closely appressed shields.
*each shield constructed of:-
radial)
non-imbricated) elements.
petaloid)
*variety of crystal constructions within the central area.

distal cross-section

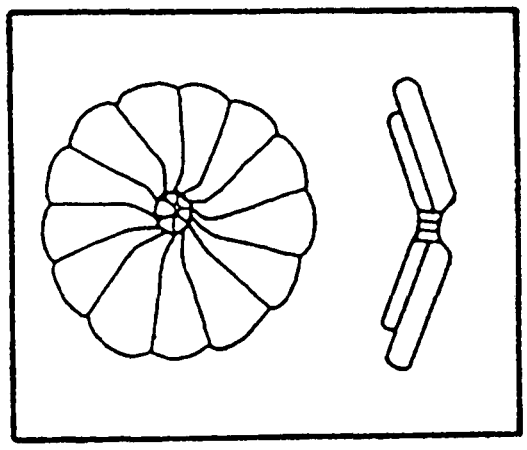

Fig. B.13. *Biscutum*, typical genus of Biscutaceae showing structural arrangement (after Reinhardt, 1965).

LM Distinguishing features : *similar to that seen under SEM conditions. However, it may not be possible to note the appressed nature of the distal and proximal shields.
*poor birefringence.

Shape : ELLIPTICAL & CIRCULAR

Range : Early Jurassic to Early Palaeocene.

Biostratigraphical : poor to moderate.

Braarudosphaeraceae

Deflandre (1947)

Description : The Braarudosphaeraceae include pentolith-shaped nannoliths, normally made up of five equal segments (Fig. B.14).

Plankton Stratigraphy : pages 358 & 452.

SEM & LM : *pentolith in shape.
Distinguishing features *normally five equally shaped segments.

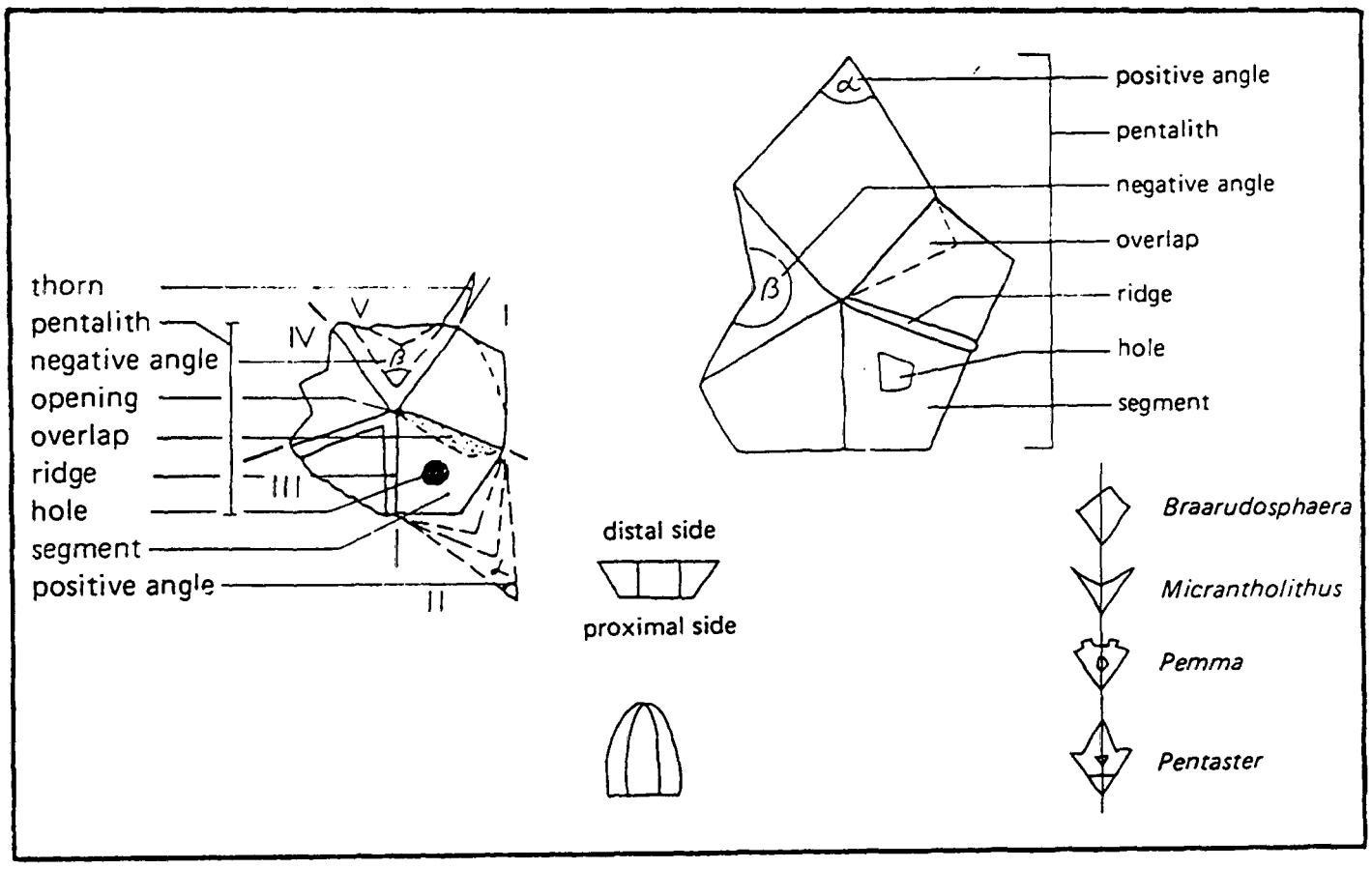

Fig. B.14. Terminology of the Braarudosphaeraceae (after Perch-Nielsen, 1985a & b).

Shape : PENTAGONAL

Range : Early Cretaceous to present day.

Biostatigraphical : moderate in the Late Mesozoic.

Calciosoleniaceae

Kamptner (1927)

Description : The Calciosoleniaceae include rhomboidal coccoliths, with calcite laths extending inward from the outer walls. Laths may meet along a central line.

Plankton Stratigraphy : pages 358 & 452.

SEM & LM Distinguishing features : *rhomboidal in shape.

Shape : RHOMBOIDAL

Range : Early Cretaceous to present day.

Biostratigraphical : poor.

Calyculaceae

Noël (1973)

Description : The Calyculaceae include elliptical and circular coccoliths with an overall shape in side view of a chalice-like-cup (cylinder) with a horizontal lip, the central area is covered with a grid (Fig. B.15).

Plankton Stratigraphy : page 358.

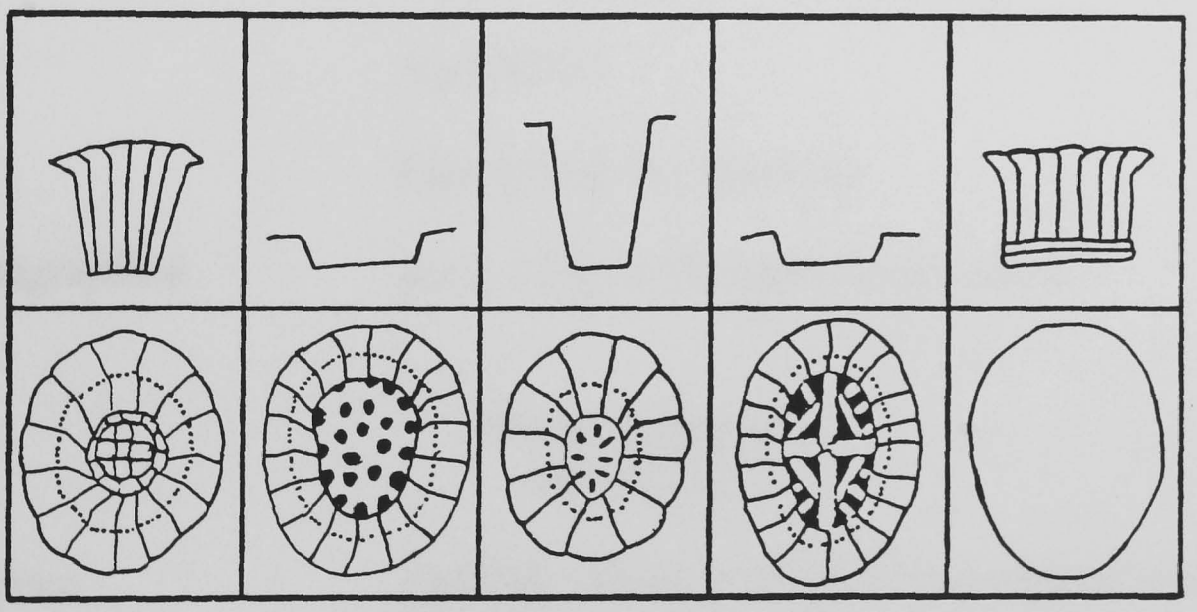

Fig. B.15. Typical Calyculaceae structural arrangements (modified from Perch-Nielsen, 1985a).

SEM Diagnostic features :
*elliptical/sub circular.
*chalice-like-shape (vase).
*cylindrical.
*narrow rim.
*central area covered by a grid.

LM Distinguishing features : *similar to that seen under SEM conditions However, it may be difficult to note the chalice-like-shape of the coccolith.

Shape	:	ELLIPTICAL, CIRCULAR, CYLINDER & VASE
Range	:	Early to Late Jurassic.
Biostratigraphical	:	poor.

Calyptrosphaeraceae
Boudreaux and Hay (1969)

Description	:	The Calyptrosphaeraceae include coccoliths and nannoliths of varying design, and are made up of uniform, small calcite crystals (holococcoliths).
Note	:	Due to the type of construction, holococcoliths have a poor survival rate within the geological record.
Plankton Stratigraphy	:	pages 359 & 453.
SEM & LM Distinguishing features	:	Due to the number of various designs, it is felt that this family should be considered along with **Incertae sedis** within the fourth search level section.
Shape	:	VARIOUS
Range	:	Late Jurassic to present day.
Biostratigraphical	:	poor, owing to the type of construction.

Ceratolithaceae
Norris (1965)

Description	:	The Ceratolithaceae includes horse-shaped nannoliths (Fig. B.16).
Plankton Stratigraphy	:	page 454.
SEM & LM Distinguishing features	:	*horseshoe-shape.
Shape	:	HORSESHOE
Range	:	Very Late Oligocene to present day.
Biostratigraphical	:	moderate to good.

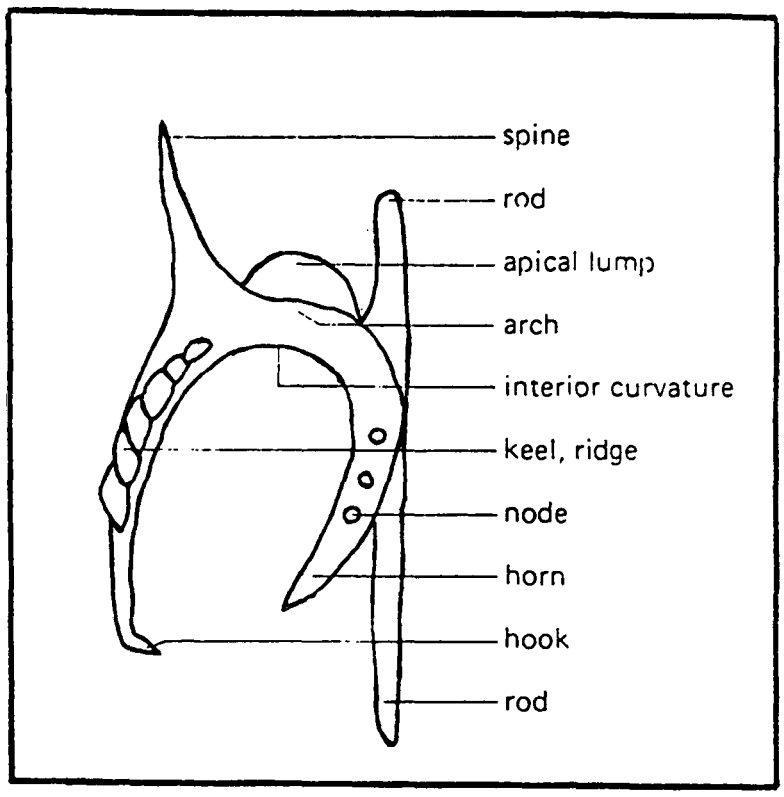

Fig. B.16. Terminology of the Ceratolithaceae (after Perch-Nielsen, 1985b).

Chiastozygaceae

Rood, Hay and Barnard (1973)

Description	:	The Chiastozygaceae include elliptical coccoliths with a rim of inclined elements and has a 'X' or an 'H' bridging the central area.
Plankton Stratigraphy	:	page 361.
SEM & LM Distinguishing features	:	*elliptical. *narrow rim of inclined elements. *central structure formed by a 'X' or an 'H'.
Shape	:	ELLIPTICAL
Range	:	Triassic/Early Jurassic to Palaeocene.
Biostratigraphical	:	poor to moderate.

Coccolithaceae

Poche (1913)

Description	:	The Coccolithaceae includes both elliptical and circular coccoliths, with a distal shield consisting of radial petaloid type elements, which is not birefringent under crossed polars. The proximal shield is smaller

consisting of one or two cycles and normally shows strong birefringence. The central area may be open or closed and possess or lack a central structure (Fig. B.17).

Plankton Stratigraphy : page 456.

SEM Distinguishing features :
*distal shield made up of radiating petaloid elements.
*elliptical.
*circular.
*proximal shield smaller than the distal shield and is constructed of two or more cycles of overlapping petaloid elements.

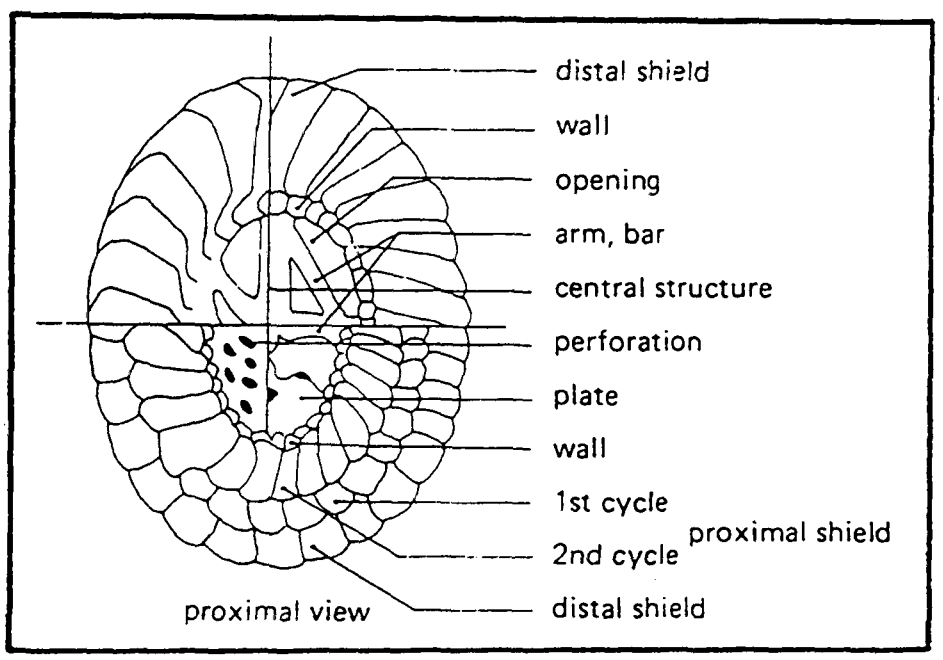

Fig. B.17. Terminology of the Coccolithaceae (after Perch-Nielsen, 1985b).

LM Distinguishing features :
*distal shield does not show birefringence under crossed polars.
*proximal shield shows strong birefringence.
*elliptical.
*circular.
*appears smaller under crossed polars, best seen under plane polars or phase contrast.

Shape : ELLIPTICAL & CIRCULAR

Range : Late Cretaceous to present day.

Biostratigraphical : very good.

Crepidolithaceae

Black (1971)

Description : The Crepidolithaceae includes elliptical-, circular- and cylindrical-shaped coccoliths/nannoliths of substantial thickness, were the outer rim consists of a ring of calcite sectors without appreciable imbrication. A proximal floor and massive distal process may be present (Fig. B.18).

Plankton Stratigraphy : page 364.

SEM & LM Distinguishing features :
*elliptical.
*circular.
*large distal process (if present/attached).
*cylindrical.
*relatively thick.

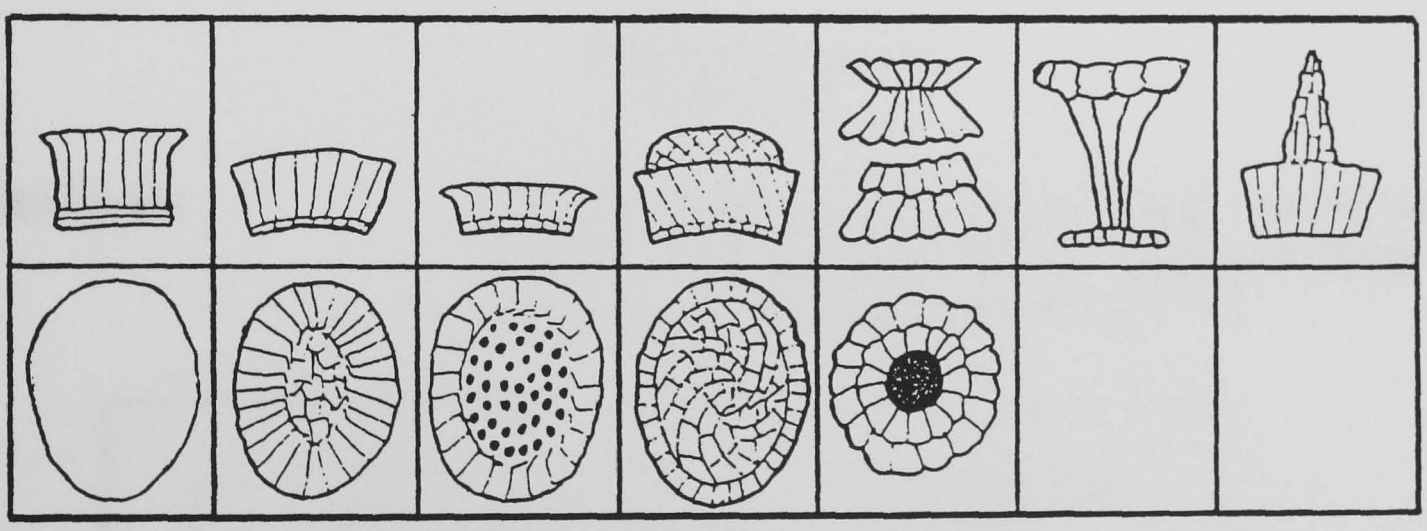

Fig. B.18. Typical Crepidolithaceae structural arrangements (modified from Perch-Nielsen, 1985a).

Shape : ELLIPTICAL, CIRCULAR & CYLINDRICAL

Range : Early Jurassic to Late Cretaceous.

Biostratigraphical : poor to moderate.

Deutschlandiaceae

Kamptner (1928)

Description : The Deutschlandiaceae include circular nannoliths with just a single shield that lacks birefringence under crossed polars, and a small central cone where the ring of elements around the cone is birefringent.

Plankton Stratigraphy	:	page 466.
SEM Distinguishing features	:	*circular. *single shield. *small central cone.
LM Distinguishing features	:	*similar to that seen under SEM conditions. However, the single shield is of poor birefringence, with the ring of elements surrounding the central cone being birefringent, best viewed under plane polars or phase contrast.
Shape	:	CIRCULAR
Range	:	Early Pliocene to present day.
Biostratigraphical	:	poor.

Discoasteraceae

Tan (1927)

Description : The Discoasteraceae include star-, rosette-, circular- and basket-shaped nannoliths which when lying flat remain dark whilst under crossed polars (Fig. B.19).

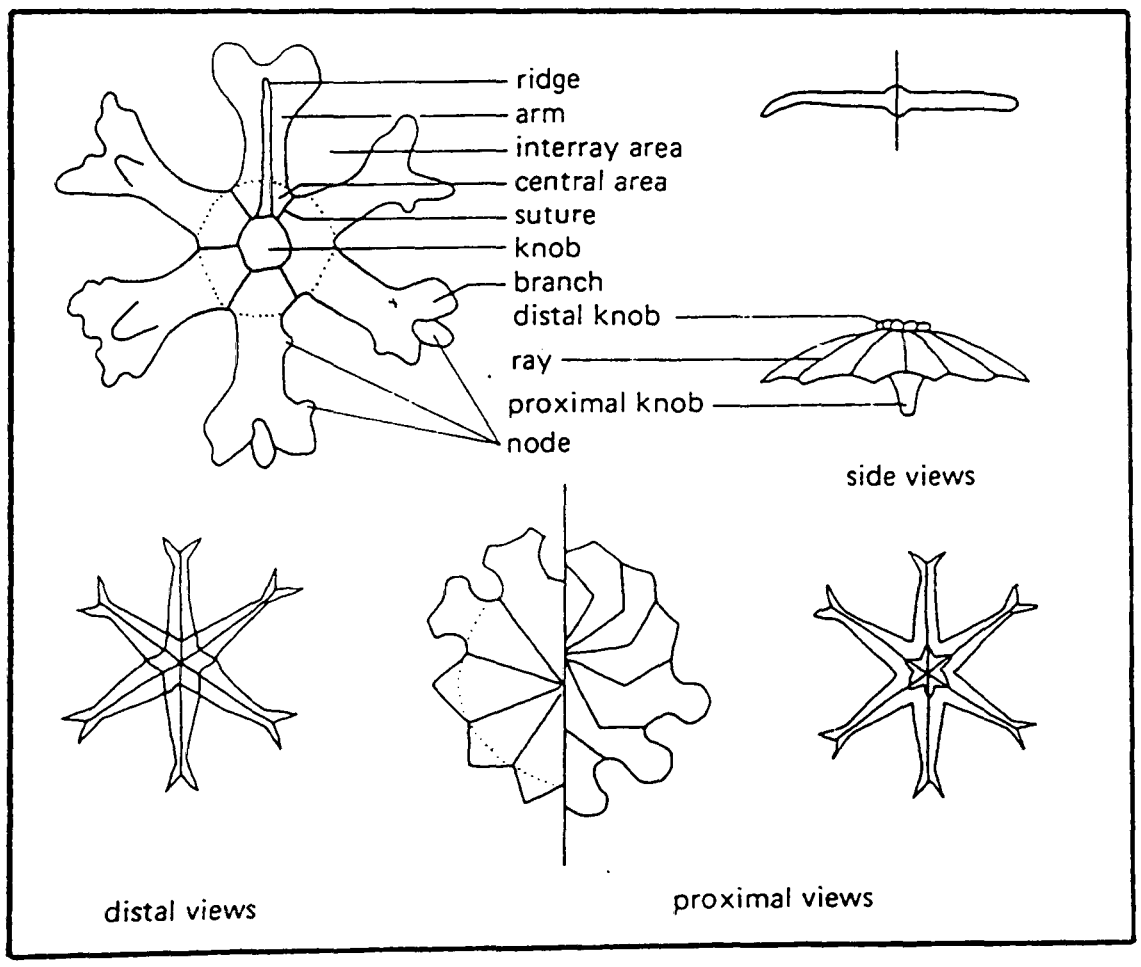

Fig. B.19. Terminology of the Discoasteraceae (after Perch-Nielsen, 1985b).

Plankton Stratigraphy : page 467.

SEM Distinguishing features :
*star.
*rosette.
*circular.
*basket.

LM Distinguishing features
*similar to that seen under SEM conditions. However, the nannolith is not birefringent and therefore best viewed under plane polars or phase contrast.

Shape : STAR, ROSETTE, CIRCULAR & BASKET

Range : Late Palaeocene to Late Pliocene.

Biostratigraphical : very good.

Eiffellithaceae
Reinhardt (1965)

Description : The Eiffellithaceae includes elliptical coccoliths with a narrow rim of inclined elements and an inner cycle of plate type elements. Within the central area there is a central 'X' or '+', and may support a central process (Fig. B.20).

Plankton Stratigraphy : page 368.

SEM Distinguishing features :
*elliptical.
*thin outer rim.
*inclined elements (rim).
*inner cycle consisting of plate type elements.
*central 'X' or '+'.
*central process may be present.

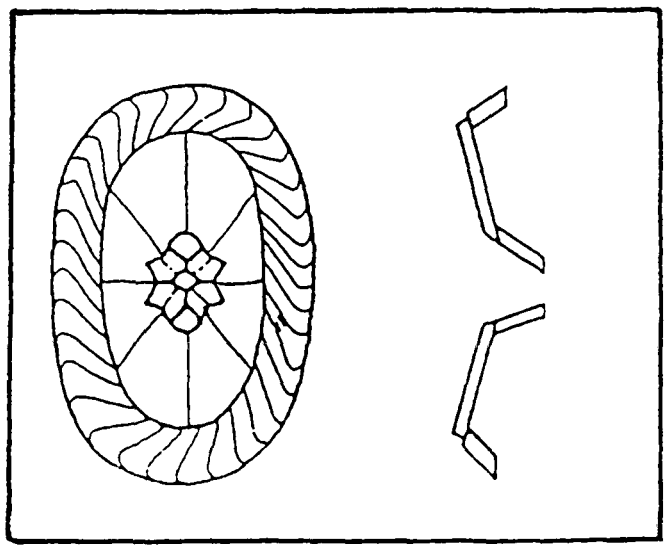

Fig. B.20. *Eiffellithus*, typical genus of Eiffellithaceae showing structural arrangement (after Reinhardt, 1965).

LM Distinguishing features : *similar to that seen under SEM conditions. However, it may be not possible to distinguish the inclined nature of the rim elements.

Shape : ELLIPTICAL

Range : Late Cretaceous.

Biostratigraphical : moderate.

Ellipsogelosphaeraceae

Noël (1965)

Description : The Ellipsogelosphaeraceae include both elliptical and circular coccoliths, the distal shield has slightly overlapping elements, whereas the proximal shield has radial arranged elements. The central area can be open, closed or bridged (Fig. B.21).

Plankton Stratigraphy : page 369.

SEM Distinguishing features :
*elliptical.
*circular.
*distal shield has slightly overlapping elements.
*proximal shield has radial arranged elements.
*central area may be open, closed or bridged.

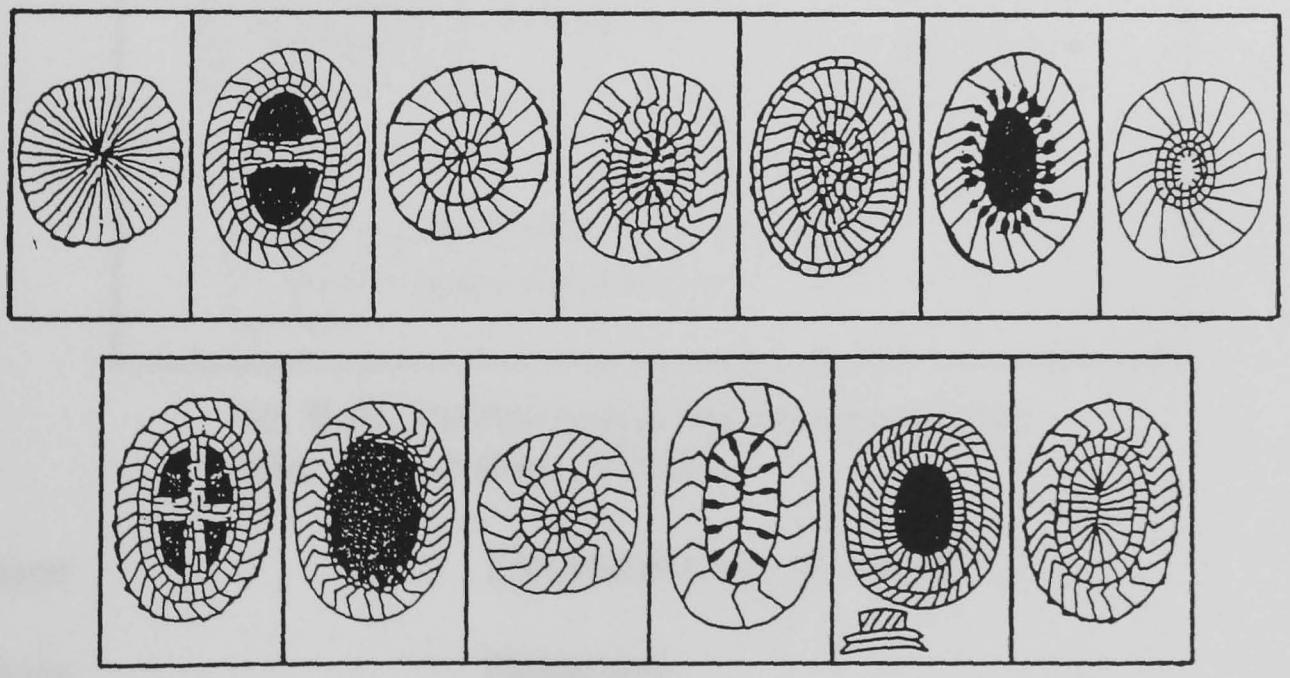

Fig. B.21. Typical Ellipsogelosphaeraceae structural arrangements (modified from Perch-Nielsen, 1985a).

LM Distinguishing features	:	*similar to that seen under SEM conditions. However, it may be not possible to distinguish the overlapping nature of the elements of the distal shield.
Shape	:	ELLIPTICAL & CIRCULAR
Range	:	Early Jurassic to Palaeocene.
Biostratigraphical	:	moderate.

Fasciculithaceae

Hay and Mohler (1967)

Description	:	The Fasciculithaceae include cylindrical nannoliths with a proximal column and a distal disc and cone (Fig. B.22).
Plankton Stratigraphy	:	page 481.
SEM & LM Distinguishing features	:	*cylindrical. *proximal column. *a disk or lateral elements. *distal cone.

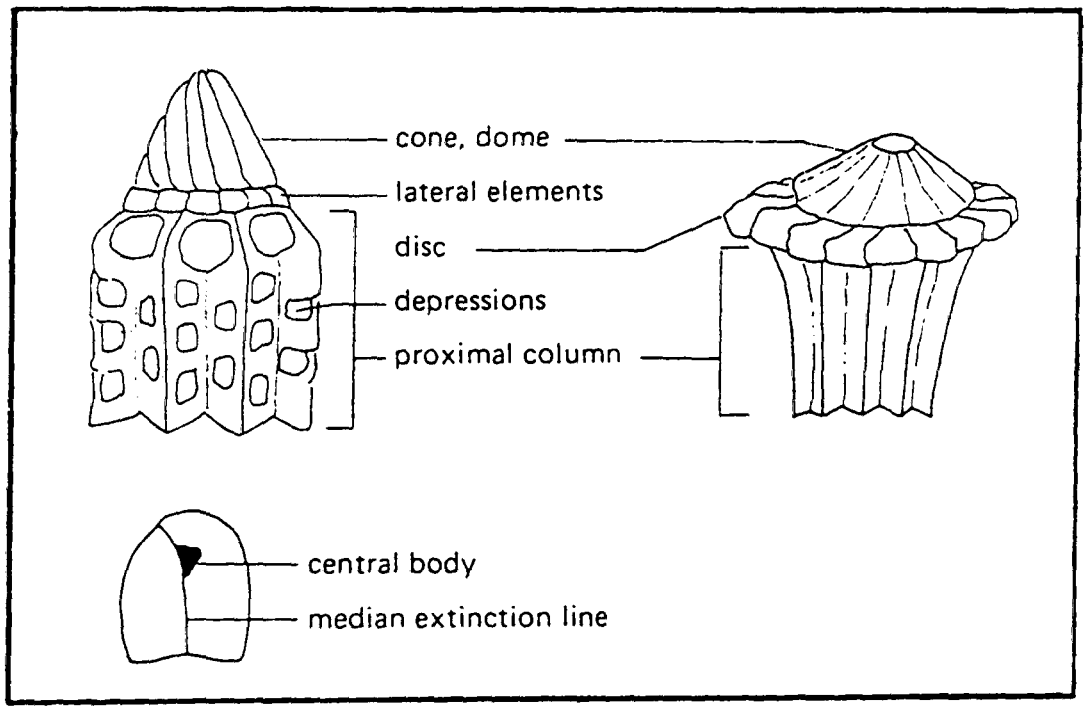

Fig. B.22. Terminology of the Fasciculithaceae (after Perch-Nielsen, 1985b).

Shape	:	CYLINDRICAL & CONE
Range	:	Palaeocene.
Biostratigraphical	:	very good.

Goniolithaceae

Deflandre (1957)

Description : The Goniolithaceae includes pentagonal-shaped composite coccoliths which have a wall composed of vertical elements enclosing a granular central area.

Plankton Stratigraphy : pages 372 & 484.

SEM & LM Distinguishing features :
*pentagonal.
*granular centre.

Shape : PENTAGONAL

Range : Late Cretaceous to Eocene.

Biostratigraphical : poor.

Helicosphaeraceae

Black (1971)

Description : The Helicosphaeraceae include spiral/helical-walled coccoliths usually with a flange. The central area can either be bridged, open or closed/filled (Fig. B.23).

Plankton Stratigraphy : page 485.

SEM & LM Distinguishing features :
*elliptical.
*spiral/helical.
*flange.
*central area
-bridge
-open
-filled/closed.

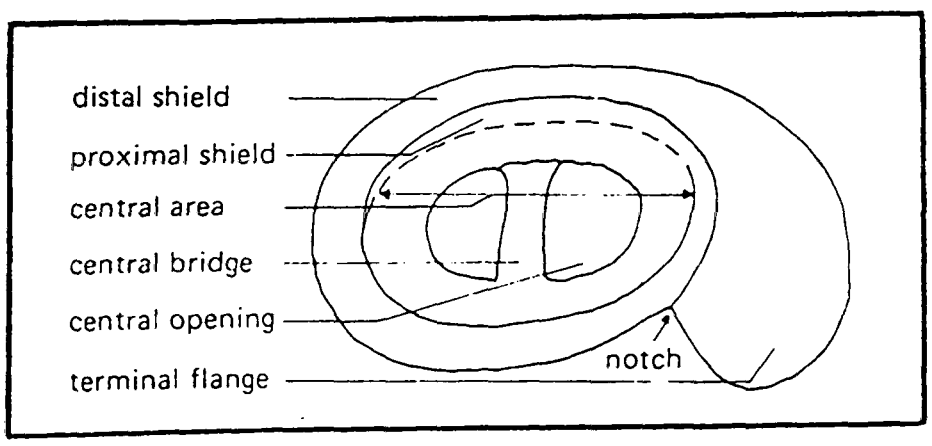

Fig. B.23. Terminology of the Helicosphaeraceae (after Perch-Nielsen, 1985b).

Shape	:	SPIRAL or HELICAL
Range	:	Eocene to present day.
Biostratigraphical	:	good.

Heliolithaceae

Hay and Mohler (1967)

Description	:	The Heliolithaceae include circular coccoliths which have two to three appressed cycles of elements, forming a cylindrical structure were the proximal is the largest and slimmest (Fig. B.24).
Plankton Stratigraphy	:	page 481.
SEM Distinguishing features	:	*circular. *cylindrical in side view. *two to three appressed cycles of elements.

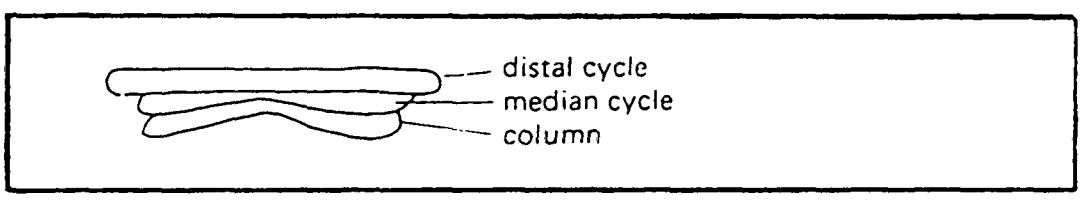

Fig. B.24. Terminology of the Heliolithaceae
(after Perch-Nielsen, 1985b)

LM Distinguishing features	:	*similar to that seen under SEM conditions. However, may have difficulty distinguishing the appressed nature of the cycles.
Shape	:	CIRCULAR & CYLINDRICAL
Range	:	Late Palaeocene.
Biostratigraphical	:	moderate to good.

Lithostromationaceae

Deflandre (1959)

Description	:	The Lithostromationaceae includes triangular, hexagonal or nearly circular nannoliths which are relatively large and have symmetrically arranged depressions.

Plankton Stratigraphy : page 494.

SEM Distinguishing features :
*triangular.
*hexagonal.
*sub-circular.
*relatively large.
*symmetrically arranged depressions.

LM Distinguishing features :
*due to height, difficult to focus and photograph at high magnification.
*if lying flat, not birefringent under crossed polars.

Shape : TRIANGULAR, HEXAGONAL or CIRCULAR

Range : Early Eocene to Late Pliocene.

Biostratigraphical : poor.

Microrhabdulaceae

Deflandre (1963)

Description : The Microrhabdulaceae include cylindrical-, rod- or spindle-shaped nannoliths (Fig. B.25).

Plankton Stratigraphy : page 372.

SEM & LM Distinguishing features :
*cylindrical.
*rod.
*spindle.

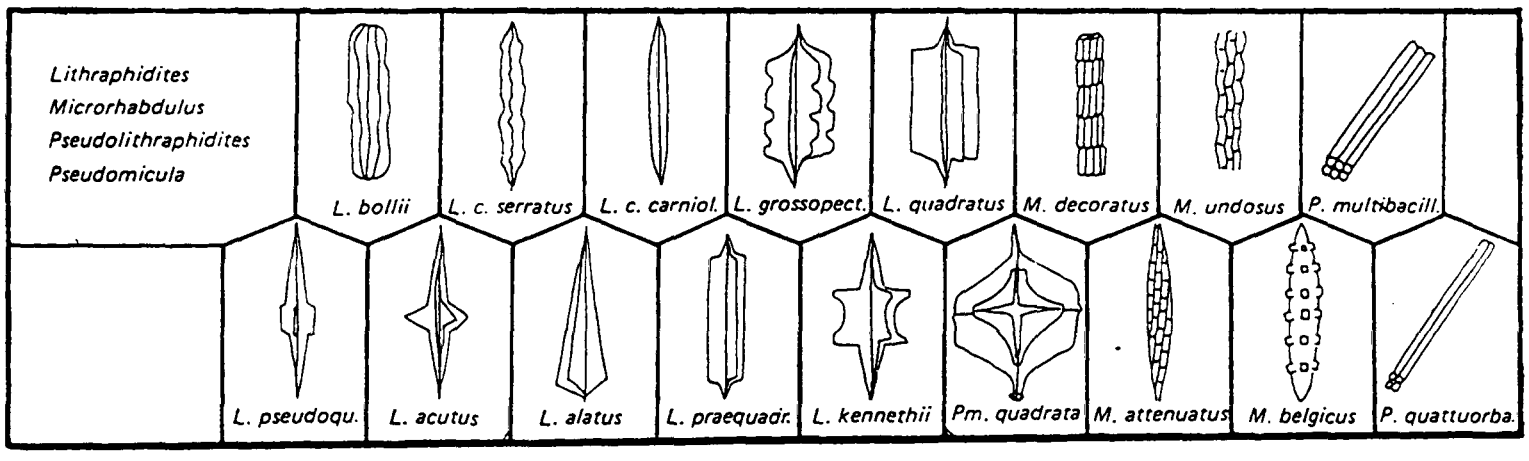

Fig. B.25. Typical Microrhabdulaceae structural arrangements (modified from Perch-Nielsen, 1985a).

Shape : CYLINDRICAL, ROD & SPINDLE

Range : Late Jurassic to Late Cretaceous.

Biostratigraphical : moderate to good.

Nannoconaceae

Deflandre (1959)

Description : The Nannoconaceae include cylindrical-, cone- or circular-shaped (end view) nannoliths, which are made up of a thick wall of wedges or plates, oriented perpendicular and spiral around an axial cavity or canal (Fig. B.26).

Plankton Stratigraphy : page 375.

SEM Distinguishing features :
*cylindrical.
*cone-shaped.
*circular (end view).

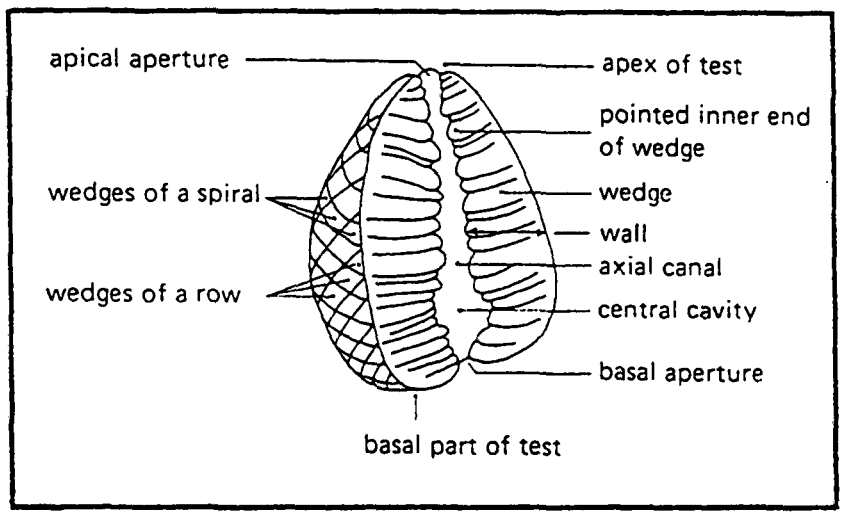

Fig. B.26. Terminology of the Nannoconaceae (after Perch-Nielsen, 1985a).

LM Distinguishing features : *similar to that seen under S.E.M. conditions, however, under crossed polars, the central cavity is visible.

Shape : CYLINDER, CONE or CIRCULAR

Range : Late Jurassic to Late Cretaceous.

Biostratigraphical : moderate to good.

Podorhabdaceae

Noël (1965)

Description : The Podorhabdaceae includes elliptical coccoliths which have a narrow rim of two to three jointive petaloid or subquadrate elements, enclosing a variety of structures, composed of many fine calcite crystals spanning a large central area. The central process, if present, may be hollow or solid (Fig. B.27).

Subfamilies	:	Podorhabdoideae	*tubular central process. *when broken leaves a hole in central area.
		Retacapsoideae	*distal shield with two cycles of elements. *proximal shield with one cycle of elements. *if present, a solid central process. *when broken leaves a closed central area.
		Cribrosphaerelloideae	*central area with a grid. *no process.
Plankton Stratigraphy	:	page 378.	
SEM Distinguishing features	:	*narrow rim. *two to three layers of jointive petaloid or subquadrate elements. *wide central area. *variety of structures within the central area. *a solid or hollow central process, commonly arising out of the centre.	

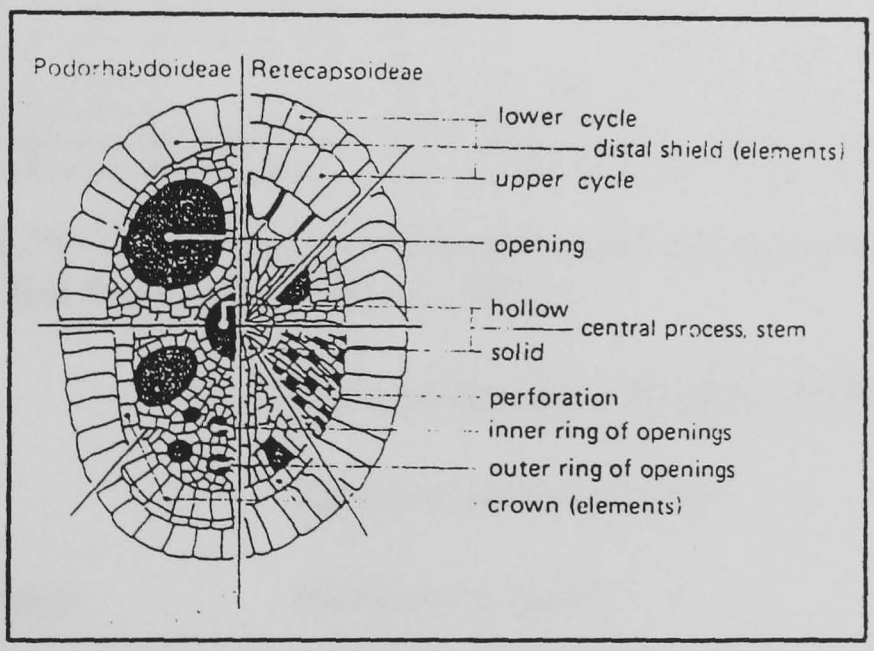

Fig. B.27. Terminology of the Podorhabdaceae (after Perch-Nielsen, 1985a).

LM Distinguishing features	:	*similar to that seen under SEM conditions. However, it may be not possible to view the detailed layering of the petaloid elements. *under crossed polars, a black cross with straight arms is seen

Shape : ELLIPTICAL

Range : Early Jurassic to Late Cretaceous.

Biostratigraphical : poor.

Polycyclolithaceae
Forchheimer (1972)

Description : The Polycyclolithaceae include cylindrical-, block-, star- or rosette-shaped nannoliths (Fig. B.28).

Plankton Stratigraphy : page 387.

SEM & LM Distinguishing features : *cylindrical.
*block.
*star.
*rosette.

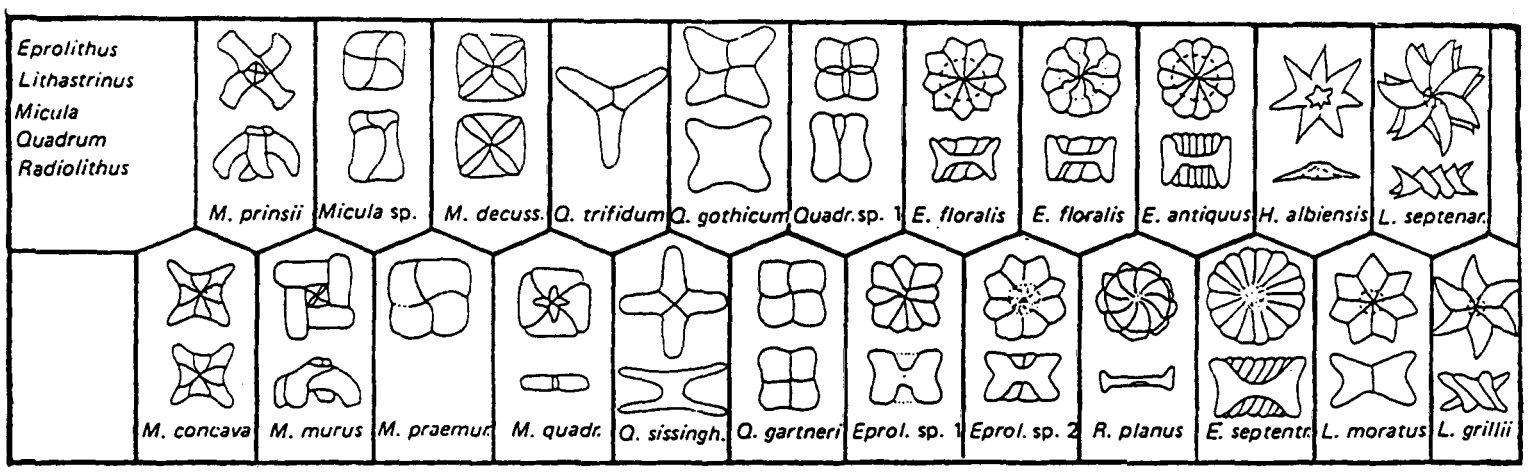

Fig. B.28. Typical Polycyclolithaceae structural arrangements (modified from Perch-Nielsen, 1985a).

Shape : CYLINDRICAL, BLOCK, STAR & ROSETTE

Range : Early to Late Cretaceous.

Biostratigraphical : moderate to good.

Pontosphaeraceae
Lemmermann (1908)

Description : The Pontosphaeraceae include elliptical coccoliths, with a wall/rim containing two cycles of elements of varying height and a large central area. In proximal view the elements are radially arranged and in the distal view the

elements are concentrically arranged. The floor of the central area is pierced by perforations/holes or thinned by depressions (Fig. B.29).

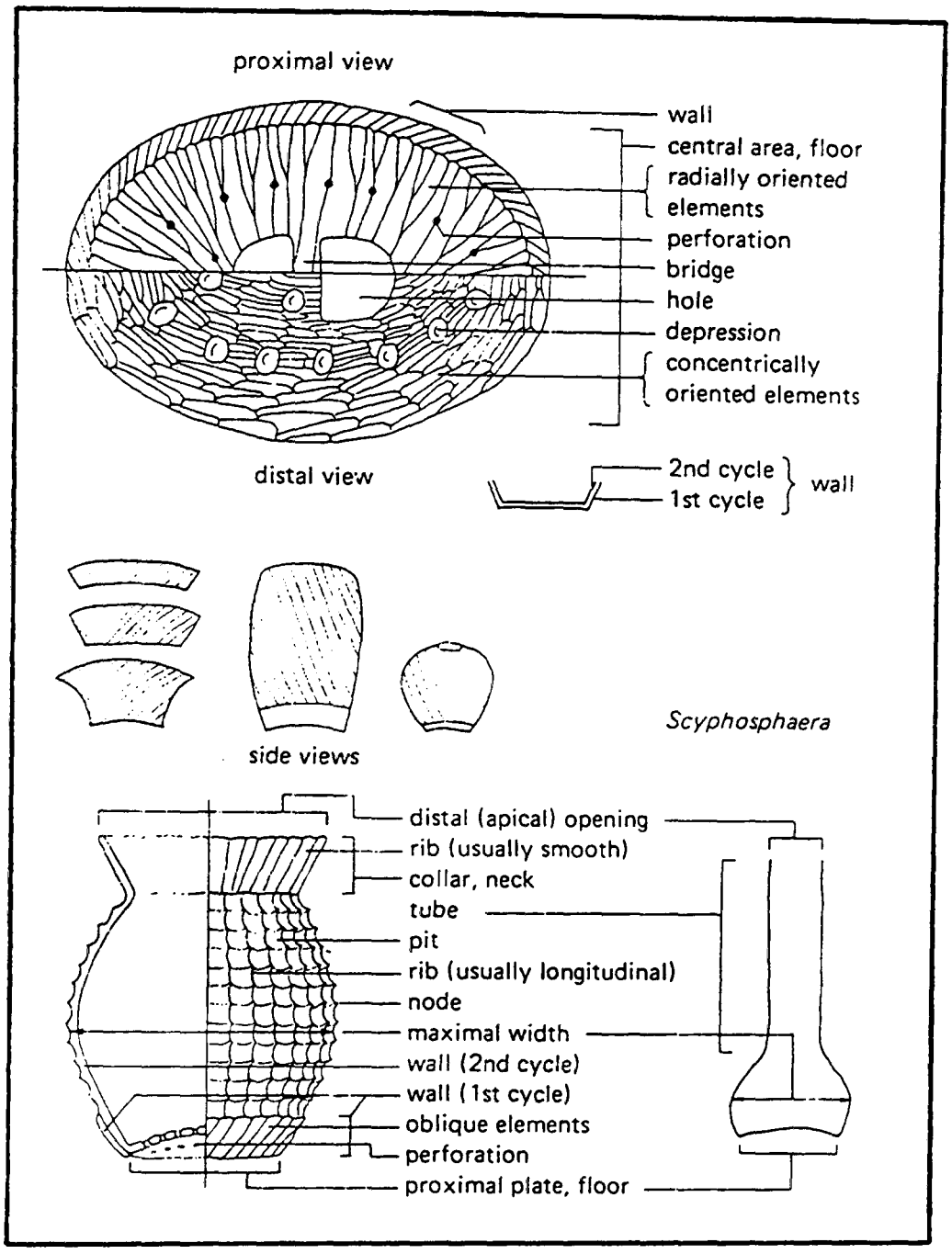

Fig. B.29. Terminology of the Pontosphaeraceae (after Perch-Nielsen, 1985b).

Plankton Stratigraphy : page 495.

SEM Distinguishing features :

*elliptical.
*vase.
*large central area.
*wall containing two cycles of elements
-proximal, elements are radial.
-distal, elements are concentric.
*wall can be low or high.
*floor of central area pierced by perforations/holes or thinned by depressions.

LM Distinguishing features	:	*similar to that seen under SEM conditions. However, it may be not possible to note that there are two cycles of wall elements.
Shape	:	ELLIPTICAL & VASE
Range	:	Palaeocene to present day.
Biostratigraphical	:	poor to moderate.

Prediscosphaeraceae

Rood, Hay and Barnard (1971)

Description	:	The Prediscosphaeraceae includes elliptical and circular coccoliths which nearly always have 16 elements in both shields. The open central area is spanned by a '+' or a 'X', supporting a central process if present (Fig. B.30).
Plankton Stratigraphy	:	page 393.
SEM & LM Distinguishing features	:	*elliptical. *circular. *open central area spanned by a '+' or a 'X'. *central process may be present. *16 elements in both shields.

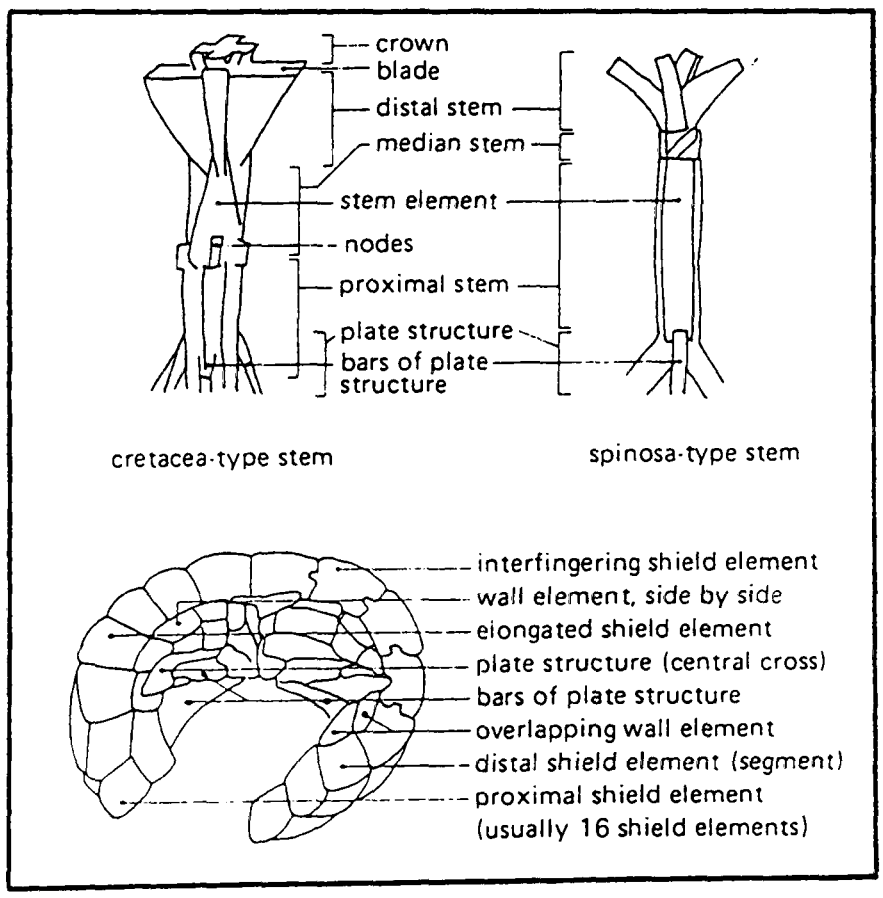

Fig. B.30. Terminology of the Prediscosphaeraceae (after Perch-Nielsen, 1985a).

Shape : ELLIPTICAL CIRCULAR & ROD

Range : Early to Late Cretaceous.

Biostratigraphical : moderate to good.

Prinsiaceae

Hay and Mohler (1967)

Description : The Prinsiaceae include elliptical and circular coccoliths, with both the proximal and distal shields being birefringent in crossed polars, and the interference figure being dextrogyre in distal view (Fig. B.31).

Plankton Stratigraphy : page 501.

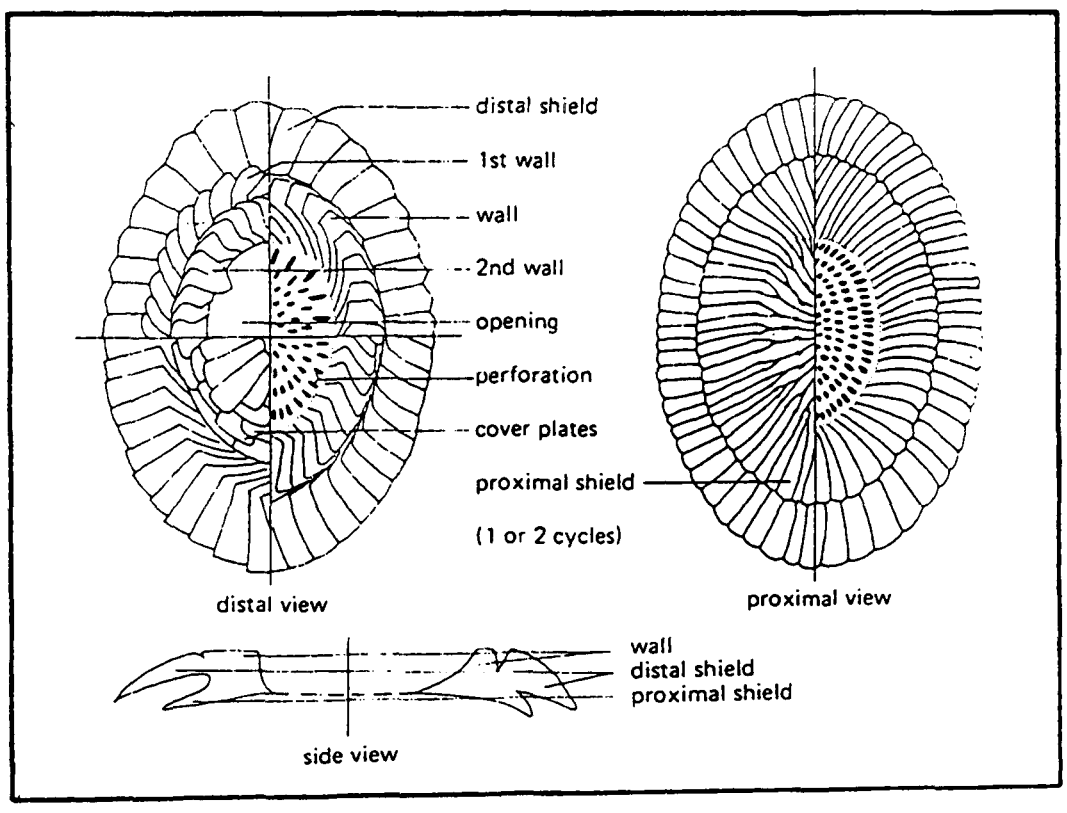

Fig. B.31. Terminology of the Prinsiaceae (after Perch-Nielsen, 1985b).

SEM Distinguishing features :
*elliptical.
*circular.
*proximal shield smaller than the distal shield
*central area
-perforations/grid/net.
-open.
-obliquely bridged.

LM Distinguishing features : *similar to that seen under SEM conditions. However, it may be not possible to see that the proximal shield is smaller than the distal shield

*interference figure between crossed polars is dextrogyre in distal view.
*both proximal and distal shields are birefringent and therefore appear as correct size under polarised and normal light, unlike the family Coccolithaceae which appears smaller under crossed polars.

Shape : CIRCULAR & ELLIPTICAL

Range : Late Cretaceous to present day.

Biostratigraphical : moderate.

Rhabdosphaeraceae

Lemmermann (1908)

Description : The Rhabdosphaeraceae includes elliptical and circular nannoliths, with a base containing one to several cycle of elements, the long/large central process rises from the base (Fig. B.32).

Plankton Stratigraphy page 515

SEM Distinguishing features :
*elliptical.
*circular.
*rod (large central process, broken off).
*one or two shields.
*central area with one to several cycles of elements.
*long/large central process.

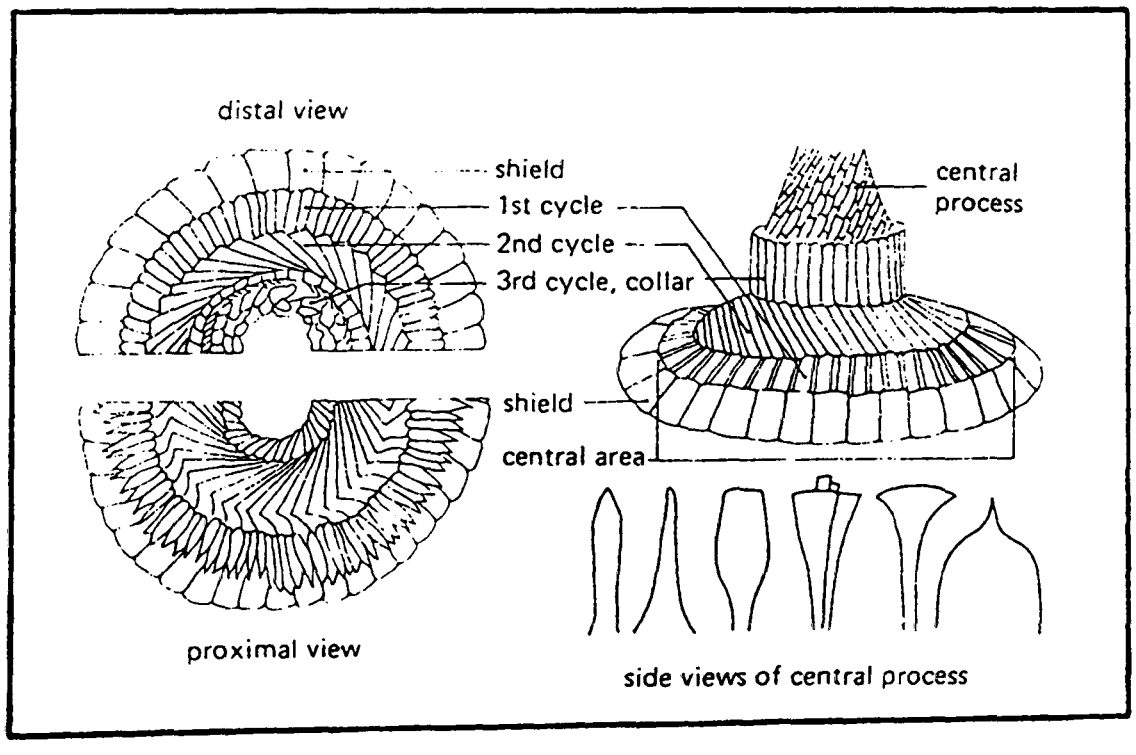

Fig. B.32. Terminology of the Rhabdosphaeraceae (after Perch-Nielsen, 1985b).

LM Distinguishing features	:	*similar to that seen under SEM conditions. However, it may be not possible to see if there is one or two shields and the detail of the central area.
Shape	:	ELLIPTICAL, CIRCULAR & ROD
Range	:	Late Palaeocene to present day.
Biostratigraphical	:	poor.

Rhagodiscaceae

Hay (1977)

Description	:	The Rhagodiscaceae includes elliptical coccoliths, with a rim/wall composed of inclined elements and a central area covered by approximately equal sized granules, a central process may be present.
Plankton Stratigraphy	:	page 394.
SEM Distinguishing features	:	*elliptical. *narrow rim of inclined elements. *central area covered by approximately equal size granules. *central process may be present.
LM Distinguishing features	:	*similar to that seen under SEM conditions. However, it may be not possible to see the detail of the central area.
Shape	:	ELLIPTICAL
Range	:	Early to Late Cretaceous.
Biostratigraphical	:	poor.

Schizosphaerellaceae

Deflandre (1959)

Description	:	The Schizosphaerellaceae includes spherical to sub spherical nannoliths, consisting of two overlapping/interlocking hemispheres.
Plankton Stratigraphy	:	page 394.

SEM & LM Distinguishing features : *spherical/sub spherical.
*two overlapping/interlocking hemispheres.

Shape : SPHERICAL

Range : Late Triassic to Late Jurassic.

Biostratigraphical : poor.

Sollasitaceae

Black (1971)

Description : The Sollasitaceae includes elliptical coccoliths consisting of two shields, with a large, open central area containing grids, bars, granules or a meshwork, but with no central process (Fig. B.33).

Plankton Stratigraphy : page 396.

SEM & LM Distinguishing features : *elliptical.
*large open central area.
*occupied by a grid, bars, granules or meshwork.
*no central process or spine.

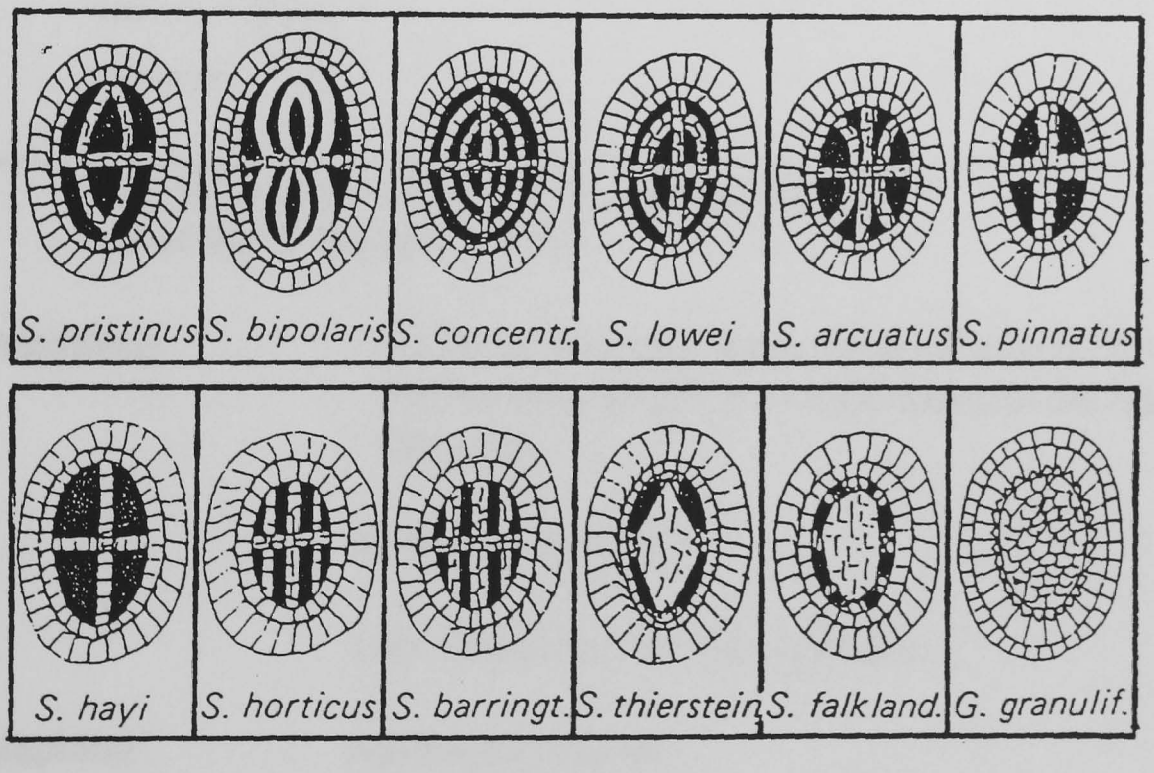

Fig. B.33. Typical Sollasitaceae structural arrangements (modified from Perch-Nielsen, 1985a).

Shape : ELLIPTICAL

Range : Early Jurassic to Palaeocene.

Biostratigraphical : poor.

Sphenolithaceae

Deflandre (1952)

Description : The Sphenolithaceae includes nannofossils which have a proximal shield/column supporting one to several tiers of lateral elements and capped by an apical or distal structure which may be elongated and/or bifurcating (Fig. B.34).

Plankton Stratigraphy : page 517.

SEM Distinguishing features :
*proximal shield/column.
*supporting one to several tiers of lateral elements.
*capped by an apical or distal structure.
*elongated or bifurcating.

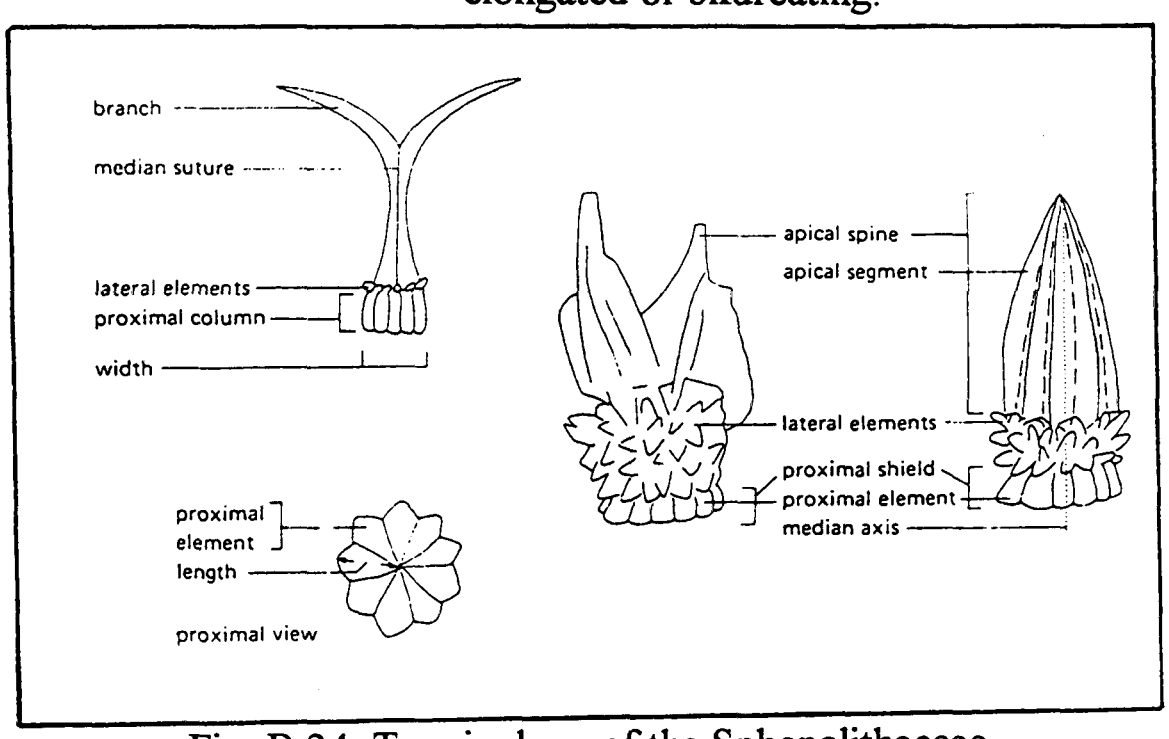

Fig. B.34. Terminology of the Sphenolithaceae (after Perch-Nielsen, 1985b).

LM Distinguishing features : *similar to that seen under SEM conditions. However, it may be not possible to see the detail of the lateral elements.

Shape : CONE & BLOCK

Range : Late Palaeocene to Late Pliocene.

Biostratigraphical : moderate to good.

Stephenolithiaceae

Black (1968) and related genera

Description : The Stephenolithiaceae includes circular, elliptical and polygonal coccoliths, were the rim/outer wall is made up

of vertically arranged elements. The central area is spanned by variously arranged elements which may support a central process. Radial spines may project from the marginal rim/outer wall (Fig. B.35).

Plankton Stratigraphy : page 397.

SEM & LM Distinguishing features :
*circular.
*elliptical.
*polygonal.
*narrow rim/outer wall made up of vertically arranged elements.
*central area spanned by radially or otherwise arranged elements.
*central process may be present.
*radial spines may project from the rim/outer wall.

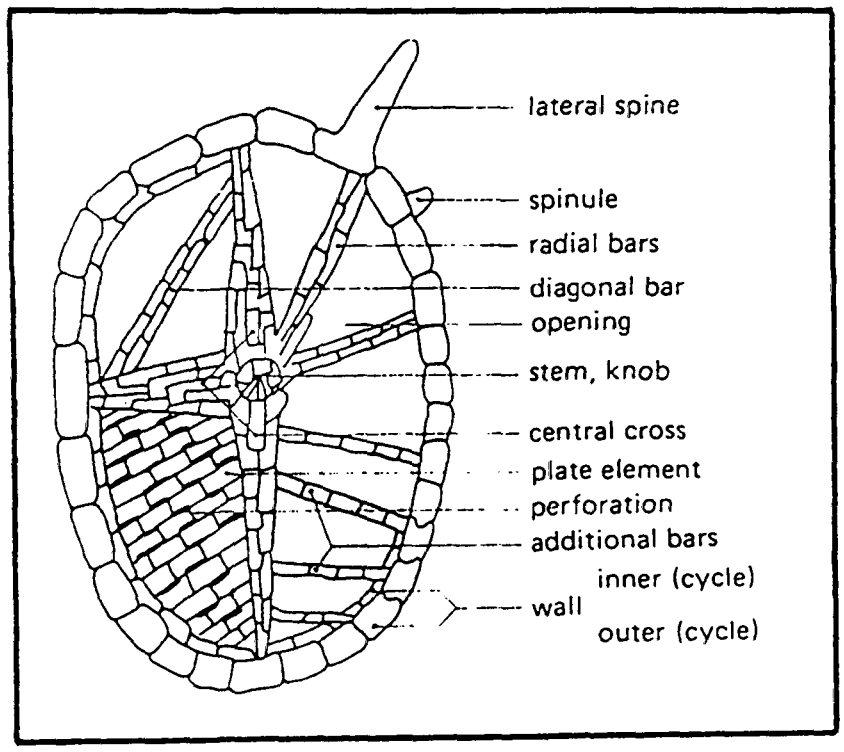

Fig. B.35. Terminology of the Stephenolithiaceae (after Perch-Nielsen, 1985a).

Shape : CIRCULAR, ELLIPTICAL & POLYGONAL

Range : Early Jurassic to Late Cretaceous.

Biostratigraphical : moderate to good.

Syracosphaeraceae

Lemmermann (1908)

Description : The Syracosphaeraceae includes elliptical coccoliths which have a complex rim/outer wall, with a central area partially closed by lath-shaped elements.

Plankton Stratigraphy : page 523.

SEM & LM Distinguishing features :
*elliptical.
*a complex rim/outer wall.
*central area partially closed by lath-shaped elements.
*central process may be available.

Shape : ELLIPTICAL

Range : Late Oligocene to present day.

Biostratigraphical : poor.

Thoracosphaeraceae
Schiller (1930)

Description : The Thoracosphaeraceae includes spherical and ovoid calcareous forms, composed of interlocking polygonal elements. An opening and/or lid may be present.

Plankton Stratigraphy : pages 406 & 524.

SEM & LM Distinguishing features :
*spherical.
*ovoid.
*one or more keels may be present.
*large opening may be present at one pole, lid also may be present.

Shape : SPHERICAL & OVOID

Range : Late Jurassic to present day.

Biostratigraphical : poor to moderate.

Triquetrorhabdulaceae
Lipps (1969)

Description : The Triquetrorhabdulaceae include spindle-shaped rods which are made up of three concave blades with triradial cross-section.

Plankton Stratigraphy : page 526.

SEM & LM Distinguishing features : *rod.
*spindle-shape.
*concave sides.

Shape : ROD

Range : Mid Eocene to Late Miocene.

Biostratigraphical : poor.

Zygodiscaceae

Hay and Mohler (1969)

Description : The Zygodiscaceae includes elliptical coccoliths which have a narrow rim/outer wall made up of narrow steeply inclined laths (elements). The central area which has no floor is spanned by either 'I', 'X' or 'H' type structures (Fig. B.36).

Plankton Stratigraphy : pages 406 & 526.

SEM Distinguishing features : *elliptical.
*narrow rim/outer wall.
*rim/outer wall made up of one or two cycles of steeply inclined laths (elements).
*'I' - 'X' - 'H' structures bridging the central area.
*lacking a floor to the placolith.

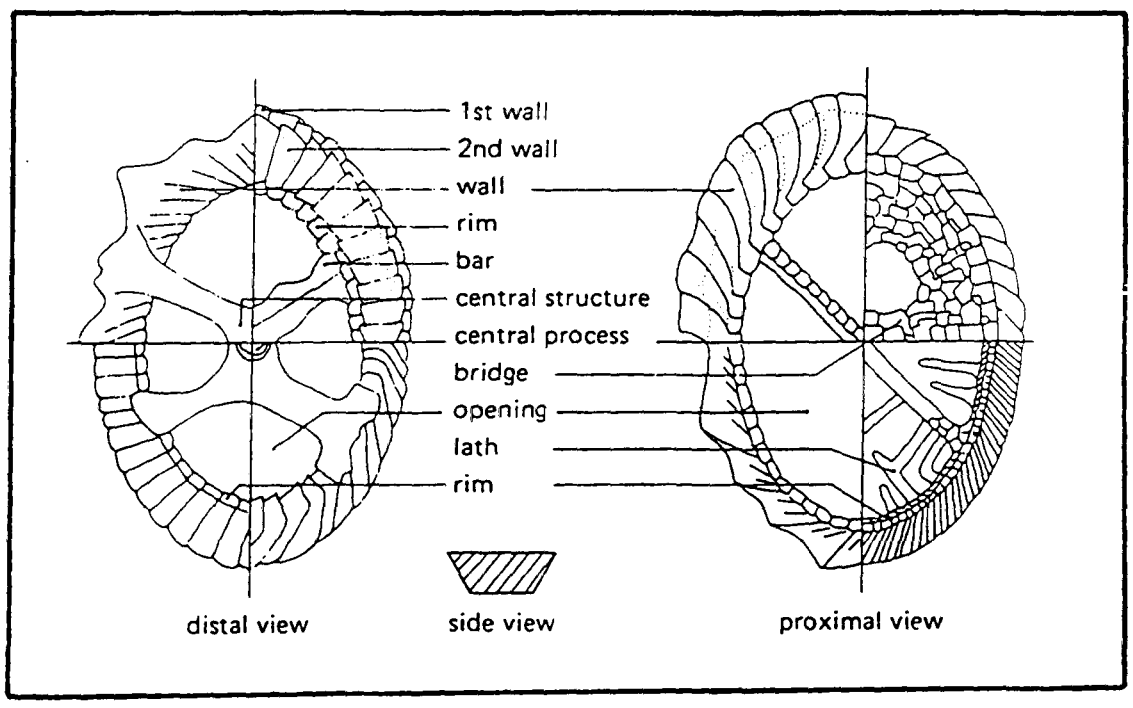

Fig. B.36. Terminology of the Zygodiscaceae (after Perch-Nielsen, 1985b).

LM Distinguishing features	:	*similar to that seen under SEM conditions. However, it may be not possible to see the detail of the rim/outer wall.
Shape	:	ELLIPTICAL
Range	:	Early Jurassic to Early Oligocene.
Biostratigraphical	:	poor to moderate.

FOURTH LEVEL SEARCH

Calyptrosphaeraceae
(Holococcoliths of various constructions)

and

Incertae sedis
(Various constructions)

NB.

If it is not possible to make a satisfactory identification at this level, especially after failing to identify at the lower levels of search, assume that the calcareous nannofossil under investigation may not be biostratigraphically important.

Calyptrosphaeraceae

Boudreaux and Hay (1969)

Description : The Calyptrosphaeraceae include coccoliths and nannoliths of varying design, and are made up of uniform, small calcite crystals (holococcoliths).

Notes : Due to the type of construction, holococcoliths have a poor survival rate within the geological record.

Apart from viewing figures B.37 and B.38, it is important to consult the relevant pages within the publication 'Plankton Stratigraphy'.

Plankton Stratigraphy : pages 359 & 453.

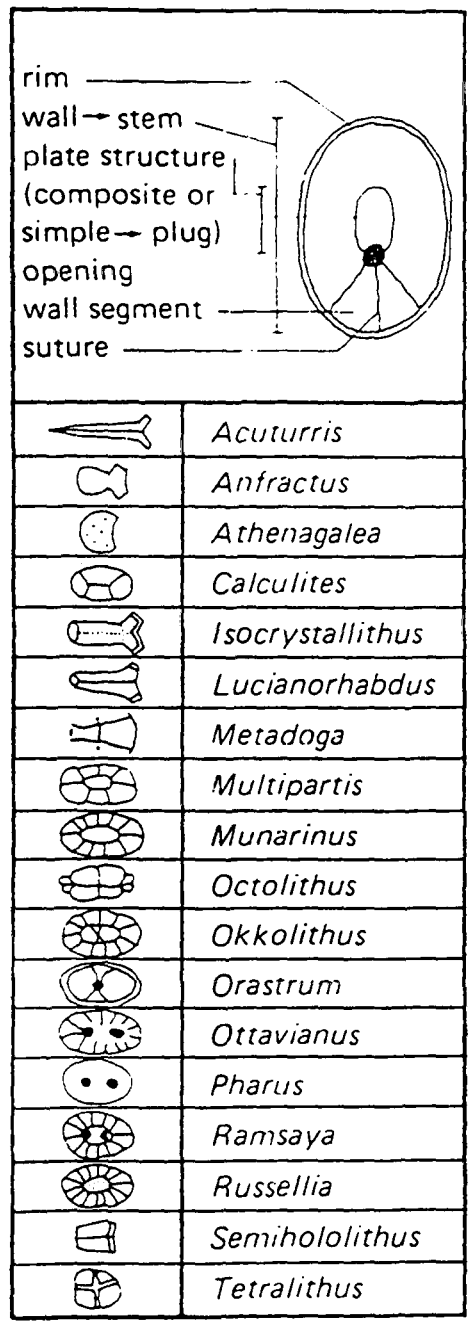

Fig. B.37. Some genera structural arrangements of the Calyptrosphaeraceae (modified from Perch-Nielsen, 1985a).

SEM & LM : Due to the number of various designs, it is difficult to note
Distinguishing features any diagnostic features that would prove useful within the Identification Key.

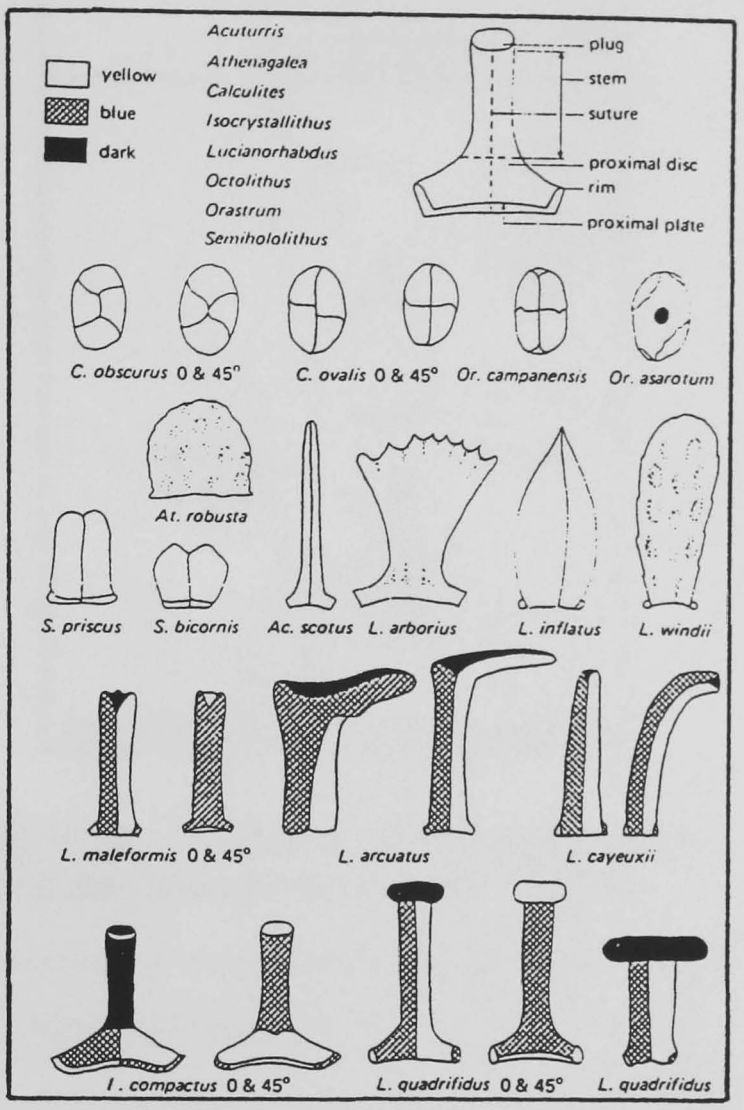

Fig. B.38. Terminology of *Lucianorhabdus* and other genera of the Calyptrosphaeraceae (modified from Perch-Nielsen, 1985a).

Shape : VARIOUS

Range : Late Jurassic to present day.

Biostratigraphical : poor, owing to the type of construction.

Incertae sedis

Notes : Within this grouping are calcareous nannofossils that belong to unrelated families.

Apart from viewing figures B.39 and B.40, it is important to consult the relevant pages within the publication 'Plankton Stratigraphy'.

Plankton Stratigraphy : pages 409 & 533.

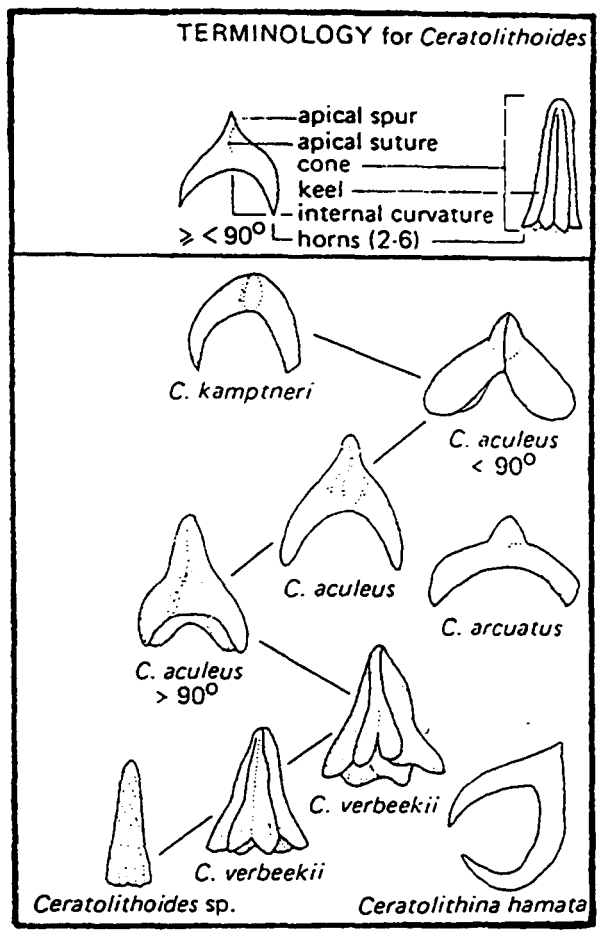

Fig. B.39. Terminology for *Ceratolithoides* (modified from Perch-Nielsen, 1985a).

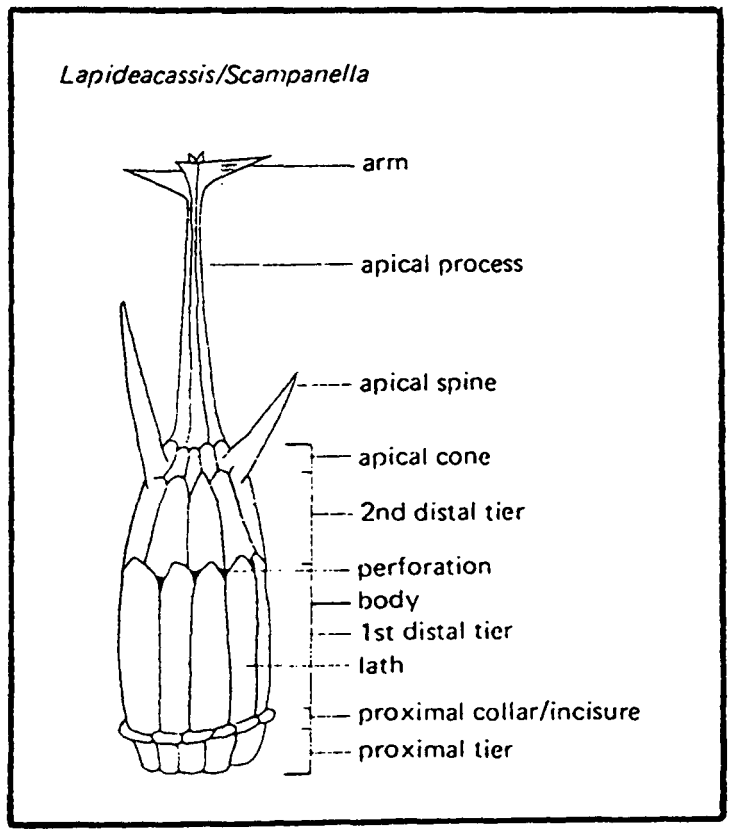

Fig. B.40. Terminology for *Lapideacassis/Scampanella* (after Perch-Nielsen, 1985b).

BIBLIOGRAPHY

Black, M. 1968. Taxonomic problems in the study of coccoliths. *Palaeontology,* **11** (5), 793-813.

Black, M. 1971. Coccoliths of the Speeton Clay and Sutterby Marl. *Proc. Yorkshire geol. Soc.,* **38** (3), 381-424.

Boudreaux, J. E. & Hay, W. W. 1969. Calcareous nannoplankton and biostratigraphy of the Late Pliocene-Pleistocene-Recent sediments of the Submarex cores. *Rev. Esp. Micropaleontol.,* **1,** 249-92.

Bukry, D. 1969. Upper Cretaceous coccoliths from Texas and Europe. *Univ. Kansas Paleontol. Contrib.,* **51** (Protista 2), 1-79.

Deflandre, G. 1947. *Braarudosphaera* nov. gen., type d'une famille nouvelle de Coccolithophoridés actuels à éléments composites. *C. r. Seances Acad. Sci. Paris,* **225,** 439-41.

Deflandre, G. 1952. Classe des coccolithophoridés. In: P. P. Grassé (ed.), *Traité de Zoologie,* vol. 1, pp. 439-70.

Deflandre, G. 1957. *Goniolithus* nov. gen., type d' une famille nouvelle de Coccolithophoridé fossiles, à éléments pentagonaux non composites. *C.r. Seavces Acad. Sci. Paris,* **244,** 2539-41.

Deflandre, G. 1959. Sur les nannofossils calcaires et leur systématique. *Rev. Micropaleontol.,* **2,** 127-52.

Deflandre, G. 1963. Sur les Microrhabdulidés, famille nouvelle de nannofossiles calcaires. *C.r. Seances Acad. Sci. Paris,* **256,** 3484-6.

Forchheimer, S. 1972. Scanning electron microscope studies of Cretaceous coccoliths from the Köpinsberg Borehole No. 1, SE Sweden. *Sver. geol. Unders.,* ser. C.668, **65** (14), 1-141.

Hay, W. W. 1977. Calcareous nannofossils. In: A. T. S. Ramsay (ed.), *Oceanic Micropalaeontology,* pp. 1055-1200. Academic Press, London.

Hay, W. W. & Mohler, H. P. 1967. Calcareous nannoplankton from early Tertiary rocks at Pont Labau, France, and Paleocene-Eocene correlations. *J. Paleontol.,* **41,** 1505- 41.

Kamptner, E. 1927. Beitrag zur Kenntnis adriatischer Coccolithophoriden. *Arch. Protistenk.,* **58,** 173-84.

Kamptner, E. 1928. Über das System une die Phylogenie der Kalkflagellaten. *Arch. Protisenk.*, **64,** 19-43.

Lemmermann, E. 1908. Flagellatae, Chlorophyceae, Coccosphaerales und Silicoflagellatae. In: K. Brandt & C. Apstein (eds.), *Nordisches Plankton,* pp. 1-40. Lipsius & Tischer, kiel and Leipzig.

Lipps, J. H. 1969. *Triquetrorhabdulus* and similar calcareous nannoplankton. *J. Paleontol.*, **43,** 1029-32.

Noël, D. 1965. *Sur les coccolithes du Jurassique Européen et d' Afrique du Nord.* Centre Nat. Rech. Sc., 209 pp.

Noël, D. 1973. Nannofossiles calcaires de sédiments jurassiques finement laminés. *Bull. Mus. natl. Hist. nat.*, ser. 3, **75,** 95-156.

Norris, R. E. 1965. Living cells of *Ceratolithus cristatus* (Coccolithophorineae). *Arch. Protistenk.*, **108,** 19-24.

Prins, B. 1979. Notes on nannology - 1. *Clausicoccus,* a new genus of fossil coccolithophorids. *INA Newsletter,* **1** (1), N-2-N-4.

Perch-Nielsen, K. 1985. Mesozoic calcareous nannofossils and Cenozoic calcareous nannofossils. In H. M. Bolli *et al.* (eds), *Plankton Stratigraphy.* pp. 329-554. Cambridge University Press, Cambridge.

Poche, F. 1913. Das System der Protozoa. *Arch. Protistenk.*, **30,** 125-321.

Reinhardt, P. 1965. Neue Familien für fossile Kalkflagellaten (Coccolithophriden, Coccolithineen). *Monatsber. Dt. Akad. Wiss. Berlin,* **7,** 30-40.

Rood, A. P., Hay, W. W. & Barnard, T. 1971. Electron microscope studies of Oxford clay coccoliths. *Eclog. geol. Helv.*, **64** (2), 245-72.

Schiller, J. 1930. Coccolithineae. In: *Dr. L. Rabenhorst's Kryptogamen-Flora von Deutschland, Österreich und der Schweiz.*, vol. 10, part2, pp. 89-267. Akad. Verlagsges., Leipzig.

Siesser, W. G. 1993. Calcareous nannoplankton. In J. H. Lipps (ed.) *Fossil Prokaryotes and Protists,* pp. 169-201, Blackwell Scientific Publications.

Tan, S. H. 1927. Discoasteridae incertae sedis. *Proc. Sect. Sc. K. Akad. Wet. Amsterdam,* **30**, 411-19.

APPENDIX C

Deep Sea Drilling Project and Ocean Drilling Project Chapters Relating to Calcareous Nannofossils

Notes

DSDP	Deep Sea Drilling Project
ODP	Ocean Drilling Project
NOT AVAILABLE	Up to the date of submission of this thesis, the author has not been able to view the volume.
++++++	There is no chapter within the volume refering to calcareous nannofossils.

DSDP or ODP	Year	Chapt./Page/Plates	Range of calcareous nannofossils	Author(s)
DSDP				
1.	1969	15/369/7	Eocene to Holocene	Bukry & Bramlette
		16/388/0	Eocene to Holocene	Hay
2.	1970	13/349/0	Late Cretaceous to Pliocene	Bukry
3.	1970	18/589/0	Cretaceous to Holocene	Bukry & Bramlette
		19/613/0	Cretaceous to Holocene	Gartner
4.	1970	17/375/0	Eocene to Pleistocene	Bukry
		23/455/0	Cretaceous to Pleistocene	Hay
5.	1970	18/487/0	Neogene	Bukry & Bramlette
		19/495/0	Neogene	Gartner
6.	1971	29/965/8	Cretaceous to Pleistocene	Bukry
		30/1005/0	Palaeogene & Neogene	Hay
7.	1971	29/1471/3	Tertiary	Martini & Worsley
		30/1509/0	Tertiary	Gartner
		31/1513/0	Tertiary	Bukry
8.	1971	13/777/6	Oligocene to Quaternary	Haq & Lipps
		14/791/0	Oligocene to Quaternary	Bukry
9.	1972	14/817/0	Eocene to Pleistocene	Bukry
		15/833/0	Eocene to Pleistocene	Gartner
10.	1973	16/375/0	Late Cretaceous to Pleistocene	Hay
		17/385/0	Late Cretaceous to Pleistocene	Bukry
11.	1972	11/427/12	Early Cretaceous	Wilcoxon
		12/459/0	Early Cretaceous to Holocene	Wilcoxon
		13/475/0	Late Jurassic to Holocene	Bukry
12.	1972	15/1003/22	Late Cretaceous to Pleistocene	Perch-Nielsen
		16/1071/0	Late Cretaceous to Pleistocene	Bukry

DSDP or ODP	Year	Chapt./Page/Plates	Range of calcareous nannofossils	Author(s)
13.	1973	33/817/0	Miocene to Pleistocene	Bukry & Gartner
14.	1972	14/421/16	Cretaceous to Pliocene	Roth & Thierstein
15.	1973	15/625/2	Cretaceous to Pleistocene	Hay & Beaudry
		16/685/0	Cretaceous to Pleistocene	Bukry
16.	1973	26/653/5	Cretaceous to Pliocene	Bukry
		31/883/0	Cretaceous to Pliocene	Gartner
17.	1973	23/695/27	Cretaceous to Holocene	Roth
18.	1973	15/569/10	Oligocene to Pleistocene	Wise
19.	1973	26/741/0	Early Cretaceous to Pleistocene	Worsley
20.	1973	12/221/6	Cretaceous to Pleistocene	Hekel
		14/307/2	Cenozoic	Bukry
21.	1973	18/641/15	Late Cretaceous to Pleistocene	Edwards
22.	1974	26/577/0	Late Cretaceous to Holocene	Gartner
23.	1974	40/1073/0	Palaeocene to Pleistocene	Boudreaux
		41/1091/0	Palaeocene to Pleistocene	Bukry
24.	1974	23/969/0	Palaeocene to Holocene	Roth
		24/995/0	Palaeocene to Holocene	Bukry
25.			NOT AVAILABLE	
26.	1974	28/619/12	Cretaceous to Holocvene	Thierstein
		29/669/0	Cretaceous to Palaeogene	Bukry
27.	1974	30/589/10	Late Cretaceous to Pleistocene	Decima
		31/623/0	Late Cretaceous to Pleistocene	Bukry
28.	1975	15/589/0	Neogene	Burns
		20/709/0	Neogene	Bukry
29.	1975	13/469/21	Palaeocene to Pleistocene	Edwards & Perch-Nielsen
30.	1975	17/549/0	Late Cretaceous to Pleistocene	Shafik

DSDP or ODP	Year	Chapt./Page/Plates	Range of calcareous nannofossils	Author(s)
31.	1975	20/531/1	Neogene	Rezak & Henry
		34/655/0	Eocene to Pleistocene	Ellis
32.	1975	24/677/1	Palaeocene to Holocene	Bukry
33.	1976	15/493/1	Cretaceous to Pliocene	Bukry
34.	1976	58/705/0	Eocene to Pliocene	Blechschmidt
35.	1976	34/557/3	Mesozoic to Cenozoic	Haq
36.	1977	8/269/89	Mesozoic to Cenozoic	Wise & Wind
		14/745/0	Cenozoic	Bilal *et al.*
37.	1977	74/909/0	Neogene	Howe
38.	1976	26/823/0	Palaeogene to Holocene	Muller
		27/843/0	Tertiary	Bukry
39.	1977	31/699/50	Cretaceous to Pleistocene	Perch-Nielsen
40.	1978	12/571/16	Mesozoic to Cenozoic	Decima *et al.*
		13/635/3	Cenozoic	Bukry
41.	1978	14/667/3	Mesozoic	Cepek
		15/689/0	Cenozoic	Bukry
It is important to note that volumes 38 to 41 inclusive have a joint supplement volume.				
38.	1978	14/141/1	Oligocene	Bilal *et al.*
39.	1978		++++++++++++++++++++	
40.	1978		++++++++++++++++++++	
41.	1978	6/913/5	Pliocene to Pleistocene	Samtleben
42.	1978	32/727/0	Neogene	Muller
43.	1979	17/507/19	Palaeocene to Pleistocene	Okada & Thierstein
		23/617/2	Palaeocene to Eocene	Haq, Okada & Lohmann

DSDP or ODP	Year	Chapt./Page/Plates	Range of calcareous nannofossils	Author(s)
44.	1978	33/703/5	Cretaceous to Holocene	Schmidt
		34/731/3	Cretaceous	Roth
		35/761/1	Jurassic	Wind
45.	1979		++++++++++++++++++++	
46.	1979		++++++++++++++++++++	
47 (pt1).	1979	3/221/11	Early Cretaceous	Wind & Cepek
		7/289/7	Neogene to Holocene	Cepek & Wind
47 (pt2).	1979	6/327/0	Palaeocene to Pleistocene	Blechschmidt
48.	1979	25/589/9	Early Cretaceous to Holocene	Muller
49.	1979	16/519/0	Oligocene to Holocene	Steinmetz
		17/533/2	Miocene to Holocene	Martini
50.	1980	7/333/0	Cenozoic	Cepek & Gartner
		8/345/0	Mesozoic	Cepek, Gartner & Cool
It is important to note that volumes 51, 52 & 53 were published together as one volume.				
51.	1980	15/815/1	Mid-Cretaceous	Gartner
		16/823/8	Cretaceous to Pleistocene	Siesser
54.	1980	20/535/0	Late Pliocene to Quaternary	Bukry
55.	1980	10/349/0	Palaeocene to Pleistocene	Takayama
It is important to note that volumes 56 & 57 were published together as one volume.				
56.	1980	25/867/2	Pliocene	Haq & Goreau
		26/875/0	Miocene to Pleistocene	Shaffer
58.	1980	7/549/0	Eocene to Pleistocene	Okada

DSDP or ODP	Year	Chapt./Page/Plates	Range of calcareous nannofossils	Author(s)
59.			NOT AVAILABLE	
60.	1982	26/507/2	Eocene to Pleistocene	Ellis
61.	1981	6/475/7	Various	Thierstein & Manivit
62.	1981	11/397/0	Mesozoic	Cepek
		13/471/1	Mid Cretaceous	Roth
63.	1981	11/445/6	Tertiary	Bukry
64.	1982	41/955/1	Miocene to Pleistocene	Aubry
65.	1983	22/487/0	Neogene	Hattner
66.	1982	23/589/14	Neogene	Stradner & Allram
67.	1982	10/383/1	Cretaceous to Pleistocene	Muzylov
68.	1982	9/325/4	Pliocene to Pleistocene	Rio
69.			NOT AVAILABLE	
70.			NOT AVAILABLE	
71.	1983	21/481/35	Mesozoic to Cenozoic	Wise
		22/551/5	Late Cretaceous	Wind & Wise
72.	1983		++++++++++++++++++++	
73.	1984	9/391/0	Cretaceous to Pleistocene	Percival
		10/425/0	Miocene	A K von Salis
74.	1984	8/475/12	Cretaceous to Palaeogene	Manivit
		14/561/0	Neogene to Quaternary	Jiang & Gartner
75.	1984	11/565/52	Cretaceous	Stradner & Steinmetz
		14/671/54	Tertiary to Holocene	Steinmetz & Stradner
76.	1983	23/573/0	Jurassic	Roth *et al.*
		25/587/6	Jurassic to Early Cretaceous	Roth
77.	1984	26/629/0	Cenozoic	Lang & Watkins
		27/649/7	Cretaceous	Watkins & Bowdler

DSDP or ODP	Year	Chapt./Page/Plates	Range of calcareous nannofossils	Author(s)
78.	1984	20/411/11	Cretaceous & Miocene to Pleistocene	Bergen
79.	1984	21/563/1	Cretaceous	Wiegand
		25/657/3	Jurassic	Wiegand
80.	1985	29/767/4	Quaternary	Pujos
81.	1984	5/403/0	Cenozoic	Backman
82.			NOT AVAILABLE	
83.			NOT AVAILABLE	
84.	1985	8/339/1	Late Cretaceous to Tertiary	Filenice
85.	1985	13/553/3	Quaternary	Pujos
		14/581/3	Cenozoic	Pujos
		15/609/0	Cenozoic	Gartner & Chow
86.			NOT AVAILABLE	
87.			NOT AVAILABLE	
It is important to note that volumes 88 and 91 were published together as one volume				
88.	1987		++++++++++++++++++++	
89.	1986	5/285/2	Late Cretaceous	Bergen
90.	1986	11/747/2	Palaeogene	Martini
		12/763/0	Miocene to Pleistocene	Lohmann
92.	1986	10/255/11	Late Cretaceous to Pleistocene	Knuttel
93.	1987	15/593/1	Neogene	Muza, Wise & Covington
		16/617/23	Cretaceous to Pleistocene	Covington & Wise
		17/661/0	Cretaceous to Palaeocene & Neogene	Lang & Wise
		18/685/5	Eocene	Applegate & Wise
		19/699/0	Palaeocene to Eocene	Jiang & Wise

DSDP or ODP	Year	Chapt./Page/Plates	Range of calcareous nannofossils	Author(s)
94.	1987	13/651/8	Miocene to Pleistocene	Takayama
95.	1987	11/359/14	Early Eocene	Valentine
96.	1986	32/601/4	Quaternary	Constans & Parker
ODP	I = Initial Report	S = Scientific Report		
101I.	1986		++++++++++++++++++++	
101S.			NOT AVAILABLE	
102I.			NOT AVAILABLE	
102S.			NOT AVAILABLE	
103I.	1987		++++++++++++++++++++	
103S.	1988	19/279/0	Cenozoic	Wei *et al.*
		20/293/29	Cretaceous	Applegate & Bergen
104I.	1987		++++++++++++++++++++	
104S.	1987	26/459/5	Oligocene to Holocene	Donnally
105I.			++++++++++++++++++++	
105S.	1989	16/245/2	Neogene	Knuttel *et al.*
		17/263/5	Cretaceous and Eocene/Oligocene	Firth
106I.			NOT AVAILABLE	
106S.			NOT AVAILABLE	
107I.			NOT AVAILABLE	
107S	1990	31/495/0	Mio/Pliocene	Muller
		32/513/0	Plio/Pleistocene	Rio *et al.*
108I	1988		++++++++++++++++++++	
108S	1989	2/9/1	Oligocene to Mid-Miocene	Olafsson
		4/35/4	Cretaceous and Cenozoic	Manivit

DSDP or ODP	Year	Chapt./Page/Plates	Range of calcareous nannofossils	Authors
109I.			NOT AVAILABLE	
109S.			NOT AVAILABLE	
110I.			NOT AVAILABLE	
110S.	1990	9/129/0	Cenozoic	Clark
111I.			NOT AVAILABLE	
111S.			NOT AVAILABLE	
112I.	1988		++++++++++++++++++++	
112S.	1990	14/217/2	Cenozoic	Martini
113I.	1988		++++++++++++++++++++	
113S			NOT AVAILABLE	
114I.			NOT AVAILABLE	
114S.	1991	7/155/0	Cretaceous to Holocene	Crux
		8/179/2	Late Eocene to Early Oligocene	Madice & Monechi
		9/193/0	Quaternary	Gard & Crux
115I.			NOT AVAILABLE	
115S.	1990	14/129/3	Palaeogene and Quaternary	Okada
		15/175/14	Late Oligocene to Pleistocene	Rio *et al.*
		16/237/3	Oligo/Miocene	Fornaciari *et al.*
		17/255/4	Quaternary	Matsuoka & Okada
116I.	1989		++++++++++++++++++++	
116S.	1990	15/165/0	Neogene	Gartner
117I.			NOT AVAILABLE	
117S.	1991	1/5/5	Neogene	Spaulding
		2/37/2	Pliocene to Quaternary	Sato *et al.*
118I.	1989		++++++++++++++++++++	
118S.	1991		++++++++++++++++++++	

DSDP or ODP	Year	Chapt./Page/Plates	Range of calcareous nannofossils	Author(s)
119I.	1989		++++++++++++++++++++	
119S	1991	26/495/6	Late Cretaceous & Cenozoic	Wei & Thierstein
		27/495/4	Early Palaeocene	Wei & Pospichal
120I.	1989		++++++++++++++++++++	
120S.	1992	21/345/5	part 1. Late Cretaceous	Watkins
		25/451/0	part 2. Cretaceous/Tertiary	Ehrendorfer & Aubry
		26/471/0	Palaeogene	Aubry
		27/493/2	Mid-Eocene to Oligocene	Firth & Wise
		28/509/2	Oligocene to Pleistocene	Wei & Wise
		29/523/2	Neogene	Wei & Wise
		30/539/0	Miocene	Beaufort & Aubry
121I.	1989		++++++++++++++++++++	
121S.	1991	5/141/8	Late Cretaceous	Resiwati
122I.	1990		++++++++++++++++++++	
122S.	1992	25/437/4	Late Triassic	Bralower *et al.*
		32/529/8	Cretaceous	Bralower & Siesser
		36/601/5	Cenozoic	Siesser & Bralower
		38/653/0	Mid-Tertiary (Braarudosphaera)	Siesser *et al.*
		40/677/0	Late Miocene to Quaternary	Siesser *et al.*
123I.	1990		++++++++++++++++++++	
123S.	1992	16/343/6	Late Cretaceous	Mutterlose
		17/369/2	Pliocene to Pleistocene	Sato *et al.*
124I.	1990		++++++++++++++++++++	
124S.	1991	10/133/5	Eocene to Holocene	Shyu & Muller
125I.	1990		++++++++++++++++++++	
125S.			NOT AVAILABLE	

DSDP or ODP	Year	Chapt./Page/Plates	Range of calcareous nannofossils	Author(s)
126I.	1990		++++++++++++++++++++	
126S.			NOT AVAILABLE	
127I.	1990		++++++++++++++++++++	
127S.			WITH VOLUME 128	
128I.			NOT AVAILABLE	
128S.	1992	10/155/0	Pleistocene	Muza
		11/171/0	Plio/Pleistocene	Rahman
129I.	1990		++++++++++++++++++++	
129S.	1992	8/179/0	Mesozoic	Erba & Covington
		9/189/0	Mid-Cretaceous	Ebra
130I.	1991		++++++++++++++++++++	
130S.	1993	6/85/1	Mesozoic	Mao & Wise
		11/179/0	Neogene	Takayama
131I.	1991		++++++++++++++++++++	
131S.	1993	1/3/0	Miocene to Holocene	Olafsson
132I.	1991		++++++++++++++++++++	
132S.	1993		++++++++++++++++++++	
133I.	1991		++++++++++++++++++++	
133S.	1993	1/3/0	Neogene	Gartner *et al.*
		2/19/3	Neogene	Wei & Gartner
134I.	1992		++++++++++++++++++++	
134S.	1994	10/179/3	Eocene to Pleistocene	Staerker
135I.	1992		++++++++++++++++++++	
135S.	1994	13/191/3	Plio/Pleistocene	Styzen
136I.	1992		++++++++++++++++++++	
136S.	1993		++++++++++++++++++++	

APPENDIX D

Calcareous Nannofossil Glossary

GLOSSARY

CALCAREOUS NANNOFOSSILS

NB. The glossary has been formulated from the descriptive terms used in the thesis and also from glossaries and text of other publications (Bukry, 1969; Brasier, 1980; Perch-Nielsen, 1985a,b and Siesser, 1993) by extracting entries which describe calcareous nannofossils. It is not the intention of this glossary to redefine any of those terms that have been extracted.

Shape Terminology *

Abcentral. Inclination of the surface (element or rim) away from the centre point of the coccosphere.
Adcentral. Inclination of the surface (element or rim) in toward centre point of the coccosphere.
Appressed shields. No gap between the distal and proximal shields.
Archaeopyle. An opening on a spherical surface (Thoracosphaeraceae, see also operculum).
Arm. Portion of crossbar between rim and centre of coccolith.
Asterolith.* Star- or rosette-shaped; projecting arms are called 'rays'.
Bar. Skeletal element crossing central area that does not pass through the centre of coccolith.
Birefringence. When a beam of light passes through a thin plate of calcite between crossed polars, the light splits into two beams, one 'fast' the other 'slow'. The difference between the corresponding relative indices will vary from poor to good, according to the direction in which the calcite is oriented relative to the crystallographic axes.
Block. Cubical or tabulate coccolith element.
Boss. Width equal to, or greater than the height.
Buttress. Calcite elements that support central stem or spine.
Calcareous nannofossils. A collective term for all the minute carbonate plates and rods
Calcareous nannoplankton. Planktic algae that bear carbonate plates and rods at some time in their life-cycle.
Calyptrolith.* Holococcolith; basket-shaped, open proximally.
Caneolith.* Disk-shaped; lath-filled central area.
Central area. Part of coccolith enclosed by rim cycle.
Central tube. Calcite elements in the form of a tube that join the distal and proximal shields together.
Ceratolith.* Horseshoe- or wishbone-shaped.
Checker board effect. Alternating square to oblong areas which are in and out of extinction.
Clockwise inclination. With sutures of elements inclined rightward as they proceed to the periphery.
Coccolith. Calcite plates forming the exterior covering of coccolithophores.
Coccolithophore. A minute, marine planktic alga belonging to the chrysophytes with two flagella and covering of minuscule calcareous plates.
Coccoshere. The more or less spherical cell covering of a coccolithophore, consisting of interlocking coccoliths
Collar. When calcite elements form a distinctive circular ring around the distal margin of an open central area.

Counter clockwise inclination. With sutures of elements inclined leftward as they proceed to the periphery.
Crenulate. A uniform rough outline.
Cribrilith.* Disk-shaped; numerous central-area perforations.
Cricolith.* Elliptical ring-shape.
Crossbar. A series of elements that cross the central area through the central point.
Crystallite. Largest structural unit acting as a single crystallographically homogeneous domain. These units lack the true crystal form of their constituent mineral - calcite.
Cycle. Ring of skeletal elements.
Cycolith.* Circular ring-shape.
Cyrtolith.* Basket-shaped, commonly with a projecting central process.
Dextral imbrication. Each element overlapping one to the right when viewed from the centre of the cycle
Dimorphic. A species with two distinct morphologic forms.
Distal view. Outward facing convex side of coccolith.
Dithecate. A coccolithophore constructed of two layers of coccoliths; each layer may contain coccoliths of different shapes.
Discolith.* Disk-shaped; thickened, raised rim; may or may not have central area perforations; definitions for this term may vary; synonymous in part with cribrilith.
Eccentricity. The measure of the variance of coccolith outline from a perfect circle: long axis/short axis.
Element. Base structural unit of coccolith, skeleton consisting of a single calcite crystallite.
Extinction line. It is part of the optic pattern formed when the calcareous nannofossil is viewed between crossed polars.
Flagellum. A relatively thin and long, protoplasmic extension from the cell of a protist or metazoan.
Form genus. A genus based on plant or algal parts with the same form or morphology.
Furrow. Long thin elongate depression, normally aligned to the long axis.
Golgi body. A membranous organelle within the cell of a eukaryote, usually containing various products of cell synthesis.
Granules. Normally found within the central area as disordered calcite elements.
Haptonema. A relatively thin and long, protoplasmic extension which may be straight or coiled and may serve for temporary attachment in the haptophyce an algae.
Helicolith.* Spiralling, overlapping marginal flange.
Heterococcoliths. A coccolith constructed of calcite crystals that differ in size and shape.
Holococcoliths. A coccolith constructed of calcite crystals that are essentially identical in size and shape.
ICBN. (See also Organ genus and Form genus), International Code of Botanical Nomenclature, the rules for naming and recognising the proper names of plant species, accepted by all botanists; used to govern the use of names in algal protists.
ICZN. International Code of Zoological Nomenclature, the rules for naming and recognising the proper names of animal species, accepted by all zoologists; used also to govern the use of names in protozoan protists.
Imbricate. See dextral and sinistral imbrication.
Inclination. See clockwise and counter clockwise inclination.
Lopadolith.* Basket-, cup-, or vase-shaped, with high rim, opening distally.
Lath. Skeletal element with one large dimension, one intermediate and one small.

Mitochondria. Conspicuous double membrane organelles within cell functioning in cell respiration.
Nannoconid.* Cone- or cylinder-shaped, with an axial canal.
Nannoliths. One of a variety of minuscule calcareous plates, probably from a planktic alga.
Operculum. A lid to cover opening on a spherical surface (Thoracosphaeraceae, see also archaeopyle).
Optic axes. The direction in crystals along which there is no double refraction.
Optic extinction patterns. The dark pattern formed by areas of a rock or fossil skeleton perpendicular or parallel to the crossed nicols of a polarising microscope that do not transmit light.
Organ genus. A generic name based on morphology of an organ from a fossil, in particular the organ of a plant, such as a leaf, flower, stem, etc., or parts of algae.
Pellicle. The external, non mineralised covering of the cell of a protist.
Pentolith.* Five four sided crystals joined to form a pentagon.
Petaloid. Petal in shape with no imbrication, but can overlap.
Placolith.* Two shields joined by a central tube.
Pleomorphic. A species with two distinct morphologic forms at different phases of the life cycle.
Prismatolith.* Polygonal prisms, solid or perforate.
Proximal view. Inward facing concave side of coccolith.
Rabdolith.* Single shield, surmounted by a stem.
Radial. Suture corresponding to radius in circular form or to straight line drawn through nearest focus or line connecting foci of elliptical form.
Rim. Peripheral cycle or cycles of elements in coccolith skeletons surrounding central area.
Scapolith.* Rhombohedral-shaped, with parallel laths in central area.
Secondary cycle. Accessory circlet of elements which instead of being concentrically within the rim cycle rests on the rim cycle, seen only in proximal view.
Shield. Single layer of elements forming entire coccolith surface.
Sinistral imbrication. Each element overlapping one to the left when viewed from the centre of the cycle.
Slit. Thin elongate opening normally oriented to the long axis
Sphenolith.* Prismatic base formed of radial crystals, surmounted by cone.
Spine. An outward protrusion from the rim or see stem for alternative description.
Stelolith.* Cylinder- or column-shaped.
Stem. Complex of elements in the form of a cylindrical prism, which may be hollow or solid, and extends from the centre of the distal side of some coccoliths.
Stephanolith.* Polygonal- or cylindrical-shaped; hollow with radiating spokes.
Stub. See boss
Suture. Boundary between skeletal elements.
Vacuoles. A globular structure in the cytoplasm of a cell; may contain food particles, fats, oils, etc., or may function to expel material from the cell.
Vesicles. See golgi body.
Zygolith.* Elliptical ring with a crossbar supporting a central process.

APPENDIX E

Sample Data

CONTENTS

Introduction

Data Tables

In numerical order

Introduction
Fig. E.2. Processing Number (D. No.)
Fig. E.3. Sampling Number (Fieldwork)
Fig. E.4. Locality Number (Fig. E.1.)

Distribution Tables

In numerical order (D. No.)

Introduction
Fig. E.5. Late Cretaceous
Fig, E.6. Palaeocene
Fig. E.7. Mid to Late Eocene
Fig. E.8. Early Miocene
Fig. E.9 Late Miocene

Miscellaneous

Fig. E.10. Samples processed to reconnaissance level only

INTRODUCTION

Appendix E is split into three sections of formalised data; Data Tables, Distribution Tables and a Miscellaneous section, which were obtained during the course of the project. The headings common to all tables are explained in detail below.

Processing Number (D. No.)

The D. No. is assigned in strict numerical order from the Department of Geological Science's Micropalaeontological Laboratory processing record file, at the start of processing the sample. The sample may have multiple processing numbers assigned to itself, but a D. No. may only be assigned one sample.

New Locality Number

The New Locality Number has been assigned to assist the reader to determine the locality of samples processed from S.W. Cyprus (Fig. E.1). However, samples collected by Dr. H. A. Armstrong at the umber quarry, Margi and Kottaphi Hill, Agrokipia, north of the Troodos Massif, have been assigned numbers 101 and 102 respectively.

Localities 12 and 19 are noted on Fig. E.1., however, even though samples are available, none were processed and therefore no information is available for those localities in the Data Tables.

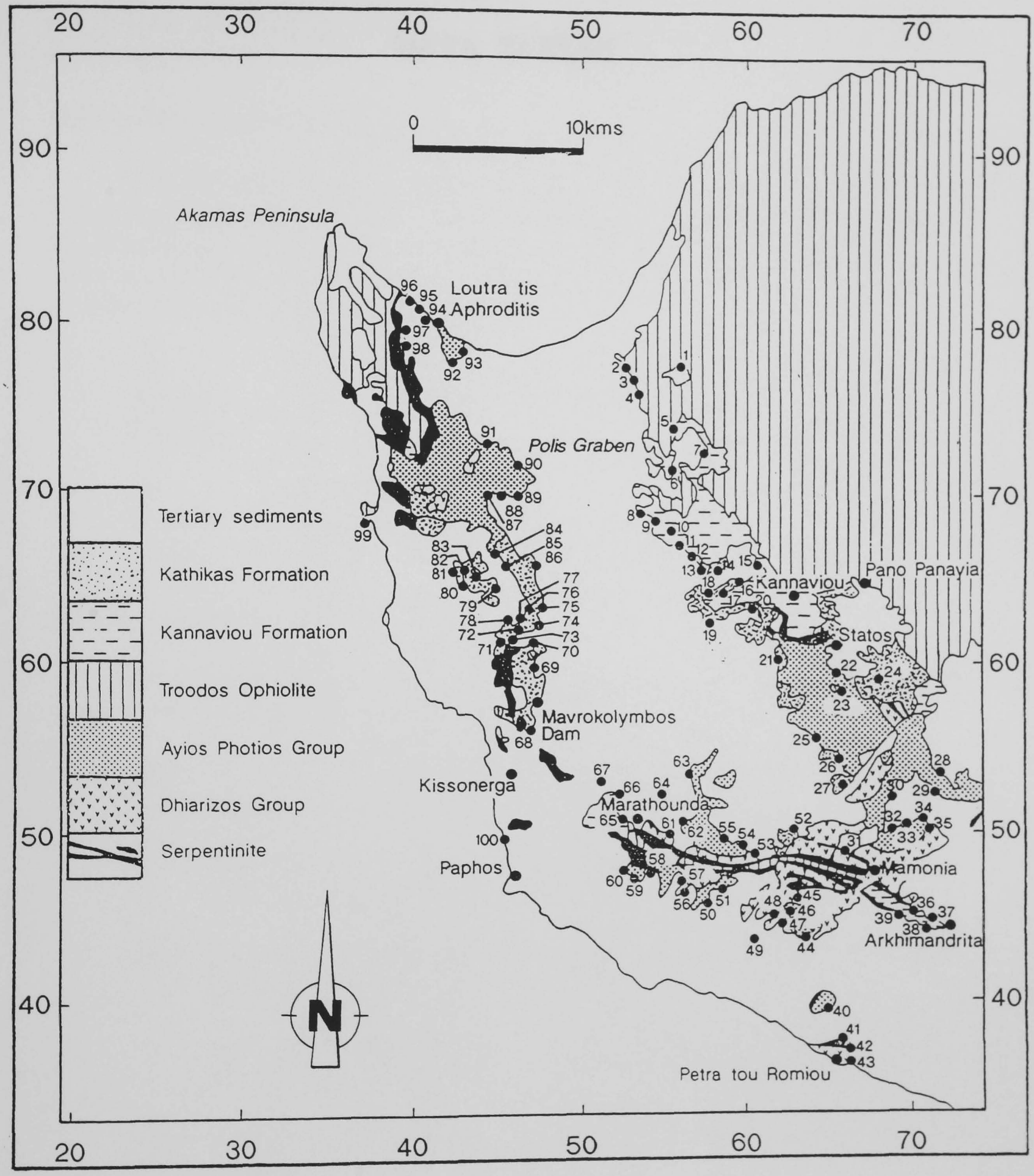

Fig. E.1. Geological map of S.W. Cyprus, displaying the sample localities.

DATA TABLES

Introduction

For information relating to headings, Processing Number, New Locality Number and Chapter, see introduction to Appendix E. Headings relating to the Data Tables only, are explained in detail below.

Old Locality Number (Fieldwork)

The first field season samples were collected within a field slip designation. However, this was found to be unworkable when processing data became available and the information needed to be filed in a more satisfactory manner. To overcome the problem, S.W. Cyprus was split into 12 field areas (A to L) and field area M for sample localities that were outside S.W. Cyprus.

CY	Prefix represents localities visited during the first field season.
A to EA	The following letter(s) is the field slip identifier.
1 to 12	The following number(s) is the locality with the field slip.
CP	Prefix represents localities visited after the first field season.
A to M	The following letter is the field area identifier.
1 to 12	The following number(s) is the locality within the field area.

Sample Number

All samples collected during the project were given a four figure number starting at 1001, with each separate field season visit having its own numerical identifier.

1992 1000,1100 and 1200 numbers for samples collected during the first field season based at the village of Mamonia.

1300 numbers for samples collected by Dr. H. A. Armstrong from the umber quarry, near the village of Margi.

1993 1400 numbers for samples collected during the second field season based at the village of Polis.

1500 numbers for samples collected by Dr. H. A. Armstrong from the Kottaphi Hill locality, near the village of Agrokipia.

1994 1600 numbers for samples collected during the third field season based at Paphos.

1994 1700 numbers for samples collected during the third year undergraduate Cyprus field visit, based at Limasol.

Grid Reference

Sampling localities are given a six figure grid reference based on the Cypriot Grid Reference System.

Lithological Key

CK	Calcareous sediments
EVAP	Evaporites
HG	Hard ground
INT	Chalk interbeds
KN	Kannaviou Formation
KT	Kathikas Formation (including chalk interbeds)
LST	Limestone
LST. B	Limestone breccia
ML	Marl
MN	'Moni Melange' type deposit
REW	Reworked horizon
R. MUD	Red mudstone
S	Sandstone (unconsolidated)
SERP	Serpentinite
SL.ST	Siltstone
T.INT	Calcareous interbed within Troodos pillow lava
TR	Troodos Complex (undifferentiated)

Age of sample relative to the Distribution Tables

UC	Late Cretaceous
P	Palaeocene
E	Eocene
LM	Early Miocene
UM	Late Miocene
X	Reconnaissance only

Thinsection and Smearslides

X = Availability
NB. During the production of smearslides, a coverslip was produced and stored for SEM investigations, if required.

Area (Records)

Based on the CP system of Old Locality Identifiers, the letter that follows the CP prefix, which represents the area identifier within S.W. Cyprus (A to M), is also the same identifier for the record files of processed data, collected from CY and CP sample localities.

PROCESSING NUMBER (D. No.)	OLD LOCALITY No.	SAMPLE NUMBER	GRID REFERENCE (CYPRUS)	LITHOLOGY	AGE	NEW LOCALITY NUMBER	THINSECTION	SMEARSLIDE	AREA (RECORDS)	CHAPTER IDENTIFIERS
60	CYBb1	1007	701454	KN	UC	37		X	J	
61	CYBb1	1008	701454	KN	UC	37	X	X	J	
62	CYBb1	1010	701454	KN	UC	37		X	J	
63	CYBb1	1012	701454	KN	UC	37		X	J	
64	CYBb1	1013	701454	KN	UC	37		X	J	
65	CYD1	1014	630437	CK	LM	44	X	X	H	P12
67	CYD2	1016	622447	CK	P	47	X	X	H	
68	CYF1	1017	394805	SERP	UC	96		X	A	
69	CYF1	1018	394805	LST	UM	96	X		A	
70	CYF1	1019	394805	LST	UM	96	X		A	
71	CYF1	1020	394805	LST	UM	96	X		A	
73	CYF1	1021	394805	LST	UM	96	X		A	
74	CYG1	1023	386774	LST	UM	97	X		A	
75	CYGI	1024	386774	LST	UM	97	X		A	
76	CYG1	1025	386774	LST	UM	97	X		A	
77	CYG1	1026	386774	LST	UM	97	X		A	
78	CYG2	1027	387764	SERP	UC	98	X	X	A	
79	CYG2	1030	387764	LST	LM	98	X	X	A	
80	CYG2	1031	387764	LST	LM	98	X	X	A	
86	CYDA5	1057	470627	KT	X	74	X		C	
87	CYBb1	1060	701454	KN	UC	37	X		J	
88	CYI1	1062	545775	TR	UC	1	X		B	
89	CYI1	1064	545775	TR	UC	1	X		B	
90	CYI1	1065	545775	LST	UM	1	X	X	B	
91	CYI1	1066	545775	LST	UM	1		X	B	
93	CYI3	1070	532750	CK	X	4		X	B	
94	CYE5	1151	522478	CT	X	59	X		E	
95	CYD3	1154	555461	CT	X	57	X		G	
96	CYBa1	1163	650390	LST	X	40	X		L	
97	MT2	1187	648547	CT	X	26	X		F	
98	CYG2	1255	387764	LST	UM	98	X	X	A	
99	CYG2	1256	387764	LST	UM	98	X	X	A	
100	CYG2	1257	387764	LST	UM	98	X	X	A	
101	CYG2	1258	387764	LST	UM	98	X	X	A	
102	CYG2	1259	387764	LST	LM	98	X	X	A	
103	CYG2	1262	387764	LST	UM	98	X	X	A	
104	CYG2	1029	387764	ML	X	98	X	X	A	
105	CYG2	1260	387764	LST.B	UM	98	X	X	A	
106	CYG2	1261	387764	LST.B	UM	98	X	X	A	
107	CYG2	1028	387764	SL.ST	X	98		X	A	
112	CYH1	1205	455713	CK	LM	90		X	A	
113	CYH1	1204	455713	CK	LM	90		X	A	
114	CYH1	1211	455713	INT	UC	90		X	A	
115	CYH2	1213	451696	CK	UC	89		X	A	
116	CYH2	1212	451696	CK	UC	89		X	A	LL3
117	CYQ1	1180	438695	CK	UC	87		X	A	LL4
118	CYCA3	1227	453653	CK	LM	85		X	C	
119	CYCA3	1226	453653	CK	LM	85		X	C	P3
120	CYCA3	1225	453653	CK	LM	85		X	C	
121	CYCA3	1224	453653	CK	LM	85		X	C	

Fig. E.2. Data table in numerical order based on Processing Number (D. No.).

PROCESSING NUMBER (D. No.)	OLD LOCALITY No.	SAMPLE NUMBER	GRID REFERENCE (CYPRUS)	LITHOLOGY	AGE	NEW LOCALITY NUMBER	THINSECTION	SMEARSLIDE	AREA (RECORDS)	CHAPTER IDENTIFIERS
122	CYCA5	1237	465655	CK	LM	86		X	C	P2
123	CYBA3	1218	422641	CK	LM	80		X	C	
124	CYBA3	1217	422641	CK	LM	80		X	C	P4
125	CYBA3	1216	422641	CK	UC	80		X	C	LL11
126	CYBA3	1215	422641	CK	UC	80		X	C	
127	CYDA3	1137	461629	HG	LM	78		X	C	
128	CYDA3	1040	461629	HG	LM	78		X	C	
129	CYDA3	1039	461629	HG	LM	78		X	C	
130	CYE5	1152	522478	CK	E	59		X	E	
131	CYE5	1151	522478	CK	E	59		X	E	
132	CYE5	1150	522478	REW	E	59		X	E	
133	CYA1	1004	662366	CK	P	42		X	L	
134	CYA1	1003	662366	CK	P	42		X	L	ML7
163	CYH1	1206	455713	MN	UC	90		X	A	
164	CYH1	1207	455713	MN	UC	90		X	A	MN1
165	CYH1	1208	455713	MN	UC	90		X	A	MN1
166	CYH1	1209	455713	INT	UC	90		X	A	
167	CYH1	1210	455713	INT	UC	90		X	A	MNI
184	CYCA1	1181	451658	CK	LM	84		X	C	
185	CYCA1	1182	451658	CK	LM	84		X	C	
186	CYBA6	1236	446643	CK	LM	79		X	C	
187	CYBA6	1235	446643	CK	LM	79		X	C	P5
188	CYBA6	1233	446643	HG	LM	79		X	C	
189	CYBA6	1232	446643	HG	LM	79		X	C	
190	CYBA6	1231	446643	HG	LM	79		X	C	
191	CYBA2	1214	437648	CK	LM	83		X	C	
192	CYBA1	1184	422646	CK	LM	81		X	C	
193	CYBA5	1221	421651	CK	LM	82		X	C	
194	CYDA3	1044	461629	CK	LM	78		X	C	
195	CYDA3	1043	461629	CK	LM	78		X	C	P6
196	CYDA3	1042	461629	CK	LM	78		X	C	
197	CYDA3	1038	461629	CK	UC	78		X	C	LL12
198	CYDA3	1139	461629	HG	LM	78		X	C	
199	CYDA10	1116	463629	CK	LM	76		X	C	
200	CYDA10	1117	463629	CK	LM	76		X	C	
201	CYDA9	1101	465629	CK	LM	75		X	C	
202	CYDA8	1100	468630	CK	LM	75		X	C	
204	CYEA1	1301	295765	KN	UC	101		X	M	
205	CYCA4	1230	454654	CK	LM	85		X	C	
206	CYCA4	1229	454654	CK	LM	85		X	C	
207	CYL1	1238	468601	CK	UC	69		X	C	LL15
215	CYJ1	1074	545718	CK	UC	6		X	B	LL7
216	CYS2	1106	546670	CK	E	11		X	B	
217	CYS3	1109	554666	CK	P	13		X	B	ML2
218	CYS4	1111	575652	CK	E	14		X	B	
219	MT2	1191	653395	CK	E	22		X	F	ML20
220	MT2	1188	655585	CK	E	23		X	F	
221	MT2	1185	639557	CK	E	25		X	F	
222	MT1	1174	712538	CK	E	28		X	I	
223	MT1	1175	707533	CK	E	29		X	1	

Fig. E.2 (cont.). Data table in numerical order based on Processing Number (D. No.).

PROCESSING NUMBER (D. No.)	OLD LOCALITY No.	SAMPLE NUMBER	GRID REFERENCE (CYPRUS)	LITHOLOGY	AGE	NEW LOCALITY NUMBER	THINSECTION	SMEARSLIDE	AREA (RECORDS)	CHAPTER IDENTIFIERS
224	MT2	1186	648547	CK	E	26		X	I	ML21
225	CYE3	1145	525510	CK	LM	65		X	D	
226	CYM3	1143	541512	CK	E	64		X	D	ML29
227	CYM2	1142	565525	CK	E	63		X	D	ML30
228	CYM1	1141	562503	CK	E	62		X	D	
229	CYE4	1148	522478	CK	E	60		X	E	
230	CYE4	1146	522478	REW	E	60		X	E	
231	CYD3	1153	555461	CK	E	57		X	E	ML14
232	CYN1	1157	588495	CK	E	55		X	F	
233	CYN2	1159	588492	CK	E	54		X	F	
234	CYD4	1156	562460	CK	E	56		X	G	
235	CYN3	1160	588490	CK	E	53		X	F	ML11
236	CYN5	1162	602478	CK	E	51		X	G	ML27
237	CYN6	1052	630513	CK	E	52		X	F	ML10
238	CYA2	1006	669369	CK	E	43		X	L	
239	CYA3	1264	665367	CK	E	42		X	L	
240	CYBa1	1164	650390	CK	E	40		X	L	ML15
241	CYBb1	1011	701454	KN	UC	37		X	J	
242	CYBb1	1059	701454	KN	UC	37		X	J	
243	CYBb2	1166	694448	CK	LM	38		X	K	
244	CYC1	1240	701458	CK	E	36		X	J	ML25
245	CYBb1	1060	701454	CK	E	37		X	J	
246	MT1	1179	619449	CK	P	47		X	H	ML6
247	MT1	1178	625451	CK	UC	46		X	H	
248	MT1	1177	630458	CK	UC	45		X	H	LL18
249	MT1	1176	657495	CK	E	31		X	I	
250	MT1	1173	700512	CK	E	33		X	I	
251	MT1	1172	701513	CK	E	33		X	I	
252	CYBb2	1165	694448	CK	LM	38		X	K	P14
253	CYI1	1067	545775	LST	UM	1		X	B	
254	CYI2	1068	528760	CK	UC	2		X	B	LL5
255	CYI2	1069	528760	CK	UC	2		X	B	
256	CPB1	1401	528760	CK	LM	2		X	B	
257	CPB2	1402	529757	CK	UC	3		X	B	
258	CPB3	1404	532750	T.INT	X	4		X	B	
259	CYI3	1071	532750	T.INT	X	4		X	B	
260	CYI3	1072	532750	T.INT	X	4		X	B	
261	CPB4	1405	550740	CK	UC	5		X	B	LL6
262	CPB4	1406	550740	CK	UC	5		X	B	
263	CYJ1	1073	545718	KN	UC	6		X	B	
264	CPB5	1407	545718	CK	E	6		X	B	ML16
265	CPB5	1408	545718	CK	E	6		X	B	
266	CPB6	1409	545674	CK	E	10		X	B	ML17
267	CPB7	1410	536678	CK	UM	9		X	B	MM3
268	CPB8	1451	560705	KN	UC	7		X	B	
269	CPB8	1452	560705	KN	UC	7		X	B	
270	CYS1	1103	542674	CK	UM	9		X	B	
271	CYS1	1104	542674	CK	E	9		X	B	
272	CYS2	1105	546670	CK	UC	11		X	B	LL9
273	CYS4	1110	575652	CK	E	14		X	B	ML18

Fig. E.2 (cont.). Data table in numerical order based on Processing Number (D. No.).

PROCESSING NUMBER (D. No.)	OLD LOCALITY No.	SAMPLE NUMBER	GRID REFERENCE (CYPRUS)	LITHOLOGY	AGE	NEW LOCALITY NUMBER	THINSECTION	SMEARSLIDE	AREA (RECORDS)	CHAPTER IDENTIFIERS
274	CYT1	1112	596660	CK	E	15		X	B	ML19
276	CPB10	1454	575643	CK	P	18		X	B	ML4
277	CYT2	1113	598650	KN	UC	16		X	B	KN1
278	CYT2	1114	598650	KN	UC	16		X	B	
279	CYT2	1115	598650	KN	UC	16		X	B	
280	CYS2	1107	546570	KN	UC	11		X	B	
281	CYS2	1108	546570	KN	UC	11		X	B	
282	MT2	1192	585640	KN	UC	17		X	B	
291	CYA1	1002	662366	KN	UC	41		X	B	
292	CYA1	1003	662366	KN	UC	41		X	L	
293	CYA2	1005	669368	KN	UC	43		X	L	
294	CYA3	1265	662366	KN	UC	42		X	L	
306	CYBb3	1168	684459	CK	E	39		X	K	
307	CYBb3	1169	684459	KN	UC	39		X	K	
308	CYBb2	1167	694448	KN	UC	38		X	K	
309	CYBb1	1009	701454	KN	UC	37		X	J	
310	CYC1	1241	701458	KN	UC	36		X	J	
311	CPA7	1437	423773	CK	UM	92		X	A	MM1
312	CPA6	1436	422782	CK	UC	93		X	A	LL1
313	CPA5	1435	402796	CK	LM	94		X	A	
314	CYF2	1022	400799	CK	E	95		X	A	
315	CPA4	1428	435733	CK	LM	91		X	A	
316	CPA1	1455	455713	CK	LM	90		X	A	P1
317	CPA1	1456	455713	CK	LM	90		X	A	
318	CPA1	1459	455713	LST	LM	90		X	A	
319	CPA1	1458	455713	LST	LM	90		X	A	
320	CPA1	1457	455713	CK	LM	90		X	A	
321	CPA1	1425	455713	LST	LM	90	X	X	A	
322	CPA1	1424	455713	LST	LM	90	X	X	A	
323	CPA1	1423	455713	LST	LM	90		X	A	
324	CPA1	1421	455713	CK	UC	90		X	A	LL2
325	CPA1	1411	455713	CK	UC	90		X	A	
326	CPA1	1412	455713	CK	UC	90		X	A	
328	CPA3	1427	439695	CK	LM	88		X	A	
329	CPA1	1414	455713	MN	UC	90		X	A	MN1
330	CPA1	1415	455713	MN	UC	90		X	A	
331	CPA1	1417	455713	MN	UC	90		X	A	
332	CPA1	1420	455713	MN	UC	90		X	A	MNI
333	CPA1	1413	455713	INT	UC	90		X	A	
334	CPA1	1416	455713	INT	UC	90		X	A	
335	CPA1	1418	455713	INT	UC	90		X	A	
336	CPA1	1419	455713	MN	UC	90		X	A	MNI
342	CPD1	1441	512547	CK	LM	67		X	D	
343	CPD2	1442	505537	CK	LM	67		X	D	
344	CYE6	1252	522509	CK	LM	66		X	D	P9
345	CYE7	1254	523510	CK	LM	66		X	D	
346	CYE6	1253	522509	KN	UC	66		X	D	
348	CPE1	1432	522478	CK	E	60		X	E	
349	CPE1	1433	522478	CK	E	60		X	E	
350	CPE2	1434	522478	CK	E	60		X	E	

Fig. E.2 (cont.). Data table in numerical order based on Processing Number (D. No.).

PROCESSING NUMBER (D. No.)	OLD LOCALITY No.	SAMPLE NUMBER	GRID REFERENCE (CYPRUS)	LITHOLOGY	AGE	NEW LOCALITY NUMBER	THINSECTION	SMEARSLIDE	AREA (RECORDS)	CHAPTER IDENTIFIERS
351	CYE1	1050	525475	CK	E	58		X	E	ML28
352	CPE1	1429	522478	REW	LM	60		X	E	
353	CPE1	1431	522478	REW	LM	60		X	E	
354	CPE1	1430	522478	INT	LM	60		X	E	
355	CYE1	1051	525475	KN	UC	58		X	E	
356	CYE5	1149	522478	REW	UC	59		X	E	
357	CYD3	1155	555461	CK	E	57		X	G	
358	CYN4	1161	596479	CK	E	50		X	G	
360	CYE4	1147	522478	REW	LM	60		X	E	
361	CPH1	1443	618448	CK	P	47		X	H	
362	CPH2	1444	623453	CK	P	46		X	H	
363	CPH2	1445	623453	CK	P	46		X	H	
364	CPI1	1446	657496	CK	E	31		X	I	ML24
365	CPI2	1447	682505	CK	E	32		X	I	ML8
366	CPI3	1448	682523	CK	E	30		X	I	ML9
367	CPI4	1449	698592	CK	E	29		X	I	ML23
368	CPI5	1450	713543	CK	E	28		X	I	ML22
369	MT1	1171	711512	CK	E	34		X	I	
370	MT1	1170	717507	CK	E	35		X	I	
371	CPF1	1470	588495	CK	E	55		X	F	ML12
372	CPF1	1471	589498	CK	E	55		X	F	
373	CPF1	1472	588505	CK	LM	55		X	F	P11
374	CPF1	1473	588508	CK	UM	55		X	F	
375	CPF1	1474	588508	CK	UM	55		X	F	
376	CPF1	1475	589509	EVAP	UM	55		X	F	
377	CPF1	1476	589512	CK	UM	55		X	F	
378	INT	1189	668601	INT	UC	24		X	F	KT3
379	INT	1190	668601	INT	UC	24		X	F	KT3
380	INT	1193	655531	KT	UC	27		X	F	KT4
381	INT	1194	655531	KT	UC	27		X	F	KT4
382	INT	1195	655531	KT	UC	27		X	F	KT4
383	INT	1196	655531	KT	UC	27		X	F	KT4
384	INT	1197	655531	KT	UC	27		X	F	KT4
385	INT	1198	655531	KT	UC	27		X	F	KT4
386	INT	1199	655531	KT	UC	27		X	F	KT4
387	INT	1200	655531	KT	UC	27		X	F	KT4
388	INT	1201	655531	KT	UC	27		X	F	KT4
389	INT	1202	655531	KT	UC	27		X	F	KT4
390	INT	1203	655531	KT	UC	27		X	F	KT4
391	CYN2	1158	588492	KN	UC	54		X	F	
393	CYBA6	1234	446643	HG	LM	79		X	C	
394	CYCA3	1223	453653	CK	LM	85		X	C	
395	CYCA4	1228	454654	CK	LM	85		X	C	
396	CYDA1	1035	468623	CK	LM	73		X	C	
397	CYDA1	1034	468623	CK	LM	73		X	C	
398	CYDA1	1033	468623	CK	LM	73		X	C	
400	CYDA3	1041	461629	S	LM	78		X	C	
401	CYDA3	1140	461629	HG	LM	78		X	C	
402	CYDA3	1138	461629	HG	LM	78		X	C	
403	CYDA5	1078	470627	CK	LM	74		X	C	

Fig. E.2 (cont.). Data table in numerical order based on Processing Number (D. No.).

PROCESSING NUMBER (D. No.)	OLD LOCALITY No.	SAMPLE NUMBER	GRID REFERENCE (CYPRUS)	LITHOLOGY	AGE	NEW LOCALITY NUMBER	THINSECTION	SMEARSLIDE	AREA (RECORDS)	CHAPTER IDENTIFIERS
404	CYDA5	1077	470627	CK	LM	74		X	C	P7
405	CYDA5	1082	470627	CK	LM	74		X	C	
406	CYDA5	1081	470627	CK	LM	74		X	C	
407	CYDA5	1080	470627	CK	LM	74		X	C	
408	CYDA5	1079	470627	CK	LM	74		X	C	
409	CYDA6	1090	470627	CK	LM	74		X	C	
410	CYDA6	1089	470627	CK	LM	74		X	C	
411	CYDA6	1091	470627	CK	LM	74		X	C	
412	CYDA6	1088	470627	CK	LM	74		X	C	
413	CYDA6	1087	470627	CK	LM	74		X	C	
414	CYDA6	1086	470627	CK	LM	74		X	C	
415	CYDA6	1085	470627	CK	LM	74		X	C	
416	CYDA7	1098	470627	CK	LM	74		X	C	
417	CYDA7	1096	470627	CK	LM	74		X	C	
418	CYDA7	1095	470627	CK	LM	74		X	C	
419	CYDA7	1097	470627	CK	LM	74		X	C	
420	CYDA12	1128	462629	CK	LM	77		X	C	
421	CYDA12	1127	462629	CK	LM	77		X	C	
422	CYDA12	1126	462629	CK	LM	77		X	C	
423	CYDA12	1125	462629	CK	LM	77		X	C	
424	CYDA12	1136	462629	HG	LM	77		X	C	
425	CYDA12	1135	462629	HG	LM	77		X	C	
426	CYDA12	1134	462629	HG	LM	77		X	C	
427	CYDA12	1133	462629	HG	LM	77		X	C	
428	CYDA12	1132	462629	HG	LM	77		X	C	
429	CYDA12	1131	462629	HG	LM	77		X	C	
430	CYDA12	1129	462629	HG	LM	77		X	C	
431	CYDA12	1130	462629	HG	LM	77		X	C	
432	CYDA11	1124	462629	CK	LM	77		X	C	
433	CYDA11	1123	462629	CK	LM	77		X	C	
434	CYDA11	1122	462629	HG	LM	77		X	C	
435	CYDA11	1121	462629	HG	LM	77		X	C	
436	CYDA11	1120	462629	HG	LM	77		X	C	
437	CYDA11	1119	462629	CK	UC	77		X	C	LL13
438	CYDA11	1118	462629	CK	UC	77		X	C	
439	CYDA1	1032	468623	R.MUD	X	73		X	C	
440	CYDA1	1036	468623	KT	UC	73		X	C	
441	CYDA2	1037	468623	KT	UC	73		X	C	
442	CYDA5	1076	470627	KT	UC	74		X	C	
443	CYDA5	1075	470627	KT	UC	74		X	C	
444	CYDA5	1084	470627	KT	UC	74		X	C	
445	CYDA5	1094	470627	KT	UC	74		X	C	
446	CYDA7	1093	470627	KT	UC	74		X	C	
447	CYDA7	1092	470627	KT	UC	74		X	C	
448	CYDA4	1053	470627	INT	UC	72		X	C	KT1
449	CYDA4	1054	470627	INT	UC	72		X	C	KT1
450	CYBA1	1182	422646	KN	UC	81		X	C	
451	CYBA5	1183	422646	KN	UC	82		X	C	
452	CYBA4	1219	426648	KN	UC	82		X	C	

Fig. E.2 (cont.). Data table in numerical order based on Processing Number (D. No.).

PROCESSING NUMBER (D. No.)	OLD LOCALITY No.	SAMPLE NUMBER	GRID REFERENCE (CYPRUS)	LITHOLOGY	AGE	NEW LOCALITY NUMBER	THINSECTION	SMEARSLIDE	AREA (RECORDS)	CHAPTER IDENTIFIERS
453	CYEA2	1501	145785	CK	LM	102		X	M	
454	CYEA2	1502	145785	CK	LM	102		X	M	
455	CYEA2	1503	145785	CK	LM	102		X	M	
456	CYEA2	1504	145785	CK	LM	102		X	M	
457	CYEA2	1505	145785	CK	LM	102		X	M	
458	CYEA2	1506	145785	CK	LM	102		X	M	
459	CYEA2	1507	145785	CK	LM	102		X	M	
460	CYEA2	1508	145785	CK	LM	102		X	M	
461	CYEA2	1509	145785	CK	LM	102		X	M	
462	CYEA2	1510	145785	CK	LM	102		X	M	
463	CYEA2	1511	145785	CK	LM	102		X	M	
464	CYEA2	1512	145785	CK	LM	102		X	M	
465	CYEA2	1514	145785	CK	LM	102		X	M	
466	CYEA2	1515	145785	CK	LM	102		X	M	
467	CYEA2	1516	145785	CK	LM	102		X	M	
468	CYEA2	1517	145785	CK	LM	102		X	M	
469	CYEA2	1518	145785	CK	UM	102		X	M	
470	CYEA2	1519	145785	CK	UM	102		X	M	
471	CYEA2	1520	145785	CK	UM	102		X	M	
472	CYEA2	1521	145785	CK	UM	102		X	M	
473	CYEA2	1522	145785	CK	UM	102		X	M	
476	CPD3	1477	539502	REW	E	61		X	D	
481	CPC1	1478	455612	CK	LM	70		X	C	
482	CPC1	1479	461609	CK	UC	70		X	C	LL14
483	CPC1	1480	463610	CK	UC	70		X	C	
484	CPC1	1481	454609	CK	UC	70		X	C	
485	CPC1	1482	450610	INT	UC	71		X	C	KT2
486	CPC2	1483	475563	CK	UC	68		X	C	LL16
487	CPL1	1484	670367	CK	E	43		X	L	ML26
488	CPL1	1485	670367	CK	E	43		X	L	ML26
489	CPL1	1486	670367	CK	E	43		X	L	ML26
490	CPL1	1487	670367	CK	E	43		X	L	ML26
491	CPL1	1488	670367	CK	LM	43		X	L	P13
492	CPL1	1489	670367	CK	LM	43		X	L	
493	CPL1	1490	670367	CK	LM	43		X	L	
494	CPL1	1491	670367	CK	LM	43		X	L	
495	CPL1	1492	670367	CK	LM	43	X	X	L	
517	CPD3	1716	539502	CK	X	61		X	D	
518	CPD3	1718	539502	CK	X	61		X	D	
519	CPL2	1715	661369	CK	E	41		X	L	
520	CPH5	1714	617455	CK	UC	48		X	H	LL17
521	CPB14	1634	555665	CK	P	13		X	B	
522	CPB14	1633	555665	CK	P	13		X	B	
523	CPH4	1645	605442	CK	LM	49		X	H	
524	CPL2	1655	661369	CK	P	41		X	H	
525	CPC3	1623	482571	CK	LM	68		X	C	
526	CPC3	1624	482571	CK	LM	68		X	C	
527	CPC3	1625	482571	CK	LM	68		X	C	
528	CPC3	1626	482571	CK	X	68		X	C	
529	CPC3	1627	482571	CK	LM	68		X	C	

Fig. E.2 (cont.). Data table in numerical order based on Processing Number (D. No.).

PROCESSING NUMBER (D. No.)	OLD LOCALITY No.	SAMPLE NUMBER	GRID REFERENCE (CYPRUS)	LITHOLOGY	AGE	NEW LOCALITY NUMBER	THINSECTION	SMEARSLIDE	AREA (RECORDS)	CHAPTER IDENTIFIERS
530	CPB12	1631	536678	CK	UM	9		X	B	
531	CPB12	1632	536678	CK	UC	9		X	B	LL8
532	CPB11	1630	528688	CK	P	8		X	B	ML1
533	CPB14	1635	555665	CK	P	13		X	B	
534	CPB14	1636	555665	CK	P	13		X	B	ML3
535	CPB16	1638	600632	CK	P	20		X	B	ML5
536	CPL2	1656	661369	CK	E	41		X	L	
537	CPL2	1654	661369	CK	E	41		X	L	ML26
538	CPA11	1629	368677	CK	UC	99		X	A	LL10
539	CPL2	1652	661369	CK	E	41		X	L	
540	CPL2	1651	661369	CK	E	41		X	L	
541	CPL2	1650	661369	CK	E	41		X	L	
565	CPC5	1801	510447	CK	UM	100		X	C	MM2
576	CPD5	1605	539502	CK	E	61		X	D	ML13
580	CPC3	1602	482571	CK	LM	68		X	C	P8
581	CPC3	1622	482571	LST	LM	68	X	X	C	
582	CPC5	1606	539502	CK	LM	61		X	D	P10
583	CPF2	1639	620594	CK	LM	21		X	F	P15
597	CPC3	1619	482571	CK	LM	68		X	C	
598	CPC3	1620	482571	CK	LM	68		X	C	
599	CPC3	1621	482571	CK	LM	68		X	C	
600	CPH4	1644	605442	CK	LM	49		X	H	
601	CPF2	1643	620594	CK	LM	21		X	F	

Fig. E.2 (cont.). Data table in numerical order based on Processing Number (D. No.).

SAMPLE NUMBER	PROCESSING NUMBER (D. No.)	OLD LOCALITY No.	GRID REFERENCE (CYPRUS)	LITHOLOGY	AGE	NEW LOCALITY NUMBER	THINSECTION	SMEARSLIDE	AREA (RECORDS)	CHAPTER IDENTIFIERS
1002	291	CYA1	662366	KN	UC	41		X	B	
1003	134	CYA1	662366	CK	P	42		X	L	ML7
1003	292	CYA1	662366	KN	UC	41		X	L	
1004	133	CYA1	662366	CK	P	42		X	L	
1005	293	CYA2	669368	KN	UC	43		X	L	
1006	238	CYA2	669369	CK	E	43		X	L	
1007	60	CYBb1	701454	KN	UC	37		X	J	
1008	61	CYBb1	701454	KN	UC	37	X	X	J	
1009	309	CYBb1	701454	KN	UC	37		X	J	
1010	62	CYBb1	701454	KN	UC	37		X	J	
1011	241	CYBb1	701454	KN	UC	37		X	J	
1012	63	CYBb1	701454	KN	UC	37		X	J	
1013	64	CYBb1	701454	KN	UC	37		X	J	
1014	65	CYD1	630437	CK	LM	44	X	X	H	P12
1016	67	CYD2	622447	CK	P	47	X	X	H	
1017	68	CYF1	394805	SERP	UC	96		X	A	
1018	69	CYF1	394805	LST	UM	96	X		A	
1019	70	CYF1	394805	LST	UM	96	X		A	
1020	71	CYF1	394805	LST	UM	96	X		A	
1021	73	CYF1	394805	LST	UM	96	X		A	
1022	314	CYF2	400799	CK	E	95		X	A	
1023	74	CYG1	386774	LST	UM	97	X		A	
1024	75	CYGI	386774	LST	UM	97	X		A	
1025	76	CYG1	386774	LST	UM	97	X		A	
1026	77	CYG1	386774	LST	UM	97	X		A	
1027	78	CYG2	387764	SERP	UC	98	X	X	A	
1028	107	CYG2	387764	SL.ST	X	98		X	A	
1029	104	CYG2	387764	ML	X	98	X	X	A	
1030	79	CYG2	387764	LST	LM	98	X	X	A	
1031	80	CYG2	387764	LST	LM	98	X	X	A	
1032	439	CYDA1	468623	R.MUD	X	73		X	C	
1033	398	CYDA1	468623	CK	LM	73		X	C	
1034	397	CYDA1	468623	CK	LM	73		X	C	
1035	396	CYDA1	468623	CK	LM	73		X	C	
1036	440	CYDA1	468623	KT	UC	73		X	C	
1037	441	CYDA2	468623	KT	UC	73		X	C	
1038	197	CYDA3	461629	CK	UC	78		X	C	LL12
1039	129	CYDA3	461629	HG	LM	78		X	C	
1040	128	CYDA3	461629	HG	LM	78		X	C	
1041	400	CYDA3	461629	S	LM	78		X	C	
1042	196	CYDA3	461629	CK	LM	78		X	C	
1043	195	CYDA3	461629	CK	LM	78		X	C	P6
1044	194	CYDA3	461629	CK	LM	78		X	C	
1050	351	CYE1	525475	CK	E	58		X	E	ML28
1051	355	CYE1	525475	KN	UC	58		X	E	
1052	237	CYN6	630513	CK	E	52		X	F	ML10
1053	448	CYDA4	470627	INT	UC	72		X	C	KT1
1054	449	CYDA4	470627	INT	UC	72		X	C	KT1
1057	86	CYDA5	470627	KT	X	74	X		C	
1059	242	CYBb1	701454	KN	UC	37		X	J	

Fig. E.3. Data table in numerical order based on Sampling Number (Fieldwork).

SAMPLE NUMBER	PROCESSING NUMBER (D. No.)	OLD LOCALITY No.	GRID REFERENCE (CYPRUS)	LITHOLOGY	AGE	NEW LOCALITY NUMBER	THINSECTION	SMEARSLIDE	AREA (RECORDS)	CHAPTER IDENTIFIERS
1060	87	CYBb1	701454	KN	UC	37	X		J	
1060	245	CYBb1	701454	CK	E	37		X	J	
1062	88	CYI1	545775	TR	UC	1	X		B	
1064	89	CYI1	545775	TR	UC	1	X		B	
1065	90	CYI1	545775	LST	UM	1	X	X	B	
1066	91	CYI1	545775	LST	UM	1		X	B	
1067	253	CYI1	545775	LST	UM	1		X	B	
1068	254	CYI2	528760	CK	UC	2		X	B	LL5
1069	255	CYI2	528760	CK	UC	2		X	B	
1070	93	CYI3	532750	CK	X	4		X	B	
1071	259	CYI3	532750	T.INT	X	4		X	B	
1072	260	CYI3	532750	T.INT	X	4		X	B	
1073	263	CYJ1	545718	KN	UC	6		X	B	
1074	215	CYJ1	545718	CK	UC	6		X	B	LL7
1075	443	CYDA5	470627	KT	UC	74		X	C	
1076	442	CYDA5	470627	KT	UC	74		X	C	
1077	404	CYDA5	470627	CK	LM	74		X	C	P7
1078	403	CYDA5	470627	CK	LM	74		X	C	
1079	408	CYDA5	470627	CK	LM	74		X	C	
1080	407	CYDA5	470627	CK	LM	74		X	C	
1081	406	CYDA5	470627	CK	LM	74		X	C	
1082	405	CYDA5	470627	CK	LM	74		X	C	
1084	444	CYDA5	470627	KT	UC	74		X	C	
1085	415	CYDA6	470627	CK	LM	74		X	C	
1086	414	CYDA6	470627	CK	LM	74		X	C	
1087	413	CYDA6	470627	CK	LM	74		X	C	
1088	412	CYDA6	470627	CK	LM	74		X	C	
1089	410	CYDA6	470627	CK	LM	74		X	C	
1090	409	CYDA6	470627	CK	LM	74		X	C	
1091	411	CYDA6	470627	CK	LM	74		X	C	
1092	447	CYDA7	470627	KT	UC	74		X	C	
1093	446	CYDA7	470627	KT	UC	74		X	C	
1094	445	CYDA5	470627	KT	UC	74		X	C	
1095	418	CYDA7	470627	CK	LM	74		X	C	
1096	417	CYDA7	470627	CK	LM	74		X	C	
1097	419	CYDA7	470627	CK	LM	74		X	C	
1098	416	CYDA7	470627	CK	LM	74		X	C	
1100	202	CYDA8	468630	CK	LM	75		X	C	
1101	201	CYDA9	465629	CK	LM	75		X	C	
1103	270	CYS1	542674	CK	UM	9		X	B	
1104	271	CYS1	542674	CK	E	9		X	B	
1105	272	CYS2	546670	CK	UC	11		X	B	LL9
1106	216	CYS2	546670	CK	E	11		X	B	
1107	280	CYS2	546570	KN	UC	11		X	B	
1108	281	CYS2	546570	KN	UC	11		X	B	
1109	217	CYS3	554666	CK	P	13		X	B	ML2
1110	273	CYS4	575652	CK	E	14		X	B	ML18
1111	218	CYS4	575652	CK	E	14		X	B	
1112	274	CYT1	596660	CK	E	15		X	B	ML19
1113	277	CYT2	598650	KN	UC	16		X	B	KN1

Fig. E.3 (cont.). Data table in numerical order based on Sampling Number (Fieldwork).

SAMPLE NUMBER	PROCESSING NUMBER (D. No.)	OLD LOCALITY No.	GRID REFERENCE (CYPRUS)	LITHOLOGY	AGE	NEW LOCALITY NUMBER	THINSECTION	SMEARSLIDE	AREA (RECORDS)	CHAPTER IDENTIFIERS
1114	278	CYT2	598650	KN	UC	16		X	B	
1115	279	CYT2	598650	KN	UC	16		X	B	
1116	199	CYDA10	463629	CK	LM	76		X	C	
1117	200	CYDA10	463629	CK	LM	76		X	C	
1118	438	CYDA11	462629	CK	UC	77		X	C	
1119	437	CYDA11	462629	CK	UC	77		X	C	LL13
1120	436	CYDA11	462629	HG	LM	77		X	C	
1121	435	CYDA11	462629	HG	LM	77		X	C	
1122	434	CYDA11	462629	HG	LM	77		X	C	
1123	433	CYDA11	462629	CK	LM	77		X	C	
1124	432	CYDA11	462629	CK	LM	77		X	C	
1125	423	CYDA12	462629	CK	LM	77		X	C	
1126	422	CYDA12	462629	CK	LM	77		X	C	
1127	421	CYDA12	462629	CK	LM	77		X	C	
1128	420	CYDA12	462629	CK	LM	77		X	C	
1129	430	CYDA12	462629	HG	LM	77		X	C	
1130	431	CYDA12	462629	HG	LM	77		X	C	
1131	429	CYDA12	462629	HG	LM	77		X	C	
1132	428	CYDA12	462629	HG	LM	77		X	C	
1133	427	CYDA12	462629	HG	LM	77		X	C	
1134	426	CYDA12	462629	HG	LM	77		X	C	
1135	425	CYDA12	462629	HG	LM	77		X	C	
1136	424	CYDA12	462629	HG	LM	77		X	C	
1137	127	CYDA3	461629	HG	LM	78		X	C	
1138	402	CYDA3	461629	HG	LM	78		X	C	
1139	198	CYDA3	461629	HG	LM	78		X	C	
1140	401	CYDA3	461629	HG	LM	78		X	C	
1141	228	CYM1	562503	CK	E	62		X	D	
1142	227	CYM2	565525	CK	E	63		X	D	ML30
1143	226	CYM3	541512	CK	E	64		X	D	ML29
1145	225	CYE3	525510	CK	LM	65		X	D	
1146	230	CYE4	522478	REW	E	60		X	E	
1147	360	CYE4	522478	REW	LM	60		X	E	
1148	229	CYE4	522478	CK	E	60		X	E	
1149	356	CYE5	522478	REW	UC	59		X	E	
1150	132	CYE5	522478	REW	E	59		X	E	
1151	94	CYE5	522478	CT	X	59	X		E	
1151	131	CYE5	522478	CK	E	59		X	E	
1152	130	CYE5	522478	CK	E	59		X	E	
1153	231	CYD3	555461	CK	E	57		X	E	ML14
1154	95	CYD3	555461	CT	X	57	X		G	
1155	357	CYD3	555461	CK	E	57		X	G	
1156	234	CYD4	562460	CK	E	56		X	G	
1157	232	CYN1	588495	CK	E	55		X	F	
1158	391	CYN2	588492	KN	UC	54		X	F	
1159	233	CYN2	588492	CK	E	54		X	F	
1160	235	CYN3	588490	CK	E	53		X	F	ML11
1161	358	CYN4	596479	CK	E	50		X	G	
1162	236	CYN5	602478	CK	E	51		X	G	ML27
1163	96	CYBa1	650390	LST	X	40	X		L	

Fig. E.3 (cont.). Data table in numerical order based on Sampling Number (Fieldwork).

SAMPLE NUMBER	PROCESSING NUMBER (D. No.)	OLD LOCALITY No.	GRID REFERENCE (CYPRUS)	LITHOLOGY	AGE	NEW LOCALITY NUMBER	THINSECTION	SMEARSLIDE	AREA (RECORDS)	CHAPTER IDENTIFIERS
1164	240	CYBa1	650390	CK	E	40		X	L	ML15
1165	252	CYBb2	694448	CK	LM	38		X	K	P14
1166	243	CYBb2	694448	CK	LM	38		X	K	
1167	308	CYBb2	694448	KN	UC	38		X	K	
1168	306	CYBb3	684459	CK	E	39		X	K	
1169	307	CYBb3	684459	KN	UC	39		X	K	
1170	370	MT1	717507	CK	E	35		X	I	
1171	369	MT1	711512	CK	E	34		X	I	
1172	251	MT1	701513	CK	E	33		X	I	
1173	250	MT1	700512	CK	E	33		X	I	
1174	222	MT1	712538	CK	E	28		X	I	
1175	223	MT1	707533	CK	E	29		X	1	
1176	249	MT1	657495	CK	E	31		X	I	
1177	248	MT1	630458	CK	UC	45		X	H	LL18
1178	247	MT1	625451	CK	UC	46		X	H	
1179	246	MT1	619449	CK	P	47		X	H	ML6
1180	117	CYQ1	438695	CK	UC	87		X	A	LL4
1181	184	CYCA1	451658	CK	LM	84		X	C	
1182	185	CYCA1	451658	CK	LM	84		X	C	
1182	450	CYBA1	422646	KN	UC	81		X	C	
1183	451	CYBA5	422646	KN	UC	82		X	C	
1184	192	CYBA1	422646	CK	LM	81		X	C	
1185	221	MT2	639557	CK	E	25		X	F	
1186	224	MT2	648547	CK	E	26		X	I	ML21
1187	97	MT2	648547	CT	X	26	X		F	
1188	220	MT2	655585	CK	E	23		X	F	
1189	378	INT	668601	INT	UC	24		X	F	KT3
1190	379	INT	668601	INT	UC	24		X	F	KT3
1191	219	MT2	653395	CK	E	22		X	F	ML20
1192	282	MT2	585640	KN	UC	17		X	B	
1193	380	INT	655531	KT	UC	27		X	F	KT4
1194	381	INT	655531	KT	UC	27		X	F	KT4
1195	382	INT	655531	KT	UC	27		X	F	KT4
1196	383	INT	655531	KT	UC	27		X	F	KT4
1197	384	INT	655531	KT	UC	27		X	F	KT4
1198	385	INT	655531	KT	UC	27		X	F	KT4
1199	386	INT	655531	KT	UC	27		X	F	KT4
1200	387	INT	655531	KT	UC	27		X	F	KT4
1201	388	INT	655531	KT	UC	27		X	F	KT4
1202	389	INT	655531	KT	UC	27		X	F	KT4
1203	390	INT	655531	KT	UC	27		X	F	KT4
1204	113	CYH1	455713	CK	LM	90		X	A	
1205	112	CYH1	455713	CK	LM	90		X	A	
1206	163	CYH1	455713	MN	UC	90		X	A	
1207	164	CYH1	455713	MN	UC	90		X	A	MN1
1208	165	CYH1	455713	MN	UC	90		X	A	MN1
1209	166	CYH1	455713	INT	UC	90		X	A	
1210	167	CYH1	455713	INT	UC	90		X	A	MNI
1211	114	CYH1	455713	INT	UC	90		X	A	
1212	116	CYH2	451696	CK	UC	89		X	A	LL3

Fig. E.3 (cont.). Data table in numerical order based on Sampling Number (Fieldwork).

SAMPLE NUMBER	PROCESSING NUMBER (D. No.)	OLD LOCALITY No.	GRID REFERENCE (CYPRUS)	LITHOLOGY	AGE	NEW LOCALITY NUMBER	THINSECTION	SMEARSLIDE	AREA (RECORDS)	CHAPTER IDENTIFIERS
1213	115	CYH2	451696	CK	UC	89		X	A	
1214	191	CYBA2	437648	CK	LM	83		X	C	
1215	126	CYBA3	422641	CK	UC	80		X	C	
1216	125	CYBA3	422641	CK	UC	80		X	C	LL11
1217	124	CYBA3	422641	CK	LM	80		X	C	P4
1218	123	CYBA3	422641	CK	LM	80		X	C	
1219	452	CYBA4	426648	KN	UC	82		X	C	
1221	193	CYBA5	421651	CK	LM	82		X	C	
1223	394	CYCA3	453653	CK	LM	85		X	C	
1224	121	CYCA3	453653	CK	LM	85		X	C	
1225	120	CYCA3	453653	CK	LM	85		X	C	
1226	119	CYCA3	453653	CK	LM	85		X	C	P3
1227	118	CYCA3	453653	CK	LM	85		X	C	
1228	395	CYCA4	454654	CK	LM	85		X	C	
1229	206	CYCA4	454654	CK	LM	85		X	C	
1230	205	CYCA4	454654	CK	LM	85		X	C	
1231	190	CYBA6	446643	HG	LM	79		X	C	
1232	189	CYBA6	446643	HG	LM	79		X	C	
1233	188	CYBA6	446643	HG	LM	79		X	C	
1234	393	CYBA6	446643	HG	LM	79		X	C	
1235	187	CYBA6	446643	CK	LM	79		X	C	P5
1236	186	CYBA6	446643	CK	LM	79		X	C	
1237	122	CYCA5	465655	CK	LM	86		X	C	P2
1238	207	CYL1	468601	CK	UC	69		X	C	LL15
1240	244	CYC1	701458	CK	E	36		X	J	ML25
1241	310	CYC1	701458	KN	UC	36		X	J	
1252	344	CYE6	522509	CK	LM	66		X	D	P9
1253	346	CYE6	522509	KN	UC	66		X	D	
1254	345	CYE7	523510	CK	LM	66		X	D	
1255	98	CYG2	387764	LST	UM	98	X	X	A	
1256	99	CYG2	387764	LST	UM	98	X	X	A	
1257	100	CYG2	387764	LST	UM	98	X	X	A	
1258	101	CYG2	387764	LST	UM	98	X	X	A	
1259	102	CYG2	387764	LST	UM	98	X	X	A	
1260	105	CYG2	387764	LST.B	UM	98	X	X	A	
1261	106	CYG2	387764	LST.B	UM	98	X	X	A	
1262	103	CYG2	387764	LST	LM	98	X	X	A	
1264	239	CYA3	665367	CK	E	42		X	L	
1265	294	CYA3	662366	KN	UC	42		X	L	
1301	204	CYEA1	295765	KN	UC	101		X	M	
1401	256	CPB1	528760	CK	LM	2		X	B	
1402	257	CPB2	529757	CK	UC	3		X	B	
1404	258	CPB3	532750	T.INT	X	4		X	B	
1405	261	CPB4	550740	CK	UC	5		X	B	LL6
1406	262	CPB4	550740	CK	UC	5		X	B	
1407	264	CPB5	545718	CK	E	6		X	B	ML16
1408	265	CPB5	545718	CK	E	6		X	B	
1409	266	CPB6	545674	CK	E	10		X	B	ML17
1410	267	CPB7	536678	CK	UM	9		X	B	MM3

Fig. E.3 (cont.). Data table in numerical order based on Sampling Number (Fieldwork).

SAMPLE NUMBER	PROCESSING NUMBER (D. No.)	OLD LOCALITY No.	GRID REFERENCE (CYPRUS)	LITHOLOGY	AGE	NEW LOCALITY NUMBER	THINSECTION	SMEARSLIDE	AREA (RECORDS)	CHAPTER IDENTIFIERS
1411	325	CPA1	455713	CK	UC	90		X	A	
1412	326	CPA1	455713	CK	UC	90		X	A	
1413	333	CPA1	455713	INT	UC	90		X	A	
1414	329	CPA1	455713	MN	UC	90		X	A	MN1
1415	330	CPA1	455713	MN	UC	90		X	A	
1416	334	CPA1	455713	INT	UC	90		X	A	
1417	331	CPA1	455713	MN	UC	90		X	A	
1418	335	CPA1	455713	INT	UC	90		X	A	
1419	336	CPA1	455713	MN	UC	90		X	A	MN1
1420	332	CPA1	455713	MN	UC	90		X	A	MN1
1421	324	CPA1	455713	CK	UC	90		X	A	LL2
1423	323	CPA1	455713	LST	LM	90		X	A	
1424	322	CPA1	455713	LST	LM	90	X	X	A	
1425	321	CPA1	455713	LST	LM	90	X	X	A	
1427	328	CPA3	439695	CK	LM	88		X	A	
1428	315	CPA4	435733	CK	LM	91		X	A	
1429	352	CPE1	522478	REW	LM	60		X	E	
1430	354	CPE1	522478	INT	LM	60		X	E	
1431	353	CPE1	522478	REW	LM	60		X	E	
1432	348	CPE1	522478	CK	E	60		X	E	
1433	349	CPE1	522478	CK	E	60		X	E	
1434	350	CPE2	522478	CK	E	60		X	E	
1435	313	CPA5	402796	CK	LM	94		X	A	
1436	312	CPA6	422782	CK	UC	93		X	A	LL1
1437	311	CPA7	423773	CK	UM	92		X	A	MM1
1441	342	CPD1	512547	CK	LM	67		X	D	
1442	343	CPD2	505537	CK	LM	67		X	D	
1443	361	CPH1	618448	CK	P	47		X	H	
1444	362	CPH2	623453	CK	P	46		X	H	
1445	363	CPH2	623453	CK	P	46		X	H	
1446	364	CPI1	657496	CK	E	31		X	I	ML24
1447	365	CPI2	682505	CK	E	32		X	I	ML8
1448	366	CPI3	682523	CK	E	30		X	I	ML9
1449	367	CPI4	698592	CK	E	29		X	I	ML23
1450	368	CPI5	713543	CK	E	28		X	I	ML22
1451	268	CPB8	560705	KN	UC	7		X	B	
1452	269	CPB8	560705	KN	UC	7		X	B	
1454	276	CPB10	575643	CK	P	18		X	B	ML4
1455	316	CPA1	455713	CK	LM	90		X	A	P1
1456	317	CPA1	455713	CK	LM	90		X	A	
1457	320	CPA1	455713	CK	LM	90		X	A	
1458	319	CPA1	455713	LST	LM	90		X	A	
1459	318	CPA1	455713	LST	LM	90		X	A	
1470	371	CPF1	588495	CK	E	55		X	F	ML12
1471	372	CPF1	589498	CK	E	55		X	F	
1472	373	CPF1	588505	CK	LM	55		X	F	P11
1473	374	CPF1	588508	CK	UM	55		X	F	
1474	375	CPF1	588508	CK	UM	55		X	F	
1475	376	CPF1	589509	EVAP	UM	55		X	F	
1476	377	CPF1	589512	CK	UM	55		X	F	

Fig. E.3 (cont.). Data table in numerical order based on Sampling Number (Fieldwork).

SAMPLE NUMBER	PROCESSING NUMBER (D. No.)	OLD LOCALITY No.	GRID REFERENCE (CYPRUS)	LITHOLOGY	AGE	NEW LOCALITY NUMBER	THINSECTION	SMEARSLIDE	AREA (RECORDS)	CHAPTER IDENTIFIERS
1477	476	CPD3	539502	REW	E	61		X	D	
1478	481	CPC1	455612	CK	LM	70		X	C	
1479	482	CPC1	461609	CK	UC	70		X	C	LL14
1480	483	CPC1	463610	CK	UC	70		X	C	
1481	484	CPC1	454609	CK	UC	70		X	C	
1482	485	CPC1	450610	INT	UC	71		X	C	KT2
1483	486	CPC2	475563	CK	UC	68		X	C	LL16
1484	487	CPL1	670367	CK	E	43		X	L	ML26
1485	488	CPL1	670367	CK	E	43		X	L	ML26
1486	489	CPL1	670367	CK	E	43		X	L	ML26
1487	490	CPL1	670367	CK	E	43		X	L	ML26
1488	491	CPL1	670367	CK	LM	43		X	L	P13
1489	492	CPL1	670367	CK	LM	43		X	L	
1490	493	CPL1	670367	CK	LM	43		X	L	
1491	494	CPL1	670367	CK	LM	43		X	L	
1492	495	CPL1	670367	CK	LM	43	X	X	L	
1501	453	CYEA2	145785	CK	LM	102		X	M	
1502	454	CYEA2	145785	CK	LM	102		X	M	
1503	455	CYEA2	145785	CK	LM	102		X	M	
1504	456	CYEA2	145785	CK	LM	102		X	M	
1505	457	CYEA2	145785	CK	LM	102		X	M	
1506	458	CYEA2	145785	CK	LM	102		X	M	
1507	459	CYEA2	145785	CK	LM	102		X	M	
1508	460	CYEA2	145785	CK	LM	102		X	M	
1509	461	CYEA2	145785	CK	LM	102		X	M	
1510	462	CYEA2	145785	CK	LM	102		X	M	
1511	463	CYEA2	145785	CK	LM	102		X	M	
1512	464	CYEA2	145785	CK	LM	102		X	M	
1514	465	CYEA2	145785	CK	LM	102		X	M	
1515	466	CYEA2	145785	CK	LM	102		X	M	
1516	467	CYEA2	145785	CK	LM	102		X	M	
1517	468	CYEA2	145785	CK	LM	102		X	M	
1518	469	CYEA2	145785	CK	UM	102		X	M	
1519	470	CYEA2	145785	CK	UM	102		X	M	
1520	471	CYEA2	145785	CK	UM	102		X	M	
1521	472	CYEA2	145785	CK	UM	102		X	M	
1522	473	CYEA2	145785	CK	UM	102		X	M	
1602	580	CPC3	482571	CK	LM	68		X	C	P8
1605	576	CPD5	539502	CK	E	61		X	D	ML13
1606	582	CPC5	539502	CK	LM	61		X	D	P10
1619	597	CPC3	482571	CK	LM	68		X	C	
1620	598	CPC3	482571	CK	LM	68		X	C	
1621	599	CPC3	482571	CK	LM	68		X	C	
1622	581	CPC3	482571	LST	LM	68	X	X	C	
1623	525	CPC3	482571	CK	LM	68		X	C	
1624	526	CPC3	482571	CK	LM	68		X	C	
1625	527	CPC3	482571	CK	LM	68		X	C	
1626	528	CPC3	482571	CK	X	68		X	C	
1627	529	CPC3	482571	CK	LM	68		X	C	
1629	538	CPA11	368677	CK	UC	99		X	A	LL10

Fig. E.3 (cont.). Data table in numerical order based on Sampling Number (Fieldwork).

SAMPLE NUMBER	PROCESSING NUMBER (D. No.)	OLD LOCALITY No.	GRID REFERENCE (CYPRUS)	LITHOLOGY	AGE	NEW LOCALITY NUMBER	THINSECTION	SMEARSLIDE	AREA (RECORDS)	CHAPTER IDENTIFIERS
1630	532	CPB11	528688	CK	P	8		X	B	ML1
1631	530	CPB12	536678	CK	UM	9		X	B	
1632	531	CPB12	536678	CK	UC	9		X	B	LL8
1633	522	CPB14	555665	CK	P	13		X	B	
1634	521	CPB14	555665	CK	P	13		X	B	
1635	533	CPB14	555665	CK	P	13		X	B	
1636	534	CPB14	555665	CK	P	13		X	B	ML3
1638	535	CPB16	600632	CK	P	20		X	B	ML5
1639	583	CPF2	620594	CK	LM	21		X	F	P15
1643	601	CPF2	620594	CK	LM	21		X	F	
1644	600	CPH4	605442	CK	LM	49		X	H	
1645	523	CPH4	605442	CK	LM	49		X	H	
1650	541	CPL2	661369	CK	E	41		X	L	
1651	540	CPL2	661369	CK	E	41		X	L	
1652	539	CPL2	661369	CK	E	41		X	L	
1654	537	CPL2	661369	CK	E	41		X	L	ML26
1655	524	CPL2	661369	CK	P	41		X	H	
1656	536	CPL2	661369	CK	E	41		X	L	
1714	520	CPH5	617455	CK	UC	48		X	H	LL17
1715	519	CPL2	661369	CK	E	41		X	L	
1716	517	CPD3	539502	CK	X	61		X	D	
1718	518	CPD3	539502	CK	X	61		X	D	
1801	565	CPC5	510447	CK	UM	100		X	C	MM2

Fig. E.3 (cont.). Data table in numerical order based on Sampling Number (Fieldwork).

NEW LOCALITY NUMBER	PROCESSING NUMBER (D. No.)	OLD LOCALITY No.	SAMPLE NUMBER	GRID REFERENCE (CYPRUS)	LITHOLOGY	AGE	THINSECTION	SMEARSLIDE	AREA (RECORDS)	CHAPTER IDENTIFIERS
1	88	CYI1	1062	545775	TR	UC	X		B	
	89	CYI1	1064	545775	TR	UC	X		B	
	90	CYI1	1065	545775	LST	UM	X	X	B	
	91	CYI1	1066	545775	LST	UM		X	B	
	253	CYI1	1067	545775	LST	UM		X	B	
2	254	CYI2	1068	528760	CK	UC		X	B	LL5
	255	CYI2	1069	528760	CK	UC		X	B	
	256	CPB1	1401	528760	CK	LM		X	B	
3	257	CPB2	1402	529757	CK	UC		X	B	
4	93	CYI3	1070	532750	CK	X		X	B	
	258	CPB3	1404	532750	T.INT	X		X	B	
	259	CYI3	1071	532750	T.INT	X		X	B	
	260	CYI3	1072	532750	T.INT	X		X	B	
5	261	CPB4	1405	550740	CK	UC		X	B	LL6
	262	CPB4	1406	550740	CK	UC		X	B	
6	215	CYJ1	1074	545718	CK	UC		X	B	LL7
	263	CYJ1	1073	545718	KN	UC		X	B	
	264	CPB5	1407	545718	CK	E		X	B	ML16
	265	CPB5	1408	545718	CK	E		X	B	
7	268	CPB8	1451	560705	KN	UC		X	B	
	269	CPB8	1452	560705	KN	UC		X	B	
8	532	CPB11	1630	528688	CK	P		X	B	ML1
9	267	CPB7	1410	536678	CK	UM		X	B	MM3
	270	CYS1	1103	542674	CK	UM		X	B	
	271	CYS1	1104	542674	CK	E		X	B	
	530	CPB12	1631	536678	CK	UM		X	B	
	531	CPB12	1632	536678	CK	UC		X	B	LL8
10	266	CPB6	1409	545674	CK	E		X	B	ML17
11	216	CYS2	1106	546670	CK	E		X	B	
	272	CYS2	1105	546670	CK	UC		X	B	LL9
	280	CYS2	1107	546570	KN	UC		X	B	
	281	CYS2	1108	546570	KN	UC		X	B	
13	217	CYS3	1109	554666	CK	P		X	B	ML2
	521	CPB14	1634	555665	CK	P		X	B	
	522	CPB14	1633	555665	CK	P		X	B	
	533	CPB14	1635	555665	CK	P		X	B	
	534	CPB14	1636	555665	CK	P		X	B	ML3
14	218	CYS4	1111	575652	CK	E		X	B	
	273	CYS4	1110	575652	CK	E		X	B	ML18
15	274	CYT1	1112	596660	CK	E		X	B	ML19
16	277	CYT2	1113	598650	KN	UC		X	B	KN1
	278	CYT2	1114	598650	KN	UC		X	B	
	279	CYT2	1115	598650	KN	UC		X	B	
17	282	MT2	1192	585640	KN	UC		X	B	

Fig. E.4. Data table in numerical order based on New Locality Number (Fig. E.1.).

NEW LOCALITY NUMBER	PROCESSING NUMBER (D. No.)	OLD LOCALITY No.	SAMPLE NUMBER	GRID REFERENCE (CYPRUS)	LITHOLOGY	AGE	THINSECTION	SMEARSLIDE	AREA (RECORDS)	CHAPTER IDENTIFIERS
18	276	CPB10	1454	575643	CK	P		X	B	ML4
20	535	CPB16	1638	600632	CK	P		X	B	ML5
21	583	CPF2	1639	620594	CK	LM		X	F	P15
	601	CPF2	1643	620594	CK	LM		X	F	
22	219	MT2	1191	653395	CK	E		X	F	ML20
23	220	MT2	1188	655585	CK	E		X	F	
24	378	INT	1189	668601	INT	UC		X	F	KT3
	379	INT	1190	668601	INT	UC		X	F	KT3
25	221	MT2	1185	639557	CK	E		X	F	
26	97	MT2	1187	648547	CT	X	X		F	
	224	MT2	1186	648547	CK	E		X	I	ML21
27	380	INT	1193	655531	KT	UC		X	F	KT4
	381	INT	1194	655531	KT	UC		X	F	KT4
	382	INT	1195	655531	KT	UC		X	F	KT4
	383	INT	1196	655531	KT	UC		X	F	KT4
	384	INT	1197	655531	KT	UC		X	F	KT4
	385	INT	1198	655531	KT	UC		X	F	KT4
	386	INT	1199	655531	KT	UC		X	F	KT4
	387	INT	1200	655531	KT	UC		X	F	KT4
	388	INT	1201	655531	KT	UC		X	F	KT4
	389	INT	1202	655531	KT	UC		X	F	KT4
	390	INT	1203	655531	KT	UC		X	F	KT4
28	222	MT1	1174	712538	CK	E		X	I	
	368	CPI5	1450	713543	CK	E		X	I	ML22
29	223	MT1	1175	707533	CK	E		X	I	
	367	CPI4	1449	698592	CK	E		X	I	ML23
30	366	CPI3	1448	682523	CK	E		X	I	ML9
31	249	MT1	1176	657495	CK	E		X	I	
	364	CPI1	1446	657496	CK	E		X	I	ML24
32	365	CP12	1447	667667	CK	E		X	I	ML8
33	250	MT1	1173	700512	CK	E		X	I	
	251	MT1	1172	701513	CK	E		X	I	
34	369	MT1	1171	711512	CK	E		X	I	
35	370	MT1	1170	717507	CK	E		X	I	
36	244	CYC1	1240	701458	CK	E		X	J	ML25
	310	CYC1	1241	701458	KN	UC		X	J	
37	60	CYBb1	1007	701454	KN	UC		X	J	
	61	CYBb1	1008	701454	KN	UC	X	X	J	
	62	CYBb1	1010	701454	KN	UC		X	J	
	63	CYBb1	1012	701454	KN	UC		X	J	
	64	CYBb1	1013	701454	KN	UC		X	J	
	87	CYBb1	1060	701454	KN	UC	X		J	
	241	CYBb1	1011	701454	KN	UC		X	J	
	242	CYBb1	1059	701454	KN	UC		X	J	

Fig. E.4 (cont.). Data table in numerical order based on New Locality Number (Fig. E.1.).

NEW LOCALITY NUMBER	PROCESSING NUMBER (D. No.)	OLD LOCALITY No.	SAMPLE NUMBER	GRID REFERENCE (CYPRUS)	LITHOLOGY	AGE	THINSECTION	SMEARSLIDE	AREA (RECORDS)	CHAPTER IDENTIFIERS
37	245	CYBb1	1060	701454	CK	E		X	J	
	309	CYBb1	1009	701454	KN	UC		X	J	
38	243	CYBb2	1166	694448	CK	LM		X	K	
	252	CYBb2	1165	694448	CK	LM		X	K	P14
	308	CYBb2	1167	694448	KN	UC		X	K	
39	306	CYBb3	1168	684459	CK	E		X	K	
	307	CYBb3	1169	684459	KN	UC		X	K	
40	96	CYBa1	1163	650390	LST	X	X		L	
	240	CYBa1	1164	650390	CK	E		X	L	ML15
41	291	CYA1	1002	662366	KN	UC		X	B	
	292	CYA1	1003	662366	KN	UC		X	L	
	519	CPL2	1715	661369	CK	E		X	L	
	524	CPL2	1655	661369	CK	P		X	H	
	536	CPL2	1656	661369	CK	E		X	L	
	537	CPL2	1654	661369	CK	E		X	L	ML26
	539	CPL2	1652	661369	CK	E		X	L	
	540	CPL2	1651	661369	CK	E		X	L	
	541	CPL2	1650	661369	CK	E		X	L	
42	133	CYA1	1004	662366	CK	P		X	L	
	134	CYA1	1003	662366	CK	P		X	L	ML7
	239	CYA3	1264	665367	CK	E		X	L	
	294	CYA3	1265	662366	KN	UC		X	L	
43	238	CYA2	1006	669369	CK	E		X	L	
	293	CYA2	1005	669368	KN	UC		X	L	
	487	CPL1	1484	670367	CK	E		X	L	ML26
	488	CPL1	1485	670367	CK	E		X	L	ML26
	489	CPL1	1486	670367	CK	E		X	L	ML26
	490	CPL1	1487	670367	CK	E		X	L	ML26
	491	CPL1	1488	670367	CK	LM		X	L	P13
	492	CPL1	1489	670367	CK	LM		X	L	
	493	CPL1	1490	670367	CK	LM		X	L	
	494	CPL1	1491	670367	CK	LM		X	L	
	495	CPL1	1492	670367	CK	LM	X	X	L	
44	65	CYD1	1014	630437	CK	LM	X	X	H	P12
45	248	MT1	1177	630458	CK	UC		X	H	LL18
46	247	MT1	1178	625451	CK	UC		X	H	
	362	CPH2	1444	623453	CK	P		X	H	
	363	CPH2	1445	623453	CK	P		X	H	
47	67	CYD2	1016	622447	CK	P	X	X	H	
	246	MT1	1179	619449	CK	P		X	H	ML6
	361	CPH1	1443	618448	CK	P		X	H	
48	520	CPH5	1714	617455	CK	UC		X	H	LL17
49	523	CPH4	1645	605442	CK	LM		X	H	
	600	CPH4	1644	605442	CK	LM		X	H	

Fig. E.4 (cont.). Data table in numerical order based on New Locality Number (Fig. E.1.).

NEW LOCALITY NUMBER	PROCESSING NUMBER (D. No.)	OLD LOCALITY No.	SAMPLE NUMBER	GRID REFERENCE (CYPRUS)	LITHOLOGY	AGE	THINSECTION	SMEARSLIDE	AREA (RECORDS)	CHAPTER IDENTIFIERS
50	358	CYN4	1161	596479	CK	E		X	G	
51	236	CYN5	1162	602478	CK	E		X	G	ML27
52	237	CYN6	1052	630513	CK	E		X	F	ML10
53	235	CYN3	1160	588490	CK	E		X	F	ML11
54	233	CYN2	1159	588492	CK	E		X	F	
	391	CYN2	1158	588492	KN	UC		X	F	
55	232	CYN1	1157	588495	CK	E		X	F	
	371	CPF1	1470	588495	CK	E		X	F	ML12
	372	CPF1	1471	589498	CK	E		X	F	
	373	CPF1	1472	588505	CK	LM		X	F	P11
	374	CPF1	1473	588508	CK	UM		X	F	
	375	CPF1	1474	588508	CK	UM		X	F	
	376	CPF1	1475	589509	EVAP	UM		X	F	
	377	CPF1	1476	589512	CK	UM		X	F	
56	234	CYD4	1156	562460	CK	E		X	G	
57	95	CYD3	1154	555461	CT	X	X		G	
	231	CYD3	1153	555461	CK	E		X	E	ML14
	357	CYD3	1155	555461	CK	E		X	G	
58	351	CYE1	1050	525475	CK	E		X	E	ML28
	355	CYE1	1051	525475	KN	UC		X	E	
59	94	CYE5	1151	522478	CT	X	X		E	
	130	CYE5	1152	522478	CK	E		X	E	
	131	CYE5	1151	522478	CK	E		X	E	
	132	CYE5	1150	522478	REW	E		X	E	
	356	CYE5	1149	522478	REW	UC		X	E	
60	229	CYE4	1148	522478	CK	E		X	E	
	230	CYE4	1146	522478	REW	E		X	E	
	348	CPE1	1432	522478	CK	E		X	E	
	349	CPE1	1433	522478	CK	E		X	E	
	350	CPE2	1434	522478	CK	E		X	E	
	352	CPE1	1429	522478	REW	LM		X	E	
	353	CPE1	1431	522478	REW	LM		X	E	
	354	CPE1	1430	522478	INT	LM		X	E	
	360	CYE4	1147	522478	REW	LM		X	E	
61	476	CPD3	1477	539502	REW	E		X	D	
	517	CPD3	1716	539502	CK	X		X	D	
	518	CPD3	1718	539502	CK	X		X	D	
	576	CPD5	1605	539502	CK	E		X	D	ML13
	582	CPC5	1606	539502	CK	LM		X	D	P10
62	228	CYM1	1141	562503	CK	E		X	D	
63	227	CYM2	1142	565525	CK	E		X	D	ML30
64	226	CYM3	1143	541512	CK	E		X	D	ML29
65	225	CYE3	1145	525510	CK	LM		X	D	
66	344	CYE6	1252	522509	CK	LM		X	D	P9

Fig. E.4 (cont.). Data table in numerical order based on New Locality Number (Fig. E.1.).

NEW LOCALITY NUMBER	PROCESSING NUMBER (D. No.)	OLD LOCALITY No.	SAMPLE NUMBER	GRID REFERENCE (CYPRUS)	LITHOLOGY	AGE	THINSECTION	SMEARSLIDE	AREA (RECORDS)	CHAPTER IDENTIFIERS
66	345	CYE7	1254	523510	CK	LM		X	D	
	346	CYE6	1253	522509	KN	UC		X	D	
67	342	CPD1	1441	512547	CK	LM		X	D	
	343	CPD2	1442	505537	CK	LM		X	D	
68	486	CPC2	1483	475563	CK	UC		X	C	LL16
	525	CPC3	1623	482571	CK	LM		X	C	
	526	CPC3	1624	482571	CK	LM		X	C	
	527	CPC3	1625	482571	CK	LM		X	C	
	528	CPC3	1626	482571	CK	X		X	C	
	529	CPC3	1627	482571	CK	LM		X	C	
	580	CPC3	1602	482571	CK	LM		X	C	P8
	581	CPC3	1622	482571	LST	LM	X	X	C	
	597	CPC3	1619	482571	CK	LM		X	C	
	598	CPC3	1620	482571	CK	LM		X	C	
	599	CPC3	1621	482571	CK	LM		X	C	
69	207	CYL1	1238	468601	CK	UC		X	C	LL15
70	481	CPC1	1478	455612	CK	LM		X	C	
	482	CPC1	1479	461609	CK	UC		X	C	LL14
	483	CPC1	1480	463610	CK	UC		X	C	
	484	CPC1	1481	454609	CK	UC		X	C	
71	485	CPC1	1482	450610	INT	UC		X	C	KT2
72	448	CYDA4	1053	470627	INT	UC		X	C	KT1
	449	CYDA4	1054	470627	INT	UC		X	C	KT1
73	396	CYDA1	1035	468623	CK	LM		X	C	
	397	CYDA1	1034	468623	CK	LM		X	C	
	398	CYDA1	1033	468623	CK	LM		X	C	
	439	CYDA1	1032	468623	R.MUD	X		X	C	
	440	CYDA1	1036	468623	KT	UC		X	C	
	441	CYDA2	1037	468623	KT	UC		X	C	
74	86	CYDA5	1057	470627	KT	X	X		C	
	403	CYDA5	1078	470627	CK	LM		X	C	
	404	CYDA5	1077	470627	CK	LM		X	C	P7
	405	CYDA5	1082	470627	CK	LM		X	C	
	406	CYDA5	1081	470627	CK	LM		X	C	
	407	CYDA5	1080	470627	CK	LM		X	C	
	408	CYDA5	1079	470627	CK	LM		X	C	
	409	CYDA6	1090	470627	CK	LM		X	C	
	410	CYDA6	1089	470627	CK	LM		X	C	
	411	CYDA6	1091	470627	CK	LM		X	C	
	412	CYDA6	1088	470627	CK	LM		X	C	
	413	CYDA6	1087	470627	CK	LM		X	C	
	414	CYDA6	1086	470627	CK	LM		X	C	
	415	CYDA6	1085	470627	CK	LM		X	C	
	416	CYDA7	1098	470627	CK	LM		X	C	

Fig. E.4 (cont.). Data table in numerical order based on New Locality Number (Fig. E.1.).

NEW LOCALITY NUMBER	PROCESSING NUMBER (D. No.)	OLD LOCALITY No.	SAMPLE NUMBER	GRID REFERENCE (CYPRUS)	LITHOLOGY	AGE	THINSECTION	SMEARSLIDE	AREA (RECORDS)	CHAPTER IDENTIFIERS
74	417	CYDA7	1096	470627	CK	LM		X	C	
	418	CYDA7	1095	470627	CK	LM		X	C	
	419	CYDA7	1097	470627	CK	LM		X	C	
	442	CYDA5	1076	470627	KT	UC		X	C	
	443	CYDA5	1075	470627	KT	UC		X	C	
	444	CYDA5	1084	470627	KT	UC		X	C	
	445	CYDA5	1094	470627	KT	UC		X	C	
	446	CYDA7	1093	470627	KT	UC		X	C	
	447	CYDA7	1092	470627	KT	UC		X	C	
75	201	CYDA9	1101	465629	CK	LM		X	C	
	202	CYDA8	1100	468630	CK	LM		X	C	
76	199	CYDA10	1116	463629	CK	LM		X	C	
	200	CYDA10	1117	463629	CK	LM		X	C	
77	420	CYDA12	1128	462629	CK	LM		X	C	
	421	CYDA12	1127	462629	CK	LM		X	C	
	422	CYDA12	1126	462629	CK	LM		X	C	
	423	CYDA12	1125	462629	CK	LM		X	C	
	424	CYDA12	1136	462629	HG	LM		X	C	
	425	CYDA12	1135	462629	HG	LM		X	C	
	426	CYDA12	1134	462629	HG	LM		X	C	
	427	CYDA12	1133	462629	HG	LM		X	C	
	428	CYDA12	1132	462629	HG	LM		X	C	
	429	CYDA12	1131	462629	HG	LM		X	C	
	430	CYDA12	1129	462629	HG	LM		X	C	
	431	CYDA12	1130	462629	HG	LM		X	C	
	432	CYDA11	1124	462629	CK	LM		X	C	
	433	CYDA11	1123	462629	CK	LM		X	C	
	434	CYDA11	1122	462629	HG	LM		X	C	
	435	CYDA11	1121	462629	HG	LM		X	C	
	436	CYDA11	1120	462629	HG	LM		X	C	
	437	CYDA11	1119	462629	CK	UC		X	C	LL13
	438	CYDA11	1118	462629	CK	UC		X	C	
78	127	CYDA3	1137	461629	HG	LM		X	C	
	128	CYDA3	1040	461629	HG	LM		X	C	
	129	CYDA3	1039	461629	HG	LM		X	C	
	194	CYDA3	1044	461629	CK	LM		X	C	
	195	CYDA3	1043	461629	CK	LM		X	C	P6
	196	CYDA3	1042	461629	CK	LM		X	C	
	197	CYDA3	1038	461629	CK	UC		X	C	LL12
	198	CYDA3	1139	461629	HG	LM		X	C	
	400	CYDA3	1041	461629	S	LM		X	C	
	401	CYDA3	1140	461629	HG	LM		X	C	
	402	CYDA3	1138	461629	HG	LM		X	C	
79	186	CYBA6	1236	446643	CK	LM		X	C	

Fig. E.4 (cont.). Data table in numerical order based on New Locality Number (Fig. E.1.).

NEW LOCALITY NUMBER	PROCESSING NUMBER (D. No.)	OLD LOCALITY No.	SAMPLE NUMBER	GRID REFERENCE (CYPRUS)	LITHOLOGY	AGE	THINSECTION	SMEARSLIDE	AREA (RECORDS)	CHAPTER IDENTIFIERS
79	187	CYBA6	1235	446643	CK	LM		X	C	P5
	188	CYBA6	1233	446643	HG	LM		X	C	
	189	CYBA6	1232	446643	HG	LM		X	C	
	190	CYBA6	1231	446643	HG	LM		X	C	
	393	CYBA6	1234	446643	HG	LM		X	C	
80	123	CYBA3	1218	422641	CK	LM		X	C	
	124	CYBA3	1217	422641	CK	LM		X	C	P4
	125	CYBA3	1216	422641	CK	UC		X	C	LL11
	126	CYBA3	1215	422641	CK	UC		X	C	
81	192	CYBA1	1184	422646	CK	LM		X	C	
	450	CYBA1	1182	422646	KN	UC		X	C	
82	193	CYBA5	1221	421651	CK	LM		X	C	
	451	CYBA5	1183	422646	KN	UC		X	C	
	452	CYBA4	1219	426648	KN	UC		X	C	
83	191	CYBA2	1214	437648	CK	LM		X	C	
84	184	CYCA1	1181	451658	CK	LM		X	C	
	185	CYCA1	1182	451658	CK	LM		X	C	
85	118	CYCA3	1227	453653	CK	LM		X	C	
	119	CYCA3	1226	453653	CK	LM		X	C	P3
	120	CYCA3	1225	453653	CK	LM		X	C	
	121	CYCA3	1224	453653	CK	LM		X	C	
	205	CYCA4	1230	454654	CK	LM		X	C	
	206	CYCA4	1229	454654	CK	LM		X	C	
	394	CYCA3	1223	453653	CK	LM		X	C	
	395	CYCA4	1228	454654	CK	LM		X	C	
86	122	CYCA5	1237	465655	CK	LM		X	C	P2
87	117	CYQ1	1180	438695	CK	UC		X	A	LL4
88	328	CPA3	1427	439695	CK	LM		X	A	
89	115	CYH2	1213	451696	CK	UC		X	A	
	116	CYH2	1212	451696	CK	UC		X	A	LL3
90	112	CYH1	1205	455713	CK	LM		X	A	
	113	CYH1	1204	455713	CK	LM		X	A	
	114	CYH1	1211	455713	INT	UC		X	A	
	163	CYH1	1206	455713	MN	UC		X	A	
	164	CYH1	1207	455713	MN	UC		X	A	MN1
	165	CYH1	1208	455713	MN	UC		X	A	MN1
	166	CYH1	1209	455713	INT	UC		X	A	
	167	CYH1	1210	455713	INT	UC		X	A	MNI
	316	CPA1	1455	455713	CK	LM		X	A	P1
	317	CPA1	1456	455713	CK	LM		X	A	
	318	CPA1	1459	455713	LST	LM		X	A	
	319	CPA1	1458	455713	LST	LM		X	A	
	320	CPA1	1457	455713	CK	LM		X	A	
	321	CPA1	1425	455713	LST	LM	X	X	A	

Fig. E.4 (cont.). Data table in numerical order based on New Locality Number (Fig. E.1.).

NEW LOCALITY NUMBER	PROCESSING NUMBER (D. No.)	OLD LOCALITY No.	SAMPLE NUMBER	GRID REFERENCE (CYPRUS)	LITHOLOGY	AGE	THINSECTION	SMEARSLIDE	AREA (RECORDS)	CHAPTER IDENTIFIERS
90	322	CPA1	1424	455713	LST	LM	X	X	A	
	323	CPA1	1423	455713	LST	LM		X	A	
	324	CPA1	1421	455713	CK	UC		X	A	LL2
	325	CPA1	1411	455713	CK	UC		X	A	
	326	CPA1	1412	455713	CK	UC		X	A	
	329	CPA1	1414	455713	MN	UC		X	A	MN1
	330	CPA1	1415	455713	MN	UC		X	A	
	331	CPA1	1417	455713	MN	UC		X	A	
	332	CPA1	1420	455713	MN	UC		X	A	MNI
	333	CPA1	1413	455713	INT	UC		X	A	
	334	CPA1	1416	455713	INT	UC		X	A	
	335	CPA1	1418	455713	INT	UC		X	A	
	336	CPA1	1419	455713	MN	UC		X	A	MNI
91	315	CPA4	1428	435733	CK	LM		X	A	
92	311	CPA7	1437	423773	CK	UM		X	A	MM1
93	312	CPA6	1436	422782	CK	UC		X	A	LL1
94	313	CPA5	1435	402796	CK	LM		X	A	
95	314	CYF2	1022	400799	CK	E		X	A	
96	68	CYF1	1017	394805	SERP	UC		X	A	
	69	CYF1	1018	394805	LST	UM	X		A	
	70	CYF1	1019	394805	LST	UM	X		A	
	71	CYF1	1020	394805	LST	UM	X		A	
	73	CYF1	1021	394805	LST	UM	X		A	
97	74	CYG1	1023	386774	LST	UM	X		A	
	75	CYGI	1024	386774	LST	UM	X		A	
	76	CYG1	1025	386774	LST	UM	X		A	
	77	CYG1	1026	386774	LST	UM	X		A	
98	78	CYG2	1027	387764	SERP	UC	X	X	A	
	79	CYG2	1030	387764	LST	LM	X	X	A	
	80	CYG2	1031	38776	LST	LM	X	X	A	
	98	CYG2	1255	387764	LST	UM	X	X	A	
	99	CYG2	1256	387764	LST	UM	X	X	A	
	100	CYG2	1257	387764	LST	UM	X	X	A	
	101	CYG2	1258	387764	LST	UM	X	X	A	
	102	CYG2	1259	387764	LST	UM	X	X	A	
	103	CYG2	1262	387764	LST	LM	X	X	A	
	104	CYG2	1029	387764	ML	X	X	X	A	
	105	CYG2	1260	387764	LST.B	UM	X	X	A	
	106	CYG2	1261	387764	LST.B	UM	X	X	A	
	107	CYG2	1028	387764	SL.ST	X		X	A	
99	538	CPA11	1629	368677	CK	UC		X	A	LL10
100	565	CPC5	1801	510447	CK	UM		X	C	MM2
101	204	CYEA1	1301	295765	KN	UC		X	M	

Fig. E.4 (cont.). Data table in numerical order based on New Locality Number (Fig. E.1.).

NEW LOCALITY NUMBER	PROCESSING NUMBER (D. No.)	OLD LOCALITY No.	SAMPLE NUMBER	GRID REFERENCE (CYPRUS)	LITHOLOGY	AGE	THINSECTION	SMEARSLIDE	AREA (RECORDS)	CHAPTER IDENTIFIERS
102	453	CYEA2	1501	145785	CK	LM		X	M	
	454	CYEA2	1502	145785	CK	LM		X	M	
	455	CYEA2	1503	145785	CK	LM		X	M	
	456	CYEA2	1504	145785	CK	LM		X	M	
	457	CYEA2	1505	145785	CK	LM		X	M	
	458	CYEA2	1506	145785	CK	LM		X	M	
	459	CYEA2	1507	145785	CK	LM		X	M	
	460	CYEA2	1508	145785	CK	LM		X	M	
	461	CYEA2	1509	145785	CK	LM		X	M	
	462	CYEA2	1510	145785	CK	LM		X	M	
	463	CYEA2	1511	145785	CK	LM		X	M	
	464	CYEA2	1512	145785	CK	LM		X	M	
	465	CYEA2	1514	145785	CK	LM		X	M	
	466	CYEA2	1515	145785	CK	LM		X	M	
	467	CYEA2	1516	145785	CK	LM		X	M	
	468	CYEA2	1517	145785	CK	LM		X	M	
	469	CYEA2	1518	145785	CK	UM		X	M	
	470	CYEA2	1519	145785	CK	UM		X	M	
	471	CYEA2	1520	145785	CK	UM		X	M	
	472	CYEA2	1521	145785	CK	UM		X	M	
	473	CYEA2	1522	145785	CK	UM		X	M	

Fig. E.4 (cont.). Data table in numerical order based on New Locality Number (Fig. E.1.).

DISTRIBUTION TABLES

Introduction

For information relating to headings, Processing Number, New Locality Number and Chapter, see introduction to Appendix E. Headings relating to the Distribution Tables only, are explained in detail below.

Preservation of calcareous nannofossils

G = GOOD (little or no alteration).
M = MODERATE (50% showing some form of alteration).
P = POOR (all showing some form of alteration).

Nannofossil Content

(field of view = 390μm).
A = ABUNDANT (>5 individuals per field of view).
C = COMMON (<5 individuals per field of view).
S = SPARSE (isolated occurrences).
N = No calcareous nannofossils found, dated by published papers.

Remarks

1). All processed samples noted within the Distribution Tables are of calcareous sediments, unless otherwise stated.
2). Serpentinite intrudes into the Kathikas Formation, but not the overlying calcareous sediments.
3). In the remarks column, reference to another processing number (D. No.), indicates the initial sample was devoid of calcareous nannofossils, with the new sample located along strike at the same horizon.

Key

A	Neptunean dykes, full of reworked flora, but is an integral part of the younger overlying lithological unit.
Maas	Reworked Maastrichtian flora.
T	Thinsection available.

Lithological Key

EVAP	Evaporites
HG	Hard ground
KN	Kannaviou Formation
Koronia	Koronia Limestone
KT	Kathikas Formation (including chalk interbeds)
MN	'Moni Melange' type deposit
REW	Reworked horizon
S	Sandstone (unconsolidated)
SERP	Serpentinite
Terra	Terra Limestone
TR	Troodos Complex (undifferentiated)

PROCESSING NUMBER (D. No.)	NEW LOCALITY NUMBER	PRESERVATION	NANNOFOSSIL CONTENT	Ellipsagelosphaera fossacincta	Sollasites horticus	Watznaueria barnesae	Biscutum constans	Discorhadus ignotus	Lithraphidites carniolensis	Stradneria crenulata	Glaukolithus compactus	Vekshinella stradneri	Placozygus fibuliformis	Corollithion signum	Eiffellithus turriseiffelii	Microrhabdulus decoratus	Cribrosphaerella ehrenbergii	Quadrum gartneri	Eiffellithus eximius	Micula staurophora	Vagalapilla compacta	Micula decussata	Calculites obscurus	Lithraphidites praequadratus	Microrhabdulus attenuatus	Retecapsa neocomiana	Prediscosphaera cretacea	Arkhangelskiella cymbiformis	Eiffellithus gorkae	Prediscosphaera grandis	Micula mura	Micula swastica	CHAPTER IDENTIFIERS	REMARKS
60	37		N																														KN
61	37		N																														KN
62	37		N																														KN
63	37		N																														KN
64	37		N																														SERP
68	96		N																														SERP
78	98		N																														KN
87	37		N																														TR
88	1		N																														TR
89	1		N																														MN
114	90	G	C			X			X	X	X		X			X	X					X				X	X						
115	89	G	C			X				X			X			X	X					X	X			X	X						
116	89	G	C			X				X	X					X	X					X	X			X	X	X				LL3	
117	87	G	A			X		X				X	X			X	X			X	X			X	X			X		X		LL4	
125	80	G	C			X				X		X	X			X	X			X					X			X			X	X	LL11	
126	80	G	C			X				X		X	X			X	X			X					X		X	X			X			
163	90		N																														MN
164	90	G	C			X			X	X			X		X	X	X					X			X			X	X			MN1	MN
165	90	G	C			X										X	X					X		X		X	X	X				MN1	MN
166	90	M	C			X				X						X	X					X				X	X						MN
167	90	G	C			X			X	X						X	X					X	X									MN1	MN
197	78	M	C			X							X		X		X			X		X					X			X		LL12	
204	101		N																														KN
207	69	P	S			X									X					X												LL15	
215	6	G	C			X							X			X	X					X			X		X	X				LL7	
241	37		N																														KN
242	37		N																														KN
247	46	P	S			X											X					X											
248	45	P	S			X				X			X																			LL18	
254	2	M	S			X				X			X		X	X				X							X				X	LL5	
255	2	M	S			X				X					X					X		X					X						
257	3		N																														
261	5	M	S			X				X						X				X		X					X	X				LL6	
262	5	M	S			X				X						X	X					X					X	X					
263	6		N																														KN
268	7		N																														KN
269	7		N																														KN
272	11	G	C			X				X			X			X	X					X					X	X				LL9	
277	16	G	A	X	X	X	X	X	X		X	X	X	X		X	X	X	X						X	X	X						KN1	KN
278	16		N																														KN
279	16		N																														KN
280	11		N																														KN
281	11	P	S			X										X	X					X											KN
282	17		N																														KN
291	41		N																														KN
292	41		N																														KN
293	43		N																														KN
294	42		N																														KN
307	39		N																														KN
308	38		N																														KN
309	37		N																														KN
310	36		N																														KN

Fig. E.5. Distribution of calcareous nannofossils viewed in the Late Cretaceous lithologies of S.W. Cyprus.

PROCESSING NUMBER (D. No.)	NEW LOCALITY NUMBER	PRESERVATION	NANNOFOSSIL CONTENT	Ellipsagelosphaera fossacincta	Sollasites horticus	Watznaueria barnesae	Biscutum constans	Discorhadus ignotus	Lithraphidites carniolensis	Stradneria crenulata	Glaukolithus compactus	Vekshinella stradneri	Placozygus fibuliformis	Corollithion signum	Eiffellithus turriseiffelii	Microrhabdulus decoratus	Cribrosphaerella ehrenbergii	Quadrum gartneri	Eiffellithus eximius	Micula staurophora	Vagalapilla compacta	Micula decussata	Calculites obscurus	Lithraphidites praequadratus	Microrhabdulus attenuatus	Retecapsa neocomiana	Prediscosphaera cretacea	Arkhangelskiella cymbiformis	Eiffellithus gorkae	Prediscosphaera grandis	Micula mura	Micula swastica	CHAPTER IDENTIFIERS	REMARKS
312	93	M	S			X				X					X	X	X					X					X	X					LL1	
324	90	M	A			X							X			X	X			X		X					X	X	X				LL2	
325	90	G	A			X							X			X	X					X					X	X						
326	90	G	A			X				X			X			X	X			X		X					X	X	X					
329	90	P	S			X				X																				X			MN1	MN
330	90	M	C			X			X	X			X		X	X	X					X			X			X	X					MN
331	90	M	C			X										X	X					X		X		X	X	X						MN
332	90	M	S			X									X																		MNI	MN
333	90	P	S			X				X												X												MN
334	90	M	C			X			X	X						X	X					X	X											MN
335	90	G	C			X			X	X			X			X	X					X			X		X	X						MN
336	90	G	C			X			X	X	X		X			X	X			X		X	X	X	X		X	X					MNI	MN
346	66		N																															KN
355	58		N																															KN
356	59		N																															REW
378	24	G	C			X			X	X						X	X			X					X		X	X					KT3	KT
379	24	G	C			X				X			X			X	X			X				X			X	X		X			KT3	KT
380	27	M	C			X				X			X		X	X	X			X			X				X	X		X			KT4	KT
381	27	M	C			X			X	X			X			X	X								X								KT4	KT
382	27	P	S			X				X			X			X	X											X					KT4	KT
383	27	M	C			X				X			X			X	X					X					X		X				KT4	KT
384	27	P	S			X				X			X		X	X	X					X	X	X			X						KT4	KT
385	27	P	S			X							X			X	X					X					X	X					KT4	KT
386	27	G	A			X			X	X			X			X	X							X			X	X		X			KT4	KT
387	27	G	A			X			X	X			X			X	X					X		X	X		X	X	X				KT4	KT
388	27	M	A			X				X			X			X	X					X					X	X					KT4	KT
389	27	G	A			X			X	X			X		X	X	X					X			X		X	X	X				KT4	KT
390	27	P	S			X			X							X	X							X			X						KT4	KT
391	54		N																															KN
437	77	M	S			X									X	X				X								X					LL13	
438	77	M	S			X				X					X	X						X						X						
440	73		N																															KT
441	73		N																															KT
442	74		N																															KT
443	74		N																															KT
444	74		N																															KT
445	74		N																															KT
446	74		N																															KT
447	74		N																															KT
448	72	M	S			X				X			X		X	X	X			X							X	X					KT1	KT
449	72	G	C			X		X								X	X								X		X	X					KT1	KT
450	81		N																															KN
451	82		N																															KN
452	82		N																															KN
482	70	M	C			X										X	X			X		X			X			X					LL14	
483	70	M	C			X							X				X					X						X						
484	70	M	C			X				X						X	X					X	X				X	X						
485	70	G	A			X			X	X			X			X	X			X		X					X	X	X	X			KT2	KT
486	68	M	A			X			X	X			X			X	X											X					LL16	
520	48	M	S			X				X			X				X					X	X				X							LL17	
531	9	M	S			X				X			X				X					X						X						LL8	
538	99	P	S			X							X				X																	LL10	

Fig. E.5 (cont.). Distribution of calcareous nannofossils viewed in the Late Cretaceous lithologies of S.W. Cyprus.

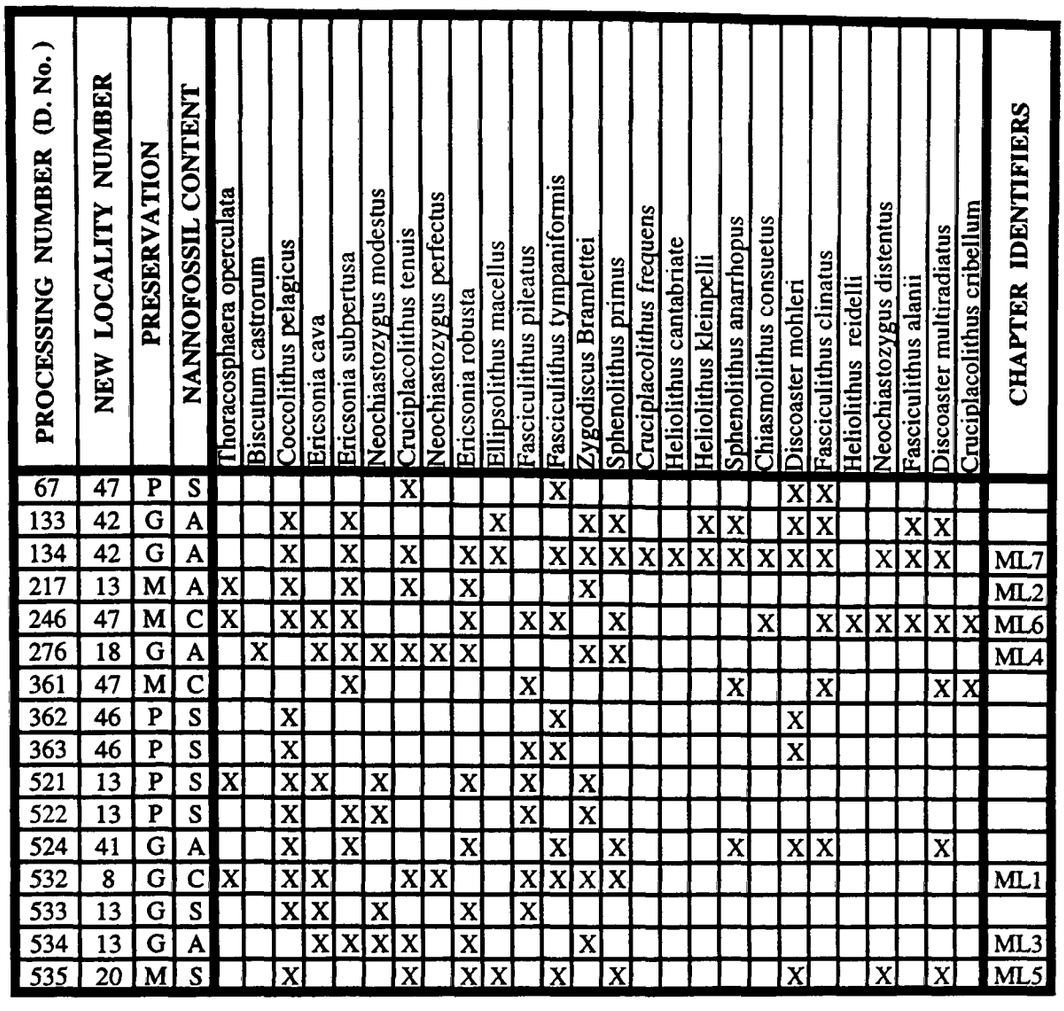

PROCESSING NUMBER (D. No.)	NEW LOCALITY NUMBER	PRESERVATION	NANNOFOSSIL CONTENT	Thoracosphaera operculata	Biscutum castrorum	Coccolithus pelagicus	Ericsonia cava	Ericsonia subpertusa	Neochiastozygus modestus	Cruciplacolithus tenuis	Neochiastozygus perfectus	Ericsonia robusta	Ellipsolithus macellus	Fasciculithus pileatus	Fasciculithus tympaniformis	Zygodiscus Bramlettei	Sphenolithus primus	Cruciplacolithus frequens	Heliolithus cantabriate	Heliolithus kleinpelli	Sphenolithus anarrhopus	Chiasmolithus consuetus	Discoaster mohleri	Fasciculithus clinatus	Heliolithus reidelli	Neochiastozygus distentus	Fasciculithus alanii	Discoaster multiradiatus	Cruciplacolithus cribellum	CHAPTER IDENTIFIERS
67	47	P	S							X					X								X	X						
133	42	G	A			X		X					X			X	X			X	X		X	X			X	X		
134	42	G	A			X		X		X		X	X		X	X	X	X	X	X	X	X	X	X		X	X	X		ML7
217	13	M	A	X		X		X		X		X				X														ML2
246	47	M	C	X		X	X	X				X		X	X		X						X		X	X	X	X	X	ML6
276	18	G	A		X		X	X	X	X	X	X				X	X													ML4
361	47	M	C					X						X							X			X				X	X	
362	46	P	S			X									X								X							
363	46	P	S			X								X	X								X							
521	13	P	S	X		X	X		X			X		X		X														
522	13	P	S			X		X	X					X		X														
524	41	G	A			X		X				X			X		X				X		X	X				X		
532	8	G	C	X		X	X			X	X			X	X	X	X													ML1
533	13	G	S			X	X		X			X		X																
534	13	G	A				X	X	X	X		X				X														ML3
535	20	M	S			X				X		X	X		X		X						X			X		X		ML5

Fig. E.6. Distribution of calcareous nannofossils viewed in the Late Palaeocene chalks of S.W. Cyprus.

PROCESSING NUMBER (D. No.)	NEW LOCALITY NUMBER	PRESERVATION	NANNOFOSSIL CONTENT	Coccolithus pelagicus	Chiasmolithus consuetus	Cruciplacolithus cribellum	Chiasmolithus californicus	Chiasmolithus solitus	Discoaster barbadiensis	Toweius gammation	Chiasmolithus grandis	Sphenolithus radians	Discoaster lodoensis	Chiasmolithus expansus	Ericsonia formosa	Sphenolithus moriformis	Reticulofenestra dictyoda	Sphenolithus spiniger	Discoaster wemmelensis	Calcidiscus protoannula	Thoracosphaera tuberosa	Coccolithus eopelagicus	Chiasmolithus medius	Cruciplacolithus vanheckae	Sphenolithus furcatolithoides	Reticulofenestra reticulata	Sphenolithus pseudoradians	Chiasmolithus modestus	Chiasmolithus nitidus	Cyclicargolithus marismontium	Reticulofenestra umbilica	Dictyococcites scrippsae	Reticulofenestra hillae	Dictyococcites bisectus	Cyclicargolithus floridanus	CHAPTER IDENTIFIERS
130	59	M	C	X								X					X					X					X		X	X	X				
131	59	M	C	X											X		X			X											X				
132	59	M	C	X													X					X										X				
216	11	M	C	X												X	X					X									X		X			
218	14	P	S	X											X															X		X	X	X		
219	22	P	S	X								X		X	X	X	X					X										X				ML20
220	23	M	S												X	X	X															X				
221	25	M	C	X								X					X				X															
222	28	P	S	X											X						X	X									X	X		X		
223	29	P	S	X											X																	X	X	X		
224	26	P	S	X								X			X	X							X									X		X		ML21
226	64	M	S	X								X			X	X	X												X		X					ML29
227	63	M	S	X	X										X	X	X						X						X			X				ML30
228	62	M	S	X				X							X					X										X		X				
229	60	M	C								X	X			X		X	X		X	X	X			X		X		X	X			X			
230	60	M	C	X												X					X	X											X		X	
231	57	M	C	X					X	X	X				X	X	X	X			X		X	X												ML14
232	55	M	C	X						X			X		X		X															X				
233	54	M	S	X					X			X					X																			
234	56	M	C	X																X		X									X	X		X	X	
235	53	M	S	X					X	X			X		X		X		X			X														ML11
236	51	M	S	X					X		X	X			X		X			X		X									X	X				ML27
237	52	M	A				X		X					X		X																				
238	43	M	C	X					X						X	X						X			X							X				
239	42	P	S	X											X																	X	X	X		
240	40	M	S	X							X	X			X	X	X	X							X											ML15
244	36	M	S	X										X	X	X				X	X											X		X		ML25
245	37	M	S	X											X	X	X																			
249	31	M	C	X								X			X		X					X										X				
250	33	P	S	X											X		X															X				
251	33	P	S	X								X			X		X					X									X					
264	6	P	S													X					X	X			X	X						X				ML16
265	6	P	S	X								X				X						X														
266	10	P	S	X												X	X			X		X										X				ML17
271	9	P	S	X								X			X																					
273	14	P	S									X					X					X				X						X				ML18
274	15	P	S	X					X						X	X						X								X	X	X				ML19
306	39	M	C								X				X	X	X															X				
314	95	P	S	X											X		X									X					X	X				
348	60	M	C	X											X			X				X	X	X								X				
349	60	M	C	X										X	X			X	X		X	X					X									
350	60	M	C	X											X		X					X	X		X							X				
351	58	G	C	X					X					X	X		X					X		X		X	X	X	X	X						ML28
357	57	M	S	X											X		X			X																
358	50	P	S	X											X		X		X			X														
364	31	M	C	X								X		X	X		X				X	X									X	X				ML24
365	32	M	C	X				X	X						X	X			X			X					X									ML8
366	30	M	S	X						X			X	X	X	X	X					X														ML9
367	29	M	C									X			X	X						X									X	X		X		ML23
368	28	M	C	X											X						X	X				X					X	X		X		ML22
369	34	M	S	X											X												X				X			X		

Fig. E.7. Distribution of calcareous nannofossils viewed in the Mid to Late Eocene chalks of S.W. Cyprus.

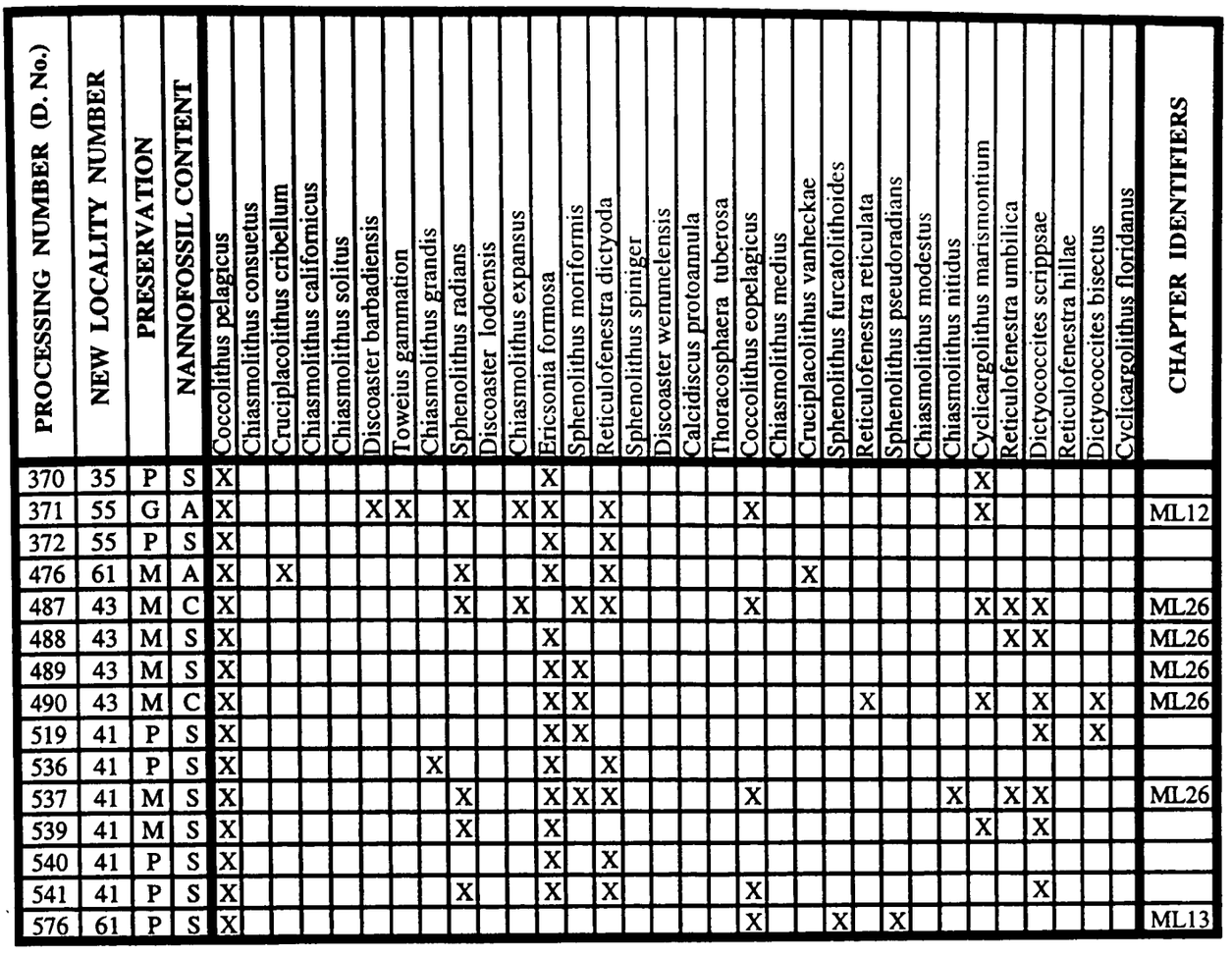

PROCESSING NUMBER (D. No.)	NEW LOCALITY NUMBER	PRESERVATION	NANNOFOSSIL CONTENT	Coccolithus pelagicus	Chiasmolithus consuetus	Cruciplacolithus cribellum	Chiasmolithus californicus	Chiasmolithus solitus	Discoaster barbadiensis	Toweius gammation	Chiasmolithus grandis	Sphenolithus radians	Discoaster lodoensis	Chiasmolithus expansus	Ericsonia formosa	Sphenolithus moriformis	Reticulofenestra dictyoda	Sphenolithus spiniger	Discoaster wemmelensis	Calcidiscus protoannula	Thoracosphaera tuberosa	Coccolithus eopelagicus	Chiasmolithus medius	Cruciplacolithus vanheckae	Sphenolithus furcatolithoides	Reticulofenestra reticulata	Sphenolithus pseudoradians	Chiasmolithus modestus	Chiasmolithus nitidus	Cyclicargolithus marismontium	Reticulofenestra umbilica	Dictyococcites scrippsae	Reticulofenestra hillae	Dictyococcites bisectus	Cyclicargolithus floridanus	CHAPTER IDENTIFIERS
370	35	P	S	X											X															X						
371	55	G	A	X					X	X		X		X	X		X					X								X						ML12
372	55	P	S	X											X		X																			
476	61	M	A	X		X						X			X		X							X												
487	43	M	C	X								X		X		X	X					X								X	X	X				ML26
488	43	M	S	X											X																X	X				ML26
489	43	M	S	X											X	X																				ML26
490	43	M	C	X											X	X										X				X		X		X		ML26
519	41	P	S	X											X	X																X		X		
536	41	P	S	X							X				X		X																			
537	41	M	S	X								X			X	X	X					X							X		X	X				ML26
539	41	M	S	X								X			X															X		X				
540	41	P	S	X											X		X																			
541	41	P	S	X								X			X		X					X										X				
576	61	P	S	X																		X			X		X									ML13

Fig. E.7 (cont.). Distribution of calcareous nannofossils viewed in the Mid to Late Eocene chalks of S.W. Cyprus.

PROCESSING NUMBER (D. No.)	NEW LOCALITY NUMBER	PRESERVATION	NANNOFOSSIL CONTENT	Coccolithus pelagicus	Pontosphaera mulipora	Sphenolithus moriformis	Dictyococcites scrippsae	Dictyococcites bisectus	Cyclicargolithus floridanus	Cyclicargolithus abisectus	Dictyococcites antarcticus	Coccolithus miopelagicus	Helicosphaera sissura	Thoracosphaera fossata	Helicosphaera kamptneri	Helicosphaera granulata	Umbilicosphaera sibogae	Discoaster variabilis	Sphenolithus heteromorphus	Reticulofenestra pseudoumbilicus	Calcidiscus macintyrei	Calcidiscus leptoporus	CHAPTER IDENTIFIERS	REMARKS
65	44	M	S	X	X		X	X	X	X	X	X			X								P12	
79	98		N																					Terra, T
80	98		N																					Terra, T
103	98		N																					
112	90	M	C	X			X		X		X	X			X									
113	90	M	C	X			X				X	X	X		X									
118	85	M	C	X			X		X						X									
119	85	M	A	X			X	X	X	X		X											P3	
120	85	M	C	X					X						X									
121	85	M	C																					REW, A
122	86	M	A	X			X	X	X	X		X											P2	
123	80	M	A	X			X	X	X	X	X	X			X									
124	80	M	A	X	X		X		X	X	X	X	X										P4	
127	78	G	A																					REW, Maas, A
128	78	G	A																					REW, Maas, A
129	78	G	A																					REW, Maas, A
184	84	M	S	X		X			X						X									
185	84	M	S	X		X		X	X						X									
186	79	M	C	X	X	X	X	X	X		X	X			X									
187	79	M	C	X	X			X	X		X	X	X		X								P5	
188	79	M	S	X					X		X	X			X									
189	79	M	S	X			X				X			X										
190	79	M	S	X					X	X		X												
191	83	P	S	X			X		X	X														
192	81	P	S	X			X		X		X													
193	82	P	S	X		X	X		X		X	X												
194	78	M	C	X	X				X	X	X	X			X									
195	78	M	C	X	X				X	X	X	X			X								P6	
196	78	M	C	X			X		X	X	X	X			X								P6	
198	78	M	C	X			X		X		X	X			X								P6	HG
199	76	M	S	X		X	X		X	X	X	X												
200	76	M	S	X	X	X	X		X	X		X			X									
201	75	P	S	X	X		X	X		X	X	X												
202	75	P	S	X			X	X			X	X												
205	85	P	S	X		X	X		X	X	X	X												
206	85	P	S	X	X	X	X		X		X	X			X									
225	65	M	C	X		X			X	X		X												
243	38	M	C	X	X	X	X	X	X	X		X			X	X	X							
252	38	M	C	X	X	X	X	X	X	X	X	X	X		X	X	X						P14	
256	2	P	S	X		X			X			X												
313	94		N																					Terra
315	91		N																					Terra
316	90	M	C	X					X		X	X	X	X	X								P1	
317	90	M	C	X			X		X		X	X		X	X								P1	
318	90		N																					Terra
319	90		N																					Terra, T
320	90		N																					Terra
321	90		N																					Terra, T
322	90		N																					Terra, T
323	90		N																					Terra
328	88	P	C	X		X			X			X		X	X		X				X	X		

Fig. E.8. Distribution of calcareous nannofossils viewed in the Early Miocene chalks of S.W. Cyprus and Kottaphi Hill, Agrokipia.

PROCESSING NUMBER (D. No.)	NEW LOCALITY NUMBER	PRESERVATION	NANNOFOSSIL CONTENT	Coccolithus pelagicus	Pontosphaera multipora	Sphenolithus moriformis	Dictyococcites scrippsae	Dictyococcites bisectus	Cyclicargolithus floridanus	Cyclicargolithus abisectus	Dictyococcites antarcticus	Coccolithus miopelagicus	Helicosphaera sissura	Thoracosphaera fossata	Helicosphaera kamptneri	Helicosphaera granulata	Umbilicosphaera sibogae	Discoaster variabilis	Sphenolithus heteromorphus	Reticulofenestra pseudoumbilicus	Calcidiscus macintyrei	Calcidiscus leptoporus	CHAPTER IDENTIFIERS	REMARKS
342	67	M	C	X					X		X	X		X			X		X	X				
343	67	M	C	X	X	X			X			X						X	X	X	X			
344	66	P	S	X					X		X	X			X								P9	
345	66	M	C	X		X			X			X			X			X						
352	60	M	A	X					X		X	X							X		X			REW
353	60	M	A	X					X			X					X		X		X			REW
354	60	M	A	X					X			X					X	X	X					REW
360	60	M	A	X		X			X		X	X		X				X						REW
373	55	G	A	X	X	X			X		X	X	X		X								P11	
393	79	P	S	X		X			X	X		X												HG
394	85	P	S	X			X	X	X		X	X												
395	85	P	S	X		X	X		X		X	X												
396	73	M	A	X	X	X	X		X	X	X	X												
397	73	M	A	X		X	X		X	X	X	X												
398	73	P	S	X			X		X	X		X												
400	78		N																					S
401	78	P	S	X			X	X	X			X											P6	HG
402	78	M	C	X			X		X		X	X			X								P6	HG
403	74	M	A	X		X	X	X	X	X			X		X									
404	74	M	A	X		X	X	X	X	X		X	X										P7	
405	74	M	C	X			X	X	X	X		X			X									
406	74	M	C	X		X	X	X	X	X		X												
407	74	M	A	X		X	X	X	X		X	X												
408	74		N																					S
409	74	M	C	X		X	X	X	X	X		X	X		X									
410	74	M	C	X		X	X	X	X	X		X	X		X									
411	74		N																					S
412	74	M	A	X			X	X	X	X		X			X									
413	74	M	S	X			X		X		X													
414	74	M	A	X		X	X	X	X		X	X			X									
415	74	M	C	X		X	X	X	X		X	X												
416	74	M	A	X			X	X	X	X	X	X			X									
417	74	M	C	X		X	X	X	X		X	X												
418	74	M	S	X			X		X			X			X									
419	74	M	A	X		X	X	X	X	X		X			X									
420	77	M	A	X	X		X	X	X		X	X												
421	77	M	A	X			X	X	X	X		X			X									
422	77	P	S	X			X		X	X														
423	77	M	A	X	X	X	X	X	X			X												
424	77	M	C	X		X	X	X	X		X	X												
425	77	M	C	X			X		X	X		X												
426	77	M	A	X		X	X	X	X		X	X												
427	77	M	A	X			X	X	X	X	X	X												
428	77	M	S	X		X		X	X			X												
429	77	P	S	X		X	X		X	X		X												
430	77	M	C	X		X	X	X	X			X												
431	77	M	C	X			X	X	X		X	X												
432	77	G	A	X	X	X	X		X	X	X	X			X									
433	77	M	C	X		X	X	X	X		X	X			X									
434	77	M	C	X			X	X	X	X	X	X												
435	77	M	C	X			X	X	X		X	X												
436	77	M	A	X		X	X	X	X	X	X	X												

Fig. E.8 (cont.). Distribution of calcareous nannofossils viewed in the Early Miocene chalks of S.W. Cyprus and Kottaphi Hill, Agrokipia.

PROCESSING NUMBER (D. No.)	NEW LOCALITY NUMBER	PRESERVATION		NANNOFOSSIL CONTENT	Coccolithus pelagicus	Pontosphaera multipora	Sphenolithus moriformis	Dictyococcites scrippsae	Dictyococcites bisectus	Cyclicargolithus floridanus	Cyclicargolithus abisectus	Dictyococcites antarcticus	Coccolithus miopelagicus	Helicosphaera sissura	Thoracosphaera fossata	Helicosphaera kamptneri	Helicosphaera granulata	Umbilicosphaera sibogae	Discoaster variabilis	Sphenolithus heteromorphus	Reticulofenestra pseudoumbilicus	Calcidiscus macintyrei	Calcidiscus leptoporus	CHAPTER IDENTIFIERS	REMARKS
453	102	P	S		X			X		X	X		X												
454	102	P	S		X					X	X		X			X									
455	102	P	S		X					X	X		X			X									
456	102	M	C		X				X	X	X	X	X	X											
457	102	P	S		X					X	X	X	X												
458	102	P	S		X					X	X		X												
459	102	M	C		X			X		X	X	X	X		X	X									
460	102	M	C		X					X		X	X			X									
461	102	P	C		X					X		X	X	X		X			X						
462	102	M	C		X					X		X	X	X	X	X									
463	102	P	C		X							X	X			X							X		
464	102	P	C		X	X				X		X	X	X		X			X		X				
465	102	P	A		X	X							X			X			X	X			X		
466	102	M	A		X							X	X		X	X			X	X					
467	102	P	S		X					X		X				X				X			X		
468	102	M	C							X		X				X		X			X				
481	70	P	S		X			X		X						X									
491	43	M	C		X	X	X	X	X		X	X	X					X			X			P13	
492	43	M	C		X	X		X			X	X	X		X	X								P13	
493	43	M	C		X	X		X	X	X	X		X			X								P13	
494	43	M	C		X	X		X		X	X	X	X			X								P13	
495	43		N																						Terra, T
523	49	P	S		X			X		X		X				X									
525	68	P	S		X				X		X		X											P8	
526	68	M	S		X					X	X	X	X			X								P8	
527	68	M	S		X			X	X	X		X	X											P8	
529	68	M	S		X		X	X			X		X	X		X								P8	
580	68	P	A		X			X	X	X	X		X			X								P8	
581	68	P	S					X				X	X											P8	Terra, T
582	61	M	C		X				X	X	X	X	X	X		X								P10	
583	21	G	A		X			X		X		X	X	X		X								P15	
597	68	M	A		X			X		X	X	X	X												
598	68	M	A		X			X		X	X	X	X												
599	68	M	C		X			X		X	X	X	X	X										P8	
600	49	M	C		X			X		X		X	X	X		X									
601	21	M	S		X			X	X	X			X			X									

Fig. E.8 (cont.). Distribution of calcareous nannofossils viewed in the Early Miocene chalks of S.W. Cyprus and Kottaphi Hill, Agrokipia.

PROCESSING NUMBER (D. No.)	NEW LOCALITY NUMBER	PRESERVATION	NANNOFOSSIL CONTENT	Pontosphaera multipora	Thoracosphaera fossata	Reticulofenestra minuta	Reticulofenestra haqii	Dictyococcites antarcticus	Helicosphaera kamptneri	Umbilicosphaera sibogae	Hayaster perplexus	Reticulofenestra pseudoumbilicus	Calcidiscus macintyrei	Calcidiscus leptoporus	Scyphosphaera apsteini	Scyphosphaera canescens	Scyphosphaera conica	Scyphosphaera recta	Scyphosphaera recurvata	Scyphosphaera turris	Coccolithus pliopelagicus	Catinaster coalitus	Rhabdosphaera procera	Sphenolithus abies	Discoaster pentaradiatus	Discoaster bellus	Helicosphaera selli	Discoaster neorectus	Amaurolithus amplificus	Sphenolithus verensis	Amaurolithus delicatus	CHAPTER IDENTIFIER	REMARKS
69	96		N																													Koronia, T.
70	96		N																														Koronia, T.
71	96		N																														Koronia, T.
73	96		N																														Koronia, T.
74	97		N																														Koronia, T.
75	97		N																														Koronia, T.
76	97		N																														Koronia, T.
77	97		N																														Koronia, T.
90	1		N																														Koronia, T.
91	1		N																														Koronia.
98	98		N																														Koronia, T.
99	98		N																														Koronia, T.
100	98		N																														Koronia, T.
101	98		N																														Koronia, T.
102	98		N																														Koronia, T.
105	98		N																														Koronia, T.
106	98		N																														Koronia, T.
253	1		N																														Koronia.
267	9	M	A	X					X				X	X		X						X		X				X				MM3	
270	9		N																														See 267
311	92	G	A	X		X	X	X	X			X	X	X		X	X			X				X	X	X		X				MM1	
374	55	P	C	X					X	X			X	X							X		X										
375	55	P	S		X				X			X			X						X		X										
376	55		N																														EVAP
377	55	P	S						X				X	X							X		X										
469	102	M	C					X	X	X		X		X									X										
470	102	M	C					X	X	X		X	X	X																			
471	102	P	S						X	X		X											X										
472	102		N																														
473	102	P	S						X	X		X												X	X								
530	9		N																														See 267
565	100	G	A		X			X	X	X	X	X	X		X	X	X	X	X	X	X		X	X	X		X	X	X	X	X	MM2	

Fig. E.9. Distribution of calcareous nannofossils viewed in the Late Miocene chalks of S.W. Cyprus and Kottaphi Hill, Agrokipia.

MISCELLANEOUS

PROCESSING NUMBER (D. No.)	OLD LOCALITY No.	SAMPLE NUMBER	GRID REFERENCE (CYPRUS)	LITHOLOGY	AGE	NEW LOCALITY NUMBER	THINSECTION	SMEARSLIDE	AREA (RECORDS)
86	CYDA5	1057	470627	KT	X	74	X		C
93	CYI3	1070	532750	CK	X	4		X	B
94	CYE5	1151	522478	CT	X	59	X		E
95	CYD3	1154	555461	CT	X	57	X		G
96	CYBa1	1163	650390	LST	X	40	X		L
97	MT2	1187	648547	CT	X	26	X		F
104	CYG2	1029	387764	ML	X	98	X	X	A
107	CYG2	1028	387764	SL.ST	X	98		X	A
258	CPB3	1404	532750	T.INT	X	4		X	B
259	CYI3	1071	532750	T.INT	X	4		X	B
260	CYI3	1072	532750	T.INT	X	4		X	B
439	CYDA1	1032	468623	R.MUD	X	73		X	C
517	CPD3	1716	539502	CK	X	61		X	D
518	CPD3	1718	539502	CK	X	61		X	D
528	CPC3	1626	482571	CK	X	68		X	C

Fig. E.10. Samples processed to reconnaissance level only (no calcareous nannofossils found).